

CRC REVIVALS

Instrumentation for Trace Organic Monitoring

Raymond E. Clement, K. W. M. Siu,
H. H. Hill

 CRC Press
Taylor & Francis Group

Instrumentation for Trace Organic Monitoring

R. E. Clement

K. W. M. Siu

H. H. Hill, Jr.



CRC Press

Taylor & Francis Group

Boca Raton London New York

CRC Press is an imprint of the
Taylor & Francis Group, an **informa** business

First published 1992 by CRC Press
Taylor & Francis Group
6000 Broken Sound Parkway NW, Suite 300
Boca Raton, FL 33487-2742

Reissued 2018 by CRC Press

© 1992 by LEWIS PUBLISHERS, INC.
CRC Press is an imprint of Taylor & Francis Group, an Informa business

No claim to original U.S. Government works

This book contains information obtained from authentic and highly regarded sources. Reasonable efforts have been made to publish reliable data and information, but the author and publisher cannot assume responsibility for the validity of all materials or the consequences of their use. The authors and publishers have attempted to trace the copyright holders of all material reproduced in this publication and apologize to copyright holders if permission to publish in this form has not been obtained. If any copyright material has not been acknowledged please write and let us know so we may rectify in any future reprint.

Except as permitted under U.S. Copyright Law, no part of this book may be reprinted, reproduced, transmitted, or utilized in any form by any electronic, mechanical, or other means, now known or hereafter invented, including photocopying, microfilming, and recording, or in any information storage or retrieval system, without written permission from the publishers.

Trademark Notice: Product or corporate names may be trademarks or registered trademarks, and are used only for identification and explanation without intent to infringe.

Library of Congress Cataloging-in-Publication Data

Instrumentation for trace organic monitoring/edited by R. E. Clement,

K. W. M. Siu, H. H. Hill, Jr.

p. cm.

Includes bibliographical references and index.

ISBN 0-87371-213-7

1. Organic compounds—Analysis. 2. Trace analysis.

3. Instrumental analysis. I. Clement, R. E. II. Siu, K. W. M.

III. Hill, H. H. (Herbert H.)

QD271.I547 1991

547.3—dc20

91-3892

A Library of Congress record exists under LC control number: 91003892

Publisher's Note

The publisher has gone to great lengths to ensure the quality of this reprint but points out that some imperfections in the original copies may be apparent.

Disclaimer

The publisher has made every effort to trace copyright holders and welcomes correspondence from those they have been unable to contact.

ISBN 13: 978-1-315-89462-1 (hbk)

ISBN 13: 978-1-351-07372-1 (ebk)

Visit the Taylor & Francis Web site at <http://www.taylorandfrancis.com> and the
CRC Press Web site at <http://www.crcpress.com>

PREFACE

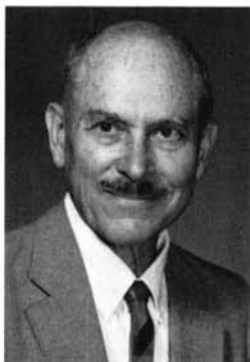
The determination of trace levels of organic substances in the environment is growing in importance. Many studies have shown that such compounds as the polycyclic aromatic hydrocarbons (PAH), polychlorinated biphenyls (PCBs), various organometallics, chlorinated dibenzo-p-dioxins (CDDs) and dibenzofurans (CDFs), cause very serious deleterious effects in animals tested under laboratory conditions. In many cases, these effects were observed when animals were exposed to only trace amounts of the chemical. The qualitative and quantitative determination of these and similar substances in the environment is therefore of considerable importance. Unfortunately, analyses for such contaminants often must be performed when the analytes are present at part-per-billion (ppb), part-per-trillion (ppt), or even part-per-quadrillion (ppq) concentrations. To complicate this task, real environmental samples are complex mixtures of hundreds of compounds, many of which may be interferences for the target analytes.

To meet the difficult analytical challenge described above, a number of instrumental analytical techniques have been developed and refined over the past 20 years. Some of these techniques are just now achieving full maturity, while others are now well-established. All are needed if we are to solve the complex problems of environmental analytical chemistry.

In this volume the advanced techniques of gas and liquid chromatography, low- and high-resolution mass spectrometry, ion mobility spectrometry, supercritical fluid extraction and chromatography, Fourier transform infrared spectroscopy, and others are described as they are used to solve complex environmental problems. These are the most important instrumental analytical techniques currently available to tackle the most difficult applications of trace organic analysis.

This book is based on a symposium to honor Professor Emeritus Francis W. Karasek which was part of the Third Chemical Congress of North America. The contents reflect the many contributions of Professor Karasek to the field of instrumental analytical chemistry.

IN HONOR OF FRANCIS W. KARASEK



Francis W. Karasek, Ph.D. received his B.Sc. degree from Elmhurst College in 1942 and his Ph.D. in 1952 from Oregon State University. Following an extended period as head of the automated analytical instrumentation group at Phillips Petroleum he moved to the University of Waterloo in Ontario, Canada as Associate Professor of analytical chemistry in 1968. He was promoted to full Professor in 1973, and was conferred the title of Professor Emeritus in 1988. Professor Karasek pioneered the development of ion mobility spectrometry, and is also known for his work in developing instrumental methodologies for the trace analysis of hazardous substances, such as the chlorinated dibenzo-p-dioxins and dibenzofurans. His most recent research efforts have led to the discovery of chemical techniques for controlling the formation of the chlorinated dioxins in municipal incineration processes, a development with major implications for environmental health and safety. Karasek brought new methods and techniques to the attention of analytical chemists via review articles and short courses. He has authored 3 books on organic trace analysis and over 250 publications, including 12 patents and 95 review papers. As an editorial associate for *Industrial Research/Development Magazine*, he has written 92 articles on new analytical instrumentation. He is the editor of the *Spectra-Physics Chromatography Review*, *Antek Application News* and was on the Editorial Board of *Analytical Letters*, *Chemosphere*, and the *International Journal of Environmental Analytical Chemistry*. Karasek's laboratory produced over 30 M.Sc.s and Ph.D.s since 1969. In 1988 he was honored by the Chemical Institute of Canada as the Fisher Scientific Award Winner for his contributions to analytical chemistry. He was also the initial winner of the Ontario Ministry of the Environment "Excellence in Science" award for analytical chemistry research for 1987-88. His honors also include the Wachmeister Chair of Science and Engineering 1984, Distinguished Professor, Bayreuth, Germany, 1986, and five visiting professorships. Professor Karasek wishes to encourage young scientists to engage in critical, analytical research directed at the solution of environmental problems. Towards this end he established in 1989 the Francis W. Karasek Award for Achievements in Environmental Science.



R. E. Clement, Ph.D., C. Chem. was awarded the Ph.D. degree from the University of Waterloo in 1981, under the supervision of Professor Emeritus F. W. Karasek. He joined the Ontario Ministry of the Environment in 1982 and is currently a senior research scientist in the Laboratory Services Branch. Dr. Clement has published 90 scientific papers, most in the dioxin/furan field, and has published or edited 4 books, including *Basic Gas Chromatography-Mass Spectrometry: Principles and Techniques*. In 1989, Dr. Clement chaired the 9th International Symposium on Chlorinated Dioxins and Related Compounds, and in 1990 served as the Associate Executive Director of the Canadian Institute for Research in Atmospheric Chemistry. He also has a strong interest in teaching environmental and analytical chemistry, for which he holds appointments as Adjunct Research Professor at Carleton University and Honorary Professor at the University of Western Ontario. He chaired a committee that developed a new Environmental Technology program at Durham College, and is active in the KEY (Knowledge of the Environment for Youth) foundation — a program to help high school teachers improve their knowledge of environmental issues. Dr. Clement serves on the Editorial Board of *Chemosphere* and is a member of ACS, CIC, ASMS, and AWMA.



K. W. M. Siu, Ph.D. obtained his doctorate in 1981 from Dalhousie University under the supervision of Walter A. Aue. He joined the then Division of Chemistry, National Research Council of Canada in 1982 as a Research Associate and became a Research officer in 1983. Dr. Siu's research interest is in the areas of chromatography and analytical mass spectrometry. In the past few years, his work has concentrated on the determination of environmentally significant organometallic species and on electrospray mass spectrometry. He has co-authored some 50 publications and given as many invited lectures in national and international conferences. He has been appointed Adjunct Professor in the Department of Chemistry, Carleton University as well as Queen's University. Dr. Siu serves on the Executive Board of the Analytical Chemistry Division, Chemical Institute of Canada and is a Contributing Editor of *Canadian Chemical News*.



H. H. Hill, Jr., Ph.D. obtained his doctoral degree in Chemistry in 1975 from Dalhousie University in Halifax, Nova Scotia under the direction of W. A. Aue. While at Dalhousie, he was a member of the Trace Analysis Research Centre and was awarded the Izaak Walton Memorial Scholarship for advanced study. Before joining the chemistry faculty at WSU in 1976, he spent a year as a postdoctoral fellow in the laboratory of F. W. Karasek at the University of Waterloo, Ontario.

His specific areas of research interests are chromatography, trace organic analysis, and ambient pressure ionization processes. For the past 15 years he has been involved in the research and development of various analytical methods such as gas chromatography, supercritical fluid chromatography, microbore liquid chromatography, supercritical fluid extraction, photoionization, flame ionization, and ion mobility spectrometry. He has published over 80 research papers on the separation and detection of trace organic compounds and recently received the Keene P. Dimick award for his research in detection methods for gas and supercritical fluid chromatography. Currently, his research focuses on the quantification and identification of mid-molecular weight range compounds (M.W. 300-3000) which are difficult to determine by traditional analytical methods.

CONTENTS

1. New Applications for IMS Detection Techniques, *A. H. Lawrence and L. Elias* 1
2. Continuous Atmospheric Monitoring of Organic Vapors by Ion Mobility Spectrometry, *G. A. Eiceman, A. P. Snyder, and D. A. Blyth*.... 13
3. Ion Mobility Spectrometry (IMS) Study of Aromatic Hydrocarbons and Nitrogen- and Sulfur-Containing Compounds, *Hiroyuki Hatano, Souji Rokushika, and Takashi Ohkawa* 27
4. Gas, Supercritical Fluid, and Liquid Chromatographic Detection of Trace Organics by Ion Mobility Spectrometry, *H. H. Hill, Jr., W. F. Siems, R. L. Eatherton, R. H. St. Louis, M. A. Morrissey, C. B. Shumate, and D. G. McMinn* 49
5. Analysis of the Headspace Vapors of Marijuana and Marijuana Cigarette Smoke Using Ion Mobility Spectrometry/Mass Spectrometry (IMS/MS), *S. H. Kim and G. E. Spangler* 65
6. The Development and Application of a High Resolution Mass Spectrometry Method for Measuring Polychlorinated Dibenzo-p-Dioxins and Dibenzofurans in Serum, *D. G. Patterson, Jr., L. R. Alexander, W. E. Turner, S. G. Isaacs, and L. L. Needham*..... 119
7. Comparison of Low Resolution, High Resolution Mass Spectrometry and Mass Spectrometry/Mass Spectrometry Techniques in the Analysis of Polychlorinated Dibenzo-p-Dioxins and Dibenzofurans, *Benjamin P.-Y. Lau, Dorcas Weber, and John J. Ryan*..... 155
8. The Evaluation of Toxicity of Water Leachates from Incinerator Flyash Using Living Human Cells and Analytical Techniques, *E. Jellum, A. K. Thorsrud, N. C. Herud, H. Y. Tong, and F. W. Karasek*.... 179
9. Determination of Organometallic Species by High Performance Liquid Chromatography-Mass Spectrometry, *J. W. McLaren, K. W. M. Siu, and S. S. Berman*..... 195
10. Advantages of an API Source for Analysis by Liquid Chromatography/Mass Spectrometry, *B. A. Thomson, A. Ngo and B. I. Shushan*.... 209
11. Parallel Column Gas Chromatography-Mass Spectrometry for the Analysis of Complex Environmental Mixtures, *J. C. Marr, J. Visentini, and M. A. Quilliam* 219

12. Current Status of Hyphenated Fourier Transform Infrared Techniques, <i>Donald F. Gurka</i>	241
13. Solvent-Free Extraction of Environmental Samples, <i>Janusz Pawliszyn</i>	253
14. Model Studies on the Solid-Supported Isolation, Derivation, and Purifi- cation of Chlorophenols and Chlorophenoxy Acetic Acid Herbicides, <i>Jack M. Rosenfeld and Y. Moharir</i>	279
15. A Surface Acoustic Wave Piezoelectric Crystal Aerosol Mass Microbalance, <i>W. D. Bowers and R. L. Chuan</i>	291
List of Authors	305
Index	309



Taylor & Francis

Taylor & Francis Group

<http://taylorandfrancis.com>

CHAPTER 1

New Applications for Ion Mobility Spectrometry Detection Techniques

A. H. Lawrence and L. Elias

The search for trace organic substances in complex organic and inorganic matrices is one of the most challenging tasks facing analytical chemists today. The presence of trace contaminants affects all aspects of our lives: the water and food we ingest, the air we breathe, the quality of the goods we produce, the environment in which we work and live—in short, our day-to-day health and security. The chemists' ability to discern these trace contaminants, which in one form or other may signify a hazard to human welfare, has been largely due to the development of highly sensitive and selective analytical instruments.

Modern instrumental analytical chemistry can be divided into two distinct categories: the first one comprises very powerful and versatile laboratory instrumentation designed for fixed-facility use and the detailed analysis of complex mixtures, e.g., GC/MS, GC/FTIR, tandem MS, etc., and the second one involves portable or easily transportable devices which are intended for field use and the detection of specific target compounds.

The Trace Vapour Detection Section of the Applied Aerodynamics Laboratory has been involved for a number of years in a program aimed at the development of rapid on-site sampling and analysis techniques for trace organic detection. This laboratory developed a portable gas chromatograph (GC) explosives detector which was subsequently transferred to industry and is now in use at all Canadian international airports.¹ In addition, a GC-based trace narcotics detector has also been developed and field tested; expected to be in production soon, the instrument is designed to detect cocaine and heroin residues in less than 2 min.²

Recently, we have investigated the feasibility of ion mobility spectrometry (IMS) as a viable field technology for trace organic detection and monitoring. Our decision was influenced by the fact that IMS offers distinct advantages, namely, good sensitivity (subpart-per-billion levels), fast response time (0.1 to 10 sec), and operation at atmospheric pressure.

ION MOBILITY SPECTROMETRY

The operation of an IMS is analogous to the operation of a time-of-flight mass spectrometer (TOF-MS), the main difference, however, being that the TOF-MS operates under vacuum whereas the IMS operates at atmospheric pressure.

The ion mobility spectrometer is comprised of a heated inlet, an ion-molecule reaction chamber containing a radioactive source or a photoionization source, an ion drift chamber, a shutter grid interposed between the reaction and drift chambers, and an ion collector (Figure 1). The sample, in vapor form, is introduced into the ion reaction chamber by means of a carrier gas (usually nitrogen or air). Trace impurities, such as water and ammonia present in the carrier gas, are ionized by the energetic electrons released from the radioactive source and a number of positive and negative reactant ions are formed, such as $(\text{H}_2\text{O})_n\text{H}^+$ and $(\text{H}_2\text{O})_n\text{O}_2^-$. These reactant ions undergo a complex series of ion-molecule reactions with the analyte, and product ions are formed. Depending on the polarity of an applied electric field, either positive or negative ions are periodically pulsed into the drift region through the gated shutter grid. In the drift region, the ions travel towards the collector through a drift gas while under the influence of the electric field. In doing so, they separate into their individual species due to their different mobilities; the transit time of a pulsed 'packet' of ions is generally in the order of 20 ms. A total ion mobility spectrum of ion current versus drift time can be generated in less than 5 sec. IMS results are usually reported in terms of drift time (millisecond) or the reduced mobility constant, $K_0(\text{cm}^2\text{V}^{-1}\text{sec}^{-1})$, according to Equation 1:

$$K_0 = d/t \cdot E (273/T)(P/760) \quad (1)$$

where t is the drift time of the ion in seconds, d is the drift length in centimeters, E is the electric field strength in volts per centimeter, P is the drift gas pressure in torr, and T is the drift gas temperature in degrees Kelvin.³

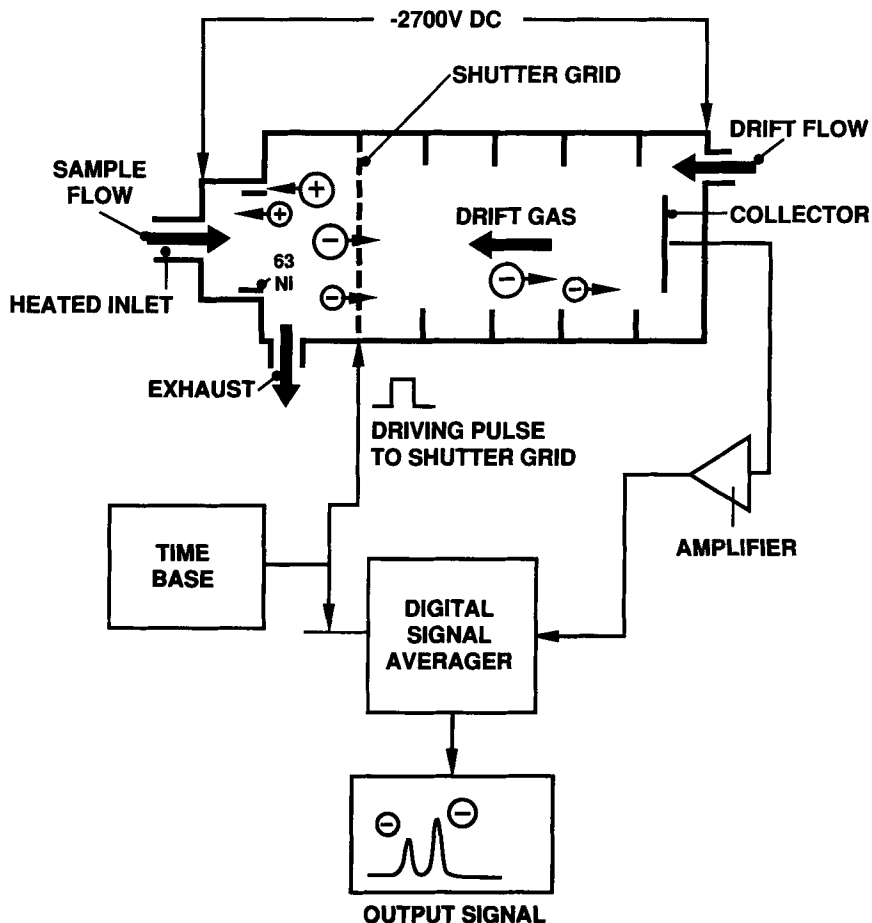


Figure 1. Schematic of ion mobility spectrometer.

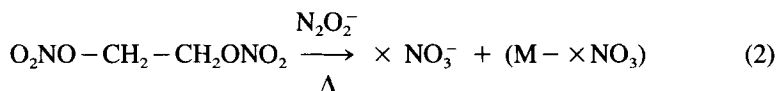
The IMS data presented in this chapter were obtained with a Phemto-Chem 100 ion mobility spectrometer (PCP Inc., West Palm Beach, FL) which contains a ^{63}Ni radioactive source, and the experimental parameters used to operate the instrument (unless indicated otherwise in the figure captions) were the same as those presented in Table 1.

APPLICATIONS RESEARCH

Although IMS has received considerable attention as a laboratory technique, it has not achieved, in our opinion, its full potential as a dedicated instrument intended for field use. We have investigated a number of interesting field applications which appear suited for IMS, as outlined below.

Detection of Hidden Bombs

A study was carried out by this laboratory on the detection of ethylene glycol dinitrate (EGDN)—the most volatile effluent in dynamite formulations—using IMS.⁴ EGDN, like other organonitrates, is electronegative in character and readily forms negative ions in IMS, but undergoes dissociative electron capture reactions and does not produce a stable molecular anion. Instead, an ion peak with a reduced mobility of 2.46 to 2.48 $\text{cm}^2\text{V}^{-1}\text{sec}^{-1}$ is produced, corresponding to the fragment ion $(\text{NO}_3)^-$ (see References 5 and 6) as in Equation 2.



This peak overlaps significantly with the peak associated with the reactant ions when air or nitrogen is used as the carrier gas, thus restricting its usefulness as an IMS marker for identification purposes.

It was shown that the addition of trace amounts of Cl^- reagent ion to the carrier stream results in increased ionization specificity and leads to the formation of a stable ion cluster $(\text{EGDN}\cdot\text{Cl})^-$ of m/z 187, which is well separated from the region of the reactant ions in the ion mobility spectra (Figure 2)⁴; in a separate set of experiments, the mass associated with the spectral peaks was determined by coupling the IMS to a quadrupole mass spectrometer. Using a double-dilution vapor source and a sample collection/injection technique developed in this laboratory,^{7,8} the minimum detectable quantity of $(\text{EGDN}\cdot\text{Cl})^-$, recorded at a signal amplitude of three times the 1σ noise, was determined to be 30 pg. The sensitivity obtained and speed of response observed pointed to a screening method based on IMS and chloride ion chemistry as a possible technique for detecting concealed explosives in various search scenarios, such as in aircraft and in airport terminals.

Table 1. Instrument Parameters

Parameter	Value
Cell length	14 cm
Drift length	8 cm
Drift voltage	± 2700 V
Carrier gas (purified air)	200 mL/min
Drift gas (purified air)	600 mL/min
Inlet and drift temperature	220°C
Pressure	atmosphere
Gate width	0.2 msec
Frequency of signal acquisition ^a	42 Hz
Delay time ^b	6 msec

^a IMS spectra were obtained by signal averaging 256 or 512 scans with a Nicolet 1170 signal averager; the half-band width of IMS peaks was 0.4 msec.

^b The time between gate opening and start of data collection.

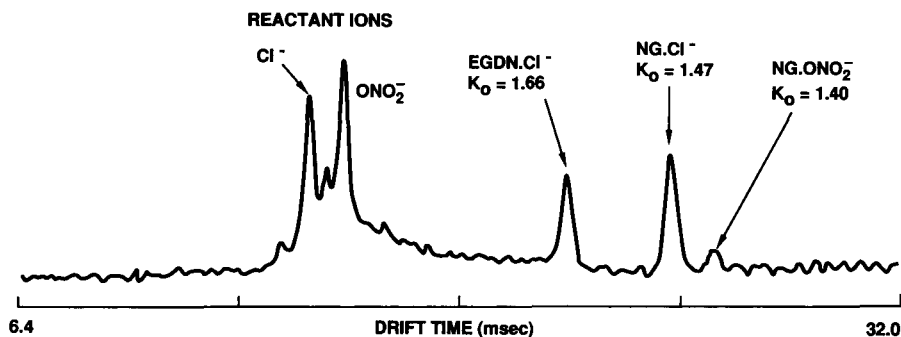


Figure 2. Negative ion mobility spectrum of headspace vapors from a dynamite sample. Carrier gas, purified air spiked with dichloromethane; inlet and drift temperature, 75°C; drift voltage, -3000 V.

Forensic and Medical Applications

Forensic chemistry makes use of a variety of sophisticated analytical instrumental techniques to trace the extremely small quantities of drugs, explosives, and poisons present in various specimens. The conventional procedure adopted in forensic case-work involves collecting the evidence at the scene (e.g., fire debris, empty vials, etc.) for subsequent chemical analyses to be performed in the laboratory. Laboratory results are often not available for several days.

A research project was undertaken by this laboratory to investigate the potential of IMS with regard to the on-site detection of drug residues on the hands of subjects by way of skin-surface sampling. A laboratory study was first carried out and revealed that, in simulated overdose situations, nanogram quantities of drug micro particulates were left on the hands following manual contact with some commercial drug tablets.^{8,9} These microscopic particles could be recovered from the hands by skin-surface sampling using a suction probe packed with a fine metallic mesh filter; when the collector probe was subsequently inserted into the heated inlet of the IMS for thermal desorption and analysis, results were obtained in 5 to 10 sec. It was found that drugs encountered in overdose cases, such as the benzodiazepines, cocaine, and the tricyclic antidepressants, have relatively high gas-phase basicity compared to other components present in the drug matrix. Consequently, these chemicals compete favorably for the positive charges available in the reaction chamber of the instrument and readily form protonated molecular or quasimolecular ions in IMS. The method can be especially valuable in those forensic investigations where a preliminary indication of the use of drugs is required.

As a follow-up to the laboratory study, a field investigation was conducted at Ottawa General Hospital in which emergency patients who had a history of drug overdose (and who consented to our sampling) had their hands 'sniffed' upon arrival in the emergency ward. Figure 3 shows positive ion mobility spectra obtained from a clean hand, a doxepin standard (a tricyclic antidepressant), and the right hand of a patient admitted to the hospital with doxepin overdose. The results of the study

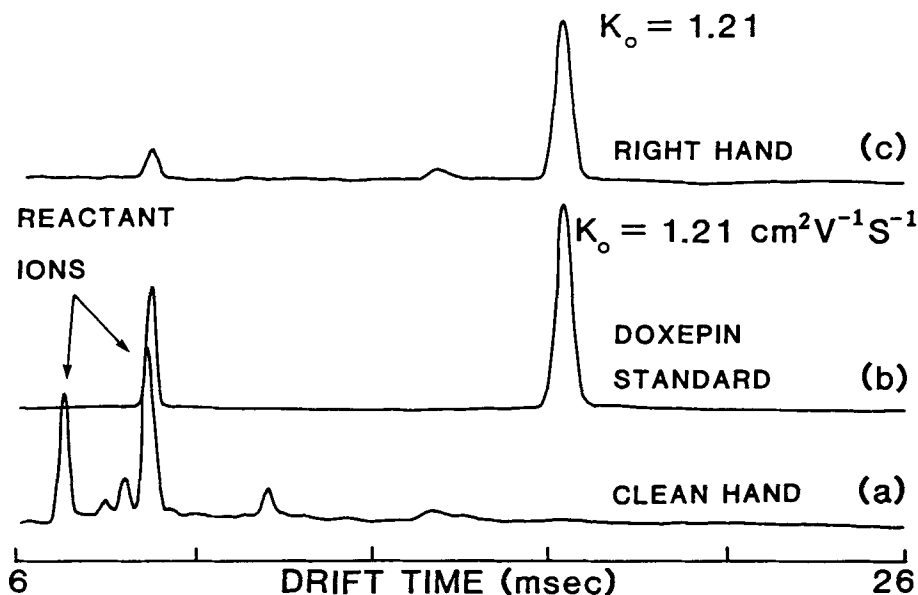


Figure 3. Positive ion mobility spectra from (a) a clean hand; (b) doxepin standard; (c) right hand of a patient admitted to hospital with doxepin overdose.

were favorable inasmuch as a high proportion of the overdose patients tested positive; these results were confirmed by urinalysis.^{11,12}

The prompt toxicological information obtained by this method is important in the management of emergency patients, and this preliminary screening test could eventually become a part of a routine physical examination.

Characterization of Plant Materials

Separation of certain wood species, under mill conditions, has been of interest to the forest products and pulp and paper industries for some time. A number of analytical techniques has been attempted (e.g., color tests) to achieve this objective with varying degrees of success. In this regard, a screening procedure was developed for the identification of black spruce, jack pine, and balsam fir (SPF).¹³ The method is based on the thermal release of vapors from the wood sample, followed by 'target compound' analysis using IMS, with IMS signatures characteristic of each wood species being obtained in a matter of seconds. Figures 4 and 5 show that the pine and fir samples give unique, salient IMS peaks at $K_o = 1.29$ and $K_o = 1.39 \text{ cm}^2 \text{ V}^{-1} \text{ sec}^{-1}$, respectively, the pine signature being obtained in the negative mode and the fir signature in the positive mode. The spruce samples display no distinguishing peaks in either mode and thus, given a SPF mix, the presence or absence of black spruce can be inferred by monitoring the peaks at 1.29 and 1.39. The method has potential for use in an industrial setting as a reliable sorting procedure

for a variety of wood species. Work is currently in progress to identify the ionic species associated with the IMS peaks by means of gas chromatography/mass spectrometry (GC/MS) and ion mobility spectrometer/mass spectrometry (IMS/MS).

The same approach was successfully applied to the detection of pentachlorophenol (PCP) in wood chips.¹³ PCP is a precursor of dioxins and its use as a fungicide has been banned by the wood industry because of its inherent health risks. It would, therefore, be highly desirable to develop a method that could be easily integrated with industrial process control systems and could quickly and reliably detect PCP in wood chips and other wood products. Figure 6 illustrates that, under the experimental conditions used, PCP is efficiently removed from the wood matrix, and its identification based on the peak at $K_0 = 1.56 \text{ cm}^2\text{V}^{-1}\text{sec}^{-1}$ (probably due to PCP molecular ion M^-) has been found to be reliable.

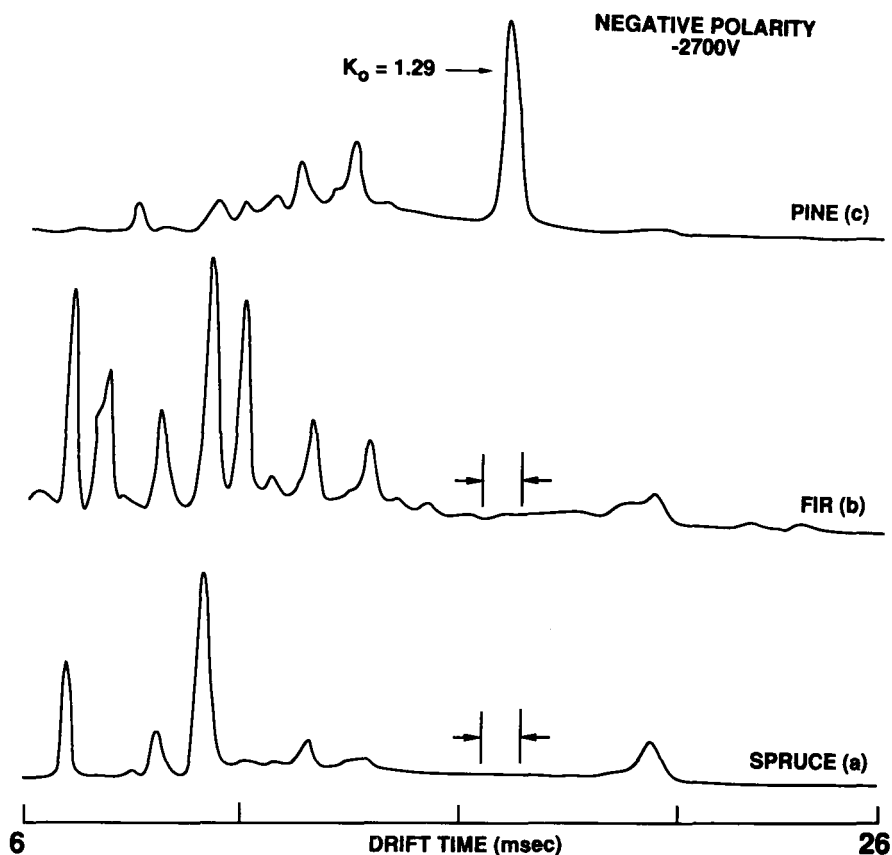


Figure 4. Negative ion mobility spectra of (a) black spruce; (b) balsam fir; (c) jack pine.

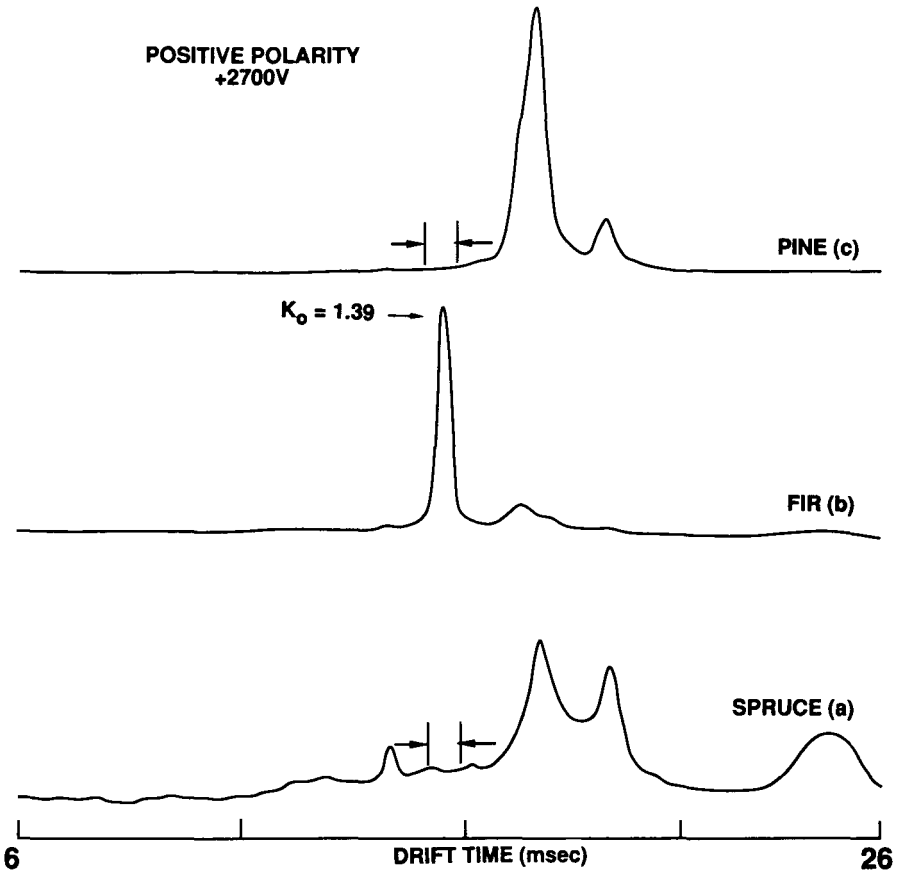


Figure 5. Positive ion mobility spectra of (a) black spruce; (b) balsam fir; (c) jack pine.

COMPACT IMS CHEMICAL SENSOR

The interest generated by the laboratory's research work has instigated a number of industrial efforts aimed at the development of compact, rugged IMS chemical sensors specifically designed for field use. The laboratory contributes to this development in researching effective sampling methodologies and sample injection techniques, as well as in the tailoring of such systems for deployment in specific applications. In addition, a compact digital signal averager for processing IMS electrometer signals has been developed and tested.¹⁴ The hardware requirements have been simplified and miniaturized by making use of a dual-ported RAM and an LCD graphics display. This signal averager has proved to function satisfactorily and reliably, exhibiting similar resolution and accuracy to that of the much larger Nicolet 1170.

RESOLUTION ENHANCEMENT OF IMS SPECTRA

A number of attempts have been made to evaluate IMS resolution.¹⁵ It is generally agreed that mobility-based separations are poorer than those that can be achieved with mass spectrometry or gas chromatography, inasmuch as the peak widths in IMS are ultimately diffusion-limited. As a result, overlapping IMS peaks are common, particularly in mixture analyses. To improve the resolution and specificity of the IMS and, as a consequence, enhance the ability of the detector to reliably handle complex samples, we have investigated the use of digital signal processing (DSP) techniques to mathematically resolve overlapping IMS peaks.¹⁰ Figures 7 and 8 illustrate the efficacy of the application of a second derivative algorithm developed here to the separation into its components of a broad, unresolved IMS peak obtained in analyzing a mixture of bromazepam and diazepam.

These results underline the advantages of implementing a DSP scheme, such as the second derivative function, in the peak detection algorithm of an IMS field instrument. Work is currently in progress to determine both effectiveness and limitations of the second derivative algorithm, as well as other algorithms such as deconvolution, adaptive filtering, and cross-correlation.

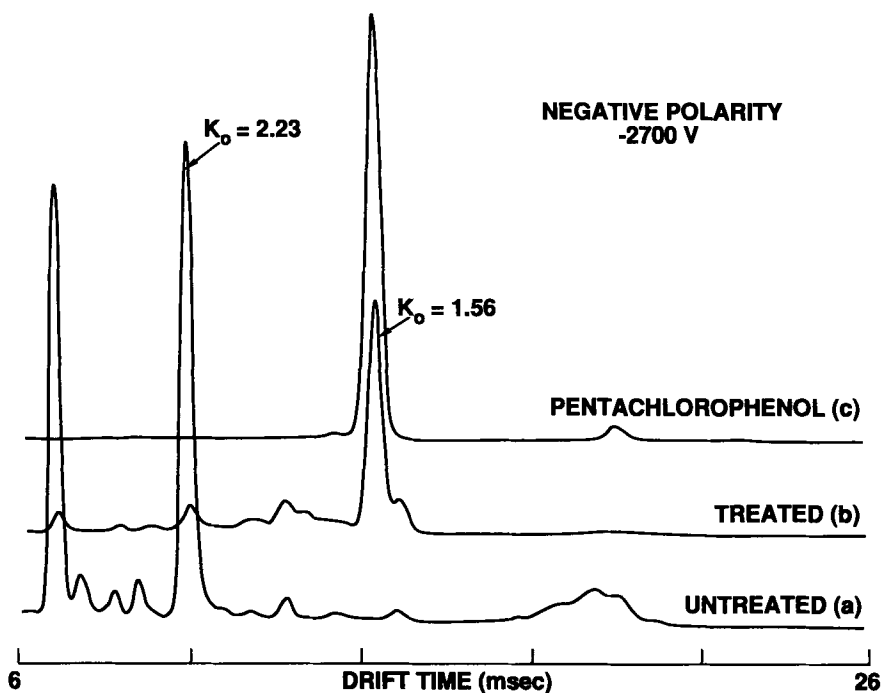


Figure 6. Negative ion mobility spectra of (a) untreated wood chips; (b) wood chips treated with pentachlorophenol (~400 ppm); (c) pentachlorophenol standard.

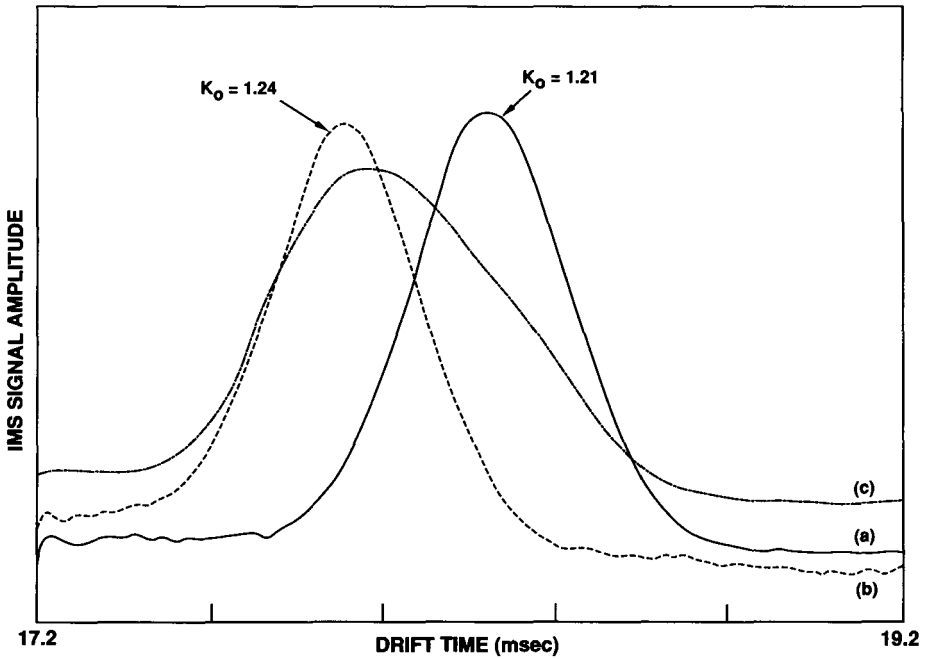


Figure 7. Positive ion mobility spectra of (a) diazepam —; (b) bromazepam -----; (c) diazepam/bromazepam mixture -·-·-. Delay time, 17.2 msec; frequency of signal acquisition, 500 Hz.

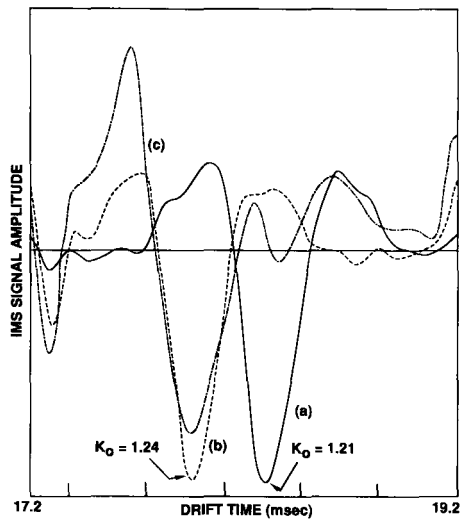


Figure 8. Second derivative positive ion mobility spectra of (a) diazepam —; (b) bromazepam -----; (c) diazepam/bromazepam mixture -·-·-. Delay time, 17.2 msec; frequency of signal acquisition, 500 Hz.

REFERENCES

1. Elias, L. "Development of a Portable Gas Chromatograph Explosives Detector," *National Research Council of Canada, LTR-UA-57 (January 1981)*.
2. Elias, L. and Lawrence, A. H. "Portable Trace Narcotics Detector for Field Use," *Can. J. Spectrosc.* 32:14A—15A (1987).
3. Carr, T. W., Ed. *Plasma Chromatography*, (New York: Plenum Publishing Corporation, 1984).
4. Lawrence, A. H. and Neudorfl, P. "Detection of Ethylene Glycol Dinitrate Vapors by Ion Mobility Spectrometry Using Chloride Reagent Ions," *Anal. Chem.* 60:104—109 (1988).
5. Asselin, M. "Detection of Dyanmite with a Plasma Chromatograph," Proceedings of the New Concept Symposium and Workshop on Detection and Identification of Explosives, Reston, VA (1978), 177—181.
6. Spangler, G. E., Carrico, J. P., and Kim, S. H. "Analysis of Explosives Residues with Ion Mobility Spectrometry," Proceedings of the International Symposium on the Analysis and Detection of Explosives, Quantico, VA (1983), 267—282.
7. Elias, L. Unpublished results (1978).
8. Lawrence, A. H. "Detection of Drug Residues on the Hands of Subjects by Surface Sampling and Ion Mobility Spectrometry," *Forensic Sci. Int.* 34:78—83 (1987).
9. Lawrence, A. H., Nanji, A. A., and Taverner, J. "Skin-Sniffing/Ion Mobility Spectrometric Analysis: A Potential Screening Method in Clinical Toxicology," *J. Clin. Lab. Anal.* 2:101—107 (1988).
10. Lawrence, A. H. "Characterization of Benzodiazepine Drugs by Ion Mobility Spectrometry," *Anal. Chem.* 61:343—349 (1989).
11. Nanji, A. A., Lawrence, A. H., and Mikhael, N. Z. "Use of Skin Surface Sampling and Ion Mobility Spectrometry as Preliminary Screening Method for Drug Detection in an Emergency Room," *J. Toxicol. Clin. Toxicol.* 25(6):501—515 (1987).
12. Nanji, A. A. and Lawrence, A. H. "Detection of Drugs in Patients with Overdose: Comparison Between Skin Surface Air Sampling and Thin Layer Chromatography," *Int. J. Clin. Pharmacol.* 26:1—3 (1988).
13. Lawrence, A. H. "Rapid Characterization of Wood Species by Ion Mobility Spectrometry," Proceedings of the 75th Annual Meeting of the Canadian Pulp and Paper Association, Montreal, (1989), B51—54.
14. Prini, A., Lawrence, A. H., and Laframboise, S. "Compact Digital Signal Averager for Ion Mobility Spectrometer (IMS) Signals," *J. Phys. E: Sci. Instrum.* 20:1422—1424 (1987).
15. Rokushika, S., Hatano, H., Baim, M. A., and Hill, H. H. "Resolution Measurement for Ion Mobility Spectrometry," *Anal. Chem.* 57:1902—1907 (1985).



Taylor & Francis

Taylor & Francis Group

<http://taylorandfrancis.com>

CHAPTER 2

Continuous Atmospheric Monitoring of Organic Vapors by Ion Mobility Spectrometry

G. A. Eiceman, A. P. Snyder, and D. A. Blyth

ABSTRACT

A hand-held commercially available ion mobility spectrometer (IMS) was used for continuous monitoring of airborne organic vapors in laboratory and field investigations. In one field study, IMS response to methylsalicylate vapors was monitored continuously through unattended operation during a 13-hr period of atmospheric turbulence to illustrate the susceptibility of point sensors to wind direction. Fluctuations under near-quiescent atmospheric conditions also were demonstrated using dimethylsulfoxide. In a third study, IMS was used to define the plume shape from a point source of dipropyleneglycolmonomethylether in a 25 m × 12 m grid downwind of the vapor source with windspeeds of 6 to 18 km/hr. Laboratory studies were used to characterize mobility spectra of individual compounds, instrumental response times, and effects of chemical interferents.

INTRODUCTION

Ion mobility spectrometry (IMS) has long been considered a technology with characteristics that portended the practical advancement as an atmospheric monitor.^{1,2} Other monitoring instruments that are based upon comparable principles of atmospheric pressure chemical ionization (APCI) of analyte include continuous, flow-through electron capture detectors (ECD)³ and APCI-mass spectrometers (MS).^{4,5} Each of these sensors is capable of rapid (<1 sec) response and excellent limits of detection (LOD) near 1 ppb for airborne vapors. However, an ECD has limited powers of selectivity and APCI-MS is expensive and not particularly mobile; however, APCI-MS instruments have been transported in large vans for atmospheric sensing.^{6,7} All processes in IMS occur in air at ambient pressure so instrumentation can be made hand-held and relatively inexpensive. Although IMS has been suggested for air monitoring, actual environmental investigations with IMS have been limited in number and scope. Watson and Kohler⁸ compared with the detection of airborne nickel carbonyl by IMS with infrared spectrometry, and Dam⁹ measured 8-hr concentration emission profiles of an unnamed toxic pollutant from an industrial point source. Preliminary examination of vapor plumes have been described using several ionization devices including a hand-held IMS suitable for continuous air monitoring.¹⁰ Nonetheless, IMS has not received much attention as a tool for atmospheric environmental monitoring, perhaps due to early reports on perceived inadequacies in resolution.¹¹ These problems seem to be due more to the particulars of APCI principles rather than to deficiencies in separations by ionic mobilities.

The initial IMS event of analyte ionization is based on electron or proton exchanges between a reservoir of reactant ions in the ion source and the analyte of interest. Due to the large collisional frequencies of ions and molecules at atmospheric pressure, ionization is competitive and ionization efficiency depends upon both capture kinetics and concentrations of neutral analytes. Exact quantitative descriptions of IMS response with mixtures is under theoretical and practical development at New Mexico State University, but only approximate predictive models are currently available. Thus, for the successful application of IMS to monitoring airborne organic vapors, the analyte of interest should have considerably greater proton or electron affinities than potential interferents. When target vapors have medium or low proton or electron affinities, interferences can occur and are evident in the mobility spectrum. In such instances, product ions may be formed through alternate ionization strategies such as photoionization.¹³ Compounds with low or medium affinities for proton or electrons can easily register strong responses in IMS so long as the ionization source is free of molecules with proton/electron affinities stronger than the analyte.

Instrumentation for IMS has recently been miniaturized and hand-held wholly portable instruments have become available for use in atmospheric monitoring.¹⁴ These IMS devices contain all supporting electronics, gas flow systems, and signal processing through an on-board computer in a package that is rugged and lightweight (Figure 1). One objective for the present work was to examine the performance of this commercial hand-held IMS with respect to quality of mobility spectra, response

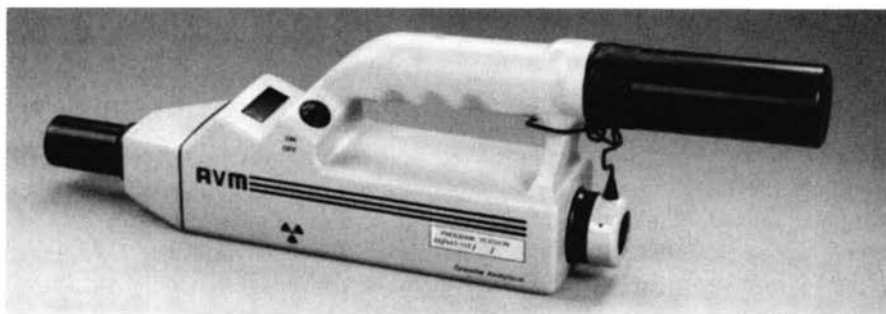


Figure 1. Photograph of a commercially available hand-held ion mobility spectrometer (Graseby Ionics, Ltd., Watford, UK).

times, and memory effects. An objective for the field component of our study was to illustrate the capabilities of IMS for airborne vapor monitoring as well as the limitations inherent with all point sensors.

EXPERIMENTAL

Instrumentation

An ion mobility spectrometer from Graseby Ionics, Ltd. (Watford, UK) was equipped with a 3-cm drift region, 10-m Ci ^{63}Ni ion source, 1-cm reaction region, and dimethylsilicone membrane inlet (Figure 2), and is available as model AVM. The IMS was operated at ambient temperature and pressure with purified air as the carrier and drift gas. Signals were processed externally using a Graseby ASP board/software designed specifically for use in an IBM PC/XT/AT-compatible microcomputer for automated continuous sensing by IMS. Other operating conditions were ion shutter pulse width, 300 msec; frequency of analysis, 13 Hz; and drift region field of 210 V/cm. A Hewlett-Packard (HP) model 3390A recording integrator was connected to the ASP board analog output and operated at 3 cm/min.

In laboratory studies, a flow tube was constructed of 8-cm diameter \times 1.5-m long rigid PVC pipe, and laboratory air doped with organic vapors was delivered through the tube to the IMS using a model 4600X System Paps fan (Pamotor, Burlingame, CA). The IMS was placed in the cross section of the flow tube at the opposite end of the pipe and the air flow was roughly 6×10^3 m³/sec or 0.3 m/sec. In field studies, the IBM PC/AT was placed in a hatchback compact automobile and was used onsite in a spacious grassland at the Edgewood Area, Aberdeen Proving Grounds. The site was equipped with line power and a portable meteorological station, model EWS (Climatronics Corp., Bohemia, NY), for continuous recording of temperature, dew point, wind speed, and wind direction.

Procedures

Laboratory Studies

Known volumes (5 to 10 μL) of organic compounds were applied as neat liquid to a tissue placed 1 cm from the flow tube fan and mobility spectra were continuously recorded at an interval of 8 sec between acquisition and storage of spectra (64 scans averaged per spectrum). Plumes of 10 to 90 sec were generated by removing the vapor source, after the appropriate delay, from the drift tube fan. Compounds obtained from Aldrich Chemical Co. (Milwaukee, WI) were dimethylsulfoxide (DMSO), dipropyleneglycolmonomethylether (DPM), triethylphosphate (TEP) and methylsalicylate (MSAL), and were selected as nontoxic simulants of pesticides. The estimated concentration of these vapors in the flow tube at steady state were estimated as 0.5 to 1 mg m^{-3} . In interferent studies, a steady-state concentration of individual vapors was generated and 200 μL of an interferent were added to a second tissue located next to the analyte vapor source, yielding pulses of 1.1 g m^{-3} for the interferent vapors. Interferents were selected to represent a broad range of compound classes or proton affinities and included hexane, benzene, methylene chloride, methanol, and ammonia. Interferents were obtained in reagent grade quality from various commercial sources.

Field Studies

The effect of wind direction on IMS sensing was measured from 4:30 PM (May 16, 1988) to 6:00 AM (May 17) during a tornado watch in eastern Maryland where a violent storm moved easterly from 4:00 to 8:00 PM. Strong winds shifted in direction from the south (0°) to the north (90°) and back (0°) as the storm front passed near the test site. A 3 m \times 3 m square plot of grass (with the longitudinal edges aligned to magnetic north) was sprayed with 50 ml of a fine mist of 40% MSAL in peanut oil (by volume). The peanut oil was added to reduce the effective vapor pressure of MSAL. The IMS was placed 3 cm from ground level at a distance

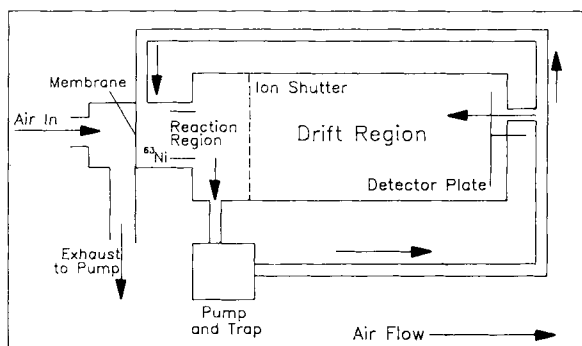


Figure 2. Schematic of the hand-held ion mobility spectrometer with membrane inlet as shown in Figure 1.

of 50 cm downwind from the NW corner of the square. Spectra were recorded continuously at 4-min intervals (2000 scans per spectrum) for 13.5 hr. Environmental conditions were wind speed, 0 to 48 km/hr; wind direction, 0 to 270°; and air temperature, 15 to 22°C.

In a second study, a point source of DPM was used to generate a plume, and mobility spectra were obtained at 0-, 2.5-, 5-, 10-, 15-, 20-, and 25-m distances downwind from the source, at elevations of 1 to 2 m from the ground along 2.5 to 5 m intervals that were perpendicular to the plume axis. The point source was a 32 cm × 28 cm sheet of tissue paper saturated with 20 mL of DPM and mounted on a wood frame. In addition, a vertical profile was obtained at 1 m from the source at elevations from 10 to 190 cm. Environmental conditions were wind speed, 8 to 16 km/hr; wind direction, 220 to 290°; and air temperature, 23°C. In a final study, neat DMSO was applied to a grass plot during a period of sunny, warm weather with stable wind speed and direction. The IMS was positioned 1 m downwind from the point source and 10 cm from ground level. Spectra were recorded continuously for 5 hr from 1:00 to 6:00 PM using 1000 scans per spectrum. Environmental conditions were wind speed, 5 to 8 km/hr; wind direction, 270°; air temperature, 20 to 22°C.

RESULTS AND DISCUSSION

Laboratory Studies

Mobility spectra from the IMS response to positive ions for DMSO, DPM, TEP, and negative ions for MSAL are shown in Figure 3 where drift times were 8.51, 8.21, 11.1, and 12.1 msec for MSAL, DMSO, DPM, and TEP, respectively. Peak widths were 0.8 to 1 msec at baseline and were comparable to laboratory-grade IMS instruments with peak widths of 0.3 to 0.6 msec at baseline.¹⁵ Spectra were simple as was expected from APCI sources, and product ions were identified with an IMS-MS as the oxygen-monomer adduct, $M^*O_2^-$, for MSAL and dimer ions, M_2H^+ , for DMSO, DPM, and TEP.¹⁶ At low concentrations for TEP and DPM, dimer ions were replaced by monomer ions, MH^+ with drift times of 9.7 and 9.8 msec, respectively. The hand-held IMS showed moderately fast response (better than 8 sec), and the ion intensities were very stable with standard deviations for peak heights of only 0.9 mV (0.3% relative standard deviation). Limits of detection were estimated as 0.01 mg m⁻³, while the linear ranges were approximately 1.5 to 2 orders of magnitude. The dynamic relationship between reactant and product ions is shown graphically in Figure 4. The movement of a vapor plume was monitored by the IMS inlet and was collected as individual mobility spectra as a function of clock time. As vapor concentrations increased, product ion intensity also increased and reactant ion (RIP) intensity declined. Afterwards, reactant ions were restored and product ion intensity decayed.

Ion intensity profiles for 10- to 90-sec deliveries of vapors to the laboratory flow tube are shown in Figure 5 for TEP. The rising slopes of product ion intensities for each plume were virtually superimposable, indicating that rates of IMS response

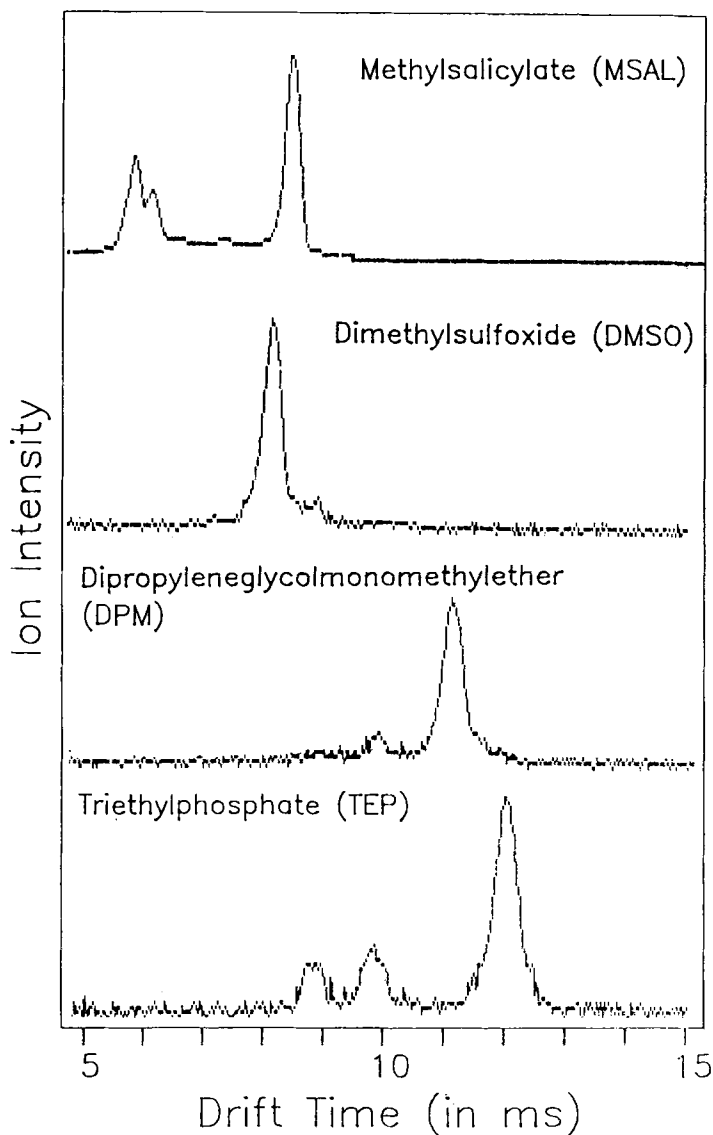


Figure 3. Mobility spectra for target vapors used in laboratory and field studies. Reduced mobilities and identities are given in the text.

to the vapors were independent of concentration on the delivery time scale. Moreover, the curves revealed that a steady-state concentration in the flow tube was achieved only after 60 sec of vapor delivery and corresponded to near saturation of the IMS. This time was influenced by the air flow and tube dimensions and was likely the result of transport-limited diffusion across the flow tube (under near

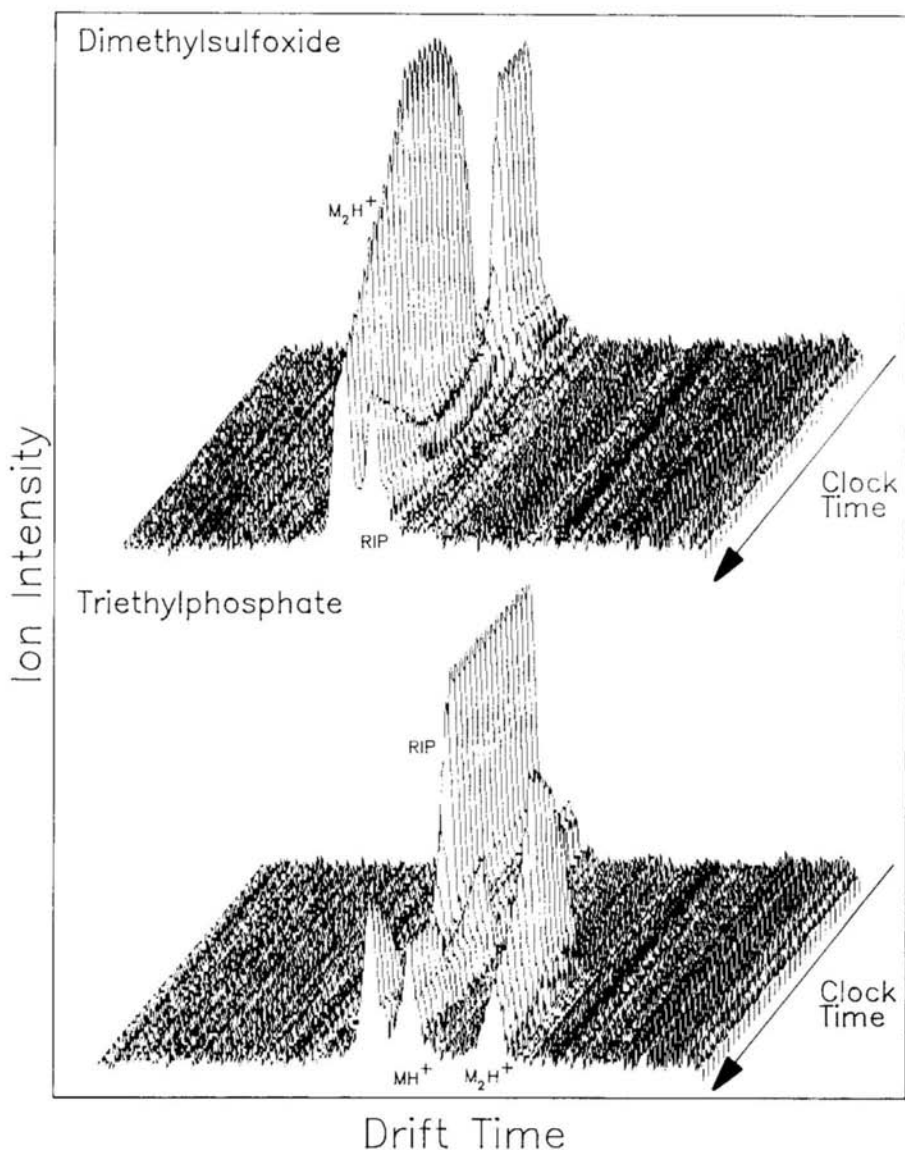


Figure 4. Profiles of mobility spectra for DMSO and TEP as their respective vapor plumes were monitored by the IMS.

laminar flow conditions) rather than hysteresis in the IMS. As expected, the reactant ion profiles were inversely proportional to those for product ions. On the trailing edge of the plume, product ion intensity decreased and the reactant ion intensity was restored after a 2-min delay for TEP. The monomer ion intensity showed good response at low TEP concentrations (either side of the plume center of mass), but was completely depleted at high concentrations of TEP through shifts in gaseous

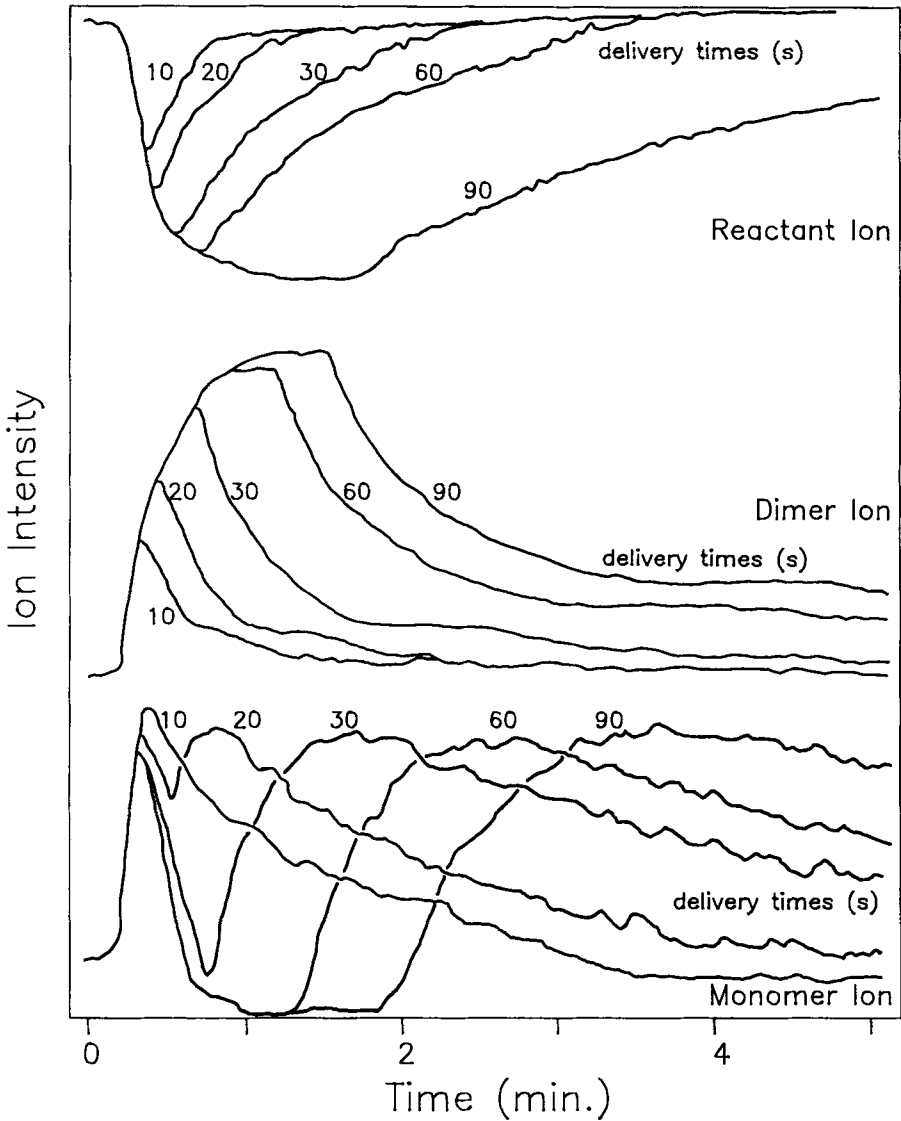


Figure 5. Ion intensities of product ions for TEP from plumes of various duration. The plumes were generated by exposing the flow tube to the vapor source for times of 10, 20, 30, 60, and 90 sec as designated on each curve. Integration ticks were retouched from the plots.

equilibrium to the dimer ion. Exact relative contributions to the memory effects from the flow tube surfaces versus that inside the IMS could not be discerned from these results, but plots suggest that gross overloading with certain compounds can disable IMS response through saturation of the ionization region. Recovery for the longest delivery of DPM was about 4 min to full restoration of reactant ions, suggesting a chemical dependence on clearance. Exact measurements on clearance rates of IMS alone were not made, but severe exposures produced complete saturation from 20 to 60 sec in duration, indicating that the long recovery times were also influenced by vapor adsorption on the flow tube. The present IMS source configuration and tube parameters were not designed for high-speed response (or rapid clearance) and these results certainly do not establish a lower limit on IMS response times. Alternate flow configurations in the ion source region may result in response times of roughly 50 msec, and ultimate response times will be governed in IMS more by fluid dynamics of air sampling than by ion chemistry or electronics.

The target compounds chosen all had large proton or electron affinities and IMS response with these compounds should not be measurably affected by other atmospheric pollutants. The product ion intensities during delivery of interferents at concentrations 1000 to 2000 \times greater than the analyte showed only a slight decrease (<10%) for DPM, DMSO, and TEP when ammonia was added to the flow tube; other potential interferents (hexane, benzene, methylene chloride, and methanol) showed no detectable influence on the product ion intensity. While APCI principles may account for much of this selectivity, the membrane inlet (Figure 2) also may have aided selectivity through the rejection of highly polar compounds such as alcohols. The continuous detection of the selected target vapors using the handheld IMS in field studies will be unaffected by these (and most other) ambient air pollutants.

Field Studies

Results from air monitoring near a section of grass contaminated with MSAL are shown in Figure 6, where product ion intensities are aligned with wind direction and speed. During this monitoring episode, fluctuations in wind direction occurred at irregular intervals (1:00 to 1:15, 2:30 to 3:00, and 3:30 to 3:45 AM) although wind speed was roughly constant. A strong response to MSAL was observed when the wind was northward (i.e., IMS downwind), but intensity fell as the wind direction reversed (passed 180°—IMS upwind). This occurred even though the IMS was within 50 cm of the contaminated grass plot. The fluctuations were especially evident in mobility spectra as shown for the monitoring interval from 3:15 to 4:20 AM. All spectra were recorded continuously and the findings demonstrated the vulnerability of point sensors to changes in wind direction.

During a sunny, warm day with a constant slight wind, DMSO on grass yielded a saturated IMS response for 2.5 hr and product ion intensity thereafter decayed only 40% during the next 2 hr (data not shown). Stability of response for DMSO intensity was measured at the beginning of the study when vapor concentrations were constant over a short period with a standard deviation of 21 mV and a relative

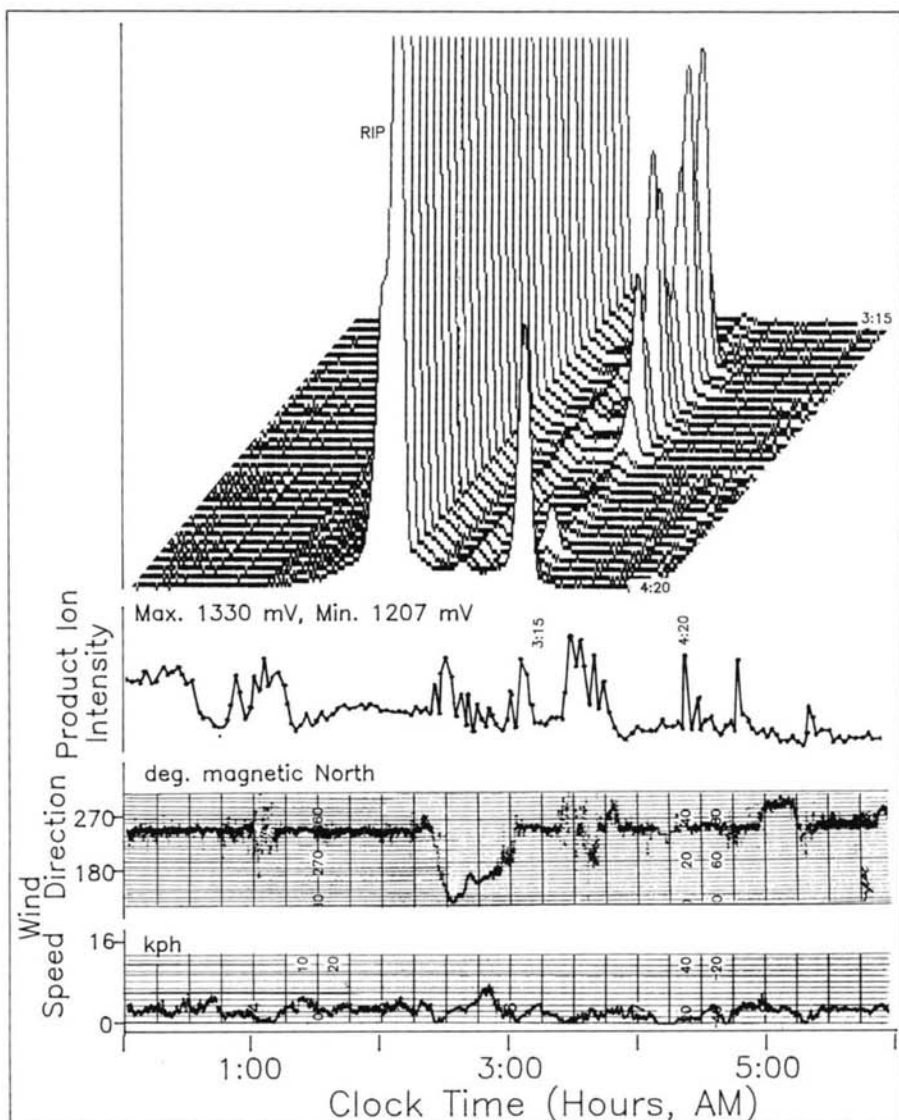


Figure 6. Product ion intensities from continuous IMS sensing near a square plot of grass contaminated with MSAL. Wind direction and speed profiles from the portable meteorological station are shown below the IMS response profile. Monitoring time frame was from midnight to 6:00 AM.

standard deviation of 7.5%. Small fluctuations were removed by averaging 1000 scans per spectrum, leaving only variations caused by wind direction and speed. Under these circumstances, which represented relatively calm wind conditions, atmospheric turbulence caused signal fluctuations that were $20\times$ greater than what was observed under controlled laboratory conditions (*vide supra*).

In a third environmental study, DPM was released continuously from a point source of vapors and the plume was evaluated downwind by moving the IMS through a region anticipated to contain DPM vapors. The results are displayed as isoconcentration contours in Figure 7, where a narrow curved region of high DPM concentration was surrounded by larger regions of lower concentrations. Since only one IMS was available and 35 positions were chosen for measurement of product ion intensity, the resolution of information about the plume was limited. Consequently, only an approximate geometry for the plume was possible, with straight lines connecting measurement positions. Resolution could be improved either by recording spectra continuously as the IMS is swept through the plume region or better still by using more than one IMS in the experiment. A third option of a greater number of sampling points was disqualified due to unacceptably long delays from analysis times of 2 min per position. This analysis time was comparatively long, but was considered necessary to signal average response due to fluctuations in wind direction and expected shifts in plume position over the sampling grid. Neither of the former options were available for the present study, and resolution was fixed at 2-m intervals for the width and 5-m intervals for length.

The plume was also interrogated at 2 m in elevation (data not shown) from ground where DPM was virtually undetected. This finding was preliminary evidence that the plume was not dispersed equally in all directions and suggested that the organic vapor sank toward the ground and was dispersed. When the IMS was brought to a distance of 1 m from the source, movement of vapors toward the ground became evident as shown in a concentration-elevation profile (Figure 7, inset) immediately downwind of the source. The implications of turbulence from a nearby shelter and poor spatial resolution render these data unsuitable for matching to plume models. However, these results illustrate the suitability of IMS as a chemical monitor for comparable or related investigations. In that regard, IMS was stable, convenient, and highly automated and permitted time resolution of plume fluctuations on the 3- to 10-sec time scale. Long-term stability in response and calibration drift in IMS will be explored in future investigations.

CONCLUSIONS

A hand-held commercial ion mobility spectrometer was shown to exhibit dynamic response to organic vapor plumes with response times better than 8 sec. Potential atmospheric pollutants with low proton/electron affinities exhibited negligible effects on IMS response against the target vapors. Continuous monitoring of airborne vapors was successfully demonstrated over a 12-hr period near a plot of contaminated soil and demonstrated both the suitability of IMS for unattended operation with advanced signal processing. The susceptibility of point sensors to fluctuation

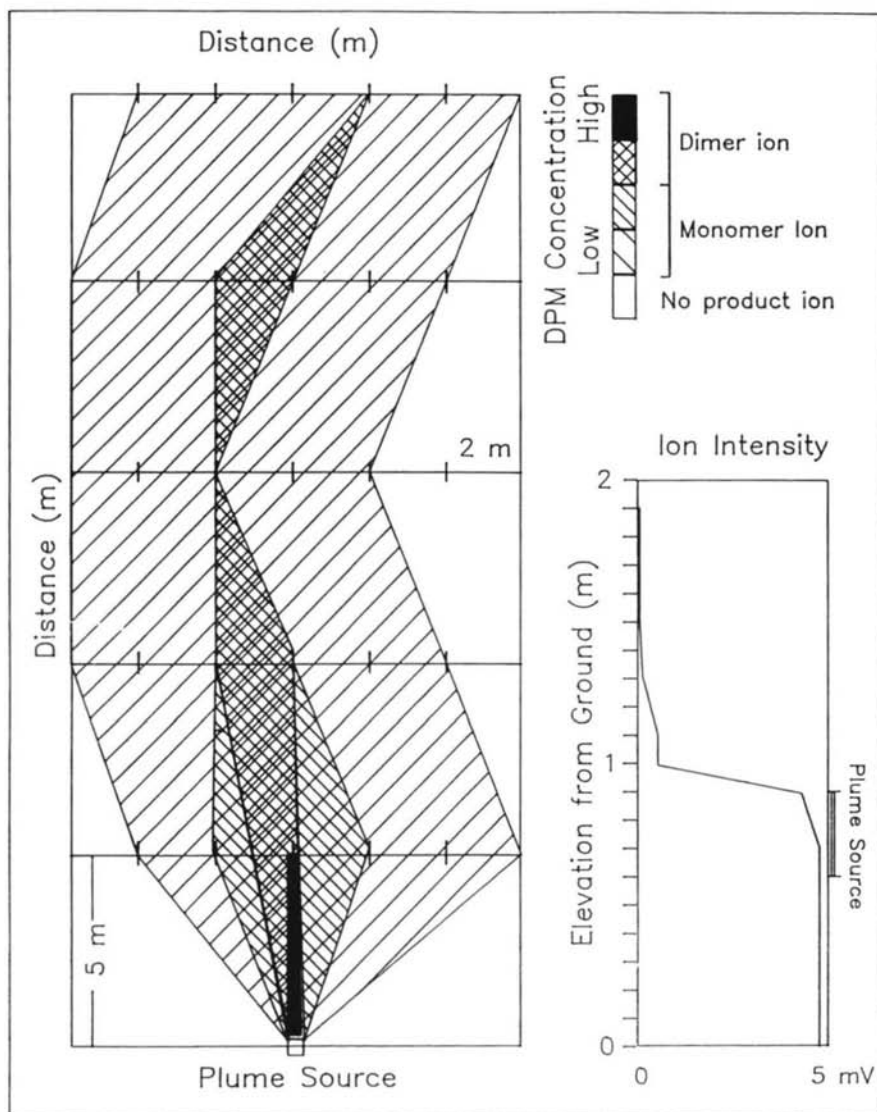


Figure 7. Estimated isoconcentration contours from IMS sensing of DPM. The point source was located approximately 1 m from ground level. The inset shows the vertical concentration profile 1 m downwind from the point source.

in wind direction was observed when the IMS inlet was upwind of the analyte vapor. Plume characterization from a point source was also demonstrated, but the incorporation of multiple IMS sensors would dramatically enhance both the speed and spatial resolution of plume mapping. Multiple point sensors surrounding a contamination site would also permit perimeter monitoring of emitted vapors without severe susceptibility to wind direction.

REFERENCES

1. Karasek, F. W. "The Plasma Chromatograph," *Res. Dev.*, 21:(3):34—37 (1970).
2. Karasek, F. W., Kilpatrick, W. D., and Cohen, M. J. "Qualitative Studies of Trace Concentrations by Plasma Chromatography," *Anal. Chem.* 43:1441—1447 (1971).
3. Benner, R. L. and Lamb, B. "A Fast Response Continuous Analyzer for Halogenated Atmospheric Tracers," *J. Atmos. Ocean. Technol.* 2(4):582—589 (1985).
4. Williams, D. T., Denely, H. V., and Lane, D. A. "On Site Determination of Sulfotep Air Levels in a Fumigating Greenhouse," *Am. Ind. Hyg. Assoc. J.* 41:647—651 (1980).
5. Williams, D. T., Denley, H. V., Lane, D. A., and Quan, E. S. K. "Real Time Monitoring of Methomyl Air Levels During and After Spraying in a Greenhouse," *Am. Ind. Hyg. Assoc. J.*, 43:190—195 (1982).
6. Karasek, F. W. "Instrumented Van Helps Profile Spread of Toxic Chemical during Mississauga Train Crash Crisis," *Can. Res.*
7. Lane, D. A., Thomson, B. A., Lovett, A. M., and Reid, N. M. "Real-Time Tracking of Industrial Emissions through Populated Areas using a Mobile APCI Mass Spectrometry System," Proceedings from the 8th International Mass Spectrometry Conference, Oslo, Norway, 1480—1489 (August 1979).
8. Watson, W. M. and Kohler, C. F. "Continuous Environmental Monitoring of Nickel Carbonyl by Fourier Transform Infrared Spectrometry and Plasma Chromatography," *Environ. Sci. Technol.* 13:1241—1243 (1979).
9. Dam, R. J. "Analysis of Toxic Vapors by Plasma Chromatography," in *Plasma Chromatography*, Carr, T. W., Ed. (New York: Plenum Press, 1984), pp. 177—214.
10. Blyth, D. A. "The Use of Ion Mobility Techniques for Detecting Organic Vapors in the Atmosphere," Proceedings of the International Symposium on Protection against Chemical Warfare Agents, June 17—19, Stockholm, 65—69.
11. Keller, R. A. and Metro, M. M. "Evaluation of the Plasma Chromatograph as a Separator-Identifier," *J. Chromatog. Sci.* 12:673—677 (1974).
12. Vandiver, V. J. "Gas Phase Reaction Rate Constants for Atmospheric Pressure Ionization in Ion Mobility Spectrometry," Ph.D. dissertation, New Mexico State University, Las Cruces, NM (1987).
13. Leasure, C. S., Fleischer, M. E., and Eiceman, G. A. "Photoionization in Air with Ion Mobility Spectrometry using a Hydrogen Discharge Lamp," *Anal. Chem.* 58:2141—2145 (1986).
14. Bradshaw, R. F. D. and Brokenshire, J. L. Tracer Vapor Detector, U.S. Patent No. 4, 317, 995 (1982).
15. Eiceman, G. A., Leasure, C. S., and Vandiver, V. J. "Negative Ion Mobility Spectrometry for Selected Inorganic Pollutants," *Anal. Chem.* 58:76 (1986).
16. Shoff, D. B. Personal communication (1988).
17. Karasek, F. W. "Plasma Chromatography," *Anal. Chem.* 46(8):710A—720A (1974).



Taylor & Francis

Taylor & Francis Group

<http://taylorandfrancis.com>

CHAPTER 3

Ion Mobility Spectrometry (IMS) Study of Aromatic Hydrocarbons and Nitrogen- and Sulfur-Containing Compounds

Hiroyuki Hatano, Souji Rokushika, and Takashi Ohkawa

ABSTRACT

Ion mobility spectrometric (IMS) analyses of aromatic hydrocarbons and nitrogen- and sulfur-containing compounds were performed by using a Pheyto-Chem 100 ion mobility spectrometer equipped with a ^{63}Ni radioactive β -source in an ionizing chamber, and nitrogen or air as carrier and drift gases in a drift tube. Positive and negative product ions were generated from sample molecules by ion-molecule reactions with reactant ions formed in the carrier gas in the ionization area. The product ions drift under atmospheric pressure down a drift tube under the influence of an electric field. The product ions of a compound are detected as a function of drift time to form an IMS.

The ion mobility spectra of nitrogen-containing heterocyclics, alkylsulfides, aromatic hydrocarbons, aromatic amines, fatty acids, and phenolic compounds were

recorded. For the positive product ions of various homologous series that included pyridine, quinoline, aniline, benzene, phenol, and their respective alkyl derivatives with various carbon chains, linear relationships between reduced mobilities of the product ions and logarithms of molecular weights of their parent compounds were found. For the various homologous series investigated, the slopes of the reduced mobility versus log molecular weight plots were very close to each other and to that observed for alkanes. The linear relationship of reduced mobility (K_0) of an ion and the molecular weight (MW) of its parent compound was expressed as:

$$K_0 = -a \log (MW) + b$$

where a is a variable that depends on the structure of the homologous series, and b depends on the properties of specific functional groups in the molecules.

The mobility of the ions depends upon not only the molecular weight, but also the size and shape of the ions. Ions of saturated heterocyclic compounds drifted slower than those of pyridine derivatives with similar molecular weights. Those of condensed-ring heterocyclic compounds traveled faster than those of saturated heterocyclic and pyridine compounds. Ions of halogenated pyridines show larger mobilities than those of alkylpyridines with similar molecular weights, which can be explained by differences of molecular sizes and shapes of the ions. Ions of isomers of halogenated pyridines were separated from each other by ion mobility spectrometry. Ions of alkylbenzene derivatives were found to show larger mobilities than those of alkylpyridines with similar molecular weights.

In general, bulky ions required larger drift times than compact ions for different compounds with the same molecular weight and same functional groups. Reduced mobilities of ions of aromatic amines increased in the order primary, secondary, and tertiary, which corresponds with the results observed for alkyl amines.

When air was used as both carrier and drift gas, reduced mobilities of both positive and negative ions for sulfur compounds were found to have linear relationships to logarithms of molecular weights, except for the negative ions of sulfide compounds.

In IMS, organic molecules are ionized at high efficiency to produce molecular ions under an atmospheric pressure ionization process. This ionization provides an ultrasensitive detection technique which was shown to be able to detect an amount of 5 femtomoles of 2,4,6-collidine.

INTRODUCTION

Ion mobility spectrometry (IMS), previously known as plasma chromatography, is defined as electrophoresis of ions in the gaseous phase. Gaseous sample compounds form ionic species by ion-molecule reactions with reactant ions produced from carrier nitrogen or air in an ionization chamber equipped with ^{63}Ni -irradiation or corona discharge. Resulting molecular ions are separated due to different mobilities of their molecular ions under an electric field of a drift tube. Extremely effective ionization is obtained because the reactions proceed under atmospheric

pressure and ultramicro separation is obtained at femtomolar amounts of samples.

Plasma chromatography was first reported by Cohen and Karasek¹ and developed further by Horning et al.,^{2,5} Karasek et al.,^{3,6-7} and Spangler et al.⁴

This paper is based on the thesis work by T. Ohkawa for his master's degree at Kyoto University.

EXPERIMENTAL

An ion mobility spectrometer, Phemto-Chem 100, P. C. P. Co., FL, was used in this study. A ⁶³Ni source with 60-keV rays was used as an irradiation source for ionization throughout these experiments. Nitrogen or air was used as carrier and drift gases.

Experimental conditions are presented in Table 1. Positive reactant ions are reported to be (H₂O)_nH⁺, (H₂O)_nNO⁺, (H₂O)_nNH₄⁺, and their N₂ clusters. Negative reactant ions are electrons, (e⁻), when nitrogen gas was used as a carrier gas. The additional negative reactant ions O₂⁻, O(H₂O)₂⁻ and CNO⁻ were also obtained when air was used as a carrier gas.²⁻⁵

Sample compounds used in these experiments are listed in Table 2.

RESULTS AND DISCUSSION

Aromatic Hydrocarbons, Phenols, and Fatty Acids

The ion mobility spectra of positive ions produced from benzene and its derivatives, and from condensed polyaromatic hydrocarbons were measured. A typical spectrum is presented in Figure 1. Reduced mobilities of the positive ions were calculated as shown in Table 3, and are plotted versus the logarithms of molecular weights in the parent compounds in Figure 2.

Linear relationships between reduced mobilities of the positive ions and logarithms of molecular weights of the homologous compounds were observed, as shown in Figure 2, and as given in the following equations:

Line k for M⁺ of alkylbenzene derivatives

$$\begin{aligned} K_o &= -2.19 \log MW + 6.41 \\ r &= -1.000 \end{aligned} \quad (1)$$

where M⁺ represents a molecular ion and r is a correlation coefficient.

Line l for MH⁺

$$\begin{aligned} K_o &= -2.10 \log MW + 6.18 \\ r &= -0.999 \end{aligned} \quad (2)$$

Line m for M⁺ of condensed aromatic homologues

$$\begin{aligned} K_o &= -1.13 \log MW + 5.47 \\ r &= -1.000 \end{aligned} \quad (3)$$

Table 1. Ion Mobility Spectrometer: Experimental Condition

Temperature ^a in drift tube	ca. 200°C
Pressure ^b in drift tube	ca. 760 mm/Hg
Flow rate of carrier gas	200 mL/min
Flow rate of drift gas	100 mL/min
Potential gradient in electric field	214.3 V/cm
Gate width	0.2 msec
Repetition period	24 msec
Average number of sweeps	64
Gas used as carrier and drift gas	Nitrogen or air

^a Measured by a chromel-alumel thermocouple.

^b Measured by a mercurial barometer.

Table 2. Sample Compounds Used in This Experiment

Compound	Supplier
Benzene	Nakarai Chemicals, Ltd.
Toluene	
o-Xylene	
m-Xylene	
p-Xylene	
Ethylbenzene	
Cumene	
Naphthalene	
2,3-Dimethylnaphthalene	Tokyo Chemical Industry Co., Ltd.
Anthracene	Nakarai Chemicals, Ltd.
Phenanthrene	
Pyrene	
Fluoranthene ^a	Tokyo Chemical Industry Co., Ltd.
1,2-Benzanthracene	Nakarai Chemicals, Ltd.
Chrysene	
3,4-Benzopyrene	
Perylene	
Pentacene	Tokyo Chemical Industry Co., Ltd.
β-Iodonaphthalene ^a	
Diphenyl ^a	Nakarai Chemicals, Ltd.
Dibenzyl	Tokyo Chemical Industry Co., Ltd.
o-Terphenyl ^a	Nakarai Chemicals, Ltd.
m-Terphenyl ^a	
p-Terphenyl	
Formic acid	Wako Pure Chemical Industries Co., Ltd.
Acetic acid	Nakarai Chemicals, Ltd.
Propionic acid	
n-Butyric acid	
iso-Butyric acid	
n-Valeric acid	
iso-Valeric acid	
n-Caproic acid	
iso-Caproic acid	Wako Pure Chemical Industries Co., Ltd.
n-Caprylic acid	
Phenol	Nakarai Chemicals, Ltd.
o-Cresol	
m-Cresol	
p-Cresol	
2,3-Xylenol	
2,4-Xylenol	
2,5-Xylenol	

Table 2 (continued). Sample Compounds Used in This Experiment

Compound	Supplier
2,6-Xylenol	
3,4-Xylenol	
3,5-Xylenol	
Pyridine	
α -Picoline	Tokyo Chemical Industry Co., Ltd.
β -Picoline	
γ -Picoline	
2,3-Lutidine	
2,4-Lutidine	
2,5-Lutidine	
2,6-Lutidine	
3,4-Lutidine	
3,5-Lutidine	Nakarai Chemicals, Ltd.
2-Ethylpyridine ^a	Tokyo Chemical Industry Co., Ltd.
3-Ethylpyridine ^a	
4-Ethylpyridine	
2,4,6-Collidine	
2-n-Propylpyridine	
2-Methyl-5-ethylpyridine	Wako Pure Chemical Industries, Ltd.
4-Benzylpyridine	Tokyo Chemical Industry Co., Ltd.
2-Chloropyridine	Nakarai Chemicals, Ltd.
4-Chloropyridine (Hydrochloride)	Tokyo Chemical Industry Co., Ltd.
2,6-Dichloropyridine	Nakarai Chemicals, Ltd.
3,5-Dichloropyridine ^a	
2-Bromopyridine	
3-Bromopyridine	
Pyrrrole	Tokyo Chemical Industry Co., Ltd.
N-Methylpyrrole	
Pyrrolidine ^a	Nakarai Chemicals, Ltd.
N-Methylpyrrolidine ^a	Tokyo Chemical Industry Co., Ltd.
Piperidine ^a	Nakarai Chemicals, Ltd.
2-Pipecoline	
4-Pipecoline	Wako Pure Chemical Industries, Ltd.
N-Ethylpiperidine ^a	
2-Ethylpiperidine ^a	
Imidazole	Nakarai Chemicals, Ltd.
Pyrimidine	
Pyrazine	
1,3,5-Triazine ^a	
5-Methylpyrimidine	Sigma Chemical Co., Ltd.
2-Methylpyrazine	Nakarai Chemicals, Ltd.
2,3,5,6-Tetramethylpyrazine	
Piperazine	
N-Methylpiperazine	
Indole	
Quinoline	
iso-Quinoline ^a	Tokyo Chemical Industry Co., Ltd.
Quinoxaline	
Quinazoline	
Phthalazine ^a	
2-Methylquinoxaline	
2,3-Dimethylquinoxaline ^a	
Benzocinnoline	
Aniline	Nakarai Chemicals, Ltd.
N-Methylaniline	
o-Toluidine	

Table 2 (continued). Sample Compounds Used in This Experiment

Compound	Supplier
m-Toluidine ^a	
p-Toluidine	
N,N-Dimethylaniline ^a	Tokyo Chemical Industry Co., Ltd.
N-Ethylaniline	Nakarai Chemicals, Ltd.
o-Ethylaniline	
p-Ethylaniline	
N-n-Propylaniline ^a	Tokyo Chemical Industry Co., Ltd.
N,N-Diethylaniline	
N-n-Butylaniline ^a	
2,6-Diethylaniline ^a	
p-n-Butylaniline ^a	
Diphenylamine	
Triphenylamine	
Dimethyl sulfide	Wako Pure Chemical Industries Co., Ltd.
Diethyl sulfide ^a	Nakarai Chemicals, Ltd.
Di-n-propyl sulfide ^a	Tokyo Chemical Industry Co., Ltd.
Di-tert-butyl sulfide ^a	
Diallyl disulfide ^a	
Di-tert-amyl disulfide ^a	
Diphenyl sulfide	
Diphenyl disulfide ^a	
p-Thiocresol ^a	Nakarai Chemicals, Ltd.
Thiophene	
Furan	
Ethyl ether	

^a Pure grade.

Line n for M⁺ of diphenyl aromatic homologues

$$K_o = -1.89 \log MW + 5.78 \quad (4)$$

$$r = -1.000$$

It has been reported that larger K is for M⁺ and different K_o of M⁺ and of MH⁺ are able to be observed by ion mobility spectrometry.⁷

Ion mobility spectra of positive ions produced from fatty acids and phenolic compounds were measured when air was used as a carrier gas, as shown in Figures 3 and 4, respectively.

Reduced mobilities of the positive ions are calculated as presented in Table 4 and presented in Figure 5 versus logarithms of molecular weights of the parent compounds. The positive ions were produced when both air and nitrogen were used as carrier gas, whereas the negative ions were only observed when using an air carrier. It is worthy to note that oxygen provides stabilization of the product ions. The linear relationships are presented as follows: Line l for positive ions of phenols

$$K_o = -2.03 \log MW + 6.07 \quad (5)$$

$$r = -1.000$$

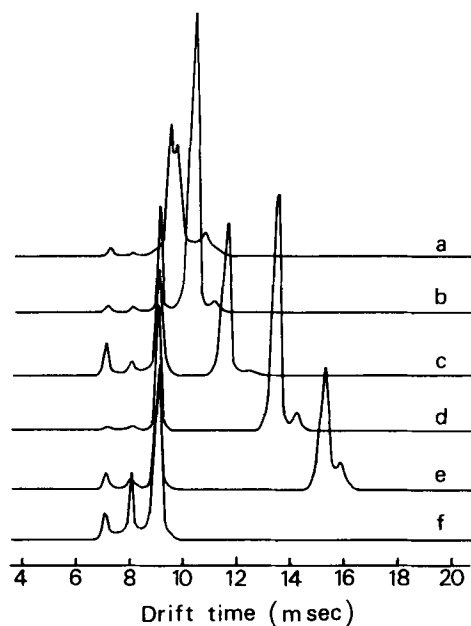


Figure 1. Ion mobility spectra of positive ions of aromatic hydrocarbons: (a) benzene, (b) toluene, (c) naphthalene, (d) anthracene, (e) 1,2-benzanthracene, and (f) reactant ions.

Table 3. Reduced Mobilities of Positive Ions of Aromatic Hydrocarbons

Compound	Molecular Weight	Reduced Mobility (K_0 , $\text{cm}^2/\text{V}\cdot\text{sec}$)	
		Positive	Negative
Benzene	78.11	2.27	2.20
Toluene	92.14		2.07
o-Xylene	106.17	1.98	1.93
m-Xylene	106.17		1.93
p-Xylene	106.17	1.98	1.93
Ethylbenzene	106.17		1.93
Cumene	120.20	1.86	1.81
Naphthalene	128.17		1.84
2,3-Dimethylnaphthalene	156.23		1.65
Anthracene			
Phenanthrene	178.23		1.58
Pyrene			
Fluoranthene	202.26		1.49
1,2-Benzanthracene	228.29		1.39
Chrysene			
3,4-Benzpyrene	252.32		1.33
Perylene			
β -Iodonaphthalene	254.07		1.61
Pentacene	278.35		1.25
Diphenyl	154.21		1.66
Dibenzyl	182.27		1.52
o-Terphenyl			
m-Terphenyl	230.31		1.31
p-Terphenyl			

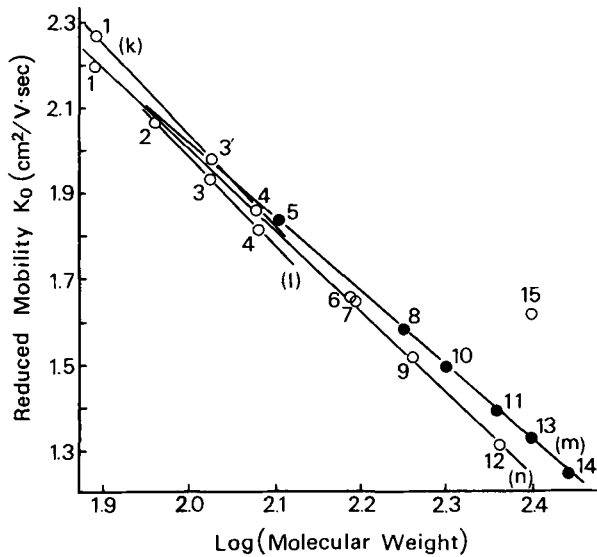


Figure 2. Relationships between reduced mobilities of the positive ions and logarithms of molecular weights of aromatic compounds. (1) Benzene; (2) toluene; (3) o-, m-, and p-xylene, ethylbenzene; (3') o- and p-xylene; (4) cumene; (5) naphthalene; (6) diphenyl; (7) 2,3-dimethylnaphthalene; (8) anthracene, phenanthracene; (9) dibenzyl; (10) pyrene, fluoranthene; (11) 1,2-benzanthrene, chrysene; (12) o-, m-, and p-terphenyl; (13) 3,4-benzopyrene, perylene; (14) pentacene; and (15) β -iodonaphthalene.

Line m for positive ions of fatty acids

$$K_0 = -2.61 \log MW + 7.29 \quad (6)$$

$$r = 0.999$$

Line n for negative ions of fatty acids

$$K_0 = -2.36 \log MW + 6.61 \quad (7)$$

$$r = -0.998$$

Separation of isomeric ions of butyric acid was performed successfully by using IMS. Drift times of ions of isobutyric acid were smaller than those of n-butyric acid. This illustrates that mobilities of isomeric ions of amines are smallest for primary amines and largest for tertiary amines. It is interesting that the reduced mobilities of product ions of fatty acids are larger than those of phenols and pyridines.

Pyridine and Heterocyclic Nitrogen Compounds

Ion mobility spectra of positive ions of pyridine and its related compounds were obtained as shown in Figure 6. Reduced mobilities of the ions of nitrogen compounds

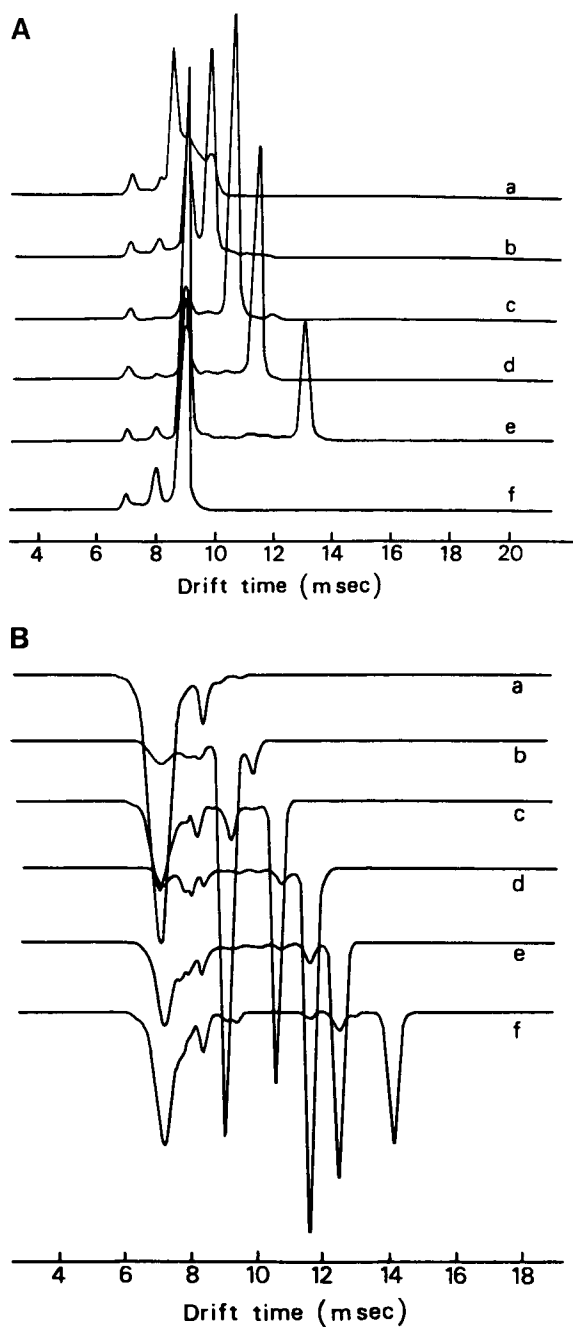


Figure 3. Ion mobility spectra of positive product ions (A) and negative product ions (B) of fatty acids; (A): (a) acetic acid, (b) n-butyric acid, (c) n-valeric acid, (d) n-caproic acid, (e) n-caprylic acid, and (f) reactant ions; (B): (a) reactant ions, (b) acetic acid, (c) n-butyric acid, (d) n-valeric acid, (e) n-caproic acid, and (f) n-caprylic acid.

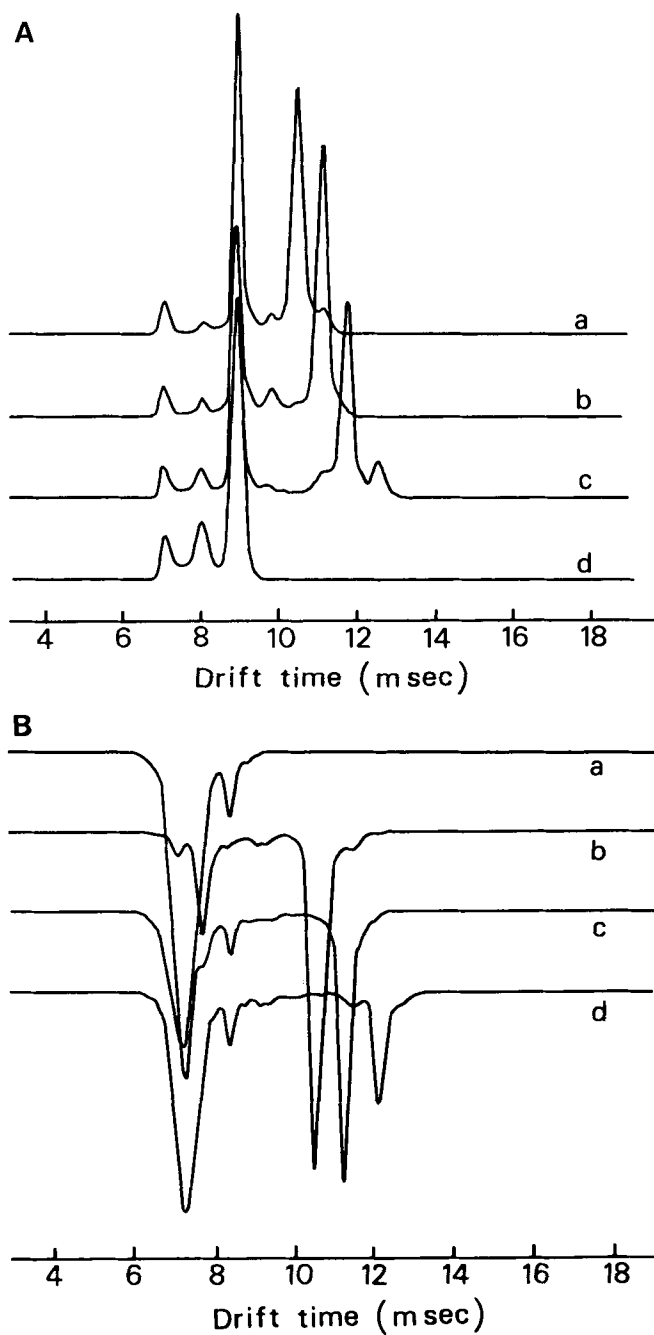


Figure 4. Ion mobility spectra of positive product ions (A) and negative product ions (B) of phenolic compounds; (A): (a) phenol, (b) o-cresol, (c) 2,3-xyleneol, and (d) reactant ions; (B): (a) reactant ions, (b) phenol, (c) o-cresol, and (d) 2,3-xyleneol.

Table 4. Reduced Mobilities of Positive Ions and Negative Ions of Fatty Acids and of Phenolic Compounds

Compound	Molecular Weight	Reduced Mobility (K_0 , cm ² /V-sec)	
		Positive	Negative
Formic acid	46.02	3.09 ^a	2.73
Acetic acid	60.05	2.57	2.38
Propionic acid	74.08	2.41	2.18
n-Butyric acid	88.11	2.23	2.01
iso-Butyric acid	88.11	2.31	2.03
n-Valeric acid	102.13	2.07	1.87
iso-Valeric acid	102.13	2.09	1.88
n-Caproic acid	116.16	1.91	1.74
iso-Caproic acid	116.16	1.94	1.75
n-Caprylic acid	144.21	1.66	1.54
Phenol	94.11	2.07	2.06
o-Cresol	108.14	1.95	1.92
m-Cresol	108.14	1.95	1.90
p-Cresol	108.14	1.95(2.02) ^b	1.90(2.01) ^b
2,3-Xylenol	122.17	1.83	1.78
2,4-Xylenol	122.17	1.83(1.89) ^b	1.78(1.87) ^b
2,5-Xylenol	122.17	1.84	1.79
2,6-Xylenol	122.17	1.84	1.81
3,4-Xylenol	122.17	1.83	1.76
3,5-Xylenol	122.17	1.83	1.76

^a Weak peak.^b Sub-peak.

with higher molecular weights were smaller than those of the compounds with lower molecular weights.

IMS separation of the positive ions of pyridine and its methyl derivatives was performed successfully as shown in Figure 7. After sample injection, a positive ion of collidine appeared at first, and cations of lutidine and picoline next, and at last, ions of pyridine. These were separated from each other depending upon proton affinity and ionizability of these compounds.

Reduced mobilities of positive ions of pyridine and its related compounds were calculated as presented in Table 5. The reduced mobilities were plotted versus the logarithms of molecular weights of the pyridine derivatives as shown in Figure 8.

The linear relationship with molecular weight of positive ions of pyridine derivatives is presented according to the following equation:

$$K_0 = -2.02 \log MW + 6.00 \quad (8)$$

$$r = -0.998$$

This line is parallel with that produced by ions of alkyl amines.^{8,9} The slope of the linear relationship corresponds to K_0 for one molar methylene group of the compound.

Ion mobility spectra of positive ions of halogenated pyridine and related halo-compounds are shown in Figure 9.

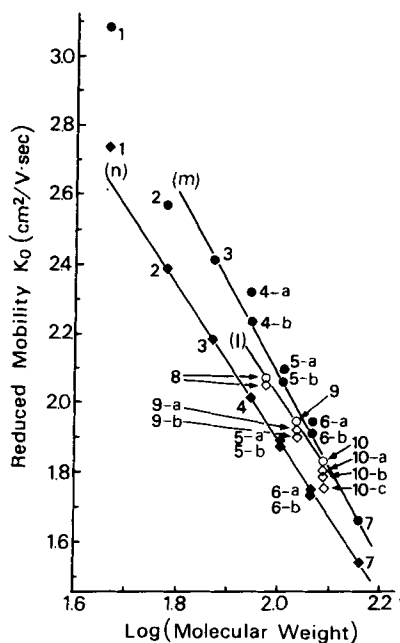


Figure 5. Relationships between reduced mobilities of positive and negative ions and logarithms of molecular weights of fatty acids and of phenolic compounds: ●: positive ions of fatty acids; ◆: negative ions of fatty acids, ○: positive ions of phenolic, and ◇: negative ions of phenolic compounds; (1) formic acid, (2) acetic acid, (3) propionic acid, (4) butyric acid (a:iso-; b:n-), (5) valeric acid (a:iso-; b:n-), (6) caproic acid (a:iso-; b:n-), (7) n-caprylic acid, (8) phenol, (9) Cresol (a:o-; b:m-, p-), and (10) xylene (a:2,6-; b:2,3-;2,4-;2,5-; c:3,4-;3,5-).

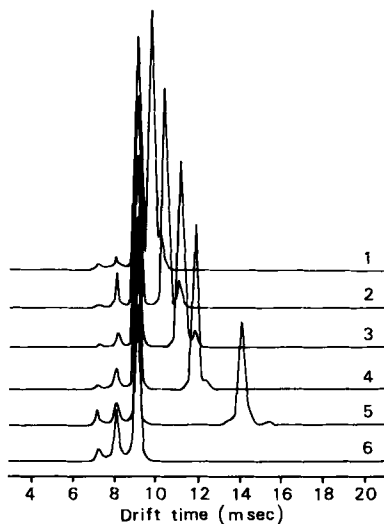


Figure 6. Ion mobility spectra of positive ions of pyridine and its methyl and benzyl derivatives; (1) pyridine, (2) α -picoline, (3) 2,3-lutidine, (4) 2,4,6-collidine, (5) 4-benzylpyridine, and (6) reactant ions.

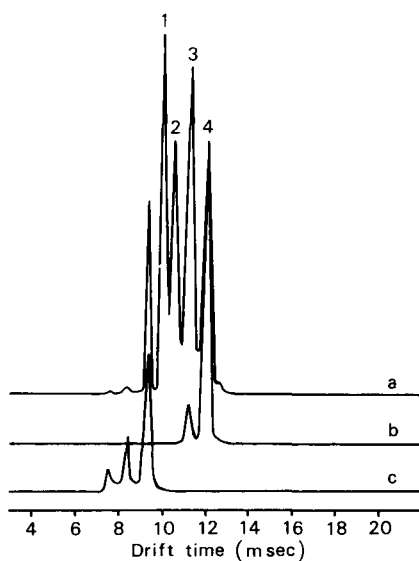


Figure 7. Ion mobility spectrometric separation of positive ions of pyridine and its methyl derivatives; immediately after (a) and after 10 min (b) of sample injection, (c) reactant ions; (1) pyridine, (2) α -picoline, (3) 2,3-lutidine, and (4) 2,4,6-collidine.

Table 5. Reduced Mobilities of Positive Ions of Pyridine and Its Related Compounds

Compound	Molecular Weight	Reduced Mobility (K_0 , $\text{cm}^2/\text{V}\cdot\text{sec}$)
Pyridine	79.10	2.16
α -Picoline	93.13	2.05
β -Picoline	93.13	2.02
γ -Picoline	93.13	2.02
2,3-Lutidine	107.15	1.91
2,4-Lutidine	107.15	1.91
2,5-Lutidine	107.15	1.91
2,6-Lutidine	107.15	1.91
3,4-Lutidine	107.15	1.91
3,5-Lutidine	107.15	1.91
2-Ethylpyridine	107.15	1.91
3-Ethylpyridine	107.15	1.89
4-Ethylpyridine	107.15	1.89
2,4,6-Collidine	121.18	1.80
2-n-Propylpyridine	121.18	1.80
2-Methyl-5-ethylpyridine	121.18	1.80
4-Benzylpyridine	169.23	1.50
2-Chloropyridine	113.55	1.96
4-Chloropyridine	113.55	1.93
2,6-Dichloropyridine	147.99	1.82
3,5-Dichloropyridine	147.99	1.76
2-Bromopyridine	158.00	1.88
3-Bromopyridine	158.00	1.83

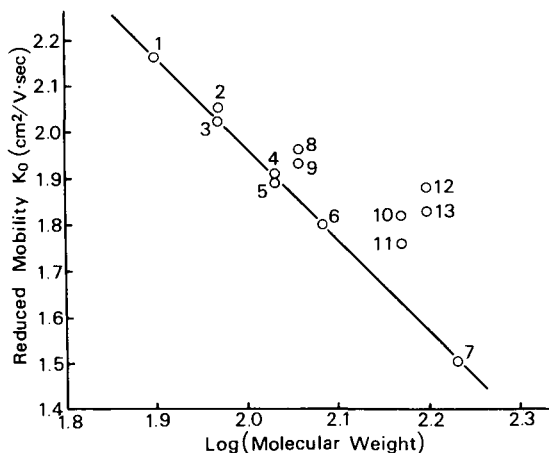


Figure 8. Relationships between reduced mobilities of positive ions and logarithms of molecular weights of pyridine and its derivatives; (1) pyridine, (2) α -picoline, (3) β - and γ -picoline, (4) lutidine, 2-ethylpyridine, (5) 3- and 4-ethylpyridine, (6) 2,4,6-collidine, 2-n-propylpyridine, 2-methyl-5-ethyl-pyridine, (7) 4-benzylpyridine, (8) 2-chloropyridine, (9) 4-chloropyridine, (10) 2,6-dichloropyridine, (11) 3,5-dichloropyridine, (12) 2-bromopyridine, and (13) 3-bromopyridine.

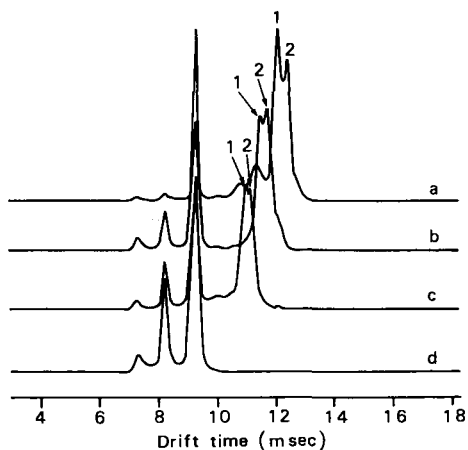


Figure 9. Ion mobility spectra of positive ions of halogenated pyridine and its derivatives; (a) 1: 2,6-dichloropyridine, 2: 3,5-dichloropyridine; (b) 1: 2-bromopyridine, 2: 3-bromopyridine; (c) 1: 2-chloropyridine, 2: 4-chloropyridine; and (d) reactant ions.

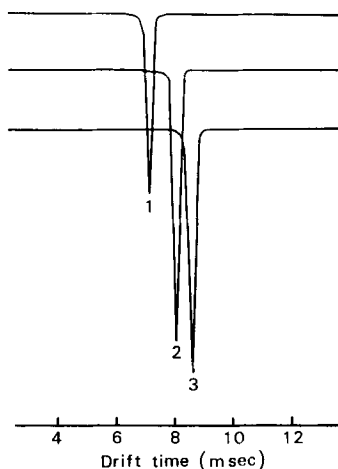


Figure 10. Ion mobility spectra of halogen ions produced from halogenated pyridines and naphthalene; (1) $K_0 = 3.01$ (Cl^- :2-chloropyridine), (2) $K_0 = 2.68$ (Br^- :2-bromopyridine), and (3) $K_0 = 2.54$ (I^- : β -iodonaphthalene).

Negative halogen ions were produced from halogenated pyridine derivatives and aromatic compounds as shown in Figure 10. No molecular product ions were observed under these conditions.

Ion mobility spectra of positive ions of heterocyclic nitrogen compounds, condensed heterocyclic compounds, and saturated cyclic compounds were observed as shown in Figure 11.

Linear relationships between reduced mobilities of the positive ions and logarithms of the molecular weights of heterocyclic nitrogen compounds are presented in Figure 12, in which the straight lines are presented by the following equation:

$$K_0 = -1.79 \log MW + 5.52 \quad (9)$$

$$r = -0.997$$

and

$$K_0 = -2.09 \log MW + 6.23 \quad (10)$$

$$r = -0.999$$

Reduced mobilities of positive ions of condensed heterocyclic and saturated cyclic compounds such as piperidine derivatives were smaller than those of unsaturated cyclic compounds, presented in Table 6. The linear relationships are presented in the following equation:

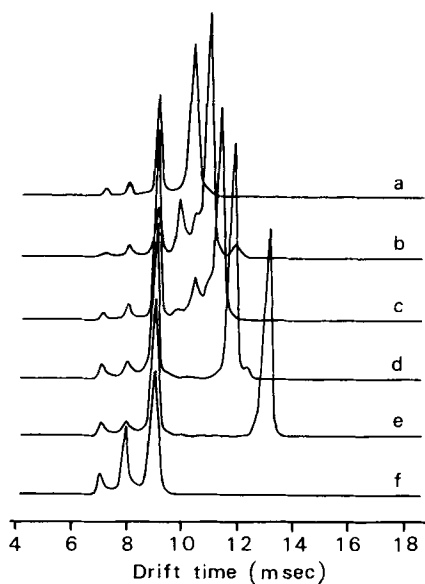


Figure 11. Ion mobility spectra of positive ions of heterocyclic nitrogen compounds; (a) pyrimidine, (b) piperidine, (c) 2-pipecoline, (d) quinoxaline, (e) 2,3-dimethylquinoxaline, and (f) reactant ions.

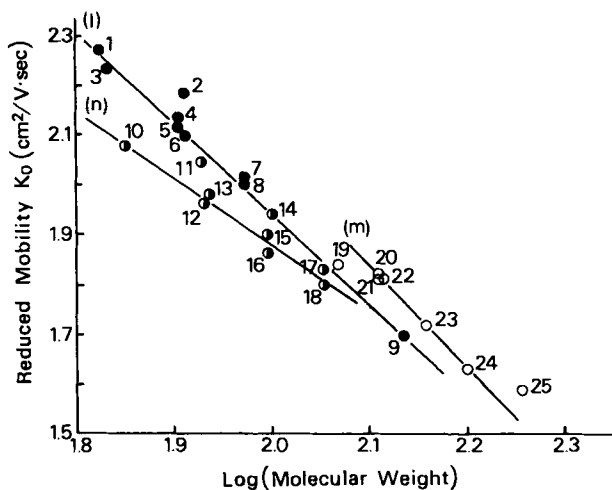


Figure 12. Relationships between reduced mobilities of positive ions and logarithms of molecular weights of heterocyclic nitrogen compounds; (1) pyrrole, (2) N-methylpyrrole, (3) imidazole, (4) pyrimidine, (5) pyrazine, (6) 1,3,5-triazine, (7) 5-methylpyrimidine, (8) 2-methylpyrazine, (9) 2,3,5,6-tetramethylpyrazine, (10) pyrrolidine, (11) N-methylpyrrolidine, (12) piperidine, (13) piperazine, (14) N-methylpiperazine, (15) 2-pipecoline, (16) 4-pipecoline, (17) N-ethylpiperidine, (18) 2-ethylpiperidine, (19) indole, (20) quinoline, (21) iso-quinoline, (22) quinoxaline, quinazoline, phthalazine, (23) 2-methylquinoxaline, (24) 2,3-dimethylquinoxaline, and (25) benzocinnoline.

Table 6. Reduced Mobilities of Positive Ions of Nitrogen-Containing Cyclic Compounds

Compound	Molecular Weight	Reduced Mobility (K_0 , cm ² /V·sec)
Pyrrole	67.09	2.27
N-Methylpyrrole	81.12	2.18
Pyrrolidine	71.12	2.08
N-Methylpyrrolidine	85.15	2.05
Piperidine	85.15	1.96
2-Pipecoline	99.18	1.90
4-Pipecoline	99.18	1.86
N-Ethylpiperidine	113.20	1.83
2-Ethylpiperidine	113.20	1.80
Imidazole	68.08	2.23
Pyrimidine	80.09	2.13
Pyrazine	80.09	2.11
1,3,5-Triazine	81.08	2.09
5-Methylpyrimidine	94.12	2.01
2-Methylpyrazine	94.12	2.00
2,3,5,6-Tetramethylpyrazine	136.22	1.70
Piperazine	86.14	1.98
N-Methylpiperazine	100.17	1.94
Indole	117.15	1.84
Quinoline	129.16	1.82
iso-Quinoline	129.16	1.81
Quinoxaline	130.15	1.81
Quinazoline	130.15	1.81
Phthalazine	130.15	1.81
2-Methylquinoxaline	144.18	1.72
2,3-Dimethylquinoxaline	158.21	1.63
Benzocinnoline	180.21	1.59

$$K_0 = -1.45 \log MW + 4.79 \quad (11)$$

$$r = -0.999$$

It was found that the reduced mobilities of positive ions of ortho-substituted compounds were larger than those of meta-substituted compounds, and those of N-substituted compounds were larger than those of ortho-substituted compounds. The sensitivity of IMS is shown in Figure 13, which shows results of experiments on the separation and detection of ions of 2,4,6-colicine. This technique provides ultra-micro sensitivity of a femtomolar level.

Aromatic Amines

Ion mobility spectra of positive ions of aromatic amines such as aniline and its derivatives are shown in Figure 14. Reduced mobilities of the positive ions are presented in Table 7.

The reduced mobilities of the positive ions of primary alkylamines were largest and those of tertiary compounds were smallest. The K_0 of the positive ions of aniline derivatives were larger than those of pyridine homologues.

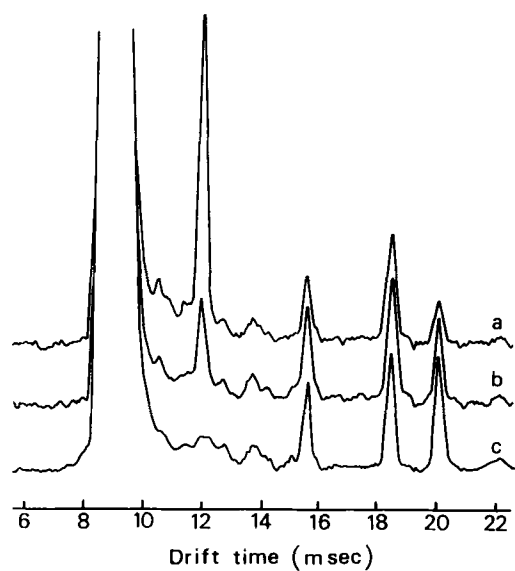


Figure 13. Sensitivity of the ion mobility spectrometry on the positive ions of 2,4,6-collidine ions; (a) 0.5 nL/mL, 1 μ L \approx 5 pmol of collidine; (b) 0.5 pL/mL, 1 μ L \approx 5 pmol of collidine; and (c) water, 1 μ L.

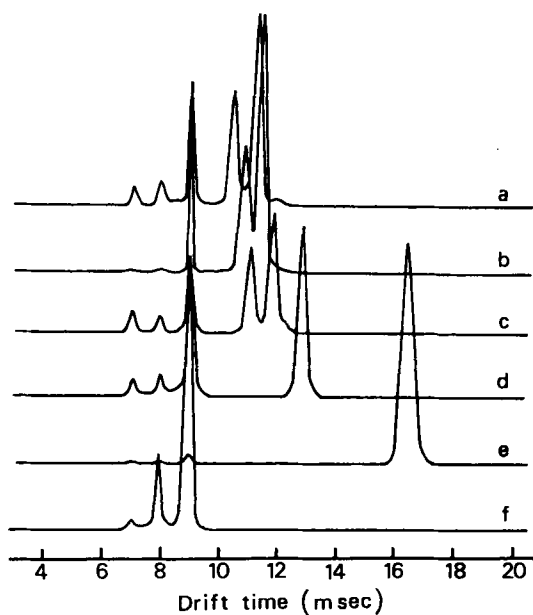


Figure 14. Ion mobility spectra of positive ions of aromatic amines; (a) aniline, (b) N-methylaniline, (c) o-toluidine, (d) N,N-diethylaniline, (e) triphenylamine, and (f) reactant ions.

Table 7. Reduced Mobilities of Positive Ions of Aromatic Amines

Compound	Molecular Weight	Reduced Mobility (K_O , $\text{cm}^2/\text{V}\cdot\text{sec}$)
Aniline	93.13	1.91 (2.06) ^a
N-Methylaniline	107.16	1.85 (1.95) ^a
o-Toluidine	107.16	1.81 (1.93) ^a
m-Toluidine	107.16	1.79 (1.93, 1.73) ^a
p-Toluidine	107.16	1.79 (1.93) ^a
N,N-Dimethylaniline	121.18	1.80 (1.87) ^a
N-Ethylaniline	121.18	1.77 (1.83) ^a
o-Ethylaniline	121.18	1.72 (1.82) ^a
p-Ethylaniline	121.18	1.67 (1.82) ^a
N-n-Propylaniline	135.21	1.69
N,N-Diethylaniline	149.24	1.66
N-n-Butylaniline	149.24	1.60
2,6-Diethylaniline	149.24	1.58 (1.65) ^a
p-n-Butylaniline	149.24	1.48 (1.60) ^a
Diphenylamine	169.23	1.55 (1.59) ^a
Triphenylamine	245.32	1.31

^a Sub-peak (refers to values in parenthesis only).

Relationships between reduced mobilities of the ions of those aniline homologues and logarithms of molecular weights of those compounds were plotted as shown in Figure 15.

Linear relationships for para-alkyl substituted anilines, for ortho-alkyl-substituted anilines and for N-alkyl-substituted anilines are expressed as follows:

Line 1 for p-substituents

$$K_O = -2.11 \log MW + 6.07 \quad (12)$$

$$r = -1.000$$

Line m for o-substituents

$$K_O = -1.61 \log MW + 5.09 \quad (13)$$

$$r = -1.000$$

Line n for N-substituents

$$K_O = -1.73 \log MW + 5.36 \quad (14)$$

$$r = -0.997$$

The results for aromatic amines were similar to those observed for aliphatic amines in that the reduced mobilities of positive ions of primary compounds were largest and for tertiary compounds were smaller.

Sulfur-Containing Compounds

Ion mobility spectra of positive ions of sulfur-containing compounds were obtained as shown in Figure 16.

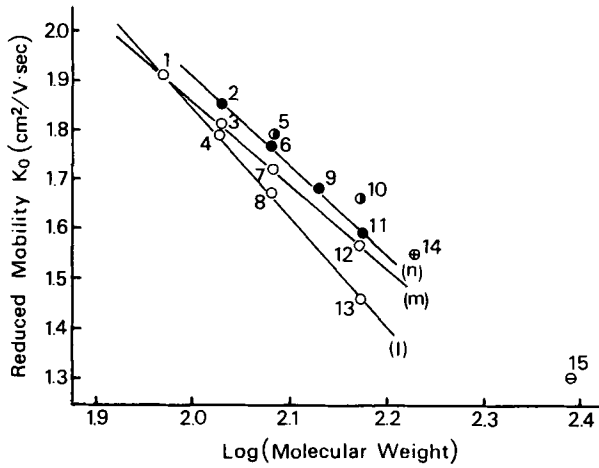


Figure 15. Relationships between reduced mobilities of positive ions and logarithms of molecular weights of aromatic amines; (1) aniline, (2) N-methylaniline, (3) o-toluidine, (4) m- and p-toluidine, (5) N,N-dimethylaniline, (6) N-ethylaniline, (7) o-ethylaniline, (8) p-ethylaniline, (9) N-n-propylaniline, (10) N,N-diethylaniline, (11) N-n-butylaniline, (12) 2,6-diethyl-aniline, (13) p-n-butylaniline, (14) diphenylamine, and (15) triphenylamine.

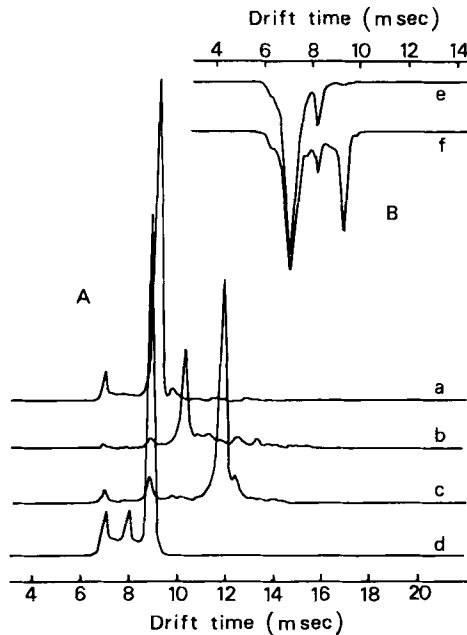


Figure 16. Ion mobility spectra of positive ions (A) and negative ions (B) of alkyl sulfides; (a) dimethyl sulfide, (b) diethyl sulfide, (c) di-n-propyl sulfide, (d) reactant ions, (e) reactant ions, and (f) dimethyl sulfide.

Table 8. Reduced Mobilities of Positive Ions of Sulfur-Containing Compounds

Compound	Molecular Weight	Reduced Mobility (K_0 , $\text{cm}^2/\text{V}\cdot\text{sec}$)	
		Positive	Negative
Dimethyl sulfide	62.13	2.36	2.32
Diethyl sulfide	90.19	2.08	2.31
Di-n-propyl sulfide	118.24	1.82	2.32
Di-tert-butyl sulfide	146.29	2.37	2.32,2.00
Diallyl disulfide	146.27	1.90	2.31
Di-tert-amyl disulfide	206.40	1.87	2.31
Diphenyl sulfide	186.27	1.54	(2.32) ^a 1.97
Diphenyl disulfide	218.33	1.54	(2.32) ^a 1.97
p-Thiocresol	124.20	(1.79) ^a	1.83
Thiophene	84.14	2.22	2.31
Furan	68.08	2.37	(2.32) ^a 2.16
Ethyl ether	74.12	2.23,2.15	2.38

^a Weak peak (refers to values in parenthesis only).

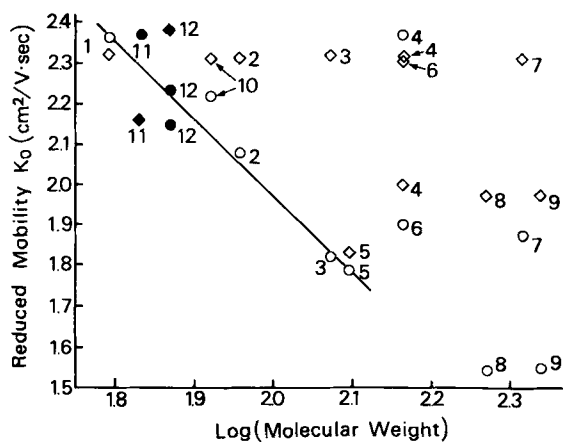


Figure 17. Relationships between reduced mobilities of positive (○) and negative (◇) ions and logarithms of molecular weights of sulfur compounds; (1) dimethyl sulfide, (2) diethyl sulfide, (3) di-n-propyl sulfide, (4) di-tert-butyl sulfide, (5) p-thiocresol, (6) diallyl disulfide, (7) di-tert-amyl disulfide, (8) diphenyl sulfide, (9) diphenyl disulfide, (10) thiophene, (11) furan, and (12) ethyl ether.

Reduced mobilities of the positive ions are presented in Table 8 and plotted versus logarithms of molecular weights of the parent compounds are shown in Figure 17.

Linear relationships between reduced mobilities of positive ions of sulfur compounds and logarithms of molecular weights of the parent compounds were observed only for the dimethyl, diethyl, and dipropyl disulfides as follows:

$$K_0 = -1.92 \log MW + 5.81 \quad (15)$$

$$r = -0.998$$

Table 9. Linear Relationships between Reduced Mobilities of the Ions and Logarithms of Molecular Weights of the Homologous Compounds Presented According to the Following Equation: $K_0 = -a \log MW + b$ (r is the Correlation Coefficient)

Homologous Compound		Figure in Text	a	b	r
1	Alkyl benzene derivatives (M^+)	4(k)	2.19	6.41	-1.000
2	Alkyl benzene derivatives (MH^+)	4(l)	2.10	6.18	-0.999
3	Condensed polycyclic aromatic hydrocarbon	4(m)	1.73	5.47	-1.000
4	Benzene phenyle derivatives	4(n)	1.89	5.78	-1.000
5	Alkyl phenol derivatives	7(l)	2.03	6.07	-1.000
6	Fatty acid (cation)	7(m)	2.61	7.29	-0.999
7	Fatty acid (anion)	7(n)	2.36	6.61	-0.998
8	Alkyl pyridine derivatives	10	2.02	6.00	-0.998
9	Alkyl diazine derivatives	14(l)	1.79	5.52	-0.997
10	Condensed heterocyclic alkyl derivatives	14(m)	2.09	6.23	-0.999
11	Alkyl piperidine derivatives	14(n)	1.45	4.79	-0.990
12	p-Alkyl aniline derivatives	16(l)	2.11	6.07	-1.000
13	o-Alkyl aniline derivatives	16(m)	1.61	5.09	-1.000
14	N-Alkyl aniline derivatives	16(n)	1.73	5.36	-0.997
15	Alkyl sulfide	18	1.92	5.81	-0.998

It was found that several sulfides such as di-tert-butylsulfide and di-tert amylsulfide seemed to decompose during the IMS ionization and drift-tube separation processes.

Ion mobility spectra of negative ions of thiophene and furans were measured. The results showed some decomposition also occurred for these compounds. The linear relationships presented already in Figures 2, 5, 8, 12, 15, and 17, and Equations 1 to 15 are summarized in Table 9.

REFERENCES

1. Cohen, M. L. and Karasek, F. W. *J. Chromatogr. Sci.* 8:370 (1970); Karasek, F. W. *Res. Dev.* 21(3):34 (1970); 21(12):25 (1970).
2. Griffin, G. W., Dzidic, I., Carroll, D. I., Stillwell, R. N., and Horning, E. C. *Anal. Chem.* 45:1240 (1973).
3. Karasek, F. W. and Denney, D. W. *Anal. Chem.* 46:633 (1974).
4. Spangler, G. E. and Collins, C. I. *Anal. Chem.* 47:403 (1975).
5. Carroll, D. I., Dzidic, I., Stillwell, R. N., and Horning, E. C. *Anal. Chem.* 47:1956 (1975).
6. Karasek, F. W., Hill, Jr., H. H., Kim, S. H., and Rokushika, S. *J. Chromatogr.* 135:329 (1977).
7. Kim, S. H., Betty, K. R., and Karasek, F. W. *J. Chromatogr.* 50:2006 (1978).
8. Karasek, F. W., Kim, S. H., and Rokushika, S. *Anal. Chem.* 50:2013 (1978).
9. Kim, S. H. and Karasek, F. W. *Anal. Chem.* 50:1784 (1978).

CHAPTER 4

Gas, Supercritical Fluid, and Liquid Chromatographic Detection of Trace Organics by Ion Mobility Spectrometry

H. H. Hill, Jr., W. F. Siems, R. L. Eatherton, R. H. St. Louis, M. A. Morrissey, C. B. Shumate, and D. G. McMinn

INTRODUCTION

F. W. Karasek and M. J. Cohen recognized the potential of ion mobility spectrometry (IMS) as a detection method for gas chromatography as early as 1970.¹ They demonstrated, through calculations, that gas flows and sensitivity requirements were compatible between a gas chromatograph and an ion mobility spectrometer. Later, F. W. Karasek and his group at the University of Waterloo demonstrated the use and potential of IMS as a chromatographic detector. The earliest experiments, performed in cooperation with R. A. Keller, coupled the IMS with a packed column gas chromatograph.² The column effluent was split between a flame ionization detector and an IMS. They found that ion mobility spectra for 10 ng of musk ambrette dissolved in benzene could be obtained even when the musk ambrette

was not completely separated from the benzene solvent. S. P. Cram and S. N. Chesler later demonstrated the ability to obtain ion mobility spectra after gas chromatographic introduction using an ion mobility instrument which could take spectra in 20 msec.³ They found that the sensitivity of the IMS was comparable to that of a flame ionization detector (FID) for freons, but provided additional utility in identifying the chromatographic effluents. The qualitative nature of the IMS after gas chromatography was investigated further by F. W. Karasek and S. H. Kim.⁴ Using selected organic acids, aldehydes, and esters, they found that characteristic ion mobility spectra could be obtained at levels between 10^{-6} and 10^{-12} g. In all of this work the ion mobility spectrometer was used primarily as an ion separation device after gas chromatographic introduction to provide additional qualitative information.

In 1977, F. W. Karasek and co-workers demonstrated the use of IMS as a dedicated detector for chromatography where specific mobility windows were monitored continuously. The resulting response, obtained as a function of time, was the chromatographic tracing rather than the ion mobility separation.⁴ Several modes of operation were presented in which flame ionization or electron capture detection (ECD) patterns could be obtained depending on whether positive or negative ions were monitored. Furthermore, tunable mobility detection of selected ions permitted the molecular selective detection of compounds after separation by gas chromatography. Limitations of the chromatograph-ion mobility interface were identified during the course of this research. Two major technical problems were identified: (1) the sensitivity of the ion mobility spectrometer was so high that contamination from column bleed, unseparated components or residual solvent could interfere with the response, and (2) the cell volume of the ion mobility spectrometer was so large that losses in chromatographic resolution occurred during the detection process.

GAS CHROMATOGRAPHIC DETECTION

Based on the pioneering research of F. W. Karasek, the first ion mobility spectrometer specifically designed as a detector for capillary gas chromatography was constructed in 1982.⁵ Shown in Figure 1, the ion mobility detector (IMD) included four salient construction modifications from earlier ion mobility spectrometers:

1. The drift gas entered the spectrometer near the collecting electrode and traveled through the drift and ionization regions before exiting through an opening in the repeller plate. In previous designs, gases entered at both ends of the instrument and exited the instrument near the center. By altering the pattern of the drift gas flow, a unidirectional gas flow was achieved which helped to keep the drift region free of contaminating neutral molecules.
2. The drift tube was completely sealed to permit undesired neutral species to be swept more efficiently from the instrument.
3. The sample was introduced into the detector between the ionization region and the drift region. As a result of this modification, the sample is swept away from the ion drift region and through the ionization with the full velocity of the drift gas flow.

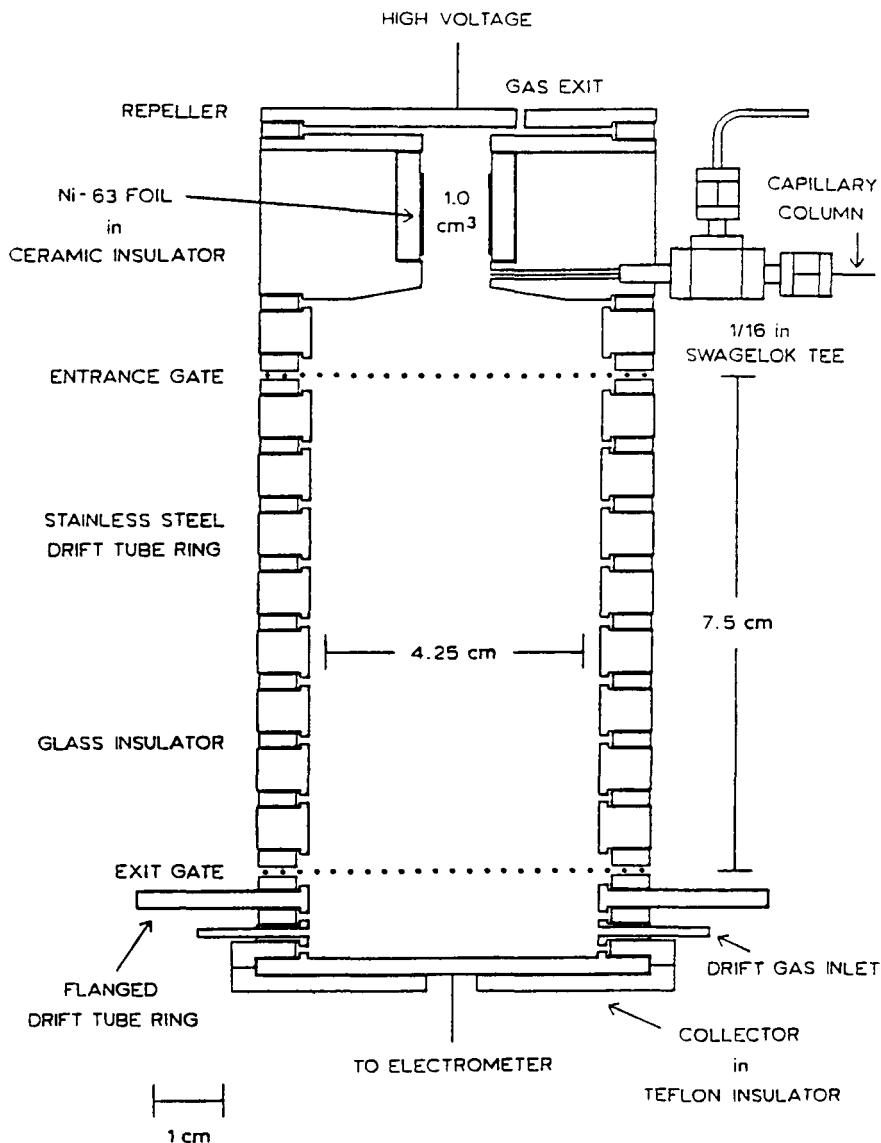


Figure 1. Schematic diagram of an ion mobility spectrometer designed as a gas chromatographic detector.

4. The detector cell volume in the ionization region was reduced to 1 cm^3 . This reduction in volume, coupled with the unidirectional countercurrent drift gas flow, reduced the residence time of a compound in the ionization region to a few tenths of a second. There was no apparent loss of sensitivity, and the integrity of the gas chromatographic separation was maintained.

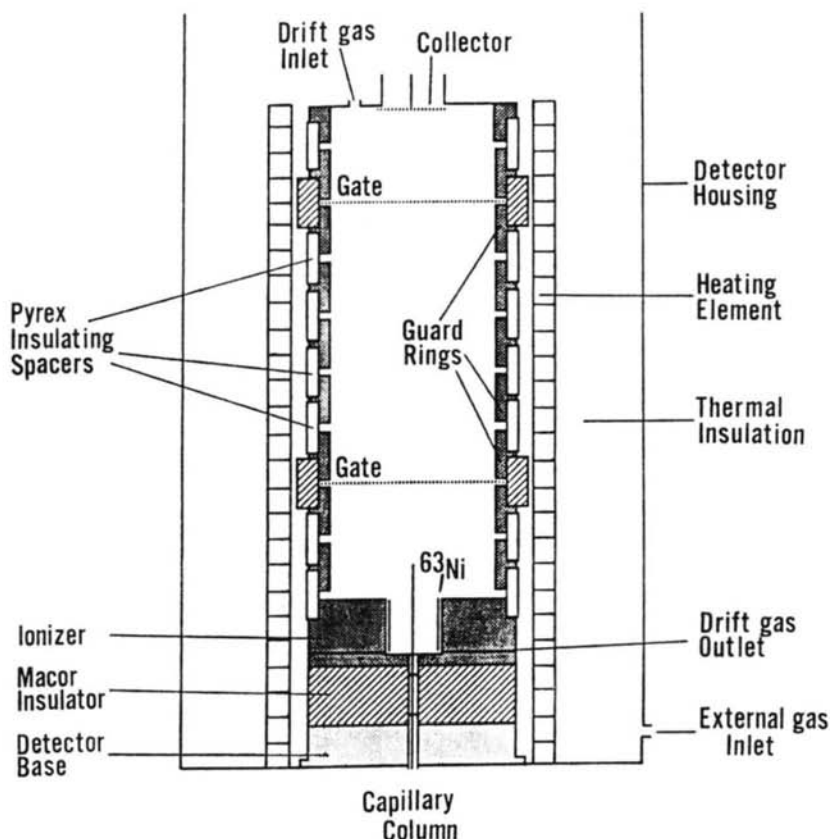


Figure 2. Ion mobility detector for capillary gas chromatography with axial sample introduction.

More recently, the detector was modified further by introducing the sample axially into the spectrometer.⁶ This concentric sample introduction approach, in combination with a unidirectional flow, permitted optimization of chromatographic resolution and detector sensitivity. Figure 2 provides a schematic diagram of this new design.

Figure 3 is an example chromatogram of super unleaded gasoline separated by capillary gas chromatography and detected using the nonselective positive ion monitoring mode.⁷ In this mode of operation, all ions which drifted with mobilities slower than those of the reactant ions were detected and produced a response on the chromatogram for all compounds which formed product ions having these characteristics. Since most organic compounds form positive product ions, the tracing in Figure 3 is considered nonselective and is similar to chromatograms obtained with a flame ionization detector. Sensitivity changes, however, as a function of the compound detected.

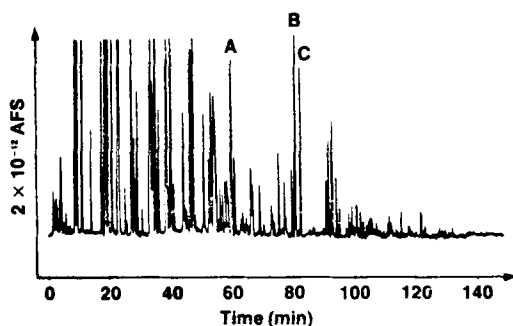


Figure 3. Nonselective positive-ion chromatogram of super unleaded gasoline of a 0.6- μ L injection with a 215:1 split. Peak A = naphthalene, peak B = 2-methylnaphthalene, and C = 1-methylnaphthalene.

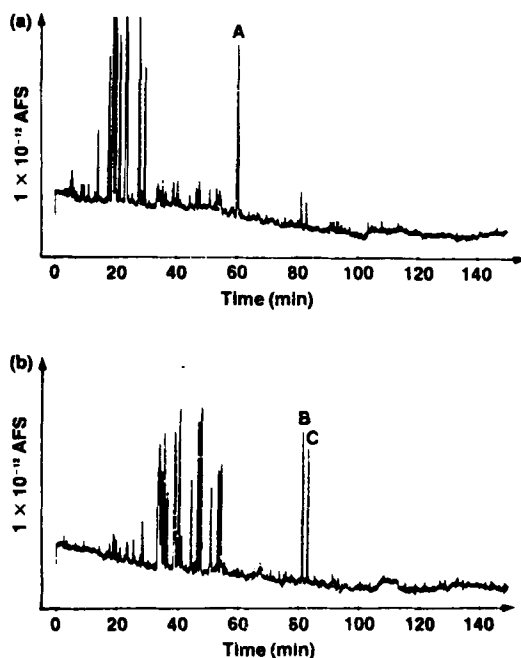


Figure 4. Selective positive-ion chromatograms of super unleaded gasoline. In tracing (a), drift times which correspond to that of naphthalene was monitored. In tracing (b), drift times which correspond to those of 2-methylnaphthalene and 1-methylnaphthalene were monitored.

A major advantage of ion mobility detection is that molecular selective detection can be achieved when the detector is tuned to monitor a narrow window of ion mobilities. For example, in tracing (a) of Figure 4, the detector has been tuned to monitor ions which drift between 6.15 and 6.50 msec. This condition provides selective detection of naphthalene in the gasoline sample. When the detector is

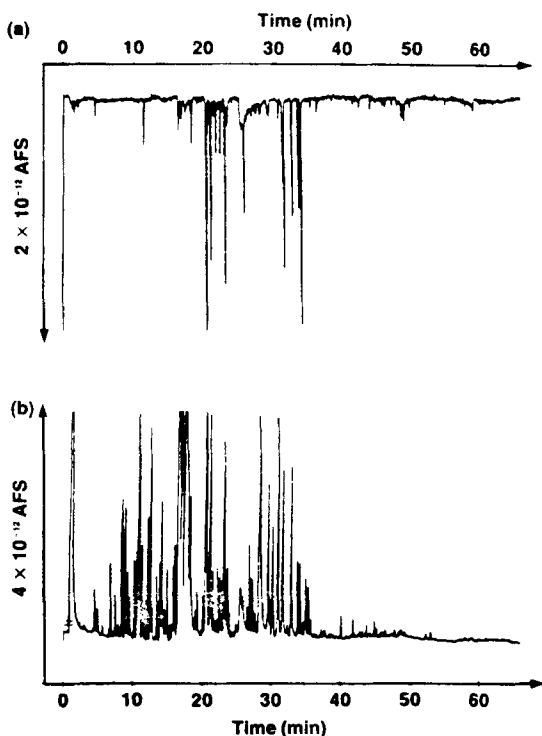


Figure 5. Negative (a) and positive (b) ions are monitored to produce ECD-like and FID-like chromatograms of peppermint oil.

tuned to monitor ions which drift between 6.55 and 6.9 msec, selective detection of the methylnaphthalenes occurs. Thus, the IMD can provide selective detection after gas chromatography when hetero-atoms are not present in the molecule.

The IMD can be operated in the negative mode as well. Figure 5 exhibits non-selective monitoring chromatograms for both negative and positive ions when peppermint oil is separated. The upper tracing is of negative ions, which provided a response similar to that expected for an electron capture detector. The lower tracing is that of positive product ions and is similar to that of a FID. By simply changing from positive to negative ions, two complementary chromatograms can be produced from the same sample.

Selectivity in the negative ion mode can be spectacular. Figure 6 shows the electron capture mode of ion mobility detection in which an Aroclor 1248 sample that has been spiked with a small quantity of 4,4'-dibromobiphenyl was separated by capillary gas chromatography.⁸ Normally it would be difficult to pick out the bromine-containing compound in this mixture. When the ion mobility detector is tuned to monitor the bromide ion, however, Figure 7 shows how easy it is to detect this compound in the presence of the Aroclor mixture.

Figure 8 compares the analysis of soil for the trace organic 2,4-dichlorophenoxyacetic acid (2,4-D) using electron capture, flame ionization, and selective ion mobility detection.⁹ In this analysis, soil samples were Soxhlet-extracted with 1:1 mixture of acetone-hexane, evaporated to near dryness, and taken up in methanol. The methyl esterification of the 2,4-D was carried out in the presence of boron trifluoride as a catalyst. Following the reaction, excess methanol was removed by rotary evaporation. The catalyst was destroyed in water and the ether was extracted from the aqueous solution with diethyl ether. This ether extract was evaporated to near dryness and dissolved in methanol. GC separation and detection was performed without further cleanup. As can be seen from the figure, both the ECD and the FID tracings exhibit considerable possibility for interference. The IMD, on the other hand, provided sensitive and selective detection for the 2,4-D methyl ester.

SUPERCRITICAL FLUID CHROMATOGRAPHIC DETECTION

From the description of the sample preparation procedure, it is obvious that the determination of 2,4-D in soil can be a time-consuming procedure. The use of an ion mobility detector decreased the analysis time because its specificity for 2,4-D obviated the need for chromatographic clean-up procedures. Nevertheless, it would be advantageous if 2,4-D could be determined without the derivatization step required in gas chromatography. One advantage of supercritical fluid chromatography (SFC) is that many compounds such as 2,4-D can be separated without forming

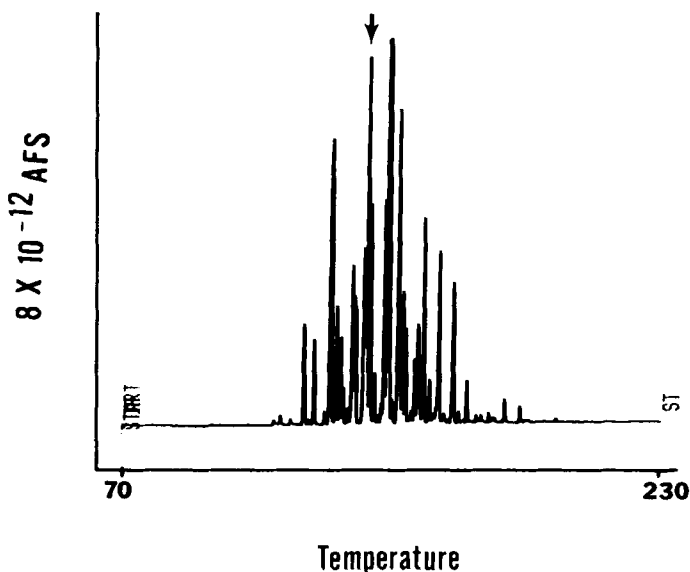


Figure 6. Electron capture ion mobility detection of Aroclor 1248 after spiking with 4,4'-dibromobiphenyl.

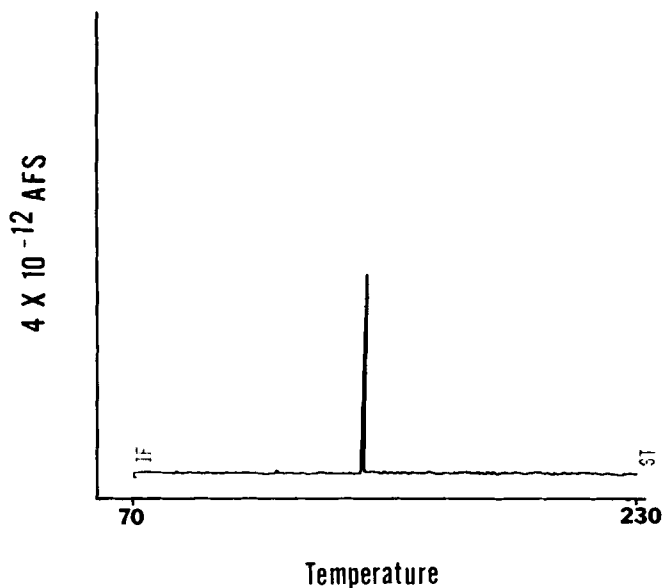


Figure 7. Bromide selective detection of Aroclor 1248 spiked with 4,4'-dibromobiphenyl.

the derivative. Figure 9 shows the ion mobility detection of underivatized 2,4-D after SFC.¹⁰

The ion mobility detector was first proposed for use with supercritical fluid chromatography in 1985¹¹ and has been evaluated both as a detector¹² and a spectrometer.¹³ One major advantage of ion mobility detection for supercritical fluid chromatography is that it responds to compounds which cannot be detected by standard spectrophotometric (i.e., UV/Vis) methods. Figure 10 shows the results of supercritical fluid chromatography of a series of methyl esters using CO_2 as the mobile phase and UV/Vis detection. Because these compounds have low molar absorptivities, no detection occurred with a Jasco UVIVDEC 100II UV detector operated at a fixed wavelength of 210 nm.

The numbered arrows on the chromatogram mark the position at which ion mobility spectra were obtained with an ion mobility spectrometer connected in series to a UV/Vis detector. Results of the IMD scans are shown in Figure 11. Scan 1 shows the ion mobility reactant ions present before injection of the methyl ester mixture. Scan 2 shows the spectrum which occurred as the solvent, cyclohexane, passed through the detector. Scan 3 shows a product ion which drifted at about 18 msec, but this ion did not match any of the known spectra for the methyl ester standards. Scan 4 shows the product ion for methyl caprate and the product ion for the unknown component of scan 3. Scans 5, 6, and 8 show typical spectra for methyl laurate, methyl myristate, and methyl stearate, respectively, while scan 7 shows the reactant ions present between the elution of methyl myristate and methyl stearate.

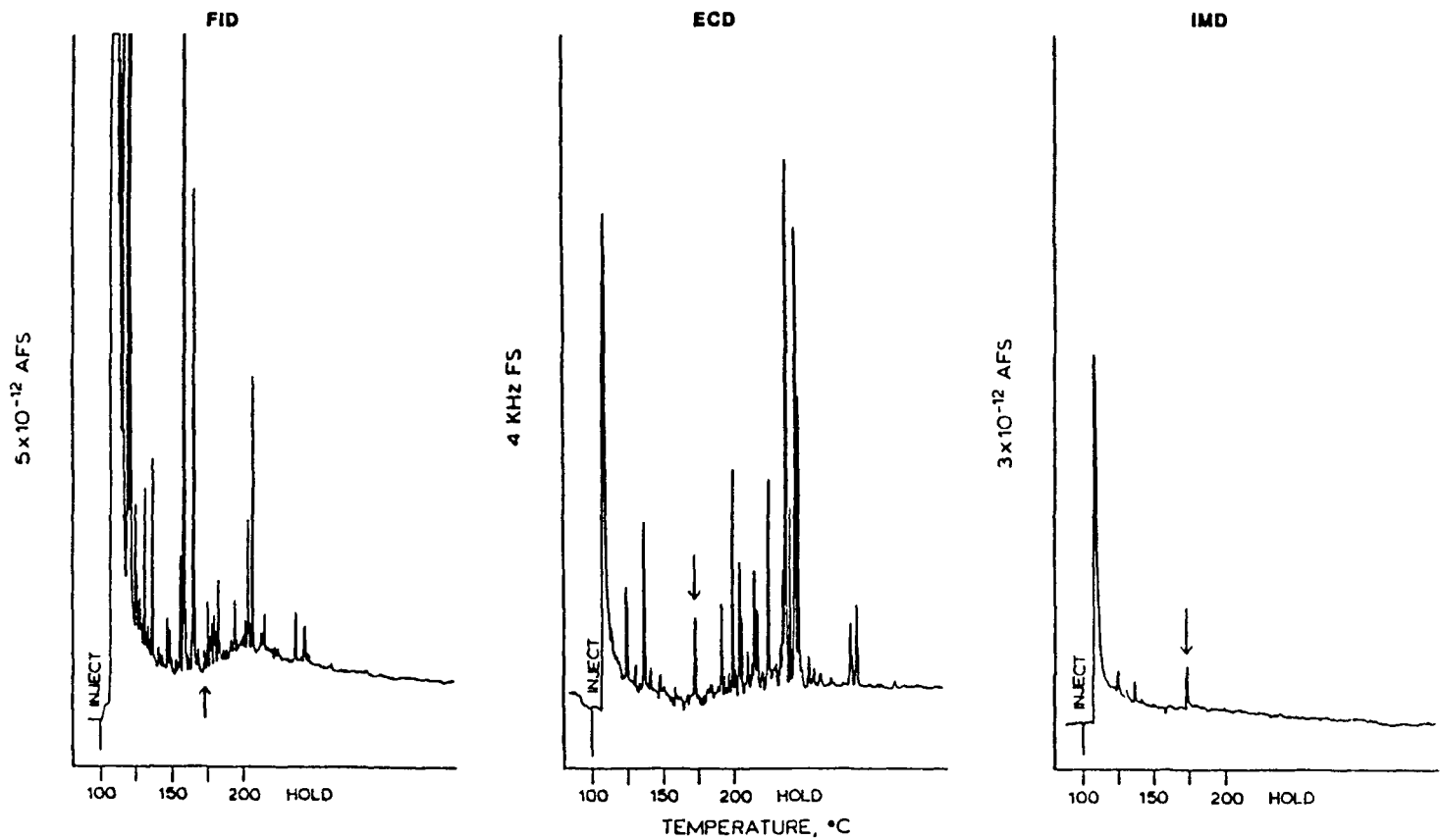


Figure 8. Electron capture, ion mobility, and flame ionization detection of 2,4-D methyl ester in a soil extract after separation by gas chromatography.

If reactant ions are monitored continuously, a supercritical fluid chromatogram can be obtained. Figure 12 shows a capillary supercritical fluid separation of polymethylsiloxane with CO_2 as the mobile phase. Drift times which correspond to those of the reactant ions were monitored continuously and a depletion of the signal as the polymethylsiloxane oligomers underwent ion-molecule reactions with the reactant ions served as the chromatographic response. In this chromatogram, oligomers with molecular weights greater than 5000 amu are detected.

Monitoring product ions can provide selective detection. Figure 13 shows the positive product ion detection of a supercritical fluid chromatographic separation of Triton-X 100. The upper tracing, representing a nonselective response, was obtained by monitoring a wide mobility window through which all of the product ions migrated. For selective detection at individual oligomers, the monitoring window is narrowed to include the migration time of the product ion from only one of the oligomers.

Although IMD is still in its infancy as a fully characterized detection system for

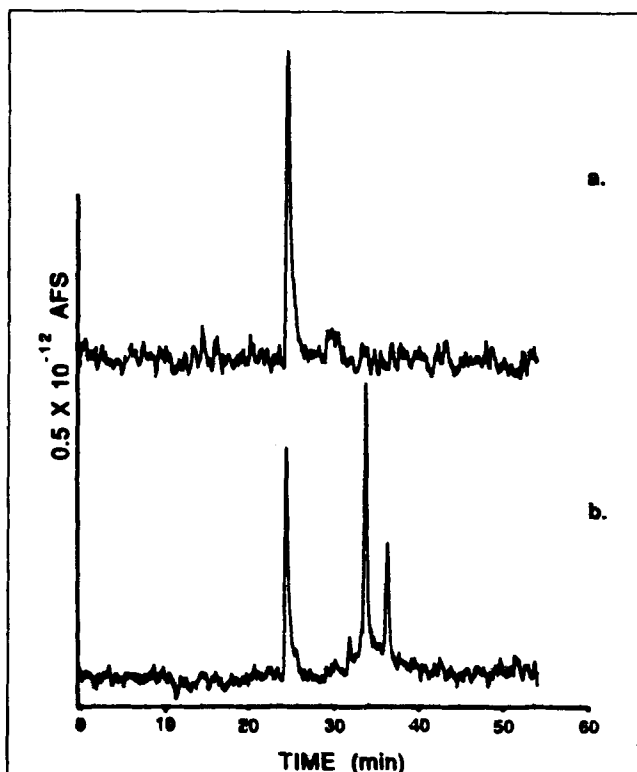


Figure 9. Selection ion mobility detection after supercritical fluid chromatographic separation of underivatized 2,4-dichlorophenoxyacetic acid extracted from soil with no column cleanup. (a) 2,4-D standard; (b) extract of soil.

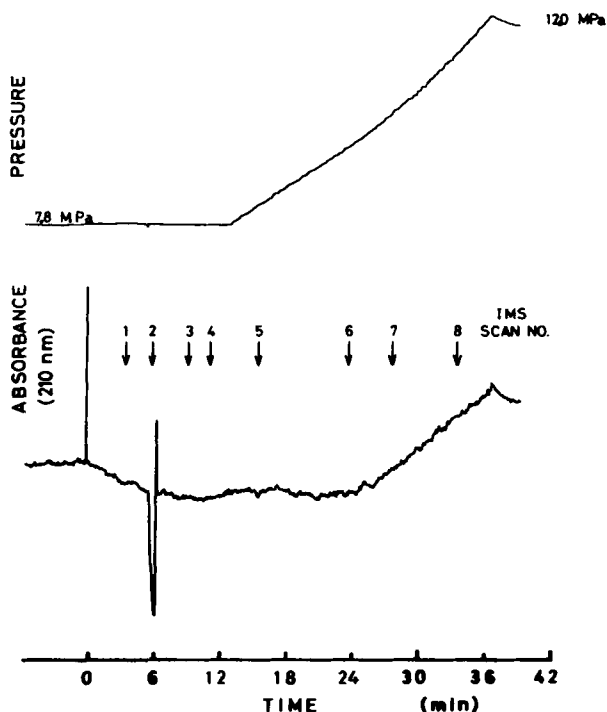


Figure 10. Supercritical fluid chromatogram of methyl esters with UV detection. Numbers mark position of IMS scans. (From S. Rokushika, H. Hatano, and H. H. Hill, Jr. *Anal. Chem.* 59:8 [1987]. With permission.)

supercritical fluid chromatography, it appears to hold promise as a versatile SFC detector. IMD has been shown to exhibit reproducible mobility data even when contaminating gases are introduced into the ionization region. It extends the range of detection beyond those compounds which can be monitored by UV/Vis detectors. It provides nonselective FID-like responses and nonselective ECD-like responses. When tuned to specific drift times, it produces molecular selective responses. Initial investigations indicate that it may be compatible with a wide variety of supercritical mobile phases. The IMD may prove to be a very useful detector for SFC.

LIQUID CHROMATOGRAPHIC DETECTION

Again, F. W. Karasek and co-workers were the first to investigate the potential of ion mobility spectrometry as a detection method for liquid chromatography.¹⁴ They used the moving belt approach as an indirect IMS to LC interface and were able to transfer and obtain spectra of the solute. The first attempt to introduce liquids directly into a IMS was made by M. Dole and co-workers^{15,16} using an electrified spray method of sample introduction. The moving belt system was limited in that it only worked well for volatile compounds while the electrified spray method introduced nonvolatiles into the drift region of the spectrometer.

Recently, a form of electrified spray called corona-spray was combined with the unidirectional flow ion mobility spectrometer to provide ion mobility spectra of compounds introduced directly into the spectrometer as liquid samples.¹⁷ Figure 14 shows a schematic of a corona-spray spectrometer where A is the fused silica liquid transfer line, B is a glass insulating sleeve, C is a gas exit port, D is a Teflon source block, E is the electrical connection, F is a stainless-steel voltage ring, G is a Teflon insulator ring, H is the ion entrance gate, I is the aperture grid, J is the ion collector screen, and K is the drift gas entrance.

Although corona-spray ion mobility spectrometry (CIMS) is only in the initial phases of investigation, early experiments seem promising. Table 1 lists some of the compounds which have been found to provide spectra in the CIMS and suggests that the technique may be applicable to a wide variety of compounds. Figure 15 shows corona-spray ion mobility spectra of methyl and butyl paraben illustrating that the separation of the product ions in the mixture is possible. Finally, Figure

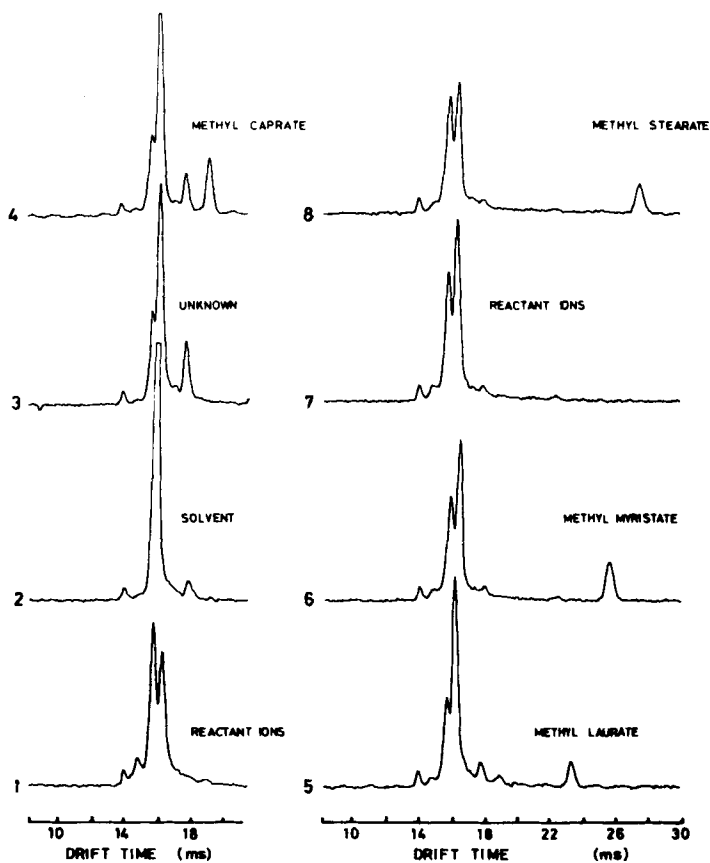


Figure 11. Ion mobility spectra corresponding to the scan numbers given in Figure 10.

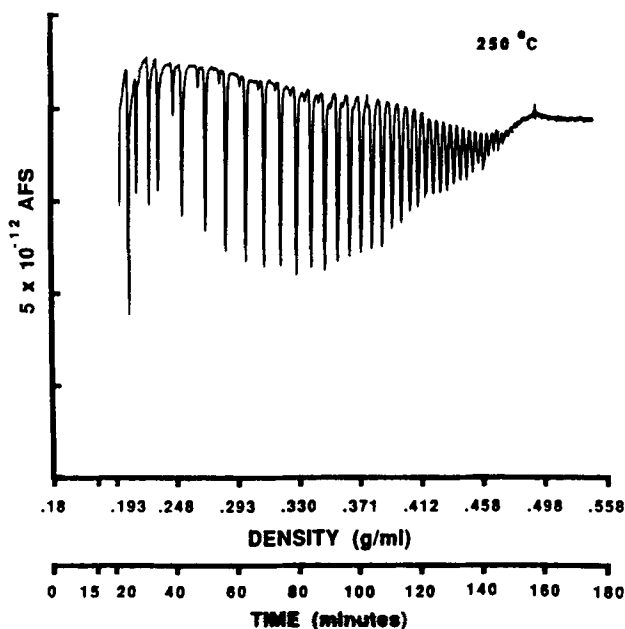


Figure 12. Supercritical fluid chromatogram of polymethylsiloxane with CO₂ as the mobile phase and ion mobility detection in the positive reactant ion depletion (PRID) mode.

16 provides a liquid chromatographic separation of methyl, propyl, and butyl parabens with corona-spray ion mobility detection in the positive reactant ion depletion monitoring mode. It should be noted here that in the CIMS no radioactive source is present. Both nebulization and ionization of the sample occurs from the corona-spray process.

Table 1. Compounds that Provided CIMS Spectra

Triisopropanolamine	Lysine
Tri-n-butylamine	Glycine
Dibenzylamine	Methionine
Diphenylamine	Asparagine
Caffeine	Alanine
Indole	Phenylethylamine
Chloropropionic acid	Acetylsalicylic acid
Aroclor 1242 (PCB)	Ascorbic acid
Trichlorobenzene	Sulfanilic acid
Trichloroacetic acid	Trichloropropionic acid
Trichlorophenoxyacetic acid	
Trinitrotoluene	
Erythromycin estolate	Lutidine
Methylparaben	Butylparaben
Phenylbutazone	Tris (THAM)
o-Cresol	Tricresol phosphate

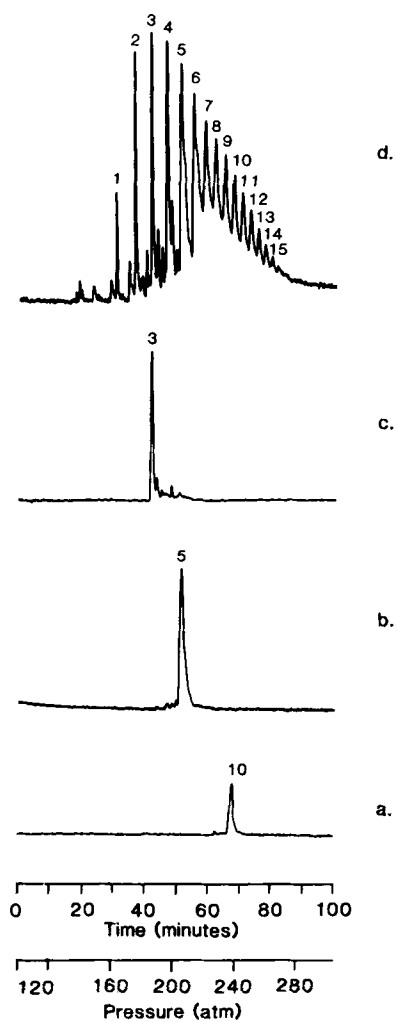


Figure 13. Supercritical fluid separation of Triton-X 100 with positive product ion mobility detection. Tracings a, b, and c represent selective positive product ion monitoring while tracing d is nonselective monitoring.

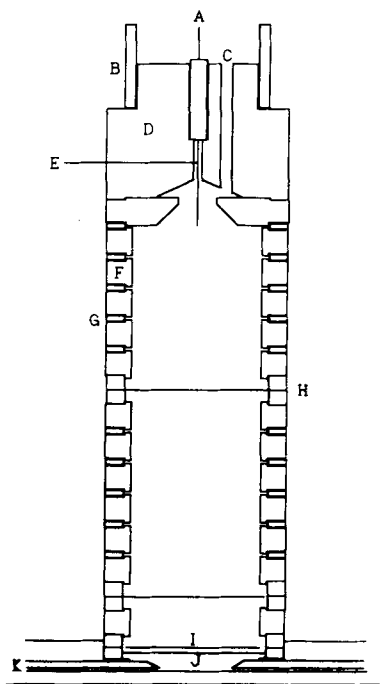


Figure 14. Schematic of corona-spray ion mobility detector.

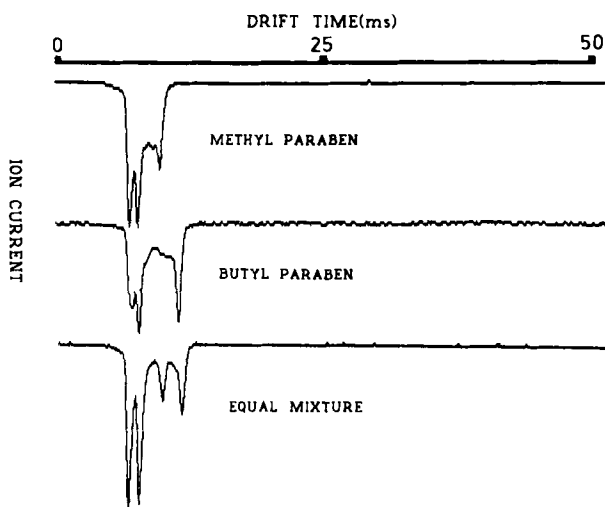


Figure 15. Corona-spray ion mobility spectra of methyl and butyl paraben: total scan time, 0.2 sec; methanol/water flow rate, 10 $\mu\text{L}/\text{min}$; drift field, 250 V/cm; needle voltage, 6500 V; nitrogen drift gas, 700 mL/min; pressure, 695 torr; temperature, 184°C.

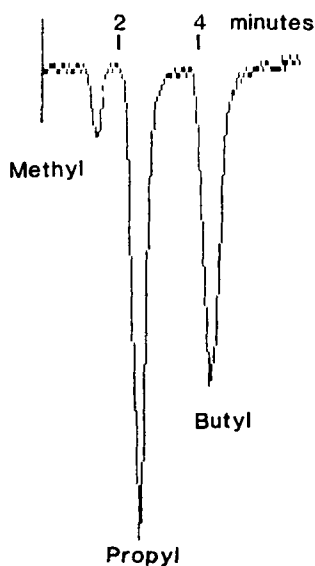


Figure 16. Corona-spray ion mobility detection of methyl, propyl, and butyl paraben after separation by liquid chromatography.

REFERENCES

1. Cohen, M. J. and Karasek, F. W. *J. Chromatogr. Sci.* 8:330 (1970).
2. Karasek, F. W. and Keller, R. A. *J. Chromatogr. Sci.* 10:626 (1972).
3. Cram, S. P. and Chesler, S. N. *J. Chromatogr. Sci.* 11:391 (1973).
4. Karasek, F. W., Hill, H. H., Kim, S. H., and Rokushika, S. *J. Chromatogr.* 135:329 (1977).
5. Baim, M. A. and Hill, H. H., Jr. *Anal. Chem.* 54:38 (1982).
6. St. Louis, R. H., Siems, W. F., and Hill, H. H., Jr. *J. Chromatogr.* 479:221 (1989).
7. St. Louis, R. H., Siems, W. F., and Hill, H. H., Jr. *LC-GC* 6(9):810 (1988).
8. St. Louis, R. H. and Hill, H. H., Jr. Manuscript in preparation.
9. Baim, M. A. and Hill, H. H., Jr. *J. Chromatogr.* 279:631 (1983).
10. Morrissey, M. A. and Hill, H. H., Jr. *J. Chromatogr. Sci.* 27:529 (1989).
11. Rokushika, S., Hatano, H., and Hill, H. H., Jr. *International Symposium on High Performance Liquid Chromatography*, Kyoto, Japan (January 28—30, 1985).
12. Eatherton, R. L., Morrissey, M. A., Siems, W. F., and Hill, H. H., Jr. *J. High Res. Chromatogr. Chromatogr. Commun.* 9:154 (1986).
13. Rokushika, S., Hatano, H., and Hill, H. H., Jr. *Anal. Chem.* 59:8 (1987).
14. Karasek, F. W. and Denny, D. W. *Anal. Lett.* 6:993 (1973).
15. Dole, M., Gupta, C. V., Mack, L. L., and Nakamae, K. *Polym. Prepr.* 18(2):188 (1977).
16. Gieniec, J., Mack, L. L., Nadamae, K., Gupta, C., Kumar, V., and Dole, M. *Biomed. Mass Spectrom.* 11(6):259 (1984).
17. Shumate, C. B. and Hill, H. H., Jr. *Anal. Chem.* 61:601 (1989).

CHAPTER 5

Analysis of the Headspace Vapors of Marijuana and Marijuana Cigarette Smoke Using Ion Mobility Spectrometry/Mass Spectrometry (IMS/MS)

S. H. Kim and G. E. Spangler

INTRODUCTION

This chapter discusses the use of ion mobility spectrometry (IMS) for the detection and analysis of vapor constituents released from marijuana before and during smoking. IMS is a technique based on ionizing the sample under atmospheric pressure conditions and recording the positive and negative ion mobility spectra of the product ions. The ionization is initiated by reactant ions which are generated in the carrier gas by β -particles (66-keV electrons) emitted from a ^{63}Ni radioactive source. When purified air (<10 ppm H_2O) is used for the carrier gas, the reactant ions are primarily $(\text{H}_2\text{O})_n\text{H}^+$ and $(\text{H}_2\text{O})_n\text{O}_2^-$ [or $(\text{H}_2\text{O})_n\text{CO}_4^-$ if a trace of CO_2 is present] clustered with nitrogen.¹⁻³ For additional information on the IMS technique (also known as plasma chromatography) the reader is referred to several excellent reviews.⁴⁻⁹

While the use of illicit drugs other than marijuana may be of greater concern, the abuse of marijuana as a psychoactive drug is still a significant problem to forensic laboratories and law enforcement officials. For these agencies, the following operational capabilities are desired:¹⁰⁻¹⁴ (1) intercepting concealed contraband in international traffic, (2) determining whether an unknown sample of plant material contains marijuana, (3) determining whether cannabis samples confiscated at different locations originate from a common lot, (4) tracing of illicit marijuana samples to their geographic origin, (5) monitoring enclosed areas (e.g., schools) for covert use of the drug, (6) safety screening a workforce for nonuse of marijuana, and (7) intrusive/nonintrusive testing of human subjects. While the presence of marijuana can usually be determined using some combination of visual examination, color tests and chromatography [thin layer (TLC), gas/liquid (GLC), high performance liquid (HPLC), and/or gas chromatography/mass spectrometry (GC/MS)],^{15,16} the preparative steps as well as the analytical procedures are often time consuming. The IMS technique offers a real-time approach to ultrasensitive detection of marijuana either as an ambient air monitor^{17,18} or as a detector providing an enhanced analytical capability to gas, supercritical, or liquid chromatography.¹⁹⁻²¹

Several investigations have been made into the chemical composition of marijuana. *Cannabis sativa L.* has been found to contain over 420 different constituents.^{22,23} Not all of these compounds are found in headspace vapors. Typical headspace chromatograms show three separate fractions based on ascending order of boiling points:²⁴ (I) a volatile fraction (bp = 20 to 80°C, mol wt <100), (II) an intermediate volatile fraction (bp = 150 to 198°C, mol wt >100), and (III) a lesser volatile fraction (bp >198°C, mol wt >200). The volatile fraction (I) consists of oxygenated compounds such as acetone (approximately 75%), methanol, acetaldehyde, ethanol, ethylacetate, and isobutylaldehyde. The intermediate volatile fraction (II) contains the monoterpene hydrocarbons such as α - and β -pinene, β -myrcene, limonene, ocimene, and β -phellandrene, etc. The less volatile fraction (III) contains the sesquiterpene hydrocarbons, such as β -caryophyllene and β -farnesene, which are believed to be responsible for the characteristic odor of marijuana and its smoke.^{24,25} The psychoactive [Δ^9 -tetrahydrocannabinol (Δ^9 -THC)] and related [cannabinol (CBN), cannabidiol (CBD), and cannabichrome (CBC)] compounds indigenous to marijuana belong to a nonvolatile fraction (bp >200°C, mol wt >300) which has not yet been detected in headspace vapors. Although concentrations will depend on the country of origin, Table 1 shows a typical profile for the headspace vapors and essential oil of marijuana.¹¹ Also Table 2 shows the composition of the nonpolar neutral fraction of marijuana smoke condensate as determined by gas chromatography.²⁵ The cannabinoids have been detected in smoke condensates.

For identification, the compounds of fractions I and II are not specific enough to allow discrimination of marijuana from other herbaceous materials.²⁶ For example, α -pinene is the major component of the oil of turpentine and limonene is the major component of orange peel. Unfortunately, 10 and 70 to 80% of the headspace vapors of marijuana at 65°C are due to fractions I and II, respectively. Since the essential oil of marijuana contains 37.5% caryophyllene compared to less

Table 1. Comparison of the Composition of Headspace Vapors of Marijuana with the Composition of Essential Oil of Marijuana^a

Component	Composition (%)	
	Head-space	Essential Oil
α -Pinene	55.5	3.9
Camphene	0.9	0.7
β -Pinene	16.4	2.2
2-Methyl-2-heptene-6-one	0.4	0.6
Δ^3 -Carene	0.6	0.1
Myrcene	8.3	1.0
α -Terpinene	<0.1	<0.1
Limonene/ β -Phellandrene	5.4	1.0
<i>cis</i> -Ocimene	1.2	0.2
<i>trans</i> -Ocimene	3.2	0.7
γ -Terpinene	<0.1	<0.1
Terpinolene	0.8	0.6
<i>p</i> -Cymene	—	0.1
Linalool	<0.1	0.5
Fenchyl Alcohol	—	0.1
Borneol	—	<0.1
<i>trans</i> - α -Bergamotene	0.7	8.0
β -Caryophyllene	3.4	37.5
β -Farnesene	0.8	9.8
α -Terpinenol	—	1.0
β -Humulene	0.7	13.9
α -Selinene	—	2.2
β -Bisabolene	—	3.2
Curcumene	—	1.4
Caryophyllene oxide	—	7.4
Total identified components	98.3	96.0

^a Hood, L. V. S., M. E. Dames, and G. T. Barry. "Headspace Volatiles of Marijuana," *Nature*. 242(5397):402-403 (1973). With permission.

than 1% for citrus oils,^{27,28} this compound has been considered as a secondary signature for marijuana. Caryophyllene is more concentrated in headspace vapors of marijuana than the involatile psychoactive components.

The saturated vapor pressures for some of the more important components of marijuana can be found in the *CRC Handbook of Chemistry and Physics*.²⁹ For fractions I and II, these vapor pressures correspond to concentrations of 6.2×10^{-7} g/mL (239 ppm) for acetone and 6.0×10^{-8} g/mL (9.9 ppm) for α -pinene.²⁹ The vapor concentration for caryophyllene can be estimated from the vapor pressure for cadinene which corresponds to 3.6×10^{-9} g/mL (0.4 ppm). Although these vapor concentrations are high compared to those which might be found in equilibrium with marijuana, they are well above the limit of detection for IMS, which is 1.0 pg or 10 ppt.^{5,30}

During the course of smoking a marijuana cigarette, 42 to 50% of the cannabinoids is pyrolyzed. Combustion may also occur since the temperature of the cigarette tip is in the range of 270 to 280°C. If one inhales during smoking, 8% of the cannabinoids are released into room air. This number increases to 31% when inhalation

Table 2. Compounds Found in the Nonpolar Neutral Fraction of Marijuana Smoke Condensate

Compound	Formula	Mol. Weight (amu)	Rel. Abund. (%)	Presence in Smoke of	
				Marijuana	Tobacco
Decane	C ₁₀ H ₂₂	142	18.0	No	Yes
A dihydrolimonene	C ₁₀ H ₁₈	138	27.0	No	Yes
Limonene	C ₁₀ H ₁₆	136	50.0	Yes	Yes
Undecane	C ₁₁ H ₂₄	156	47.0	Yes	Yes
Nicotine	C ₁₀ H ₁₄ N ₂	162	60.0	No	Yes
Solanone	C ₁₃ H ₂₂ O	194	24.0	No	Yes
β-Caryophyllene	C ₁₅ H ₂₄	204	65.5	Yes	No
α-Bergamotene	C ₁₅ H ₂₄	204	28.2	Yes	No
Humulene	C ₁₅ H ₂₄	204	40.5	Yes	No
A sesquiterpene	C ₁₅ H ₂₄	204	16.2	Yes	No
β-Farnesene	C ₁₅ H ₂₄	204	18.0	No	Yes
A sesquiterpene	C ₁₅ H ₂₄	204	15.0	Yes	No
A dehydrosesquiterpene	C ₁₅ H ₂₂	202	40.0	Yes	No
A sesquiterpene alcohol	C ₁₅ H ₂₆ O	222	14.5	Yes	No
Norphytene	C ₁₈ H ₃₈	266	30.0	Yes	Yes
A solanone-like ketone	C ₁₈ H ₃₂ O	264	25.0	Yes	Yes
Neophytadiene	C ₂₀ H ₃₈	278	75.2	Yes	Yes
A nonadecene	C ₁₉ H ₃₈	266	16.0	Yes	Yes
An eicosadiene	C ₂₀ H ₃₈	278	16.0	Yes	Yes
An eicosadiene	C ₂₀ H ₃₈	278	15.8	Yes	No
An eicosatetrane	C ₂₀ H ₃₄	274	25.0	No	Yes
Cannabicitran	C ₂₁ H ₃₀ O ₂	314	15.8	Yes	No
Cannabidiol	C ₂₁ H ₃₀ O ₂	314	55.0	Yes	No
Cannabichromene	C ₂₁ H ₃₀ O ₂	314	34.0	Yes	No
Δ ⁹ -Tetrahydrocannabinol	C ₂₁ H ₃₀ O ₂	314	100.0	Yes	No
Cannabinol	C ₂₁ H ₂₆ O ₂	310	50.0	Yes	No
Heptacosane	C ₂₇ H ₅₆	380	16.5	Yes	Yes
Nonacosane	C ₂₉ H ₆₀	408	50.0	Yes	Yes
An isomer of Hentriacontane	C ₃₁ H ₆₄	436	24.0	No	Yes
Hentriacontane	C ₃₁ H ₆₄	436	45.0	No	Yes

^a Novotny, M., F. Merli, D. Wiesler, M. Fencel, and T. Saeed. "Fractionation and Capillary Gas Chromatographic-Mass Spectrometric Characterization of the Neutral Components in Marijuana and Tobacco Smoke Condensates," *J. Chromatog.* 238:141—150 (1982).

does not accompany smoking.³¹ Karasek et al. found that Δ⁹-THC produced a very strong positive ion response with a mobility peak of 1.06 ± 0.02 cm²/V/sec when 10⁻⁷ and 10⁻⁹ g of sample was injected into the instrument.³²

ION-MOLECULE REACTIONS

When applying IMS to the detection of marijuana, it is very important to consider the use of appropriate reactions for the ionization of the sample. From this point of view, IMS is related to chemical ionization (CI) mass spectrometry which has had a long-held goal of developing functional-group selective ion-molecule reactions. Most CI studies to date, including IMS, rely on exothermic proton transfer as the method of ionization. Exothermic proton transfer reactions proceed with near collision frequency, but exhibit little functional group selectivity.

The proton transfer reaction mechanism is implemented in IMS by using hy-

dronium reactant ions which have a proton affinity of 723.8 kJ/mol.^{33,34} The open literature abounds with examples showing that the hydronium reactant ion can be used to ionize a large number of organic compounds using IMS.³⁵ The reason for this is that most organic compounds, particularly if they contain nucleophilic groups, have a proton affinity greater than water. On the other hand, this success also leads to a problem in that selective ionization of a mixture of compounds in IMS is not always possible.³⁶ This consideration has led to the development of IMS as a gas chromatographic detector.¹⁹ Furthermore after the proton has transferred, rearrangement and bond cleavage in the product ion is possible as might be anticipated from the principles of organic chemistry.³⁷⁻⁴² For these reasons, it is desirable to consider other ion molecule reactions which might be used in IMS for specific ionization.

Two alternative ion-molecule reactions which have been developed for IMS involve the use of ammonia⁴³ and acetone^{44,45} as reagent gases. When ammonia is used as an ionizing gas in chemical ionization mass spectrometry (CIMS), the ammonium ion can either (1) transfer a proton to a more basic acceptor, (2) form an adduct ion via electrophilic attachment to molecules with basicities similar to ammonia, and (3) if the acceptor possesses a good leaving group, such as an halide, hydroxy, or alkoxy group, displace the group with ammonia.^{46,47} Because of its rather high basicity (having a proton affinity of 857.1 kJ/mol),^{33,34} the ammonium ion is less likely to enter into proton transfer reactions with several important classes of compounds (e.g., alkanes, alkenes, ethers, acids, thio-compounds, alkyl halides, and alkyl aromatic compounds). Ammonia CI has been used to differentiate aldehydes from ketones since aldehydes form Schiff bases while ketones do not.⁴⁸ Ammonia CI has also been used to differentiate some meta-disubstituted aromatics from the ortho and para isomers.⁴⁶ This is useful since more acidic reagent gases often allow the differentiation of ortho-substituted aromatics from the meta or para isomers.⁴⁹ Hydrogen/deuterium exchange in ammonia CI has also been used to count active hydrogens to provide a simple method for differentiating primary, secondary, and tertiary amines.⁵⁰⁻⁵²

Similarly, the use of acetone as a reagent gas in IMS provides specificity of ionization.^{44,45} Mass spectrometric studies have shown that a protonated dimer ion of acetone is easily formed under high pressure conditions such as in the reactor of an IMS.^{53,54} Although the proton affinity of acetone (824.5 kJ/mol)^{33,34} is less than ammonia, the proton affinity of the protonated dimer ion of acetone (about 950 kJ/mol) is greater due to contributions from the heat of solvation. When acetone is used as the reagent gas, two reactions, i.e., proton transfer and association (perhaps involving cluster exchange), are observed.⁴⁵ The efficiency of proton transfer and/or association is dependent upon the concentration of acetone in the reactor and proton transfer may even not be observed when using high concentrations of acetone.

EXPERIMENTAL

Ion Mobility Spectrometer/Mass Spectrometer

The Ion Mobility Spectrometer/Mass Spectrometer (IMS/MS) instrument was an ETG, Inc. ion mobility spectrometer coupled to an EXTREL quadrupole mass spectrometer. A schematic of the system is shown in Figure 1. The IMS was constructed using a conventional stacked ring design with closed ceramic insulator rings separating adjacent bias rings. The drift gas was preheated to 200°C and was circulated in spiraled tubing inside the IMS cell housing before entering the drift region. Two thermocouples (one near the Faraday plate and another near the shutter grid) were used to measure the drift temperature. Center holes in the aperture grid and collector allowed ions to pass from the ion mobility spectrometer and through a 25- μm pinhole into the mass spectrometer. Mobility spectra were collected using an electronically floated electrometer coupled to a Tracor TN-1500 signal averager. The experimental conditions typically used for the investigations are shown in Table 3.

The mass spectrometer was designed to sample high pressure ionization sources and was functionally similar to that described by McKeown and Siegel.⁵⁵ Two-stage pumping was used in the vacuum system. The ion optics were contained in the first vacuum chamber, which was evacuated by a 500-L/sec turbomolecular pump to 1.5×10^{-4} torr. The ion optics (a series of electrostatic lenses) focused the ions entering the vacuum chamber onto the entrance aperture of the quadrupole mass spectrometer. The quadrupole mass filter was in the second vacuum chamber, which was evacuated by a 6-in. diffusion pump to maintain a base pressure of 4×10^{-6} torr. Between the pinhole and the electrostatic lenses was a wire mesh cylindrical basket (biased 6.9 V relative to the pinhole) which allowed extraction of the ions from the expanding gases behind the pinhole. An on-axis, saturated high-gain, continuous dynode (Channeltron) electron multiplier was used for ion counting. Ratemeter conversion of the electronically discriminated and standardized pulses from the Channeltron created a simulated analog signal which drove an oscilloscope display or a strip chart recorder. On other occasions, the transistor-transistor logic (TTL) pulses from the ratemeter were fed to the multichannel scaler input of a Tracor TN-1500 signal averager. Other experimental conditions are given in Table 3.

Four types of data were collected from the IMS/MS system: (1) ion mobility spectra collected from the Faraday plate of the IMS, (2) total ion mobility spectra (TIMS) collected from the electron multiplier of the mass spectrometer operated in the RF-only mode, (3) mass spectra (MS) of the total ion current (i.e., shutter grid open) of the IMS, and (4) mass identified mobility spectra (MIMS), where the shutter grid of the IMS was pulsed and the mass spectrometer was tuned to a specific mass. Typically the IMS/MS data were collected in the order listed, but it is the comparison of the MIMS data with TIMS data that allowed correlation of ion mass with mobility.

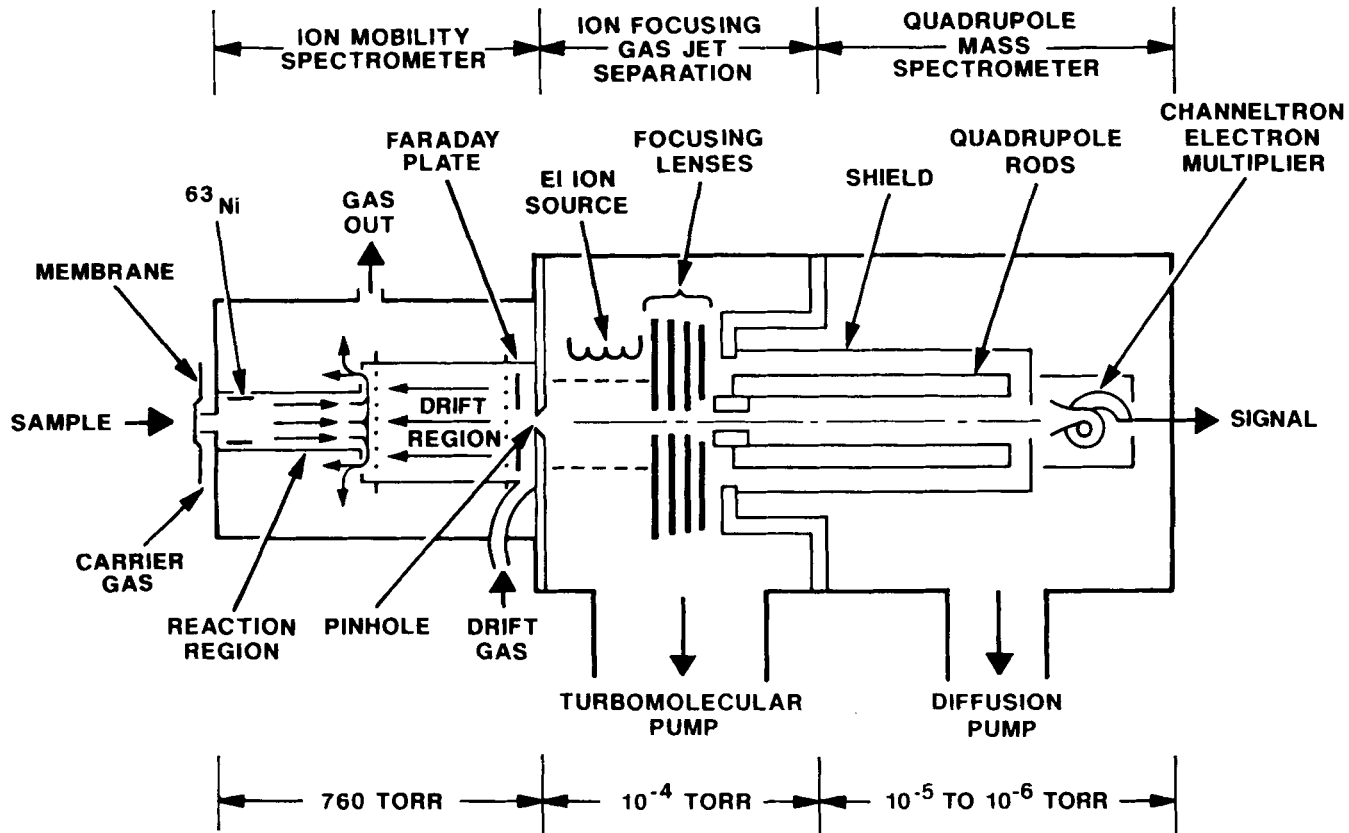


Figure 1. Schematic of the ion mobility spectrometer/mass spectrometer system.

The sample inlet for the IMS/MS was a single-stage membrane inlet.³ This inlet consisted of two aluminum blocks which sandwiched a membrane between two Viton gaskets. Channels provided on the inner surfaces of the blocks allowed sample gas to flow across the external surface of the membrane and the carrier gas for the IMS to flow across the internal surface of the membrane. The external flow was either ambient air drawn into the inlet by means of a suction pump or purified air delivered to the inlet by a purified air generator. Sample vapors contained in the ambient or purified sample gas permeated the membrane to be swept into the reactor of the IMS by the carrier gas. The membrane was MEM-100 unbacked dimethylsilicone (25 μm thick) supplied by General Electric Co., Membrane Products, Schenectady, NY. This membrane allows ambient air to be sampled by the IMS without compromising the purity requirements of the carrier and drift gases. While the membrane inlet was heated independently of the IMS cell, it was maintained at cell temperature unless otherwise noted.

The sample inlet was also designed to allow injection of sample behind the membrane using a sample probe or syringe.⁵⁶ This injection port was used for the analysis of the cannabinoids.

Gases

Purified air from an AADCO (Rockville, MD) pure air generator was used for the carrier and drift gases. This generator purified ambient air using a "heatless desorption" compression/decompression cycle on molecular sieve. Hydrocarbons were removed from the purified air using a methane reactor and a 1.8 m \times 0.95 cm o.d. column of thermally activated 13X molecular sieve, $\text{Na}_{86}[(\text{AlO}_2)_{86}(\text{SiO}_2)_{106}] \times \text{H}_2\text{O}$, was inserted between the reactor and the IMS cell.

Table 3. Experimental Conditions

Characteristic	Measurements
Ion mobility spectrometer	
Reactor length	6.9 cm
Reactor voltage	1500 V
Drift length	10.92 cm
Drift voltage	2150 V
Sample gas	200 cm^3/min
Carrier gas (purified air)	200 cm^3/min
Drift gas (purified air)	800 cm^3/min
Drift temperature	25—200°C
Reaction temperature	25—206°C
Membrane temperature	25—200°C
Pressure	Atmospheric
Mass Spectrometer	
Inlet pressure	1.5×10^{-4} torr
Chamber pressure	4×10^{-6} torr
Resolution	$\Delta m = 1$ (low mass) $\Delta m = 2-3$ (high mass)

Before the experiments, the 13X molecular sieve column was activated by 24-hr baking at 200°C under a flow of prepurified nitrogen (11 ppm water, 5 ppm carbon dioxide, 20 ppm argon). The pure air delivered to the IMS had a water content of 1.4 to 1.9 ppm as monitored by a DuPont 303 Moisture Monitor (Analytical Instruments Division, Wilmington, DE).

Reagent Gases

The reagent gases necessary to generate the ammonium and acetone reactant ions were introduced into the carrier gas of the IMS using a permeation tube.⁵⁷ The permeation tube consisted of a Teflon tube which contained the reagent (0.25-in. o.d., 1 in. long) and a Swagelok cap which sealed one end of the Teflon tube. After the permeation tube was filled with reagent, the open end of the Teflon tube was sealed with a 1-mL polypropylene membrane and inserted into a 0.25-in. Swagelok tee. The other two ends of the tee were coupled to the carrier gas line to allow the permeation of reagent vapors into the carrier gas flowing across the polypropylene membrane. The temperature of the permeation tube was room temperature.

A solution of 0.1% of ammonium hydroxide in water was used to introduce ammonia vapors into the carrier gas and reagent grade acetone was used to introduce acetone vapors into the carrier gas.

Samples

The samples were α -pinene, d-limonene, β -myrcene, t-caryophyllene, caryophyllene oxide, cannabinal (CBN), cannabidiol (CBD), and Δ^9 -THC purchased from Sigma Chemical Company, St. Louis, MO. As received, α -pinene was a clear liquid with an odor between orange peel and weak turpentine; t-caryophyllene was a clear liquid with a weak odor between cloves and turpentine; caryophyllene oxide, CBN, and CBD were powders; and the Δ^9 -THC was in solution (95%) with ethanol. Solutions (10^{-4} g/mL) of the cannabinoids in ethanol were used for analysis of these compounds.

The marijuana were caches confiscated by the U.S. Coast Guard as a result of their extradition activities. Three samples were tested; one captured from a Bayliner boat and two originating from Jamaica.

The marijuana cigarettes and smoke condensate were supplied by the Naval Research Laboratories with analyses traceable to the Research Triangle Institute, Research Triangle Park, NC. The cigarettes contained Mississippi-grown Mexican marijuana, and the smoke condensate was accompanied with the following analyses:

●Solids	9.22% (W/V)
● Δ^9 -THC	4.32 mg/mL or 0.43% (W/V)
●CBD	0.6 mg/mL or 0.06% (W/V)
●CBN	0.6 mg/mL or 0.06% (W/V)

Smoking Apparatus

The smoking apparatus is shown in Figure 2. The smoke was generated by a marijuana cigarette mounted above stopcock B and sampling began by opening stopcocks B and C and closing stopcock A to draw air through the cigarette. This caused marijuana smoke to be delivered to the mixing chamber whose content was sampled by the suction pump associated with the membrane inlet of the IMS. When smoke arrived at the membrane, data collection began. If the smoke concentration became too high, stopcock A was reopened to provide dilution. Depending on test results, the mixing chamber and sample transfer lines could both be heated to minimize adsorption.

RESULTS

Hydronium Reactant Ions

Figure 3 shows IMS/MS data for the positive reactant ions at 205°C. Spectra A and B are the total ion mobility and corresponding mass spectra obtained when purified air was used for sample gas (i.e., exterior of the membrane is purged with purified air) and spectra C and D are the total ion mobility and mass spectra obtained when laboratory air was used for the sample gas. The major reactant ion has a reduced mobility (K_0) of 2.58 cm²/V/sec and the ions with $m/e = 37, 65,$ and 93 were shown with MIMS to contribute to this ion mobility peak. These ions are consistent with the formula $(N_2)_m(H_2O)_nH^+$ where $n = 1$ and $m = 0, 1,$ and 2 . In spectrum C, the ammonium ion (reduced mobility 3.29 cm²/V/sec and $m/e = 18$) is increased in amplitude. Results similar to these were obtained for other IMS cell temperatures except that reduced mobility decreased with decreasing temperature.

Figure 4 shows IMS spectra collected against headspace vapors of α -pinene, d-limonene, and β -myrcene at 150°C. For these signatures, the vapor was introduced into the sample gas by drawing laboratory air over the neck of a reagent bottle capped with perforated tinfoil. Two peaks with reduced mobilities 2.23 to 2.25 and 1.76 to 1.79 cm²/V/sec are observed at low vapor concentration, and a third peak with reduced mobility 1.21 to 1.22 cm²/V/sec is observed at high vapor concentration. The corresponding mass spectra for the monoterpenes are shown in Figure 5. Two product ions with $m/e = 81$ and 137 (MH^+) are common to all three isomers. These ions were shown with MIMS data to contribute to the ion mobility peaks with reduced mobilities 2.23 to 2.25 and 1.76 cm²/V/sec, respectively. In addition, higher mass ions with $m/e = 246$ to $247, 260,$ and 274 to 275 are observed in the mass spectrum for α -pinene, d-limonene, and β -myrcene, respectively. In this region of the mass spectrum, the data for β -myrcene were consistent and reproducible, but not for d-limonene and α -pinene.

Figure 6 shows IMS data collected against headspace vapors of t-caryophyllene. A strong ion mobility peak with a reduced mobility of 1.45 cm²/V/sec along with a weak shoulder at 1.40 cm²/V/sec is observed. The MIMS data of Figure 7 shows

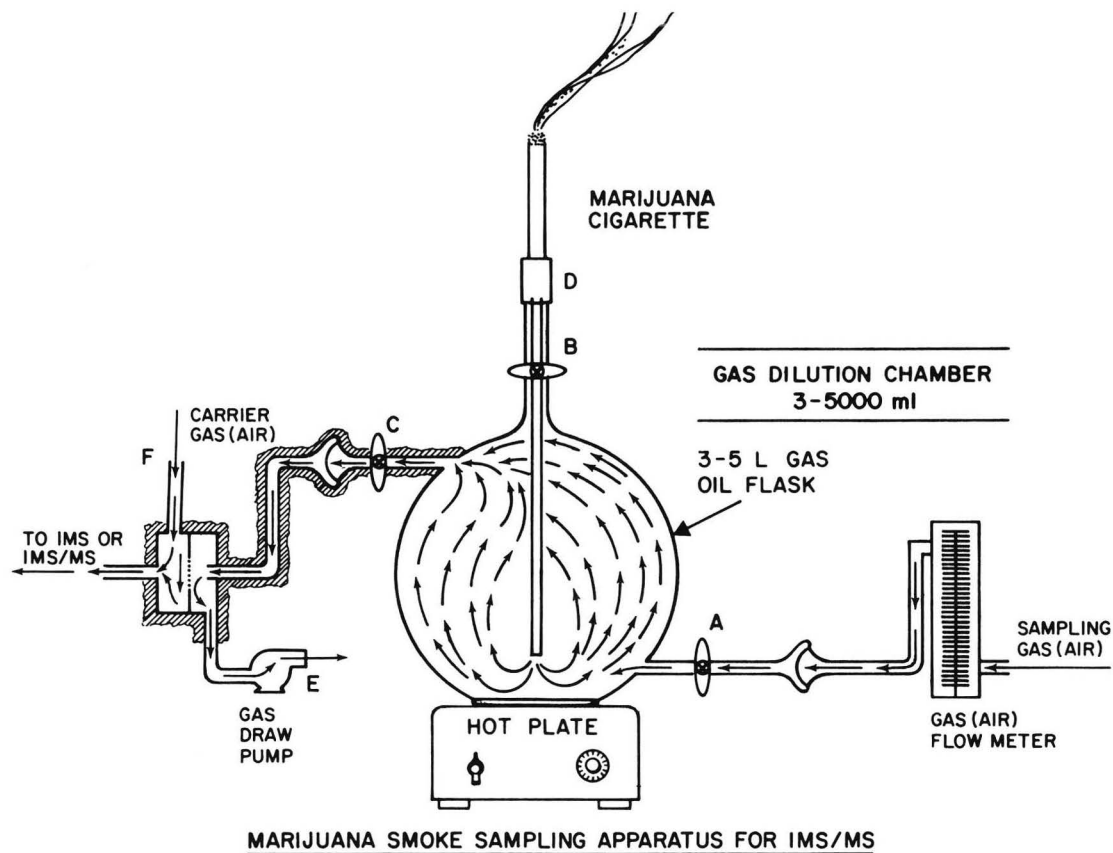


Figure 2. Smoking apparatus used to sample vapors in smoke from a marijuana cigarette.

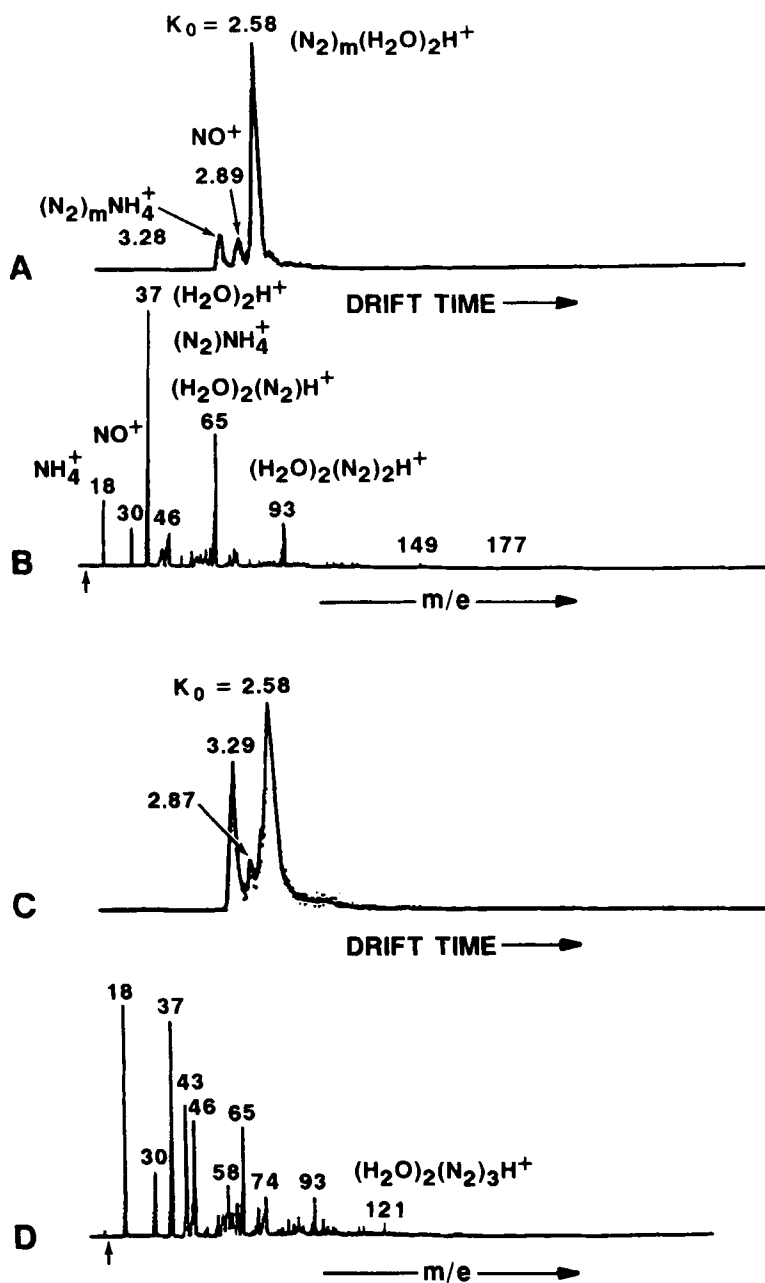


Figure 3. Hydronium reactant ions for an IMS cell temperature of 205°C. Spectra A and B are the total ion mobility spectrum and mass spectrum respectively while sampling purified air. Spectra C and D are the total ion mobility spectrum and mass spectrum, respectively, while sampling laboratory air.

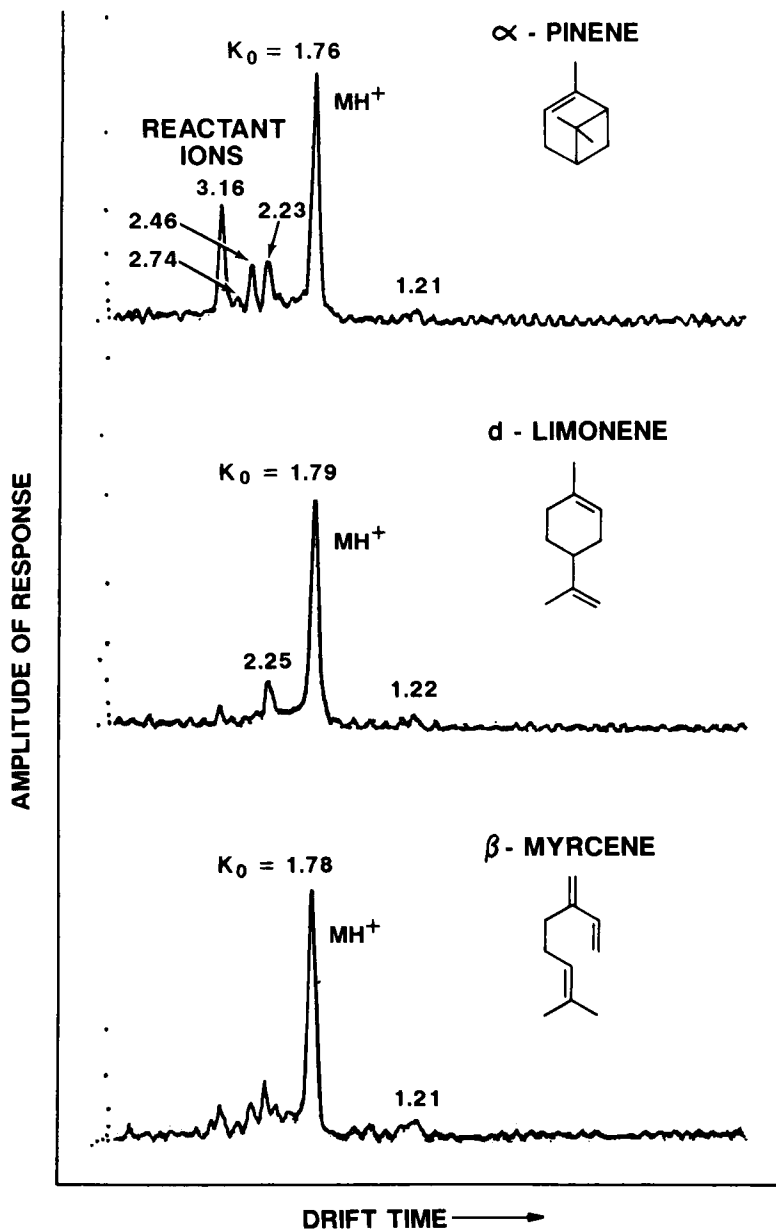


Figure 4. Ion mobility spectra of α -pinene, d-limonene, and β -myrcene using hydronium reactant ions and an IMS cell temperature of 150°C.

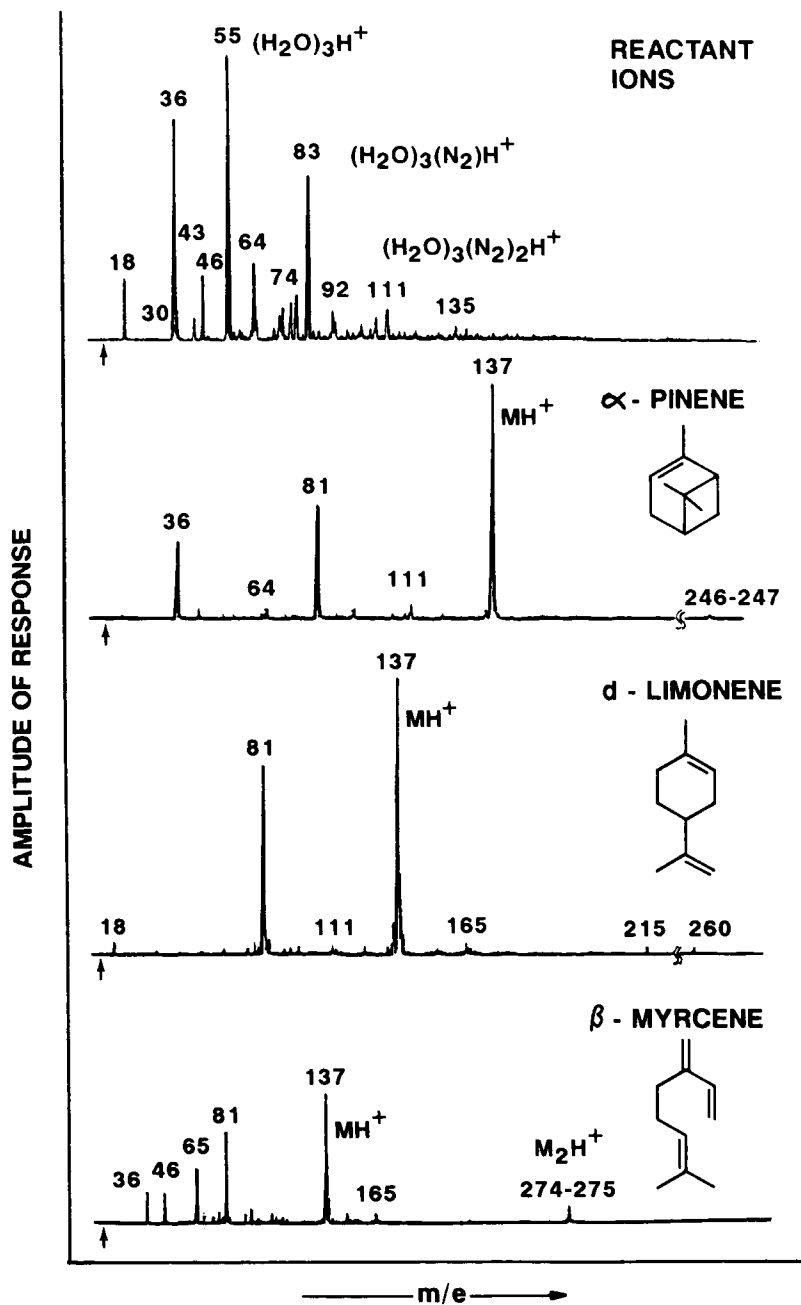


Figure 5. Mass spectra of α -pinene, d-limonene, and β -myrcene using hydronium reactant ions and an IMS cell temperature of 150°C.

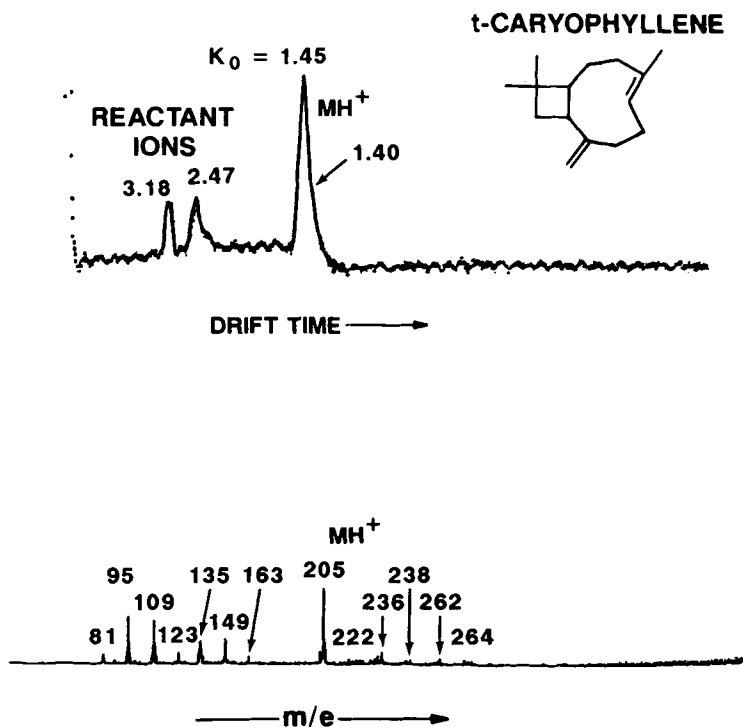


Figure 6. Ion mobility spectrum (top) and mass spectrum (bottom) of *t*-caryophyllene using hydronium reactant ions and an IMS cell temperature of 150°C.

that the MH^+ ion with $m/e = 205$ and another ion with $m/e = 238$ contribute to the $1.45\text{-cm}^2/\text{V}/\text{sec}$ peak and the ions with $m/e = 221$ to 222 contribute to the $1.40\text{-cm}^2/\text{V}/\text{sec}$ peak. Figure 8 shows IMS spectra collected against headspace vapors of caryophyllene oxide. The data are very similar to *t*-caryophyllene except for a more pronounced $1.40\text{-cm}^2/\text{V}/\text{sec}$ peak. The major ion in the mass spectrum for caryophyllene oxide has $m/e = 204$, which corresponds to a loss of oxygen from the molecule. The ion with $m/e = 221$ to 222 is either MH^+ of caryophyllene oxide or a molecular ion (M^+) of caryophyllene. Caryophyllene is easily oxidized to caryophyllene oxide in air.⁵⁸

While the negative ion spectrum was monitored, no negative ions were observed from the terpenes throughout this work.

Figure 9 shows IMS spectra collected against 5- μL injections of the cannabinoid solutions into the injection port of the membrane inlet. The injection was accomplished by heating the inlet to 206°C, depositing the sample on a stainless-steel wire and, after evaporating the solvent at room temperature, desorbing the sample into the heated injection port. A strong ion mobility peak with reduced mobility $1.08\text{ cm}^2/\text{V}/\text{sec}$ is observed from all the cannabinoids. The mass spectra of Figure 10 show that the protonated monomer ions MH^+ are observed from each of these compounds. The ions with $m/e = 315$ were shown to contribute to the $1.08\text{ cm}^2/\text{V}/\text{sec}$ with mass identified mobility data (see Figure 11 for Δ^9 -THC).

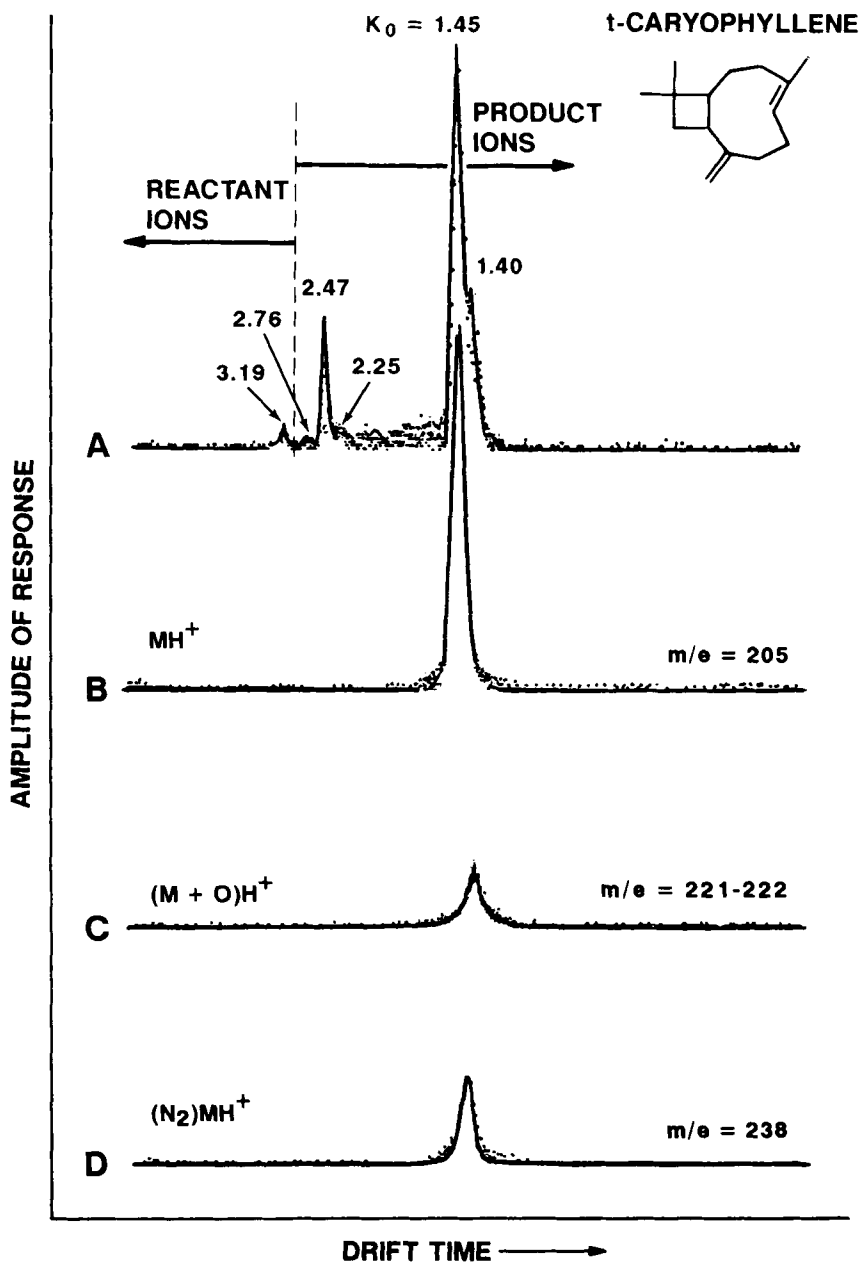


Figure 7. Mass identified mobility data (spectra B to D) of the t-caryophyllene response (spectrum A) of Figure 6.

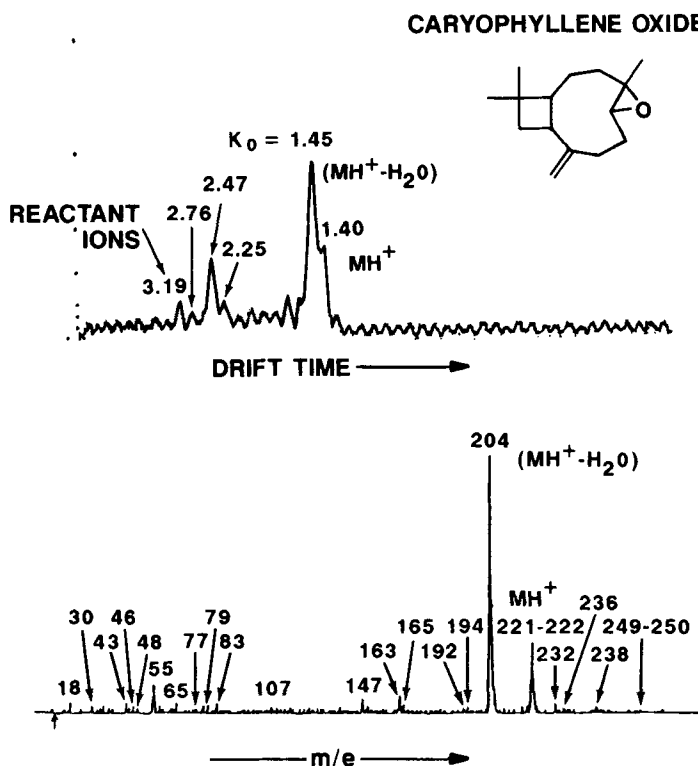


Figure 8. Ion mobility spectrum (top) and mass spectrum (bottom) of caryophyllene oxide using hydronium reactant ions and an IMS cell temperature of 150°C.

Figure 12 shows negative ion mobility spectra for the cannabinoids. Similar to the positive ion spectra, a prominent IMS peak with a reduced mobility 1.07 cm²/V/sec is observed. The mass spectra of Figure 13 show that the negative ion response is due to (M-H)⁻ product ions resulting from an hydride abstraction reaction between the (H₂O)_nO⁻, (H₂O)_nCO₃⁻, and (H₂O)CO₄⁻ reactant ions and the cannabinoid sample.

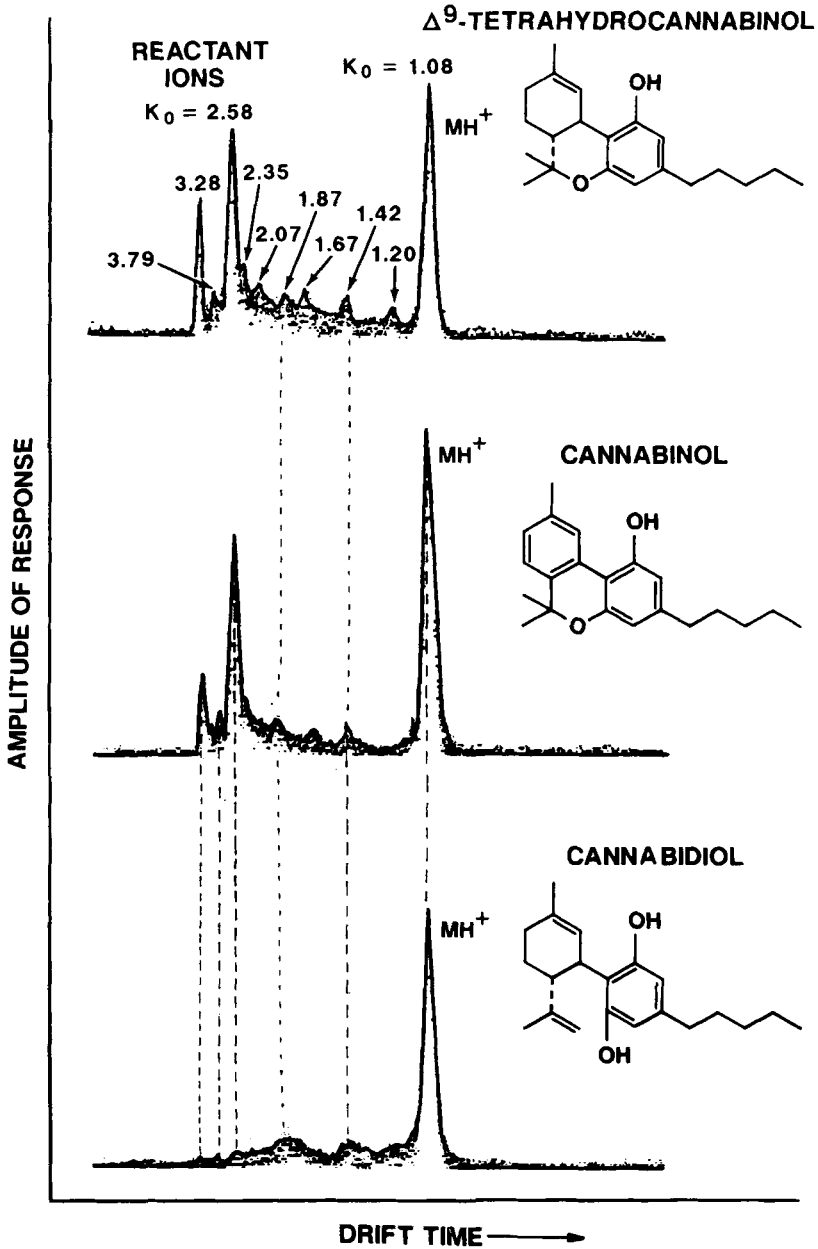


Figure 9. Total ion mobility spectra of three cannabinoids using hydronium reactant ions and an IMS cell temperature of 206°C.

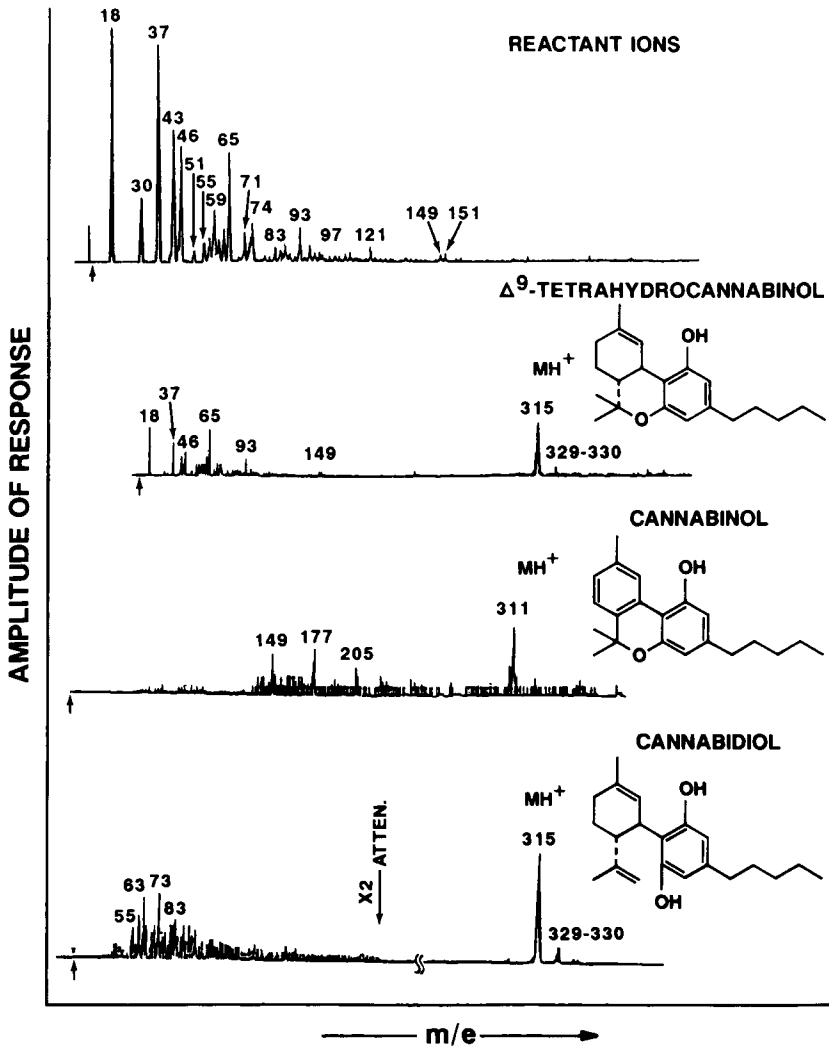


Figure 10. Mass spectra of three cannabinoids using hydronium reactant ions and an IMS cell temperature of 200°C.

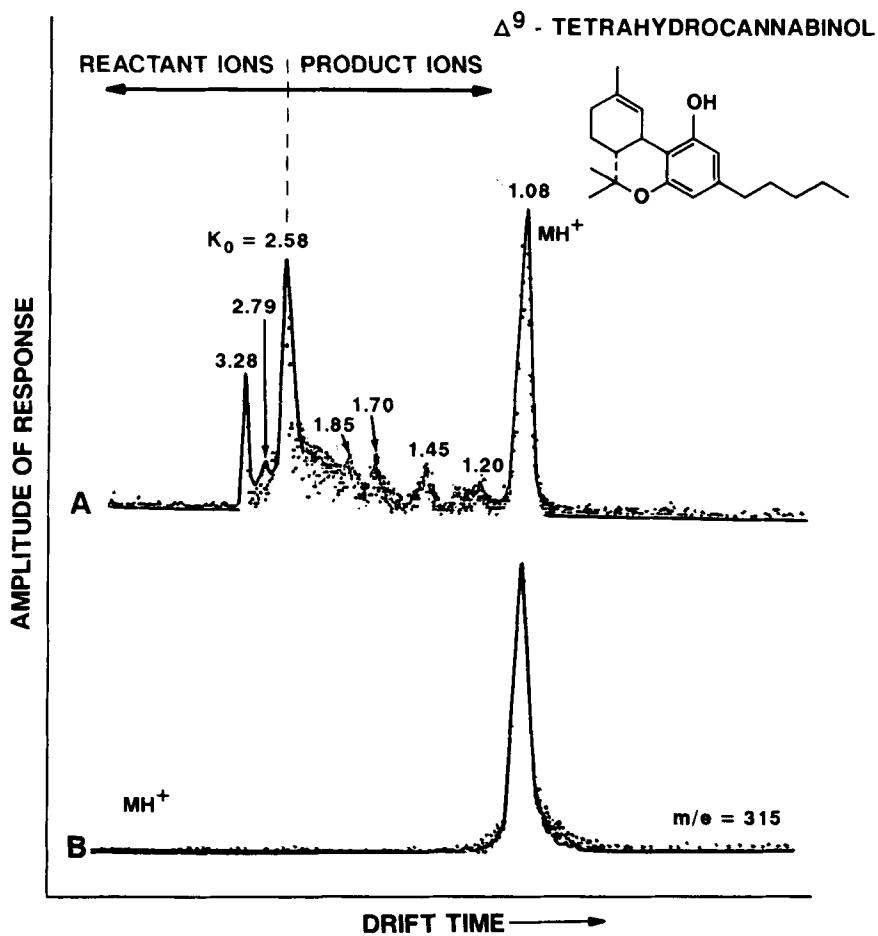


Figure 11. Mass identified mobility data (spectrum B) of the Δ^9 -tetrahydrocannabinol response (spectrum A) of Figure 9.

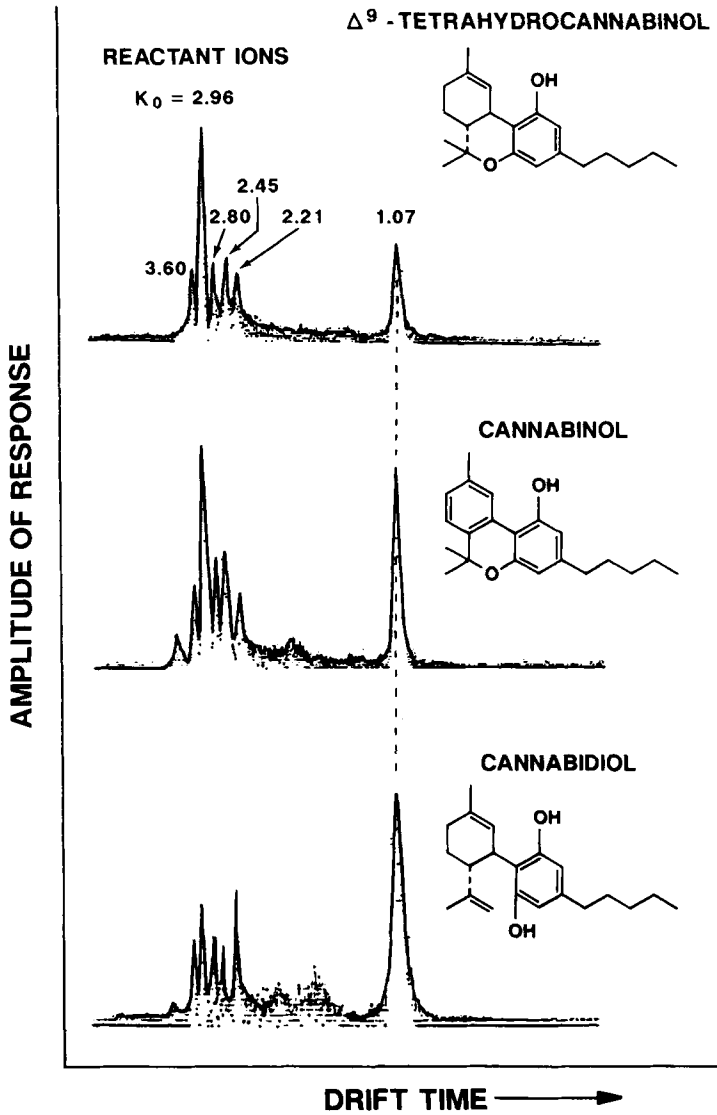


Figure 12. Total ion mobility spectra of three cannabinoids using oxygen anion reactant ions and an IMS cell temperature of 206°C.

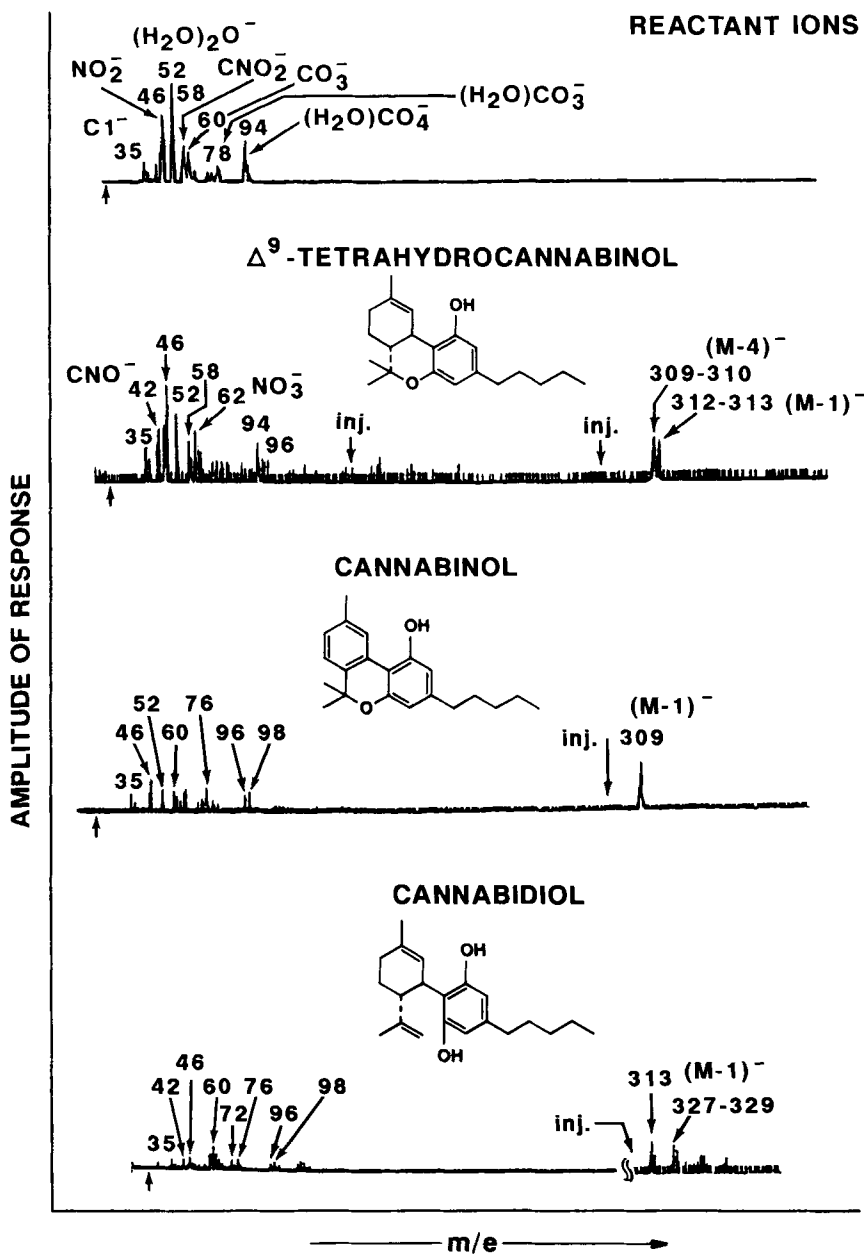


Figure 13. Mass spectra of three cannabinoids using oxygen anion reactant ions and an IMS cell temperature of 200°C.

Ammonium Reactant Ions

Figure 14 shows IMS/MS data for the ammonium reactant ion. Like the hydronium reactant ion, the ions are clusters involving water and molecular nitrogen. The extent of clustering is temperature sensitive with the centroid of the clusters residing on $(\text{H}_2\text{O})_2(\text{N}_2)_2\text{NH}_4^+$ at 27.5°C and NH_4^+ at 191°C. The temperature dependence observed for the reduced mobilities of the ammonium reactant ion is

Temperature	Reduced Mobility (Abundance)	
	$(\text{NH}_3)(\text{NH}_4^+)$	$(\text{H}_2\text{O})_n(\text{N}_2)_m\text{NH}_4^+$
27.5°C	2.32(7%)	2.20(93%)
50°C	2.43(3%)	2.29(97%)
100°C	3.10(1%)	2.57(99%)
190°C		3.22(100%)

These differ slightly from previously published values.⁶

Figure 15 shows the response of the IMS/MS to headspace vapors of sec t-caryophyllene. The product ion has a reduced mobility of 1.45 cm²/V/sec and a mass of 205 (see Figure 16) which corresponds to the protonated monomer ion of t-caryophyllene. This result indicates that the product ion formed from t-caryophyllene has a greater proton affinity than ammonia under the conditions employed in this work. The sensitivity of IMS to t-caryophyllene using ammonium reactant ions was not as great as using hydronium reactant ions, but the differences in sensitivity were insignificant compared to acetone reactant ions. The origin of the peaks with reduced mobilities between 2.16 and 1.59 cm²/V/sec is presently unknown.

Figure 17 shows IMS/MS data collected against a 5- μL injection of the Δ^9 -THC solution into the IMS. An ion mobility peak with reduced mobility of 1.08 cm²/V/sec is observed. The mass identified mobility data of Figure 18 show that the ions with $m/e = 313$ and 317 contribute to the 1.08-cm²/V/sec peak. While reduced mobility is the same as that observed from Δ^9 -THC using hydronium reactant ions, the mass of the ions differ and correspond to $(M - 1)^+$ and $(M + 3)^+$, respectively. There is also some evidence in the spectrometric data of Figure 17 that the peak amplitude ratio for the m/e 18 (NH_4^+) to 36 $[(\text{H}_2\text{O})\text{NH}_4^+]$ ions decrease compared to the unreacted reactant ion distribution (see Figures 14 and 17). This suggests that the unclustered ammonium ion participates preferentially in the reaction.

The results of Figure 19 show that the other cannabinoids produced IMS spectra similar to Δ^9 -THC analogous to hydronium reactant ion results (see Figure 9). Mass spectra collected on these responses showed that, similar to Δ^9 -THC, the responses were due to $(M + 3)^+$ ions. No difference in sensitivity to the cannabinoids was observed when using ammonium reactant ion chemistry versus hydronium reactant ion chemistry.

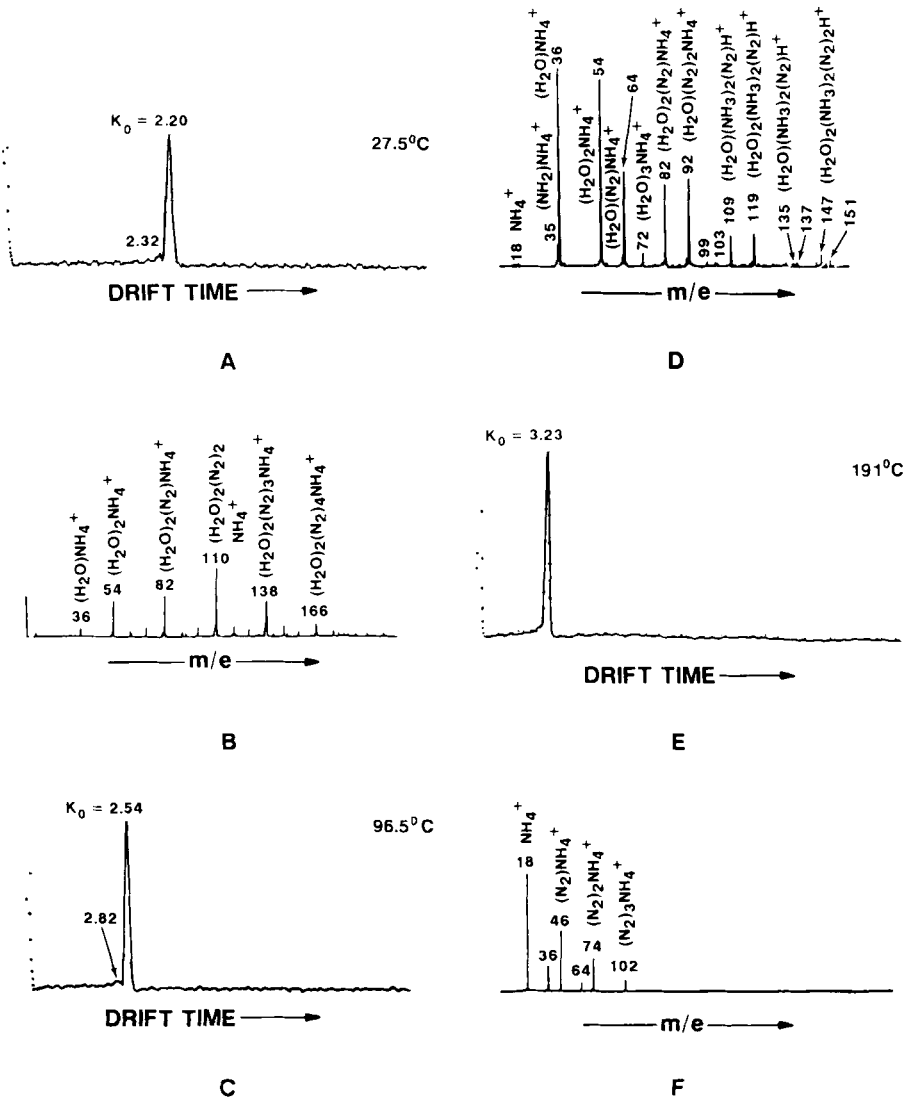


Figure 14. Ammonium reactant ions for three IMS temperatures. Spectra A, C, and E are ion mobility spectra, and spectra B, D, and F are mass spectra collected while sampling purified air.

Acetone Reactant Ions

Figure 20 shows the IMS/MS spectrum for the acetone reactant ion which is a protonated dimer ion with a reduced mobility of $2.09 \text{ cm}^2/\text{V}/\text{sec}$ and mass 117.

Figure 21 shows the IMS/MS response to headspace vapors of t-caryophyllene using acetone reactant ions. A peak with a reduced mobility of $1.45 \text{ cm}^2/\text{V}/\text{sec}$ was

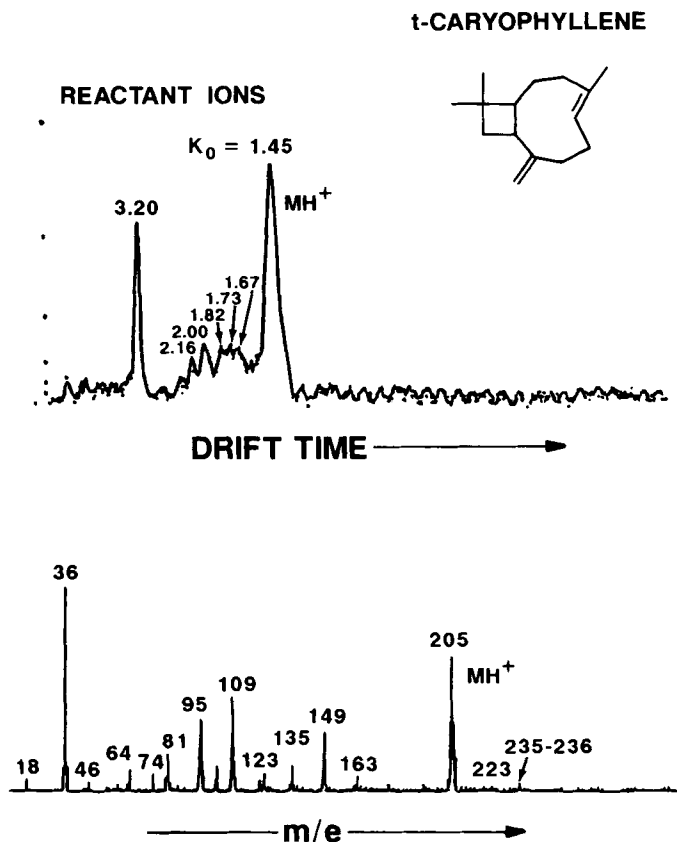


Figure 15. Ion mobility spectrum (top) and mass spectrum (bottom) of t-caryophyllene using ammonium reactant ions and an IMS cell temperature of 191°C.

observed with ions having a mass of 205 (MH^+) contributing to the peak. As evidenced by the poor response of Figure 21, IMS is less sensitive to t-caryophyllene when acetone reactant ions are used versus hydronium or ammonium reactant ions. When the IMS cell was challenged in the same manner with headspace vapors of t-caryophyllene using acetone versus hydronium reactant ions, the MH^+ response was 20 times greater for hydronium reactant ions than for acetone reactant ions.

When the concentration of the t-caryophyllene was increased, the response of Figure 22 was obtained. Two ion mobility peaks are observed with reduced mobilities 1.45 $cm^2/V/sec$ (major) and 1.78 $cm^2/V/sec$ (minor). The MIMS data of Figure 23 shows that the two ions with $m/e = 204$ (M^+) and 205 (MH^+) both contribute to the 1.45- $cm^2/V/sec$ peak. Although acetone has a lower proton affinity than ammonia [whose ammonium ion transfers its proton to t-caryophyllene (see Figure 15)], it appears that acetone preferentially forms a dimer ion with another molecule of acetone rather than transferring its proton to caryophyllene. Increasing

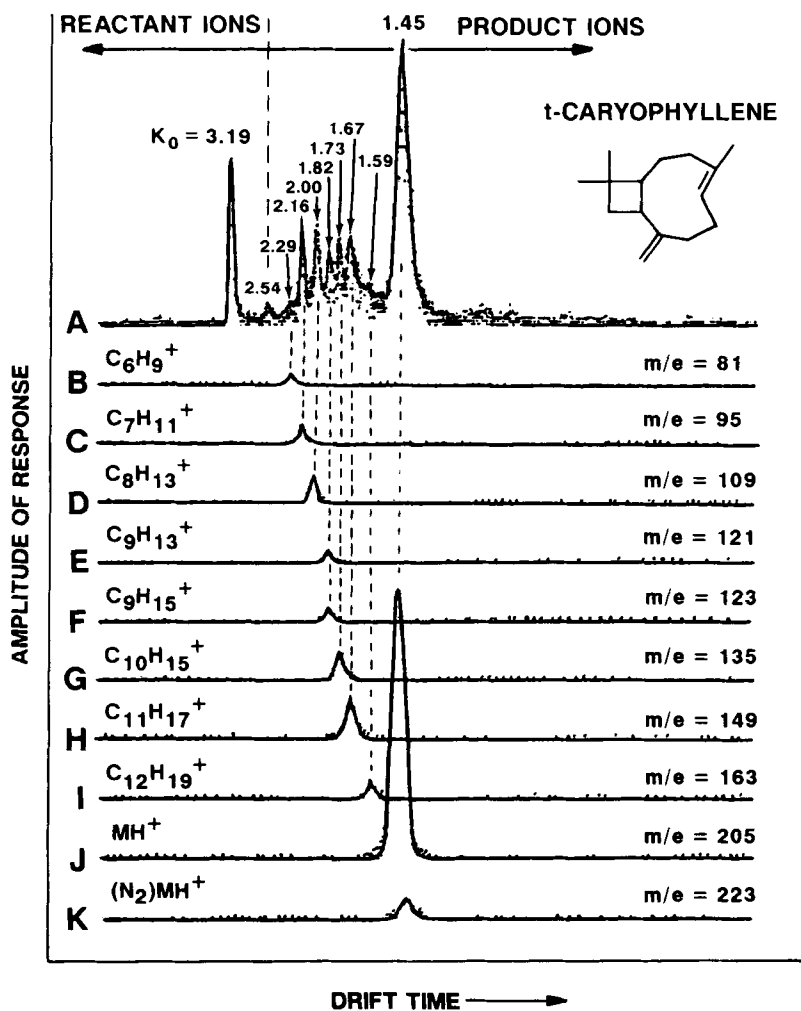


Figure 16. Mass identified mobility data (spectra B to K) of the t-caryophyllene response of Figure 15.

the concentration of t-caryophyllene increases the competitiveness of caryophyllene for the proton (Figure 22). Even though the ions have the same mobility as the protonated monomer ions of the monoterpenes, the ions contributing to the $1.78 \text{ cm}^2/\text{V}/\text{sec}$ peak could not be identified.

The IMS data collected on Δ^9 -THC using acetone reactant ion chemistry are shown in Figure 24. The data is presented along with similar data collected using hydronium and ammonium reactant ions for comparison. An ion mobility peak with a reduced mobility of $1.08 \text{ cm}^2/\text{V}/\text{sec}$ is observed for all three reactant ions. While no mass spectrometric data were collected on Δ^9 -THC using acetone reactant ions, the cannabinoids are most likely ionized through proton transfer reactions.

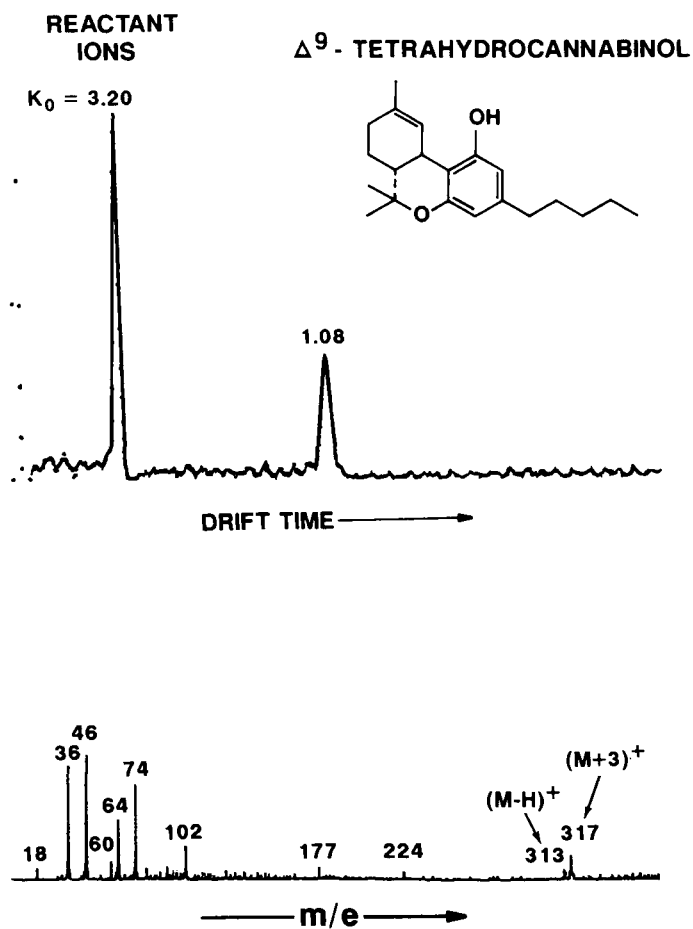


Figure 17. Ion mobility spectrum (top) and mass spectra (bottom) of Δ^9 -tetrahydrocannabinol using ammonium reactant ions and an IMS cell temperature of 189°C.

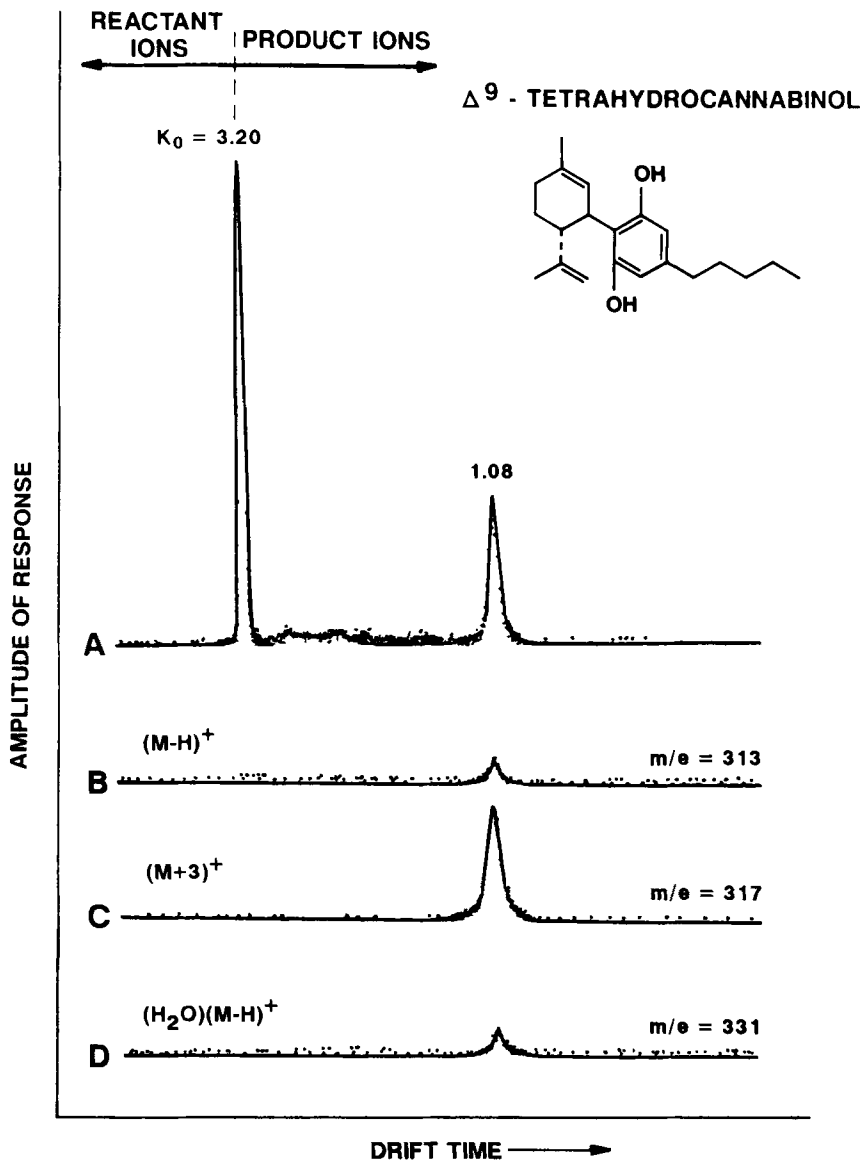


Figure 18. Mass identified mobility data (spectra B to D) of the Δ^9 -tetrahydrocannabinol response (spectrum A) of Figure 17.

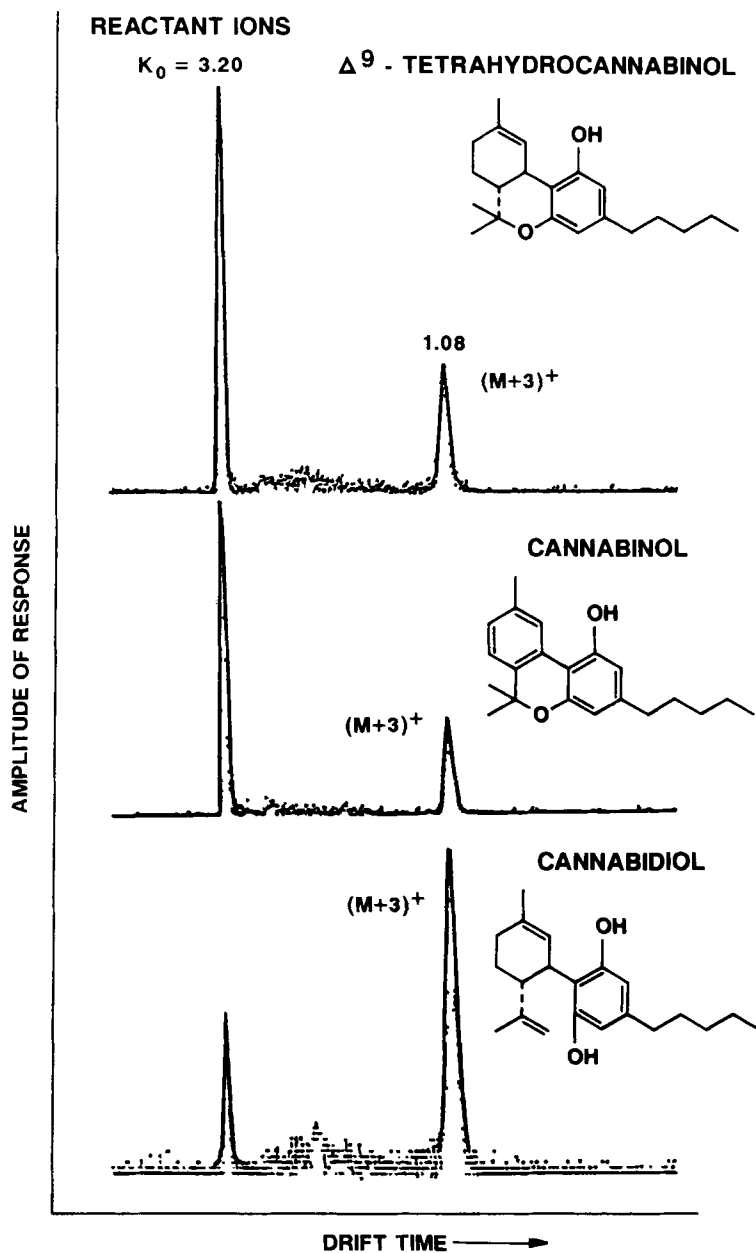


Figure 19. Ion mobility spectra of three cannabinoids using ammonium reactant ions and an IMS cell temperature of 190°C.

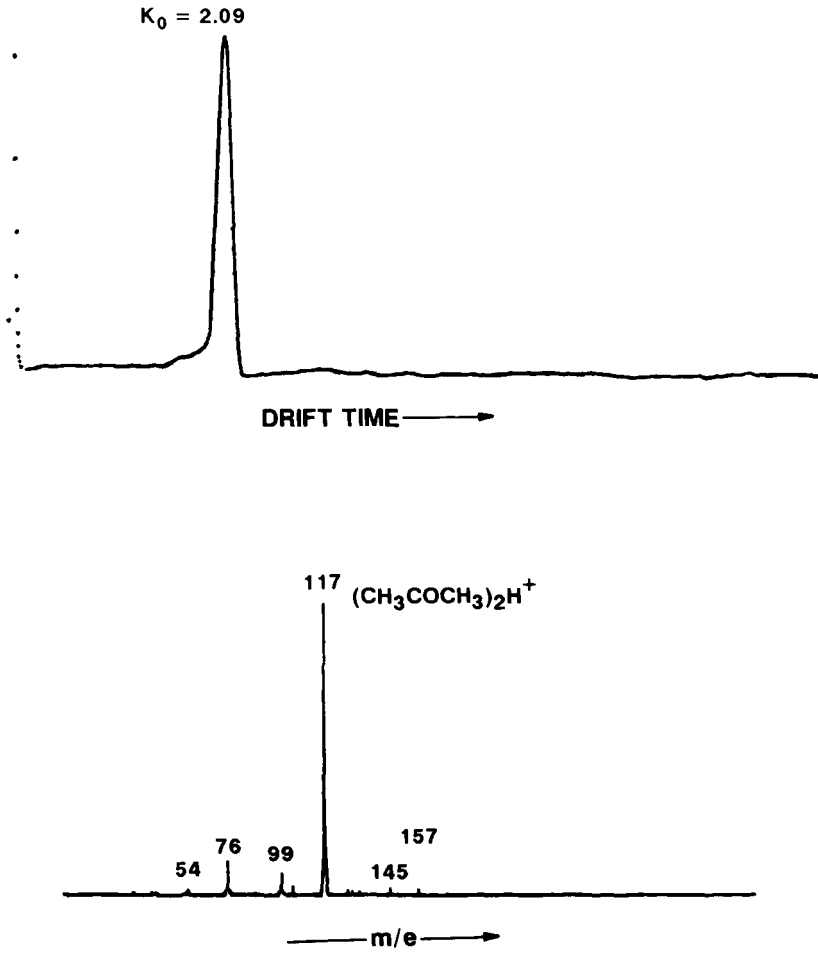


Figure 20. Acetone reactant ions for an IMS cell temperature of 189°C. The top spectrum is the ion mobility spectrum, and the bottom spectrum is the mass spectrum collected while sampling purified air.

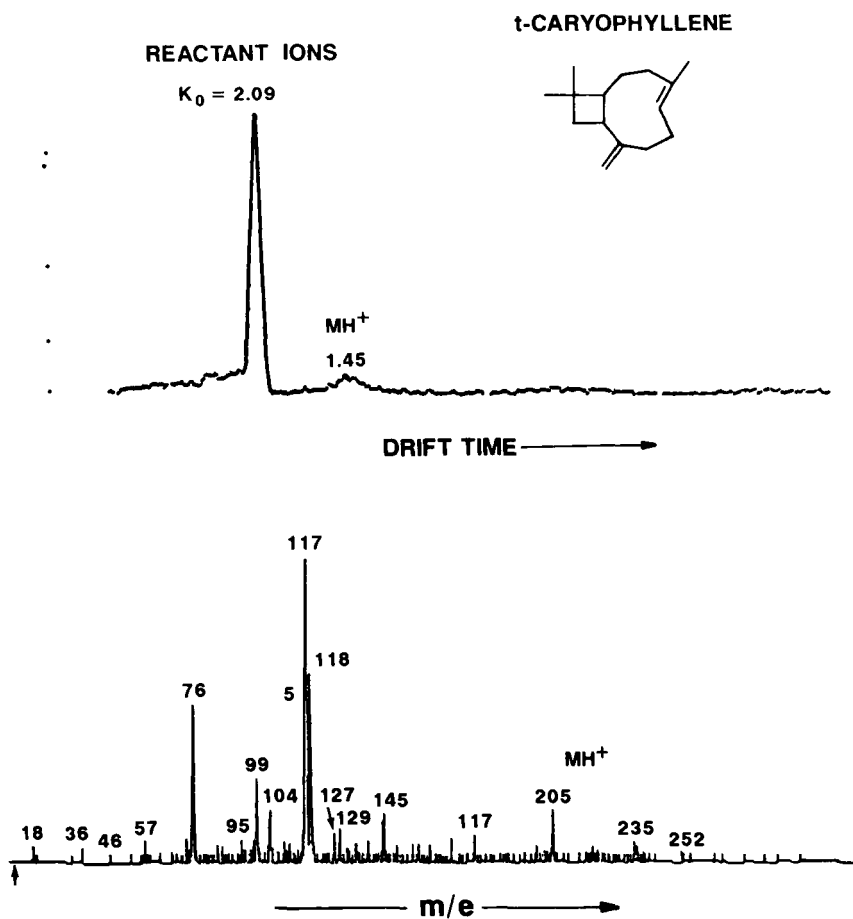


Figure 21. Ion mobility spectrum (top) and mass spectrum (bottom) of t-caryophyllene (moderate concentration) using acetone reactant ions and an IMS cell temperature of 190°C.

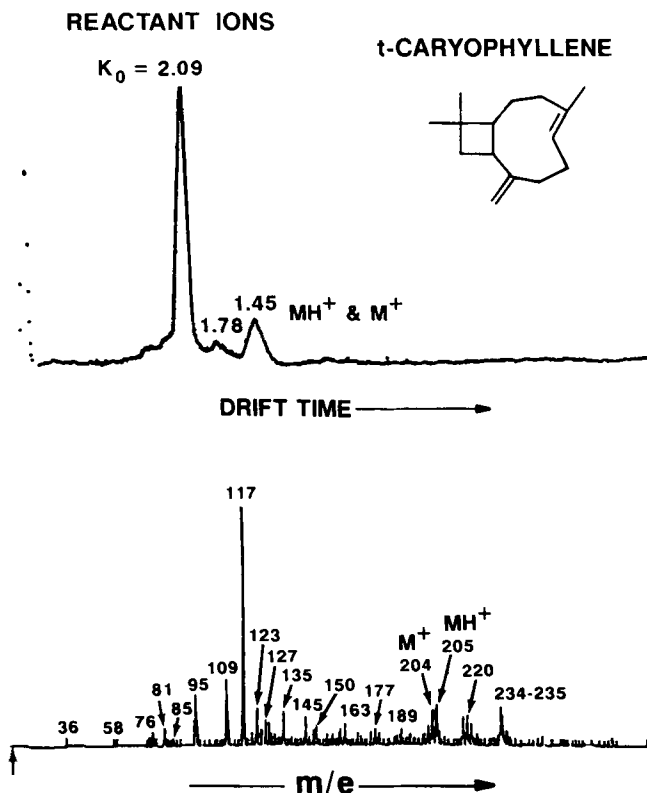


Figure 22. Ion mobility spectrum (top) and mass spectrum (bottom) of t-caryophyllene (very high concentration) using acetone reactant ions and an IMS cell temperature of 190°C.

Temperature Studies

Except possibly for acetone chemistry whose dimer ion has only a weak tendency to cluster with water, the reactant ions investigated during this study cluster easily with water. Since the heat of solvation adds to the proton affinity for the ion and since the extent of clustering is temperature sensitive, the proton affinity of the reactant ion will change with temperature. Because larger clusters are formed at lower temperatures than at higher temperatures, the proton affinity of the reactant ion will increase as the temperature decreases.

Also the ability of a reactant ion to undergo proton transfer reactions with a sample molecule increases as the difference in their proton affinities increase. This affect is shown in Figure 25 for t-caryophyllene. As the drift temperature of the IMS cell is increased, the proton affinities of the hydronium and ammonium reactant ions decrease to allow more efficient ionization of t-caryophyllene. Tests showed that the drift temperatures 50 and 100°C are needed to obtain a significant IMS

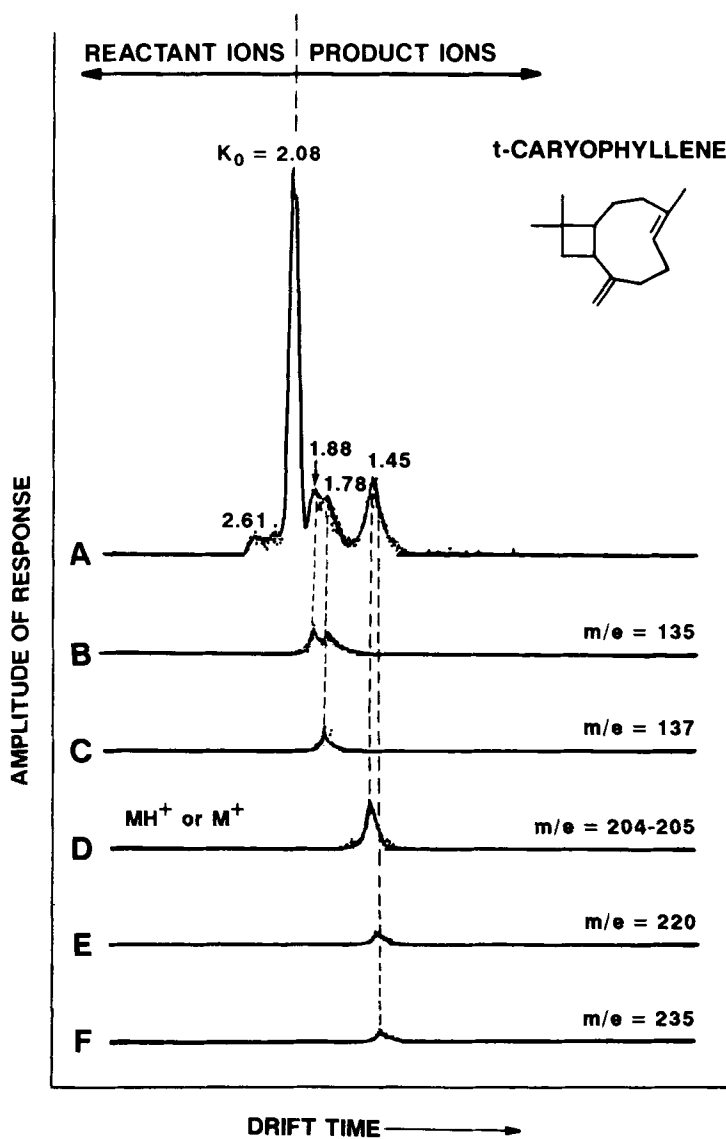


Figure 23. Mass identified mobility data (spectra B to F) of the t-caryophyllene response (spectrum A) of Figure 22.

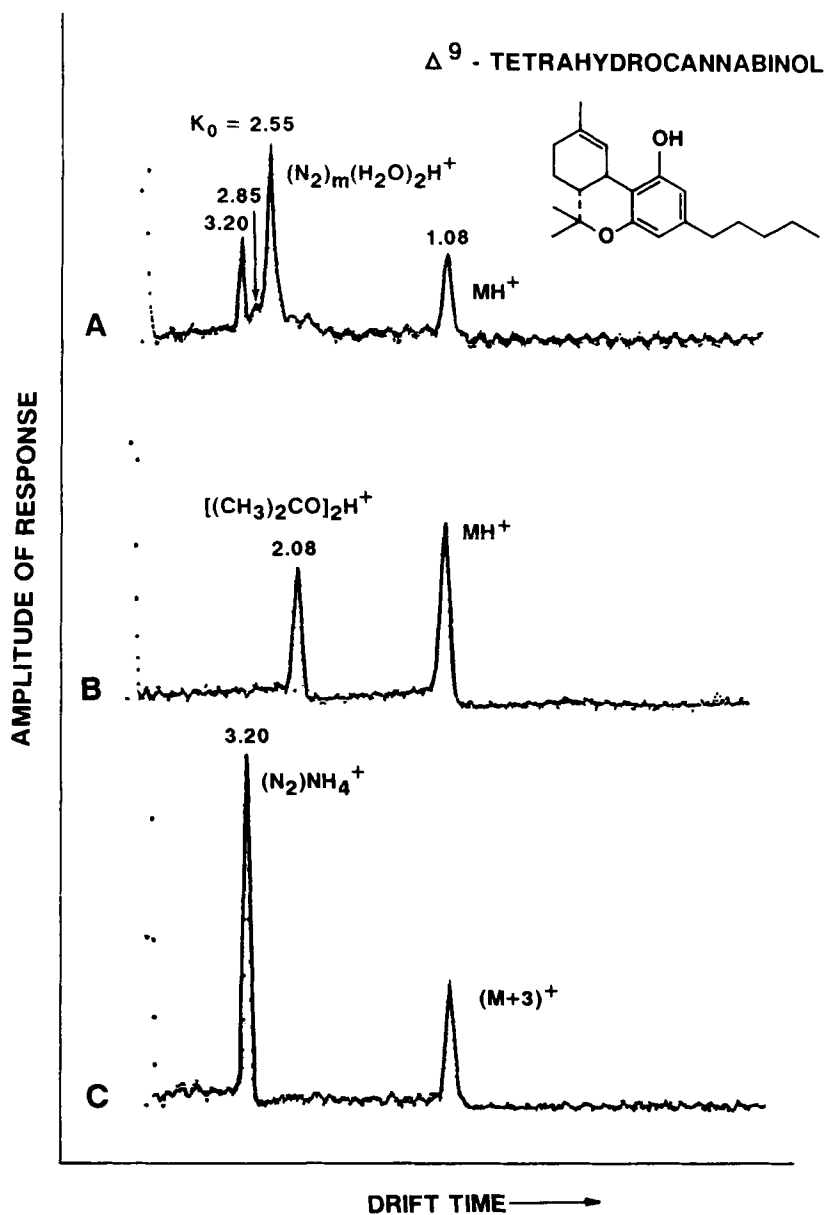


Figure 24. Ion mobility spectra of Δ^9 -tetrahydrocannabinol using hydronium (spectrum A), ammonium (spectrum B), and acetone (spectrum C) reactant ions and an IMS cell temperature of 204°C.

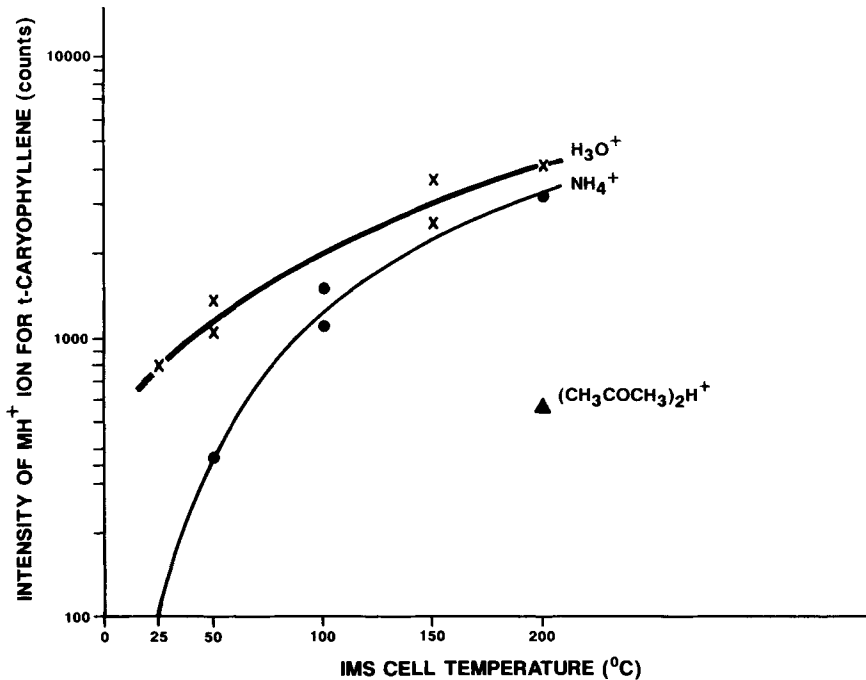


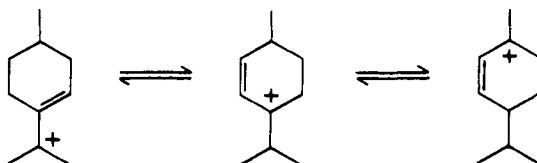
Figure 25. Variation of the MH^+ response of t-caryophyllene with IMS cell temperature using the three reactant ions of this study.

response from t-caryophyllene using hydronium and ammonium reactant ions, respectively. Because the proton affinity of the protonated acetone dimer ion is high, ionization of t-caryophyllene using this reactant ion can only occur for higher drift temperatures ($\geq 200^\circ\text{C}$).

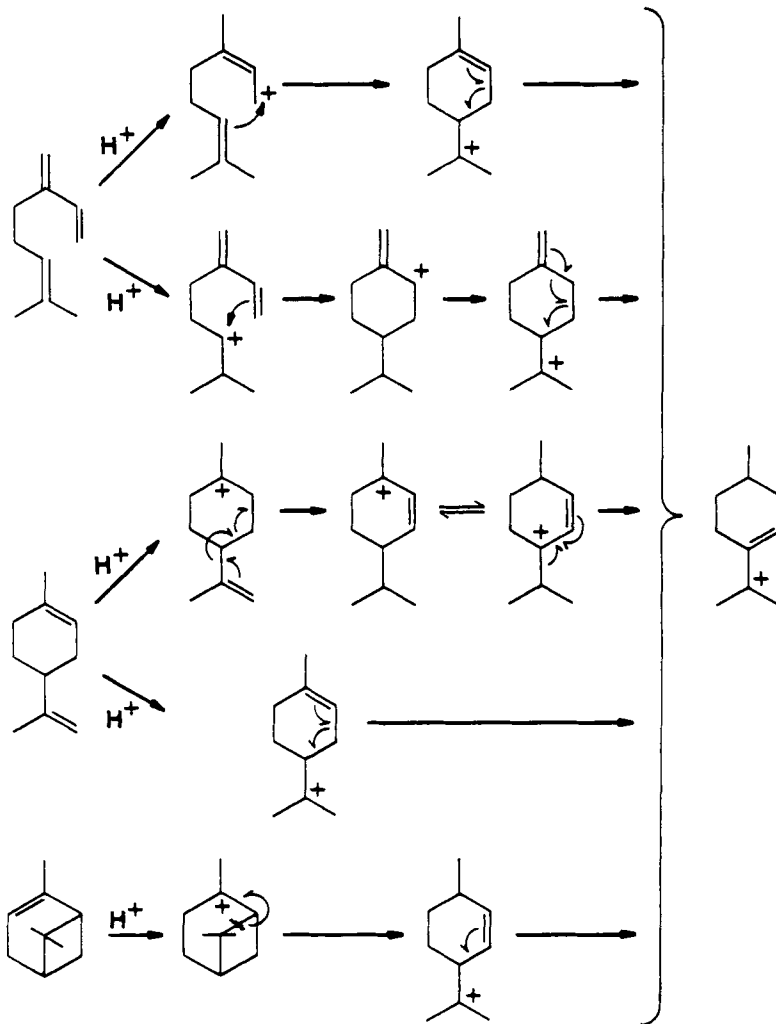
DISCUSSION

Monoterpenes

The monoterpenes, β -myrcene, d-limonene, and α -pinene, all undergo proton transfer reactions to yield protonated monomer ions (MH^+). The proton initially attacks an olefinic double bond,^{59,60} but later migrates between stable configurations such as:

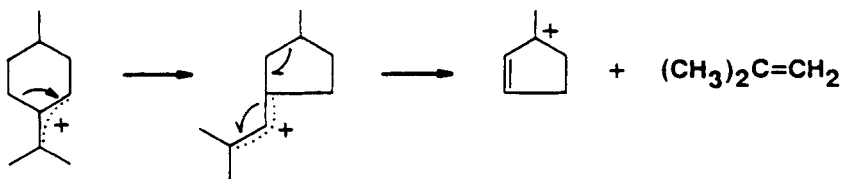


For each of these three configurations, the positive charge is located on a tertiary carbon allylic to a double bond. The reaction sequences which could terminate into the above structures are as follows:



As evidenced by the ion with $m/e = 81$ in the mass spectra of Figure 5, the protonated molecular ion also undergoes decomposition. It is first noted the product ion with $m/e = 81$ differs from the fragment ions with $m/e = 68$ to 69 and 93 observed in electron impact mass spectrometry.⁶¹ This difference is related to the formation of odd-electron molecular ions (M^+) in electron impact mass spectrometry and protonated even-electron molecular ions (MH^+) in chemical ionization mass spectrometry.⁶²

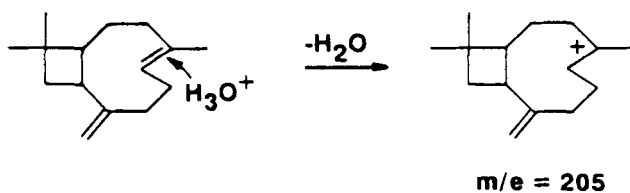
Unlike the reverse Diehls-Alder reaction which is typically used to explain fragmentation of odd-electron molecular ions (M^+) for simple monoterpenes,⁶³ a ring contraction mechanism better describes the fragmentation observed for protonated even-electron ions.⁶⁴⁻⁶⁶ For β -myrcene, d-limonene, and α -pinene, the migration of positive charge around the cyclohexyl ring of the protonated molecular ion eventually leads to rearrangement and fragmentation:



The rearranged ion provides a new structure which allows the allylic charge to migrate between two tertiary carbons. The cyclopentenium ion is known to be very stable, thermodynamically.^{67,68}

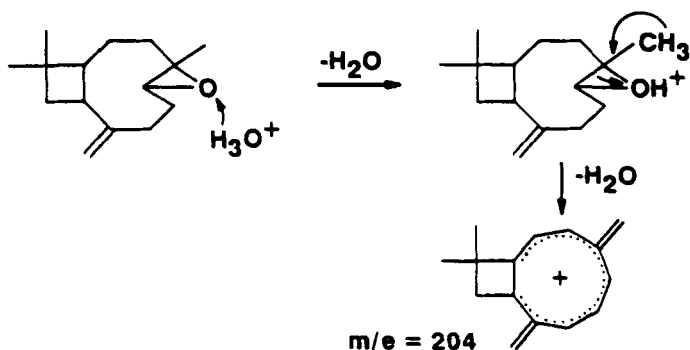
Caryophyllene

The ions with $m/e = 205$ in Figures 6, 15, and 21 are due to protonation of *t*-caryophyllene:



The reduced mobility for these ions is $1.45 \text{ cm}^2/\text{V}/\text{sec}$. In high concentration, *t*-caryophyllene may also undergo charge exchange reactions with precursor ions, such as N_4^+ , to yield an M^+ ion at $m/e = 204$ (see Figure 22).

The ions with $m/e = 204$ observed for caryophyllene oxide in Figure 8 suggests that water is eliminated after this compound is protonated:



The reduced mobility for the ions with $m/e = 221$ is $1.40 \text{ cm}^2/\text{V}/\text{sec}$ and the reduced mobility for the ions with $m/e = 204$ is $1.45 \text{ cm}^2/\text{V}/\text{sec}$.

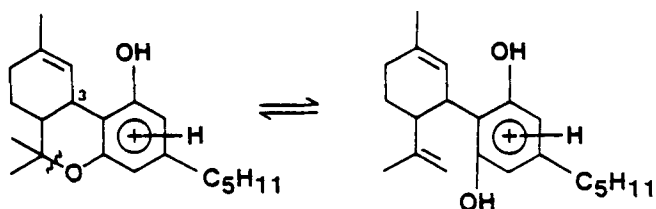
The other peaks observed in the spectra for the caryophyllenes correspond to ions typical of terpenes. Sesquiterpenoids often undergo fragmentations similar to corresponding monoterpenoids and produce similar ions.⁶⁹ The specific mechanisms for fragmentation of *t*-caryophyllene are not established.

Cannabinoids

As evidenced by ions with a mass corresponding to MH^+ in Figure 10, the cannabinoids are ionized by proton transfer from the hydronium reactant ion. For Δ^9 -THC and CBN, the site of attachment can be either the double bond of the cyclohexyl ring, the ether oxygen, the hydroxyl group, or the phenolic aromatic ring. While Buttrill has proposed substituent protonation for phenol, Kebarle argues ring protonation based on proton transfer equilibrium measurements which seem to be supported by the deuterium exchange experiments of Hunt.⁷⁰⁻⁷² Harrison determined that there is a difference of approximately 63 kJ/mol between the proton affinity of the etheric oxygen in anisole (approximately 770 kJ/mol) and that of the aromatic ring (approximately 833 kJ/mol).⁷³ Furthermore, disubstitution as occurs in resorcinol increases ring basicity compared to phenol. This is consistent with Hunt, who observed that deuterium is easily incorporated into the aromatic ring of resorcinol.⁷² Consequently, protonation of the phenolic aromatic ring in Δ^9 -THC and CBN appears to be favored over protonation of the hydroxyl group and that this tendency is increased for the resorcinol ring of CBD.

The cannabinoids can also be viewed as higher derivatives of anisole with an ether oxygen having a proton affinity greater than that of anisole (perhaps equivalent to an ether with a methyl group replaced by a *t*-butyl group). Since the proton affinity of *t*-BuOMe (852.1 kJ/mol) is greater than the proton affinity of $(\text{Me})_2\text{O}$ (807.4 kJ/mol) by 44.7 kJ/mol ,³⁴ the ether oxygen in Δ^9 -THC and CBN may be 44.7 kcal/mol greater than the ether oxygen in anisole. That is, the proton affinity of the ether oxygen in Δ^9 -THC and CBN (approximately 815 kJ/mol) is 18 kJ/mol less than the proton affinity of the phenolic aromatic ring.

Similarly an estimate can be made on the proton affinity for the cyclohexyl ring in Δ^9 -THC and CBD, and the toluol ring in CBN by noting that the proton affinities for isopropylbenzene, isobutylene, and 1-methylcyclohexene are 816.3 , 823.8 , and 836.4 kJ/mol , respectively.³⁴ That is, the proton affinities for the cyclohexyl rings in Δ^9 -THC and CBN are very close to the proton affinity of the phenolic rings for these compounds and the proton affinity of the toluol ring in CBN is less than the proton affinity of the phenolic ring in that compound. Since, as noted earlier, the proton affinity of a resorcinol aromatic ring is greater than the proton affinity of a phenolic aromatic ring, the site of protonation for the cannabinoids appears to be the phenolic aromatic ring with the product ion resonating between the following structures:

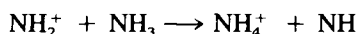
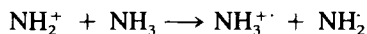
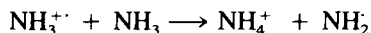
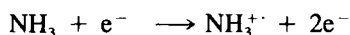


Cleavage of the C–O bond is a direct result of the electron withdrawing characteristics of the protonated phenolic ring.

Since the proton affinity of acetone (824.5 kJ/mol) is less than the proton affinity of the cannabinoids,³⁴ the reaction mechanism involved for the ionization of the cannabinoids using acetone reactant ions is presumed to be similar to that described earlier for the hydronium reactant ions. On the other other hand, the formation of $(M+3)^+$ and $(M-1)^+$ ions from the cannabinoids using ammonium reactant ions is a surprise. Because the ammonium ion has a proton affinity (857.1 kJ/mol) greater than the cannabinoids,³⁴ electrophilic attachment of NH_4^+ is expected.⁴⁷ The fact that an $(M+18)^+$ ion is not observed suggests that the excited $[\text{M}\cdots\text{H}\cdots\text{NH}_3]^+^*$ complex has a short lifetime and the site for protonation is the phenolic aromatic ring. It is known that although benzene, toluene, and 1,2,3-trimethylbenzene have proton affinities of 769, 795, and 828 kJ/mol, respectively, they do not undergo attachment reactions under ammonia CI conditions.⁴⁷

In general, several reactions can be postulated between the ammonium reactant ion and the cannabinoids which would lead to $(M+3)^+$ ions: (1) displacement of CH_3 by NH_4^+ , (2) addition of NH_3 and NH_4^+ with the elimination of two CH_4 's (3) addition of three hydrogens, and (4) replacement of CH_3 by H_2O . The displacement and elimination reactions of (1) and (2) are not considered feasible because the mechanism would involve an attack by the ammonium ion on the quarternary carbon with the elimination of one or both of the geminated methyl groups. Such an attack is inconsistent with the site of protonation described earlier and would result in cleavage of the C–O bond with formation of a stable tertiary amine (i.e., no elimination of methyl groups). To evaluate the other two reaction mechanisms, it is necessary to discuss the reactant ions.

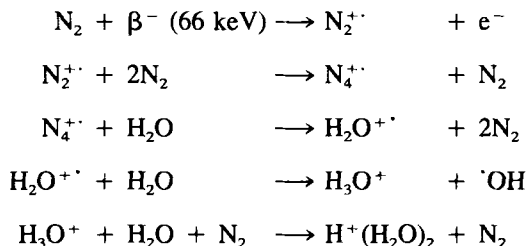
For the low pressures employed in mass spectrometry, Westmore and Alauddin present the following reaction sequence for the ionization of ammonia in chemical ionization mass spectrometry.⁴⁷



Products of these reactions include hydrogen radicals which can participate in subsequent hydrogenation reactions. For example, after the cannabinoids are ionized and the C–O bond is cleaved, olifinic bonds are available for reduction. This reduction could be accomplished by hydrogen radicals or a concerted attack by several ammonia molecules as described by Das, Reddy, Vairamani, Madhusudhanan, Fraïsse, and Tabet.⁷⁴ While in principle these reactions may be possible, the likelihood of generating hydrogen radicals from ammonia under atmospheric pressure conditions and the dependence of Das et al.'s mechanism on conjugated bonds near an activating site must be reconsidered. Without rearrangement, the product ions formed upon protonation of the cannabinoids do not contain conjugated bonds. It is therefore difficult to imagine how Das et al.'s mechanism would apply to this problem. In order to address the question of hydrogen radical generation, the reactions leading to the formation of ammonium reactant ions under atmospheric pressure conditions in IMS must be considered.

For ion mobility spectrometry a ⁶³Ni radioactive source emits 66 keV beta particles (electrons) for ionization. While the energy of these beta particles is certainly sufficient to initiate the reactions described earlier for the generation of ammonium reactant ions, the efficiency for direct ionization of ammonia is greatly reduced over, say, a mechanism involving N₂^{+·} precursor ions in the ionization of ammonia. Typically, a vapor concentration of approximately 100 ppb is used in IMS to generate a saturation response (i.e., only ammonium ions are observed) to ammonium vapors. This means that when a beta particle is emitted by the ⁶³Ni source, it has 1 in 10⁷ chances of ionizing an ammonia molecule as opposed to a nitrogen or oxygen molecule.

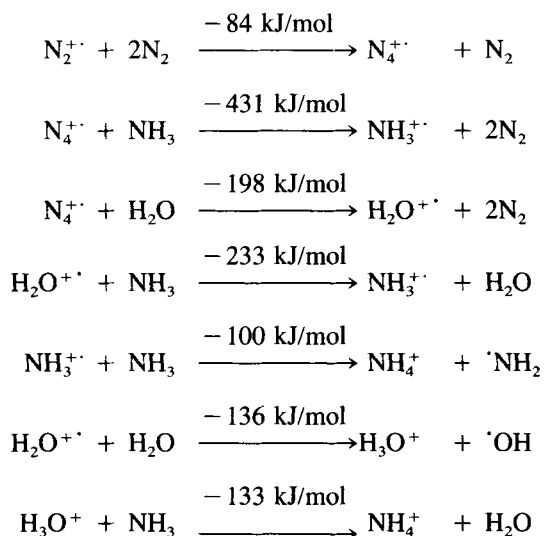
To emphasize this point, similar considerations were given to the generation of hydronium reactant ions in the carrier gas of an IMS which typically contains 3 ppm of water. The reactions which have been proposed for the generation of these reactant ions are as follows:⁷⁵



The reactions proceed through N₂^{+·} and N₄^{+·} precursor ions which eventually exchange charge with water to yield H₂O^{+·}. Similarly, it is improbable that beta particles will ionize ammonia molecules directly and form ammonium reactant ions.

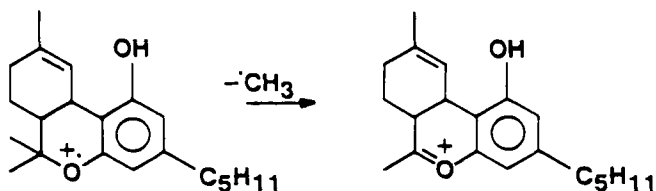
A series of reactions which can be proposed for the generation of ammonium reactant ions from N₂^{+·} is as follows:



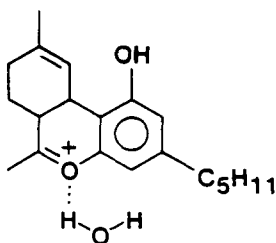


The heats of reaction are calculated using handbook values for the heat of formation for the various species,⁷⁶ proton affinities for water and ammonia,³⁴ and assuming that the heat of formation of $\text{N}_4^{+\cdot}$ from $\text{N}_2^{+\cdot}$ is -0.87 eV (-84 kJ/mol).⁷⁷ The reactions are similar to those for hydronium reactant ions until charge exchange takes place between $\text{N}_4^{+\cdot}$ and water. At this point, the charge exchange can involve either water or ammonia. The thermodynamic data indicate that the formation of $\text{NH}_3^{+\cdot}$ is exothermic over the formation of $\text{H}_2\text{O}^{+\cdot}$ ion by 233 kJ/mol and the ammonium reactant ion arises from the intermediate $\text{NH}_3^{+\cdot}$ ion for all reasonable concentrations of ammonia which might be used to generate ammonium reactant ions in IMS. Since the charge exchange of $\text{N}_2^{+\cdot}$ with ammonia to yield $\text{NH}_2^{+\cdot}$ and a hydrogen radical is endothermic by 24.1 kJ/mol , it is more difficult to generate hydrogen radicals under the atmospheric pressure conditions of IMS than the vacuum conditions of mass spectrometry.⁷⁶ This conclusion is also true if the reaction of negative reactant ions with ammonia to produce hydrogen radicals is considered.

The result of this finding is that hydrogenation by hydrogen radicals is probably secondary to reactions of the sample with NH_4^+ and $\text{NH}_3^{+\cdot}$. Since it has already been noted that NH_4^+ does not react with the cannabinoids because of the high proton affinity of ammonia, the reaction of the cannabinoids with $\text{NH}_3^{+\cdot}$ are probably important. A possible reaction of this type involves allowing charge exchange between $\text{NH}_3^{+\cdot}$ and the cannabinoid with the elimination of one of the geminated methyl groups similar to that observed in electron impact mass spectrometry.⁷⁸⁻⁸¹ The resulting product ion is



Because the positive charge is localized on the oxygen of the product ion, water clustering is possible:



This leads to an $(M+3)^+$ ion from the cannabinoid. Ring closure is obviously necessary to produce a similar ion from CBD.

Finally, the $(M-1)^+$ ions observed from the cannabinoids in the presence of ammonia are most likely due to hydride anion abstraction from an allylic (e.g., #3) position of cannabinoid molecule. While a more careful series of mechanistic studies are needed, the abstraction might be accomplished with the NH_4^+ reactant ion which would dissociate into ammonia and hydrogen.

Using water and acetone reagent gases, negative ionization of the cannabinoids yields an $(M-1)^-$ ion. This ion is formed as a result of proton abstraction by the $(\text{H}_2\text{O})_2\text{O}^-$, $(\text{H}_2\text{O})_n\text{CO}_3^-$, and $(\text{H}_2\text{O})\text{CO}_4^-$ reactant ions to form a phenoxide ion.⁸²⁻⁸⁴ Phenoxide ions were not observed in the presence of ammonia which appears to change the identity of the negative reactant ions.

APPLICATION TO MARIJUANA DETECTION

Using the IMS/MS system, the headspace vapors in the equilibrium with confiscated marijuana were sampled by inserting the inlet of the IMS through a hole punctured in the polypropylene bags containing the samples. Vapors were drawn from these bags across the membrane of the IMS/MS by means of a suction pump. Also, smoke from a burning cigarette of marijuana was sampled using the smoking apparatus of Figure 2.

Figure 26 shows the responses obtained by sampling headspace vapors from three samples of marijuana. For both hydronium and ammonium reactant ions, the responses displayed a major peak with a reduced mobility of $1.45 \text{ cm}^2/\text{V}/\text{sec}$ which corresponds to caryophyllene (see Figures 6 and 15). The mass spectral data of Figure 27 shows that the protonated molecular ion of caryophyllene, m/e 205, was indeed observed from the samples. Also appearing in the spectra are ions with masses 81 and 137 and an ion mobility peak with reduced mobility $1.78 \text{ cm}^2/\text{V}/\text{sec}$. These ions can be attributed to the monoterpenes (see Figures 4 and 5).

Figures 28 through 30 show the response to the IMS/MS to marijuana cigarette smoke using hydronium, ammonium, and acetone reactant ions, respectively. In each case, an ion with a reduced mobility $1.10 \text{ cm}^2/\text{V}/\text{sec}$ was observed corresponding to Δ^9 -THC (see Figures 9, 19, and 24). This was verified by collecting

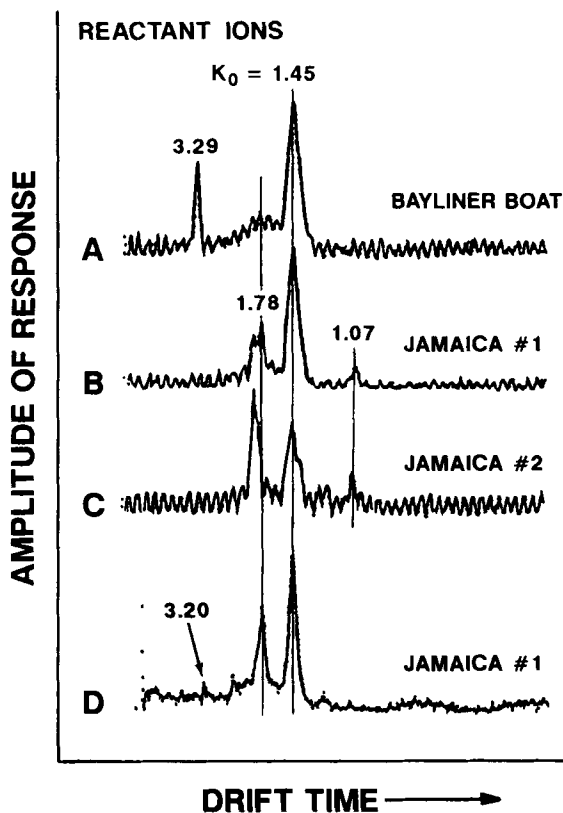


Figure 26. Ion mobility spectra collected against headspace vapors of three confiscated marijuana samples. Spectra A to C were collected using hydronium reactant ions and an IMS cell temperature of 150°C, and spectrum D was collected using ammonium reactant ions and an IMS cell temperature of 190°C.

the mass spectra of Figure 31 using ammonium reactant ions. The ions with $m/e = 316$ to 317 are the $(M^+ - \text{CH}_3 + \text{H}_2\text{O})^+$ ions associated with Δ^9 -THC in Figure 18. Figure 32 shows mass identified mobility data collected against the marijuana cigarette smoke.

A comparison of data shows that the Δ^9 -THC is hardly detected in cigarette smoke using hydronium reactant ions. Acetone reactant ions are a little better in that a good response to Δ^9 -THC is obtained if the smoke concentration is not too high. However, the ammonium reactant ion allows good detection of Δ^9 -THC over a wide range of smoke concentration. The reason for this success is related to the intermediate proton affinity of the ammonium reactant ion and perhaps the greater stability of the secondary ion formed from the cannabinoids using ammonia chemistry. The low proton affinity of the hydronium reactant ion allows it to ionize a larger number of compounds in marijuana smoke which masks the Δ^9 -THC response. The large size of the acetone reactant ion shifts the interferences to longer drift

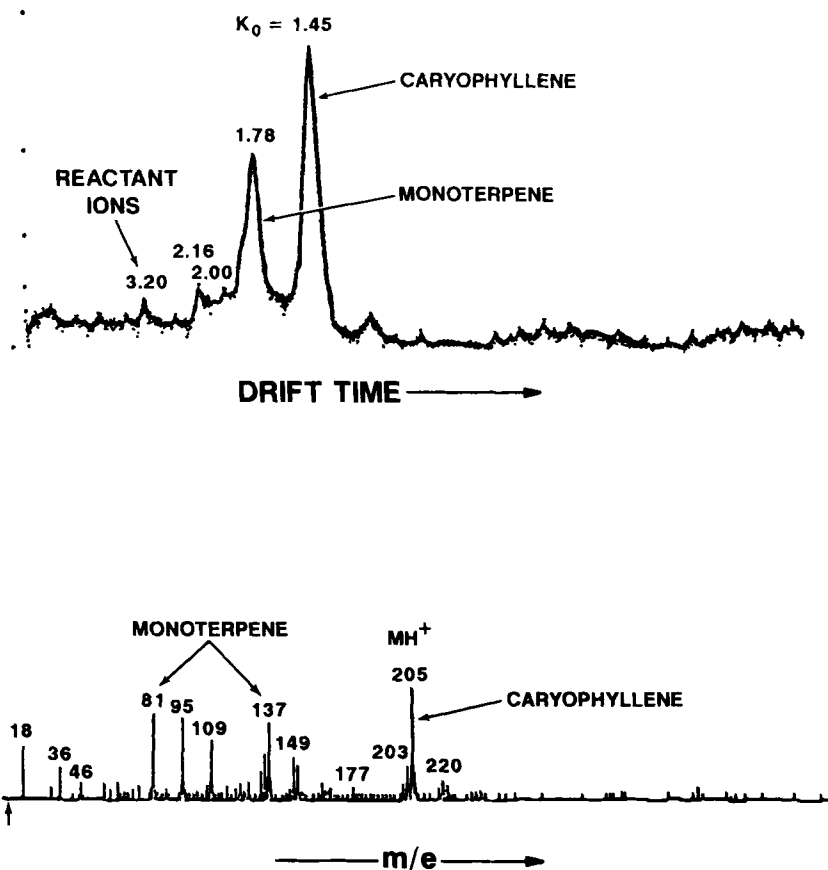


Figure 27. The ion mobility spectrum (top) and the mass spectrum (bottom) collected against headspace vapors of a confiscated marijuana sample using ammonium reactant ions and an IMS cell temperature of 190°C.

times to again mask the Δ^9 -THC response. The ammonium reactant ion has a higher proton affinity than the hydronium reactant ion to reduce the effects of smoke interference and is smaller in size than the acetone reactant ion to minimize shifts in drift time due to ion clustering. Because the secondary ions formed from the cannabinoids in the presence of ammonia are not protonated species, they are more stable against interferences of high proton affinity which compete with protonated species for charge.

Another result of these detection experiments was that Δ^9 -THC was not observed in the headspace vapors of marijuana, but was observed in marijuana cigarette smoke. This can be explained on the basis that the cannabinoids are present in the plant as their carboxylic acid derivative (the so-called A-acids) which decarboxylate

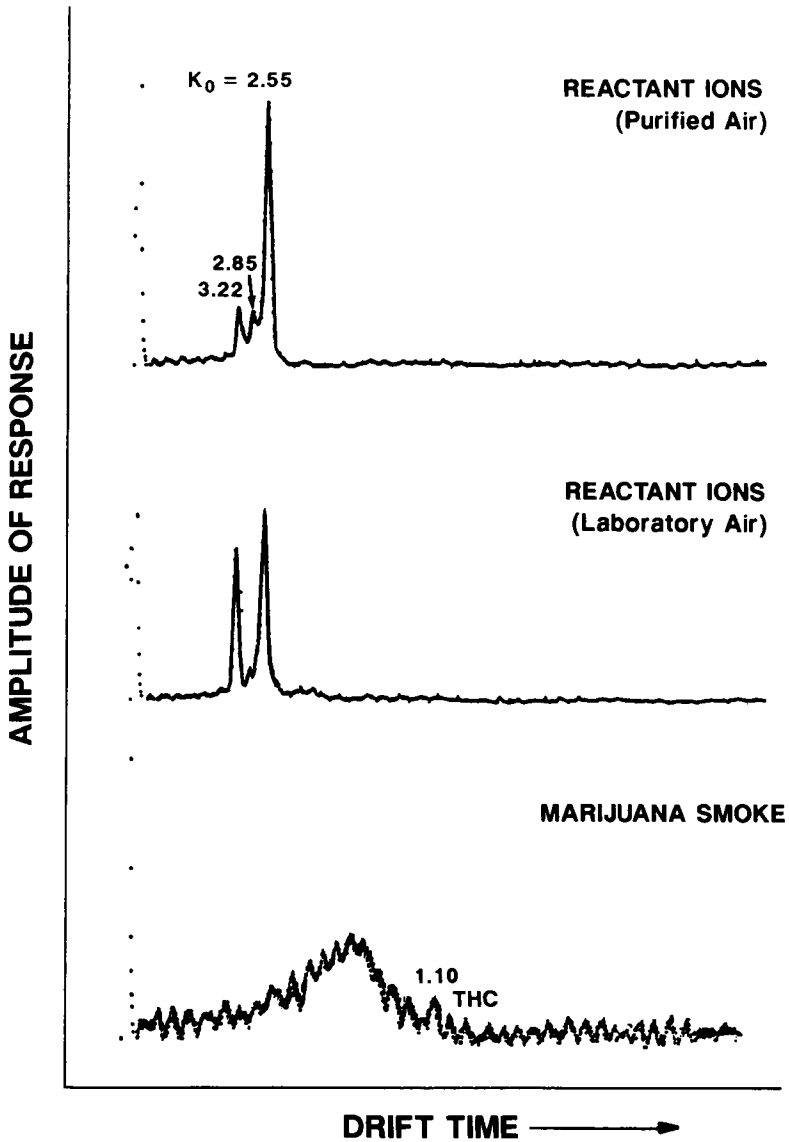


Figure 28. Ion mobility spectrum of marijuana smoke using hydronium reactant ions and an IMS cell temperature of 189°C . The top two spectra show reactant ion spectra for purified air and laboratory air before sampling smoke.

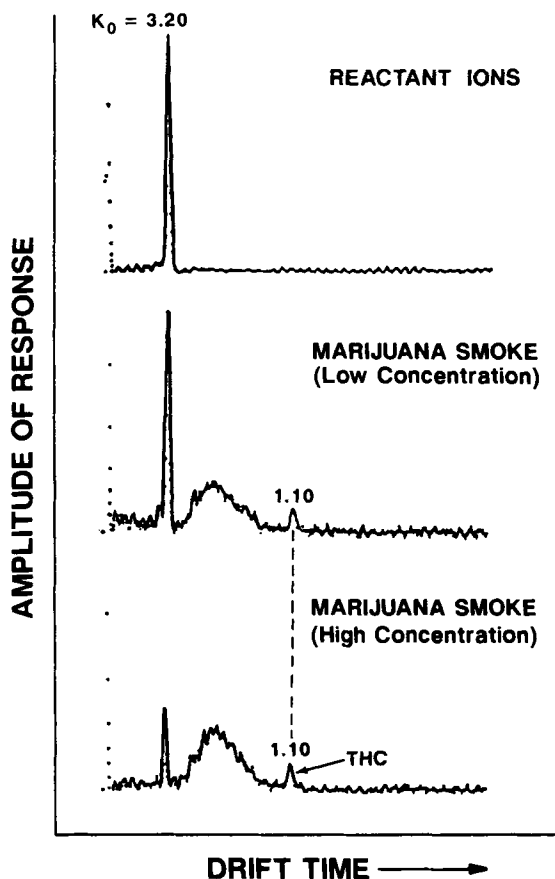


Figure 29. Ion mobility spectrum of marijuana smoke using ammonium reactant ions and an IMS cell temperature of 189°C. The top spectrum shows the reactant ions before sampling smoke.

slowly at room temperature.⁸¹ However, Δ^9 -THC can be released in cigarette smoke because the rate of decarboxylation increases in the high temperature zone of the cigarette tip.⁸⁵

CONCLUSIONS

The data of Tables 1 and 2 show that two fractions of marijuana can be used for its detection. These are the sesquiterpenes, specifically β -caryophyllene, and the cannabinoids, specifically Δ^9 -tetrahydrocannabinol.

IMS/MS reference data collected on these compounds showed that both can be detected using hydronium and ammonium reactant ions. However, ammonium reactant ions were shown to be superior for the detection of Δ^9 -THC in marijuana smoke. Reasonable reaction mechanisms suggest that the improved ionization ca-

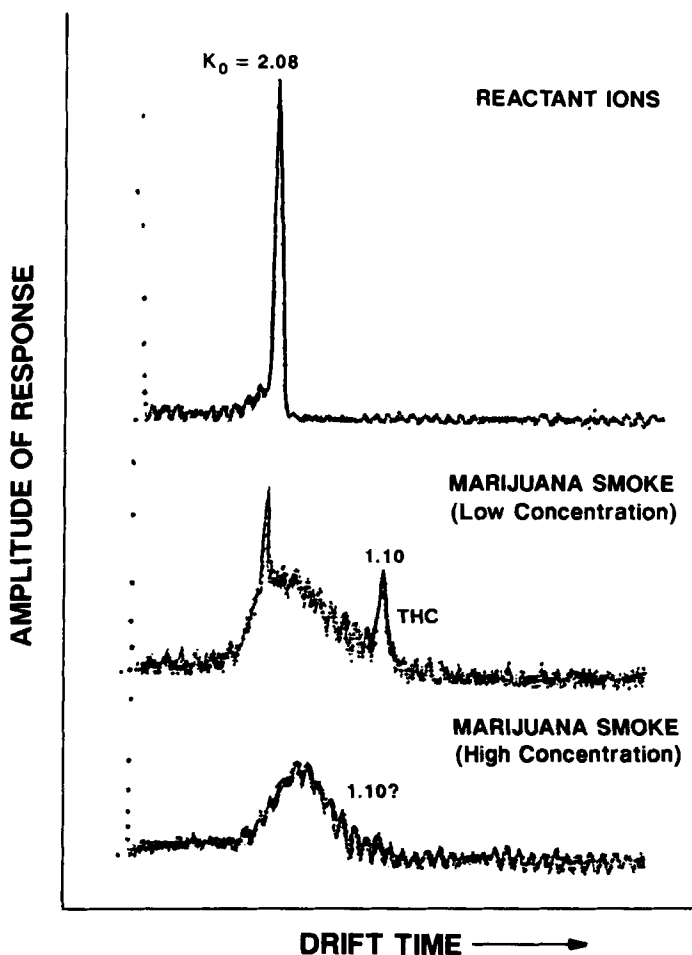


Figure 30. Ion mobility spectrum of marijuana smoke using acetone reactant ions and an IMS cell temperature of 189°C. The top spectrum shows the reactant ions before sampling smoke.

pabilities of ammonium reactant ions over hydronium reactant ions is due to reaction mechanisms unique to the ammonium reactant ion and a stable secondary ion derived from the cannabinoids in the presence of ammonium reactant ions.

ACKNOWLEDGMENTS

This research was supported in part by the U.S. Coast Guard R&D Center, Avery Point, Groton, CT and the U.S. Naval Research Laboratory, Washington, DC.

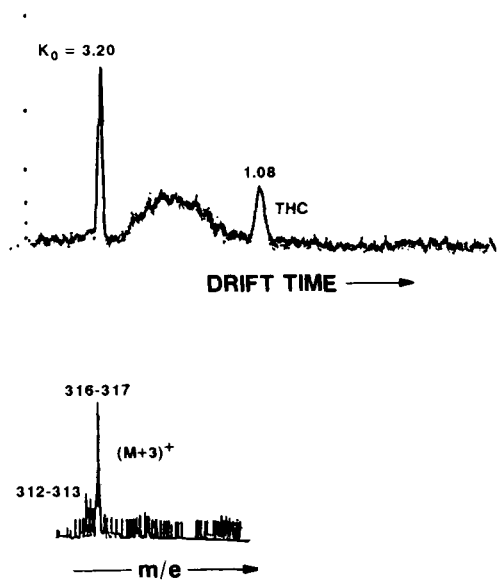


Figure 31. The ion mobility spectrum (top) and the mass spectrum (bottom) collected against marijuana smoke using ammonium reactant ions and an IMS cell temperature of 188°C.

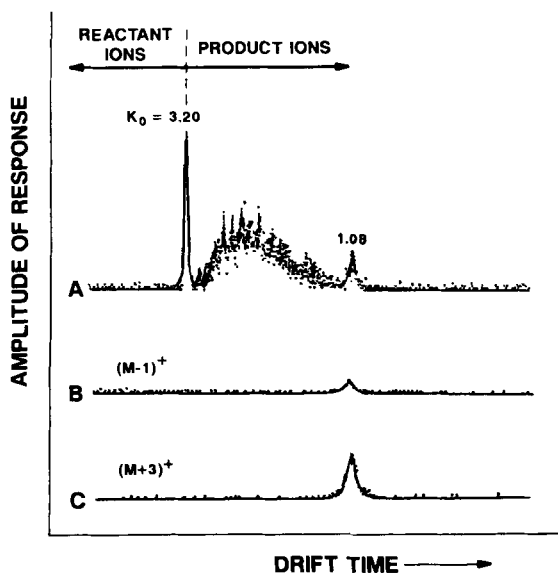


Figure 32. Mass identified mobility data (spectra B and C) of the marijuana smoke response (spectrum A) of Figure 31.

REFERENCES

1. Griffin, G. W., I. Dzidic, D. I. Carroll, R. N. Stillwell, and E. C. Horning. "Ion Mass Assignments Based on Mobility Measurements, Validity of Plasma Chromatographic Mass Mobility Correlations," *Anal. Chem.* 45(7):1204—1209 (1973).
2. Kim, S. H., K. R. Betty, and F. W. Karasek. "Mobility Behavior and Composition of Hydrated Positive Reactant Ions in Plasma Chromatography with Nitrogen Carrier Gas," *Anal. Chem.* 50(14):2006—2012 (1978).
3. Spangler, G. E., and J. P. Carrico. "Membrane Inlet for Ion Mobility Spectrometry (Plasma Chromatography)," *Int. J. Mass Spectrom. Ion Phys.* 52:267—287 (1983).
4. Cohen, M. J., and F. W. Karasek. "Plasma Chromatography—A New Dimension for Gas Chromatography and Mass Spectrometry," *J. Chromatog. Sci.* 8(6):330-337 (1970).
5. Karasek, F. W. "Plasma Chromatography," *Anal. Chem.* 46(8):710A-720A (1974).
6. Kim, S. H. "Fundamental Aspects of Plasma Chromatography," Ph.D. Thesis, University of Waterloo, Ontario, Canada (1977).
7. Carr, T. W., Ed. *Plasma Chromatography* (New York: Plenum, 1984).
8. Witkiewicz, Z., and E. Stryszak. "Plasma Chromatography. I. The Physicochemical Fundamentals of Plasma Chromatography and the Apparatus Involved," *Chem. Anal. Warsaw.* 30:491—518 (1985).
9. Witkiewicz, Z., and E. Stryszak. "Plasma Chromatograph. II. Analytical Applications of Plasma Chromatography," *Chem. Anal. Warsaw.* 30(5—6):683 (1985).
10. Novotny, M., M. L. Lee, C.-E. Low, and A. Raymond. "Analysis of Marijuana Samples from Different Origins by High-Resolution Gas-Liquid Chromatography for Forensic Application," *Anal. Chem.* 48(1):24—29 (1976).
11. Hood, L. V. S., and G. T. Barry. "Headspace Volatiles of Marijuana and Hashish: Gas Chromatographic Analysis of Samples of Different Geographic Origin," *J. Chromatog.* 166:499—506 (1978).
12. Manolis, A., L. J. McBurney, and B. A. Bobbie. "The Detection of Δ^9 -Tetrahydrocannabinol in the Breath of Human Subjects," *Clin. Biochem.* 16:229—233 (1983).
13. Fenimore, D. C., R. R. Freeman, and P. R. Loy. "Determination of Δ^9 -Tetrahydrocannabinol in Blood by Electron Capture Gas Chromatography," *Anal. Chem.* 45(14):2331—2335 (1973).
14. Foltz, R. L., K. M. McGinnis, and D. M. Chinn. "Quantitative Measurement of Δ^9 -Tetrahydrocannabinol and Two Major Metabolites in Physiological Specimens Using Capillary Column Gas Chromatography Negative Ion Chemical Ionization Mass Spectrometry," *Biomed. Mass Spectrom.* 10(5):316—323 (1983).
15. Gough, T. A., and P. B. Baker. "Identification of Major Drugs of Abuse Using Chromatography," *J. Chromatog. Sci.* 20:289—329 (1983).
16. Gudzinowicz, B. J., M. J. Gudzinowicz, J. Hologgitas, and J. L. Driscoll. "The Analysis of Marijuana Cannabinoids and Their Metabolites in Biological Media by GC and/or GC-MS Techniques," *Adv. Chromatog.* 18:197—265 (1980).
17. Carrico, J. P., A. W. Davis, D. N. Campbell, J. E. Roehl, G. R. Sima, G. E. Spangler, K. N. Vora, and R. J. White. "Chemical Detection and Alarm for Hazardous Chemicals," *Am. Lab.* 18(2):152—163 (1986).
18. Blythe, D. A. "A Vapour Monitor for Detection and Decontamination Control," in *Proc. Int. Symp. Protection Against Chemical Warfare Agents* (Stockholm, Sweden:National Defence Research Institute, 1983), pp. 65—69.
19. Baim, M. A., and H. H. Hill, Jr. "Tunable Selective Detection for Capillary Gas Chromatography by Ion Mobility Monitoring," *Anal. Chem.* 54(1):38—43 (1982).

20. Eatherton, R. L., M. A. Morrissey, W. F. Siems, and H. H. Hill, Jr. "Ion Mobility Detection after Supercritical Fluid Chromatography" *J. High Res. Chromatogr. Chromatogr. Commun.* 9:154—160 (1986).
21. Hill, H. H., Jr., W. F. Siems, R. L. Eatherton, R. St. Louis, M. A. Morrissey, and C. B. Shumate. "Gas, Supercritical Fluid and Liquid Chromatographic Detection of Trace Organics by EMS," 3rd Chemical Congress of North America and 195th ACS National Meeting, Toronto, Canada, June 1988.
22. Turner, C. E., M. A. Elsohly, and E. G. Boeren. "Constituents of Cannabis sativa L. XVII. A Review of the Natural Constituents," *J. Nat. Prod.* 43:169—234 (1980).
23. Turner, C. E., O. J. Bouwsma, S. Billets, and M. A. Elsohly. "Constituents of Cannabis sativa L., XVIII. Electron Voltage Selected Ion Monitoring Study of Cannabinoids," *Biomed. Mass Spectrom.* 7(6):247—256 (1980).
24. Hood, L. V. S., M. E. Dames, and G. T. Barry. "Headspace Volatiles of Marijuana," *Nature* 242(5397):402—403 (1973).
25. Novotny, M., F. Merli, D. Wiesler, M. Fencel, and T. Saeed. "Fractionation and Capillary Gas Chromatography-Mass Spectrometric Characterization of the Neutral Components in Marijuana and Tobacco Smoke Condensates," *J. Chromatog.* 238:141—150 (1982).
26. Riba, M. L., J. P. Tathy, J. Mathieu, and L. Torres. "A Simple, Efficient Device for Determining Terpenes Present as Traces in the Atmosphere," *Int. J. Environ. Anal. Chem.* 20:255 (1985).
27. Shaw, P. E., and M. G. Moshonas. "Mass Spectrometry for the Identification of Citrus Flavor Components," *Mass Spectrom. Rev.* 4:397—420 (1985).
28. Hunter, G. L. K., and W. B. Brogden, Jr. "A Rapid Method for Isolation and Identification of Sesquiterpene Hydrocarbons in Cold-Pressed Grapefruit Oil," *Anal. Chem.* 36(6):1122—1123 (1964).
29. Weast, R. C., Ed. *CRC Handbook of Chemistry and Physics* (Boca Raton, FL: CRC Press, Inc., 1983), p. D199—D218.
30. Spangler, G. E., and P. A. Lawless. "Ionization of Nitrotoluene Compounds in Negative Ion Plasma Chromatography," *Anal. Chem.* 50:884—892 (1978).
31. Truitt, E. B., Jr. "Biological Disposition of Tetrahydrocannabinols," *Pharm. Rev.* 23:273—278 (1971).
32. Karasek, F. W., D. E. Karasek, and S. H. Kim. "Detection of Lysergic Acid Diethylamide, Δ^9 -Tetrahydrocannabinol and Related Compounds by Plasma Chromatography," *J. Chromatog.* 105:345—352 (1975).
33. Kebarle, P. "Ion Thermochemistry and Solvation from Gas Phase Ion Equilibria," *Ann. Rev. Phys. Chem.* 28:445—476 (1977).
34. Aue, D. H., and M. T. Bowers. "Stabilities of Positive Ions from Equilibrium Gas-Phase Basicity Measurements," in *Gas Phase Ion Chemistry*, Vol. 2, M. T. Bowers, Ed. (New York: Academic Press, Inc., 1979) Chapter 9.
35. Shumate, C., R. H. St. Louis, and H. H. Hill, Jr. "Table of Reduced Mobility Values from Ambient Pressure Ion Mobility Spectrometry," *J. Chromatog.* 373:141—173 (1986).
36. Metro, M. M., and R. A. Keller. "The Plasma Chromatograph as a Separation-Identification Technique," *Sepr. Sci.* 9(6):521—539 (1974).
37. Karasek, F. W., O. S. Tatone, and D. W. Denney. "Plasma Chromatography of the n-Alkyl Halides," *J. Chromatog.* 87:137—145 (1973).
38. Karasek, F. W., D. W. Denney, and E. H. DeDecker. "Plasma Chromatography of Normal Alkanes and Its Relationship to Chemical Ionization Mass Spectrometry," *Anal. Chem.* 46(8):970—973 (1974).

39. Karasek, F. W., A. Maican, and O. S. Tatone. "Plasma Chromatography of n-Alkyl Acetates," *J. Chromatog.* 110:295—300 (1975).
40. Karasek, F. W., and S. H. Kim. "Identification of the Isometric Phthalic Acids by Mobility and Mass Spectra," *Anal. Chem.* 47(7):1166—1168 (1975).
41. Spangler, G. E., S. H. Kim, J. P. Carrico, and J. Epstein. "The Analysis of Organophosphorous Nerve Agents using Ion Mobility Spectrometry/Mass Spectrometry (IMS/MS)," Technical report submitted on contract DAAK11-80-C-0024, Chemical Systems Laboratory, Aberdeen Proving Ground, MD (February 1983).
42. Kim, S. H., G. E. Spangler, J. Epstein, and A. W. Davis. "The Analysis of Isopropyl and Pinacolyl Methylphosphonofluoridate using Ion Mobility Spectrometry/Mass Spectrometry IMS/MS," Report CRDEC-CR-88070, Chemical Research Development and Engineering Center, Aberdeen Proving Ground, MD (June 1988).
43. Kim, S. H., F. W. Karasek, and S. Rokushika. "Plasma Chromatography with Ammonium Reactant Ions," *Anal. Chem.* 50(1):152—155 (1978).
44. Spangler, G. E., D. N. Campbell, and J. P. Carrico. "Acetone Reactant Ions for Ion Mobility Spectrometry," paper presented at the Pittsburgh Conference and Exposition on Analytical Chemistry and Applied Spectroscopy, Atlantic City, NJ, March 9, 1983.
45. Spangler, G. E., S. H. Kim, D. N. Campbell, and J. Epstein. "Ionization of Organophosphonates using Acetone Reactant Ions for Ion Mobility Spectrometry," Technical report submitted to the Chemical Research, Development and Engineering Center, Aberdeen Proving Grounds, MD (April 1988).
46. Keough, T., and A. J. DeStefano. "Factors Affecting Reactivity in Ammonia Chemical Ionization Mass Spectrometry," *Org. Mass Spectrom.* 16(12):527—533 (1981).
47. Westmore, J. B., and M. M. Alauddin. "Ammonia Chemical Ionization Mass Spectrometry," *Mass Spectrom. Rev.* 5:381—465 (1986).
48. Hunt, D. F., "Selective Reagents for Chemical Ionization Mass Spectrometry," in *Progress in Analytical Chemistry: Applications of New Techniques of Analysis*, Vol. 6, I. L. Simmons and G. W. Ewing, Eds. (New York: Plenum, 1973), pp. 359—376.
49. Milne, G. W. A., and M. J. Lacey. "Modern Ionization Techniques in Mass Spectrometry," *CRC Crit. Rev. Anal. Chem.* 4:45—104 (1974).
50. Hunt, D. F., C. N. McEwen, and R. A. Upham. "Chemical Ionization Mass Spectrometry. II. Differentiation of Primary, Secondary, and Tertiary Amines," *Tetrahedron Lett.* 4539—4542 (1971).
51. Hunt, D. F., and S. K. Sethi. "Gas-Phase Ion/Molecule Isotope Exchange Reactions: Methodology for Counting Hydrogen Atoms in Specific Organic Structural Environments by Chemical Ionization Mass Spectrometry," *J. Am. Chem. Soc.* 102:6953—6963 (1980).
52. Lin, Y. Y., and L. L. Smith. "Active Hydrogen by Chemical Ionization Mass Spectrometry," *Biomed. Mass Spectrom.* 6:15—18 (1979).
53. Munson, M. S. B. "Reactions of Gaseous Bronstead Acids," *J. Am. Chem. Soc.* 87(23):5313—5317 (1965).
54. MacNeil, K. A. G., and J. H. Futrell. "Ion-Molecule Reactions in Gaseous Acetone," *J. Phys. Chem.* 76(3):409—415 (1972).
55. McKeown, M., and M. W. Siegel. "Atmospheric Pressure Ionization Mass Spectrometry," *Am. Lab.* 7:89—99 (1975).
56. Spangler, G. E., J. P. Carrico, and S. H. Kim. "Analysis of Explosives and Explosive Residues with Ion Mobility Spectrometry," in *Proceedings of the International Symposium on the Analysis and Detection of Explosive* (Quantico, VA: FBI Academy, 1983), pp. 267—282.

57. Miguel, A. H., and D. F. S. Natusch. "Diffusion Cell for the Preparation of Dilute Vapor Concentrations," *Anal. Chem.* 47(9):1705—1707 (1975).
58. Hirao, K. *Chemistry of Flavor Synthesis* (Tokyo, Japan: Sasaki Publishing Co., 1948), pg. 63.
59. Field, F. H., and M. S. B. Munson. "Chemical Ionization Mass Spectrometry. V. Cycloparaffins." *J. Am. Chem. Soc.* 89:4272—4280 (1967).
60. Field, F. H. "Chemical Ionization Mass Spectrometry," in *Ion Molecule Reactions*, Vol. 1, J. L. Franklin, Ed. (New York: Plenum Press, 1972), Chapter 6.
61. Ryhage, R., and E. von Sydow. "Mass Spectrometry of Terpenes. I. Monoterpene Hydrocarbons," *Acta Chem. Scand.* 17(7):2025—2035 (1963).
62. McLafferty, F. W. *Interpretation of Mass Spectra*, 2nd ed. (Reading, MA: W. A. Benjamin, Inc., 1973), pp. 66—68.
63. Weinberg, D. S., and C. Djerassi. "Mass Spectrometry in Structural and Stereochemical Problems. LXXXVIII. Rearrangements of Simple Terpenes on Electron Impact," *J. Org. Chem.* 31:115—119 (1966).
64. Field, F. H. "Chemical Ionization Mass Spectrometry. VIII. Alkenes and Alkynes," *J. Am. Chem. Soc.* 90(21):5649 (1968).
65. Wesdemiotis, C., R. Wolfschutzand, and H. Schwarz. "Zur Isomerisierung von Cyclohexyl—/Methylcyclopentylkationen in der Gasphase," *Tetrahedron* 36:275—278 (1980).
66. Kingston, E. E., J. S. Shannon, and M. J. Lacey. "Rearrangements in Chemical Ionization Mass Spectrometry," *Org. Mass Spectrom.* 18(5):183—192 (1983).
67. Lossing, F. P., and J. C. Traeger. "Free Radicals by Mass Spectrometry XLVI. Heats of Formation of C₅H₇ and C₅H₈ Radicals and Cations," *Int. J. Mass Spectrom. Ion Phys.* 19:9—22 (1976).
68. Wolkoff, P., J. L. Holmes, and F. P. Lossing. "Ubiquitous [Cyclopentenium]⁺ Formation from C₆H₁₀ Molecular Ions by Methyl Loss and from Higher Homologues," in *Advances in Mass Spectrometry*, Vol. 8A, A. Quale, Ed. (London: Heyden & Son, Inc., 1980), pp. 743—747.
69. Enzell, E. R., R. A. Appleton, and I. Wahlberg. "Terpenes and Terpenoids," in *Biochemical Applications of Mass Spectrometry*, G. R. Waller, Ed. (New York: John Wiley & Sons, Interscience, 1972), Chapter 13.
70. Martinson, D. P., and S. E. Buttrill, Jr. "Determination of the Site of Protonation of Substituted Benzenes in Water Chemical Ionization Mass Spectrometry," *Org. Mass Spectrom.* 11:762—772 (1976).
71. Lau, Y. K., and P. Kebarle. "Substituent Effects on the Intrinsic Basicity of Benzene: Proton Affinities of Substituted Benzenes," *J. Am. Chem. Soc.* 98:7452—7453 (1976).
72. Hunt, D. F., and S. K. Satinder. "Gas Phase Ion/Molecule Isotope-Exchange Reactions: Methodology for Counting Hydrogen Atoms in Specific Organic Structural Environments by Chemical Ionization Mass Spectrometry," *J. Am. Chem. Soc.* 102:6953—6963 (1980).
73. Benoit, F. M., and A. G. Harrison. "Predictive Value of Proton Affinity. Ionization Energy Correlations Involving Oxygenated Molecules," *J. Am. Chem. Soc.* 99:3980—3984 (1977).
74. Das, K. G., A. M. Reddy, M. Vairamani, K. P. Madhusudhanan, D. Fraisse, and J. C. Tabet. "Reduction of Olefinic Bond under Ammonia Chemical Ionization," *Tetrahedron* 40(20):4085—4088 (1984).
75. Griffin, G. W., I. Dzidic, D. I. Carroll, R. N. Stillwell, and E. C. Horning. "Ion Mass Assignments Based on Mobility Measurements. Validity of Plasma Chromatographic Mass Mobility Correlations," *Anal. Chem.* 45(7):1204—1209 (1973).

76. Rosenstock, H. M., K. Draxl, B. W. Steiner, and J. T. Herron. "Energetics of Gaseous Ions," *J. Phys. Chem. Ref. Data* 6 (Suppl. 1):1—783 (1977).
77. Varney, R. N., M. Pahl, and T. D. Mark. "Properties of the Ionic Systems N_4^+ , O_4^+ , and O_4^- ," *Acta Phys. Aust.* 38:287—294 (1973).
78. H. Budzikiewicz, R. T. Alpin, D. A. Lightner, C. Djerassi, R. Mechoulam, and Y. Gaoni, "Massenspektroskopie und Ihre Anwendung auf Strukturelle und Stereochemische Probleme. LXVIII. Massenspektroskopische Untersuchung der Inhaltstoffe von Haschisch," *Tetrahedron* 21:1881—1888 (1965).
79. Claussen, U., H.-W. Fehlhaber, and F. Korte. "Haschisch. XI. Massenspektrometrische Bestimmung von Haschisch-Inhaltstoffen. II," *Tetrahedron* 22:3535—3543 (1966).
80. Harvey, D. J., "The Mass Spectra of The Trimethylsilyl Derivatives of 1 - and 6 -Tetrahydrocannabinol," *Biomed. Mass Spectrom.* 8(12):575—578 (1981).
81. Harvey, D. J. "Mass Spectrometry of the Cannabinoids and Their Metabolites," *Mass Spectrom. Rev.* 6:135—229 (1987).
82. Dzidic, I., D. I. Carroll, R. N. Stillwell, and E. C. Horning. "Atmospheric Pressure Ionization (API) Mass Spectrometry: Formation of Phenoxide Ions from Chlorinated Aromatic Compounds," *Anal. Chem.* 47(8):1308—1312 (1975).
83. Karasek, F. W., S. H. Kim, and H. H. Hill, Jr. "Mass Identified Mobility Spectra of p-Nitrophenol and Reactant Ions in Plasma Chromatography," *Anal. Chem.* 48(8):1133—1137 (1976).
84. Carroll, D. I., I. Dzidic, E. C. Horning, and R. N. Stillwell. "Atmospheric Pressure Ionization Mass Spectrometry" *Appl. Spectros. Rev.* 17(3):337—406 (1981).
85. Truitt, D. B., Jr. "Biological Disposition of Tetrahydrocannabinols," *Pharm. Rev.* 23:273—278 (1971).



Taylor & Francis

Taylor & Francis Group

<http://taylorandfrancis.com>

CHAPTER 6

The Development and Application of a High Resolution Mass Spectrometry Method for Measuring Polychlorinated Dibenzo-p-Dioxins and Dibenzofurans in Serum*

D. G. Patterson, Jr., L. R. Alexander, W. E. Turner, S. G. Isaacs,
and L. L. Needham

INTRODUCTION

Worldwide public concern of the toxicity of polychlorinated dibenzo-p-dioxins (PCDDs) and dibenzofurans (PCDFs) has catalyzed extensive research in many toxicologically related areas. New findings are reported yearly in several scientific meetings, including one international meeting, which concentrates primarily on PCDDs and PCDFs. One of these compounds, 2,3,7,8-tetrachlorodibenzo-p-dioxin (2,3,7,8-TCDD), has been called the most toxic compound synthesized by humans. 2,3,7,8-TCDD is only one of the 22 TCDDs and only one of 75 (mono-octa) PCDDs — there are 135 PCDFs.

* Use of trade names is for identification only and does not constitute endorsement by the Public Health Service or the U.S. Department of Health and Human Services.

None of these chemicals are produced for commercial purposes, but chlorinated dibenzo-p-dioxins and dibenzofurans are produced as trace contaminants in several chemical processes, primarily during the synthesis of chlorinated phenols. For example, 2,3,7,8-TCDD is a by-product in the synthesis of 2,4,5-trichlorophenol, an intermediate in the production of 2,4,5-trichlorophenoxyacetic acid and hexachlorophene. Trace levels of these compounds are also produced during the incineration of waste materials, combustion of leaded gasoline, and the bleaching of wood pulp.

Thus, these compounds can enter the environment by a variety of means. Once there, they are remarkably stable, and many of these compounds, especially those that are substituted with chlorine at the 2,3,7,8 positions and that are also the most toxic, bioaccumulate in the human foodchain. These compounds can generally be found at the parts-per-trillion (ppt) levels in the lipid stores of humans, especially those living in an industrialized society. For example, 2,3,7,8-TCDD is normally found in the adipose tissue and serum of adults at levels below 20 ppt.¹

Because of their lipophilic nature, PCDDs and PCDFs tend to accumulate in the lipid stores of the body. Adipose tissue has been the matrix of choice for measuring these compounds at trace levels because of its high lipid content.²⁻¹⁵ In our first study, we used adipose tissue taken at autopsy to assess body burden levels of 2,3,7,8-TCDD in individuals from the general population in Utah and Georgia.¹⁰ The adipose tissue method was then applied to a study of Missouri residents who had been residentially, recreationally, or occupationally exposed to 2,3,7,8-TCDD-contaminated oils.^{1,9,14} The participation rate in the Missouri study was much less than what we anticipated. We decided, therefore, to develop and validate a serum method to increase the participation rate for large-scale epidemiologic studies.

PCDDs and PCDFs were first measured in the blood of workers from the sawmill, leather, and textile industries by Rappe et al.¹⁶ More recently, Rappe et al. have reported a method for analyzing a large amount of plasma for PCDDs and PCDFs and its application to studies of Vietnam veterans.¹⁷⁻¹⁹ Results from analyzed blood samples taken from occupationally exposed workers in Germany were presented by Selenka.²⁰ Pöpke et al. presented a whole-blood method of analysis for PCDDs and PCDFs at the Dioxin-88 Conference in Umea, Sweden.²¹ We have also recently described a method for PCDD and PCDF analysis in serum,^{22,23} as well as the results of several serum matrix validation studies.²³⁻²⁹ Our serum method is currently being used to measure PCDDs and PCDFs in participants of large-scale epidemiologic studies designed to detect adverse effects in populations with potentially excessive exposure to these compounds.

These studies (U.S. Air Force Ranch Hand; National Institute for Occupational Safety and Health (NIOSH) Occupational Workers; Seveso, Italy, residents) that have detailed medical information, as well as laboratory measurements of PCDDs and PCDFs, offer the best opportunity to find any possible correlation between health effects and exposure.

EXPERIMENTAL

Sample Cleanup and Mass Spectrometry

The Centers for Disease Control (CDC) serum method has been previously presented for 2,3,7,8-TCDD²² and validated for the other PCDDs and PCDFs.²³ Therefore, we will present only a general description of the method. The serum (50 g) was spiked with a mixture of carbon-13-labeled PCDDs and PCDFs and equilibrated at room temperature for 30 min. The serum was extracted with a mixture of saturated ammonium sulfate (100 mL), ethanol (100 mL), and hexane (100 mL), and the hexane layer was then separated. The aqueous phase was again extracted with fresh hexane, and the hexane layers were back-extracted with concentrated sulfuric acid. The hexane extract was then washed with water, dried, and applied to column number one of a five-column cleanup procedure developed by Smith and Stalling³⁰ and modified and semiautomated in our laboratory^{31,32} for human samples. The final sample extract was concentrated to less than 1 mL, then 1 μ L of dodecane was added before it was concentrated to dryness. Just before mass spectral analysis, it was reconstituted to 5 μ L with toluene containing ¹³C₆-1,2,3,4-TCDD as an external standard. The total lipid content of the sample was calculated by a summation procedure²² using the analytically determined concentrations of the individual lipids (total cholesterol, free cholesterol, phospholipids, and triglycerides).

Analyses were conducted on one of three mass spectrometry (MS) systems — VG ZAB-2F, VG-70S, or a VG-70SE — each equipped with a VG 11/250J data system and a Hewlett-Packard 5890 gas chromatograph (GC). The high resolution instrument systems were operated at 10K resolution as defined by a 10% overlap using the peak match unit. Multiple group analyses consisted of two groups — in the first, *m/z* 292.98241 of PFK was used as the reference compound and, in the second, *m/z* 342.97922 of PFK. Injections were 2 μ L of 5 μ L of toluene containing 250 pg of ¹³C₆-1,2,3,4-TCDD. The GC and MS analyzers were operated under computer control to calibrate, acquire raw data, detect and integrate peaks, and print out chromatograms and ASCII output files that are transferred to rBase for DOS data storage on the Division of Environmental Health Laboratory Sciences (EHLS) network system. The analyses were conducted in an isomer-specific mode, with a 60-m, 0.25-mm i.d., 0.2- μ m film thickness SP 2331 capillary column. The GC injector was at 240°C, and the interface was 250°C. The initial column temperature of 100°C was held for 2 min, then programmed to 220°C at 25°C/min and held for 2 min, and then programmed 250°C at 15°C/min and held for 54.2 min. Sixty-five ion fragments were monitored for the 15 PCDD/PCDF analytes. Seven channels were monitored for each analyte: one channel for ¹³C₆-1,2,3,4-TCDD, which was added to each sample to assess the instrument resolving power;²⁷ two channels for the two lockmasses (one to centroid, the other to actually measure the response); and four channels to monitor the native and carbon-13-labeled internal standards. The total run time was 1 hr and 10 min, which represents an adjustment to move the octachlorodibenzo-*p*-dioxin (OCDD) from the previous run away from one of the ion fragments. We calibrated the instrument and checked the resolution

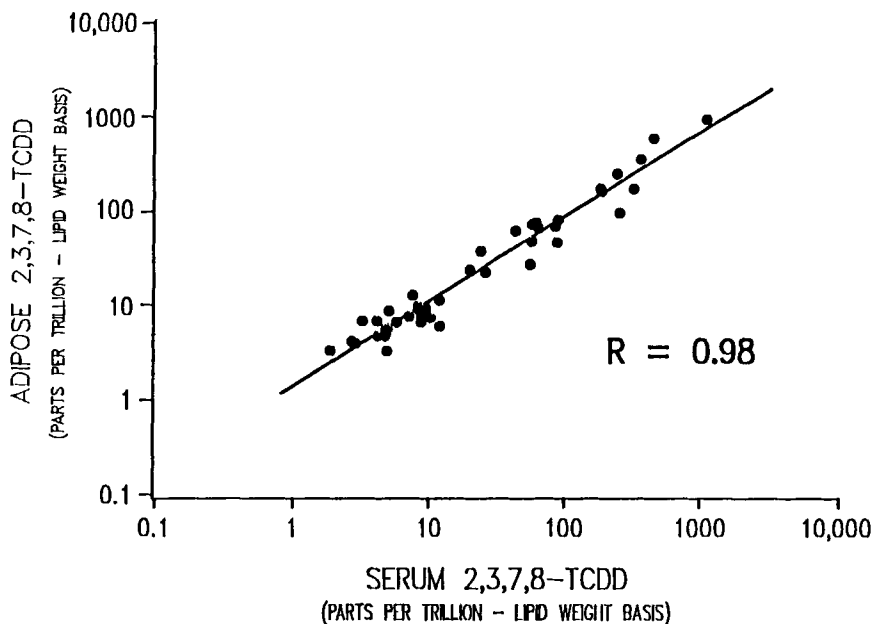


Figure 1. Correlation between human serum (lipid-weight) and adipose tissue (lipid-weight) concentrations of 2,3,7,8-TCDD from Missouri participants.

between each injection using $\sim 0.5 \mu\text{L}$ of 250 high-boiling PCR in the septum reservoir. Each analyte was quantitated by the isotope-dilution technique using linear calibration curves established for each analyte.²⁹

To minimize the possibility for carryover or cross-contamination of samples and analytical standards, the analysts used a separate syringe for each analytical standard. In addition, a glass syringe was used to analyze an unknown or quality control (QC) sample only one time.

Method Validation Studies

Serum and Adipose Tissue Correlation

To assess how well adipose tissue and serum levels of 2,3,7,8-TCDD correlated, we analyzed 2,3,7,8-TCDD in paired serum and adipose tissue samples collected from 50 persons in the State of Missouri.²⁴ The adipose tissue and serum levels ranged over nearly three orders of magnitude (Figure 1). The correlation analysis was performed for the concentration of 2,3,7,8-TCDD in adipose tissue, on both a whole-weight and lipid-weight basis, and the concentration of 2,3,7,8-TCDD in serum on a whole-weight basis and a total-lipid or lipid-fraction-weight basis. The best correlation ($r = 0.976$) was found for adipose tissue 2,3,7,8-TCDD on a lipid-weight basis, with serum 2,3,7,8-TCDD on a total-lipid-weight basis (Figure 1). Adjusting for various serum lipid fractions (total cholesterol; total triglyceride; high,

low, or very low density lipoproteins) did not improve the correlation over adjusting for serum total lipids.

On a whole-weight basis for both adipose tissue and serum 2,3,7,8-TCDD levels, the mean of the partitioning ratios was 158 to 1 (standard deviation = 75.1, standard error = 10.6). On a lipid-weight basis for both adipose tissue and serum, the mean of the partitioning ratio was 1.09 (standard deviation = 0.39, standard error = 0.06). The 95% confidence interval about the mean was 0.97 to 1.21, which includes 1.0. On the basis of these data, a one-to-one partitioning ratio of 2,3,7,8-TCDD between the lipids in adipose tissue and the lipids in serum cannot be excluded. In the past, measurement of 2,3,7,8-TCDD in adipose tissue has been generally accepted as representing the body-burden concentration of 2,3,7,8-TCDD. The high correlation between serum and adipose tissue levels that we measured in this study indicates that serum 2,3,7,8-TCDD is a valid measurement of 2,3,7,8-TCDD body-burden concentrations. The Missouri study^{9,33} allowed us to obtain paired serum and adipose tissue samples from individuals with a wide range of 2,3,7,8-TCDD levels (1.9 to 1,090 ppt). The correlation between serum and adipose tissue of the other PCDDs and PCDFs has not been studied because we could not find a large enough study population with wide ranges of these other congeners. Several results on a few individuals, however, suggest that the higher chlorinated PCDDs and PCDFs may not partition 1:1 on a lipid-adjusted basis.^{34,35} The higher chlorinated PCDDs and PCDFs were higher in their serum on a lipid-adjusted basis than in their adipose tissue on a lipid-adjusted basis.

In Vivo- and In Vitro-Bound PCDDs and PCDFs

As part of our method validation studies, we determined the partitioning of tritiated 2,3,7,8-TCDD (when added in vitro to whole blood) among the cellular, serum protein, and lipoprotein components of blood.²⁵ In three experiments, radioactive ³H-2,3,7,8-TCDD, added to whole blood or to plasma that was recombined with red blood cells (RBCs), was totally recovered in the plasma fraction after we removed the RBCs. We determined that the white blood cellular population contained less than 5% of the ³H-2,3,7,8-TCDD added to the whole blood. Because tritium was quenched by hemoglobin and the serum, the absolute analytical measurement error was 5%. The recoveries of ³H-2,3,7,8-TCDD averaged between 84 and 89% (n = 3) in the lipoprotein fraction from whole blood and reconstituted blood. The distribution of the ³H-2,3,7,8-TCDD among the various lipoprotein subfractions indicated a greater percentage associated with low density lipoproteins (LDL) (55.3% ± 9.03%) than with very low density lipoproteins (VLDL) (17.4% ± 9.07%) or high density lipoproteins (HDL) (27.3% ± 10.08%). The protein fraction (> 1.26 g/mL) contained between 11 and 16% of the added tracer. Column chromatography of the protein fraction (~15% of the total radioactivity added to whole blood) indicated that most of the ³H-2,3,7,8-TCDD in this fraction was associated with proteins in the molecular weight range of <70,000 Da. The major peak corresponded to the elution profile of human serum albumin.

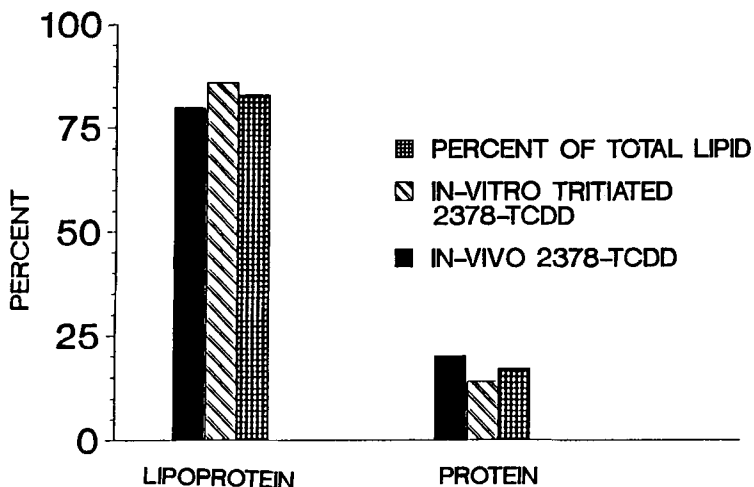


Figure 2. The in vivo and in vitro distribution of 2,3,7,8-TCDD in human serum.

We extended our validation studies to determine the in vivo distribution of the PCDDs and PCDFs in the various compartments of blood.²³ The distribution of 2,3,7,8-TCDD between the lipoprotein and protein fractions of serum is shown in Figure 2. The data in Figure 2 illustrate that 2,3,7,8-TCDD distributes between these two blood compartments according to the respective lipid content of the fraction. We have previously found a very good correlation for 2,3,7,8-TCDD partitioning between adipose tissue and serum when both are adjusted for their respective lipid content.²⁴

Unlike 2,3,7,8-TCDD, however, the higher chlorinated PCDDs and PCDFs do not appear to partition according to the lipid content of the fractions. As the degree of chlorination of the PCDD or PCDF increases, the percentage associated with the protein fraction also increases (see Figures 3 and 4). Because of the literature reports of the distribution of PCBs and pesticides,³⁶ this result was not anticipated. Our results suggest a more specific binding to the protein fraction for the PCDDs and PCDFs than for the PCBs. This may possibly explain the lack of a 1:1 correlation for the higher chlorinated PCDDs and PCDFs between adipose tissue and serum.^{34,35} Because very few paired samples of adipose tissue and serum have been analyzed, however, more work needs to be done to verify the lack of a 1:1 correlation for the higher chlorinated PCDDs and PCDFs over a wide range of concentrations.

We also estimated the PCDD and PCDF content of the RBCs by analyzing 100 g of washed RBCs that had been separated from the plasma fraction. An average of 9% (range of 6 to 13%) of the PCDDs and PCDFs in whole blood were associated with the RBC fraction.³⁷

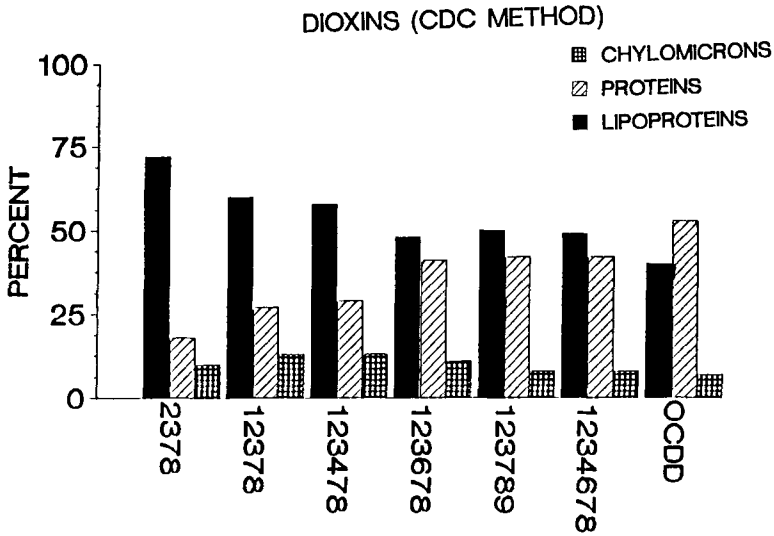


Figure 3. The in vivo distribution of PCDDs in human blood fractions.

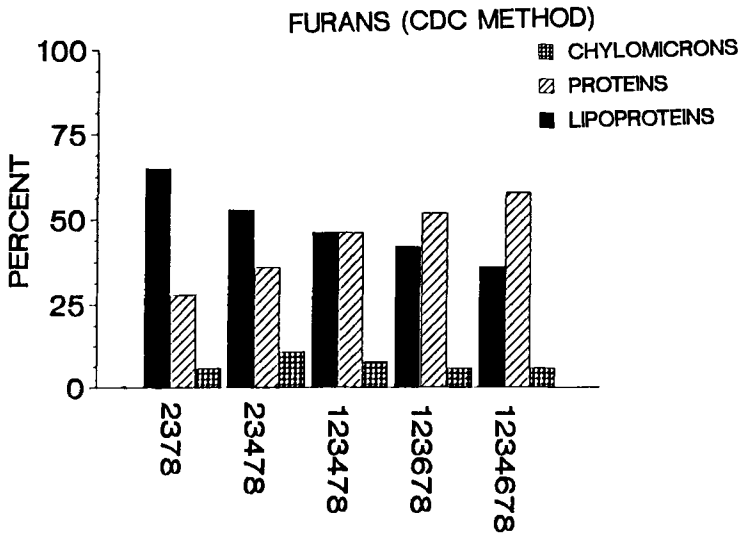


Figure 4. The in vivo distribution of PCDFs in human blood fractions.

Fasting Versus Nonfasting Blood Samples

Hansson et al.³⁸ studied PCDD and PCDF levels in pre- and postfasting blood in Vietnam veterans. The men “ate a light dinner” and donated 100 to 200 mL of blood. They then fasted for 16 to 18 hr and again donated 100 to 200 mL of blood. The results showed a small average increase for 2,3,7,8-TCDD of 13.5% in the postfast samples (the level in four men decreased and in nine men increased). Because the percent change for six men with levels below 5 ppt could be within the experimental error, the authors also calculated an average increase of 11.3% for the remaining seven men (the level decreased in two men and increased in five men). The authors concluded that “the overall pattern is consistent with a small increase in the blood levels in most cases upon which is superimposed a combination of individual variability among the subjects and analytical variability as well.”

Because dioxin measurements in the general population require a great deal of serum, we conducted a study for measuring the relationship between serum levels of PCBs; p,p'-DDE; and hexachlorobenzene.³⁹ Twenty healthy adult humans had serum samples drawn on four occasions within a 24-hr period — after a 12-hr overnight fast, 4 to 5 hr after a high-fat breakfast, at midafternoon, and the next morning after another 12-hr fast. Nonfasting samples had 22 to 29% higher mean concentrations ($p < 0.05$) than did fasting samples for PCBs (4.81 versus 3.74 ng/g serum wt), hexachlorobenzene (0.163 versus 0.134 ng/g serum wt), and p,p'-DDE (6.74 versus 5.37 ng/g serum wt). Total serum lipids were estimated from measurements of total cholesterol, free cholesterol, triglycerides, and phospholipids, and were 20% higher in nonfasting samples than in fasting samples (7.05 g/L versus 5.86 g/L). When PCBs, hexachlorobenzene, and p,p'-DDE concentrations were corrected by total serum lipids, results from fasting and nonfasting samples were not statistically different. Because of the differences in these chlorinated hydrocarbon concentrations observed with different sample collection regimens, we concluded that meaningful comparison of data on measurements of toxicants in serum required standardizing collection procedures or correcting by total serum lipid levels.

Quality Assurance

Quality assurance (QA) of analytical measurements has two essential elements.²⁸ The first is quality control (QC), which involves developing and adhering to standard operating procedures for all aspects of method performance. The second is quality assessment, which involves the use of techniques (e.g., control charts) to assess the quality of the measurement process and the results.

Quality Control

We have developed a standard operating procedures (SOP) manual that provides detailed procedures for all aspects of data and sample handling, sample cleanup, and MS.²⁸ A database (Dioxin1) has been set up on an IBM-PC network using rBase for DOS (Microrim, Inc.). The database is used for storage, retrieval, and analysis

of all data from the Dioxin Group projects. Data are entered into one of four files: (1) demographic data file (Special Activities Branch — one medical technologist), (2) lipid data file (Clinical Biochemistry Branch — two medical technologists), (3) sample cleanup data file (Toxicology Branch — eight chemists, using six automated extraction systems), and (4) mass spectral data file (Toxicology Branch — six mass spectrometer operators, using five mass spectrometers). Figure 5 shows an overview of supervisory controls and access to the Dioxin1 database. Sample

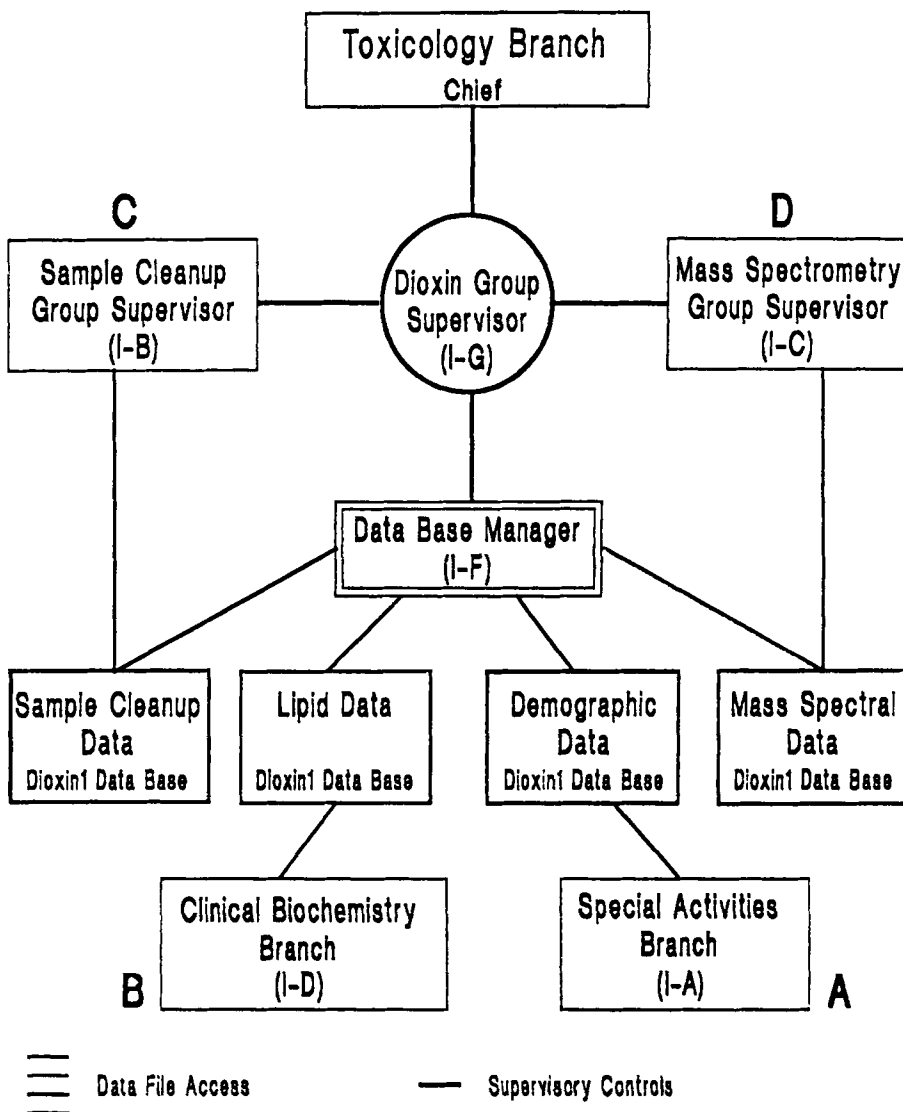


Figure 5. Supervisory controls and access to the dioxin1 database.

and data flow to and from the four groups have been previously described in detail.²⁸ Three levels of password protection are used in the database. Level one allows the data from each group to be entered, edited, and printed. Level two is used by the group supervisor. After the supervisor has checked the data to ensure proper entry, the data are verified by entering initials and the date. Once the data are verified, they can no longer be edited, except by the database manager, who has the level three password. Verified data cannot be changed by the database manager except by written request from the appropriate supervisor, which has been approved by the Dioxin group supervisor.

Quality Assessment

After the information from each of the various groups has been entered, edited, and verified in the Dioxin database, the four files are merged by the database manager and transferred from the PC network to our IBM 3091 mainframe computer. This composite disc file contains more than 70 variables associated with each analyte and sample type (e.g., 15 different PCDDs and PCDFs, blanks, standards, QC, unknown samples) and is updated weekly. This system allows timely access to the data for quality assessment activities.

All of our data manipulations are carried out using the Statistical Analysis System (SAS Institute, Inc.). Because of the many and varied types of reports, data plots, and statistical treatments used in our overall quality assurance program, a modular approach has been adopted. A custom program has been written for each function, each of which can be run independently of the others as needed. A few examples of these quality assessment functions are given below for 2,3,7,8-TCDD. Each function can also be applied to each of the other PCDDs and PCDFs.

Calibration Curves A series of 16 analytical standards are used to establish linear calibration curves for each analyte using the isotope-dilution techniques.²⁹ An example of the calibration curve for 2,3,7,8-TCDD on one of our instruments plotted over three different ranges is shown in Figure 6.

QC Materials One of the most important features of our QC program is the use of matrix-based materials that are well characterized for PCDD and PCDF concentrations to ensure that the analytical system is in control. Ten human serum pools that have been dispensed into various sized aliquots can be inserted into an analytical run. The statistical data for 2,3,7,8-TCDD in these pools are given in Table 1 and for all of the PCDDs and PCDFs from one pool in Table 2.

QC Concentration and Isotope Ratios QC charts graphically document the performance of the analytical system. Figure 7 shows a portion of the concentration QC chart for Pool J along with the 95 and 99% confidence intervals established for this pool. Figures 8 and 9 show a portion of the QC charts established for 2,3,7,8-TCDD and ¹³C₁₂-2,3,7,8-TCDD isotope ratios. These charts and confidence intervals are used to decide if an analytical run or individual sample is in control.

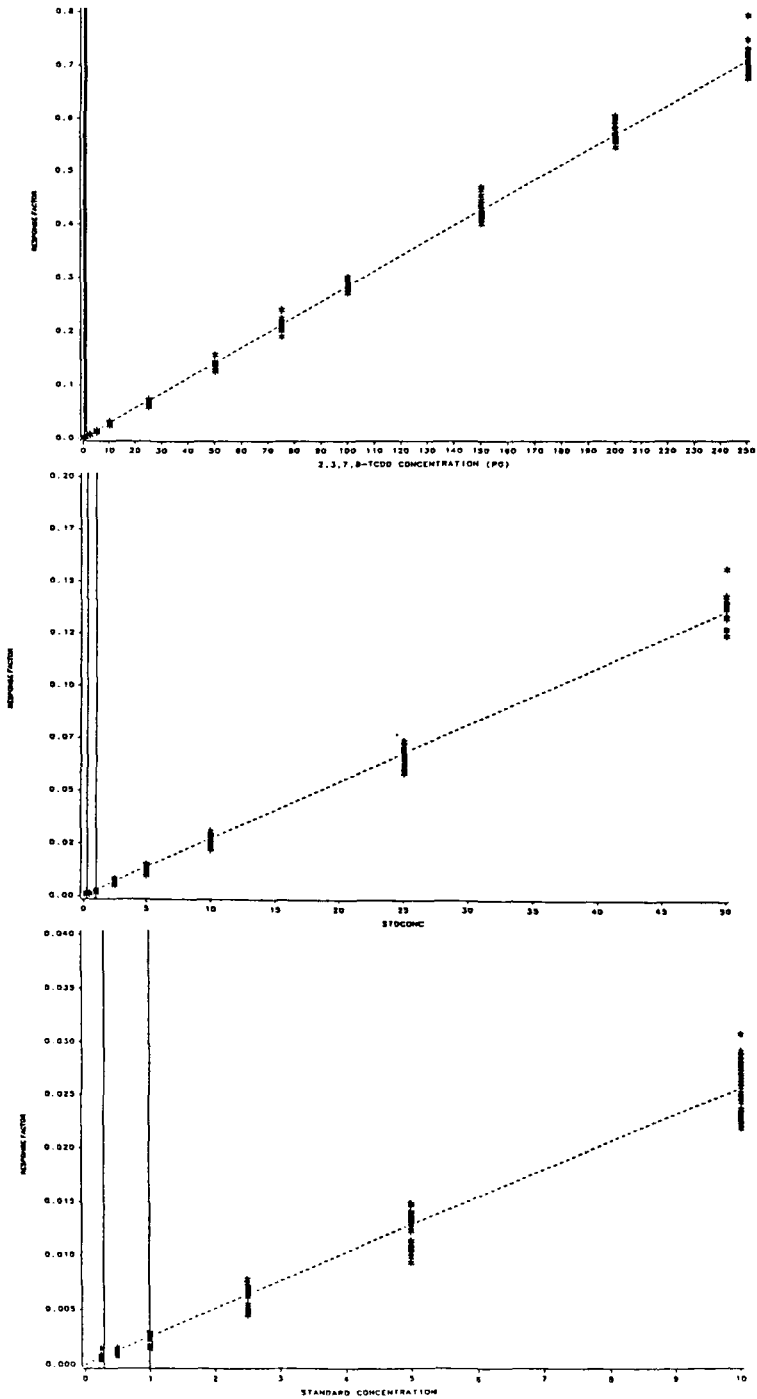


Figure 6. 2,3,7,8-TCDD standard curve for the ZAB-2F over three different ranges (n = 1000).

Chromatographic Isomer Specificity and Instrument Resolving Power We use the external $^{13}\text{C}_6$ -1,2,3,4-TCDD standard, which is spiked into every sample before mass spectral analysis, to monitor the chromatographic isomer specificity. Figure 10 shows a portion of the QC chart that monitors the retention time of $^{13}\text{C}_6$ -1,2,3,4-TCDD relative to $^{13}\text{C}_{12}$ -2,3,7,8-TCDD. The decrease in chromatographic separation between these two compounds over time is evident in the QC chart. We also use the (P + 6) ion m/z 331.9078 of $^{13}\text{C}_6$ -1,2,3,4-TCDD and m/z 331.9368 of $^{13}\text{C}_{12}$ -2,3,7,8-TCDD to demonstrate 10,000 resolving power (RP) for each mass spectral analysis. To completely separate these two ions requires >11,400 RP and, therefore, at 10,000 RP the ratio of the peak on the $^{13}\text{C}_{12}$ -2,3,7,8-TCDD (331.9368) channel due to $^{13}\text{C}_6$ -1,2,3,4-TCDD to the peak on the $^{13}\text{C}_6$ -1,2,3,4-TCDD (331.9078) channel can be plotted for each analysis. Figure 11 shows a portion of the instrument RP chart along with the upper 95 and 99% confidence intervals which are used to ensure that the instrument remains at 10,000 RP during the analysis of each sample. The external standard $^{13}\text{C}_6$ -1,2,3,4-TCDD has also been added to each of our analytical standards, and we use the ratio between $^{13}\text{C}_6$ -1,2,3,4-TCDD and $^{13}\text{C}_{12}$ -2,3,7,8-TCDD to calculate the percent recovery of the internal standard for each sample that is analyzed.

Table 1. Statistical Data for 2,3,7,8-TCDD (ppq) in the Human Serum QC Pools

	H ^a	I ^b	J ^b	K ^a	L ^a	M ^b	N ^a	O ^b	P ^a
Mean (ppq)	6830	25.8	22.1	69.1	1930	20.8	164.4	18.8	168.7
SD	640	3.4	3.4	9.0	300	3.2	13.2	3.3	22.7
CV (%)	9.4	13	15.3	13.1	15.5	15.3	8.0	17.4	13.5
n	8	20	105	134	22	150	38	165	34
Sample size (g)	10	200	100	100	10	100	100	100	50

^a Spiked serum.

^b Normal nonspiked serum.

Table 2. Statistical Data for PCDDs and PCDFs (ppq) in Human Serum QC Pool-P (50-g Samples)

Congener	Mean	SD	N	CV	LOD ^a	LOQ ^b
2378D	168.7	22.7	34	13.5	6	14
12378D	197.4	23.3	42	11.8	9	21
123478D	206.6	28.7	40	13.9	6	14
123678D	506.2	58.5	41	11.5	6	14
123789D	187.8	25.3	40	13.5	6	14
1234678D	761.9	90.6	42	11.9	15	35
OCDD	5,472	934	8	17.1	33	77
2378F	143.1	14.9	38	10.4	6	14
12378F	ND	—	43	—	15	35
23478F	42.5	7.8	28	18.4	6	14
123478F	61.8	11.8	22	19.0	6	14
123678F	41.5	9.7	26	23.3	6	14
123789F	ND	—	43	—	6	14
234678F	ND	—	43	—	6	14
1234678F	155.8	19.3	24	12.4	6	14
1234789F	ND	—	43	—	9	21

^a LOD is limit of detection for a 100-g sample.

^b LOQ is limit of quantification for a 100-g sample.

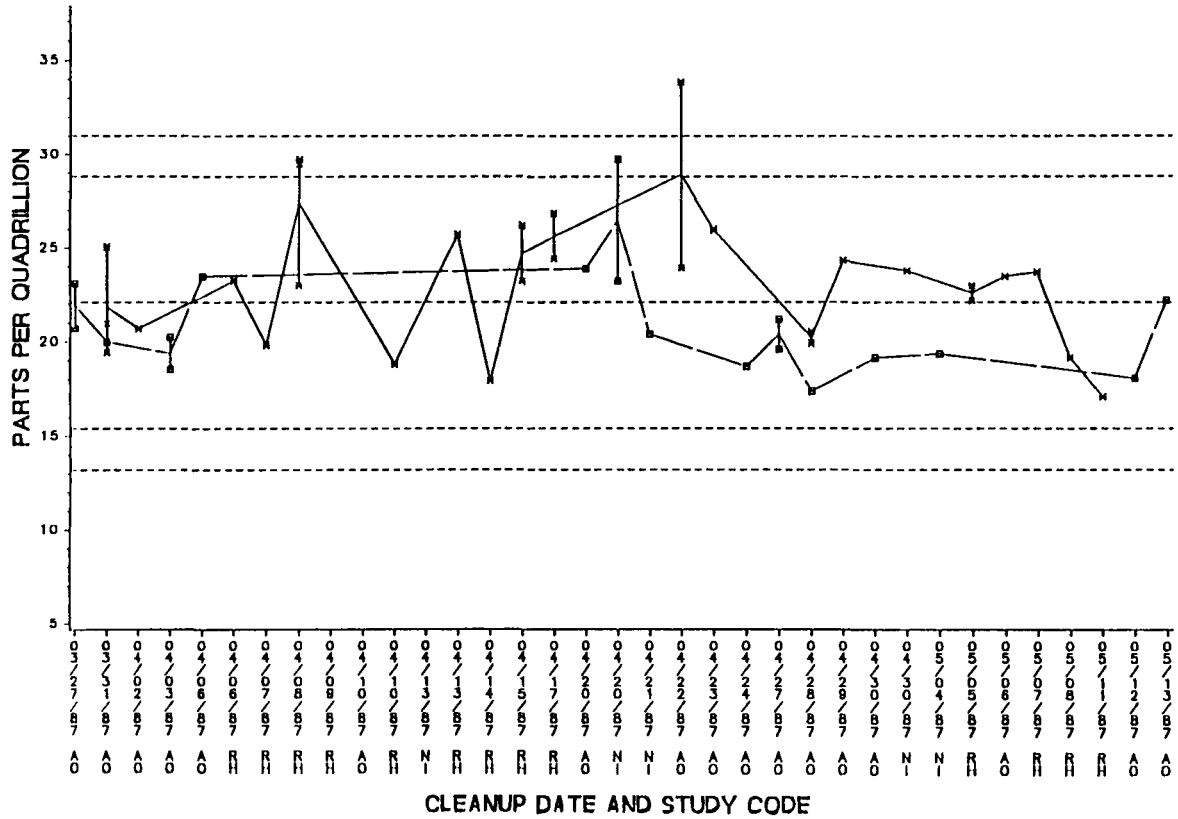


Figure 7. A portion of the serum 2,3,7,8-TCDD concentration QC Pool J chart for two mass spectrometers. Mean = 22.1; SD = 3.39; CV = 15.3

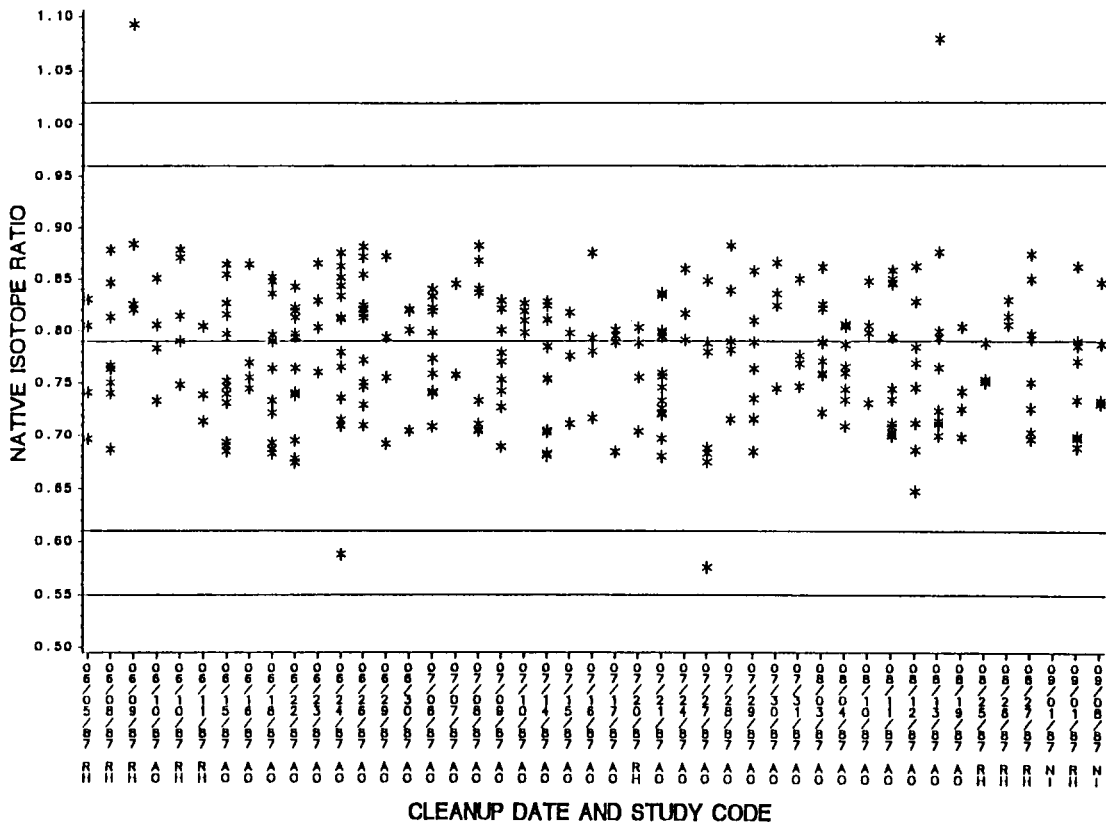


Figure 8. A portion of the m/z 320/322 (2,3,7,8-TCDD) isotope ratio chart for QC and unknown samples.

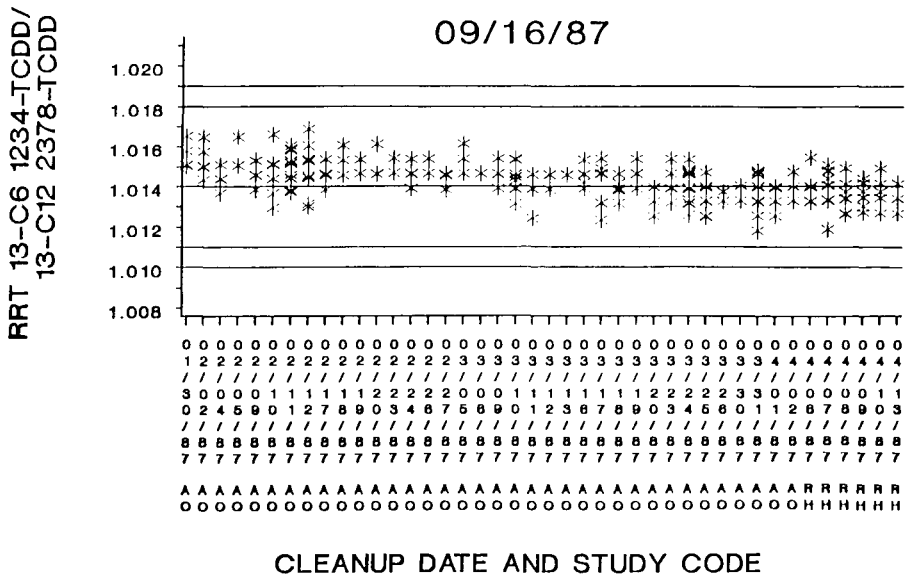


Figure 10. A portion of the chromatographic isomer specificity index chart for QC and unknown samples.

Percent Recovery of the Internal Standard The recovery of the internal standard is used not only as a QC parameter to assess the acceptability of a particular analysis, but also to assess potential bias in the method. Figures 12 and 13 show that the concentration in both QC material and unknown samples is independent of the internal standard recovery. Recovery of the internal standard as low as 10% still provides acceptable quantification (Figure 12). Sample sizes of less than 10 to 200 g are provided to the laboratory from various studies. Figure 14 illustrates that the recovery of the internal standard is independent of the sample size.

Study Sample Size Figure 15 illustrates that the concentrations calculated from various sample sizes are unbiased over a range of sample sizes from the Agent Orange Validation Study.⁴⁰ The lower sample weights (<60 g) were generally repeat analyses from individuals whose first sample (>60 g) was rejected because one or more of the QC requirements was not met.

Signal-to-Noise Ratio The sensitivity of the MS can vary from day-to-day, and thus the signal-to-noise (S/N) ratio for detected peaks will also vary. Figure 16 shows a position of the chart used to monitor this ratio, which shows that because of the use of an isotopically labeled internal standard (isotope-dilution mass spectrometry), the calculated concentration remains fairly stable over a wide range of S/N ratios.

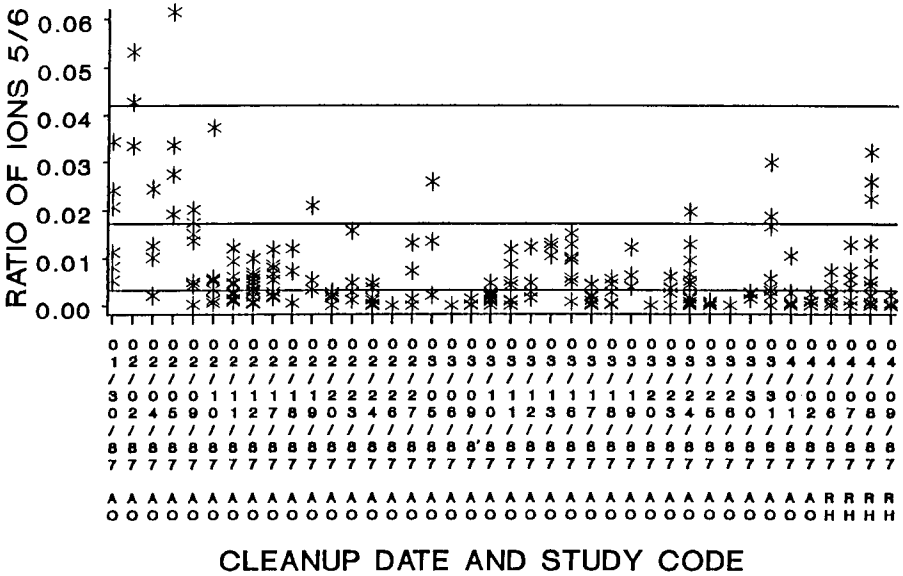


Figure 11. A portion of the instrument resolving power chart for QC and unknown samples.

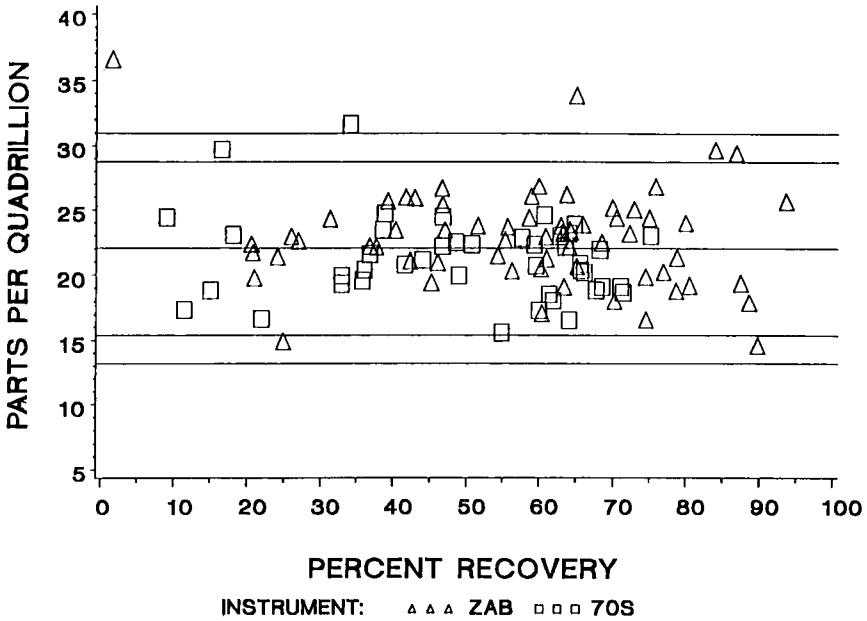


Figure 12. Percent recovery of the internal standard versus the concentration in QC Pool J for two instruments.

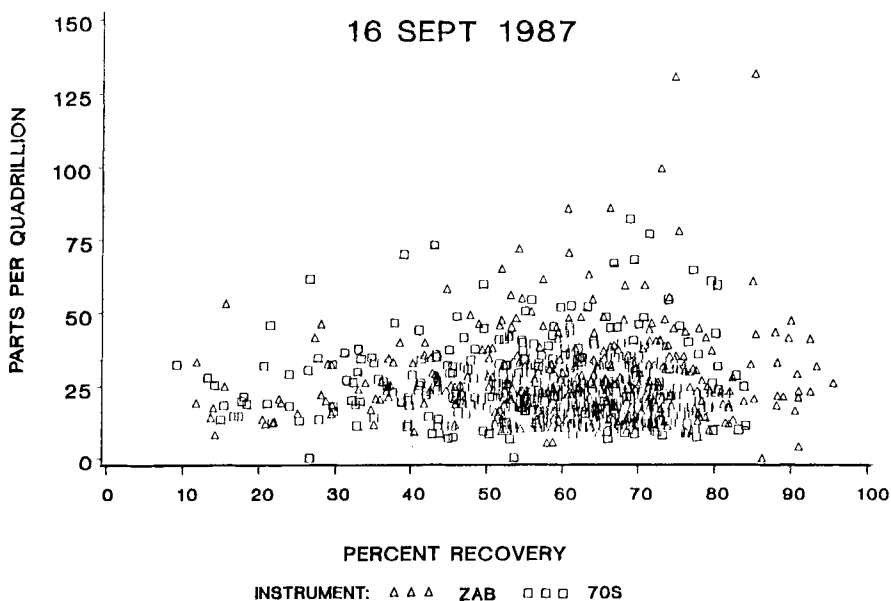


Figure 13. Percent recovery of the internal standard versus the concentration in Agent Orange serum samples.

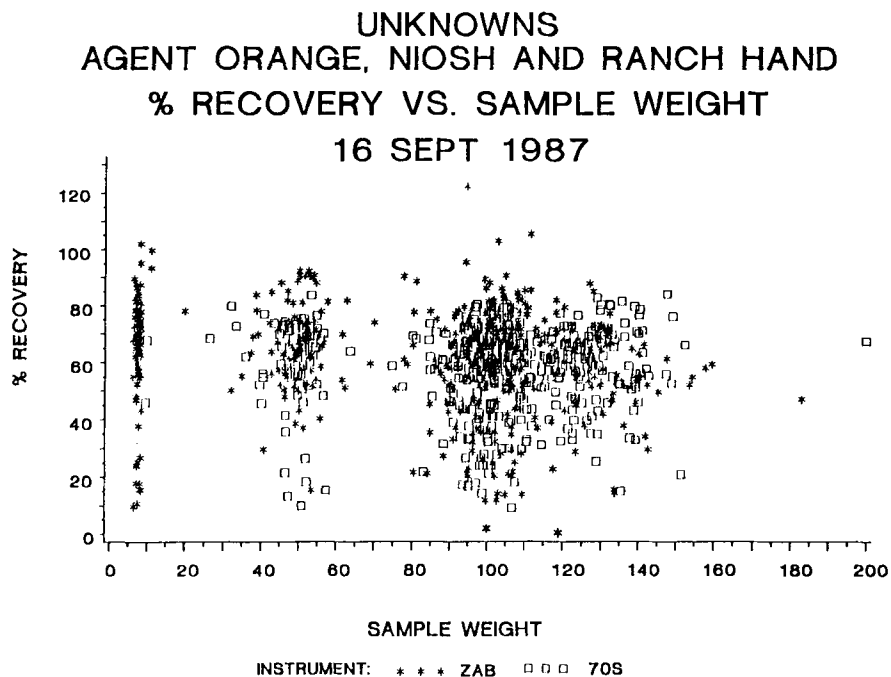


Figure 14. Percent recovery of the internal standard versus the sample weight from various studies.

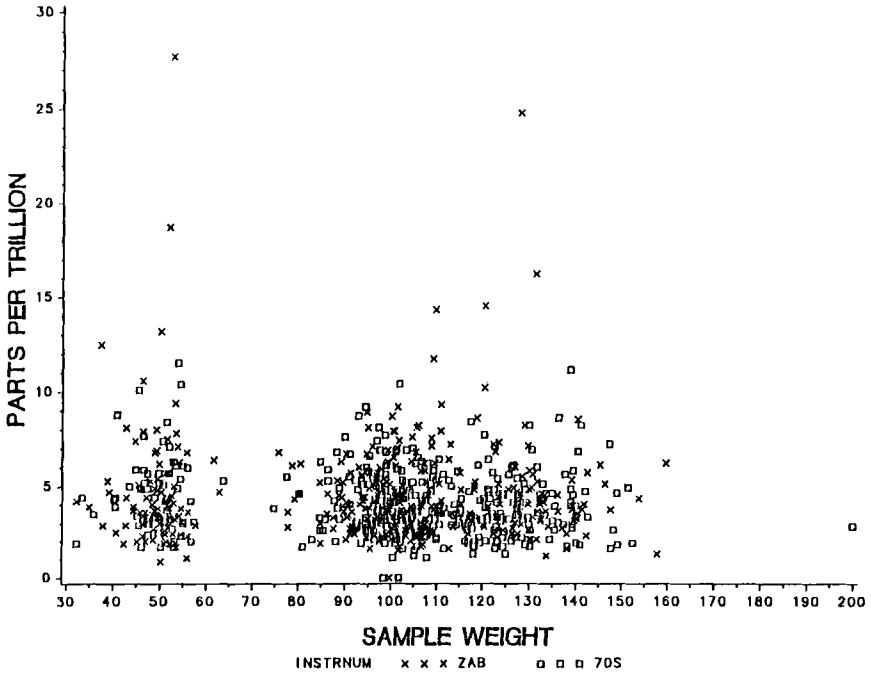


Figure 15. Concentration of 2,3,7,8-TCDD versus sample weight for samples from the Agent Orange validation study.

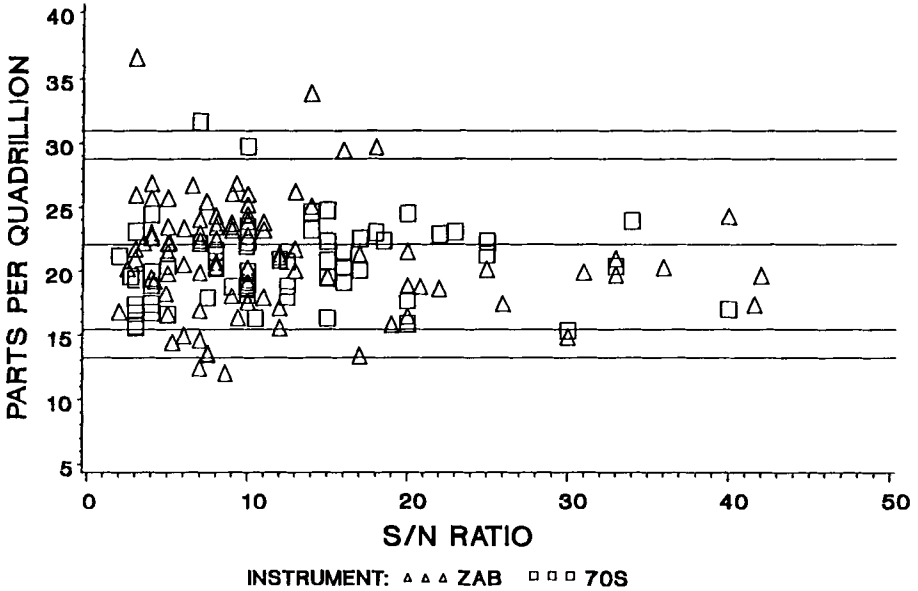


Figure 16. Concentration of 2,3,7,8-TCDD versus signal-to-noise ratio for QC Pool J.

Summary of Quality Assessment Functions All of the quality assessment functions outlined previously have options that allow an examination of each function for individual PCDDs and PCDFs as well as for individual analysts, MS operators, cleanup apparatus, time periods, and studies. Overall, the aforementioned quality assessment functions are used to document that the analytical measurement system is operating in a state of statistical control. In addition to this documentation, a sample or QC material is not considered reportable unless it meets all of the numerous, previously reported criteria for a valid result.^{22,27} All of these criteria have been incorporated into a computer program that is used by the Dioxin group supervisor to facilitate the final study data review. The output of this program identifies those variables that do not meet specifications.

Method Performance

With regular routine maintenance of the mass spectrometers, a limit of detection (LOD) of 6 ppq and a limit of quantification (LOQ) of 14 ppq for a 100-g sample containing 2,3,7,8-TCDD can be achieved for routine samples. The LODs/LOQs for the PCDDs and PCDFs are given in Table 2 and have been calculated by methods described previously.⁴¹⁻⁴³ Figure 17 illustrates the expected false positive/negative rate at the LOD (~5.5%) and LOQ (~0.5%) at the 95% confidence level. Figures 18 and 19 illustrate the within-vial reproducibility on the same instrument for QC and unknown samples, while Figure 20 shows duplicate analyses from the same

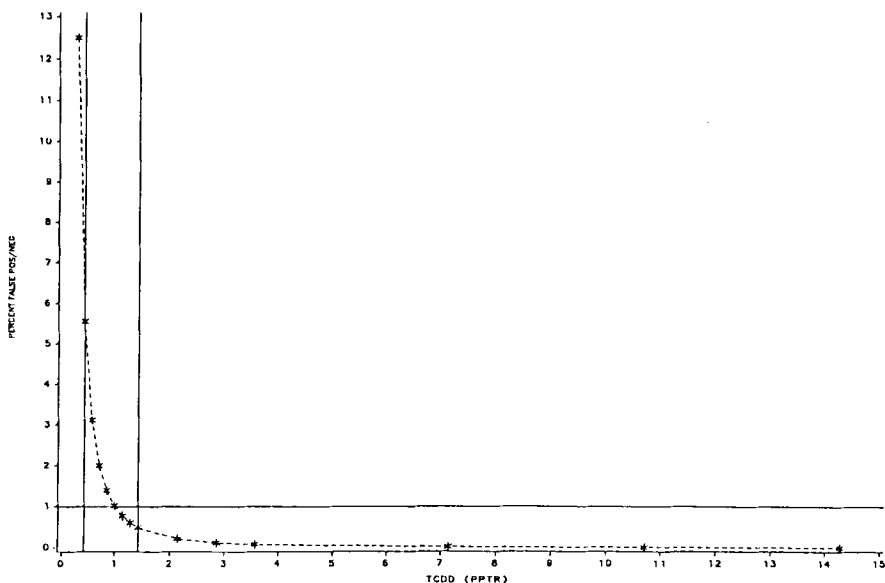


Figure 17. False positive/negative rate versus concentration for 2,3,7,8-TCDD.

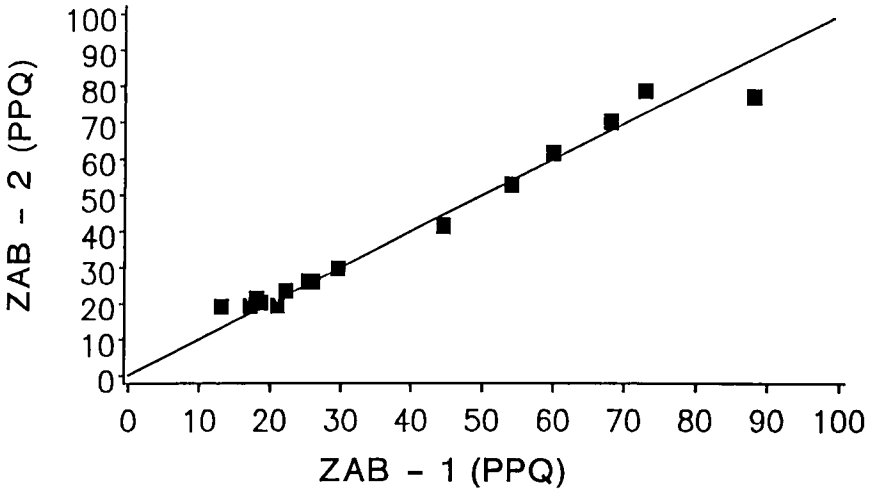


Figure 18. Duplicate analyses of the same QC sample extract on the same mass spectrometer.

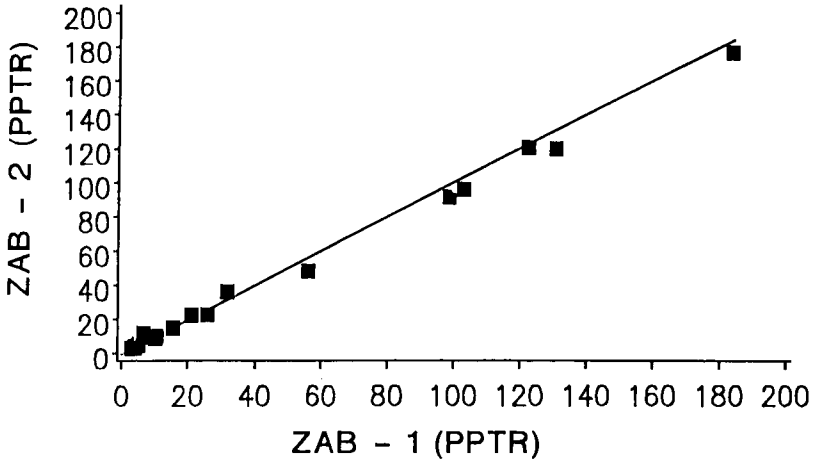


Figure 19. Duplicate analyses of the same unknown sample extract on the same mass spectrometer.

sample extract on two different mass spectrometers. The data shown in Figures 18 to 20 represent the worst case since all data were plotted, including analyses that did not meet all of our QC requirements. In general, about 20% of the samples do not meet one or more of our many quality control requirements on the first analysis. Approximately 80% of these samples will meet all QC requirements upon repeat mass spectral analysis.

RESULTS FROM VARIOUS STUDIES

Vietnam Veterans

From 1962 to 1970, the herbicide Agent Orange [a 1:1 mixture of 2,4-dichlorophenoxyacetic acid (2,4-D) and 2,4,5-trichlorophenoxyacetic acid (2,4,5-T) in diesel oil] was used as a defoliant in Vietnam. The herbicide was contaminated from less than 1 to greater than 20 ppm with 2,3,7,8-TCDD, which was formed as an unintentional by-product during the manufacture of 2,4,5-T. Many Vietnam veterans expressed concern that their health may have been adversely affected by exposure to Agent Orange and its 2,3,7,8-TCDD contaminant. In response to these concerns, the U.S. Congress passed in 1979 Public Law 96-151 (HR 3892) mandating epidemiologic studies of possible health effects in Vietnam veterans due to exposure to herbicides.

New Jersey⁴⁴ and Massachusetts,⁴⁵ the CDC,^{40,46-49} the U.S. Air Force,⁵⁰⁻⁵² and the Veterans Administration (VA)² have all conducted studies on Vietnam veterans. Gross et al.,² in a VA-sponsored study, were the first to measure 2,3,7,8-TCDD levels in the adipose tissue of Vietnam veterans some 10 years after their exposure had ceased. The results of this study showed that several veterans who were classified as "heavily exposed" had 2,3,7,8-TCDD levels above the levels in a group of veterans classified as "nonexposed." This finding, along with the study by Rappe et al.⁵³ showing detectable levels of PCDFs in the blood of survivors of the Yusho incident in Japan about 11 years after their exposure ceased, suggested that elevated levels of 2,3,7,8-TCDD might still be measured in veterans many years after their exposure. The veterans in studies that actually measured 2,3,7,8-TCDD

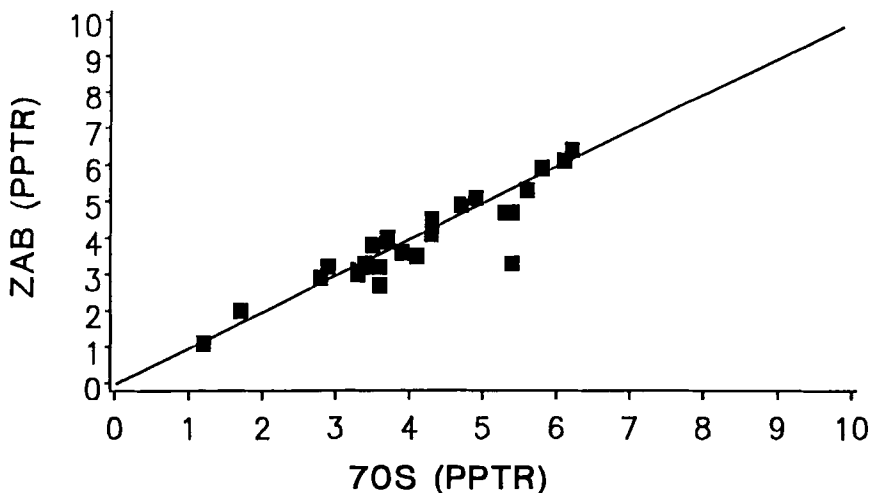


Figure 20. Duplicate analyses of the same unknown sample extract on two different mass spectrometers.

body burden levels can be subdivided into two groups: (1) those veterans who handled Agent Orange as part of their military duties (Operation Ranch Hand), and (2) those veterans who served in a combat role but did not directly handle Agent Orange (ground troops). The largest such studies have been conducted by the CDC and the U.S. Air Force in collaboration with the CDC.

Ground Troops

A large-scale study of U.S. Army veterans was conducted by the CDC⁴⁰ to determine if military records could be used to identify veterans exposed to Agent Orange. The CDC compared current serum 2,3,7,8-TCDD levels of Vietnam veterans with exposure estimates based on military records and with TCDD levels of veterans not serving in Vietnam. The indirect exposure measures were as follows: (1) weighted number of days within 2 km of an Agent Orange spray within 6 d after the spray, (2) weighted number of days within 2 km of a previous Agent Orange spray, (3) the same scores for sprays with unknown herbicide agents, (4) the number of days in five heavily sprayed areas, and (5) two self-reported measures of exposure. None of the indirect measures of exposure and neither type of self-reported exposure identified Vietnam veterans who were likely to have currently elevated serum TCDD levels. The distributions of current TCDD levels were nearly identical (Figure 21) in Vietnam (mean 4.2 ± 2.6 ppt, $n = 646$) and non-Vietnam (mean 4.1 ± 2.3 ppt, $n = 97$) veterans. Two Vietnam veterans had levels above 20 ppt as shown in Figure 21 (TCDD levels in individuals from the general population generally are below 20 ppt).¹ These two men each reported their health status as "excellent" and did not attribute any health problems to Agent Orange exposure.

Agent Orange Handlers

In 1978, the U.S. Air Force responded to the Congressional mandate with the Air Force Health Study of all 1,267 members of the Air Force Ranch Hand unit and a series of matched controls. The two groups were given detailed physical examinations in 1982,⁵⁴ 1985,⁵⁵ and 1987 to 1988. These same veterans will be examined again in 1992, 1997, and 2002. In 1987, the Air Force, in collaboration with CDC, conducted a pilot study to evaluate the Air Force exposure index for Ranch Hand veterans. The pilot study measured 2,3,7,8-TCDD levels in 150 Ranch Hand veterans and in 50 controls. The results from this study showed a large difference between the mean level in the Ranch Hand veterans (49 ppt, $n = 147$) and the controls (5 ppt, $n = 49$). Also, the distribution of levels in the two groups differed markedly (Figure 22) and indicates that some Ranch Hand personnel have had above background 2,3,7,8-TCDD exposure. As the data plotted in Figure 22 shows, however, approximately 38% of the Ranch Hand veterans had levels less than 20 ppt, which is within the range normally found in unexposed populations.¹ The Air Force decided to analyze the serum from nearly all members of the Ranch Hand unit for 2,3,7,8-TCDD. These analyses will be completed in 1991, at which

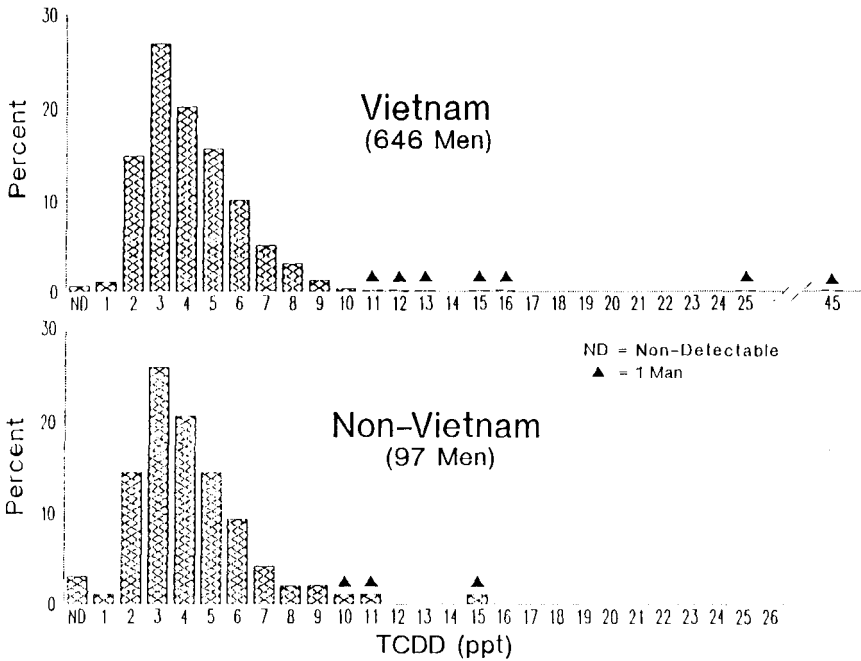


Figure 21. Serum 2,3,7,8-TCDD levels of Vietnam and non-Vietnam veterans in the Agent Orange validation study.

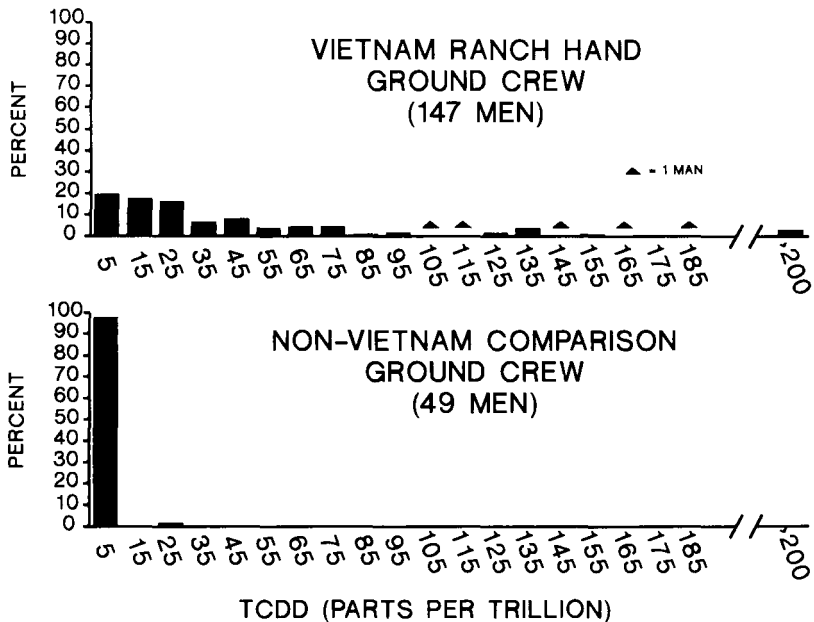


Figure 22. Serum 2,3,7,8-TCDD levels of Ranch Hand and control veterans in the 1987 Air Force health study.

time the relationship between TCDD levels and the many health status parameters measured in the Ranch Hand Study will be determined.

Two other studies funded by the States of New Jersey⁴⁴ and Massachusetts⁴⁵ have determined PCDD and PCDF levels in small cohorts of Vietnam veterans (ground troops and Agent Orange handlers). Both studies found that Agent Orange handlers had elevated 2,3,7,8-TCDD levels in blood and adipose tissue, but ground troops were within the normal background range. These results are consistent with the CDC and Air Force studies.

2,3,7,8-TCDD Half-Life in Humans

The half-life of 2,3,7,8-TCDD in most animals is much less than 1 year with some variability among species. The half-life in monkeys has been reported to be just over 1 year (391 days).⁵⁶ There are several studies which indicate that the half-life in humans may be longer than 1 year. The finding of elevated 2,3,7,8-TCDD levels in occupationally exposed workers many years after their exposure ceased was used to suggest that 5 to 8 years was a more reasonable estimate of TCDD half-life in humans.⁹ A researcher who had ingested radiolabeled 2,3,7,8-TCDD estimated a half-life of 5.8 years based on his urinary and fecal excretion.⁵⁷ Because of the very limited half-life data available, the CDC in collaboration with the U.S. Air Force conducted a study of Vietnam veterans to better estimate the half-life of 2,3,7,8-TCDD in humans.⁵⁰ In this study, 2,3,7,8-TCDD levels were determined for 36 Ranch Hand veterans in serum collected in 1987 as well as in serum from the same individuals which had been collected and stored since 1982. The median half-life for these 36 Ranch Hand veterans was 7.1 years (95% confidence interval about the median of 5.8 to 9.6 years).

A half-life of 7 years in humans suggests that about two to four 2,3,7,8-TCDD half-lives have elapsed since the potential exposure of Vietnam veterans to Agent Orange and that 2,3,7,8-TCDD can serve as a biological marker for previous TCDD exposure in Vietnam veterans.

Seveso, Italy

In July of 1976, an explosion occurred at a factory producing 2,4,5-trichlorophenol in Meda, Italy, which resulted in contamination with 2,3,7,8-TCDD of parts of the towns of Seveso, Meda, Cesano Maderno, and Desio. Within 20 d of the explosion, Italian authorities had evacuated all families from the area immediately surrounding the explosion site (Zone A) and had taken measures to minimize exposure of nearby residents (Zone B). The blood and adipose tissue of one person (resident within Zone A) who died from pancreatic adenocarcinoma 7 months after the explosion were measured for 2,3,7,8-TCDD. Her 2,3,7,8-TCDD levels (whole-weight bases) were 1840 ppt in adipose tissue and 6 ppt in blood.⁵⁸

In April 1988, Italian scientists and the CDC agreed to analyze 30 of the more than 30,000 serum samples (1 to 3 mL) that had been collected from residents of four zones during July 1976 through 1985. This pilot study⁵⁹ was to assess whether

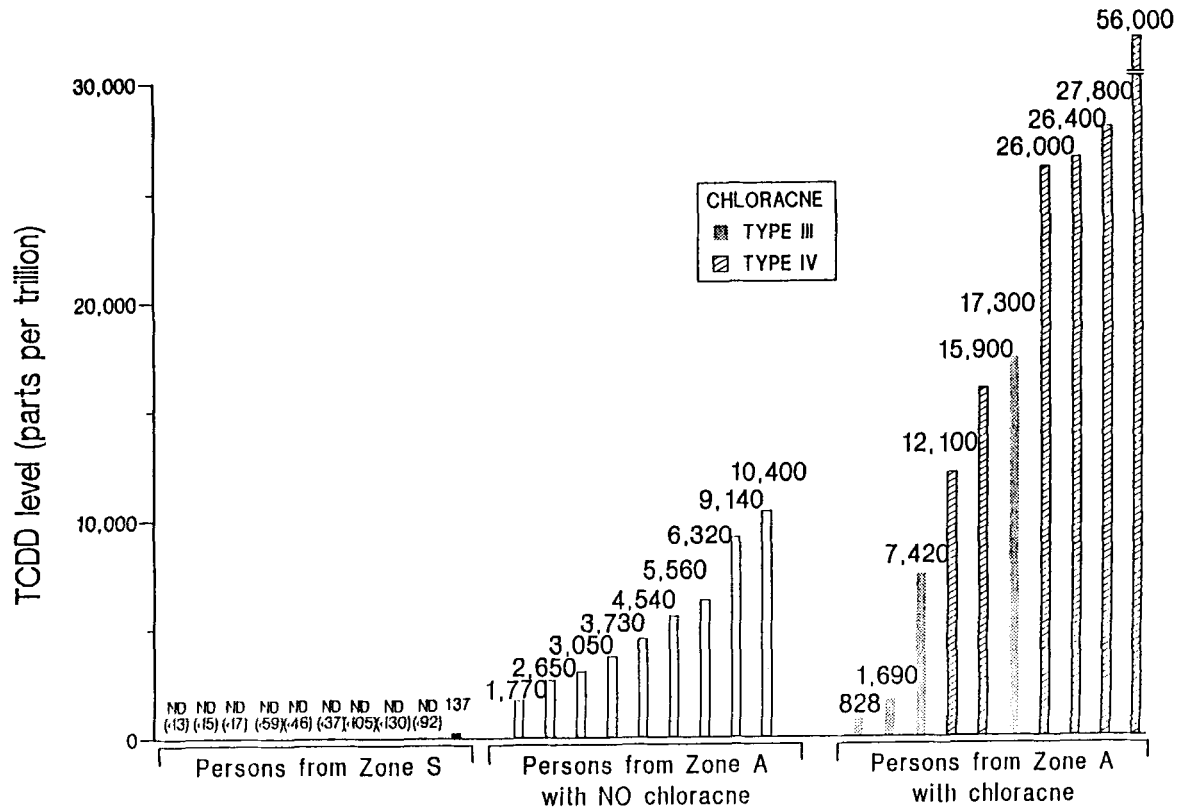


Figure 23. Serum 2,3,7,8-TCDD levels of Zone A residents (with and without chloracne) and controls (Zone non-ABR) Seveso, Italy.

serum methodology developed at the CDC²² could be used to measure 2,3,7,8-TCDD in these low-volume samples. The pilot study analyzed serum samples from (1) 10 Zone A residents who had the most severe types (III or IV) of chloracne, (2) 10 Zone A residents who had not developed chloracne, and (3) 10 persons from Zone non-ABR (a control zone outside the contaminated area). All of these samples, which had been collected in 1976 and stored since then at -30°C , were analyzed at the CDC without any sample identification.

The 2,3,7,8-TCDD levels detected in some of these samples are the highest ever reported in humans (Figure 23). The seven highest levels ($>12,000$ ppt) are from children who developed the most severe types of chloracne.⁶⁰ As seen in Figure 23, however, no apparent threshold level for chloracne is obvious, although the people (mostly children) who developed chloracne had on average much higher levels of 2,3,7,8-TCDD than those (mostly adults) that did not.

The potentially exposed populations and selected controls underwent physical examinations from 1976 to 1985. Although some liver function tests in some of the populations were outside the normal concentration range, any such result was only transient in nature.⁶¹ The only abnormal clinical finding has been chloracne. Because some of the potential adverse health effects may have a longer latency period, approximately 250 more of these stored serum samples will be analyzed for 2,3,7,8-TCDD. These data will contribute to our knowledge of the half-life of 2,3,7,8-TCDD in men, women, boys, and girls. These results will also be forthcoming in 1991.

The planned analysis of additional stored samples from this incident could provide more detailed information concerning half-life of TCDD in humans (children versus adults, men versus women). In addition, because most residents of the contaminated areas underwent extensive medical examinations from 1976 to 1985, analysis of additional samples would allow a correlation of TCDD levels with any potential adverse health effects.

Missouri

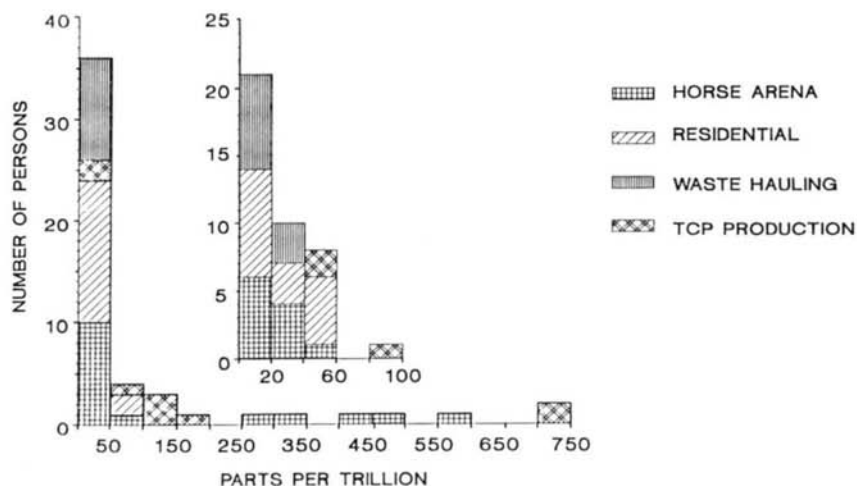
A chemical plant in Verona, MO produced 2,4,5-T from 1968 to 1969, sat idle for a year, and then produced hexachlorophene until the plant was closed in December 1971. Approximately 29 kg of 2,3,7,8-TCDD-contaminated sludge wastes produced at the Verona plant were mixed with waste oils and inadvertently sprayed in 1971 for dust control on areas of eastern Missouri (horse arenas, parking lots, and residential roads). More than 250 sites in Missouri are suspected of having been contaminated and 45 have been documented to have had greater than 1 ppb 2,3,7,8-TCDD in the soil (two thirds of these sites are residential). Between 1983 and 1985, the Missouri Department of Health compiled a central listing of more than 2000 persons who believed that they had been exposed to TCDD.

During 1985 to 1986, a study of adipose tissue levels of 2,3,7,8-TCDD in Missouri residents was conducted under a cooperative agreement between the Missouri Department of Health and the CDC (funded by an interagency agreement with the Agency for Toxic Substances and Disease Registry).^{9,33} The exposed group

Table 3. Adipose Tissue 2,3,7,8-TCDD Levels in ppt in Exposed and Control Participants, Missouri, 1986

Exposure Status	N	Range	Mean	SD	Median
TCP production	9	41.9—750	245	287	122
Horse arena	16	5.0—577	145	202	24.1
Residential	16	5.2—59.1	26.8	18.9	19.5
Waste removal	10	3.7—25.8	12.4	8.3	9.0
Controls	128	ND—20.2	7.0	4.0	6.1

consisted of 51 individuals who were classified into one of four exposure categories: (1) production of 2,4,5-trichlorophenol; (2) transportation of contaminated wastes, maintenance, or employment with a trucking company that had used contaminated oil for dust control; (3) involvement with horses in contaminated arenas; and (4) residents of areas sprayed with contaminated oil. The control group consisted of 128 persons who donated 20 g of omental adipose tissue during elective abdominal surgery at one of three hospitals in Kansas City, St. Louis, or Springfield. All but one of the participants had detectable adipose tissue levels of 2,3,7,8-TCDD as shown in Table 3. The distributions of the 2,3,7,8-TCDD levels are shown in Figure 24. The range of adipose tissue 2,3,7,8-TCDD levels for persons with no known exposure was nondetectable to 20.2 ppt. Ninety-five percent of the levels were 16.6 ppt or less. No significant differences by sex, race, or city of residence, or by rural, suburban, or urban status were noted. In the control group, the mean and median adipose tissue 2,3,7,8-TCDD levels increased about 20% per decade of age for both males and females (see Figure 25). This is consistent with the findings of other studies.^{10,11}

**Figure 24.** Adipose tissue 2,3,7,8-TCDD levels in exposed persons from Missouri, 1986.

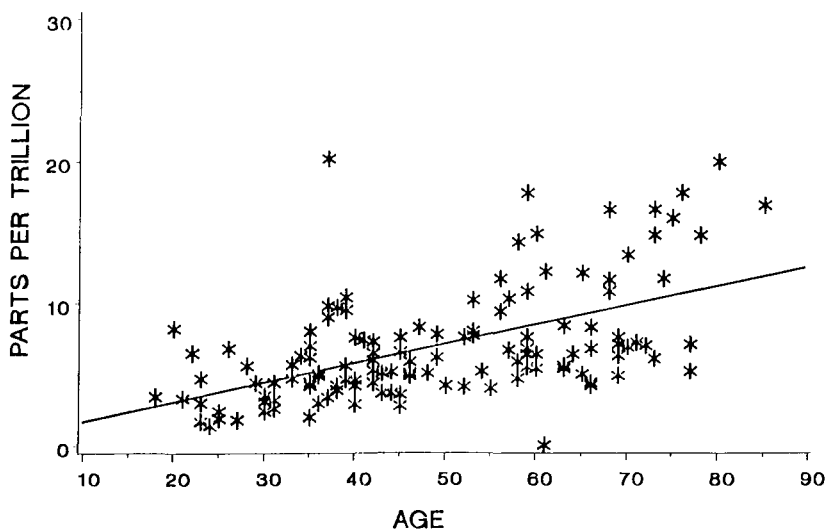


Figure 25. Correlation of adipose tissue 2,3,7,8-TCDD levels with age from 128 general Missouri residents.

Differences were significant in levels for the persons with no known exposure versus 51 exposed persons and for three of the four exposure categories (TCP production, horse arena, and residential exposure). Twenty-two (43%) of the 51 exposed participants had levels less than the highest level of the control participants. Significantly, these individuals (43%) were thought to have been exposed to 2,3,7,8-TCDD on the basis of epidemiologic evidence, but they did not show evidence of exposure on the basis of objective laboratory data. An objective measure of exposure is needed to minimize misclassification before looking at outcomes such as health effects.

Occupationally Exposed Populations

Occupationally exposed populations have been examined for 2,3,7,8-TCDD levels in both the United States and Germany. Without the identification being known, the CDC analyzed 381 serum samples for 2,3,7,8-TCDD, including 246 for all the PCDDs and PCDFs. The last report on this study,⁶² which is being conducted by the Centers for Disease Control's National Institute for Occupational Safety and Health, gave TCDD results in 143 workers who were employed at plants that manufactured chemicals contaminated with TCDD and in 54 referents. These levels are given in Table 4. The mean time interval between the last known exposure and the collection of the blood specimen was 24 and 17 years for the New Jersey and Missouri plants, respectively. Of particular note in this study is that the 2,3,7,8-TCDD levels in the workers significantly correlated with duration of exposure to the TCDD-contaminated processes ($r = 0.83$, $p < 0.0001$). The full report, including health effects, on this study is scheduled to be released in 1991.

Table 4. 2,3,7,8-TCDD Levels (ppt) in Serum Lipids of Workers and Referents

	New Jersey Plant			Missouri Plant	
	Production Workers	Office Workers	Referents	Workers	Referents
N	103	8	41	32	13
Mean	293.4	12.5	8.0	177.2	7.1
Geometric Mean	76.8	11.0	6.9	80.7	6.2
Median	84.0	11.0	5.3	108.6	6.4
Range	2—3390	7—26	2—20	3—1290	2—17

Summary of Human Levels

In general, the background levels of 2,3,7,8-TCDD reported in the literature are less than 20 ppt (see Table 5). Levels reported in Vietnam veterans who handled Agent Orange; residents of Seveso, Italy; and occupationally exposed workers have been substantially above this background level (see Figure 26). A number of large epidemiologic studies (Air Force Ranch Hand, NIOSH Workers, Seveso) that have detailed medical information and a laboratory measurement of 2,3,7,8-TCDD serum levels are still ongoing. These studies offer the best opportunity to find any possible correlation between health effects and 2,3,7,8-TCDD exposure.

Table 5. Concentration of 2,3,7,8-TCDD in Human Adipose Tissue and Serum from Individuals with No Known Exposure to 2,3,7,8-TCDD

Source of Specimen	N	Whole Weight Basis		Mean Age	Ref.
		Mean (ppt)	Range (ppt)	(Range)	
Adipose tissue from elective surgical patients in Missouri, 1985	128	7.0(6.1 ^a)	ND ^b , 1.4—20.2	49.0 (18—85)	9 33
Adipose tissue from (autopsy) Georgia and Utah, 1984	35	7.1 ^a	2.7—19	55.8 (16—85)	10
Adipose tissue from (autopsy) sudden deaths in St. Louis, MO	35	7.2 ^a	2.2—20.5	41.5 (15—88)	11
Adipose tissue from (autopsy) the general Canadian adult population, 1976	25	6.4 ^c	ND, 2.0—13	39.7	3
Adipose tissue from (adult controls) Binghamton, NY	8	7.2	1.4—17.7	—	3
Adipose tissue from hospital patients, Umea, Sweden	31	3.0	0—9	—	4
Adipose tissue composites ^d from the EPA FY'82 NHATS Repository, 1982	46	5.0 ^e	ND—10	—	8
Adipose tissue from cancer patients in Japan, 1985	12	9.0	6—18	—	7
Adipose tissue from general surgical patients in Shanghai, China, 1984	7	ND	Detection limit 2 ppt	54	13
Adipose tissue from (autopsy) general adult population in southern Japan, 1984	6	6.6 ^f	ND—9.7	59 (46—70)	6

Table 5 (continued). Concentration of 2,3,7,8-TCDD in Human Adipose Tissue and Serum from Individuals with No Known Exposure to 2,3,7,8-TCDD

Source of Specimen	N	Whole Weight Basis		Mean Age	Ref.
		Mean (ppt)	Range (ppt)	(Range)	
Adipose tissue from (autopsy) accidental death or illness in Japan	17	13.2	2.6—33	49.5 (27—74)	15
Adipose tissue from (autopsy) general adult population in Munich, FRG	44	5.9 ^{e,g}	ND(<1)—18.2	60.5 (15—85)	64,65
Adipose tissue from general adult population in Hamburg, FRG, 1986	21	—	1.5—18	—	66
Adipose tissue from U.S. Army controls (non-Vietnam)	7	3.2	1—5	—	45
Adipose tissue from Veteran controls, 1978	4	5.1	3—8	—	2
Serum from New Jersey controls, 1987	19	8.2 ^h	3.7—17.1	54	63
Serum from elective surgical patients in Missouri, 1985	21	7.6 ^h	1.9—26.0	42.5 (19—70)	22
Serum from U.S. Army Veterans (non-Vietnam), 1987	97	4.1 ^h	ND—15	39 (33—46)	40
Serum from U.S. Air Force (non-Vietnam) controls, 1987	49	4.8 ^{h,i}	2—9.7	49	51
Blood from general population in Hamburg, FRG	10	4.0 ^l	ND(<1.5)—9.1	37.1 (24—48)	21

^a Geometric mean.

^b Not detected.

^c Mean of 25 positive samples; 21 samples were NDs.

^d Composites from more than 900 specimens.

^e Lipid-adjusted basis.

^f Mean of four positives, 2-NDs.

^g Mean of 22 positive samples; 22 samples were ND (<1).

^h Serum on a lipid-adjusted basis.

ⁱ Excludes one person (21.3 ppt) documented to have had exposure to industrial chemicals.

^j Whole blood on lipid-adjusted basis.

ACKNOWLEDGMENTS

These studies were supported in part by funds from the Comprehensive Environmental Response, Compensation, and Liability Act Trust Fund through an inter-agency agreement with the Agency for Toxic Substances and Disease Registry, U.S. Public Health Service.

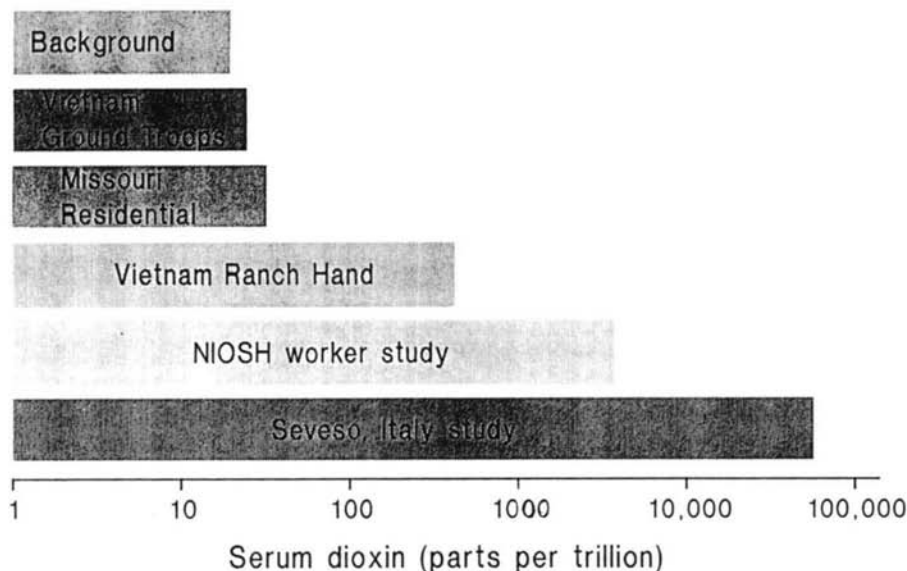


Figure 26. Ranges of measured serum 2,3,7,8-TCDD levels in selected studies.

REFERENCES

1. Patterson, D. G., Jr., M. A. Fingerhut, and D. R. Roberts. "Levels of Polychlorinated Dibenzo-p-dioxins (PCDDs) and Dibenzofurans (PCDFs) in Workers Exposed to 2,3,7,8-TCDD," *Am. J. Ind. Med.* 16:135—146 (1989).
2. Gross, M. L., J. O. Lay, and P. A. Lyon. "2378-TCDD Levels in Adipose Tissue of Vietnam Veteran," *Environ. Res.* 33:261—268 (1984).
3. Schechter, A., J. J. Ryan, and G. Gitlitz. "Chlorinated Dioxin and Dibenzofuran Levels in Human Adipose Tissue From Exposed and Control Populations," in *Chlorinated Dioxins and Dibenzofurans in Perspective*, C. Rappe, G. Choudhary, and L. H. Keith, Eds. (Chelsea, MI: Lewis Publishers, 1986), pp. 51—65.
4. Rappe, C., M. Nygren, G. Lindstrom, and M. Hansson. "Dioxins and Dibenzofurans in Biological Samples of European Origin," *Chemosphere* 15:1635—1639 (1986).
5. Nygren, M., C. Rappe, and G. Lindstrom. "Identification of 2378-Substituted PCDDs and PCDFs in Environmental and Human Samples," in *Chlorinated Dioxins and Dibenzofurans in Perspective*, C. Rappe, G. Choudhary, and L. H. Keith, Eds. (Chelsea, MI: Lewis Publishers, 1986), pp. 17—34.
6. Ryan, J. J. "Variation of Dioxins and Furans in Human Tissues," *Chemosphere* 15:1585—1593 (1986).
7. Ono, M., T. Wakimoto, R. Tatsukawa, and Y. Masuda. "PCDDs and PCDFs in Human Adipose Tissues of Japan," *Chemosphere* 15:1629—1634 (1986).
8. Stanley, J. S., K. E. Boggess, J. Onstot, and T. M. Sack. "PCDDs and PCDFs in Human Adipose Tissue From the EPA FY 82 NHATS Repository," *Chemosphere* 15:1605—1612 (1986).

9. Patterson, D. G., Jr., R. E. Hoffman, L. L. Needham et al. "Levels of 2378-TCDD in Adipose Tissue of Exposed and Control Persons in Missouri — An Interim Report," *JAMA* 256:2683—2686 (1986).
10. Patterson, D. G., Jr., J. S. Holler, S. J. Smith et al. "Human Adipose Data for 2378-TCDD in Certain U.S. Samples," *Chemosphere* 15:2055—2060 (1986).
11. Graham, M., F. G. Hileman, R. G. Orth et al. "Chlorocarbons in Adipose Tissue from a Missouri Population," *Chemosphere* 15:1595—1600 (1986).
12. Rappe, C., R. Anderson, P. A. Bergquist et al. "Overview on Environmental Fate of Chlorinated Dioxins and Dibenzofurans. Sources, Levels, and Isomeric Pattern in Various Matrices," *Chemosphere* 16:1603—1618 (1987).
13. Ryan, J. J., A. Schecter, and Y. Masuda. "Comparison of PCDDs and PCDFs in the Tissue of Yusho Patients with Those from the General Population in Japan and China," *Chemosphere* 16:2017—2025 (1987).
14. Needham, L. L., D. G. Patterson, Jr., C. C. Alley et al. "PCDD and PCDF Levels in Persons with High and Normal Levels of 2378-TCDD," *Chemosphere* 16:2027—2031 (1987).
15. Ogaki, J., K. Takayama, H. Miyata, and T. Kashimoto. "Levels of PCDDs and PCDFs in Human Tissues and Various Foodstuffs in Japan," *Chemosphere* 16:2047—2056 (1987).
16. Rappe, C., M. Nygren, H. R. Buser, and T. Kauppinen. "Occupational Exposure to Polychlorinated Dioxins and Dibenzofurans," in *Chlorinated Dioxins and Related Compounds*, O. Hutzinger, R. W. Frei, E. Merian, and F. Pocchiari, Eds. (Oxford: Pergamon Press, 1982), pp. 495—513.
17. Nygren, M. "Analysis of PCDDs and PCDFs in Human Adipose Tissue and Blood," PhD Thesis, Department of Organic Chemistry, University of Umea, Sweden (1988).
18. Kahn, P. C., M. Gochfeld, M. Nygren et al. "Dioxins and Dibenzofurans in Blood and Adipose Tissue of Agent Orange Exposed Vietnam Veterans and Matched Controls," *JAMA* 259:1661—1667 (1988).
19. Schecter, A., J. D. Constable, J. V. Bangert et al. "Isomer Specific Measurement of Polychlorinated Dibenzodioxin and Dibenzofuran Isomers in Human Blood from American Vietnam Veterans Two Decades after Exposure to Agent Orange." *Chemosphere* 18:531—538 (1989).
20. Selenka, F. "Chlorinated Dioxins and Furans in 225 Blood Samples from Occupational Exposed and Non-exposed Persons in Western Germany," presented at Dioxin-86, Fukuoka, Japan, September 16—19, 1986.
21. Pöpke, O., M. Ball, Z. A. Lis, and K. Scheunert. "PCDD/PCDF in Whole Blood Samples of Unexposed Persons," *Chemosphere* 19:941—948 (1989).
22. Patterson, D. G., Jr., L. Hampton, C. R. Lapeza, Jr. et al. "High-Resolution Gas Chromatographic/High-Resolution Mass Spectrometric Analysis of Human Serum on a Whole-Weight and Lipid Basis for 2,3,7,8-TCDD," *Anal. Chem.* 59:2000—2005 (1987).
23. Patterson, D. G., Jr., P. Furst, L. O. Henderson et al. "Partitioning of In-Vivo Bound PCDDs/PCDFs Among Various Compartments in Whole Blood," *Chemosphere* 19:135—142 (1989).
24. Patterson, D. G., Jr., L. L. Needham, J. L. Pirkle et al. "Correlation between Serum and Adipose Levels of 2378-TCDD in 50 Persons From Missouri," *Arch. Environ. Contam. Toxicol.* 17:139—143 (1988).

25. Henderson, L. O., and D. G. Patterson, Jr. "Distribution of 2378-TCDD in Human Whole Blood and Its Association with, and Extractability from, Lipoproteins," *Bull. Environ. Contam. Toxicol.* 40:604—611 (1988).
26. Needham, L. L., D. G. Patterson, Jr., J. L. Pirkle et al. "The Basis for Measuring 2378-TCDD in Serum," *Chemosphere* 18:425—430 (1989).
27. Patterson, D. G., Jr., W. E. Turner, L. R. Alexander et al. "The Analytical Methodology and Method Performance for the Determination of 2378-TCDD in Serum for the Vietnam Veteran Agent Orange Validation Study, the Ranch Hand Validation and Half-Life Studies, and Selected NIOSH Worker Studies," *Chemosphere* 18:875—882 (1989).
28. Turner, W. E., S. G. Isaacs, L. R. Alexander, and D. G. Patterson, Jr. "A Quality Assurance Program for Measuring 2378-TCDD in Human Serum," *Chemosphere* 18:1009—1016 (1989).
29. Patterson, D. G., Jr., P. Fürst, and L. R. Alexander. "Analysis of Human Serum for PCDDs/PCDFs: A Comparison of Three Extraction Procedures," *Chemosphere* 19:89—96 (1989).
30. Smith, L. M., and D. L. Stalling. "Determination of Part-Per-Trillion Levels of Polychlorinated Dibenzofurans and Dioxins in Environmental Samples," *Anal. Chem.* 56:1830—1842 (1984).
31. Patterson, D. G., Jr., J. S. Holler, C. R. Lapeza, Jr. et al. "High-Resolution Gas Chromatographic/High-Resolution Mass Spectroscopic Analysis of Human Adipose Tissue for 2378-TCDD," *Anal. Chem.* 58:705—713 (1986).
32. Lapeza, C. R., Jr., D. G. Patterson, Jr., and J. A. Liddle. "An Automated Apparatus for the Extraction and Enrichment of 2378-TCDD in Human Adipose," *Anal. Chem.* 58:713—716 (1986).
33. Andrews, J. S., Jr., W. A. Garrett, D. G. Patterson, Jr. et al. "2,3,7,8-TCDD Levels in Adipose Tissue of Persons with No Known Exposure and in Exposed Persons," *Chemosphere* 18:495—502 (1989).
34. Pöpke, O., M. Ball, Z. A. Lis, and K. Scheunert. "Comparison of PCDD/PCDF Levels in Whole Blood and Adipose Tissue Samples of Persons Exposed to Contaminated Indoor Air," *Chemosphere*, in press.
35. Schecter, A., J. J. Ryan, J. D. Constable et al. "Partitioning of 2,3,7,8-Chlorinated Dibenzo-p-dioxins and Dibenzofurans between Adipose Tissue and Plasma Lipid of 20 Massachusetts Vietnam Veterans," *Chemosphere* 20:951—958 (1990).
36. Matthews, H. B., J. R. Surlis, J. G. Carver, and M. W. Anderson. "Halogenated Biphenyl Transport by Blood Components," *Fund. Appl. Toxicol.* 4:420—428 (1984).
37. Patterson, D. G., Jr., W. E. Turner, S. G. Isaacs, and L. R. Alexander. "A Method Performance Evaluation and Lessons Learned After Analyzing More than 5,000 Human Adipose Tissue, Serum, and Breast Milk Samples for Polychlorinated Dibenzo-p-dioxin (PCDDs) and Dibenzofurans (PCDFs)," *Chemosphere* 20:829—836 (1990).
38. Hansson, M., C. Rappe, M. Gochfeld et al. "Effects of Fasting on Blood Levels of 2,3,7,8-TCDD and Related Compounds," *Chemosphere* 18:525—530 (1989).
39. Phillips, D. L., J. L. Pirkle, V. W. Burse, J. T. Bernert, Jr., L. O. Henderson, and L. L. Needham, "Chlorinated Hydrocarbon Levels in Human Serum: Effects of Fasting and Feeding," *Arch. Environ. Contam. Toxicol.* 18:495—500 (1989).
40. Centers for Disease Control Veterans Health Studies Group. "Serum 2378-TCDD Levels in U.S. Army Vietnam-Era Veterans," *JAMA* 260:1249—1254 (1988).
41. Lang, G. L., and J. D. Winfordner. *Anal. Chem.* 55:712A—724A (1983).

42. Keith, H. K. *Anal. Chem.* 55:2210—2218 (1983).
43. Taylor, J. K. *Chem. Tech.* (December 1986), pp. 756—763.
44. Kahn, P. C., M. Gochfeld, M. Nygren et al. "Dioxins and Dibenzofurans in Blood and Adipose Tissue of Agent Orange Exposed Vietnam Veterans and Matched Controls," *JAMA* 259:1661—1667 (1988).
45. Schechter, A., J. D. Constable, J. V. Bangert et al. "Elevated Body Burdens of 2,3,7,8-Tetrachlorodibenzodioxin in Adipose Tissue of United States Vietnam Veterans," *Chemosphere* 18:431—438 (1989).
46. Centers for Disease Control Vietnam Experience Study. "Health Status of Vietnam Veterans. I. Psychosocial Characteristics," *JAMA* 259:2701—2707 (1988).
47. Centers for Disease Control Vietnam Experience Study. "Health Status of Vietnam Veterans. II. Physical Health," *JAMA* 259:2708—2714 (1988).
48. Centers for Disease Control Vietnam Experience Study. "Health Status of Vietnam Veterans. III. Reproductive Outcomes," *JAMA* 259:2715—2719 (1988).
49. Centers for Disease Control Vietnam Experience Study. "Postservice Mortality Among Vietnam Veterans," *JAMA* 257:790—795 (1987).
50. Pirkle, J. L., W. H. Wolfe, D. G. Patterson, Jr. et al. "Estimates of the Half-Life of 2,3,7,8-TCDD in Ranch Hand Veterans," *J. Toxicol. Environ. Health* 27:165—171 (1989).
51. Centers for Disease Control. "Serum Levels of 2,3,7,8-TCDD in Vietnam Veterans of Operation Ranch Hand," *MMWR* 37:309—311 (1988).
52. Lathrop, G. D., W. H. Wolfe, R. A. Albanese, and P. M. Moynahan. "Epidemiologic Investigation of Health Effects in Air Force Personnel Following Exposure to Herbicides: Study Protocol," USAF School of Aerospace Medicine, National Technical Information Service, Document AD A 122 250 (1982).
53. Rappe, C., M. Nygren, H. R. Buser et al. "Identification of PCDDs and PCDFs in Human Samples: Occupational Exposures and Yusho Patients," in *Human and Environmental Risks of Chlorinated Dioxins and Related Compounds*, R. E. Tucker, A. L. Young, and A. P. Gray, Eds. (New York: Plenum Press, 1983), pp. 241—253.
54. Lathrop, G. D., W. H. Wolfe, R. A. Albanese, and P. M. Moynahan. "An Epidemiologic Investigation of Health Effects in Air Force Personnel Following Exposure to Herbicides: Baseline Morbidity Study Results," USAF School of Aerospace Medicine, National Technical Information Service, Document AD A 138 340 (1984).
55. Lathrop, G. D., S. G. Machado, T. G. Karrison et al. "Air Force Health Study: An Epidemiologic Investigation of Health Effects in Air Force Personnel Following Exposure to Herbicides: Final Report," USAF School of Aerospace Medicine, National Technical Information Services, Document AD A 188 262 (1987).
56. Bowman, R. E., S. L. Schantz, N. C. A. Weerasinghe et al. "Chronic Dietary Intake of 2,3,7,8-Tetrachlorodibenzo-p-Dioxin (TCDD) at 5 or 25 Parts Per Trillion in the Monkey: TCDD Kinetics and Dose-Effect Estimate of Reproductive Toxicity," *Chemosphere* 18:243—252 (1989).
57. Poiger, H., and C. Schlatter. "Pharmacokinetics of 2,3,7,8-TCDD in Man," *Chemosphere* 15:1489—1494 (1986).
58. Facchetti, S., A. Fornari, and M. Montagna. "Distribution of 2,3,7,8-TCDD in the Tissues of a Person Exposed to the Toxic Cloud at Seveso," *Forensic Environ. Appl.* 1:1406—1444 (1981).
59. Centers for Disease Control. "Preliminary Report: 2,3,7,8-TCDD Exposure to Humans — Seveso, Italy," *MMWR* 37:733—736 (1988).

60. Mocarelli, P., D. G. Patterson, Jr., A. Marocchi, and L. L. Needham. "Pilot Study (Phase II) For Determining Polychlorinated Dibenzo-p-dioxin (PCDD) and Polychlorinated Dibenzofuran (PCDF) Levels in Serum of Seveso, Italy Residents Collected at the Time of Exposure: Future Plans," *Chemosphere* 20:967—974 (1990).
61. Mocarelli, P., A. Marocchi, P. Brambilla et al. "Clinical Laboratory Manifestations of Exposure to Dioxin in Children: A Six-Year Study of the Effects of an Environmental Disaster Near Seveso, Italy," *JAMA* 256:2687—2695 (1986).
62. Sweeney, M. H., M. A. Fingerhut, D. G. Patterson, Jr. et al. "Comparison of Serum Levels of TCDD in TCP Production Workers and in an Unexposed Comparison Group," *Chemosphere* 20:993—1000 (1990).
63. Fingerhut, M. A., M. H. Sweeney, D. G. Patterson, Jr. et al. "Levels of 2,3,7,8-TCDD in the Serum of U.S. Chemical Workers Exposed to Dioxin Contaminated Products: Interim Results," *Chemosphere* 19:835—840 (1989).
64. Thoma, H., W. Mücke, and E. Kretschmer. "Untersuchung von Humanfettproben auf PCDD/F," *VDI-Berichte* 634:383—387 (1987).
65. Thoma, H., W. Mücke, and E. Kretschmer. "Concentrations of PCDD and PCDF in Human Fat and Liver Samples," *Chemosphere* 18:491—498 (1989).
66. Beck, H., K. Eckart, and W. Mathar. "Levels of PCDDs and PCDFs in Adipose Tissue of Occupationally Exposed Workers," *Chemosphere* 18:507—516 (1989).

CHAPTER 7

Comparison of Low Resolution, High Resolution Mass Spectrometry, and Mass Spectrometry/Mass Spectrometry Techniques in the Analysis of Polychlorinated Dibenzo-p-Dioxins and Dibenzofurans

Benjamin P.-Y. Lau, Dorcas Weber, and John J. Ryan

ABSTRACT

Four different mass spectrometric approaches — low resolution mass spectrometry (LRMS), high resolution mass spectrometry (HRMS), mass spectrometry/mass spectrometry (MS/MS) using a hybrid instrument, and MS/MS using a triple quadrupole instrument — were compared with respect to detection limits and specificity for the analysis of polychlorinated dibenzo-p-dioxins (PCDDs) and polychlorinated dibenzofurans (PCDFs) in the same set of samples. Low resolution MS offered the best sensitivity, but subpicogram detection limits were still achievable by HRMS and MS/MS techniques. The specificity of the latter two methods was

comparable and superior to the LRMS technique. Adduct ion formation and exchange reactions between the target compound and reagent ions in the Townsend discharge chemical ionization source were observed in the positive ion mode. These ion-molecule reactions may lead to some interference problems for other target compounds, especially when below nominal mass resolution is used.

INTRODUCTION

Sensitivity and specificity are two major considerations in choosing the proper mass spectrometric technique for ultratrace analysis of polychlorinated dibenzo-p-dioxins (PCDDs) and dibenzofurans (PCDFs). The analyst not only has to detect target compounds at extremely low levels in complex biological or environmental matrices, but also has to unequivocally identify them. In recent years, the demands for lower detection limits and better specificity have been ever increasing. Modern instrumentation and methodologies are designed to achieve the ultimate limits of both. Several new mass spectrometric techniques, including negative ion chemical ionization¹⁻⁴ and tandem mass spectrometry (MS/MS),⁵⁻⁷ etc., have been introduced. Review articles on the gas chromatography/mass spectrometry analyses of PCDFs/PCDDs have been published.⁸⁻¹⁰

Due to the extreme toxicity of these compounds, their detection limits in foods and biological samples should be at least in the low picogram per gram (or part per trillion) levels. In our laboratory, regardless of which instrument or what technique was used at the time when these experiments were performed, the minimum absolute detection limits (signal-to-noise ratio better than 3:1) of better than 1 pg of 2,3,7,8-tetrachlorodibenzo-p-dioxin (TCDD) and 3 pg of octachlorodibenzo-p-dioxin (OCDD) were required (recently, these detection limit requirements have been lowered by five- to tenfold). In addition to the conventional low resolution mass spectrometry (LRMS), highly specific methods using high resolution mass spectrometry (HRMS) and MS/MS were also developed. In this chapter, four different mass spectrometric approaches (namely, LRMS, HRMS, and MS/MS using a hybrid instrument and a triple quadrupole instrument) are compared first in terms of detection limit and then specificity, and then by analyses of a set of samples consisting of reagent blanks, fish tissue, monkey fat, and human tissue.

EXPERIMENTAL

Sample Preparation

Samples were prepared according to the method published elsewhere.¹¹⁻¹³ In general, homogenized samples (in acetone-hexane, 2:1 v/v) were extracted with hexane after the addition of isotopically labeled internal standards. Extracts were then defatted with concentrated sulfuric acid, cleaned-up by Florisil chromatography and a carbon column (for monkey fat and Japanese Yusho liver samples), concentrated to 25 μ L, and submitted for GC/MS or MS/MS analysis.

Standard Solutions

Two standard solutions were employed throughout the study. Both solutions contained (1.) all 2,3,7,8-substituted isomers with degree of chlorination ranged from 4 to 8 (tetra- to octahomologues); (2.) the first and the last eluting isomers (as determined on a DB-5 column) for each homologue group to aid in defining the retention time windows in the selected ion monitoring (SIM) and multiple reaction monitoring (MRM) experiments; and (3.) ^{37}Cl -isotopically labeled PCDFs and ^{13}C -labeled PCDDs as internal standards. The composition of these solutions and the concentration of internal standards are listed in Table 1. The first solution contained only the native PCDFs/PCDDs at a concentration of 5 pg/ μL for each congener and was used as a quantitation standard. The concentration of native PCDFs and PCDDs in the second solution varied from 1 to 3 pg/ μL depending on the estimated minimum detection limit (MDL) of each congener. The latter solution was labeled as the "MDL standard solution" and was used to check the detection

Table 1. Composition of Standard Mixture Solutions

No. of Cl	Congeners	Isomers	Internal Standard (Concentration)	
4	TCDF	1,3,6,8	^{37}Cl -2378-TCDF (4 pg/ μL)	
		2,4,6,8		
		2,3,6,8		
		2,3,7,8		
		3,4,6,7		
	TCDD	1,3,6,8	^{13}C -2378-TCDD (2.9 pg/ μL)	
		1,3,6,9		
		1,3,7,8		
		1,2,7,9		
		2,3,7,8		
5	PnCDF	1,2,4,7,8	^{37}Cl -23478-PnCDF (4 pg/ μL)	
		1,2,3,6,7		
		2,3,4,7,8		
		1,2,3,8,9		
	PnCDD	1,2,4,6,8	^{37}Cl -12378-PnCDD (4 pg/ μL)	
		1,2,4,7,8		
		1,2,3,7,8		
		1,2,3,8,9		
6	HxCDF	1,2,3,4,6,8	^{37}Cl -123478-HxCDF (4 pg/ μL)	
		1,2,3,4,7,8		
		2,3,4,6,7,8		
		1,2,3,4,8,9		
	HxCDD	1,2,4,6,7,9	^{37}Cl -123489-HxCDF (4 pg/ μL)	
		1,2,3,6,8,9		
		1,2,3,6,7,8		
		1,2,3,7,8,9		
7	HpCDF	1,2,3,4,6,7,8	^{13}C -123678-HxCDD (4.6 pg/ μL)	
		1,2,3,4,6,8,9		
		1,2,3,4,7,8,9		
	HpCDD	1,2,3,4,6,7,9		^{13}C -123789-HxCDD (4.0 pg/ μL)
		1,2,3,4,6,7,8		
		1,2,3,4,6,7,8		
8	OCDF	^{13}C -1234678-HpCDD (4.4 pg/ μL)		
	OCDD		^{13}C -OCDD (20.0 pg/ μL)	

limits of the instrument. In this report, quantitation was performed based on the external standard method. Amounts of PCDFs/PCDDs in the samples were calculated in absolute concentration terms (picograms per microliter) and were not corrected for recoveries or sample size.

General Conditions For a Magnetic Sector Instrument

Low resolution, high resolution, and hybrid MS/MS experiments were conducted on a VG Analytical 70EQ mass spectrometer (hybrid MS/MS with EBQQ configuration). A dedicated electron impact ionization (EI) source with electron energies of 28 to 35 eV for LRMS and MS/MS and 70 eV for HRMS was used. At low electron energy, the ionization of the helium carrier gas was suppressed, thus promoting the ionization of target compounds. The emission current was set at 500 μA , and the ion source temperature was maintained at 250°C. Mass spectrometer resolution (10% valley definition) was set at 1000 for low resolution and 10,000 for high resolution experiments. Multigroup SIM in the LRMS and HRMS modes, as well as the MRM in the MS/MS mode were controlled by a VG 11/250 data system based on a DEC PDP 11/24 computer. Tetra- to octachlorinated congeners of PCDFs and PCDDs were monitored in three groups: tetra- and pentachlorinated congeners in the first group, followed by the second group of hexa- and heptachlorinated congeners, and then the octachlorinated congeners. The retention time windows for each group were determined by injecting a standard mixture containing the first and the last elution isomers of tetra- to octachlorinated congeners. Ion switching within the same group was achieved by accelerating voltage switching with a settling time of 20 msec and a dwell time of 80 msec for each ion. A Varian 6000 gas chromatograph was directly interfaced to the ion source of the mass spectrometer. A 30-m DB-5 (J & W Scientific) fused silica column (0.25 mm i.d., 0.25- μm film thickness) was used. The head pressure of the helium carrier gas was set at 96.6 kPa (14 psi). The GC column was held at the initial temperature of 80°C then programmed to 180°C at 30°C/min followed by another ramp of 5°C/min to 280°C.

Hybrid MS/MS Conditions

When the VG 70EQ mass spectrometer was operated in the MS/MS mode, the front end resolution was maintained at least 1000, whereas the quadrupole resolution was kept at nominal mass resolution at all times. Argon was used as the collision-induced dissociation (CID) gas. Daughter ions at m/z 225 and 190 corresponding to $[\text{M}-\text{Cl}]^+$ and $[\text{M}-2\text{Cl}]^+$ from the molecular ion of hexachloro-1,3-butadiene (Figure 1) were used routinely to tune the instrument in the MS/MS mode and double check the mass calibration of the quadrupole. Optimum conditions for collision energy and CID gas pressure were established by using 1,2,3,4-TCDD as a model compound. Strict molecular ion transmission ($\text{M} \rightarrow \text{M}$) and other CID reactions: $\text{M} \rightarrow [\text{M}-\text{COCl}]$ and $\text{M} \rightarrow [\text{M}-2\text{COCl}]$ were monitored in the optimization experiments. Plots of the responses from these three reactions versus collision

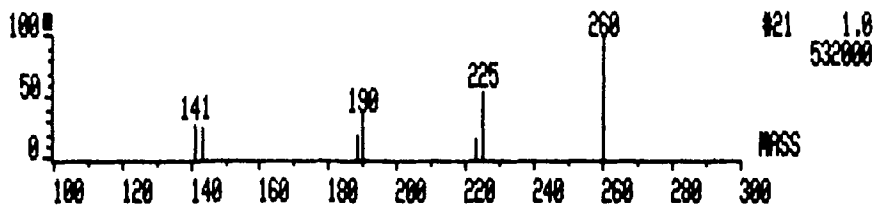


Figure 1. Daughter ion spectrum of hexachloro-1,3-butadiene.

energy (at a fixed CID gas pressure of 6×10^{-7} torr as indicated by the analyzer pressure gauge) and these responses versus collision gas pressure (at a fixed collision energy of 18 eV) indicated that the optimal values for the collision energy and the gas pressures were 17 to 20 eV and 6 to 7×10^{-7} torr, respectively. These optimal conditions are similar to those reported by Schellenberg et al.¹⁵ Masses of parent/daughter ion pairs for the multiple reaction monitoring of PCDFs/PCDDs are listed in Table 2.

Triple Quadrupole MS/MS Conditions

A SCIEX TAGA 6000E triple quadrupole mass spectrometer was employed as the second MS/MS system. A low-pressure Townsend discharge chemical ionization (CI) source employing preheated (280°C) “zero” grade air as reagent gas was used to ionize compounds eluting from the GC column. NO^+ , O_2^+ , and N_2^+ are the major reagent ions responsible for the ionization of PCDFs/PCDDs. Positive molecular ions formed through charge exchange reactions were selected by the first quadrupole and then fragmented in the collision gas cell using argon as a CID gas. Since a liquid-helium based cryogenic pumping system is used, gas molecules introduced into the system have to be heavier than helium, otherwise the pumping efficiency will be dramatically reduced. For this reason, only nitrogen can be used as the GC carrier gas and the head pressure was set at 28 kPa (4 psi). A 20-m DB-

Table 2. Parent/Daughter Ion Pairs for the Multiple Reaction Monitoring of PCDFs and PCDDs Using a Hybrid MS/MS

No. of CI	PCDFs	PCDDs
	Parent/Daughter	Parent/Daughter
4	304 → 241	320 → 257
	312 → 247 (³⁷ Cl)	332 → 268 (¹³ C)
5	340 → 277 ^a	356 → 293 ^a
	348 → 283 (³⁷ Cl)	368 → 304 (¹³ C) ^a
6	374 → 311 ^a	390 → 327 ^a
	384 → 319 (³⁷ Cl)	402 → 338 (¹³ C) ^a
7	408 → 345 ^a	424 → 361 ^a
		436 → 372 (¹³ C) ^a
8	442 → 379 ^a	458 → 395 ^a
		470 → 406 (¹³ C) ^a

^a [M + 2] ions.

5 (J & W Scientific, 0.32 mm i.d.) fused silica column was directly interfaced to the CI source. The GC oven temperature was programmed from 100 (1-min hold) to 180°C at 25°C/min, and then to 260°C at 5°C/min. The GC interface probe and the ion source temperature were maintained at 275 and 150°C, respectively. In order to achieve the detection limit requirements of at least 1 pg of 2,3,7,8-TCDD and 3 pg of OCDD, the resolution of both quadrupole analyzers has to be deliberately reduced to approximately 3 Da wide at half-height.

RESULTS AND DISCUSSION

Comparison of Detection Limits

Low and High Resolution Mass Spectrometry

Using the "MDL standard mixture" described earlier and a dedicated EI source optimized for PCDFs/PCDDs, selected LRMS responses from 1 pg of tetrachlorodibenzofuran (TCDF) and TCDDs as well as that from 3 pg of octachlorodibenzofurans (OCDFs) and OCDD are shown in Figure 2. A minimum detection limit of 50 fg TCDD can be achieved routinely at low resolution (RP = 1000).

Increasing the resolution from 1000 to 10,000 reduced the absolute peak height by a factor of 20 to 50. However, the baseline signal from chemical background also dropped substantially so that the signal-to-noise ratio did not reduce to the same extent. Figure 2 shows the responses of the same "MDL PCDF/PCDD mixture" at 10,000 resolution and at 70 eV, indicating detection limit requirements of 1 pg for TCDD and 3 pg for OCDD can still be easily met. It is likely that by reducing the electron energy to the range of 25 to 35 eV, even better sensitivity would be achievable.

GC/CI/MS/MS on a Triple Quadrupole System

Since 1983, a GC/CI/MS/MS method⁶ based on the use of the SCIEX TAGA 6000E triple quadrupole system has been used as a rapid screening method in our laboratory for the determination of PCDFs/PCDDs in a great variety of samples. Figure 3 shows the sensitivities obtained from a mixture of 5 pg each of PCDFs and PCDDs standards. In this example, the loss of COCl (63 mass units) from the two isotope peaks of the molecular ion of each compound were monitored. For example, parent/daughter ion pairs of m/z 304/241 and m/z 306/243 were both monitored for TCDF, whereas m/z 320/257 and 322/259 were monitored for TCDD. It should be noted that the theoretical ratio between two isotopic parent/daughter ion pairs for each compound in MS/MS mode is not the same as the corresponding molecular isotope ratio as observed in conventional MS. For instance, in the case of TCDD, the intensity ratio of the two isotopic parent/daughter ion pairs (m/z 320/257 and 322/259) should be 1.03 (100%/97%, see Table 3) instead of the ratio of 0.77 (between m/z 320 and 322), as in the case of conventional GC/MS/SIM method. Table 3 lists the theoretical relative intensity ratios of major parent/daughter ion

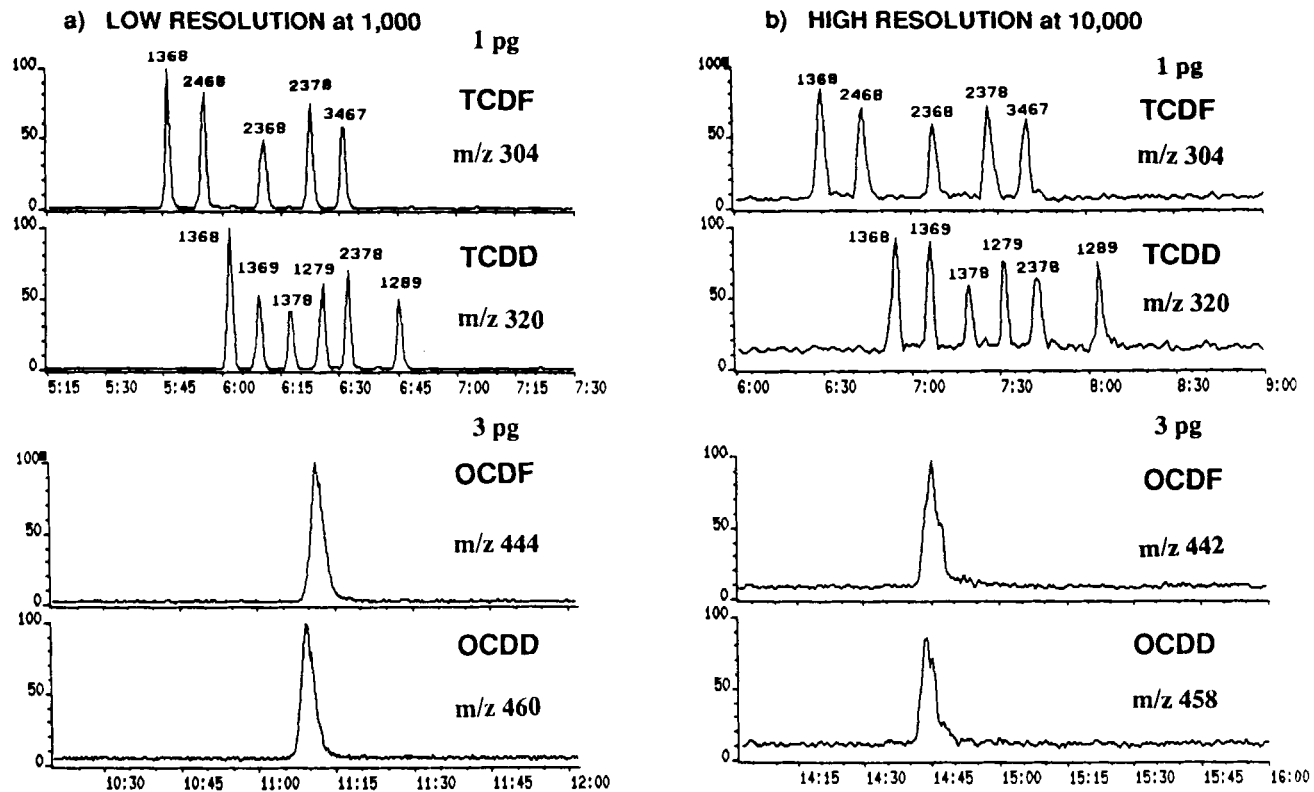


Figure 2. Responses of 1 pg TCDFs, TCDDs and 3 pg of OCDF, OCDD from (a) low resolution mass spectrometry (RP = 1000) and (b) high resolution mass spectrometry (RP = 10,000).

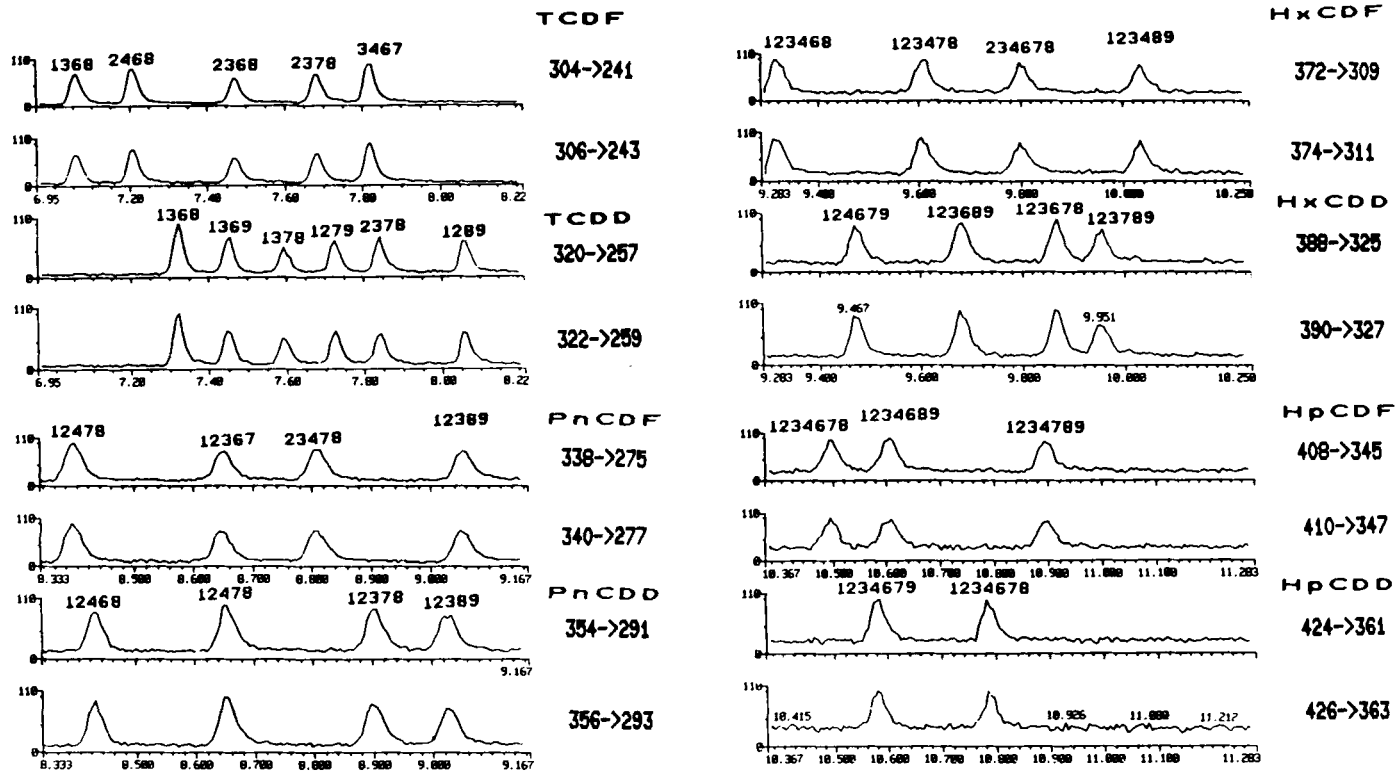


Figure 3. Responses of a standard mixture of PCDFs and PCDDs (5 pg each) obtained from triple quadrupole MS/MS (TAGA 6000E).

pairs for all PCDD congeners (same for PCDFs) in the MS/MS mode. It was found that the experimental ratios from the TAGA are quite different from those values in Table 3 due to the low mass resolution settings (>3 Da wide at half-height) as described in the experimental section.

GC/MS/MS/MRM on a Hybrid System

Figure 4 shows the response of a 1-pg 1,2,3,4-TCDD injection obtained from our hybrid MS/MS system. The mass chromatograms from the multiple reaction monitoring (MRM) of three CID reactions: $M \rightarrow M$ (unfragmented molecular ion), $M \rightarrow [M - \text{COCl}]$ and $M \rightarrow [M - 2\text{COCl}]$, show that the signal-to-noise ratio (S/N) better than 80:1 can be obtained from 1 pg of 1,2,3,4-TCDD. By extrapolation, the detection limit can be estimated as approximately 40 fg with $S/N = 3$. Typical responses of PCDFs and PCDDs from the same 5 pg standard mixture as described before are shown in Figures 5a and 5b, respectively. Parent/daughter ion pairs corresponding to the loss of a COCl from one of the isotope peaks within the molecular ion cluster of each PCDF and PCDD congener were monitored. Peaks derived from ^{37}Cl -labeled PCDF and ^{13}C -labeled PCDD internal standards are shaded in these figures. In general, the detection limits from the hybrid MS/MS are comparable to or even better than that from HRMS at 10,000 resolution.

Applications

A set of samples consisting of reagent blanks and extracts of catfish tissue, monkey fat, and human liver were analyzed by the four different MS techniques. For comparison purposes, the first three techniques were performed on the same instrument.

As shown in Table 4, some weak signals were detected by LRMS and hybrid MS/MS from a reagent blank. They all have the correct retention times as compared to their corresponding internal standards. Because these two MS techniques offer better detection limits than the other two, it is not certain whether these subpicogram quantities are interferences or genuine PCDFs/PCDDs present as contaminants. Based on our past experience, the latter case is more likely because we have observed occasionally low level cross-contamination from glassware or reagents. Extreme care has to be taken to ensure the reagent blank is clean at sub-parts per trillion levels. Thus, it is our general practice to include a reagent blank as a quality assurance sample in every batch of samples to ensure that analytical contaminants or interferences are kept below our required detection limits.

Analysis of a catfish sample with minimum chromatographic cleanup provided a good demonstration of the specificity of the different MS methods. Table 5 is a summary of these results. Considerable interferences were observed in the LRMS mode, especially for the TCDD and TCDF congeners. Mass chromatograms for TCDF, TCDD, and pentachlorodibenzofuran (PnCDF) from these four MS approaches are displayed in Figures 6, 7, and 8, respectively. It should be noted that the retention time spans for the hybrid and triple quadrupole MS/MS methods are

Table 3. Theoretical Relative Isotope Ratio for the [M-COCl] Ions of Chlorinated Dibenzo-p-dioxins in the MS/MS Analysis (Multiple Reaction Monitoring Mode)

No. of Cl	Congeners	Parent → Daughter	% Rel. Abund.	Rel. Ratios
4	TCDD	320 → 257	100.0%	1.00
		322 → 259	97.5%	.98
		324 → 261	31.7%	0.33
		326 → 263	3.4%	0.03
5	PnCDD	354 → 291	77.1%	0.77
		356 → 293	100.0%	1.00
		358 → 295	48.5%	0.49
		360 → 297	10.5%	0.11
6	HxCDD	388 → 325	61.9%	0.62
		390 → 327	100.0%	1.00
		392 → 329	65.4%	0.65
		394 → 331	21.1%	0.21
7	HpCDD	396 → 333	3.4%	0.03
		422 → 359	51.9%	0.52
		424 → 361	100.0%	1.00
		426 → 363	81.2%	0.81
8	OCDD	428 → 365	35.2%	0.35
		430 → 367	8.6%	0.09
		456 → 393	44.0%	0.44
		458 → 395	100.0%	1.00
		460 → 397	97.2%	0.97
		462 → 399	52.5%	0.52
		464 → 401	17.0%	0.17
		466 → 403	3.3%	0.03

Note: Same set of relative isotope ratios for respective PCDF homologues.

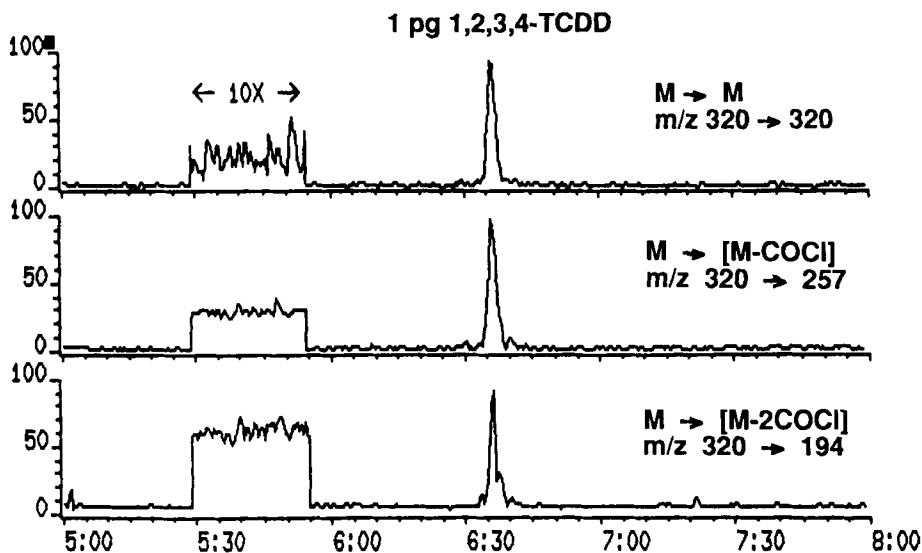


Figure 4. Multiple reaction monitoring mass chromatograms from 1 pg of 1,2,3,4-TCDD injection obtained from a hybrid MS/MS system.

Table 4. Comparison of Results from Four Different Mass Spectrometric Methods on a Reagent Blank Sample

	Low Resolution	High Resolution	Hybrid MS/MS	TAGA
2378-TCDF	~0.09(0.02)	n.d.(0.2)	trace(0.2)	n.d.(1.6)
2378-TCDD	n.d.(0.06)	n.d.(0.2)	n.d.(0.4)	n.d.(1.5)
12468-PnCDF	n.d.(0.04)	n.d.(0.5)	n.d.(0.3)	n.d.(2.6)
23478-PnCDF	~0.06(0.04)	n.d.(0.5)	trace(0.3)	n.d.(2.6)
12378-PnCDD	n.d.(0.12)	n.d.(0.8)	n.d.(0.6)	n.d.(3)
123478-HxCDF	~0.1(0.06)	n.d.(0.9)	n.d.(0.3)	n.d.(3)
123678-HxCDD	n.d.(0.09)	n.d.(1.2)	n.d.(0.6)	n.d.(6)
123789-HxCDD	n.d.(0.09)	n.d.(1.2)	n.d.(0.6)	n.d.(6)
1234678-HpCDF	n.d.(0.05)	n.d.(0.6)	n.d.(1.8)	n.d.(3)
1234689-HpCDF	n.d.(0.05)	n.d.(0.6)	n.d.(1.8)	n.d.(3)
1234789-HpCDF	n.d.(0.05)	n.d.(0.6)	n.d.(1.8)	n.d.(3)
1234789-HpCDD	~0.2(0.05)	n.d.(0.5)	n.d.(1.6)	n.d.(2)
1234678-HpCDD	n.d.(0.05)	n.d.(0.5)	n.d.(1.6)	n.d.(2)
OCDF	n.d.(0.2)	n.d.(1.6)	n.d.(1.0)	n.d.(2.6)
OCDD	~0.8(0.3)	2.2(1.9)	1.8(1.3)	trace(3)

Note: Amounts listed are in picograms per microliter, no recovery correction, followed by MDL in brackets. n.d. = not detected (MDL).

narrower than the LRMS and HRMS methods. The peak shape may appear graphically wider, but the actual peak widths in terms of absolute time are very similar. As shown in these figures, interference peaks observed in LRMS are reduced or eliminated by switching to high resolution MS or hybrid MS/MS for better specificity. For example, a peak corresponding to 38 pg of 1,2,4,6,8-PnCDF was detected in low resolution mode (Figure 8), whereas it was shown to be a false positive by HRMS and hybrid MS/MS. The triple quadrupole MS/MS also did not pick up this interference peak (which had a retention time outside the window displayed in

Table 5. Comparison of Results from Four Different Mass Spectrometric Methods on a Catfish Sample

	Low Resolution	High Resolution	Hybrid MS/MS	TAGA
2378-TCDF	Int.(0.02)	2.3(0.2)	4.4(0.2)	2.4(1.6)
2378-TCDD	Int.(0.06)	6.9(0.2)	7.3(0.4)	3.7(2.6)
12468-PnCDF	38(0.04)	n.d.(0.5)	n.d.(0.3)	n.d.(1.3)
23478-PnCDF	15(0.04)	6.4(0.5)	6.2(0.3)	3.3(1.3)
12378-PnCDD	8.5(0.12)	3.7(0.8)	6.0(0.6)	2.1(2)
123478-HxCDF	~0.5(0.06)	n.d.(0.9)	0.3(0.3)	n.d.(3)
123678-HxCDD	6.3(0.09)	3.0(1.2)	4.7(0.6)	trace(3)
123789-HxCDD	1.0(0.09)	1.5(1.2)	1.4(0.6)	n.d.(3)
1234678-HpCDF	~0.6(0.05)	n.d.(0.6)	n.d.(1.8)	n.d.(3)
1234689-HpCDF	n.d.(0.05)	n.d.(0.6)	n.d.(1.8)	n.d.(3)
1234789-HpCDF	n.d.(0.05)	n.d.(0.6)	n.d.(1.8)	n.d.(3)
1234789-HpCDD	1.0(0.05)	1.5(0.5)	n.d.(1.6)	n.d.(2.5)
1234678-HpCDD	2.4(0.05)	2.1(0.5)	2.1(1.6)	n.d.(2.5)
OCDF	~0.2(0.2)	1.5(1.6)	1(1.0)	n.d.(3)
OCDD	3.4(0.3)	2.5(1.9)	4.7(1.3)	trace(3)

Note: Amounts listed are in picograms per microliter, no recovery correction, followed by MDL in brackets. Int. = interference. n.d. = not detected (MDL).

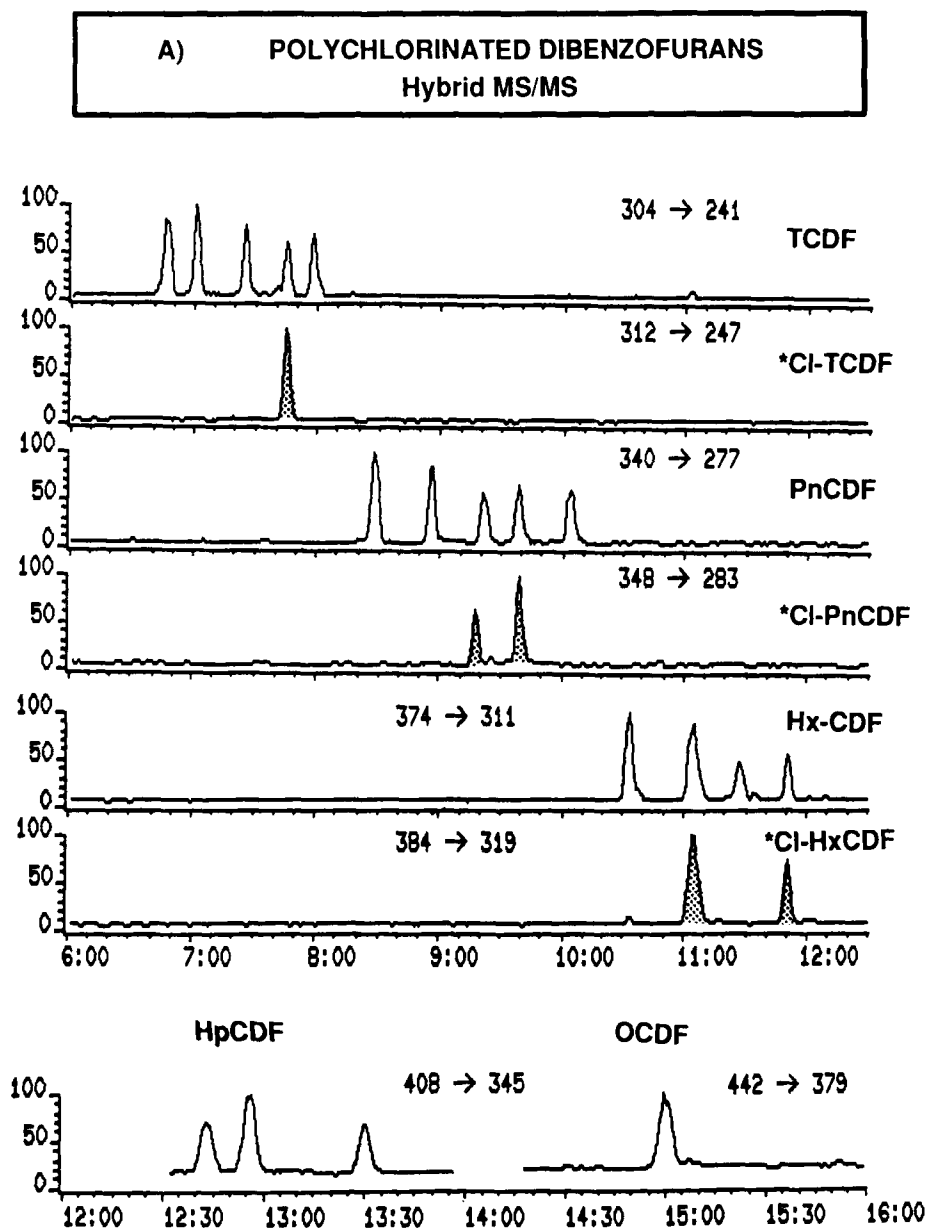
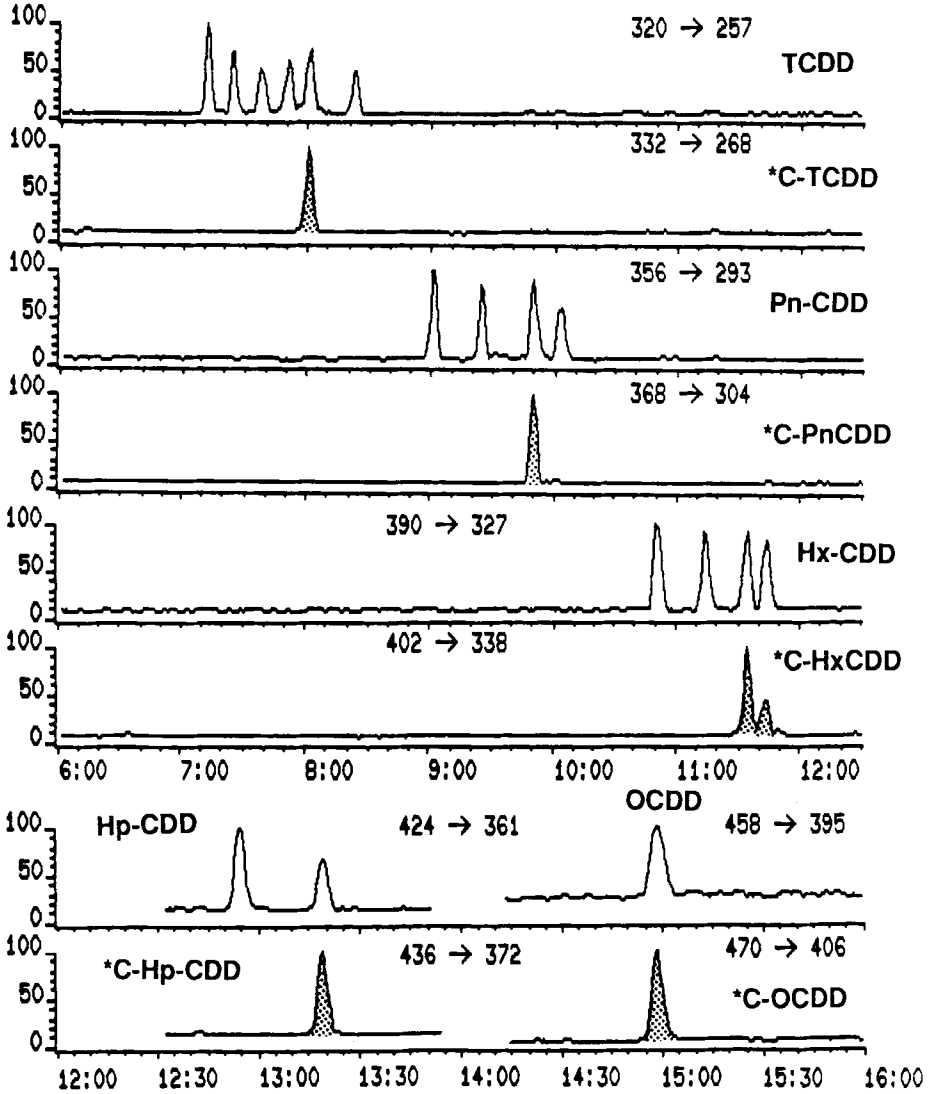


Figure 5. (A) Typical responses of PCDFs (each at 5 pg level) from a hybrid MS/MS system.

**B) POLYCHLORINATED DIBENZO-p-DIOXINS
Hybrid MS/MS**



(B) Typical responses of PCDDs (each at 5 pg level) from a hybrid MS/MS system.

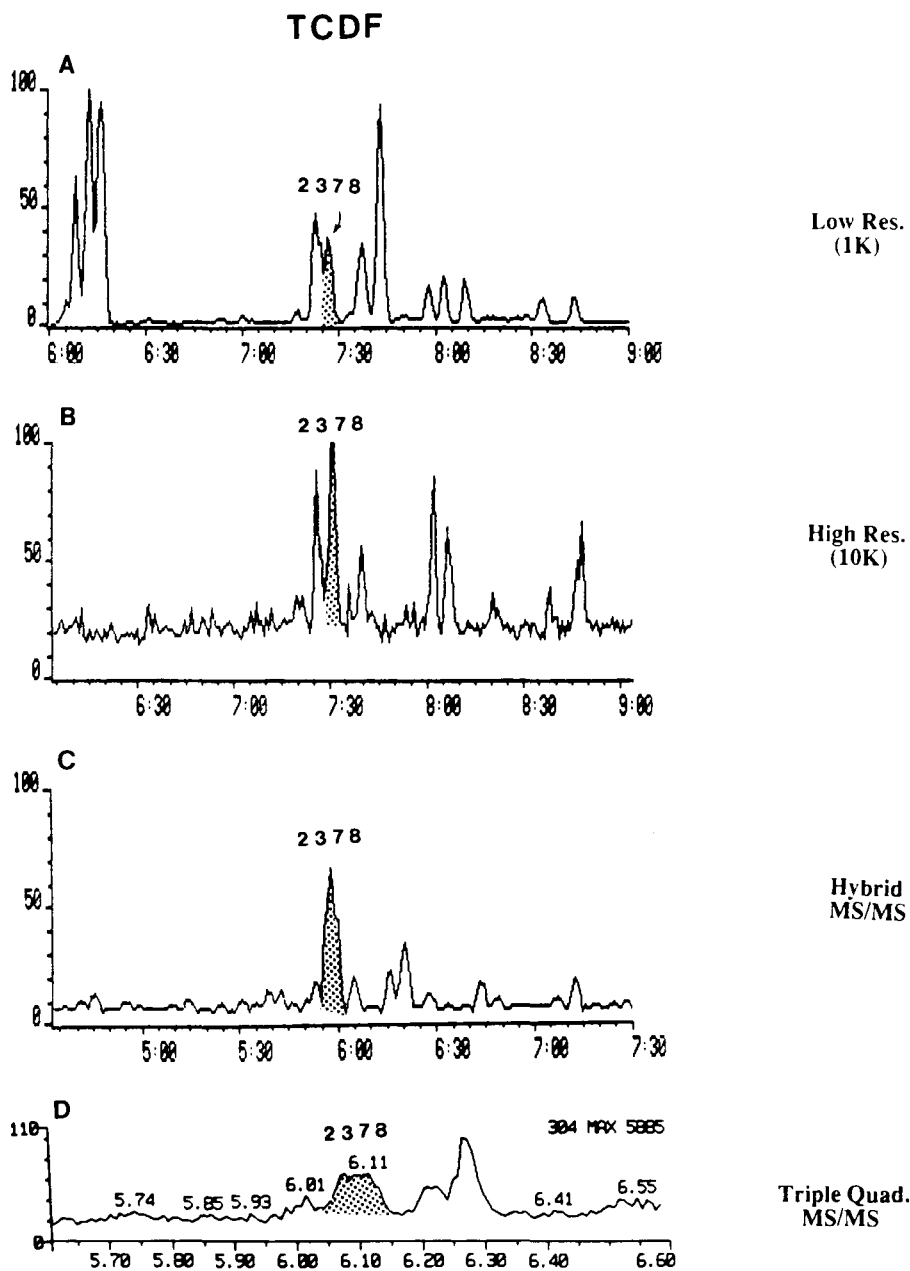


Figure 6. Mass chromatograms of TCDF in a catfish sample obtained from (A) LRMS, (B) HRMS, (C) hybrid MS/MS, and (D) triple quadrupole MS/MS.

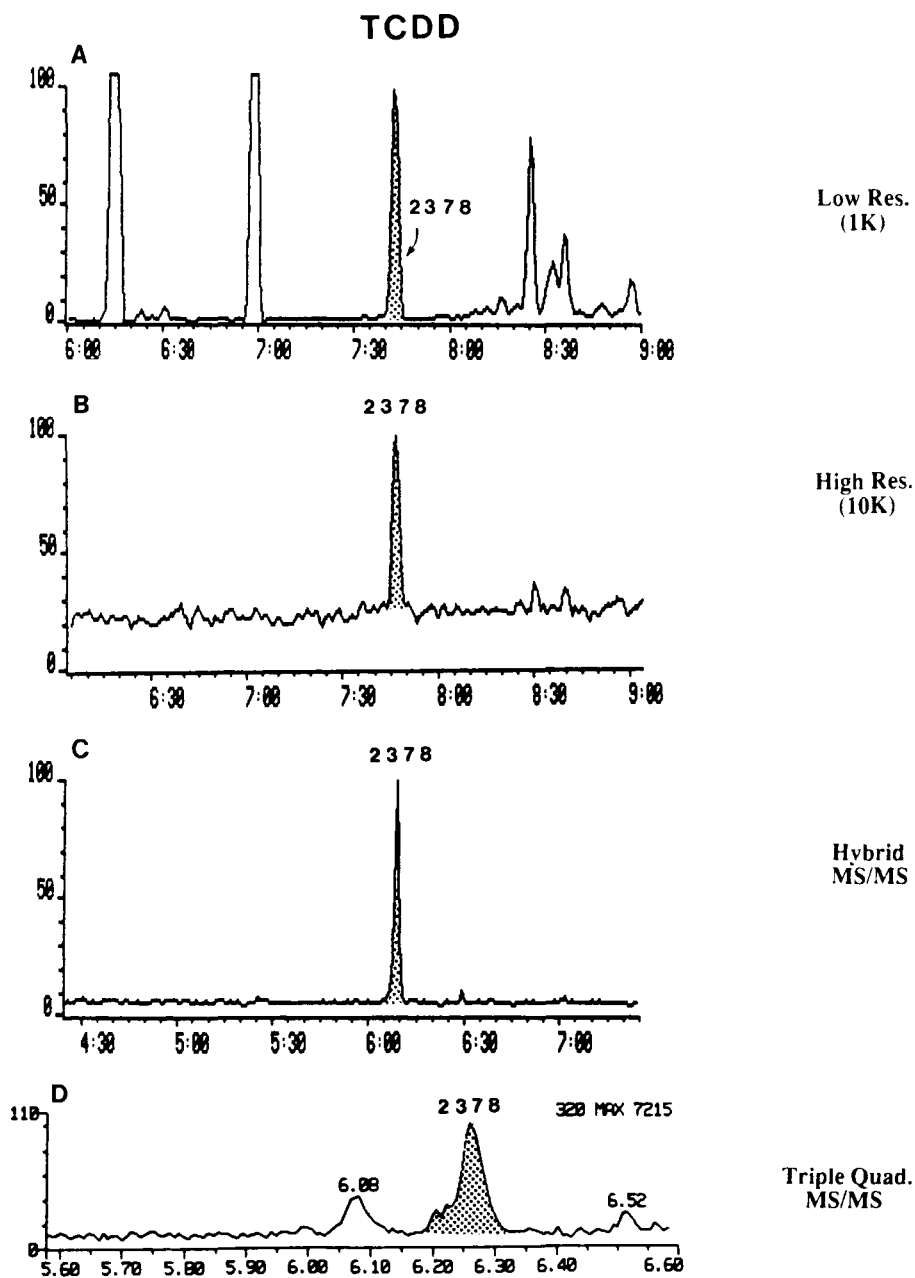


Figure 7. Mass chromatograms of TCDD in a catfish sample obtained from (A) LRMS, (B) HRMS, (C) hybrid MS/MS, and (D) triple quadrupole MS/MS.

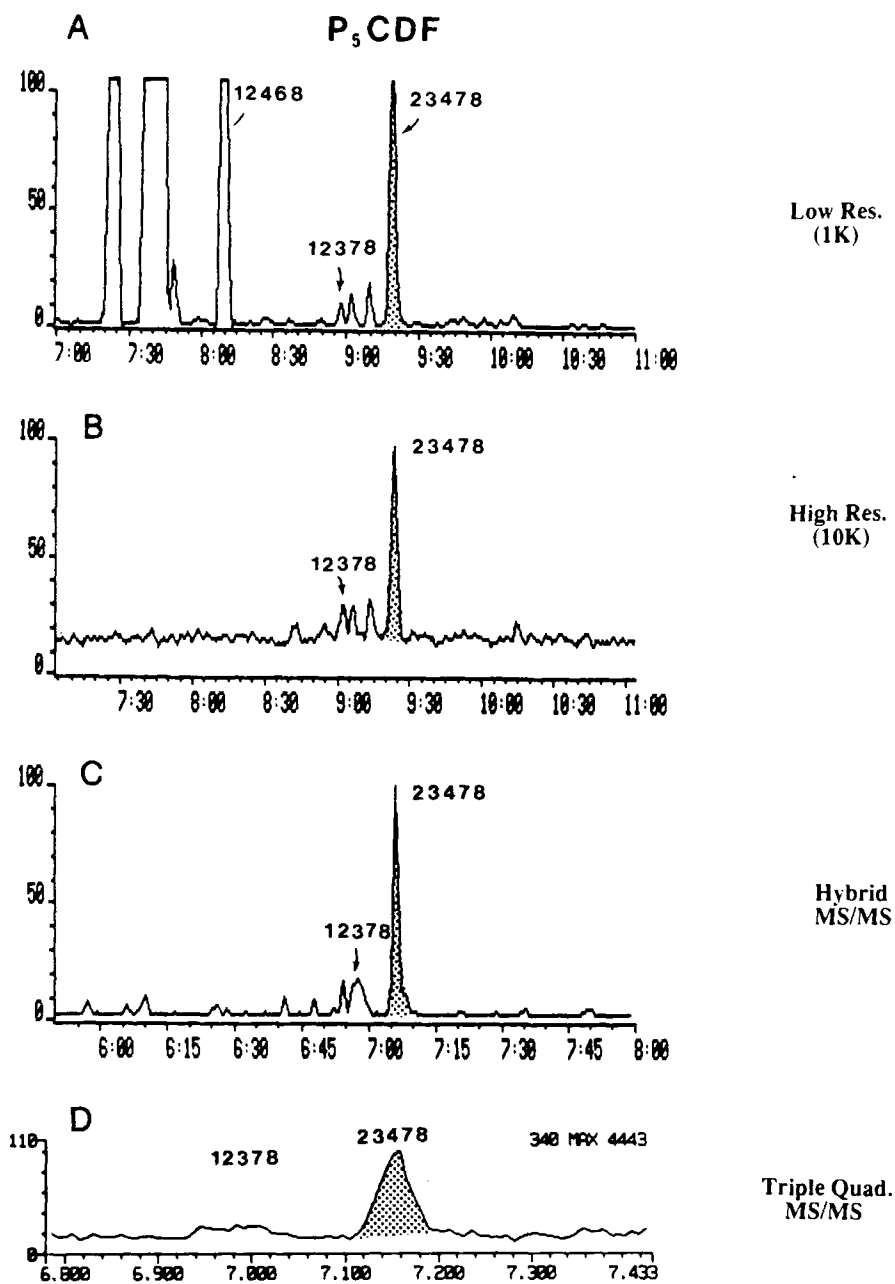


Figure 8. Mass chromatograms of PnCDF in a catfish sample obtained from (A) LRMS, (B) HRMS, (C) hybrid MS/MS, and (D) triple quadrupole MS/MS.

Figure 8). Low resolution MS also found 15 pg of 2,3,4,7,8-PnCdf in this catfish sample. However, both HRMS and hybrid MS/MS detected only 6 pg of this congener. Triple quadrupole MS/MS found 3.3 pg. A similar problem was observed in the low resolution TCDD trace (Figure 7). A large interference peak was observed in the mass chromatograms of TCDD and PnCdf at the retention time slightly earlier than that of the ^{13}C -2,3,7,8-TCDD internal standard. High resolution MS and hybrid MS/MS each detected only one peak representing 6.9 and 7.3 pg of 2,3,7,8-TCDD, respectively. Both cases indicate that real 2,3,4,7,8-PnCdf and 2,3,7,8-TCDD peaks can be obscured under chemical interference peaks. If these data are rejected simply based on the incorrect isotope ratios from the low resolution results, a false negative result would have been reported.

Table 6 displays the summary of results from a monkey fat sample. Good agreement among the four MS methods was obtained except for an interference peak in LRMS with a retention time very close to that of 2,3,7,8-TCDF and diverse values of OCDD for all methods (this may be due to the adsorption problem in the splitless injector or a slight carry over between GC injections). As shown in Figure 9, the low-level TCDF interference peak observed in LRMS was still detected in the HRMS mode although it was reduced to the noise level and did not meet the signal-to-noise ratio criterion (3:1) for detection. No peak was detected in this sample by both hybrid and triple quadrupole MS/MS modes. This example shows that in some cases, the MS/MS approach is superior to the HRMS method. We cannot provide any explanation of why the OCDD results from the triple quadrupole MS/MS deviate so much from the other methods.

Extraordinarily high levels of penta-, hexa-, and hepta-CDFs in a Japanese Yusho liver sample presented an unique problem for the analysis of PCDFs by the TAGA triple quadrupole mass spectrometer. Using "zero grade" air as the reagent gas,

Table 6. Comparison of Results from Four Different Mass Spectrometric Methods on a Monkey Fat Sample

	Low Resolution	High Resolution	Hybrid MS/MS	TAGA
2378-TCDF	Int.(0.02)	n.d.(0.2)	n.d.(0.2)	n.d.(0.3)
TCDD (not 2378-)	~0.7(0.06)	~0.5(0.2)	~0.3(0.4)	n.d.(0.8)
23478-PnCdf	~0.2(0.04)	~0.6(0.5)	~0.6(0.3)	trace(0.5)
12378-PnCDD	n.d.(0.12)	n.d.(0.8)	n.d.(0.6)	n.d.(0.5)
123478-HxCDF	5.3(0.06)	5.9(0.9)	6.3(0.3)	4.8(0.9)
123678-HxCDD	1.5(0.09)	1.0(1.2)	2.1(0.6)	1.5(0.9)
123789-HxCDD	n.d.(0.09)	n.d.(1.1)	n.d.(0.6)	n.d.(0.9)
1234678-HpCDF	~0.3(0.05)	~0.8(0.6)	n.d.(1.8)	trace(0.9)
1234689-HpCDF	~0.3(0.05)	n.d.(0.6)	n.d.(1.8)	n.d.(0.9)
1234789-HpCDF	~0.1(0.05)	n.d.(0.6)	n.d.(1.8)	n.d.(0.9)
1234789-HpCDD	n.d.(0.04)	n.d.(0.5)	n.d.(1.6)	n.d.(0.6)
1234678-HpCDD	1.8(0.04)	2.9(0.5)	3.0(1.6)	1.5(0.6)
OCDF	n.d.(0.2)	n.d.(1.6)	n.d.(1.0)	n.d.(0.9)
OCDD	37(0.3)	21(1.9)	12(1.3)	6.8(2)

Note: Amounts listed are in picograms per microliter, no recovery correction, followed by MDL in brackets. Int. = interference. n.d. = not detected (MDL).

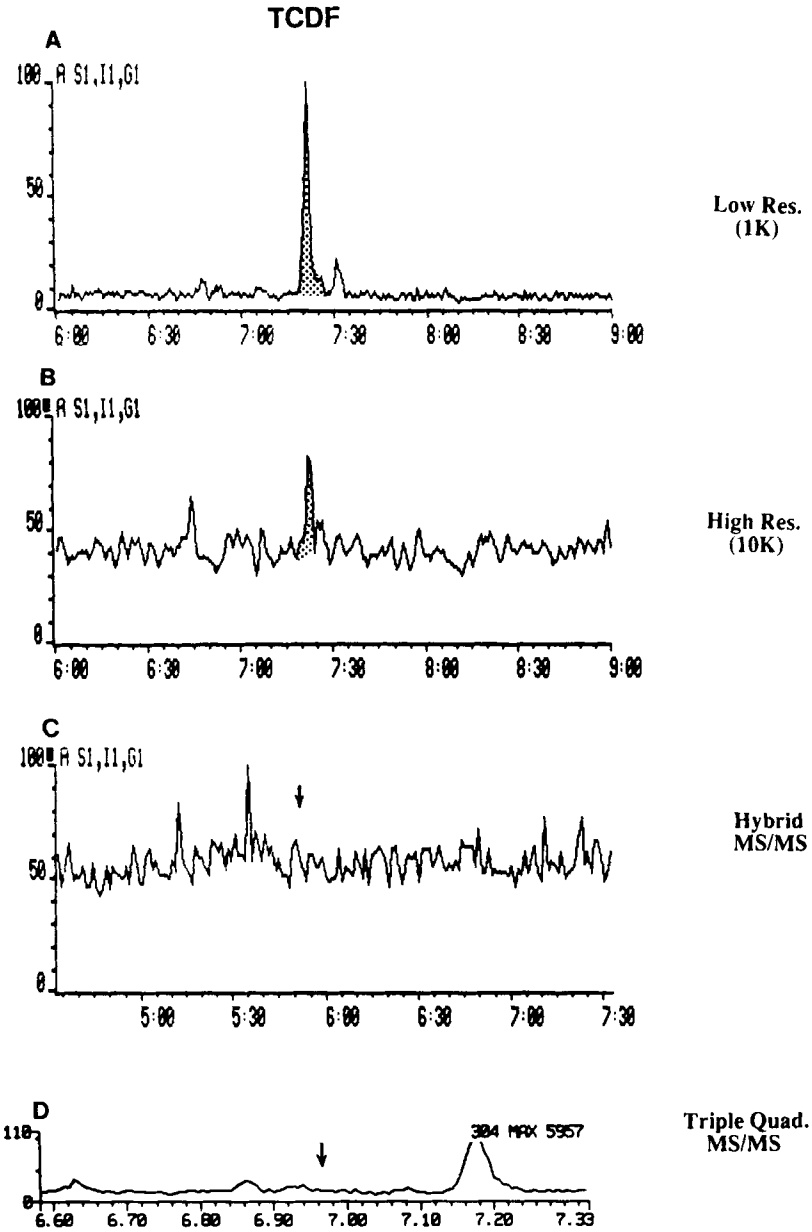


Figure 9. Mass chromatograms of TCDF in a monkey fat sample obtained from (A) LRMS, (B) HRMS, (C) hybrid MS/MS, and (D) triple quadrupole MS/MS.

reagent ions generated in the Townsend discharge CI source of the TAGA are dominated by N_2^+ , O_2^+ , and NO^+ . A great majority of the PCDFs/PCDDs are ionized through charge exchange reactions. However, ion-molecule reactions between target molecules and reagent ions lead to some undesirable by-products. For example, interaction of O_2^+ and PCDFs produces $[M + O]^+$ ions which are equivalent to PCDDs in terms of accurate mass and fragmentation pattern. This in situ formation of "pseudo-dioxins" in the Townsend discharge source obviously creates some problems because, without separation by capillary GC, no common mass spectrometric method can differentiate these ions from the native dioxins present in the sample. Although $[M + O]^-$, $[M + O - H]^-$, and $[M + O_2]^-$ are commonly observed in the negative ion mode,¹⁶⁻¹⁷ the occurrence of $[M + O]^+$ is very rare in the literature (it was reported in the case of 2,3-diphenylisobenzofuran).¹⁸ This unusual adduct ion formation is evident in the Yusho liver sample. As shown in Figure 10(c) and (g), erroneous pentachlorodibenzo-p-dioxin (PnCDD) and hexachlorodibenzo-p-dioxin (HxCDD) peaks at retention times of 7.2 and 7.95 min, respectively, were detected with exactly the same retention times as the corresponding PnCDF and hexachlorofuran (HxCDF) peaks. Based on their relative peak heights, the yield of these "pseudo-dioxins" is estimated to be around 1%. When the concentration of native PCDFs in the sample is low, these 1% "pseudo-dioxins" will be below detection limits. However, for very high PCDF concentrations such as in the Yusho case (266 $\mu\text{g}/\mu\text{L}$ of PnCDF and 1130 $\mu\text{g}/\mu\text{L}$ of HxCDF), even 1% production of these adduct ions becomes a significant interference in the determination of PCDDs. So far no good technique has been found to alleviate this problem. Diluting the sample can minimize the effect, but unfortunately at the same time the detection limit of other PCDDs is reduced to unacceptable levels. Under these circumstances, it is recommended that samples be reanalyzed using electron ionization, preferably at high resolution. Figure 11 shows the HRMS results of the same sample in which no artifactual PCDDs were observed. Table 7 shows the comparison of results from the four MS methods on this Yusho liver sample.

Other adduct ions, $[M + NO]^+$ (or $[M + 30]$) from native PCDFs, will also interfere with the determination of ^{13}C -labeled dioxin internal standards (28 mass units higher than the molecular ion of PCDFs) in LRMS. For example, the $[M + NO]^+$ of TCDF (m/z 334) will have the same nominal mass as the second isotope peak of ^{13}C -labeled TCDD ($^{37}\text{Cl}^{35}\text{Cl}_3^{13}\text{C}_{12}\text{H}_4\text{O}_2$, m/z 334). Although this should not be a problem for MS/MS because of the mass difference between the corresponding daughter ions resulting from the loss of COCl ($^{12}\text{COCl}$ for the former case and $^{13}\text{COCl}$ for the latter), the reduced resolution used in the triple quadrupole MS/MS presented an interference problem. As shown in Figure 10(d) and (h), weak signals were detected at the ^{13}C -PnCDD and ^{13}C -HxCDD internal standard traces exactly at the same retention times (7.2 and 7.95 min, respectively) as the corresponding native 2,3,4,7,8-PnCDF and 1,2,3,4,7,8-HxCDF.

In addition to the adduct ion formation, it is observed that reagent ions O_2^+ and NO^+ will also exchange with a chlorine atom of the molecular ion. These exchanged ions, equivalent to $[M + O - \text{Cl}]^+$ (or $[M - 19]$) and $[M + \text{NO} - \text{Cl}]^+$ (or

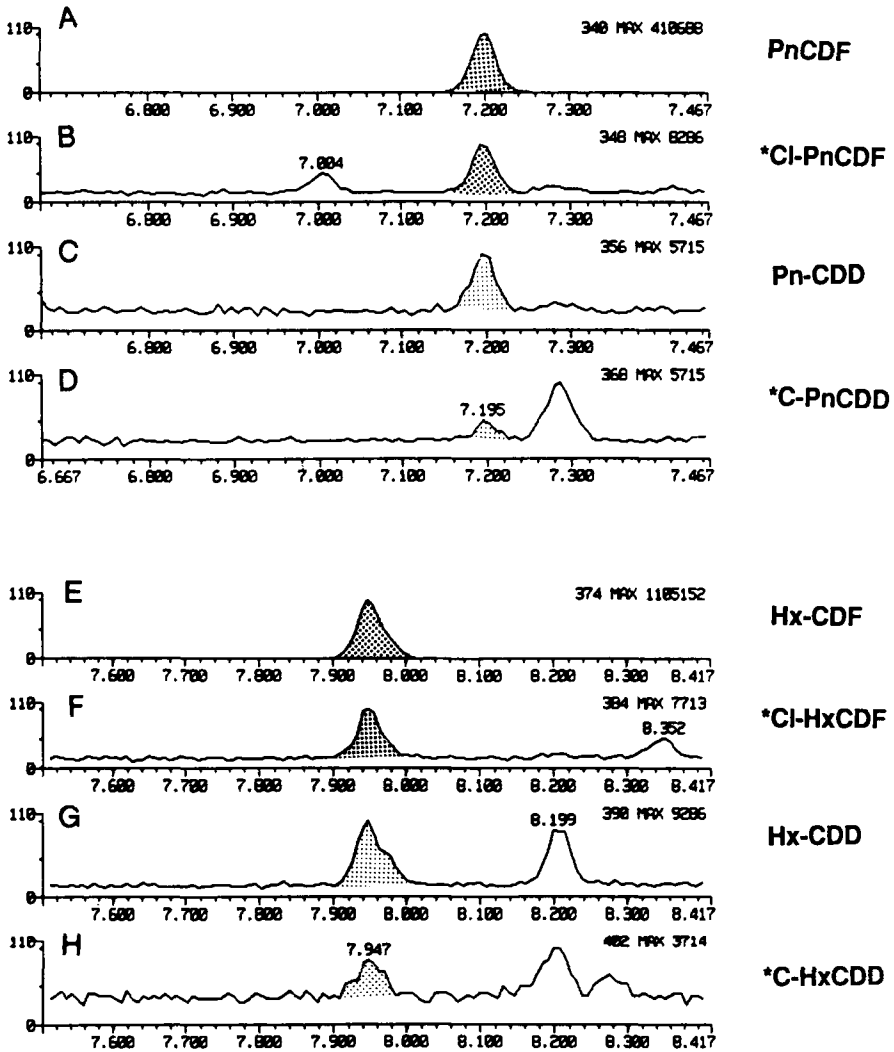


Figure 10. Multiple reaction monitoring mass chromatograms of PnCDF and PnCDD from a Japanese (Yusho) liver sample.

[M-5]), should be well separated from other target compounds or internal standards if nominal mass resolution or better can be maintained. However, this was not the case for the triple quadrupole MS/MS operated at extremely low resolution. Table 8 is a summary of possible interferences from these adduct and exchanged ions. Gas chromatographic separation becomes the only means to determine whether these ions will affect the quantitation. Interpretation of results from the TAGA triple quadrupole mass spectrometer, therefore, has to be undertaken with caution. Consideration of GC retention times allows the designation of these peaks as false positives in most instances.

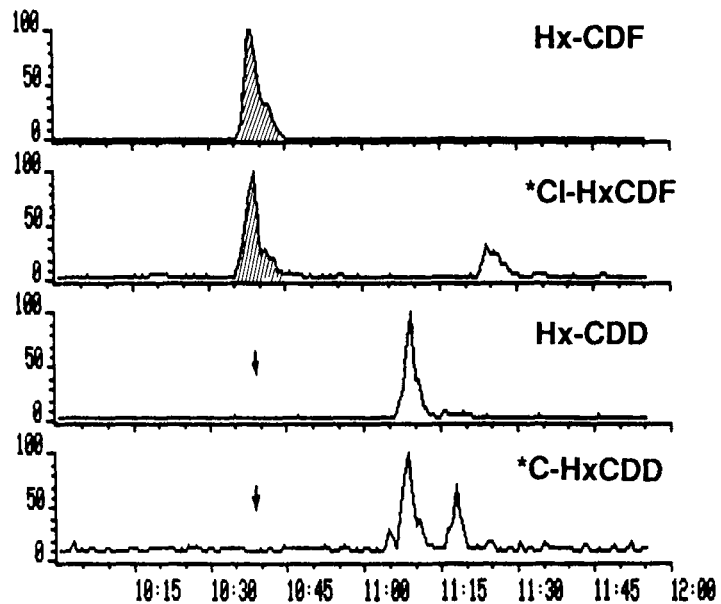
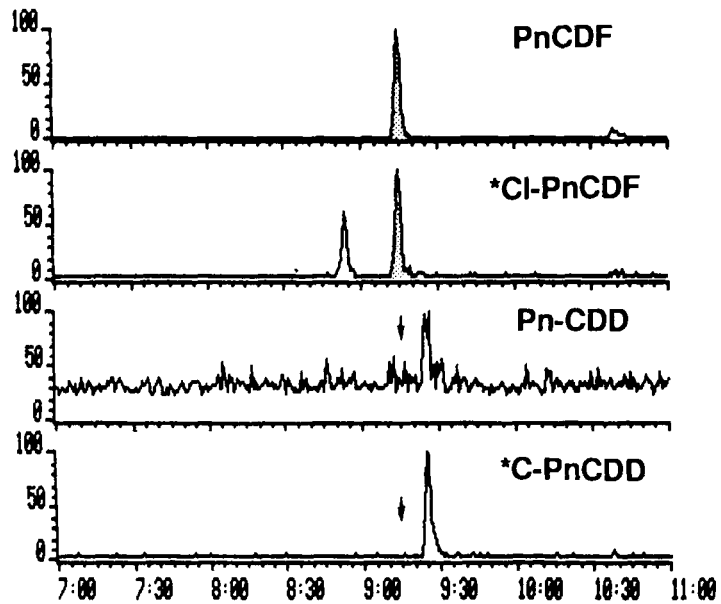


Figure 11. High resolution mass chromatogram of PnCDF and Pn-CDD from a Yusho liver sample (same as Figure 10).

Table 7. Comparison of Results from Four Different Mass Spectrometric Methods on a Yusho Liver Sample

	Low Resolution	High Resolution	Hybrid MS/MS	TAGA
2378-TCDF	~0.05(0.02)	n.d.(0.2)	n.d.(0.2)	n.d.(0.3)
2378-TCDD	n.d.(0.06)	n.d.(0.2)	n.d.(0.4)	n.d.(0.3)
23478-PnCdf	290(0.04)	240(0.5)	310(0.3)	270(0.6)
12378-PnCDD	~0.4(0.12)	~0.6(0.8)	~0.5(0.6)	n.d.(0.6)
123478-HxCDF	1400(0.06)	1100(0.9)	870(0.3)	1100(0.6)
123678-HxCDD	11(0.09)	4.6(1.1)	9.7(0.6)	8.6(0.6)
123789-HxCDD	~0.2(0.09)	n.d.(1.1)	n.d.(0.6)	n.d.(0.6)
1234678-HpCDF	270(0.05)	270(0.6)	220(1.8)	190(1.5)
1234689-HpCDF	n.d.(0.05)	n.d.(0.6)	n.d.(1.8)	n.d.(1.5)
1234789-HpCDF	16(0.05)	10(0.6)	10(1.8)	9(1.5)
1234789-HpCDD	n.d.(0.05)	n.d.(0.5)	n.d.(1.6)	n.d.(2)
1234678-HpCDD	3.4(0.05)	3.3(0.5)	2.4(1.6)	n.d.(2)
OCDF	~0.5(0.2)	n.d.(1.6)	n.d.(1)	n.d.(2.6)
OCDD	110(0.3)	48(1.9)	46(1.3)	59(3)

Note: Amounts listed are in picograms per microliter, no recovery correction, followed by MDL in brackets. n.d. = not detected (MDL).

Table 8. Interferences From the Production of Adduct Ions in the Townsend Discharge CI Source

Target Compounds	Interferences	%Yield of Adducts	Diff. ^a (Da)
Native PCDDs	[M + O]([M + 16]) of native PCDFs	~1—10%	0
¹³ C-PCDDs	[M + NO]([M + 30]) ^b of native PCDFs	<0.5%	2
³⁷ Cl-PCDFs (penta- & hexa-)	[M + O - Cl]([M - 19]) ^b of [M + 2] of ¹³ C-PCDDs (penta- & hexa-)	~45—75%	-1 & 1
¹³ C-PCDFs	[M + NO - Cl]([M - 5]) ^b of native PCDDs	~50%	1
Native TCDF	[M + NO - ³⁷ Cl]([M - 7]) ^b of ³⁷ Cl-TCDF	<2%	-1
[M + 2] of PnCdf	[M + NO - ³⁷ Cl]([M - 7]) ^b of ³⁷ Cl-PnCdf	~15%	-1

^a Mass difference between the molecular ion of the target compounds (column 1) and the interference adduct ions (column 2).

^b Interference occurs only when below nominal mass resolution is used.

CONCLUSION

It has been demonstrated from these experiments that LRMS may not provide enough specificity for the analysis of PCDFs and PCDDs in complex biological matrices. The potential of a MS/MS system for improving the specificity is quite apparent. The hybrid MS/MS system offers a slightly better detection limit and equivalent or better specificity than the HRMS method. In addition, it offers the opportunity of selecting the parent ion under low or medium resolution conditions. This provides an additional dimension to the selectivity of the analysis. However, it should also be pointed out that the MS/MS approach does have several drawbacks.

1. The cost of a MS/MS system (triple quadrupole, hybrid, or multiselector instruments) is much higher than the single analyzer system. It also requires a higher degree of expertise to operate the instrument and interpret the data.
2. The results are more susceptible to variation in operating parameters such as CID gas pressure fluctuation, slight off-focus of daughter ions, and so forth. Additional stable isotope-labeled internal standards need to be incorporated (preferably one for every analyte) into the analytical scheme.
3. The daily tuning and optimization in MS/MS mode are normally more difficult than the conventional MS, mainly due to the lack of a suitable general reference compound which has exact MS/MS properties as the target compounds.
4. There is a general belief that the additional specificity provided by the MS/MS method can be substituted for some chemical cleanup steps. Based on our five years of experience in using the MS/MS technique for the analysis of PCDFs/PCDDs, no simplification of sample cleanup can be achieved. Our detailed spiking studies indicated that the matrix or co-extractive materials injected onto the GC column will have a serious adverse effect on the quantitation of target compounds at ultratrace levels. This phenomenon is generally referred to as the matrix effect. In other words, sample cleanup still has a very significant role to play in producing reliable data.

Special attention has to be given to the ion chemistry within the Townsend discharge source when air or oxygen is used as a reagent gas. In the case of using the TAGA MS/MS system, reducing the mass resolution improves the detection limits, but also makes this technique more susceptible to interferences due to the adduct ion formation or exchange reactions between reagent ions and target compounds.

REFERENCES

1. Dougherty, R. C. "Negative Chemical Ionization Mass Spectrometry: Applications in Environmental Analytical Chemistry," *Biomed. Mass Spectrom.* 8:283 (1981).
2. Miles, W. F., Gurprasad, N. P., and Malis, G. P. "Isomer-Specific Determination of Hexachlorodibenzo-p-dioxins by Oxygen Negative Chemical Ionization Mass Spectrometry, Gas Chromatography, and High-Pressure Liquid Chromatograph," *Anal. Chem.* 57:1133 (1985).
3. Krofmacher, W. A., and Mitchum, R. K., "Atmospheric Pressure Ionization Mass Spectrometry of the Polychlorinated Dibenzo-p-dioxins," *Org. Mass Spectrom.* 19(7):299 (1984).
4. Tondeur, Y., Warren, N. N., Campana, J. E., and Missler, S. R. "A Hybrid HRGC/MS/MS Method for the Characterization of Tetrachlorinated-p-dioxins in Environmental Samples," *Biomed. Environ. Mass Spectrom.* 14:449—456 (1987).
5. Bursey, M. M., and Hass, J. R. "Tandem Mass Spectrometry for Environmental Problems" in *Tandem Mass Spectrometry*, McLafferty, F. W., Ed. (New York: John Wiley & Sons, Inc., 1983), pp. 465—478.

6. Sakuma, T., Gurprasad, N., Tanner, S. D., Ngo, A., Davidson, W. R., Mcleod, H. A., Lau, B. P.-Y., and Ryan, J. *Chlorinated Dioxins and Dibenzofurans in the Total Environment. II*, Keith, L. H., Rappe, C., and Choudhary, G., Eds. (Stoneham, MA: Butterworth Publishers, 1985), pp. 139—152.
7. Mahle, N. H., and Shadoff, L. A. "The Mass Spectrometry of Chlorinated dibenzo-p-dioxins," *Biomed. Environ. Mass Spectrom.* 9(2):45—60 (1982).
8. Webster, G. R. B., Olie, K., and Hutzinger, O. "Polychlorodibenzo-p-dioxins and Polychlorodibenzofuran," in *Mass Spectrometry in Environmental Sciences*, Karasek, F. W., Hutzinger, O., and Safe, S., Eds. (New York: Plenum Press, 1985), pp. 257—296.
9. Clement, R. E., and Tosine, H. M. "The Gas Chromatography/Mass Spectrometry Determination of Chlorodibenzo-p-dioxin and Dibenzofurans," *Mass Spectrom. Rev.* 7:593—636 (1988).
10. Crummett, W. B., Lamparski, L. L., and Nestruck, T. J. "Review and Trends in the Analysis for PCDD/PCDF," *Toxicol. Environ. Chem.* 12:111—135 (1986).
11. Ryan, J. J., Williams, D. T., Lau, B. P.-Y., and Sakuma, T. "Analysis of Human Fat Tissue for 2,3,7,8-Tetrachloro-dibenzo-p-dioxin and Chlorinated Dibenzofuran Residues," in *Chlorinated Dioxins and Dibenzofurans in the Total Environment. II*, Choudhary, G., Keith, L. H., and Rappe, C., Eds. (Stoneham, MA: Butterworth Publishers, 1985), pp. 205—213.
12. Lebel, G. L., Williams, D. T., Ryan, J. J., and Lau, B. P.-Y. "Evaluation of XAD-2 Resin Cartridge for Concentration/Isolation of Chlorinated Dibenzo-p-dioxins and Furans from Drinking Water at the Parts-per-Quadrillion Level," in *Chlorinated Dioxins and Dibenzofurans in Perspective*, Rappe, C., Choudhary, G., and Keith, L. H., Eds. (Ann Arbor: Lewis Publishers, Inc., 1986), pp. 329—341.
13. Ryan, J., Lau, B. P.-Y., Hardy, J. A., Stone, W. B., O'Keefe, W. B., and Gierthy, J. F. "2,3,7,8-Tetrachloro-dibenzo-p-dioxin and Related Dioxins and Furans in Snapping Turtle (*Chelydra Serpentina*) Tissue," *Chemosphere* 15:537 (1986).
15. Schellenberg, D. H., Bobbie, B. A., Reiner, E. J., and Taguchi, V. Y. "Optimization of MS/MS Parameters for the Determination of Chlorinated Dibenzo-p-dioxins and Dibenzofurans in Environmental Samples," in proceedings of the 36th ASMS Conference on Mass Spectrometry and Allied Topics, San Francisco, CA, June 5—10, 1988, p. 238.
16. Budzikiewicz, H. "Negative Chemical Ionization (NCI) of Organic Compounds," *Mass Spectrom. Rev.* 5:345—380 (1986).
17. Harrison, A. G. *Chemical Ionization Mass Spectrometry* (Boca Raton, FL: CRC Press, Inc., 1983), pp. 80.
18. Hunt, D. F., Brumely, W. C., Stafford, G. C., and Botz, F. K. "Analysis of Polycyclic Aromatic Hydrocarbons by Pulsed Positive-Negative Ion CIMS with Oxygen as the Reagent Gas," in *Mass Spectrometry, Part B*, Merritt, C., Jr., and McEwen, C. N., Eds. (New York: Marcel Dekker, Inc., 1980), pp. 327—328.

CHAPTER 8

The Evaluation of Toxicity of Water Leachates from Incinerator Flyash Using Living Human Cells and Analytical Techniques

E. Jellum, A. K. Thorsrud, N. C. Herud, H. Y. Tong, and F. W. Karasek

ABSTRACT

This study concerns the possibility of polychlorodibenzo-p-dioxins (PCDDs), polychlorodibenzofurans (PCDFs), and other organic and inorganic compounds entering the environment through the leaching of municipal incinerator flyash into water.

To simulate the conditions by which flyash comes into contact with water, a Soxhlet extraction of flyash using water as solvent was chosen because of its simulation of the circulation of rainwater in nature and because of its efficient use of a small volume of water and minimum glass surface. Following the extraction, a simple benzene-water partitioning step was used to transfer the organic compounds in the water extracts into organic solvent for subsequent GC and GC/MS analysis. Good recovery of PCDDs at the 2-ppt level was obtained using benzene partitioning.

The inorganic compounds in the water leachate were determined directly by inductively coupled plasma (ICP) techniques.

The analytical results for organic compounds in the water extracts show that PCDDs and PCDFs enter water through leaching in minimum quantities. These compounds were found in water at the 1- to 400-ppt level and are at very low concentration compared to the amount of PCDDs and PCDFs typically present adsorbed on the surface of this flyash.

The study also included identification of other organic compounds that were leached from the flyash into the water extracts. Identification of these organic compounds was accomplished using the techniques of GC/FID, GC/EIMS, GC/PICIMS, and GC/NICIMS. These compounds were present at higher concentrations than the PCDDs and PCDFs, and many were chlorinated. A total of 61 were found.

The extraction procedure described in this report provides a quick and easy method for the determination of the extent of potential leaching from samples such as flyash. The method does not take into account factors such as soil attenuation and temperature, but it does provide a means of evaluating leaching under the most favorable conditions. The rate of leaching in nature from rain and ground water is very inefficient compared to the leaching occurring in a Soxhlet extractor, so that the organic compounds and their concentration found in this study represent the limiting circumstances for leachate.

The water extracts of the flyash show a marked toxicity towards human cells, as demonstrated by changes in the two-dimensional electrophoretic pattern of proteins synthesized by fibroblasts in culture. The toxicity was the same whether or not the organic compounds had been removed prior to the water leaching. The water extracts contained higher concentrations (parts per million) of inorganic compounds, particularly lead, cadmium, antimony, and arsenic. These compounds present in the leachates explain the toxicity of the water extract of the flyash. The conclusion of this study is that the leaching of heavy metal compounds into the ground water most likely represents a more important pollution problem than the leaching of dioxins and other organic compounds. The latter compounds are relatively insoluble in water and are firmly adsorbed to the flyash particles and are present only in trace quantities (parts per trillion) in the water leachates.

INTRODUCTION

In large cities throughout the world, municipal waste is disposed of by incineration. The amount of urban waste disposed of in this manner worldwide is large. Canada, for example, disposes of an estimated 3 million ton of waste by incineration annually. A fine inorganic particulate matter known as flyash is formed in the combustion zone of the incinerator. This product is precipitated electrostatically from effluent gases and is usually disposed in landfills. Approximately 35,000 ton of flyash are produced for each million ton of waste incinerated. It is therefore important to study the environmental and health effects of flyash.

The composition of flyash has been studied extensively. It is composed of 70 to 95% inorganic matter such as SiO_2 , Al_2O_3 , Na_2O , and Fe_2O_3 ,¹ along with small

amounts of heavy metals such as Pb, Hg, Zn, and As. Adsorbed on the inorganic matter are more than 600 organic compounds in the parts-per-million to parts-per-billion range, many of which have been identified. These compounds include hydrocarbons, phthalates, polycyclic aromatic hydrocarbons (PAHs), and polychlorinated organic compounds.²

Some of the organic compounds, especially those containing chlorine, identified in flyash are known to be toxic. Of special concern are two classes of compounds known as polychlorinated dibenzo-p-dioxins (PCDDs) and polychlorinated dibenzofurans (PCDFs). Because of the different numbers of chlorine atoms and the different substitution patterns possible, 75 PCDD and 135 PCDF congeners exist, most of which are found on flyash. Some PCDD congeners, especially 2,3,7,8-tetrachlorodibenzo-p-dioxin (2378-TCDD) are extremely toxic.³ In addition, it is known that large amounts of the heavy metals present in flyash are toxic. Because these hazardous compounds are found in municipal flyash, regardless of the design of the incinerator or the type of garbage burned, the effect of flyash residue in the environment is an important issue.

More than 98% of the flyash is trapped by electrostatic precipitators and has to be disposed of in some manner. Most often it is buried in landfill sites. This method of disposal seems the most economical and practical. However, the flyash buried in a landfill site is constantly exposed to rain and ground water, which presents the possibility of leaching out toxic organic and inorganic compounds. It is important to know whether PCDDs and PCDFs and other organic pollutants and toxic metals are removed by water leaching and the relative toxicity of these pollutants. Little investigation has been done to examine this question.

In this study flyash samples were extracted extensively with benzene to remove all organic compounds and thereby to obtain a "cleaned" flyash. Cleaned and uncleaned flyash were then extracted with water, and the effect of water leachates on human living fibroblasts and leukocytes was tested. The results of these experiments, combined with a knowledge of the content of organic and inorganic compounds in the various leachates, should lead to a conclusion whether it is the dioxins and other such compounds, or the heavy metals on the flyash, that represent a contamination hazard to the ground water by flyash buried in landfills.

EXPERIMENTAL

Solvents and Standards

All solvents used were distilled in glass, UV grade, supplied by Caledon Laboratories (Georgetown, Ontario, Canada), with the exception of the water, which was deionized tap water. The standards of 1,2,3,4-tetrachlorodibenzo-p-dioxin (1234-TCDD), 1,2,3,4,7,8-hexachlorodibenzo-p-dioxin (123478-H₆CDD), 1,2,3,4,6,7,8-heptachlorodibenzo-p-dioxin (1234678-H₇CDD), and octachlorodibenzo-p-dioxin (OCDD) were all purchased from Ultra Scientific (Hope, RI). The standard of 1,2,3,4,7-pentachlorodibenzo-p-dioxin (12347-P₅CDD) was obtained from Cambridge Isotope Laboratories Inc. (Woburn, MA). All glassware was cleaned by

ultrasonic agitation in water and detergent powder (Canadian Laboratory Supplies) for 30 min. The glassware was rinsed with copious amounts of tap water followed by deionized water, prior to drying at 250°C for 3 hr. The glassware was rinsed three times with benzene, three times with dichloromethane, and allowed to air dry completely immediately before use.

Sample Collection

The flyash from three quite different incinerators were studied: a municipal incinerator in Toronto, Ontario, Canada; another from Machida, Japan; and the third from a copper smelter in Noranda, Quebec, Canada. The flyash samples were collected in kilogram amounts by grab sampling from the electrostatic precipitator of the incinerators studied and were stored at room temperature, away from ultraviolet and visible light.

Extraction of Flyash with Water

All flyash samples were extracted by using deionized water at a pH of 7 as the solvent in a Soxhlet extraction apparatus. The Soxhlet apparatus was cleaned by operating it with 30 mL of benzene for 1 hr prior to use, followed by a 300-mL deionized water run for several hours to ensure the removal of contaminants. A 50-g sample of flyash was placed in a coarse porosity fitted glass extraction thimble and extracted for 48 hr with 400 mL water in the Soxhlet apparatus. After the extraction, the Soxhlet apparatus was dismantled, and the Soxhlet extractor and the outside of the thimble were rinsed with 50 mL water to remove all traces of flyash. This water was added to that already in the round-bottom flask. The same glass surfaces were then rinsed with a 50-mL volume of benzene, which was placed in a separatory funnel. The thimble was emptied, and all visible traces of flyash were removed by rinsing the thimble under the deionized water tap. The thimble was then used to filter all the water previously collected, which was then transferred to the separatory funnel. Several water rinses of the round-bottom flask were also filtered through the thimble into the separatory funnel. The thimble was again rinsed under the tap to remove any particulate matter, then 25 mL of benzene were forced through the thimble by applying positive pressure at the top of the thimble with a rubber bulb. The round-bottom flask was rinsed several times with a total of 25 mL of benzene, which was added to the separatory funnel.

A magnetic Teflon stir bar was used in conjunction with a hot plate/stirrer to mix the water constantly. The heating mantle was placed on top of the hot plate/stirrer. The vortex of the water was kept close to the bottom of the flask to ensure good heat transfer.

The extraction was performed in duplicate, and an extraction blank, which used the same method but omitted the flyash, was also run.

ORGANIC COMPOUND ANALYSIS

Benzene-Water Partitioning

After the Soxhlet extraction, enough benzene was added to the separatory funnel to bring the total volume of benzene to 150 mL, and this volume was used as the first of three 150-mL aliquots of benzene used for solvent extraction. The three aliquots of benzene extract were combined, and the volume was reduced to approximately 15 mL by rotary evaporation under aspirator vacuum. The extract was then transferred to a cone-bottom flask with a Pasteur pipette, followed by several benzene rinses of the round-bottom flask, and the volume was further reduced to approximately 5 mL in the same manner. The top phase in the cone (the benzene phase) along with several benzene rinses were transferred by Pasteur pipette to a small cone-bottom flask, taking care not to transfer any of the aqueous phase. The volume in the flask was reduced to approximately 1 mL using rotary evaporation under aspirator vacuum and then transferred with several benzene rinses to a calibrated 1 mL reacti-vial. The volume was reduced to near dryness under a gentle stream of high-purity nitrogen, reconstituted to 20 μ L, and the vial was sealed and stored at -15°C .

Gas Chromatographic Analysis

GC analyses were carried out on a Hewlett-Packard HP 5880A gas chromatograph equipped with a flame ionization detector (FID) and an electron capture detector (ECD). A cool on-column injector and a 30 m \times 0.32 mm i.d. Durabond DB-5 fused silica capillary column (J & W Scientific, Rancho Cordova, CA) were used for both the FID and ECD analyses. A microcomputer data system and cartridge tape allows storage of chromatographic information for further calculations. The GC conditions for both methods of detection were as follows: injection port temperature at less than 50°C , column temperature programmed from 80 to 300°C at $5^{\circ}\text{C}/\text{min}$ with initial 1-min and final 10-min isothermal periods, detector temperature 350°C , and helium carrier gas flow rate 3 mL/min at room temperature.

Gas Chromatographic/Mass Spectrometric Analysis

GC/MS analyses were performed using a Hewlett-Packard HP 5987A GC/MS system with an HP 1000 data system and an HP 7914 Winchester disk drive.

For the electron ionization (EI) mode, an ionized voltage of 70 eV and a source temperature of 250°C were used. A direct interface kept at 300°C linked the HP 5880A to the mass spectrometer. Both linear scanning (50 to 500 amu) and selected ion monitoring (SIM) were used. Using SIM, it is possible to monitor up to five different groups of ions with up to 20 selected ions in each group. The system provided for data acquisition, and storage allows the reconstruction of chromatograms at any mass in the scan range. During or after a run, the mass spectrum of any peak on the total ion chromatogram (TIC) trace may be obtained. To help

identify compounds by their mass spectra, there is a library search system which incorporated a probability-based matching system (PBM) based on 70,000 reference spectra as well as a self-training interpretive retrieval system (STIRS).

The column used was a 30 m \times 0.25 mm Durabond DB-5 fused silica capillary column (J & W Scientific, Rancho Cordova, CA). The GC conditions were the same as those used for the GC analysis.

The GC/MS was also operated in the chemical ionization (CI) mode. The reagent gas for CI was methane. The source temperature for positive ion chemical ionization (PICl) was 200°C, and it was 100°C for negative ion chemical ionization (NICl).

Dioxin Recovery Study

Since the dioxins exhibit one of the lowest solubilities of the organic compounds, the following recovery study was performed.

A benzene solution containing 5.0 ng/ μ L 1234-TCDD and 4.7 ng/ μ L OCDD was diluted to various concentrations. Each solution was used to spike a 250-mL aliquot of water in a round-bottom flask. Each aqueous solution was well shaken and allowed to sit for 30 min. The dioxins were solvent extracted in a separatory funnel with 3 \times 100-mL aliquots of benzene. A 25-mL volume of benzene was then used to rinse the round-bottom flask and the separatory funnel. All of the benzene was combined, and the volume was reduced to approximately 15 mL with rotary evaporation under aspirator vacuum. The extract was transferred to a cone-bottom flask with several benzene rinses, and the volume was further reduced to approximately 5 mL by the same method. The organic phase was transferred by Pasteur pipette to a small pear shape flask, along with several benzene rinses, taking care not to transfer any of the aqueous phase. The volume of the benzene extract was reduced to approximately 1 mL by rotary evaporation under aspirator vacuum and transferred to a 1-mL reacti-vial along with several benzene rinses. The volume of the benzene in the reacti-vial was reduced under a gentle stream of high purity nitrogen just to the point of dryness, and 20 μ L of benzene was added to the vial before sealing it and storing it at -15°C.

Further recovery studies were performed on a PCDD standard mixture containing 1234-TCDD, 12347-P₅CDD, 123478-H₆CDD, and 1234678-H₇CDD, all at concentrations of approximately 50 ppb in benzene. A 10- μ L volume of this solution was used to spike a 250-mL volume of water to give a final concentration for each dioxin component of approximately 2 ppt. The flask was shaken and allowed to sit for 30 min, then solvent extracted in a separatory funnel with 2 \times 50-mL aliquots of benzene. A 25-mL volume of benzene was used to finally rinse the separatory funnel, then the total volume of benzene was reduced to dryness in the manner described here and diluted to 20 μ L with benzene.

To determine the recovery of dioxins in water, each sample and respective standard was injected on the HP 5880 GC using ECD detection. The only difference in chromatographic conditions from those previously described was the temperature program, which was as follows: 80 to 200°C at 20°C/min, then programmed from

200 to 300°C at 6°C/min. There were 1-min initial and 5-min final isothermal periods.

The corresponding peak areas of the various dioxin standards were used to determine the percentage of dioxin recovered by the solvent extraction. The recovery studies were performed in duplicate.

INORGANIC COMPOUND ANALYSIS

Inductively Coupled Plasma

Two different samples were used to study the toxicity effects of inorganic compounds leached from flyash. The first sample was the water extract from Soxhlet extraction of the original flyash with water. The second flyash sample was one in which all organic compounds had been removed by a prior Soxhlet extraction with benzene. The water leachates obtained by water Soxhlet extraction of these two samples were condensed to 50 mL prior to performing the inorganic analyses and toxicity tests.

The metal content of flyash and water leachates was determined by inductively coupled plasma emission spectrometry (ICP) using a Perkin Elmer Model Plasma 2 ICP instrument (Norwalk). The flyash was dissolved in aqua regia (HCl/HNO₃ 3/1 v/v) containing hydrofluoric acid at a temperature of 120°C for 4 hr in a sealed container under pressure. After cooling, boric acid was added to dissolve eventual fluoride precipitate. Two reference samples, National Bureau of Standards NBS 1633a and Coal Flyash, were included as controls. The water leachates contained a precipitate, which was partly acid-insoluble. After vigorous homogenization, aliquots were withdrawn and dried at 105°C overnight for determination of dry material. This was subsequently dissolved in aqua regia and hydrofluoric acid and treated in the same way as flyash.

Two-Dimensional Gel Electrophoresis

An ISO-DALT system (Electro-Nucleonics, Oak Ridge, TN), as described by Anderson and Anderson,^{4,5} was used for high resolution two-dimensional polyacrylamide gel electrophoresis. The ISO apparatus allows isoelectric focusing of 20 samples at a time, and the DALT tank for SDS-electrophoresis in the second dimension holds 20 slab gels.

The analytical procedure is basically as described by Anderson's group at Argonne National Laboratory.^{4,5} Cells (lymphocytes/fibroblasts) are radiolabeled by culturing in media supplemented with ³⁵S-methionine and are lysed in urea/NP-40/mercaptoethanol/ampholyte dissociation buffer mentioned here.⁶

Toxicity Test Using Human Cells and Two-Dimensional Electrophoresis

In this test, human living cells, particularly fibroblasts or freshly isolated peripheral blood leucocytes in culture, are utilized.⁷ These cells are allowed to grow

and synthesize proteins in the absence and presence of the added compound(s) to be tested, in this case water leachates. During the incubation period, the proteins become radiolabeled as the incubation medium contains ^{35}S -methionine. After two-dimensional (2-D) and autoradiography, changes in the 2-D protein profile are readily seen if the added chemicals have had toxic or mutagenic effects. In principle, the target of harmful chemicals may be the genes (DNA), the transcription process to m-RNA, the various RNAs involved in protein synthesis, the ribosomes, and the many enzymes involved in the making of new proteins. Attack at any one or more of these steps may lead to alteration of the cellular protein pattern. In practice the effects of adding increasing amounts of a toxic or mutagenic mixture are one or more of the following: (1) the synthesis of the majority of the 2000 proteins seen on the 2-D gels are gradually and easily blocked; (2) the production of a limited number of proteins are virtually unchanged (resistant to the chemical); and (3) new proteins are being formed.

RESULTS AND DISCUSSION

In nature, there is a constant circulation of water — vaporization, condensation, and precipitation. This circulation is similar to the basic process of a Soxhlet extractor. Therefore, the Soxhlet extraction of flyash with water is a good simulation of leaching flyash with water in nature. In a thimble, flyash always contacts fresh-water which is condensed. By recycling, a significant amount of organic and inorganic compounds can be gradually removed from the flyash, even those with low solubilities in water. A relatively small amount of water provides a highly efficient extraction of organic compounds in a Soxhlet extraction procedure. Eventually, these compounds removed from flyash can be accumulated in the water extract to a detectable quantity. This also reflects the phenomenon of nature, in which the organic compounds are gradually leached away by water from the flyash.

In addition to the low solubility of organic compounds in water, many trace organic compounds have a strong tendency to adsorb on a glass surface. When large glass surface areas are involved in a water sample preparation, the loss of organic compounds due to such adsorption could be significant. This loss usually leads to low recovery and poor reproducibility. This adsorption problem has been effectively minimized using a Soxhlet extractor rather than the large volume glassware apparatus required when a large amount of water is involved. In addition, all glassware surfaces which made contact with the water extract were carefully rinsed with benzene, and then these benzene aliquots were collected for organic compound analysis.

For the organic compound analysis, a simple benzene-water partitioning procedure was used to transfer the organic compounds from the water extracts into benzene for the subsequent analysis. This method minimizes the loss of trace organic compounds that usually occurs during a complicated procedure and also provides a high transfer efficiency due to the greater solubility of most organic compounds in benzene compared to water. This partitioning procedure was not applied to the water leachate used for inorganic compound testing.

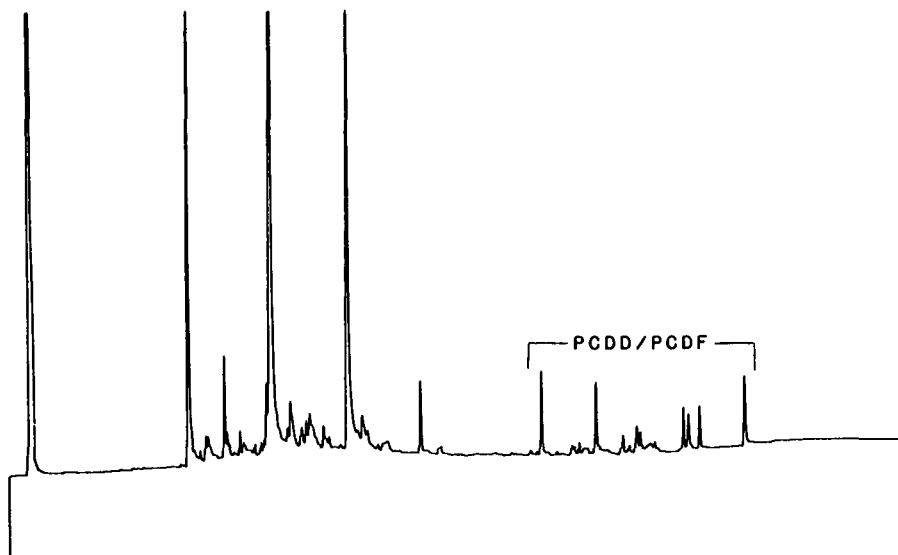


Figure 1. GC/ECD chromatogram of organic compounds in the water extract of a flyash sample showing PCDD/PCDF compounds are present.

Dioxins Found in Water Extracts

A total of seven Soxhlet extractions of flyash were carried out. Those seven extracts were analyzed for PCDDs and PCDFs after benzene-water partitioning. The analytical techniques used included GC/ECD, GC/EIMS, GC/NICIMS, and GC/PICIMS. In these seven water extracts, PCDDs were detected in five samples by GC/ECD and were more positively identified in two samples by GC/EIMS and GC/NICIMS. Dioxins reported by GC/ECD in Table 1 refer to detection of at least one of H₆CDD, H₇CDD, and OCDD. For most samples more than one of the PCDDs were identified by GC/ECD.

GC/ECD analysis provided high sensitivity, in the picogram range for PCDDs and PCDFs. However, because of the presence of interfering compounds in the water extract, tetrachlorodioxins (TCDDs) and pentachlorodioxins (P₅CDDs) could not be positively identified on the GC/ECD chromatograms for some samples. There were less interfering peaks in the elution region of hexachlorodioxins (H₆CDDs), heptachlorodioxins (H₇CDDs), and octachlorodioxins (OCDDs) on the GC/ECD chromatograms. Therefore, a typical pattern of H₆CDD, H₇CDD, and OCDD, which was usually observed in a benzene-extract of flyash, could be easily recognized on a GC/ECD chromatogram of the extract sample containing PCDD. Figure 1 shows a typical GC/ECD chromatogram of the water extraction sample containing PCDD; none of these PCDD compounds appear in the water blank.

The GC/MS system used in this study had a lower sensitivity for PCDD determination than GC/ECD. GC/MS with selected ion monitoring (GC/MS/SIM) was used with electron impact ionization (GC/EIMS/SIM) and with negative ion chem-

ical ionization (GC/NICIMS/SIM). PCDDs and PCDFs were identified in three water extraction samples by GC/EIMS/SIM and/or GC/NICIMS/SIM. Since two characteristic ions, [M] and [M + 2], were monitored for each PCDD and PCDF congener, the presence of PCDDs and PCDFs, indicated by GC/MS analysis, is reasonably positive evidence that PCDDs and PCDFs are present in water extraction samples. No PCDDs or PCDFs were found in the water blank.

A large variation exists in the concentrations of PCDDs and PCDFs found among these seven extraction samples. This is most likely caused by the problems encountered in trace analysis at the part-per-trillion level. The differences among flyash samples from batch to batch could be another reason for the variation. Therefore, an exact quantification of PCDDs and PCDFs in all the water extracts was not attempted in this study. Based on the results obtained from some samples, the concentration of PCDDs leached into water is estimated to be in the 1- to 400-ppt range as shown in Table 1.

The recovery of PCDDs using reference standards in the benzene-water partitioning procedure was investigated. The concentration level of PCDD standards in water was progressively lowered to the detection limit of GC/ECD. Due to interferences, this recovery study was limited to H₆CDD, H₇CDD, and OCDD standards. GC/MS was not used because of the greater sensitivity provided by the electron capture detector. The data given in Table 1 show a good recovery of PCDD at the 2-ppt level from a reference sample.

Based on the results obtained from both the analysis of PCDDs in water extracts and study of PCDD recovery, two conclusions can be reached. First, PCDDs and PCDFs can be leached from flyash by water at pH 7. Second, the precise quantity of PCDDs and PCDFs leached by water from flyash is difficult to determine because the levels of PCDDs and PCDFs are very low, and at such low levels, their tendency to adsorb onto glassware can present a significant loss.

Table 1. Concentration of PCDDs Extracted in Water from Flyash (parts per trillion)

Sample	Method of Determination	TCDD	P ₅ CDD	H ₆ CDD	H ₇ CDD	OCDD
LF-5	GC/NICIMS/SIM	5	106	301	360	212
	GC/EIMS/SIM	53	136	219	265	132
	GC/ECD	IN	IN	125	153	335
LF-6	GC/EIMS/SIM	ND	ND	ND	69	50
	GC/ECD	IN	IN	40	43	251
LF-7	GC/ECD	IN	IN	17	8	5
Reference standard	GC/EIMS/SIM	—	—	2	2	2
				(98) ^a	(61) ^a	(80) ^a

Notes: IN — Unable to quantify due to interferences.

ND — Non-detectable at the instrument detection limit.

^a — Percent recovery.

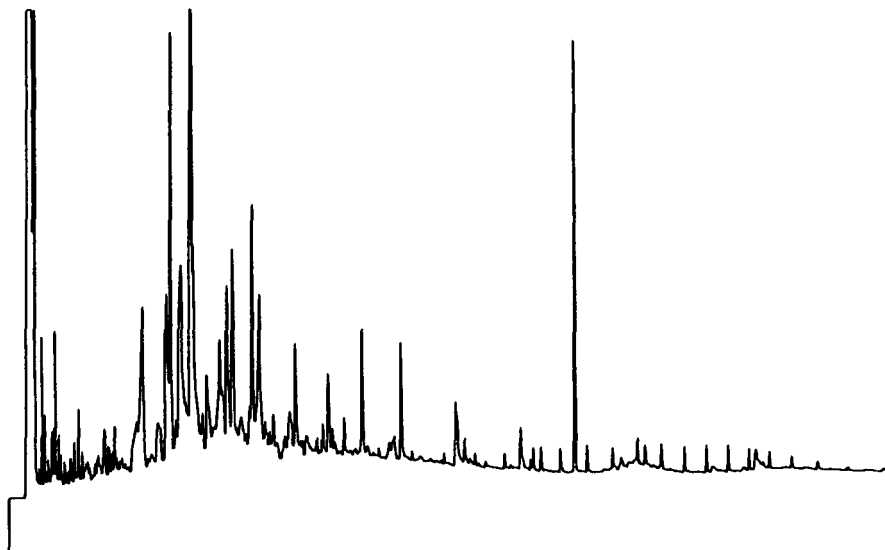


Figure 2. GC/FID chromatogram of total organic compounds in the water extract of a flyash sample.

Identification of Organic Compounds in Water Extracts

In this study many organic compounds have been found in water extracts. Five analytical techniques were used for such analysis. They included GC/FID, GC/ECD, GC/EIMS, GC/PICIMS, and GC/NICIMS. The identification of most compounds was based on the data obtained from the three GC/MS analyses. The data of GC/FID and GC/ECD were used to facilitate the identification for some compounds.

Figure 2 shows the GC/FID traces of organic compounds in one of the water extracts. Table 2 lists the organic compounds as identified using the method mentioned here. Not listed are 18 compounds that could not be identified based on the available information and 22 n-hydrocarbons with molecular weights between 198 and 520. In addition to the PCDDs and PCDFs, many compounds containing a nitrogen and hydroxyl group were found in water extracts. Some of these are not found in the benzene extract of flyash.

TOXIC EFFECT OF INORGANIC COMPOUNDS IN LEACHATE

Using a benzene solvent and Soxhlet extraction of organic compounds from flyash, it has been shown that the organic extract contains parts per million to parts per billion of PCDD, PCDF, and other organic compounds, including PAH, that exhibit all the effects of toxic, mutagenic behavior by the human cell test.⁷ Since the water contains many of the same toxic organic chemicals but at a much lower concentration and mixed with much larger amounts of extracted inorganic com-

pounds, a special and very simple approach to measuring the relative toxicity of organic and inorganic compounds in the leachate was adopted. Two water leachate samples were produced for each flyash: one in which the flyash sample used was the original with adsorbed organic compounds present; the other was the same flyash after organic compounds had been removed by a benzene solvent Soxhlet extraction. The first leachate contains both organic compounds, as described here previously, and inorganic compounds; the second contains only inorganic constituents. Comparison of the toxicity test results of these two will permit evaluation of the relative toxicity of the two compound classes.

The original flyash samples contain percent amounts of many heavy metals as shown in Table 3. Quite measurable parts-per-million-quantities were present in the water leachates produced by the Soxhlet extraction procedure, with Pb and Cd being present in the largest amounts. The toxic effect on these metal compounds as measured by the toxicity test on a water extract of the flyash after all organic compounds had been removed is seen in Figure 3. It can be observed that increasing amounts of this leachate have a profound effect on the pattern of proteins generated by the human fibroblasts. Figure 4 shows the same data for a leachate sample of the same flyash prior to removal of the organic compounds. Comparison of the data in Figures 3 and 4 reveals no difference in toxicity as measured by the toxicity test between these two samples of water leachate.

CONCLUSION

In this study we have shown that water extracts of incinerator flyash have a marked toxicity towards human cells, as demonstrated by changes in the two-dimensional pattern of proteins synthesized by fibroblasts in culture. The toxicity

Table 2. Organic Compounds Found in Water Extract

Compound	Molecular Weight
Dichloropropenamide	139
Octene ketone	126
Ethyl benzene	106
Tetrachloropentene	206
Trichlorophenol	196
Hydroxy methoxy benzaldehyde	152
Ethenyl tetrachlorobenzene	240
Trichlorocresol	240
Dimethoxy benzaldehyde	166
Dimethyl phthalate	194
Tetrachlorophenol	230
Dichloroethenyl methyl benzene or its isomer	186
Dichlorobenzamide	189
Methyl benzene dicarboxylic acid	180
Dimethyl biphenyl	182
Dichlorobenzamide	189
Caffeine	194
Dimethoxy phenanthrene	238
Dioctyl phthalate	390
Pentachlorochrysene	404

Table 3. Results of ICP Analysis of Flyash Samples and Their Water Leachate

Source	Metal Content (Weight Percent of the Flyash)								
	Pb	As	Sb	Se	Cd	Ni	Cr	Cu	Hg
Ontario 1	2.60	0.015	0.08	<0.01	0.065	0.005	0.055	0.099	0.1
Machida 2	0.46	0.006	<0.005	<0.01	0.006	0.020	0.022	0.47	0.05
Noronda 3	23.0	1.00	0.53	0.06	2.40	0.050	<0.005	12.0	<0.05
Microgram Metal per Gram of Water Leachate									
Water leachate of flyash									
Ontario 1	230	7.8	8.8	<10	140	<0.3	0.4	0.60	
Machida 2	130	<2	7.8	<10	140	<0.3	<0.3	0.56	

Water leachate Ontario 1: Dry content 26%

Water leachate Machida 2: Dry content 28%

Note: NBS 1633a and NBS coal flyash were used to calibrate the instrument, Perkin Elmer Model Plasma 2.

was the same whether or not the organic compounds had been removed (benzene extraction) prior to the water leaching. By means of ICP-analyses, it was found that the water extracts contained larger amounts of inorganic compounds (parts per million), particularly lead, cadmium, antimony, and arsenic, compared to the organic compounds (parts per trillion). These inorganic compounds present in the leachates explain the toxicity of the water extract of the flyash. The conclusion of this study is therefore that the leaching of heavy metal compounds into the ground water most likely represents a more important pollution problem than the leaching of dioxins and other organic compounds. The latter compounds are relatively insoluble in water, are firmly adsorbed to the flyash particles, and are present only in trace quantities (parts per trillion) in the water leachates.

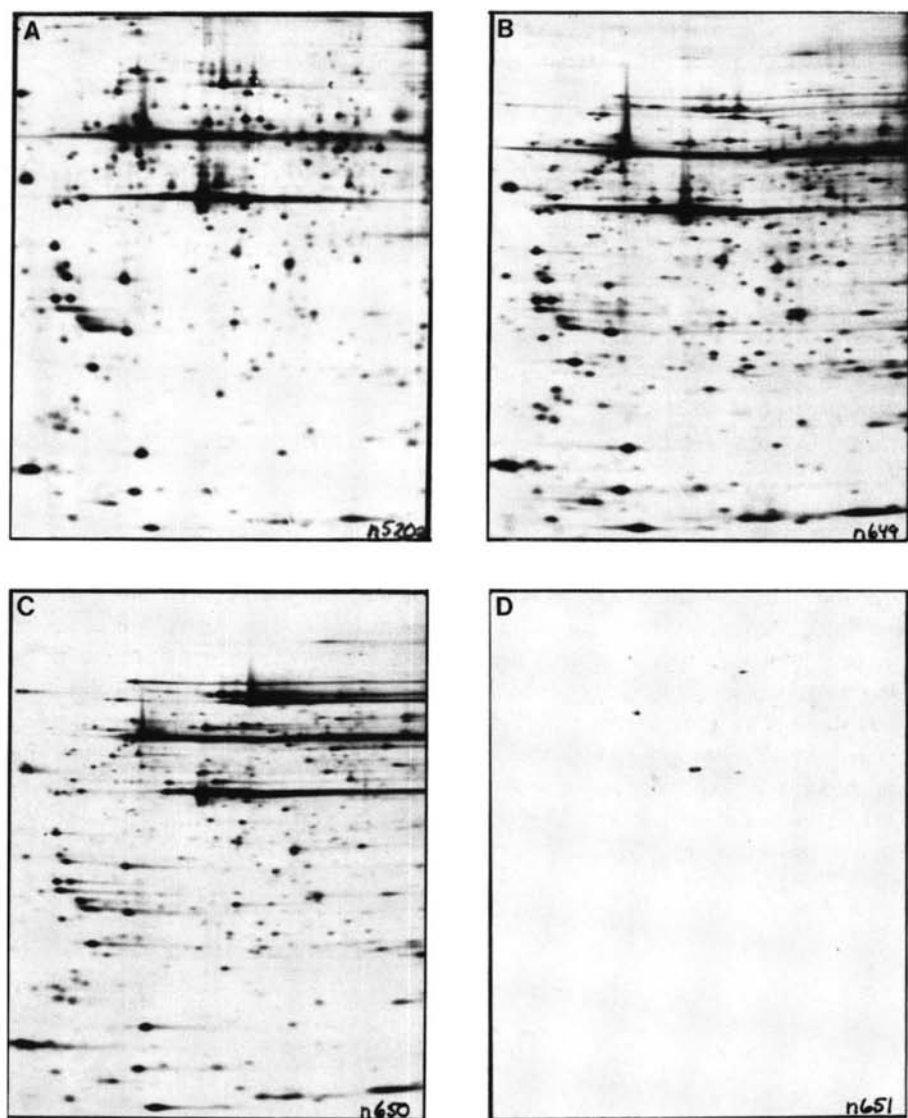


Figure 3. Effect of water extract of flyash (Ontario) on the 2-D protein pattern of human cells (fibroblasts). (A) No extract added; (B) 10 μ L extract added; (C) 25 μ L; (D) 50 μ L.

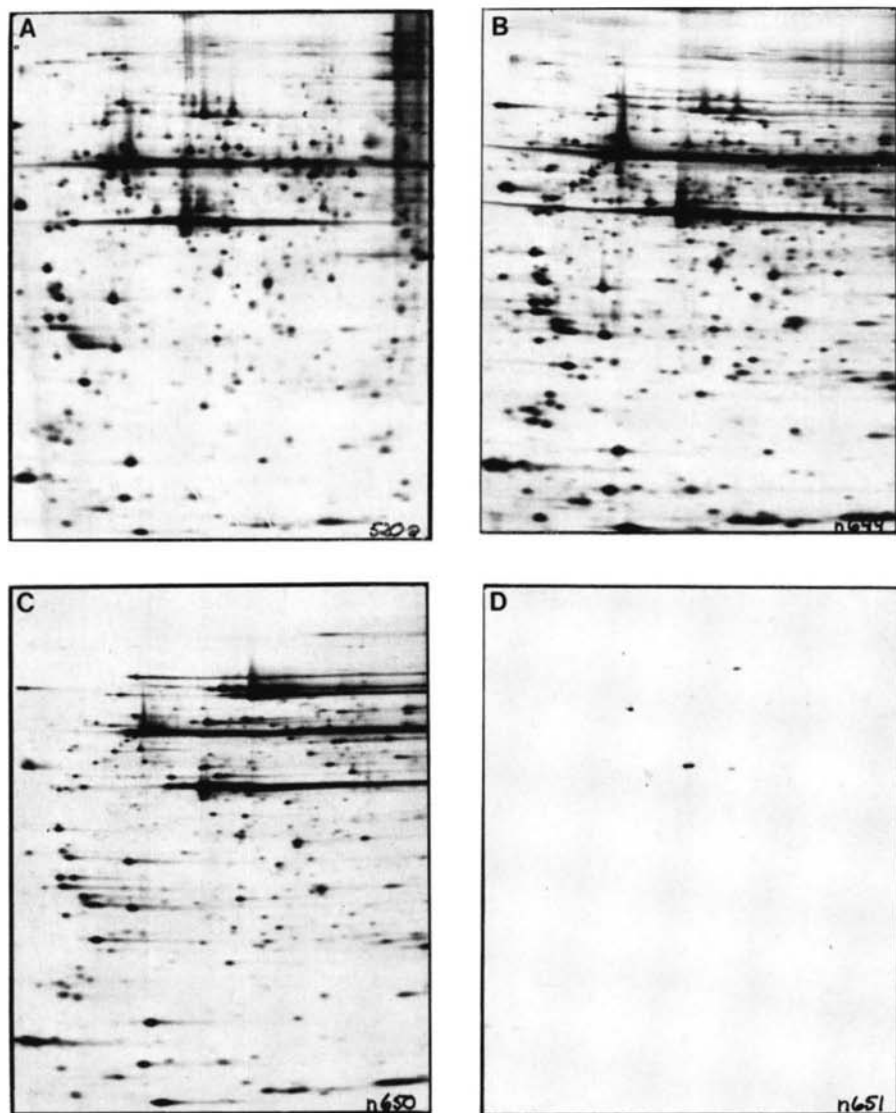


Figure 4. Effect of water extract of cleaned flyash (Ontario) on the 2-D protein pattern of human cells (fibroblasts). (A) No extract added; (B) 10 μL extract added; (C) 25 μL ; (D) 50 μL .

REFERENCES

1. Rubel, F. N. "Incineration of Solid Waste," in *Pollution Technology Review No. 13* (Part Ridge, NJ: Noges Data Corp., 1974), p. 56.
2. Tong, H. Y., D. L. Shore, and F. W. Karasek. "Identification of Organic Compounds Obtained from Incineration of Municipal Waste by High-Performance Liquid Chromatographic Fractionation and Gas Chromatography-Mass Spectrometry," *J. Chromatogr.* 285:423—441 (1984).
3. Karasek, F. W., and F. I. Onuska. "Dioxin Analysis by GC/MS Techniques," *Anal. Chem.* 54:309A (1982).
4. Anderson, N. G., and N. L. Anderson. "Analytical Techniques for Cell Fractions. XXI. Two-Dimensional Analysis of Serum and Tissue Proteins: Multiple Isoelectric Focusing," *Anal. Biochem.* 85:331—340 (1978).
5. Anderson, N. L., and N. G. Anderson. "Analytical Techniques for Cell Fractions. XXII. Two-Dimensional Analysis of Serum and Tissue Proteins: Multiple Gradient-Slab Electrophoresis," *Anal. Biochem.* 85:341—354 (1978).
6. Grimstad, I. A., A. K. Thorsrud, and E. Jellum. "Marker Polypeptides Distinguishing Between Cancer Cell Clones with High and Low Potential for Spontaneous Metastasis in Murine Fibrosarcoma Cells," *Cancer Res.* 48:572—577 (1988).
7. Jellum, E., A. K. Thorsrud, and F. W. Karasek. "Two-Dimensional Electrophoresis for Determining Toxicity of Environmental Substances," *Anal. Chem.* 55:2340 (1983).

CHAPTER 9

Determination of Organometallic Species by High Performance Liquid Chromatography-Mass Spectrometry*

J. W. McLaren, K. W. M. Siu, and S. S. Berman

INTRODUCTION

Recent advances in liquid sample introduction in mass spectrometry have resulted in tremendous growth of high performance liquid chromatography (HPLC)-mass spectrometry (MS). The marriage of the two seemingly incompatible but powerful techniques has been made possible by development of interfacing techniques such as thermospray¹ and particle beam,² and more recently the inductively coupled plasma (ICP)³ and electrospray (ES).⁴

The two major areas of incompatibility between HPLC and MS are solvent loading and the use of involatile buffer salts. The regular-bore liquid chromatography flow rate is typically 1 mL/min, which translates to approximately 1 L/min of vapor

* NRCC 32910.

after evaporation. A vapor loading as high as this puts tremendous stress on the vacuum system of the mass spectrometer. Successful coupling of LC to MS is made possible by employing differential pumping to cope with heavy solvent loading, introducing only a minor fraction of the column effluent into the mass spectrometer, and/or selectively concentrating the analytes at the interface. To effect separation, ion exchange and ion pairing chromatography often require the use of involatile buffer salts. Due to their low vapor pressure, these salts cannot be effectively pumped away and therefore should be excluded from the mass spectrometric vacuum system.

The recent success of coupling high performance liquid chromatography to inductively coupled plasma mass spectrometry and electrospray mass spectrometry is due largely to solving of the incompatibility problem. One of the most important features of these newer mass spectrometers is that they are designed to accommodate a sample inlet/interface at atmospheric pressure. Consequently, the solvent vapor does not increase the loading of the mass spectrometer. Further, the entrance of solvent and buffer salts is effectively minimized in the interface region.

In the field of environmental trace metal determination, it has been increasingly clear that for some elements more informative conclusions can be drawn only when the actual species are known because of their widely different degrees of toxicity and bioavailability. Arsenic, tin, mercury, and lead are some of the better known examples. High performance liquid chromatography-inductively coupled plasma mass spectrometry (HPLC-ICP-MS) and high performance liquid chromatography-electrospray mass spectrometry (HPLC-ESMS) lend themselves readily to trace metal speciation. The species are first efficiently separated and then selectively detected. The two stages of this tandem approach compensate for and complement each other. The chromatographic separation furnishes the mass spectrometer with reasonably pure samples for identification and quantification, whereas mass spectrometry permits sensitive and selective detection of analytes partially resolved from matrix materials.

ICP-MS and ESMS occupy the extremes of the ionization energy spectrum in mass spectrometry. The high temperature of the ICP results in the complete breakdown of most molecules into atoms, elemental ions, or simple polyatomic species; at least partial ionization is achieved for all elements with ionization potentials less than that of argon. Thus, the ICP mass spectrometer can be thought of as a very sensitive element-specific detector for HPLC. In contrast, the electrospray process involves neither dissociation of molecular nor ionization of neutral species. In fact, electrospray is best described as a desorption process for pre-formed ions in solution. In other words, the analyte has to exist in solution as ions to be amenable to electrospray mass spectrometry. Due to the relative simplicity (lack of fragmentation) of electrospray mass spectra, it is often desirable to introduce additional selectivity in the detection system; this can be achieved by adding another mass spectrometric stage, i.e., by performing tandem mass spectrometry.

In the following sections, HPLC-ICP-MS and HPLC-ESMS will be briefly introduced, and their parallel application in our laboratory to the determination of organometallic species in marine materials will be described.

HPLC-ICP-MS

Inductively coupled plasma mass spectrometry is a relatively new technique for elemental and isotopic analysis which combines the power of the inductively coupled argon plasma as an atomization and ionization source with the sensitivity and selectivity of mass spectrometry. The normal method of sample introduction is by nebulization of aqueous solutions. A stream of argon carries the sample aerosol into the toroidal plasma where, in a 5,000 to 10,000-K environment, vaporization of the solvent, volatilization of solid aerosol particles, and breakdown of molecular species into atoms and ions occur over the span of a few milliseconds. At least partial ionization is achieved for all elements whose first ionization potential is less than that of argon (15.78 eV); for many elements, close to complete ionization is achieved. A fraction of the ions in the plasma are extracted by an interface which comprises two water-cooled orifices, machined from nickel, platinum, aluminum, or other suitable metal, separated by a few millimeters. The region between the two orifices is maintained at a pressure of 1 to 5 torr by a roughing pump. After passage through the second orifice, the ions enter a region of higher vacuum (about 10^{-5} to 10^{-6} torr) maintained by diffusion pumping, turbomolecular pumping, or helium cryopumping. This mass analyzer section contains a series of electrostatic ion lenses, a quadrupole mass filter, and a continuous dynode (channeltron) detector.

ICP-MS offers a number of distinct advantages as a detection technique for inorganic or organometallic species separated by HPLC, especially when compared with other atomic spectroscopic techniques. While all these techniques have more than adequate selectivity for most HPLC applications, none except perhaps graphite furnace atomic absorption spectrometry (GFAAS) can rival the detection power of ICP-MS. Detection limits in aqueous solution for ICP-MS usually fall in the range of 10 to 100 ng/mL for continuous sample introduction. The principal advantages of ICP-MS over GFAAS in this context are its capability for simultaneous multi-element monitoring and the much greater ease of interfacing. HPLC apparatus can be directly coupled to typical ICP-MS sample introduction systems, most of which are designed to accommodate solution flow rates of 1 to 3 mL/min; all that is normally required is a short length of narrow-bore Teflon tubing.

Several recent reports⁵⁻¹⁵ have demonstrated the practical utility of inductively coupled plasma mass spectrometry as a sensitive and selective on-line detection method for HPLC in trace element speciation studies. Compatibility of the instrumentation with a range of mobile phases typically used in ion pairing, ion exchange, and size exclusion HPLC has been established. Reported applications include the study of cadmium speciation in cooked and uncooked pig kidney,^{8,9} the determination of methylmercury in an albacore tuna research material and of thimerosal in contact lens sterilizing solutions,^{10,11} the identification and quantification of arsenic species in human urine,^{12,13} and the determination of gold drug metabolites and related metals in human blood.¹⁴

While offering extremely attractive selectivity and sensitivity, the use of ICP-MS as the detection technique does, however, place some constraints on the choice of chromatographic conditions which may not apply to more conventional HPLC

Table 1. Important Arsenic Species in Clinical and Environmental Samples, in Order of Decreasing Toxicity

As (III)	
As (V)	
Monomethylarsonic acid (MMA)	
Dimethylarsinic acid (DMA)	
Arsenobetaine	$(\text{CH}_3)_3\text{As}^+ \text{CH}_2\text{COO}^-$
Arsenocholine	$(\text{CH}_3)_3\text{As}^+ \text{CH}_2\text{CH}_2\text{OH}$
Tetramethylarsonium (TMA)	$(\text{CH}_3)_4\text{As}^+$

detectors. The limited tolerance of ICP-MS instrumentation to solutions with high-dissolved solids may necessitate the use of a relatively low concentration of buffer salts in the mobile phase in some ion chromatographic applications. In addition, the introduction of some organic solvents is much more difficult than aqueous sample introduction; extremely volatile solvents such as tetrahydrofuran may easily overload and extinguish the ICP with solvent vapor, and introduction of aromatic solvents such as toluene can result in deposition of soot on, and eventual blockage of, the sampling orifices unless an auxiliary flow of oxygen is introduced to promote combustion. While the introduction of nonaqueous solvents does not in general present insurmountable difficulties, it does add to the experimental difficulty. It is not surprising, therefore, that the majority of successful HPLC-ICP-MS applications have been accomplished with reversed phase, size exclusion, or ion chromatographic procedures in which the mobile phase solvent was either water or a methanol/water mixture.

In our laboratory, HPLC-ICP-MS has been applied to speciation studies for arsenic^{6,7} and tin¹⁵ in marine samples. In the remainder of this section, we shall use our own experience and that of others to illustrate the power of ICP-MS as a detection technique for the determination of ionic and organometallic species in clinical and environmental samples.

Arsenic

HPLC-ICP-MS has been applied to the quantification of arsenic species in a dogfish tissue reference material^{6,7} and to the determination of arsenic species in human urine.^{12,13} The major species of interest are listed in Table 1. Human metabolism of inorganic arsenic results in the production of dimethylarsinic acid (DMA), with methylarsonic (MMA) as an intermediate; the presence of arsenobetaine (AB) has been observed in a number of marine crustacea and fish, and in the urine of humans after consumption of these seafoods. The inorganic forms of arsenic are by far the most toxic; arsenobetaine, arsenocholine (AC), and tetramethyl arsonium (TMA) are essentially nontoxic, while MMA and DMA occupy an intermediate position on the scale. Observation of significant amounts of inorganic arsenic species in human urine is normally an indication of unacceptably high intake.

Some details of the chromatographic procedures used for arsenic speciation by HPLC-ICP-MS are summarized in Table 2. It is possible to use reversed phase

chromatography, with either anion-pairing or cation-pairing reagents, depending upon the pH, anion exchange chromatography, or size exclusion chromatography. The various mobile phases are predominantly aqueous, with at most 30% methanol, and usually 5% or less. The introduction of these mobile phases requires only minor modifications to the ICP operating conditions appropriate for 100% aqueous solutions (e.g., a 10 to 20% increase in the radio frequency power input). The reported detection limits are remarkably consistent, considering the variety of ICP-MS instrumentation and experimental conditions employed; the range of values for each method primarily reflects differences in retention times for the various species. Since no single method permits the resolution of all of the arsenic species in Table 1, the choice of method must be based on some prior information as to which species are likely to be present in the sample or the most important.

Two problems in the determination of arsenic species employing ICP-MS detection have been reported. The more serious of these concerns the possible isobaric interference of a polyatomic species, $^{40}\text{Ar}^{35}\text{Cl}$, with monoisotopic ^{75}As . This problem has been shown to be significant in applications to human urine samples, which contain about 1% chloride. Shibata and Morita¹³ observed spurious chloride peaks in both anion pairing and size exclusion chromatograms of human urine; in the former case, the peak would overlap any peak for MMA, and in the latter, the peak

Table 2. Applications of HPLC-ICP-MS to Arsenic Speciation

Chromatographic Conditions	Application	Detection Limits (pg)	Ref.
Ion pair chromatography Mobile phase: 5 mM tetrabutylammonium phosphate in water/methanol (95:5), pH 7.1	Standard solutions only. As (III) not resolved from MMA	80—200	5
Ion pair chromatography Mobile phase: 10 mM sodium dodecyl sulfate in water/methanol/acetic acid (92.5:5:2.5), pH 2.5	Determination of arsenobetaine and other arsenic species in dogfish muscle	30—300	7
Anion exchange chromatography Mobile phase: 15 mM ammonium dihydrogen phosphate/1.5 mM ammonium acetate in water/methanol (70:30), pH 5.75	Arsenic speciation in human urine	36—96	12
Ion pair chromatography Mobile phase: 10 mM tetraethylammonium hydroxide in water/methanol (99.95:0.05), pH 6.8	Arsenic speciation in human urine	20—50	13
Ion pair chromatography Mobile phase: 10 mM sodium butyl sulfate/4 mM tetramethylammonium hydroxide/4 mM malonic acid in water/methanol (99.95:0.05), pH 3.0	Arsenic speciation in human urine	20—50	13
Size exclusion chromatography Mobile phase: 25 mM tetramethylammonium hydroxide/25 mM malonic acid in water, pH 6.8	Arsenic speciation in human urine	100—150	13

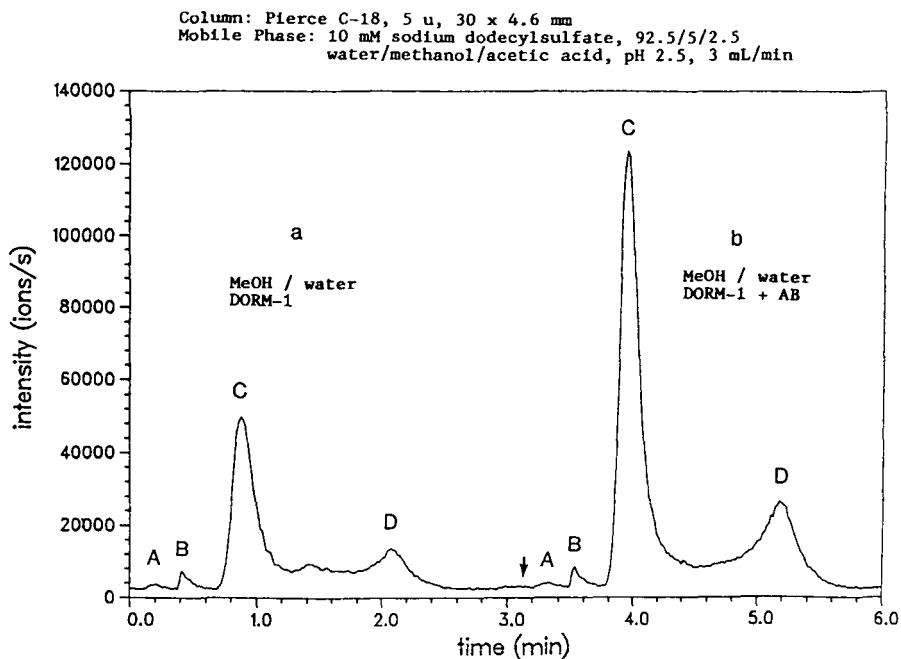


Figure 1. Cation pairing HPLC-ICP-MS chromatograms of extracts of (a) unspiked and (b) spiked samples of the dogfish muscle reference material DORM-1. (From Beauchemin, D., M. E. Bednas, S. S. Berman, J. W. McLaren, K. W. M. Siu, and R. E. Sturgeon. *Anal. Chem.* 60:2209—2212 [1988]. With permission.)

was not well resolved from the arsenobetaine peak. Heitkemper and co-workers¹⁴ encountered similar problems in the use of anion exchange chromatography. They also experienced incompatibility of the ICP-MS instrumentation with phosphate buffers; at 50-mM concentration, salt deposition on the nickel sampling orifices caused rapid pitting and clogging. This problem was greatly reduced by the use of aluminum rather than nickel orifices and the lowering of the phosphate concentration to 15 mM.

Beauchemin and co-workers⁶ evaluated both ion pairing and anion exchange chromatography, and selected cation pairing as the most appropriate methodology for the quantification of arsenic species in a dogfish muscle tissue,⁷ which contains arsenobetaine. Chromatograms for spiked and unspiked samples of this material are shown in Figure 1. Peaks were identified by coinjection of standards with the sample solution; inorganic arsenic and MMA coeluted with the void volume (peak A), peak B was found to be DMA, while peaks C and D were both associated with arsenobetaine, which apparently pairs with some anion in the sample in addition to the dodecyl sulfate in the mobile phase. Quantification of arsenobetaine at $15.7 \pm 0.8 \mu\text{g As/g}$ was achieved by applying the method of standard additions to the sum of the areas of peaks C and D, while a value of $0.47 \pm 0.02 \mu\text{g As/g}$ for

DMA was obtained by applying the same method to peak B. A great advantage of this approach was that a relatively crude extract could be used because of the very selective nature of ICP-MS detection.

Tin

The importance of determining the chemical speciation of tin in environmental samples is well recognized; of particular concern is the possible presence of tributyltin compounds.¹⁶ While the toxicity of tributyltin to aquatic organisms, especially to filter-feeding shellfish such as oysters, is well established, knowledge about the rate and mechanism of breakdown to inorganic tin in the environment is incomplete, although it appears to proceed through the dibutyl and monobutyl species. Tributyltin can be readily separated from inorganic tin and many other organotin species by HPLC¹⁷ and detected by a variety of spectroscopic techniques.¹⁸⁻²² Two recent reports by Suyani and co-workers^{23,24} indicated the potential of HPLC-ICP-MS for the determination of alkyltin and aryltin compounds in environmental samples.

Some details of the chromatographic procedures used for tin speciation by HPLC-ICP-MS are summarized in Table 3. It is possible to use either ion pairing or cation exchange chromatography. Suyani and co-workers^{23,24} evaluated both approaches and achieved the best detection limits with an ion pairing technique in which the mobile phase was sodium dodecyl sulphate in a water/propanol/acetic acid (94:3:3) mixture. A serious limitation of this approach is that it is applicable only to alkyltin compounds with alkyl groups containing less than four carbon atoms. McLaren and co-workers¹⁵ preferred cation exchange chromatography, with a mobile phase of ammonium citrate in methanol/water (60:40). This methodology was incorporated into a procedure for the quantification of both tributyltin (TBT) and dibutyltin (DBT) in a harbor sediment reference material (PACS-1). These were determined to be

Table 3. Application of HPLC-ICP-MS to Tin Speciation

Chromatographic Conditions	Application and Comments	Detection Limits (pg)	Ref.
Cation exchange chromatography Mobile phase: 180 mM ammonium citrate in methanol/water (60:40), pH 6	Determination of tributyltin and dibutyltin in a harbor sediment	20—40	15
Cation exchange chromatography Mobile phase: 100 mM ammonium acetate in methanol/water (85:15)	Standard mixtures of triaryl- and trialkyltin compounds	400—1000	23
Ion pair chromatography Mobile phase: 4 mM sodium pentane sulfonate in methanol/water/acetic acid (80:19:1), pH 3.0	Standard mixtures of triaryl- and trialkyltin compounds	400—1000	23
Ion pair chromatography Mobile phase: 20—100 mM sodium dodecyl sulphate/0—10 mM KF in water/propanol/ acetic acid (94:3:3)	Standard mixtures of methyltin compounds; standard mixtures of trimethyl-, triethyl-, and tripropyltin	26—126	24

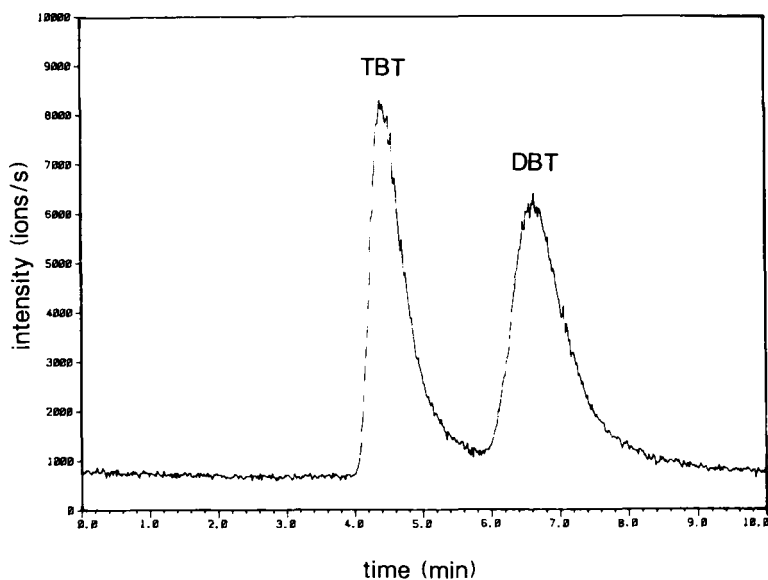


Figure 2. Cation exchange HPLC-ICP-MS chromatogram of an extract of the harbor sediment reference material PACS-1, showing peaks for tributyltin (TBT) and dibutyltin (DBT). See Table 3 for chromatographic conditions.

1.18 ± 0.15 and 1.19 ± 0.14 $\mu\text{g Sn/g}$, respectively. The chromatogram of an unspiked extract of this material is shown in Figure 2. No problems of plasma instability were encountered with methanol/water mixtures containing up to 70% methanol. The addition of oxygen to the nebulizer gas stream, as reported by Suyani et al.,²³ did not appear to be necessary; there was no observable deposition of soot on the interface after several hours of continuous operation. Furthermore, solutions of up to 0.3 M ammonium citrate could be run for long periods with no observable drop of instrumental performance. The remarkably high tolerance of the instrument for ammonium citrate would appear to be a serendipitous effect related to the relatively high volatility of this salt and/or its breakdown products.

Both Suyani et al.²³ and McLaren et al.¹⁵ reported some difficulties in controlling tin blank levels. The latter group was forced to abandon an attempt to determine monobutyltin at the same time as the dibutyl- and tributyl-species. A pH step gradient procedure for the elution of all three species was developed, but at the lower pH (3) required for elution of monobutyltin, the background signal rose considerably, probably because of elution of inorganic tin adsorbed onto the column from the mobile phase at the higher pH (6). Suyani et al.²³ encountered even more severe problems in an ion pairing chromatographic procedure. Gradual accumulation of

tin compounds from the mobile phase gave rise to an unacceptably high background signal throughout the entire chromatogram, which significantly degraded detection limits for all tin species. It would appear that a method to remove tin contaminants in the mobile phase prior to separation should be developed for future work.

HPLC-ESMS

Like ICP-MS, electrospray mass spectrometry is also a relatively new technique, although the electrospray phenomenon has been known for decades. In ESMS, an aqueous-based solution is passed through a capillary tube (typically 50 to 100 μm i.d.) biased to 3 to 4 kV, the optimum flow rate being 5 to 50 $\mu\text{L}/\text{min}$. Droplets emerging from the tube are charged. As they evaporate, the charges (ions) are brought more closely to one another due to reduction of the droplets' surface area. Ion evaporation into the gas phase occurs when coulombic repulsion among the ions overcomes their solvation forces. Electrospray is, therefore, an ion desorption rather than an ionization technique. For mass spectrometric detection, a small fraction of the spray is sampled through an orifice. The volume immediately surrounding the orifice is flushed by a stream of dry nitrogen, which keeps the orifice clean and prevents the entrance of solvent and buffer salts. The sampled ions are then declustered and focused in the lens region and mass analyzed by using a quadrupole mass filter. In more sophisticated instruments, a second mass analyzing stage may be added. This tandem mass spectrometric approach allows structural identification of electrospray-generated ions and provides a much enhanced level of selectivity in analysis.

Electrospray is seen as a uniquely effective sample introduction method for nonvolatile and/or thermally labile species that are ionized in solution for mass spectrometric analysis. Traditionally, determination of these samples has been difficult if not impossible. Electrospray permits their introduction into the mass spectrometer with little or no decomposition. Two types of analytes have received particular attention, macromolecules such as proteins and oligonucleotides,^{25,26} and organometallic species.^{27,28} For the latter, most of the work has been done on arsenic and tin species.

Arsenic

As detailed in the previous section, arsenobetaine, arsenocholine, and tetramethylarsonium are some of the environmentally and toxicologically important organoarsenic species. They have been found in a number of marine fauna and are believed to be metabolic products of these animals. A HPLC-ESMS method has been developed for the determination of these three species, which exist as cations in acidic solutions, and therefore are amenable to separation by dynamic cation exchange.²⁹ Figure 3 shows chromatograms of an injection of a mixture of AB, AC, and TMA. To make flow rates compatible, the column effluent was split and only 5% (50 $\mu\text{L}/\text{min}$) was routed into the electrospray interface. The chromatograms shown were results of selected reaction monitoring (SRM) by means of tandem

mass spectrometry. For each species, the molecular ion or protonated molecular ion (e.g., m/z 179 for AB) was selected by the first mass analyzer and fragmented in a reaction chamber (the second quadrupole of a triple quadrupole spectrometer); the principal fragment ion was then monitored by the second mass analyzer (e.g., m/z 120, the trimethylarsine ion, for AB and TMA). In this way, the tandem mass spectrometer monitored a fragmentation reaction or a collision-induced dissociation pathway almost specific to each species. In SRM, chemical interference can be encountered only if the matrix ion yields a fragment ion of the same m/z that is being monitored by the second mass analyzer. By judicious choice of experimental conditions and fragmentation reactions monitored, this is rarely a problem. Figure 3 was obtained with 1 ng As of each of the three organoarsenic species. The minimum detectable amounts (MDAs) as determined by using SRM are dependent on the efficiency of the collision-induced dissociation processes and are therefore highly variable. In the present example, the MDA for AB was estimated to be about 20 pg As, those for AC and TMA were about ten times higher.

This procedure has been applied to the quantification of AB in the dogfish muscle tissue²⁹ that was previously mentioned. The measured concentration of 15.7 ± 0.4 $\mu\text{g As/g}$ is practically identical to that obtained by using HPLC-ICP-MS.⁷

LC-MS/MS

Column: 5 μ PRP-1 Eluent: 20/80 methanol/water
containing 1mM octane sulphonate, 10 mM ammonium
citrate and 1 mM ammonium acetate, 1 mL/min, 1/20 split

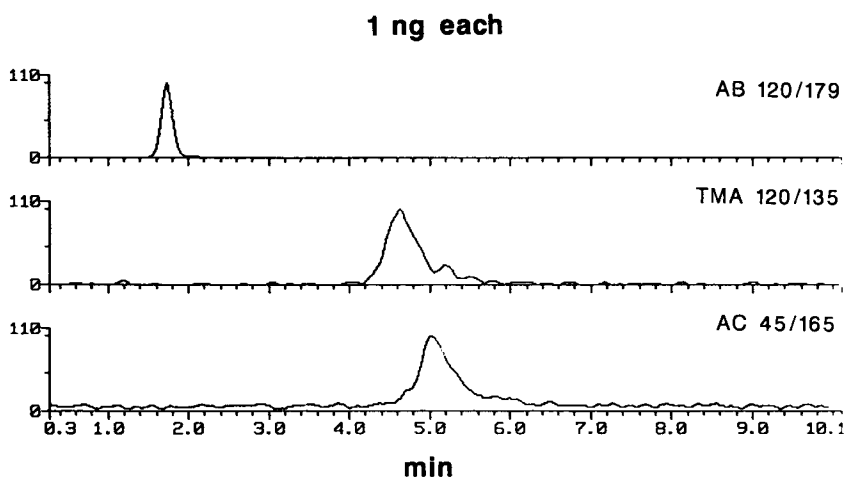


Figure 3. Dynamic ion exchange separation of arsenobetaine, tetramethyl arsonium, and arsenocholine.

Tin

ESMS has been employed for the quantification of tributyltin in the harbor sediment reference material (PACS-1) previously mentioned.³⁰ Tributyltin compounds are partially ionized in a protic solvent to yield an anion and the tributyltin cation, which is amenable to electrospray (and, evidently, cation exchange as well as cation pairing chromatography). No separation, however, was found necessary in this application as the collision-induced dissociation of tributyltin cation (m/z 291) to its most abundant fragment ion (m/z 179) is highly selective. The samples were introduced, in the form of crude extracts, into a flow stream of methanol containing 1 mM ammonium acetate for electrospray. PACS-1 was found to contain $1.29 \pm 0.07 \mu\text{g Sn/g}$ as tributyltin, which agreed well with the concentration determined by HPLC-ICP-MS (see earlier) and other techniques.³¹ The MDA was about 15 pg Sn absolute and about 0.2 $\mu\text{g Sn/g}$ of sediment. Some typical results are shown in Figure 4.

CONCLUSIONS

For organometallic speciation, few, if any, analytical techniques can rival HPLC-ICP-MS and HPLC-ESMS for combined sensitivity and selectivity. Between the two, sensitivity is approximately comparable. As previously discussed, these two mass spectrometric techniques attain selectivity differently. In HPLC-ICP-MS, the capacity of the ICP for nearly complete breakdown of molecular species into elemental ions allows the mass spectrometer to function as an element-specific detector. In HPLC-ESMS, selectivity of detection of a particular molecular ion among others with the same nominal mass/charge ratio is enhanced by taking advantage of characteristics of its structure or reactivity, e.g., through the use of tandem mass spectrometry. The major reasons for the relatively small number of reported applications to date is the fairly recent introduction and the rather high cost of both types of instrumentation.

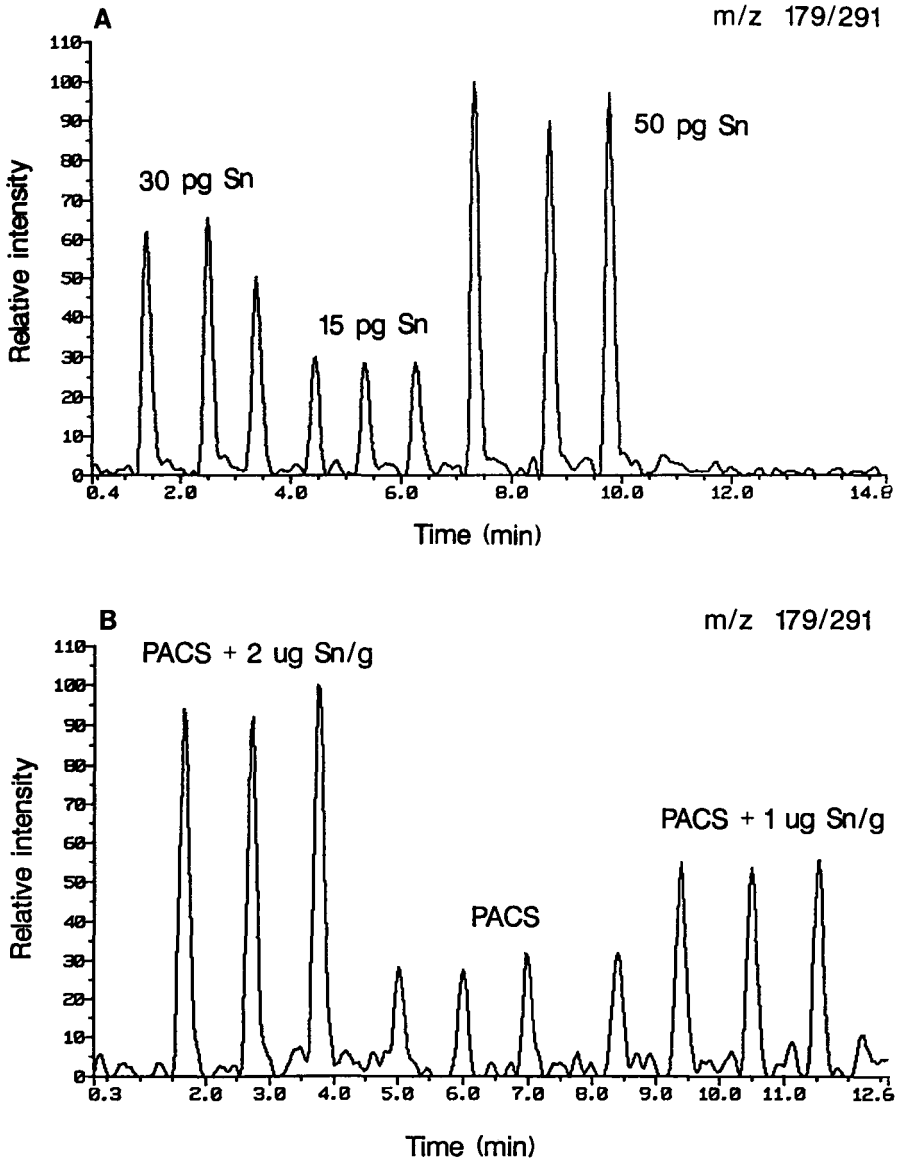


Figure 4. Flow injection analysis of tributyltin. (A) Standard solutions, (B) PACS-1 extracts containing various amounts of tributyltin spikes. (From Siu, K. W. M., P. S. Maxwell, and S. S. Berman. *J. Chromatogr.* 475:373—379 [1989]. With permission.)

REFERENCES

1. Blakley, C. R., M. J. McAdams, and M. L. Vestal. "Crossed-Beam Liquid Chromatograph-Mass Spectrometer Combination," *J. Chromatogr.* 158:261—276 (1978).
2. Willoughby, R. C., and R. F. Browner. "Monodisperse Aerosol Generation Interface for Combining Liquid Chromatography with Mass Spectroscopy," *Anal. Chem.* 56:2626—2631 (1984).
3. Houk, R. S. "Mass Spectrometry of Inductively Coupled Plasmas," *Anal. Chem.* 58:97A—105A (1986).
4. Yamashita, M., and J. B. Fenn. "Electrospray Ion Source. Another Variation on the Free-Jet Theme," *J. Phys. Chem.* 88:4451—4459 (1984).
5. Thompson, J. J., and R. S. Houk. "Inductively Coupled Plasma Mass Spectrometric Detection for Multielement Flow Injection Analysis and Elemental Speciation by Reversed-Phase Liquid Chromatography," *Anal. Chem.* 58:2541—2548 (1986).
6. Beauchemin, D., J. W. McLaren, K. W. M. Siu, and S. S. Berman. "Determination of Arsenic Species by High Performance Liquid Chromatography — Inductively Coupled Plasma Mass Spectrometry," *J. Anal. At. Spectrom.* 4:285—289 (1989).
7. Beauchemin, D., M. E. Bednas, S. S. Berman, J. W. McLaren, K. W. M. Siu, and R. E. Sturgeon. "Identification and Quantitation of Arsenic Species in a Dogfish Muscle Reference Material for Trace Elements," *Anal. Chem.* 60:2209—2212 (1988).
8. Dean, J. R., S. Munro, L. Ebdon, H. M. Crews, and R. C. Massey. "Studies of Metalloprotein Species by Directly Coupled High-Performance Liquid Chromatography Inductively Coupled Plasma Mass Spectrometry," *J. Anal. At. Spectrom.* 2:607—610 (1987).
9. Crews, H. M., J. R. Dean, L. Ebdon, and R. C. Massey. "Application of High-Performance Liquid Chromatography — Inductively Coupled Plasma Mass Spectrometry to the Investigation of Cadmium Speciation in Pig Kidney Following Cooking and In Vitro Gastro-intestinal Digestion," *Analyst* 114:895—899 (1989).
10. Bushee, D. S. "Speciation of Mercury Using Liquid Chromatography with Detection by Inductively Coupled Plasma Mass Spectrometry," *Analyst* 113:1167—1170 (1988).
11. Bushee, D. S., J. R. Moody, and J. C. May. "Determination of Thimerosal in Biological Products by Liquid Chromatography with Inductively Coupled Plasma Mass Spectrometric Detection," *J. Anal. At. Spectrom.* 4:773—775 (1989).
12. Heitkemper, D., J. Creed, J. Caruso, and F. L. Fricke. "Speciation of Arsenic in Urine Using High-Performance Liquid Chromatography with Inductively Coupled Plasma Mass Spectrometric Detection," *J. Anal. At. Spectrom.* 4:279—284 (1989).
13. Shibata, Y., and M. Morita. "Speciation of Arsenic by Reversed-Phase High Performance Liquid Chromatography — Inductively Coupled Plasma Mass Spectrometry," *Anal. Sci.* 5:107—109 (1989).
14. Matz, S. G., R. C. Elder, and K. Tepperman. "Liquid Chromatography with an Inductively Coupled Plasma Mass Spectrometric Detector for Simultaneous Determination of Gold Drug Metabolites and Related Metals in Human Blood," *J. Anal. At. Spectrom.* 4:767—771 (1989).
15. McLaren, J. W., K. W. M. Siu, J. W. Lam, S. N. Willie, P. S. Maxwell, A. Palepu, M. Koether, and S. S. Berman. "Applications of ICP-MS in Marine Analytical Chemistry," *Fresenius J. Anal. Chem.* 337:721—728 (1990).
16. Thompson, J. A. J., M. G. Sheffer, R. C. Pierce, Y. K. Chau, J. J. Cooney, W. R. Cullen, and R. J. Maguire. "Organotin Compounds in the Aquatic Environment," National Research Council of Canada (NRCC) Publication No. 22494 (1985).

17. Jewett, K. L., and F. E. Brinckman. "Speciation of Trace Di- and Triorganotins in Water by Ion-Exchange HPLC-GFAA," *J. Chromatogr. Sci.* 19:583—593 (1981).
18. Burns, D. T., F. Glockling, and M. Harriott. "Investigation of the Determination of Tin Tetraalkyls and Alkyltin Chlorides by Atomic-Absorption Spectrometry after Separation by Gas — Liquid or High-Performance Liquid — Liquid Chromatography," *Analyst* 106:921—930 (1981).
19. Ebdon, L., S. J. Hill, and P. Jones. "Speciation of Tin in Natural Waters Using Coupled High-Performance Liquid Chromatography — Flame Atomic-Absorption Spectrometry," *Analyst* 110:515—517 (1985).
20. Krull, I. S., and K. W. Panaro. "Trace Analysis and Speciation for Methylated Organotins by HPLC — Hydride Generation — Direct Current Plasma Emission Spectroscopy," *Appl. Spectrosc.* 39:960—968 (1985).
21. Langseth, W. "Speciation of Alkyltin Compounds by High Performance Liquid Chromatography with a Cyanopropyl-Bonded Silica Column," *J. Chromatogr.* 315:351—357 (1984).
22. Ebdon, L., and J. I. Garcia Alonso. "Determination of Tributyltin Ions in Estuarine Waters by High-Performance Liquid Chromatography with Fluorimetric Detection Using Morin in a Micellar Solution," *Analyst* 112:1551—1554 (1987).
23. Suyani, H., J. Creed, T. Davidson, and J. Caruso. "Inductively Coupled Plasma Mass Spectrometry and Atomic Emission Spectrometry Coupled to High-Performance Liquid Chromatography for Speciation and Detection of Organotin Compounds," *J. Chromatogr. Sci.* 27:139—143 (1989).
24. Suyani, H., D. Heitkemper, J. Creed, and J. Caruso. "Inductively Coupled Plasma Mass Spectrometry as a Detector for Micellar Liquid Chromatography: Speciation of Alkyltin Compounds," *Appl. Spectrosc.* 43:962—967 (1989).
25. Covey, T. R., R. F. Bonner, and B. I. Shushan. "The Determination of Protein, Oligonucleotide and Peptide Molecular Weights by Ion-Spray Mass Spectrometry," *Rapid Commun. Mass Spectrom.* 2:249—256 (1988).
26. Mann, M., C. K. Meng, and J. B. Fenn. "Interpreting Mass Spectra of Multiply Charged Ions," *Anal. Chem.* 61:1702—1708 (1989).
27. Siu, K. W. M., G. J. Gardner, and S. S. Berman. "Atmospheric Pressure Chemical Ionization and Electrospray Mass Spectrometry of Some Organoarsenic Species," *Rapid Commun. Mass Spectrom.* 2:69—71 (1988).
28. Siu, K. W. M., G. J. Gardner, and S. S. Berman. "Atmospheric Pressure Chemical Ionization and Ion-Spray Mass Spectrometry of Some Organotin Species," *Rapid Commun. Mass Spectrom.* 2:201—204 (1988).
29. Guevremont, R., K. W. M. Siu, G. J. Gardner, S. S. Berman. "Electrospray Ionization of Ion Exchange and Ion Pairing Chromatographic Eluents for Tandem Mass Spectrometry," Proceedings of the 38th American Society for Mass Spectrometry, Tucson, AZ, June 3—8, 1990.
30. Siu, K. W. M., G. J. Gardner, and S. S. Berman. "Ionspray Mass Spectrometry/Mass Spectrometry: Quantitation of Tributyltin in a Sediment Reference Material for Trace Metals," *Anal. Chem.* 61:2320—2322 (1989).
31. Siu, K. W. M., P. S. Maxwell, and S. S. Berman. "Extraction of Butyltin Species and Their Gas Chromatographic Determination as Chlorides in a Sediment Certified Reference Material for Trace Metals, PACS-1," *J. Chromatogr.* 475:373—379 (1989).

CHAPTER 10

Advantages of an API Source for Analysis by Liquid Chromatography/Mass Spectrometry

B. A. Thomson, A. Ngo, and B. I. Shushan

INTRODUCTION

While atmospheric pressure ionization (API) has attracted occasional interest over the past several years as an attractive method in principle for coupling a liquid chromatograph to a mass spectrometer, it is only recently that the full potential has begun to be demonstrated. The advantages are readily apparent — ability to cope with large amounts of organic and aqueous solvents without taxing a pumping system and high sensitivity associated with atmospheric pressure chemical ionization. In fact, these points, while important, are not those which are responsible for a renewed interest in atmospheric pressure ionization LC/MS. Rather it is the ability of new inlet methods to vaporize and ionize thermally labile compounds which is generating renewed interest.

The first demonstration of atmospheric pressure LC/MS was supplied by Horning et al.¹ using a home-built system. The outlet of a liquid chromatograph was simply

coupled to a small heated cell where both solvent and analyte were vaporized, with the vapor swept by a gas stream into an atmospheric pressure corona discharge. Good sensitivity was demonstrated for some simple steroids. Several years later, a different approach to API/LC/MS was demonstrated, using an interface developed for the SCIEX® TAGA 6000 MS/MS System.^{2,3} In this interface, termed the Heated Nebulizer, the liquid is sprayed into a heated quartz tube, where droplets containing both solvent and analyte are flash vaporized before being ionized by a corona discharge. This method has the advantage of minimizing the thermal decomposition of labile compounds and providing a gentle ionization which yields primarily quasimolecular ions. Good sensitivity and specificity have been demonstrated for compounds such as drugs in biological fluids.⁴ More recently, electrospray⁵ and ion spray⁶ have aroused interest as atmospheric pressure ion sources which can be coupled to liquid separation methods such as liquid chromatography and capillary zone electrophoresis (CZE). Electrospray and ion spray are both techniques in which ions are emitted directly from the liquid into the gas phase, a process which has been termed ion evaporation.^{7,8} While the same process is operative in thermospray, it is a phenomenon which is more easily controlled and employed at atmospheric pressure. The real advantage of a high pressure source is that small droplets can be readily evaporated without the addition of extra heat, thus avoiding the need to heat the liquid above ambient temperature. Thermal processes which complicate thermospray are therefore not encountered, and in addition, multiply charged ions appear to be more readily generated at ambient temperature. This has the advantage of allowing high molecular weight compounds which contain multiple basic or acidic groups to be analyzed with a relatively low mass quadrupole mass spectrometer. Impressive sensitivity has been demonstrated for compounds such as peptides and polynucleotides with molecular weights of more than 20,000 Da, by detecting multiply charged ions.⁹

It is the purpose of this chapter to review the two major methods of API/LC/MS. Compounds with a variety of functional groups have been used to explore features such as sensitivity and characteristics of the mass spectral information.

EXPERIMENTAL

The SCIEX heated nebulizer LC/MS inlet consists of a sprayer coupled to a heated desolvation/vaporization region, in a probe configuration which interfaces to the API source of the TAGA 6000 MS/MS System (Figure 1). The effluent from the LC flows through narrow bore stainless-steel tubing directly into the nebulizer, where it is converted into a fine mist by a stream of high velocity air or nitrogen. Droplets are swept by the nebulizing gas plus an auxiliary flow of air into an electrically heated quartz tube where they are rapidly vaporized. The heated vapor (solvent plus analyte) is carried into the reaction region of the API source, where the sample is chemically ionized at atmospheric pressure. The vaporizer is temperature controlled to maintain a sufficiently high temperature such that droplets are vaporized at a rate which allows intact organic molecules to be desorbed from

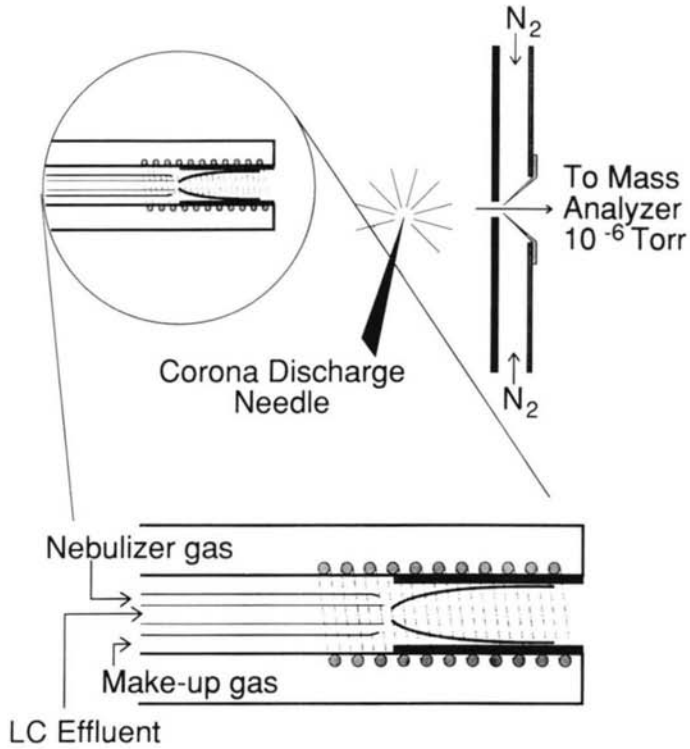


Figure 1. Schematic view of the heated nebulizer LC/MS inlet.

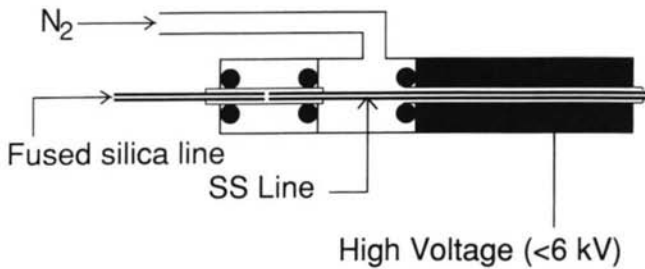


Figure 2. Schematic view of the ion spray LC/MS inlet.

the droplets or particles with minimal thermal decomposition. When the temperature is too low, the vaporization process is slower, and pyrolysis or decomposition may compete with vaporization. The process of rapid spray evaporation thus acts to preserve the molecular identity of involatile and relatively thermally labile compounds and to form a molecular vapor in the carrier gas suitable for gentle chemical ionization. The optimum temperature of the vaporizer is relatively independent of both analyte and solvent composition, so that temperature programming is not required during gradient LC runs. For optimum performance, the probe position is tuned (via controls on the ion source) for maximum signal on a test compound and then left fixed. This provides stable and reproducible operation without daily adjustments of inlet conditions.

In the API source, a current-controlled corona discharge ionizes solvent molecules and buffer salts, which act as reagent ions to ionize the analyte molecules. In the positive mode, reagent ions typically consist of ammonium clustered with water, acetonitrile, or methanol, producing MH^+ product ions from analytes which are basic. In the negative mode, reagent ions consist of solvated oxygen ions or acetate ions, which generate $(M-H)^-$. Chemical ionization is very efficient at atmospheric pressure due to the high collision frequency, thus leading to high sensitivity for polar compounds.

Ions are sampled from the API source through a gas curtain into the vacuum chamber. The gas curtain (consisting of UHP nitrogen) prevents any solvent or sample from entering the analyzer region, thus maintaining the cleanliness of the vacuum system and analyzer components. Clustered solvent molecules are removed from the analyte ions as they pass through the gas curtain and the free jet expansion into the vacuum. Ions are focused into a tandem quadrupole mass analyzer assembly for analysis by MS or MS/MS. Pumping is provided by a cryogenic system driven by a closed cycle helium refrigerator which does not require any consumable gases or liquids.

The ion spray inlet (Figure 2) is also configured as a probe which interfaces with the API source. It consists of a nebulizer, but does not subject the analyte to any heat. A high voltage (typically 3 to 6 kV) is applied to the sprayer, so that highly charged droplets are formed by the nebulization process. The stainless-steel nebulizer is connected via fused silica tubing to the LC, maintaining electrical isolation of the nebulizer from the grounded pump. The highly charged droplets exit directly into the plenum chamber of the API source, with the spray being directed toward the sampling orifice but somewhat off axis (by a few millimeters). No corona discharge is employed. Instead, the droplets evaporate, emitting ions directly into the gas phase as they shrink. The emitted ions consist of charged buffer and analyte ions which are preformed in the solvent. These ions are then sampled through the gas curtain in exactly the same manner as described for the corona discharge.

The ion spray inlet is thus specifically suited for the detection of compounds which are in a charged state in the LC solvent. This applies to the wide variety of biochemically interesting compounds, including drugs, amino acids, proteins, nu-

cleotides, etc., and even compounds that are only weakly acidic or basic can be detected by appropriate adjustment of pH. Certain neutral compounds, such as some steroids, may also be detected by virtue of the fact that they evaporate attached to buffer ions (such as ammonium or acetate), and then retain the charge when the cluster is broken.

As with the heater nebulizer, performance is optimized by adjusting the inlet position in the source for maximum signal. The probe position is independent of the analyte and solvent, although it can be somewhat dependent on the liquid flow. The nebulizer voltage is optimum at about 6 kV for low molecular weight singly charged ions and 4 kV for very high molecular weight multiply charged ions. At the higher voltage of 6 kV, a gas phase corona discharge is initiated around the nebulizer, which seems to reduce sensitivity for multiply charged species.

Operational characteristics of the heated nebulizer and ion spray inlets are somewhat different. The heated nebulizer functions well at liquid flow rates up to 1.5 mL/min, with up to 100% water. It therefore interfaces well with standard 4.1-mm LC columns. The ion spray inlet functions optimally at flow rates of 200 μ L/min and below, although it can be operated at higher flow rates with reduced sensitivity. Ion spray therefore is best interfaced with 1- or 2-mm columns for LC/MS applications. It can also, however, be operated at flow rates down to 1 μ L/min and below, conditions which are ideal when only limited sample volumes are available. If separation is not required, the sample can be introduced by a syringe drive, so that analysis can be performed with only a few microliters of sample.

RESULTS

In order to compare the characteristics of the two inlets, a variety of compounds were introduced via flow injection through each inlet. The characteristics of interest are mass spectra (positive and negative mode) and relative sensitivity. Amounts injected were typically in the 10 to 100 ng range, although up to 1 μ g was injected in some cases where poor sensitivity was obtained for a particular compound/inlet combination.

MASS SPECTRA

Several types of compounds were analyzed in both the positive and negative mode using both inlets. All compounds produced base peaks of the quasimolecular ions, and many could be detected in both ionization modes and with both inlets. Table 1 summarizes the mass spectral data.

Methionine is a simple amino acid with both basic and acidic functional groups. With the heated nebulizer, both $(M+1)^+$ and $(M-1)^-$ ions were observed with approximately equal intensity, with no decomposition products. With the ion spray, both ions were also observed, although their relative sensitivities were pH dependent as expected.

Guanosine is a relatively involatile and thermally labile compound, basic in nature. The heated nebulizer produced both $(M+1)^+$ and $(M-1)^-$ ions as base

peaks at the 1 μg level, with some response at m/z 152 in the positive mode (evidence of thermal decomposition). Only a weak response was observed in either mode at the 100 ng level. Ion spray, however, produced exclusively $(M+1)^+$ and $(M-1)^-$ at levels down to at least 10 ng (still well above the detection limit). The observation of a negative ion is surprising in view of the absence of any strong acidic group on the molecule.

Reserpine produced a relatively weak $(M-1)^-$ ion, but a strong $(M+1)^+$ ion with the heated nebulizer, with no evidence of thermal decomposition or fragmentation. By ion spray, a strong $(M+1)^+$ ion was also observed, with only a very weak response obtained in the negative mode.

Dexamethasone, a nonionic steroid, gave a strong response at $(M+1)^+$ in the positive mode with the heated nebulizer and some response at m/z 333 from thermal breakdown. A weaker response was observed in the negative mode, with $(M-1)^-$ as the base peak. Ion spray also produced some response at $(M+1)^+$ ion, but a strong response at $(M+\text{CH}_3\text{COO})^-$ in the negative mode. This unexpected result (given the nonionic character of the molecule) is attributed to the evaporation of an acetate/dexamethasone cluster from the charged droplet.

Tetrabutylammonium chloride (TBA) was included as an example of salt which should work well by ion spray, but have little or no thermal volatility. As expected, ion spray showed a very strong response at m/z 242 in the positive mode, from the intact cation. The heated nebulizer results were surprising, however, in that a base peak at m/z 242 was also obtained, along with some response at m/z 186 from protonated tributylamine. The presence of the intact cation may be due to direct ion evaporation occurring in the heated nebulizer, since there is no obvious explanation for this ion as a protonated species.

Table 1. Mass Spectra

Compound	Ions Observed			
	Ion Spray		Heated Nebulizer	
	Positive	Negative	Positive	Negative
Methionine (mol wt = 149)	150 (100) 191 (30)	148 (100) 208 (8)	150 (100) 191 (20)	148 (100)
Guanosine (mol wt = 283)	284 (100) 306 (10) 325 (5)	282 ^a	284 (100) 152 (10)	282 (100) 342 (15)
Reserpine (mol wt = 608)	609 (100)	607 ^a	609 (100)	607 ^a
Dexamethasone (mol wt = 392)	393 (100)	451 (100) 427 (35) 481 (10)	393 (100) 419 (25) 333 (25)	391 (100) 433 (25) 361 (15)
Tetrabutylammonium Chloride (cation mol wt = 242)	242 (100)	NA	242 (100) 186 (40)	NA

Note: NA = Not analyzed.

^a Full spectrum not recorded.

Sensitivity

In order to explore the relative sensitivities among the five test compounds (methionine, guanosine, reserpine, dexamethasone, and TBA), each was introduced through both inlets in a flow-injection mode and the responses measured. In all cases, the mobile phase was 50/50 MeCN/H₂O 10⁻³M CH₃COOH, and samples were dissolved in the mobile phase. The flow rates were 1.0 mL/min for the heated nebulizer and 0.1 mL/min for the ion spray. The standard solutions were 100 ng/ μ L with 1 μ L injected except for TBA, which was injected at 1 ng/ μ L for the ion spray measurement because of the very high response obtained.

The results for positive and negative mode are shown in Table 2 for both inlets. The positive mode responses by ion spray are all comparable, except for TBA, which is three orders of magnitude more sensitive than the others. While higher sensitivity would be expected because it is a salt and fully ionized and is somewhat surface active (therefore concentrating at the surface of an evaporating drop), the magnitude is somewhat surprising. Also surprising is the fact that the sensitivity to dexamethasone (neutral in solution) is nearly as high as that to the other three more basic compounds. In the negative mode, larger differences in sensitivity are observed by ion spray, not unexpected since only methionine has an acid group. The fact that the sensitivity of dexamethasone (observed as an acetate adduct as shown in Table 1) is 10 times higher than that of methionine is due to the acid nature of the solution. At neutral pH, the sensitivity towards methionine is higher, and towards dexamethasone, lower than that under the acidic conditions used here.

For the heated nebulizer, sensitivity depends on the vaporization efficiency and on the gas phase acidity/basicity. In the positive mode, only guanosine exhibits a sensitivity which is significantly different from that of methionine. This appears to be due to poor vaporization at lower levels, since 1 μ g of guanosine produced as large a signal as 1 μ g of methionine in the positive mode. As suggested previously, the sensitive detection of the TBA cation is presumed to be due to direct ion evaporation in the heated nebulizer probe. In the negative mode, the sensitivities of guanosine, reserpine, and dexamethasone are less than that of methionine, since all three lack a strong acidic hydrogen.

Overall, the results show that all test compounds can be detected with both inlets. Given the different natures of the compounds, the relative uniformity of response is encouraging. It is clear, however, that an optimum mode (positive or negative) and inlet can be selected for each compound for best sensitivity.

Table 2. Relative Sensitivities

Compound	Molar Sensitivity Relative to Methionine MH ⁺			
	Ion Spray		Heated Nebulizer	
	Positive Mode	Negative Mode	Positive Mode	Negative Mode
Methionine	1.0	0.7	1.0	0.8
Guanosine	0.98	0.08	0.07	0.008
Reserpine	2.0	0.06	2.9	0.08
Dexamethasone	0.95	7.0	1.4	0.2
TBA	1400	—	2.5	—

Methionine, a relatively volatile compound with both basic and acidic functional groups, works well by either ion spray or the heated nebulizer, in both ionization modes. Guanosine, because of its very low volatility and low thermal stability, works best by ion spray in the positive mode. Reserpine, more basic than acidic, works well with both inlets in the positive mode. Dexamethasone works best in the positive mode with the heated nebulizer, but best in the negative mode by ion spray. TBA is obviously best detected in the positive mode by ion spray.

No effort was made to determine detection limits for the compounds, although the responses obtained at 100 ng suggest low to subnanogram detectabilities for methionine, guanosine, reserpine, and dexamethasone, and low picogram to subpicogram detectability for TBA (using the optimum inlet and mode of ionization).

SUMMARY

This survey of some of the characteristics of two LC/MS inlets clearly demonstrates that API/LC/MS has a wide range of potential applications for chemical analysis. It is particularly suitable for the analysis of biochemical compounds which are polar and semivolatile or involatile in nature.

One of the significant observations of this study is that compounds which are quite different in their chemical characteristics can be sensitively detected with one inlet and one ionization mode without adjustment of instrumental conditions. This is obviously important for the analysis of unknown compounds and mixtures with many components. While no one combination of inlet and ionization mode is universal, any one can be generally useful. With some knowledge of the type of compound to be detected, the optimum configuration can be selected for the analysis. Availability of both the heated nebulizer and the ion spray inlets provides the capability for detecting nearly any compound of interest.

Much still needs to be understood about the fundamental mechanisms involved in the ion evaporation process. Further studies which explore effects of mobile phase, pH, and concentration should be useful in determining how best to select LC conditions which provide optimum separation and optimum sensitivity with the ion spray inlet.

REFERENCES

1. Horning, E. C., D. I. Carroll, I. Dzidic, K. D. Haegele, M. G. Horning, and N. Stillwell. "Atmospheric Pressure Ionization (API) Mass Spectrometry, Solvent-Mediated Ionization of Samples Introduced in Solution and in a Liquid Chromatograph Effluent Stream," *J. Chromatogr. Sci.* 12:725—729 (1974).
2. Covey, T. R., E. D. Lee, A. P. Bruins, and J. D. Henion. "Liquid Chromatography/Mass Spectrometry," *Anal. Chem.* 58:1451A—1461A (1986).
3. Thomson, B. A., and L. Danylewych-May. "Design and Performance of a New Total Liquid Introduction LC/MS Interface," paper presented at the 31st Annual Conference on Mass Spectrometry and Allied Topics, Boston, MA, May 8—13, 1983.

4. Covey, T. R., E. D. Lee, and J. D. Henion. "High-Speed Liquid Chromatography/Tandem Mass Spectrometry for the Determination of Drugs in Biological Samples," *Anal. Chem.* 58:2453—2460 (1986).
5. Whitehouse, C. M., R. N. Dreyer, M. Yamashita, and J. B. Fenn. "Electrospray Interface for Liquid Chromatographs and Mass Spectrometers," *Anal. Chem.* 57:675—679 (1985).
6. Bruins, A. P., L. D. G. Weidolf, J. D. Henion, and W. L. Budde. "Determination of Sulfonated Azo Dyes by Liquid Chromatography/Atmospheric Pressure Ionization Mass Spectrometry," *Anal. Chem.* 59:2647—2652 (1987).
7. Iribarne, J. V., and B. A. Thomson. "On the Evaporation of Small Ions from Charged Droplets," *J. Chem. Phys.* 64(6):2287—2294 (1976).
8. Iribarne, J. V., P. J. Dziedzic, and B. A. Thomson. "Atmospheric Pressure Ion Evaporation-Mass Spectrometry," *Int. J. Mass Spectrom. and Ion Phys.* 50:331—347 (1983).
9. Covey, T. R., R. F. Bonner, B. I. Shushan, and J. D. Henion. "Determination of Protein, Oligonucleotide and Peptide Molecular Weights by Ion Spray Mass Spectrometry," *Rapid Commun. Mass Spectrom.* 2(11):249—256 (1988).



Taylor & Francis

Taylor & Francis Group

<http://taylorandfrancis.com>

CHAPTER 11

Parallel Column Gas Chromatography-Mass Spectrometry for the Analysis of Complex Environmental Samples*

J. C. Marr, J. Visentini, and M. A. Quilliam

INTRODUCTION

Concern about the presence of hazardous chemicals in the environment and the threat that they pose to man and nature, has led to great demands on the chemist and his analytical tools to detect and measure such substances at lower and lower concentrations. Contaminants such as polychlorinated biphenyls (PCBs), polychlorinated dibenzodioxins (PCDDs), and polycyclic aromatic compounds (PACs) present a particularly difficult challenge due to their structural diversity. For example, PACs encompass a very large range of compounds, as shown in Figure 1.¹ In addition to the parent polycyclic aromatic hydrocarbons (PAHs), substitutions for hydrogen at various ring positions by alkyl, nitro, and other groups, or heteroatom substi-

* NRCC No. 31310.

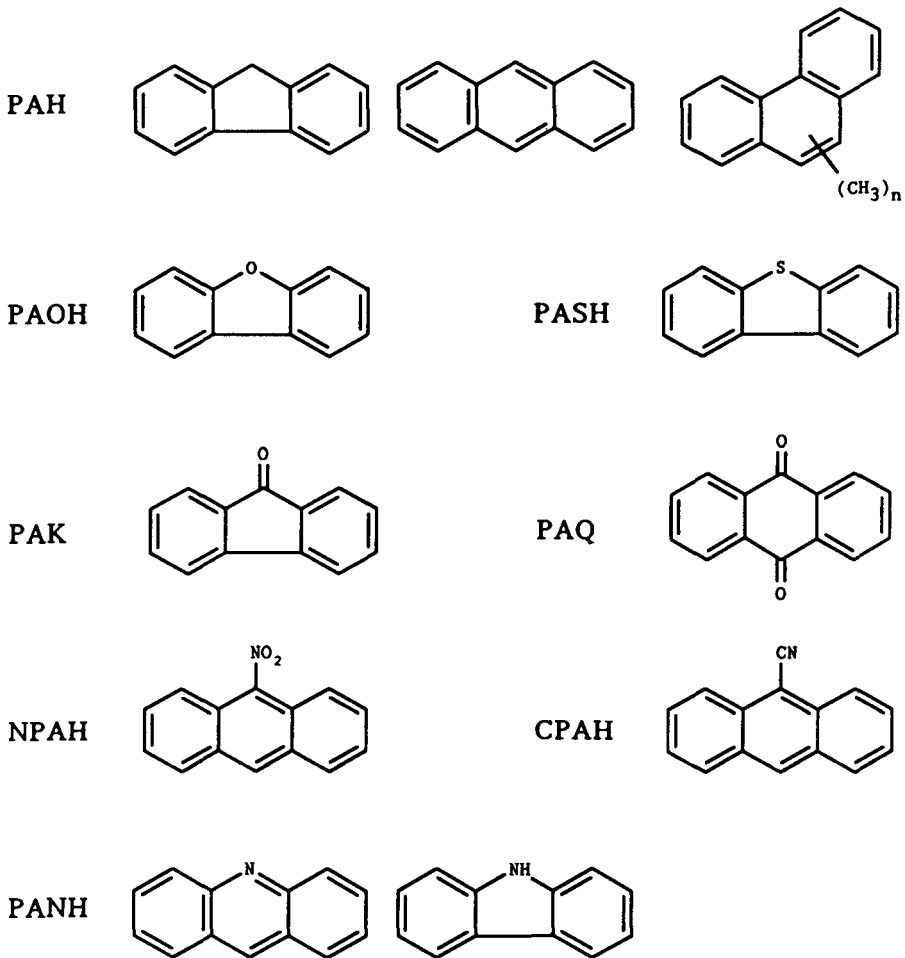


Figure 1. Representative structures of polycyclic aromatic compounds (PACs) found in the environment. For simplicity, each different class has been represented by an acronym (PAH = polycyclic aromatic hydrocarbons; PAOH = polycyclic aromatic oxygen heterocyclics; PASH = polycyclic aromatic sulfur heterocyclics; PAK = polycyclic aromatic ketones; PAQ = polycyclic aromatic quinones; NPAH = nitro polycyclic aromatic hydrocarbons; CPAH = cyano polycyclic aromatic hydrocarbons; PANH = polycyclic aromatic nitrogen heterocyclics).

tutions for carbon by oxygen, nitrogen, or sulfur, produce a variety of compound classes. It is evident that for each of these different classes of PACs, there are large numbers of possible structures, particularly isomeric ones. PACs are of particular concern due to the known or suspected carcinogenic nature of many of these compounds.^{2,3} Since carcinogenicity has been shown to be dependent upon structural features such as shape, size, steric factors, and type of substituent,¹ it is important to have information on the individual PAC in the sample.

The selection of an analytical method suitable for the analysis of contaminants in the environment is constrained by a number of factors such as the nature of the sample and analytes, the information required, the required precision and accuracy of the results, and the availability of suitable equipment. We will examine some of these factors here and then propose a novel instrumental analytical approach that we believe can be useful in certain situations.

First, it is important to recognize that the chemical composition of environmental samples such as airborne particulate matter and sediments is very complex, consisting of hundreds of organic and inorganic components. The complexity of the organic components, both in number and in structure, means that organic analytical methods must provide a high overall resolving power. Thus, high resolution chromatographic methods, such as capillary column gas chromatography (GC) or high performance liquid chromatography (HPLC), are widely used in environmental analytical chemistry.^{4,5} However, it is rare that a single chromatographic technique provides sufficient resolution for the detailed analysis of a typical environmental sample. One solution is to use one or more low resolution separation steps (usually termed a "cleanup") prior to GC or HPLC analysis in order to reduce interferences. It is also possible to improve the effective resolving power of a chromatographic method by using a detector with high detection selectivity. For example, the use of a fluorescence detector with HPLC can allow the analysis of certain target analytes (e.g., benzo[a]pyrene) with minimal sample fractionation. On the other hand, the use of extensive fractionation prior to analysis and/or selective detection may be too restrictive for some studies since this does not allow "broad-spectrum" determination of a variety of substances in a sample. In this regard, the mass spectrometer (MS) has played a very important role in environmental organic analytical chemistry because it can be used in both universal and selective detection modes.

A second factor that must be considered in method selection is the fact that compounds of interest are generally present at trace levels in extremely complex matrices. It is, therefore, very important to use detectors that provide high sensitivity. Thus, detectors such as the electron capture detector have allowed the analysis of chlorinated hydrocarbons at extremely low levels. Again, the mass spectrometer plays an important role because of its high sensitivity, especially in certain modes of operation, such as selected ion monitoring and with certain types of ionization such as negative ion chemical ionization.

Third, due to the legal and toxicological implications of detecting hazardous contaminants in environmental samples, methods must be available to provide a high degree of confidence in confirmation of compound identity and in accurate quantitation. Usually this requires the use of a spectroscopic detector such as a mass spectrometer that can provide structural information.

From these considerations it is not surprising that combined GC-MS is widely used in environmental analytical chemistry. Similarly, we expect to see HPLC-MS used a great deal more in this area since the technique has matured rapidly over the last few years and is now a viable alternative for the analysis of many environmental contaminants.⁶ Of course the particular strength of HPLC-MS lies in the

analysis of compounds too involatile for GC-MS. In general it can be assumed that results generated by a mass spectrometry-based technique are more reliable, in both a qualitative and quantitative sense, than the corresponding results from single-parameter detector systems. This is simply because the analyst can have a great deal more confidence that the analytical signal is produced solely by the analyte of interest. For example, it was shown that the critical analysis of PAC in marine sediment reference materials was best accomplished with either GC-MS or HPLC-MS, rather than with GC using flame ionization detection (FID) or HPLC using UV adsorption detection (UVD).⁷ This is easy to understand since there is a high probability that the recognized peaks in nonselective detector chromatogram of a complex environmental sample are actually combinations of two or more components. Since the retention volume range for a chromatographic system is fixed, the severity of peak overlap increases as the number of components increases.⁸ Therefore, an analysis with a single-parameter detector (e.g., GC-FID) may not provide sufficient resolution to permit accurate identification or quantitation of individual components. This is well illustrated by the GC-FID and HPLC-UVD chromatograms of a marine sediment reference material extract, shown in Figure 2. It is clear that there are hundreds of components in this sample, despite its having been taken through an extensive clean-up procedure to isolate PACs. The fact that there are more detectable peaks in the GC trace indicates that there is severe overlap in the HPLC trace. However, GC-MS analysis shows that there is a considerable degree of coelution even in the high resolution GC chromatogram.

MULTIDIMENSIONAL TECHNIQUES

The use of multidimensional techniques is a valuable way to increase the resolution and the quality of information provided by an analysis. Multichannel detection systems are particularly useful since they can monitor more than one signal at a time and offer greater versatility when determining a diverse range of compounds. For example, the ultraviolet diode array detector (DAD) can provide simultaneous multiwavelength monitoring or even continuous UV spectral acquisition.⁹ The most popular multichannel detector is the mass spectrometer since, as indicated earlier, it offers both selective and general detection capabilities and provides excellent structural information. Continuous acquisition of full mass spectra can be used for the identification of sample components, while single mass chromatograms may be generated for selective detection. The mass spectrometer may also be used in the high sensitivity selected ion monitoring mode where only the intensities of characteristic ions are recorded as a function of time. GC-MS is routinely used for the detection of PACs in environmental samples.^{5,10,11} The combination of two or more spectroscopic detectors combined with chromatography can increase the confidence of identification even further. For example, it has been shown that HPLC with simultaneous acquisition of UV and mass spectra can be very effective for the analysis of complex mixtures of PACs.⁹

Multidimensional chromatography techniques have tremendous potential in organic analysis. The most popular approach is "orthogonal" chromatography, which

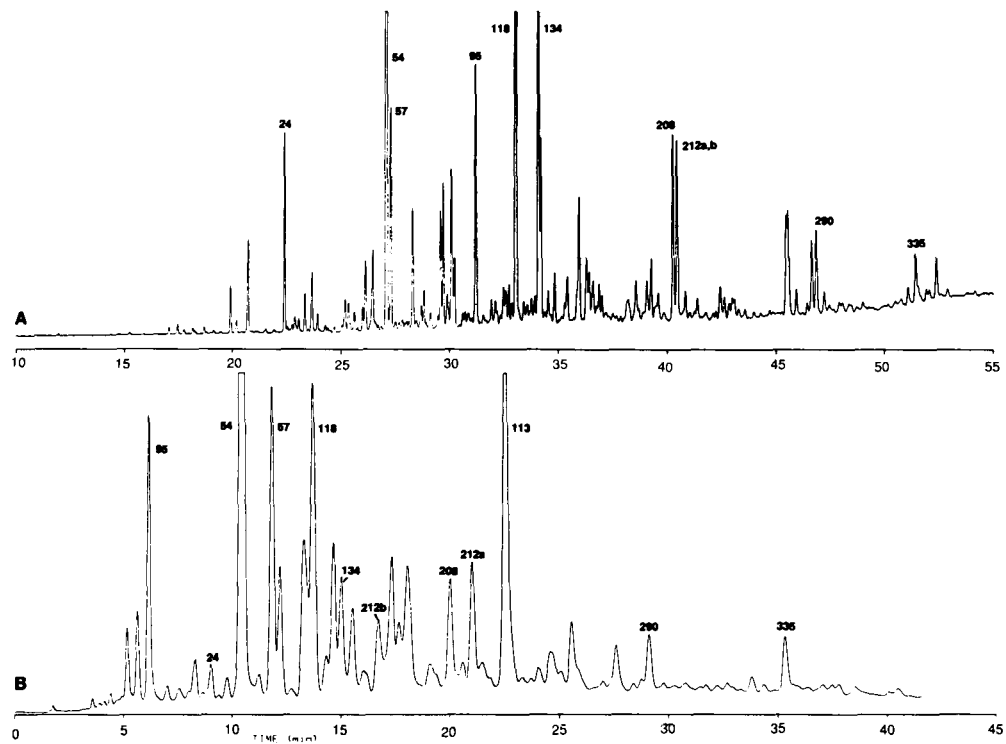


Figure 2. Analysis of the PAC fraction isolated from the marine sediment reference material HS-3 by capillary column GC-FID with a SPB-5 stationary phase (A), and HPLC-UV-D (254 nm) with gradient elution on a Vydac 201TP5 stationary phase (B). See Table 1 for peak identities.

involves using two columns of different separation selectivity (i.e., different stationary phases) with an arrangement to allow a fraction of the effluent from one column to be transferred to the second column. This may be accomplished on-line with an automatic switching valve or off-line with a preparative fraction collection system followed by injection into the second column. Two-dimensional GC analysis¹² is a common method, and commercial equipment is available. The use of preparative HPLC to isolate the fractions of interest prior to analysis by GC is another widely used two-dimensional technique which is very useful when selected compound classes are to be characterized. For example, due to the observed mutagenicity of PAH derivatives, several studies have characterized polycyclic aromatic ketones and quinones^{13,14} and nitrated PAH^{15,16} in airborne particulate samples using preparative HPLC fractionation followed by GC-MS. Although orthogonal chromatography provides a tremendous increase in the overall resolving power of the method, it also increases substantially the number of operations involved in the analysis of large numbers of analytes. This method is therefore best suited to target compound analysis.

The use of two or more GC capillary columns in parallel, each connected to its own detector, is a multidimensional approach that has received only limited attention.^{12,17-21} As illustrated in Figure 3, a sample may be injected into one injector port and then split onto two columns with different separation selectivities (i.e., different stationary phases). Of course it is also possible to generate the same information by performing two separate analyses at different times or on two separate instruments. The resulting chromatograms provide complementary information. If two components are not separated on one column, there is a good chance that they will be on the second column. In addition, by matching the retention times of peaks in the two different chromatograms with those of standards, it is possible to confirm the identities of components. However, it is obvious that the method is limited to relatively simple mixtures if only single-channel detection systems are used. For PAC mixtures from environmental samples, we have found that a parallel column GC-FID experiment is useful only for confirmation of the major components in these complex samples.²² Peaks representing minor components are difficult to correlate from one chromatogram to the other. This finding leads naturally to the instrumental method upon which we wish to focus on, for example, parallel column gas chromatography with mass spectrometric detection.

PARALLEL COLUMN GC-MS

Combining the technique of parallel column chromatography with multichannel detection can generate an abundance of data useful for the identification of components in a complex mixture. The multichannel detector can allow the detection of individual compounds even if complete chromatographic resolution has not been achieved on either column. Figure 4 is an example of the information provided by a parallel column GC-MS experiment using a mixture of PCB standards. It can be seen that the separation selectivities of the two GC columns were quite different and that the extra dimension of information provided by the mass spectra of the

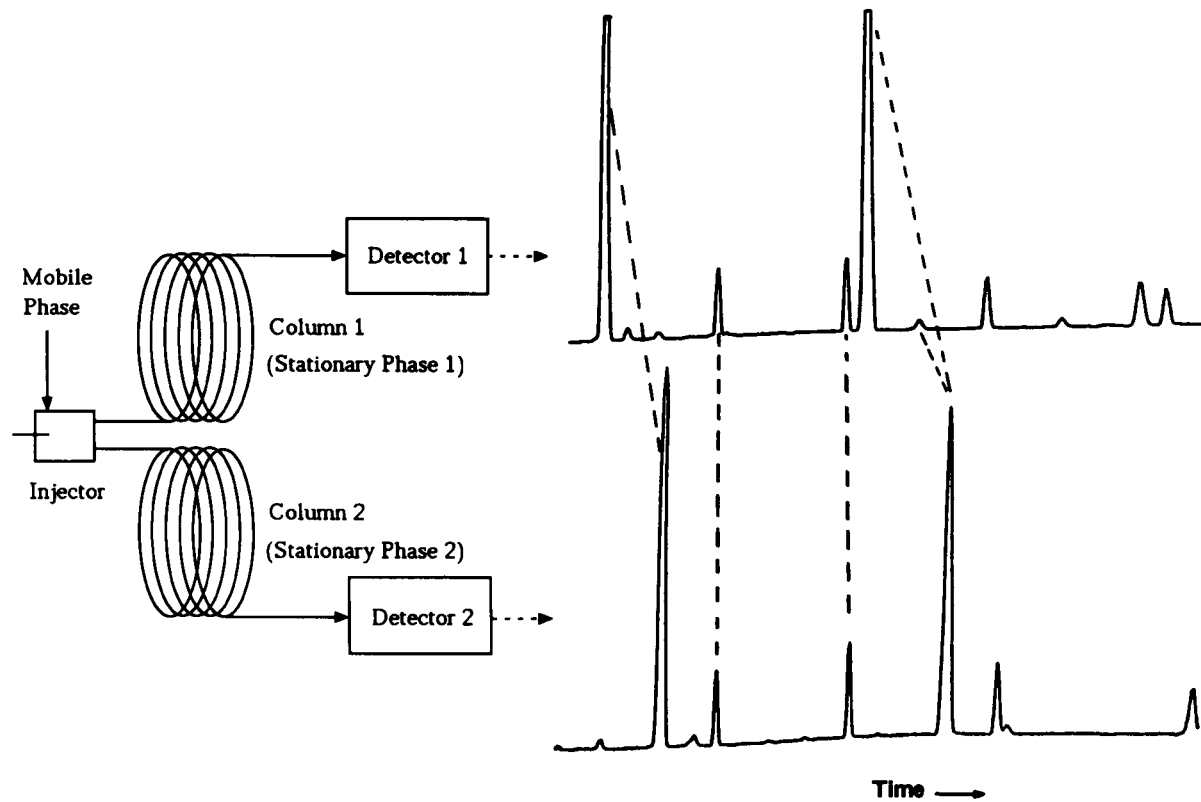


Figure 3. Schematic of a parallel column chromatography experiment. After injection, the sample is split between two columns. Chromatograms are acquired simultaneously from the two detectors.

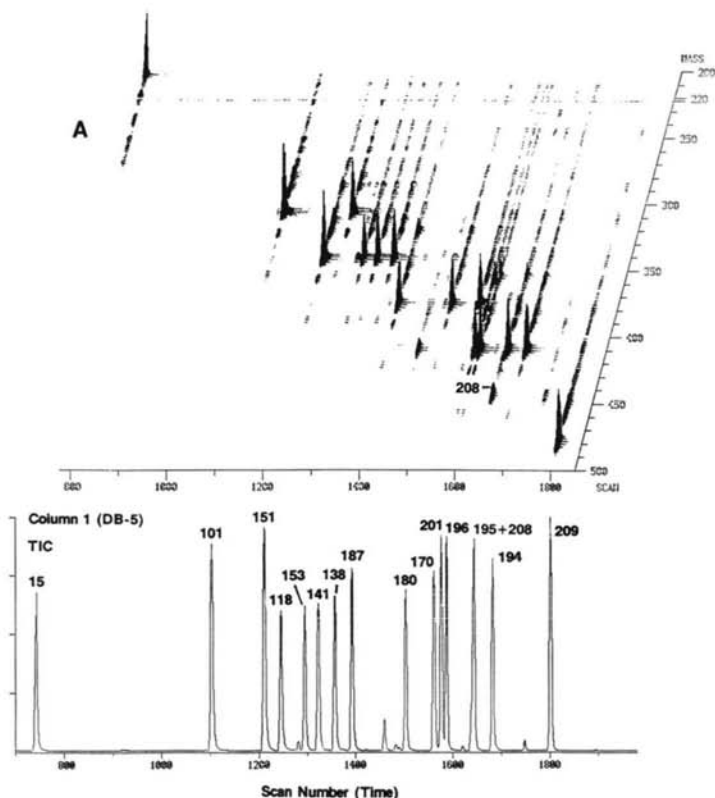


Figure 4. Analysis of a PCB standard mixture (CLB-1D from the Marine Analytical Chemistry Standards Program) by parallel column GC-MS (negative ion CI, methane/oxygen) using DB-5 (A) and DB-210 (B) stationary phases. Two data sets were generated in two separate analyses on the same instrument. The peaks are annotated with the IUPAC number system for PCB congeners.

individual peaks facilitated assignment of peak identities. It was also possible to detect unresolved components that would not have been observed with a single-parameter detector. For example, PCB-208 was identified as an impurity in the mixture. This compound could not be resolved from the other compounds by either GC column; however, the mass spectrometer provided the additional resolution required for its detection. The mass spectrum and the retention times on the two columns allowed its identification.

Kowalsky and co-workers²³ have described the combination of two or more chromatographic separations in parallel combined with multichannel detection and multivariate data analysis as "third-order chromatography." Data are collected as a function of time, column type, and detector channel. For parallel column GC-MS, these variables are scan number, column type, and m/z ratio. The application of this method to real-world complex mixtures has never been reported to our knowledge. Therefore, we decided to test the viability of this method for the analysis of PACs in complex environmental samples.

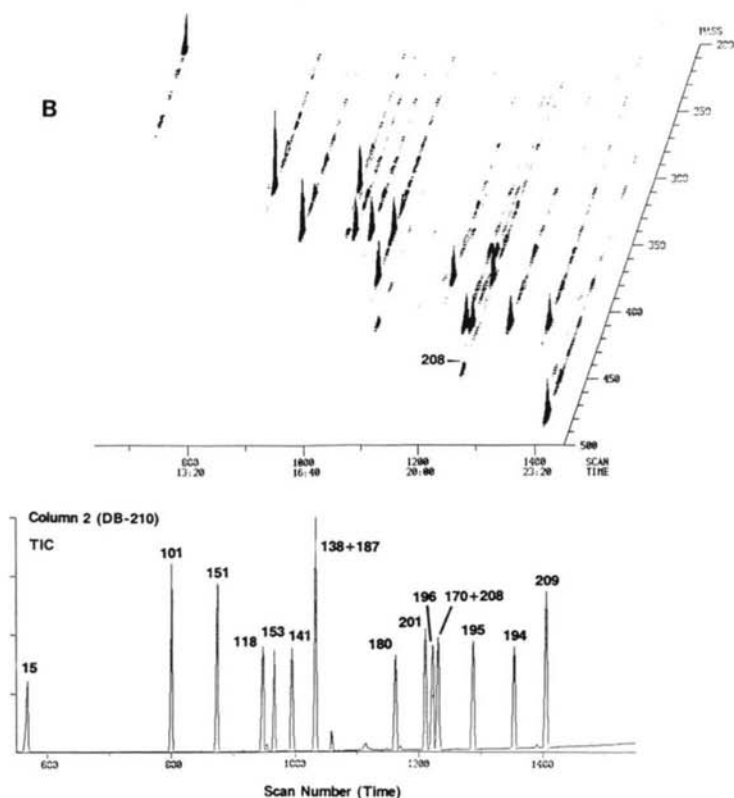


Figure 4B.

The PAC fractions from several different samples have been analyzed by this technique, using various GC columns with different selectivities and a mass spectrometer as the detector. The results presented in this paper are for a marine sediment reference material (HS-3) supplied by the Marine Analytical Chemistry Standards Program (MACSP) of the National Research Council of Canada. The U.S. National Institute of Standards and Technology (NIST) urban dust sample (SRM-1649) has also been analyzed extensively by us using this method of analysis.²² The use of reference materials provided a number of advantages for this study. Their compositions and matrices are just as complex as typical environmental samples, but they are available in bulk quantities. Therefore, replicate analyses may be performed on exactly the same material each time, and other laboratories can analyze the same sample by alternate methods to verify results. Confirmation of any quantitative results is also possible since the concentrations of some components are certified. The information obtained from these reference materials proved very useful when examining actual real-world samples, such as airborne particulate matter from Canadian cities.²²

One of the first concerns in this study was to determine which two columns would provide the most useful complementary separations for the sediment PACs. Three fused silica capillary columns were investigated, each with a different stationary phase and hence a slightly different separation selectivity. The stationary phases, in order of increasing polarity, were SPB-1 (methyl silicone), SPB-5 (5% phenyl-methyl silicone), and SPB-608 (40% phenyl-methyl silicone). Figure 5 shows the total ion chromatograms (TIC) from the three GC-MS analyses of the PAC fraction isolated from the HS-3 marine sediment reference material. As illustrated, even after the extensive cleanup that was used to isolate the PAC fraction, the chromatograms were still very complex. An important point to note is that it is very easy to match the large peaks in these TIC traces, but it is very difficult to make conclusive matches of smaller peaks.

A GC-MS analysis in the full scan mode produces a tremendous amount of data (e.g., 3500 scans resulting in approximately 4 MB of data for each of the data sets in Figure 5). A major concern is to be able to organize these data and turn them into useful information. To illustrate the type of information available, Figure 6

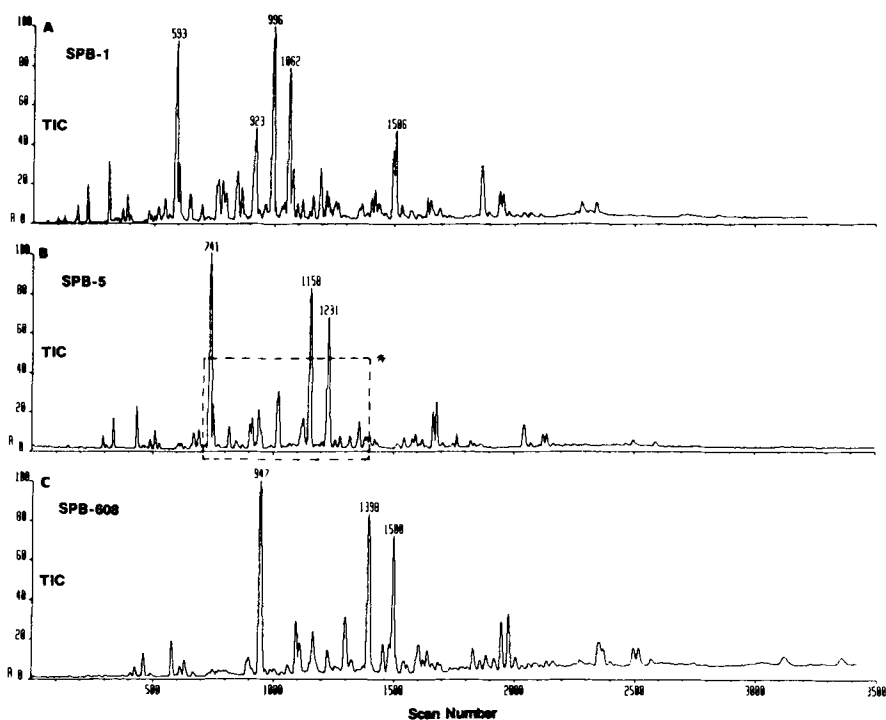


Figure 5. Total ion chromatograms (TIC) for the parallel column GC-MS analysis (electron ionization) of the PAC fraction isolated from the marine sediment reference material HS-3. The marked region * is expanded in Figure 6. (Columns: SPB-1 [A], SPB-5 [B], and SPB-608 [C]).

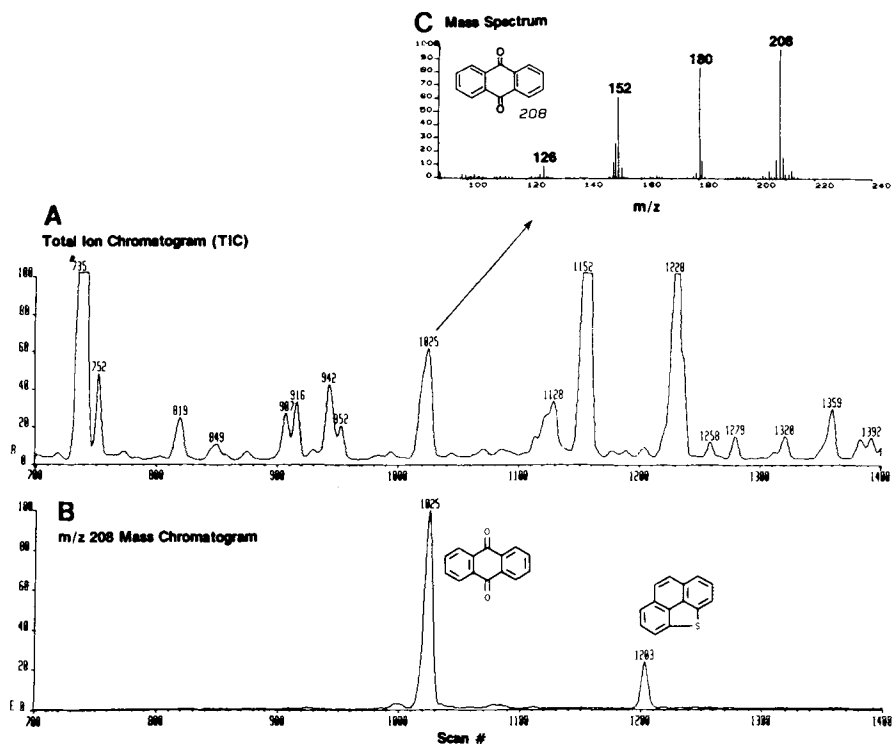


Figure 6. An expansion of marked region * in Figure 5B showing the type of information available from a GC-MS analysis. This includes the TIC (A), the m/z 208 mass chromatogram (B), and the mass spectrum of 9,10-anthraquinone (C). (Column: SPB-5)

shows an expansion of a region of the TIC for the SPB-5 column analysis in Figure 5. For this analysis, mass spectra were acquired once every second. The mass spectrum for the peak at scan 1025 (shown as an inset in Figure 6) shows that the compound has a molecular ion at m/z 208 and major fragment ions at m/z 180 and 152. Such successive losses of two 28-amu fragments (CO) is highly characteristic of quinones. A match of the retention time and the mass spectrum with those of a standard compound allowed the peak to be assigned as 9,10-anthraquinone. Also shown in Figure 6 is a mass chromatogram reconstructed from the data set by plotting the intensity of m/z 208 as a function of scan number. This chromatogram allows selective detection of anthraquinone. It should be noted that another peak in the m/z 208 mass chromatogram at scan 1203 is due to another compound with a molecular weight of 208, phenanthro[4,5-bcd]thiophene. This compound is easily distinguished from anthraquinone by its longer retention time and by its mass spectrum which has no fragment ions at m/z 180 and 152. Examination of the m/z 180 and 152 mass chromatograms (data not shown) shows that a peak is observed in each trace maximizing at scan 1025 and not at scan 1203. (As shown later, it

is possible to extract the pure mass spectrum of each compound by identifying all ions that reach a maximum intensity at the same scan number.)

Unfortunately, a few peaks in the TIC of this sample correspond to a single compound. As illustrated in Figure 7, the fairly symmetrical peak in the TIC at scan 693 is actually due to three closely eluting compounds. The mass spectrum taken at scan 693 (point B) is difficult to interpret. Examination of the mass spectra on the sides of the TIC peak proves that it is not due to a single component. The earlier mass spectrum at the point marked A indicates a PAC with a molecular ion of 196, while the one at point C shows a PAC with a molecular ion of 184. The mass chromatograms presented in Figure 7 show very clearly that the TIC peak is due to a compound of molecular weight 184 with a peak maximum at scan 694 and two isomeric compounds of molecular weight 196 with peak maxima at scans 691 and 698. This example indicates the power of GC-MS to further resolve compounds that are not completely separated by the chromatography.

Examination of individual mass chromatograms is a useful way to compare separations achieved with different columns and to correlate peaks from one column to the other. Figure 8 shows an expansion of the m/z 184 and 196 mass chro-

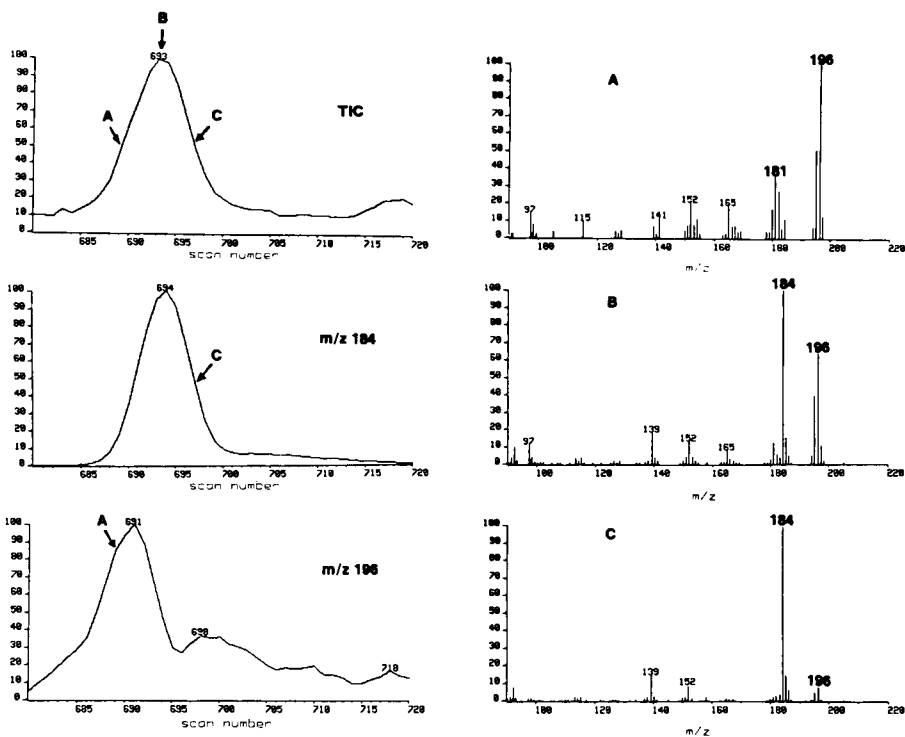


Figure 7. Examination of one peak in the TIC in Figure 5B, showing that there are three compounds coeluting under one TIC peak. (Column: SPB-5)

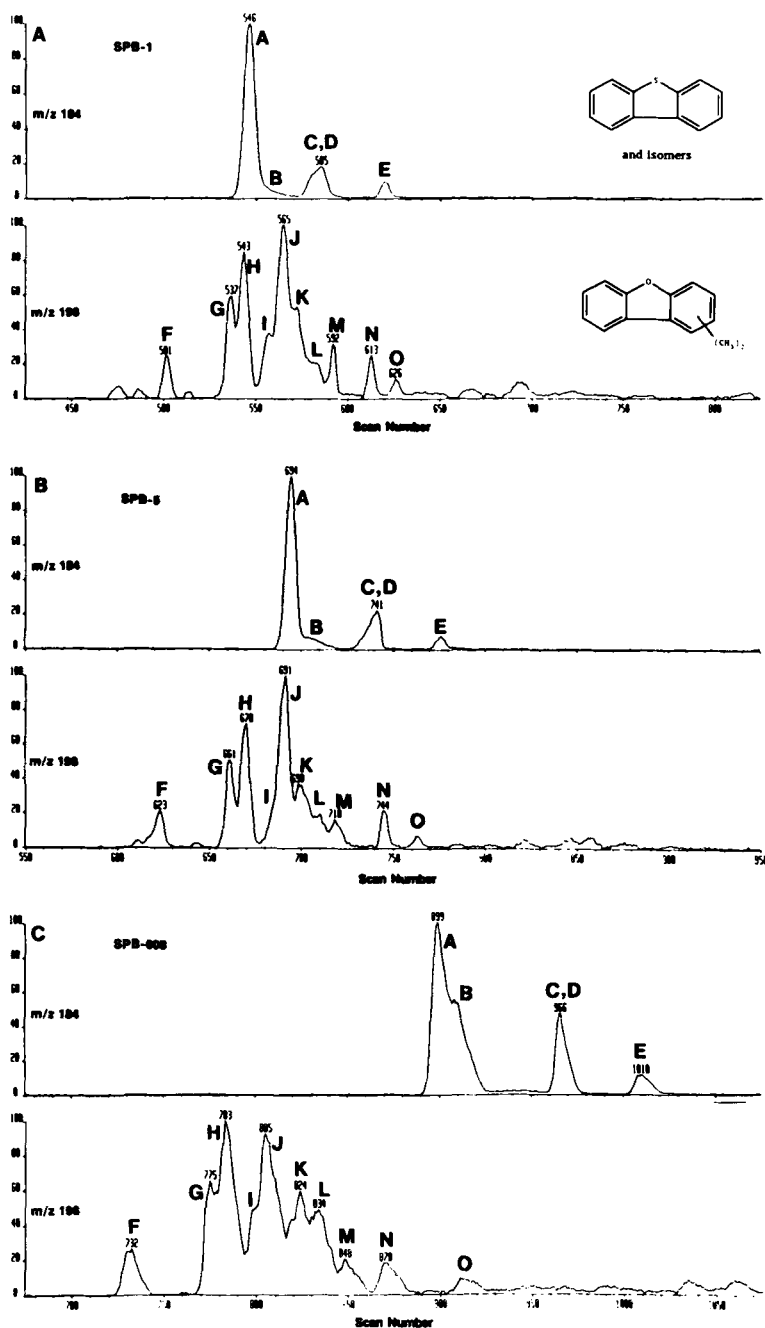


Figure 8. An illustration of the different separation selectivities shown by the three different GC columns. This shows the m/z 184 and 196 mass chromatograms over a narrow scan range from each of the data sets shown in Figure 5.

matograms for the GC-MS analyses performed on the three different columns (see Figure 5). The peaks in the m/z 184 trace are due to several different isomers of dibenzothiophene, while those in the m/z 196 trace are due to a complex mixture of dimethyl or ethyl dibenzofurans. It is quite easy to correlate peaks in the respective mass chromatograms for each column by using peak heights. From Figure 8 it is also possible to see that there is a dramatic change in the relative separations of the two classes of compounds in going from one column to the next due to the differing selectivities of each stationary phases. From data such as these we have found that the stationary phases with the most complementary separations were SPB-5 and SPB-608.

The vast amount of data acquired by a parallel column GC-MS analysis requires that the effective means of data management and analysis be developed. The procedures used should minimize the personnel time involved in organizing the data and maximize utilization of the available information. Methods such as searching the TIC for detectable peaks are not adequate for identifying the majority of the components. Minor components in a complex sample are easily missed if they coelute with major components. In addition, mass spectra may be very confusing due to coelutions. Clearly there is a need for an automated data processing program that can identify signals due to individual compounds and extract their mass spectra. Some programs of this type have been reported previously in the literature, the best known being the Biller-Biemann enhancement routine.²⁴ This procedure takes advantage of the fact that all molecular and fragment ions that belong to a particular compound reach a maximum at the same time in the mass spectrometer, i.e., at the same scan number. Peak profile analysis of all mass chromatograms in the data set thus identifies all ions common to a compound's spectrum, practically free of contributions from unresolved substances such as peak tails or column bleed. Different versions of the Biller-Biemann routine are available on many commercial mass spectrometry data systems. We have found that such programs are fairly successful for the detection of major components and enhancement of their spectra, but have severe problems with minor components in complex mixtures. This is mainly due to the fact that these programs generally incorporate simple peak detection algorithms, based on detection of a peak maximum after a mass chromatogram signal rises above a prescribed threshold. These routines have difficulty in recognizing partially resolved compounds with common ions (e.g., isomers) that give rise to multicomponent mass chromatograms such as those in Figure 8. Also, it is difficult to apply the algorithms in situations where there is a low signal-to-noise ratio. One of the goals of our research was to develop a program that uses a more sophisticated peak detection algorithm, similar to those used in modern chromatographic data systems. Such an algorithm would examine peak shape, so that spurious peaks due to noise could be filtered out and closely eluting peaks could be detected in mass chromatograms. Even peak shoulders are detectable by such algorithms. As a first step in this direction, a semiautomated peak detection routine was developed. This procedure relies upon the skills of an experienced chromatographer in recognizing peaks due to individual compounds in mass chromatograms

produced automatically by the mass spectral data system. The data generated from this analysis were compiled using a commercial spreadsheet program (LOTUS-123, Lotus Corp.) on an MS-DOS-based microcomputer. Identification of the PAC was achieved using retention indices (RIs), molecular ions, and key fragment ions. The process followed the following basic steps:

1. Automated plotting of all mass chromatograms from the data set for each chromatographic column, using a program written on the mass spectral data system. Many of the peak maximum in the mass chromatograms are automatically annotated by the MS data system.
2. Manual measurements are performed on minor peaks and shoulders not recognized by the data system.
3. Manual entry of scan numbers for peak maxima and peak heights, for each and every mass chromatogram, into a LOTUS-123 spreadsheet.
4. Sorting of the spreadsheet according to scan number. This identifies all the unique mass spectra in the data set.
5. Automated plotting of all the unique mass spectra by the MS data system.
6. Manual assignment of molecular ions, isotope peaks, and fragment ions. This is relatively easy with a PAC since the molecular ion is usually the most abundant high mass peak in the spectrum.
7. Calculation of retention indices for each component using spreadsheet template programming.
8. Comparison of results between the two GC-MS analyses using the different columns, correlation of peaks between the two sets of chromatograms, and compilation of all the results into a final table.
9. Assignment of tentative identities according to spectra and retention indices.

Obviously, this is a highly tedious operation when performed manually. However, the programs written for the MS data system significantly reduced the time required to process the results. These programs were usually run overnight when the computer was not required for mass spectrometer control and data acquisition. The use of LOTUS-123 greatly facilitated data management. The ability to produce templates and macro programs for automated calculation of retention indices and sorting of data was particularly useful. We are currently exploring programs for totally automated chromatographic peak detection and compilation of the results. An expert system programming approach may be the best route.

Retention indices were very useful in the assignment of peak identities. They were calculated with a spreadsheet template using a modified version of the method developed by Lee and co-workers.²⁵ A great many PAC retention indices based on this system have been presented in this literature, mostly on columns equivalent to the SPB-5 column used in this study.^{25,34} Excellent interlaboratory reproducibility (<0.5% RSD) is possible with this retention index system, and this allows the identification of compounds even when standards are not available in one's own laboratory. Unfortunately, the total number of PAC standards available to researchers is minor compared to the thousands of different compounds observed in real-world samples. Often it is not possible to conclusively assign a peak identity,

especially if there are a large number of isomeric possibilities. For example, through examination of mass spectra, it was possible to assign the set of peaks in a m/z 196 mass chromatogram (see Figure 8) as C₂-alkyl (ethyl or dimethyl) substituted dibenzofurans, but it was not possible to assign individual structures because of the lack of standards.

Table 1 presents a small portion of the information generated from the parallel column GC-MS analysis of the marine sediment reference material PAC fraction. Over 350 individual compounds were detected by combining data from the SPB-5 and SPB-608 data sets. Of these, 41 were firmly identified by a match of mass spectra and retention indices with those of standards. Tentative identities have been assigned for many more, but without standards it is only possible to indicate general structures.

This procedure has also been applied to several other samples such as the NIST urban dust reference material (SRM-1649) and a typical urban airborne particulate sample collected in Hamilton, Ontario.²² Over 500 PACs were detected in the former which proved to be extremely complex; over 300 compounds were detected in the latter.

Table 1. A Portion of the Data Set Produced by the Parallel Column GC-MS Analysis of the PAC Fraction of the MACSP Marine Sediment Reference Material (HS-3)

Cmpd No.	Scan Number		RI SPB-5	Mol. Wt.	Relative Conc'n	Tentative Identity
	SPB-5	SPB-608				
1	54	106	218.1	142	*	2-Methylnaphthalene
2	68	156	219.9	143	*	Methyl-quinoline/isoquinoline
3	73	142	220.5	142	*	1-Methylnaphthalene
4	148	233	230.0	154	**	Biphenyl
6	203	277	236.9	156	*	C ₂ -alkyl-naphthalene
15	294	425	248.3	154	***	Acenaphthene
17	308	493	250.0	153	**	153PANH
19	338	460	253.7	168	****	Dibenzofuran
24	436	577	265.6	166	****	Fluorene
30	490	613	272.0	182	***	Methyl-dibenzofuran
31	511	631	274.5	182	***	Methyl-dibenzofuran
33	528	667	276.5	182	**	Methyl-dibenzofuran
35	599	737	284.7	180	*	Methyl-fluorene
36	609	746	285.9	180	**	Methyl-fluorene
37	619	763	287.0	180	*	Methyl-fluorene
40	623	732	287.4	196	*	C ₂ -alkyl-dibenzofuran
41	638	794	289.1	180	*	Methyl-fluorene
42	661	775	291.7	196	**	C ₂ -alkyl-dibenzofuran
43	670	783	292.7	196	**	C ₂ -alkyl-dibenzofuran
44	673	889	293.1	180	***	9-Fluorenone
45	673	774	293.1	181	**	Methyl-carbazole
47	685	800	294.4	196	*	C ₂ -alkyl-dibenzofuran
48	691	805	295.1	196	**	C ₂ -alkyl-dibenzofuran
49	694	899	295.4	184	****	Dibenzo[b,d]thiophene
50	699	824	295.9	196	*	C ₂ -alkyl-dibenzofuran
51	705	909	296.6	184	*	Naphtho[1,2-b]thiophene
54	741	945	300.5	178	*****	Phenanthrene
55	742	966	300.7	184	**	Naphtho[2,1-b]thiophene
57	752	949	301.7	178	*****	Anthracene
59	772	988	303.9	179	**	Acridine

Table 1 (continued). A Portion of the Data Set Produced by the Parallel Column GC-MS Analysis of the PAC Fraction of the MACSP Marine Sediment Reference Material (HS-3)

Cmpd No.	Scan Number		RI	Mol. Wt.	Relative Conc'n	Tentative Identity
	SPB-5	SPB-608				
60	776	1010	304.3	184	*	Naphtho[2,3-b]thiophene
62	801	999	307.0	194	*	Methyl-fluorenone
64	819	1093	308.9	167	****	Carbazole
67	845	1053	311.7	193	*	Methyl-179PANH
68	845	1034	311.7	198	*	Methyl-184PASH
69	849	1058	312.1	204	**	1-Phenyl-naphthalene
71	856	1061	312.8	194	*	Methyl-fluorenone
72	874	1061	314.7	198	*	Methyl-184PASH
75	890	1106	316.4	198	*	Methyl-184PASH
77	901	1126	317.5	194	*	Methyl-fluorenone
78	907	1095	318.1	192	****	Methyl-phenanthrene/anthracene
80	912	1128	318.7	198	*	Methyl-184PASH
81	916	1108	319.1	192	****	Methyl-phenanthrene/anthracene
82	929	1140	320.4	192	**	Methyl-phenanthrene/anthracene
83	934	1178	320.9	181	*	Methyl-carbazole
85	942	1165	321.8	190	****	4H-Cyclopenta[def]phenanthrene
87	945	1150	322.1	192	***	Methyl-phenanthrene/anthracene
88	952	1160	322.8	192	***	Methyl-phenanthrene/anthracene
92	994	1173	327.1	212	*	C ₂ -alkyl-184PASH
94	1019	1225	329.7	204	****	2-Phenyl-naphthalene
95	1026	1298	330.4	208	****	9,10-Anthraquinone
96	1026	1194	330.4	212	*	C ₂ -alkyl-184PASH
98	1043	1220	332.2	206	*	C ₂ -alkyl-phenanthrene/anthracene
101	1064	1260	334.3	212	*	C ₂ -alkyl-184PASH
102	1070	1239	334.9	206	*	C ₂ -alkyl-phenanthrene/anthracene
103	1085	1256	336.5	206	**	C ₂ -alkyl-phenanthrene/anthracene
105	1091	1266	337.1	206	*	C ₂ -alkyl-phenanthrene/anthracene
107	1105	1293	338.5	206	*	C ₂ -alkyl-phenanthrene/anthracene
108	1113	1299	339.3	206	***	C ₂ -alkyl-phenanthrene/anthracene
110	1119	1353	339.9	204	**	Methyl-190PAH
111	1121	1305	340.1	206	**	C ₂ -alkyl-phenanthrene/anthracene
113	1128		340.9	256	**	Sulfur (S8)
114	1130	1326	341.1	206	**	C ₂ -alkyl-phenanthrene/anthracene
115	1134	1407	341.5	204	**	204PAK
116	1141	1343	342.2	206	*	C ₂ -alkyl-phenanthrene/anthracene
117	1151	1370	343.2	206	*	C ₂ -alkyl-phenanthrene/anthracene
118	1158	1395	343.9	202	*****	Fluoranthene
119	1161	1413	344.2	222	*	Methyl-anthraquinone
121	1164	1401	344.5	206	*	C ₂ -alkyl-phenanthrene/anthracene
122	1177	1375	345.9	218	**	218PAOH
123	1184	1480	346.6	206	*	C ₂ -alkyl-phenanthrene/anthracene
124	1188	1483	347.0	206	*	C ₂ -alkyl-phenanthrene/anthracene
126	1190	1388	347.2	218	*	218PAOH
128	1203	1478	348.5	208	***	Phenanthro[4,5-bcd]thiophene
132	1219	1480	350.2	222	**	Methyl-anthraquinone
134	1231	1498	351.4	202	*****	Pyrene
136	1236	1487	351.9	204	***	Methyl-190PAH
137	1236	1456	351.9	218	****	218PAOH
140	1258	1497	354.2	218	***	218PAOH
143	1278		356.3	220	*	C ₃ -alkyl-phenanthrene/anthracene
144	1279	1509	356.4	218	***	218PAOH
148	1312	1557	359.8	218	**	218PAOH
149	1320	1541	360.7	216	**	Benzofluorene or methyl-202PAH
150	1320	1541	360.7	216	**	Benzofluorene or methyl-202PAH

Table 1 (continued). A Portion of the Data Set Produced by the Parallel Column GC-MS Analysis of the PAC Fraction of the MACSP Marine Sediment Reference Material (HS-3)

Cmpd No.	Scan Number		RI SPB-5	Mol. Wt.	Relative Conc'n	Tentative Identity
	SPB-5	SPB-608				
151	1322	1543	360.9	230	*	Methyl-216PAH or C ₂ -alkyl-202PAH
155	1351	1594	363.9	216	***	Benzofluorene or methyl-202PAH
159	1359	1603	364.7	216	****	Benzofluorene or methyl-202PAH
160	1361	1557	365.0	232	**	Methyl-218PAOH
162	1383	1624	367.3	216	***	Benzofluorene or methyl-202PAH
166	1392	1640	368.2	216	***	Benzofluorene or methyl-202PAH
168	1403	1662	369.4	218	*	218PAOH
170	1405	1610	369.6	232	**	Methyl-218PAOH
171	1418	1662	371.0	218	*	218PAOH
172	1424	1685	371.6	216	***	Benzofluorene or methyl-202PAH
173	1425	1638	371.7	232	**	Methyl-218PAOH
174	1435	1695	372.8	216	**	Benzofluorene or methyl-202PAH
175	1449	1658	374.3	232	*	Methyl-218PAOH
184	1520	1779	381.9	230	*	Benzofluorenone
190	1547	1831	384.9	230	***	Benzofluorenone
194	1573	1870	387.7	230	*	Methyl-216PAH or C ₂ -alkyl-202PAH
195	1580	1858	388.5	234	***	234PASH
197	1588	1882	389.4	230	**	Methyl-216PAH or C ₂ -alkyl-202PAH
199	1595	1877	390.1	226	***	Benzo[ghij]fluoranthene
200	1595	1885	390.1	228	***	Benzo[c]phenanthrene
201	1608	1895	391.6	229	**	Benzo[c]acridine
205	1622	1916	393.1	230	***	Benzofluorenone
207	1639	1925	395.0	234	**	234PASH
208	1669	1947	398.4	228	****	Benzo[a]anthracene
211	1682	2007	399.9	217	**	Benzo[a]carbazole
212	1683	1977	400.0	228	*****	Chrysene and triphenylene
215	1699	1964	401.8	242	*	Methyl-228PAH
219	1708	2006	402.8	228	**	Naphthacene
222	1725	2067	404.8	230	*	Methyl-216PAH or C ₂ -alkyl-202PAH
224	1747	2035	407.3	242	**	Methyl-228PAH
227	1764	1827	409.3	?	***	Dialkyl-phthalate
235	1800	2061	413.5	242	*	Methyl-228PAH
236	1808	2063	414.4	242	*	Methyl-228PAH
237	1822	2089	416.1	242	**	Methyl-228PAH
238	1836	2114	417.7	242	**	Methyl-228PAH
241	1851	2135	419.5	242	*	Methyl-228PAH
244	1862	2138	420.8	254	*	Phenyl-178PAH or binaphthyl
249	1870	2156	421.7	242	*	Methyl-228PAH
255	1904	2190	425.7	254	*	Phenyl-178PAH or binaphthyl
272	2044	2350	442.3	252	***	Benzo[j]fluoranthene
273	2045	2355	442.4	252	***	Benzo[b]fluoranthene
274	2046	2371	442.4	252	**	Benzo[k]fluoranthene
280	2074	2368	445.8	268	*	268PAOH
281	2075	2401	445.9	252	**	252PAH
284	2109	2424	449.9	268	*	268PAOH
286	2125	2496	451.7	252	***	Benzo[e]pyrene
290	2140	2518	453.4	252	***	Benzo[a]pyrene
293	2165	2570	456.3	252	**	Perylene
297	2184	2499	458.5	266	*	Methyl-252PAH
303	2220	2526	462.5	266	*	Methyl-252PAH
304	2228	2574	463.4	266	*	Methyl-252PAH
306	2252	2613	466.1	266	*	Methyl-252PAH
331	2466	3053	489.8	276	*	276PAH
332	2466	3034	489.8	278	*	278PAH

Table 1 (continued). A Portion of the Data Set Produced by the Parallel Column GC-MS Analysis of the PAC Fraction of the MACSP Marine Sediment Reference Material (HS-3)

Cmpd No.	Scan Number		RI SPB-5	Mol. Wt.	Relative Conc'n	Tentative Identity
	SPB-5	SPB-608				
335	2500	3122	493.5	276	**	Indeno[123-cd]pyrene
336	2509	3136	494.4	278	*	Dibenz[a,h]anthracene
339	2545	3234	498.4	278	*	Benzo[b]chrysene
340	2560	3281	500.0	278	*	Picene
343	2592	3359	501.2	276	**	Benzo[ghi]perylene

Note: Only the most abundant compounds detected with the SPB-5 and SPB-608 columns are presented here. A total of 357 compounds were detected. The relative concentrations are indicated on an exponential scale (the concentrations of the certified compounds range from 1.3 µg/g for dibenz[a,h]anthracene to 85 µg/g for phenanthrene).

CONCLUSIONS

The application of parallel column GC-MS and the semiautomated peak detection routine to the analysis of environmental samples results in substantial improvements in the detection and identification of individual PACs. In principle this approach can be extended to any chromatographic method coupled to a multidimensional detector. For example, the unique selectivity of HPLC can be utilized to help resolve compounds not separable by GC. Although the HPLC-UVD chromatogram of the marine sediment PAC presented in Figure 2 was very complicated, the *m/z* 252 chromatograms generated from GC-MS and LC-MS analyses (see Figure 9) show the power of LC-MS in resolving isomers that cannot be completely separated using GC-MS. Parallel column chromatography can therefore be accomplished very well by a combination of GC-MS and LC-MS data sets since the two techniques produce complementary information.

ACKNOWLEDGMENTS

The authors gratefully acknowledge funding from the Ontario Ministry of the Environment, the Natural Sciences and Engineering Research Council, and the National Research Council of Canada (contract #09SC.31028-4-5320Y).

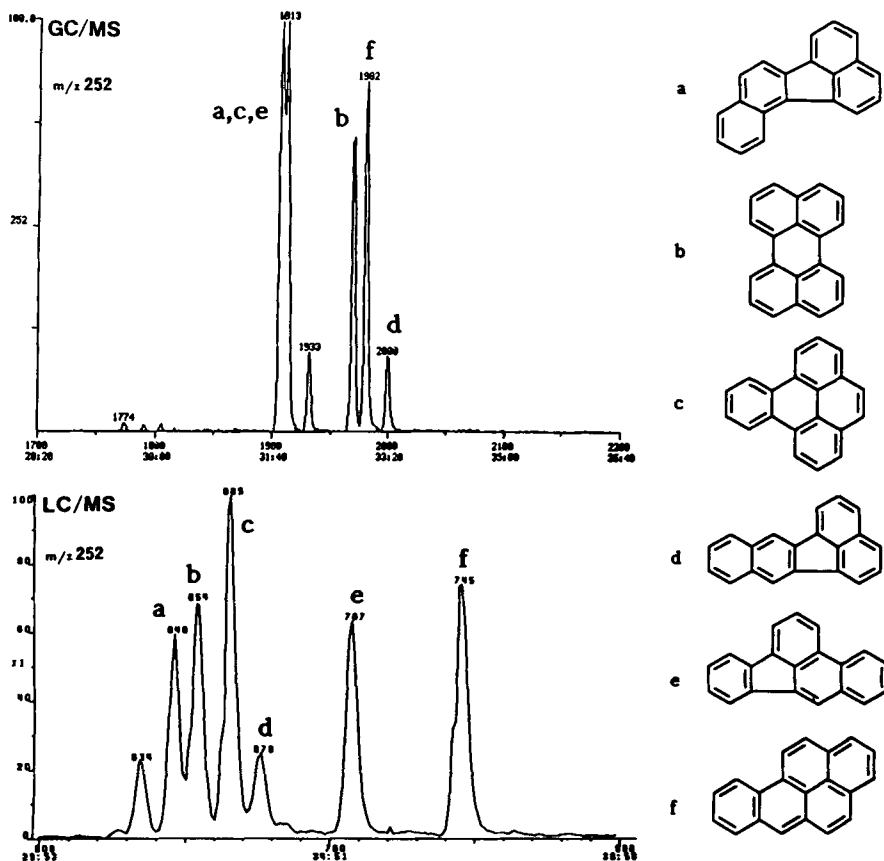


Figure 9. A comparison of the GC-MS and HPLC-MS m/z 252 mass chromatograms produced for the marine sediment reference material PAC fraction (see Figure 2 for the corresponding GC-FID and HPLC-UVD chromatograms). These traces show that HPLC gave superior separation selectivity for the isomeric PAH of molecular weight 252.

REFERENCES

1. Lee, M. L., M. V. Novotny, and K. D. Bartle. *Analytical Chemistry of Polycyclic Aromatic Compounds* (New York: Academic Press, 1981).
2. Chrisp, C. E., and G. L. Fisher. "Mutagenicity of Airborne Particles," *Mutat. Res.* 76:143—164 (1980).
3. Dehnen, W., N. Pitz, and R. Tomingas. "The Mutagenicity of Airborne Particulate Pollutants," *Cancer Lett.* 4:5—12 (1977).
4. May, W. E., and S. A. Wise. "Liquid Chromatographic Determination of Polycyclic Aromatic Hydrocarbons in Air Particulate Extracts," *Anal. Chem.* 56:225—232 (1984).
5. Wise, S. A., B. A. Benner, S. N. Chesler, L. R. Hilpert, C. R. Vogt, and W. E. May. "Characterization of the Polycyclic Aromatic Hydrocarbons from Two Standard Reference Material Air Particulate Samples," *Anal. Chem.* 58:3067—3077 (1986).

6. Yergy, A. L., C. G. Edmonds, I. A. S. Lewis, and M. L. Vestal. *Liquid Chromatography/Mass Spectrometry: Techniques and Applications* (New York: Plenum Press, 1990).
7. Sim, P. G., R. K. Boyd, R. M. Gershey, R. Guevremont, W. D. Jamieson, M. A. Quilliam, and R. J. Gergely. "A Comparison of Chromatographic and Chromatographic/Mass Spectrometric Techniques for the Determination of Polycyclic Aromatic Hydrocarbons in Marine Sediments," *Biomed. Environ. Mass Spectrom.* 14:375—381 (1987).
8. Davis, J. M., and J. C. Giddings. "Statistical Theory of Component Overlap in Multicomponent Chromatograms," *Anal. Chem.* 55:418—424 (1983).
9. Quilliam, M. A., and P. G. Sim. "Determination of Polycyclic Aromatic Compounds by High Performance Liquid Chromatography with Simultaneous Mass Spectrometry and Ultraviolet Diode Array Detection," *J. Chromatogr. Sci.* 26:160—167 (1988).
10. Lao, R. C., R. S. Thomas, and J. L. Monkman. "Computerized Gas Chromatographic-Mass Spectrometric Analysis of Polycyclic Aromatic Hydrocarbons in Environmental Samples," *J. Chromatogr.* 112:681—700 (1975).
11. Schuetzle, D., F. S.-C. Lee, T. J. Prater, and S. B. Tejada. "The Identification of Polynuclear Aromatic Hydrocarbon (PAH) Derivatives in Mutagenic Fractions of Diesel Particulate Extracts," *Intern. J. Environ. Anal. Chem.* 9:93—144 (1981).
12. Bertsch, W. "Methods in High Resolution Gas Chromatography. Two-Dimensional Techniques," *J. High Res. Chromatogr.* 1:85—90 (1978).
13. Ramdahl, Th. "Polycyclic Aromatic Ketones in Environmental Samples," *Environ. Sci. Technol.* 17:666—670 (1983).
14. Pierce, R. C., and M. Katz. "Chromatographic Isolation and Spectral Analysis of Polycyclic Quinones: Application to Air Pollution Analysis," *Environ. Sci. Technol.* 10:45—51 (1976).
15. D'Agostino, P. A. "The Analysis of Nitro Polycyclic Aromatic Hydrocarbons in Diesel Exhaust and Urban Airborne Particulate Samples," PhD Thesis, McMaster University, Hamilton, Canada (1983).
16. D'Agostino, P. A., D. R. Narine, B. E. McCarry, and M. A. Quilliam. "Cleanup and Analysis of Nitrated Polycyclic Aromatic Hydrocarbons in Environmental Samples," in *Polynuclear Aromatic Hydrocarbons: Formation, Metabolism and Measurement*, M. Cooke and A. J. Dennis, Eds. (Columbus, OH: Batelle Press, 1983), pp. 365—377.
17. Ligon, W. V., and R. J. May. "Target Compound Analysis by Two-Dimensional Gas Chromatography-Mass Spectrometry," *J. Chromatogr.* 294:77—86 (1984).
18. Sevcik, J. "Application of a Multi-Dimensional Switching System (MDSS) to Coal Tar Analysis," *J. High Res. Chromatogr.* 3:25—27 (1980).
19. Kugler, E., Halang, R. Schlenkermann, H. Webel, and R. Langlais. "Simultaneous Three-Dimensional Gas-Liquid Chromatography on Wall-Coated Glass-Capillary Columns," *Chromatogr.* 18:438—443 (1977).
20. Scott, B. F., and F. I. Onuska. "Analysis for Polychlorinated Biphenyls by Dual Capillary Column Gas Chromatography," *J. Microcolumn Separations* 1:119—124 (1989).
21. Lefevre, M. F., B. J. Verhaeghe, D. M. Declerck, and A. P. De Leenheer. "Automated Profiling of Urinary Organic Acids by Dual-Column Gas Chromatography and Gas Chromatography/Mass Spectrometry," *Biomed. Environ. Mass Spectrom.* 15:311—322 (1988).

22. Marr, J. C. "The Analysis of Polycyclic Aromatic Compounds in Urban Airborne Particulate Samples," Ph.D. thesis, McMaster University, Hamilton, Canada (1989).
23. Ramos, L. S., J. E. Burger, and B. R. Kowalski. "Third-Order Chromatography: Multivariate Analysis of Data from Parallel-Columns with Multichannel Detection," *Anal. Chem.* 57:2620—2625 (1985).
24. Biller, J. E., and K. Biemann. "Reconstructed Mass Spectra: A Novel Approach for the Utilization of Gas Chromatograph-Mass Spectrometer Data," *Anal. Lett.* 7:515—528 (1974).
25. Lee, M. L., D. L. Vassilaros, C. White, and M. Novotny. "Retention Indices for Programmed-Temperature Capillary-Column Gas Chromatography of Polycyclic Aromatic Hydrocarbons," *Anal. Chem.* 51:768—773 (1979).
26. Vassilaros, D. L., R. C. Kong, D. W. Later, and M. L. Lee. "Linear Retention Index System for Polycyclic Aromatic Compounds: Critical Evaluation and Additional Indices," *J. Chromatogr.* 252:1—20 (1982).
27. Campbell, R. M., and M. L. Lee. "Capillary Column Gas Chromatographic Determination of Nitro Polycyclic Aromatic Compounds in Particulate Extracts," *Anal. Chem.* 56:1026—1030 (1984).
28. Willey, C., M. Iwao, R. N. Castle, and M. L. Lee. "Determination of Sulfur Heterocycles in Coal Liquids and Shale Oils," *Anal. Chem.* 53:400—407 (1981).
29. Konig, J., E. Balfanz, W. Funcke, and T. Romanowski. "Determination of Oxygenated Polycyclic Aromatic Hydrocarbons in Airborne Particulate Matter by Capillary Gas Chromatography and Gas Chromatography/Mass Spectrometry," *Anal. Chem.* 55:599—603 (1983).
30. Korhonen, I. O. O., and M. A. Lind. "Gas-Liquid Chromatographic Analyses. XXXIV. Separation and Retention Indices with Retention Increments of Some Nitrated Polynuclear Aromatic Hydrocarbons on a Low-Polarity (SE-30) Capillary Column," *J. Chromatogr.* 322:71—81 (1985).
31. Rostad, C. E., and W. E. Pereira. "Kovats and Lee Retention Indices Determined by Gas Chromatography/Mass Spectrometry for Organic Compounds of Environmental Interest," *J. High Res. Chromatogr.* 9:328—334 (1986).
32. Schmid, E. R., G. Bachlecher, K. Varmuza, and H. Klus. "Determination of Polycyclic Aromatic Hydrocarbons, Polycyclic Aromatic Sulfur and Oxygen Heterocycles in Cigarette Smoke Condensate," *Fres. Z. Anal. Chem.* 322:213—219 (1985).
33. Ramdahl, Th., J. Arey, B. Zielinska, R. Atkinson, and A. M. Winer. "Analysis of Dinitrofluoranthenes by High Resolution Capillary Gas Chromatography/Mass Spectrometry," *J. High Res. Chromatogr.* 9:515—517 (1986).
34. Tuominen, J., K. Wickstrom, and H. Pyysalo. "Determination of Polycyclic Aromatic Compounds by GLC-Selected Ion Monitoring (SIM) Technique," *J. High Res. Chromatogr.* 9:469—471 (1986).

CHAPTER 12

Current Status of Hyphenated Fourier Transform Infrared Techniques

Donald F. Gurka

INTRODUCTION

The term “hyphenated techniques” was coined by the late Tomas Hirschfeld within a classic review article.¹ These techniques can be as simple as a gas chromatograph linked to a mass spectrometer (GC/MS) or as complicated as a gas chromatograph linked to a Fourier transform infrared (FT-IR) and a mass spectrometer (GC/FT-IR/MS).²

Currently, the Environmental Protection Agency monitors a few hundred extractable, GC-volatile organic compounds by GC/MS (target approach). This approach characterizes only a small subset of volatile organics, uses quadrupole GC/MS alone, and is dependent on the availability of authentic standards for GC retention time confirmation, quantitation, and user-created reference spectra (quadrupole mass spectra are not easily reproducible from spectrometer to spectrometer). In light of the 9×10^6 chemicals currently registered under the Chemical Abstract

Service³ and the estimated yearly increase in this number of about 4×10^5 ,⁴ it is easily realized that new approaches to environmental organic monitoring are badly needed.

The Need for Fourier Transform Infrared Techniques

Gas chromatography/Fourier transform infrared spectrometry (GC/FT-IR) has been shown to be a viable alternative, or a supplementary technique, to GC/MS for environmental analysis.^{5,6} The isomer discrimination and functional group capability of this technique provide useful information which is not easily obtained from the GC/MS method. Until recently, the GC/FT-IR technique did not have the sensitivity to monitor weak infrared absorbers at the low nanogram range, but newer FT-IR systems have been described which can identify the very weakly absorbing polynuclear aromatics (PAHs) at the 25—50 ng level,⁷ thereby ensuring the capability to routinely monitor most environmental contaminants at the low nanogram level. Figure 1 shows a prototype GC/FT-IR, exhibiting low nanogram sensitivities, which was built for the Environmental Monitoring Systems Laboratory at Las Vegas (EMSL-LV) by the University of California at Riverside.⁸ Figure 2 shows the FT-IR spectra of low nanogram quantities of four environmental priority pollutants measured on a 1987 vintage, commercially available GC/FT-IR system with sensitivity comparable to that of the prototype. Evaluation of the qualitative capabilities of GC/FT-IR have taken precedence over quantitative studies, but recent work indicates quantitative precision comparable to that of total ion chromatogram GC/MS.^{9,10} Further work on the applicability of the infrared absorption coefficient approach to on-the-fly GC/FT-IR is required to determine its feasibility for environmental monitoring. Work dedicated to this end is being funded by the EMSL-LV and is being carried out at the University of California at Riverside.¹¹ Preliminary results indicate the capability to quantitate to within $\pm 25\%$ of the true concentration even when a reference spectrum of the unknown compound is not available.¹² Such a "semiquantitation" approach, used in conjunction with FT-IR group frequencies, could be the basis of a broad screening approach to environmental monitoring.⁸

Directly Linked GC/FT-IR/MS

Although GC/FT-IR is a particularly powerful tool when used alone, it is even more powerful when linked to a mass spectrometer to create the technique known as GC/FT-IR/MS. A diagram of a prototype system is shown in Figure 3. Although the FT-IR component of this prototype was relatively insensitive (about 800 ng of PAH required for identification), the system provided confirmed qualitative information (identification or compound class) on 41% of the jointly detected analytes found in six real environmental samples.¹³ The improved sensitivity of the newer infrared systems should greatly enhance the performance of such a linked system.

Commercially available linked systems were displayed by two companies at the 1987 Pittsburgh Conference.¹⁴ In principle, these linked systems offer the following

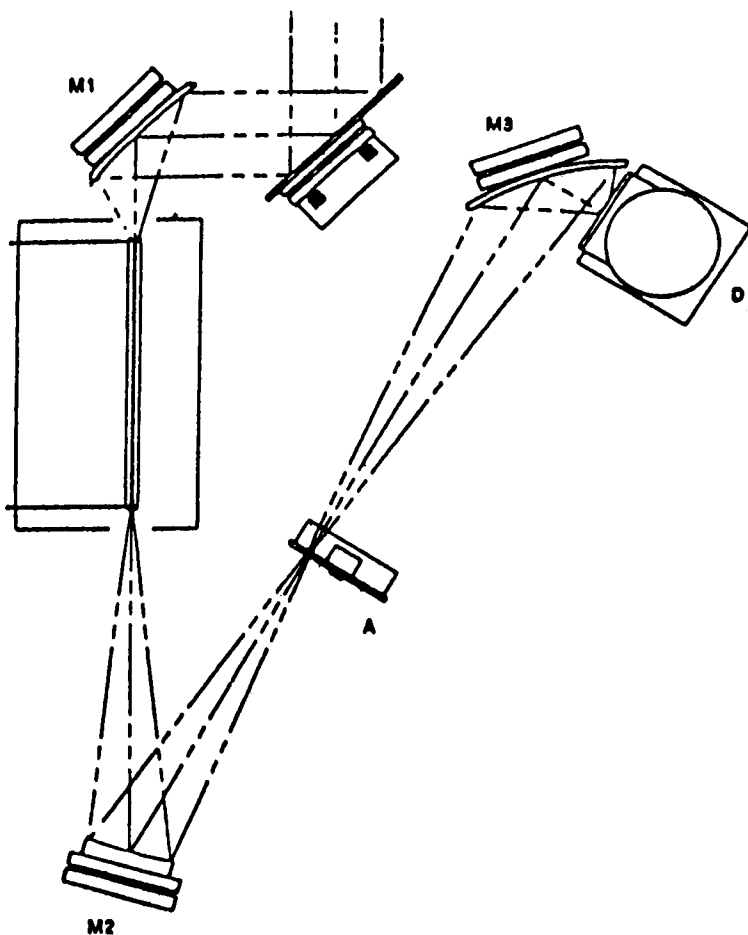


Figure 1. Prototype GC/FT-IR interface which utilizes a small focal area detector and which minimizes the lightpipe "blackbody" sensitivity effect. (From Gurka, D. F., R. Titus, P. R. Griffiths, D. E. Henry, and A. Giorgetti. *Anal. Chem.* 59:2362 [1987]. With permission.)

advantages for environmental analysis when minimizing the need for authentic standards by:

1. Using FT-IR to confirm quadrupole mass spectrometry instead of the standard GC retention time approach.
2. Using FT-IR to decrease the uncertainties associated with quadrupole-to-quadrupole spectral transferability (quadrupole GC/MS environmental analysis is invariably carried out with a user-created library).
3. Using FT-IR absorption coefficients to minimize the need for quantitation standards.

Table 1 shows the historical relationship, to date, between FT-IR and MS relative sensitivities.

Matrix Isolation Fourier Transform Infrared Spectrometry

Unlike the lightpipe GC/FT-IR technique which is on the fly, the newer technique of matrix isolation/gas chromatography Fourier transform infrared (MI/GC/FT-IR) utilizes a static GC eluate which is trapped in a frozen matrix of argon, on a rotating gold disk, at 12 K.¹⁵ The argon strip is about 100- μm wide, presenting a highly concentrated analyte to the FT-IR sample beam. This high concentration, in conjunction with the signal averaging obtainable with a static sample, permits sensitivities approaching that of GC/MS. See Figure 4 for the infrared spectrum of 1,2,3,4-tetrachlorodibenzodioxin (30-min signal averaging). Because the spectrometer optics are oriented away from the gold collection disk, FT-IR data cannot be collected in real time and a GC split to a flame ionization detector must be employed. Table 2 shows a comparison of the lightpipe and MI/GC/FT-IR techniques. The lightpipe technique has the advantage of higher sample throughput and analyte spectra which tend to look like the reference spectra regardless of lightpipe concentrations. The MI/GC/FT-IR approach is more sensitive than the lightpipe approach, but produces spectra which may be concentration dependent, especially for protic compounds.¹⁶ Thus, the analyte spectrum may not look like the reference spectrum, if the two are measured at different concentrations, presenting a real problem for environmental unknowns. However, if the analyte concentrations are known *before* MI/GC/FT-IR analysis, the appropriate extract dilutions can be made.

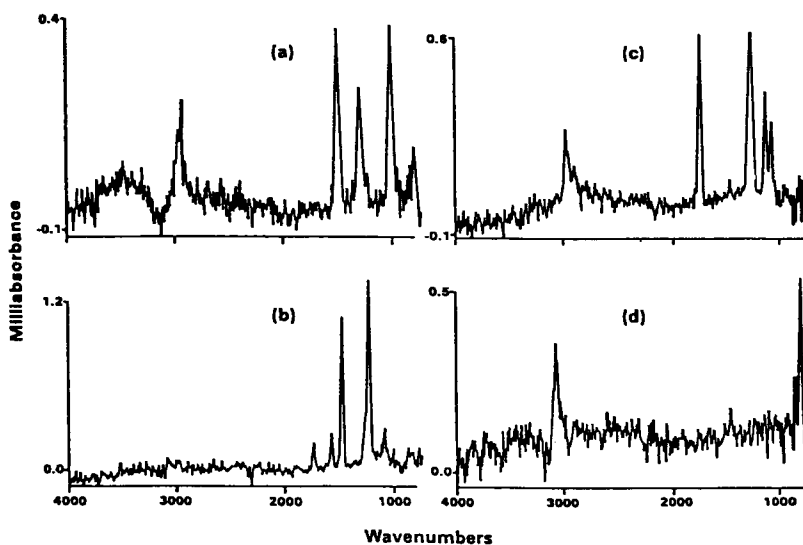


Figure 2. GC/FT-IR spectra of (a) 5 ng of *N*-nitrosodimethylamine, (b) 5 ng of 4-chlorophenyl phenyl ether, (c) 5 ng of di-*n*-butyl phthalate, and (d) 25 ng of phenanthrene. (From Gurka, D. F., and S. M. Pyle. *Environ. Sci. Technol.* 22:913 [1988]. With permission.)

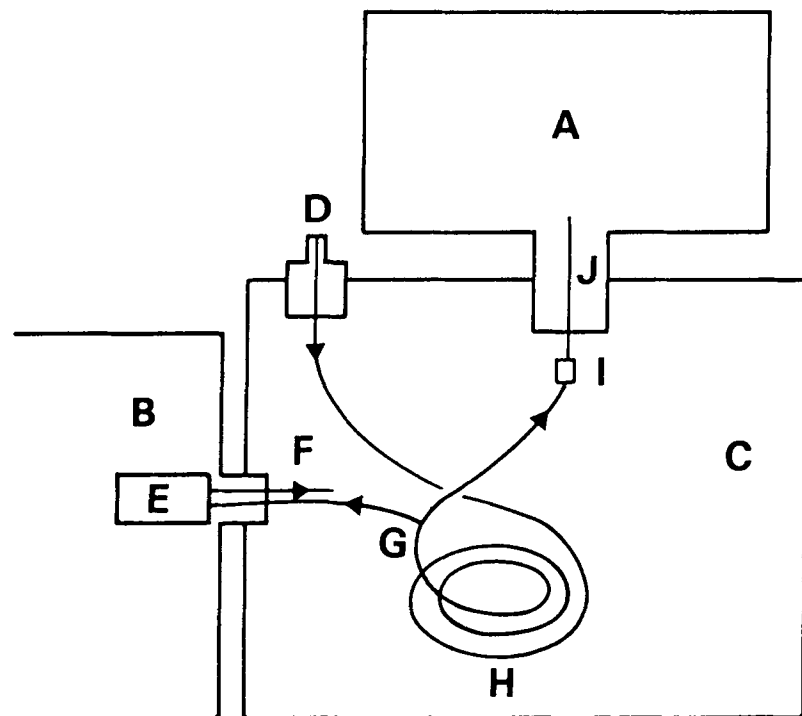


Figure 3. GC/FT-IR/MS interface: (a) MSD, (b) FT-IR interface, (c) GC oven, (d) on-column injector, (e) light pipe assembly, (f) effluent vent, (g) splitter, (h) 30 m \times 0.32 mm DB5 column, (i) 0.3 m \times 0.23 mm DB5 coated line, (j) MSD interface. (From Gurka, D. F., and R. Titus. *Anal. Chem.* 58:2189 [1986]. With permission.)

Griffiths has designed a cryotrapping interface which is more economical than MI/GC/FT-IR, produces almost real-time spectra and operates at liquid nitrogen temperatures.¹⁷ See Figure 5 for a schematic of this interface which has been described as producing spectra which are qualitatively similar to KBr spectra and thus not requiring a new reference database. Utilizing a nonspectral interface, in conjunction with supercritical fluid (SCF) and GC chromatography, Griffiths has succeeded in chromatographing the GC-volatile and nonvolatile fraction of a 2,4,5-T stillbottom extract, with a single injection (see Figure 6 for the combined SCF, GC chromatogram). Figure 7 shows the SCF/FT-IR spectrum of indole acetic acid, a nonvolatile compound, measured on the FT-IR interface.

Table 1. Progress in Improving the Relative Sensitivity of Lightpipe GC/FT-IR to that of Full Scan Quadrupole GC/MS^a

Interface Type and MCT Detector Wavenumber Cutoff	Relative Response Factor Range (MS/FT-IR)	Ref.
1982 Commercial capillary (700/cm)	40 ^a —440 ^b	6
1986 Prototype capillary (700/cm)	3—34	8
1987 Commercial capillary (750/cm)	1—11	9

Note: Based on a full scan. GC/MS minimum identifiable quantity (MIQ) of 5 ng of phenanthrene (50 to 400 amu).

^a Strong infrared absorber (i.e., nitro compound).

^b Weak infrared absorber (i.e., PAH).

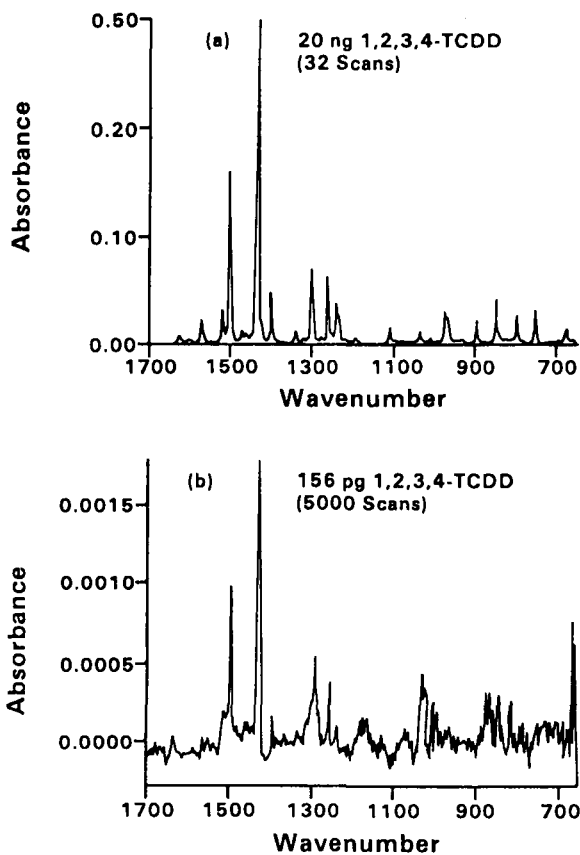


Figure 4. MI/GC/FT-IR spectrum of 156 pg of 1,2,3,4-tetrachlorodibenzodioxin with about 30 min of signal averaging. (From Wurrey, C. J., *Appl. Spectroscopy*, 42:359 [1988]. With permission.)

Table 2. Comparison of Lightpipe and Matrix Isolation GC/FT-IR

Parameter	Lightpipe/GC/FT-IR	Matrix Isolation/GC/FT-IR ^a
Sample throughput	Real time	Post run, limited by gold collection disk
Reference data-base	9000	3000 spectra. May be dependent on analyte/matrix concentration
Sensitivity	5—25 ng on the fly	Picogram with extensive signal averaging; nanogram without extensive signal averaging

^a Each of these parameters can lower sample throughput.

Computer Software for Hyphenated FT-IR Techniques

Although sophisticated computer software is available to process GC/MS data (e.g., the probability-based matching algorithm¹⁸ and GC/FT-IR data [GIFTS]¹⁹), no commercial software is currently available to process the data generated by a directly linked GC/FT-IR/MS system. Wilkins has described a preliminary version of such software,²⁰ but much remains to be accomplished if linked GC/FT-IR/MS is to become a routine environmental monitoring tool. This work includes the optimization of reference spectral databases (separate volatile and nonvolatile compound spectra), eliminate spectra of research chemicals (over 80% of CIS-NIH-NBS mass spectra), add relevant new reference spectra from the FT-IR, MS community, investigate the utilization of nuclear magnetic resonance data in conjunction with GC/FT-IR/MS spectra, and finally to pursue prediction of molecular structure from spectral data.²¹ Research is currently being funded to pursue each of these research goals.²²

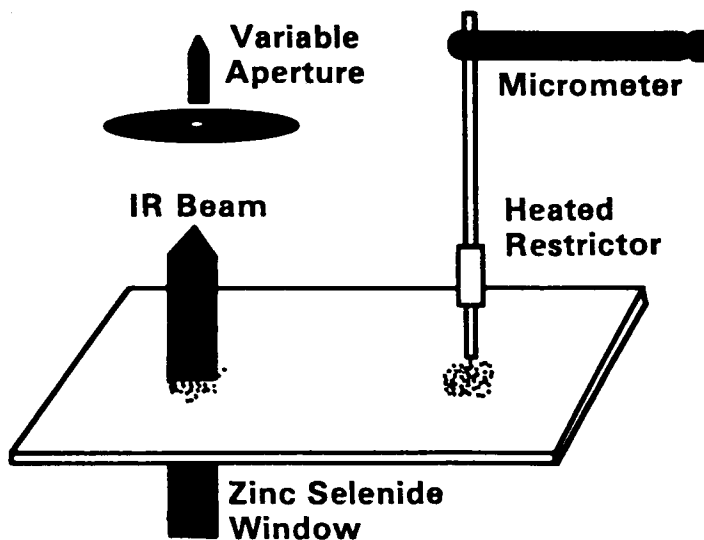


Figure 5. Diagram of FT-IR cryo-trapping interface designed by Peter Griffiths under Cooperative Agreement CR-812258 to the U.S. EPA's Environmental Monitoring Systems Laboratory at Las Vegas.

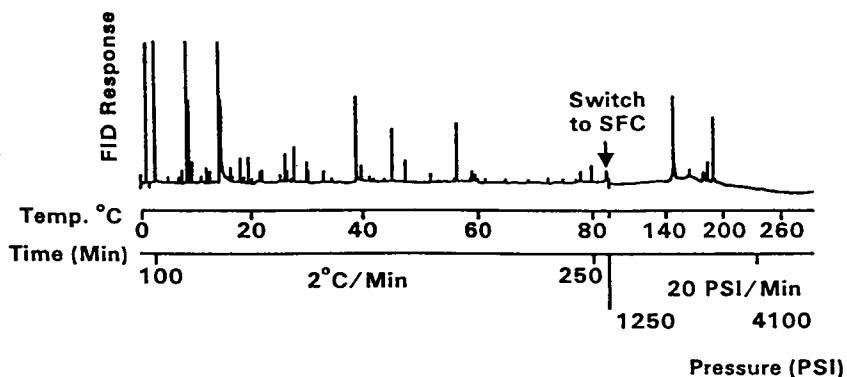


Figure 6. Combined GC, SCF chromatogram of a 2,4,5-T herbicide still bottom extract (From U.S. EPA Cooperative Agreement CR-812258).

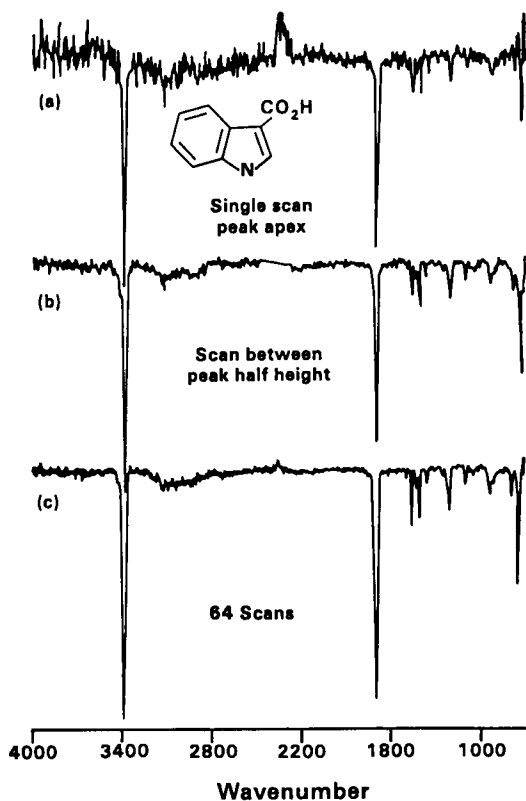


Figure 7. SCF/FT-IR spectrum of indole acetic acid measured on the cryo-trapping interface (From U.S. EPA Cooperative Agreement CR-812258).

Table 3. Current Status of the Private Sector

Company	Hyphenated FT-IR System	Ref.
Hewlett-Packard	GC/FT-IR (IRD) with sensitivity 5—25 ng Developing GC/FT-IR/MS software using STIRS and ca. 800 GC/IR group frequencies	27,28
Mattson-Hewlett Packard	Marketing GC/MI-FT-IR/MSD system	14
Nicolet	Marketing flow-cell SCF/FT-IR: nonvolatile applica- tions	29
Digilab	Cryotrapping GC/FT-IR system with sensitivity 0.5 pg to 1 ng	30

Status of the Private Sector

Table 3 shows the current status of commercially marketed, hyphenated FT-IR instrumentation. It can be seen that linked GC/FT-IR/MSD is close to becoming a realized, environmental monitoring tool. Lacking, but being actively pursued, is the computer software required to provide an integrated linked system. Such an integrated system provided the impetus for the EPA's acceptance of quadrupole GC/MS systems in the late 1970s.²³

The situation for hyphenated FT-IR systems capable of determining nonvolatile organics is worse than that for GC-volatiles. However, some progress is underway within the private sector, indicating that a potential market for such systems is perceived.

Future Horizons

Future hyphenated FT-IR commercialization possibilities include FT-IR linked with a single separation device (HPLC/FT-IR, SCF/FT-IR), multiseparation systems (GC/HPLC/FT-IR, GC/SCF/FT-IR), and separation devices linked to several detectors (HPLC/FT-IR/MS, SCF/FT-IR/MS). Very little has been achieved with linking FT-IR systems to detectors other than mass spectrometers. Preliminary results on GC and HPLC/NMR look promising,^{24,25} but NMR/FT-IR combinations have yet to be reported. Apparently, the private sector does not yet envision a viable market for hyphenated NMR systems.

Another system with far-reaching analytical potential is helium plasma elemental analysis coupled to FT-IR. Such a system would provide element-specific and empirical formula data to supplement the functional group and isomeric specific information obtainable from GC/FT-IR. These plasma systems have been the subject of much recent research,²⁶ and new systems are expected to reach the commercial market very soon. Figure 8 shows the plasma elemental and FT-IR chromatograms of an environmentally contaminated soil sample.

In conclusion, the field of hyphenated FT-IR instrumentation is a fertile field which is likely to expand to the mutual benefit of the environment and the private sector. Decreases in capitalization costs associated with miniaturization and major improvements in computerization are expected to provide impetus to this expansion.

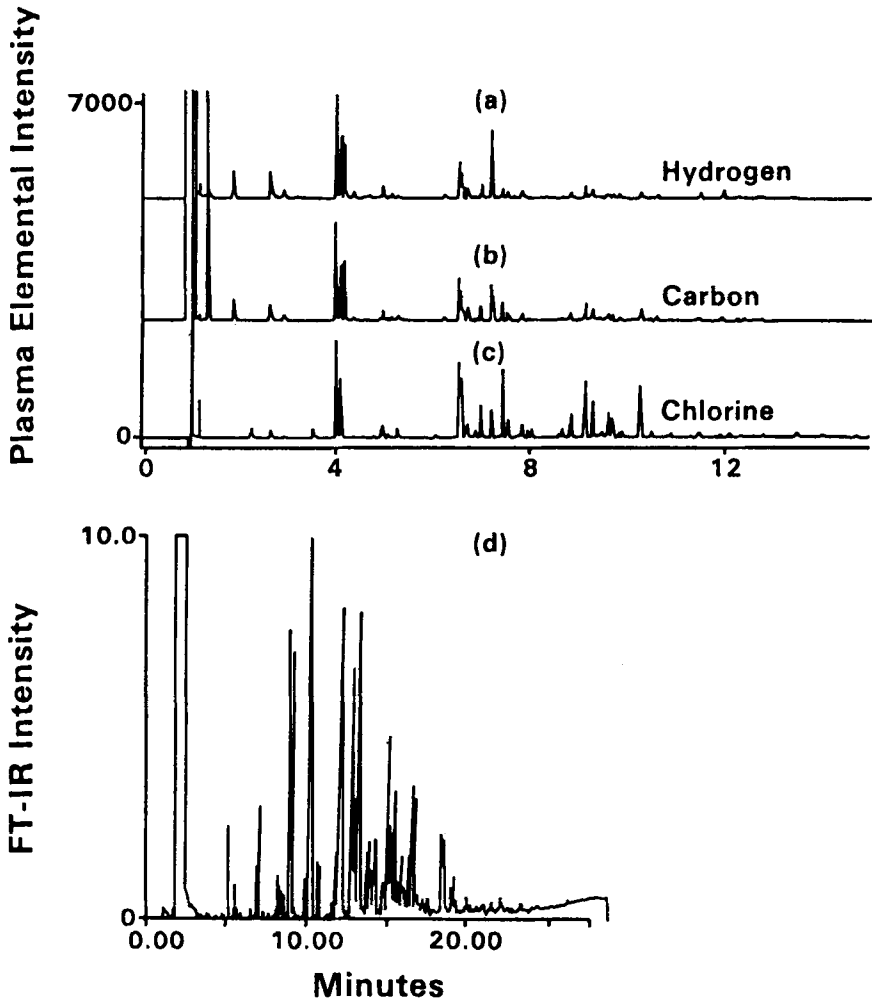


Figure 8. Plasma elemental intensity chromatograms for (a) hydrogen, (b) carbon, and (c) chlorine for a soil sample; (d) shows the FT-IR chromatogram for the same sample. (The author would like to thank Michael Wilson and Bruce Quimby of the Hewlett Packard Corporation, Avondale, PA, for the plasma chromatogram.)

ACKNOWLEDGMENT

Although the research described in this article has been funded wholly or in part by the United States Environmental Protection Agency, it has not been subjected to Agency review and therefore does not necessarily reflect the views of the Agency, and no official endorsement should be inferred. Mention of trade names or commercial products does not constitute endorsement or recommendation for use.

REFERENCES

1. Hirschfeld, T. "The Hyphenated Methods," *Anal. Chem.* 52:297A—312A (1980).
2. Wilkins, C. L. "Linked Gas Chromatography-Infrared-Mass Spectrometry," *Anal. Chem.* 59:571A—581A (1987).
3. *Opportunities in Chemistry* (Washington, D.C.: National Research Council, 1986), p. 4.
4. Arcos, J. C. "Structure Activity Relationships," *Environ. Sci. Technol.* 21:743—745 (1987).
5. Gurka, D. F., and L. D. Betowski. "Gas Chromatography/Fourier Transform/Infrared Spectrometric Identification of Hazardous Waste Extract Components," *Anal. Chem.* 54:1819—1824 (1982).
6. Gurka, D. F., M. Hiatt, and R. Titus. "Analysis of Hazardous Waste and Environmental Extracts by Capillary Gas Chromatography/Fourier Transform Infrared Spectrometry and Capillary Gas Chromatography/Mass Spectrometry," *Anal. Chem.* 56:1102—1110 (1984).
7. Henry, D. E., A. Giorgetti, A. M. Haefner, P. R., Griffiths, and D. F. Gurka. "Optimizing the Optical Configuration for Light-Pipe Gas Chromatography/Fourier Transform Infrared Spectrometry Interfaces," *Anal. Chem.* 59:2356/2361 (1987).
8. Gurka, D. F., R. Titus, P. R. Griffiths, D. E. Henry, and A. Giorgetti. "Evaluation of an Improved Single-Beam Gas Chromatography/Fourier Transform Infrared Interface for Environmental Analysis," *Anal. Chem.* 59:2362—2369 (1987).
9. Gurka, D. F., and S. M. Pyle. "Qualitative and Quantitative Environmental Analysis by Capillary Column Gas Chromatography/Fourier Transform Infrared Spectrometry," *Environ. Sci. Technol.* 22:963—968 (1988).
10. Gurka, D. F., I. Farnham, B. B. Potter, S. Pyle, R. Titus, and W. Duncan. "The Quantitation Capability of a Directly Linked Gas Chromatography/Fourier Transform Infrared/Mass Spectrometry System," *Anal. Chem.* 61:1584—1589 (1989).
11. Cooperative Agreements CR-811730 and CR-814909 between the U.S. Environmental Protection Agency's Environmental Monitoring Systems Laboratory at Las Vegas and the University of California at Riverside.
12. Haefner, A. M., and P. R. Griffiths. "Quantification of GC/FT-IR Without the Need for Identification," Abstract No. 076, presented at the 39th Pittsburgh Conference, New Orleans, LA, February 22, 1988.
13. Gurka, D. F., and R. Titus. "Rapid Screening of Environmental Extracts by Directly Linked Gas Chromatography/Fourier Transform Infrared/Mass Spectrometry," *Anal. Chem.* 58:2189—2194 (1986).
14. Borman, S. "Hyphenated MS at the Pittsburgh Conference," *Anal. Chem.* 59:769A—774A (1987).
15. Mamantov, G., A. A. Garrison, and E. L. Wehry. "Analytical Applications of Matrix Isolation Fourier Transform Infrared Spectrometry," *Appl. Spectrosc.* 36:339—347 (1982).
16. Coleman, W. M., III, and B. M. Gordon. "Examination of the Matrix Isolation Fourier Transform Infrared Spectra of Organic Compounds. X," *Appl. Spectrosc.* 42:671—674 (1988).
17. Fuocco, R., K. H. Shafer, and P. R. Griffiths. "Capillary Gas Chromatography/Fourier Transform Infrared Microspectrometry at Subambient Temperature," *Anal. Chem.* 3249—3254 (1986).

18. Pesyna, G. M., R. Venkatarghavan, H. E., Dayringer, and F. W. McLafferty. "Probability Based Matching System Using a Large Collection of Reference Mass Spectra," *Anal. Chem.* 48:1362—1368 (1976).
19. de Haseth, J. A., and T. L. Isenhour. "Reconstruction of Gas Chromatograms from Interferometric Gas Chromatography/Infrared Spectrometry Data," *Anal. Chem.* 49:1977—1981 (1977).
20. Cooper, J. R., I. C. Bowater, and C. L. Wilkins. "Gas Chromatography/Fourier Transform Infrared/Mass Spectrometry Using a Mass Selective Detector," *Anal. Chem.* 58:2791—2796 (1986).
21. Zupan, J., M. Penca, D. Hadzi, and J. Marsel. "Combined Retrieval System for Infrared, Mass, and Carbon-13 Nuclear Magnetic Resonance Spectra," *Anal. Chem.* 49:2141—2145 (1977).
22. Cooperative Agreement CR-814755-01 between the U.S. Environmental Protection Agency's Environmental Monitoring Systems Laboratory and the University of California at Riverside.
23. Gurka, D. F., L. D. Betowski, T. A. Hinnners, E. M. Heithmar, R. Titus, and J. M. Henshaw. "Environmental Applications of Hyphenated Quadrupole Techniques," *Anal. Chem.* 60:454A—465A (1988).
24. Buddrus, J., and H. Herzog. "Coupling of Chromatography and NMR," *Org. Magn. Res.* 15:211—213 (1981).
25. Laude, D. A., Jr., and C. L. Wilkins. "Reverse-Phase High Performance Liquid Chromatography/Nuclear Magnetic Resonance Spectrometry in Protonated Solvents," *Anal. Chem.* 59:546—551 (1987).
26. Uden, P. C. "Element-Selective Chromatographic Detection by Plasma Atomic Emission Spectroscopy," *Trends Anal. Chem.* 6:238—246 (1987).
27. Kwok, K. S., R. Venkatarghavan, and F. W. McLafferty. "Computer Aided Interpretation of Mass Spectra. III. A Self-Training Interpretative and Retrieval System," *J. Am. Chem. Soc.* 95:4185—4194 (1973).
28. James, J. Personal communication, Hewlett Packard Corp., Scientific Instruments Div., Palo Alto, CA (1987).
29. "Instrumentation '87," *Chem. Eng. News*, 54 (1987).
30. Griffiths, P. R. Personal communication, University of California at Riverside (1987).

CHAPTER 13

Solvent-Free Extraction of Environmental Samples

Janusz Pawliszyn

INTRODUCTION

The first step in organic analysis of environmental samples involves separating the components of interest from such matrices as soil, water, flyash, tissue, or other material. This process is achieved traditionally by using liquid extractions. For example, water samples are usually extracted with organic solvent. Similarly, solid samples are leached with an organic solvent in a Soxhlet apparatus. Methods based on solvent extraction are often time consuming, difficult to automate, and are very expensive since they require high purity organic solvents and waste disposal fees are high. In addition to the long extraction times and usually high toxicity of the organic liquids, extraction processes are highly nonselective. Therefore, sequential chromatographic techniques must very often be used to separate complex mixtures after extraction. This significantly increases the overall analysis time and cost.

In this chapter we discuss three new developments in the sample preparation methodology which eliminate use of organic solvents. One of them is a modification of the solid phase extraction (SPE) technique which uses chemically modified fused silica fibers in place of SPE cartridges. This approach is an attempt to simplify and shorten the procedures involving transfer of analytes from the aqueous samples directly into the injection port of a gas chromatograph. The other recent development which is discussed is analytical scale supercritical fluid extraction. This method is able to separate the components of interest from the solid matrix over an order of magnitude faster when compared to the Soxhlet method of extraction. Finally, a gas extraction technique based on the hollow fiber membranes is discussed. This technique facilitates removal of the volatile organics from aqueous samples and subsequent on-line chromatographic analysis.

The primary goal of this presentation is to discuss the principles and concepts behind these solvent-free techniques and instrumentation.

SOLID PHASE MICROEXTRACTION WITH FUSED SILICA FIBERS

The analytical procedures involving solid phase extraction employ disposable plastic cartridges packed with the material which is commonly used in HPLC columns. The operation of solid phase extraction consists of several steps. After the activation procedure and removal of excess organic solvent, the water matrix sample is passed through the cartridge. During this process the organic components are then adsorbed on the chemically modified silica surface. Both molecules of interest as well as interferences are retained. The desorption process is done "digitally." First, a selective solvent is chosen to remove interferences. Finally, using the appropriate elution condition, the analyte is washed out from the cartridge. From that point on, the analytical procedure is identical to that used in solvent extraction, which first calls for preconcentration of the analyte followed by the injection of the mixture into the appropriate high resolution chromatographic instrument.

The main advantages of the solid phase extraction approach over liquid-liquid extraction are speed, low cost, the ability to apply a variety of elution conditions to achieve the desired selectivity, and the concentration effect achieved with this technique.^{1,2} Small volumes of organic solvent are used in the washing and elution steps which significantly reduces the volume of waste. The rigid bonded silica material allows solvent of different polarities to be applied without the shrinking or swelling effects customary for resins. pH restrictions which apply to HPLC packings are not as strict in solid phase extraction due to the disposable nature of the cartridges. However, solid phase extractions often suffer from high blank values.^{3,4} In addition there is considerable variation between the products offered by different manufacturers and between the lots from the same source.

The most time-consuming step in analysis involving solid phase extraction is the desorption of the organic analyte and the sample transfer into the high resolution chromatographic instrument. Thermal desorption can replace this process, but current methods require extensive modification of the chromatographic injector or the

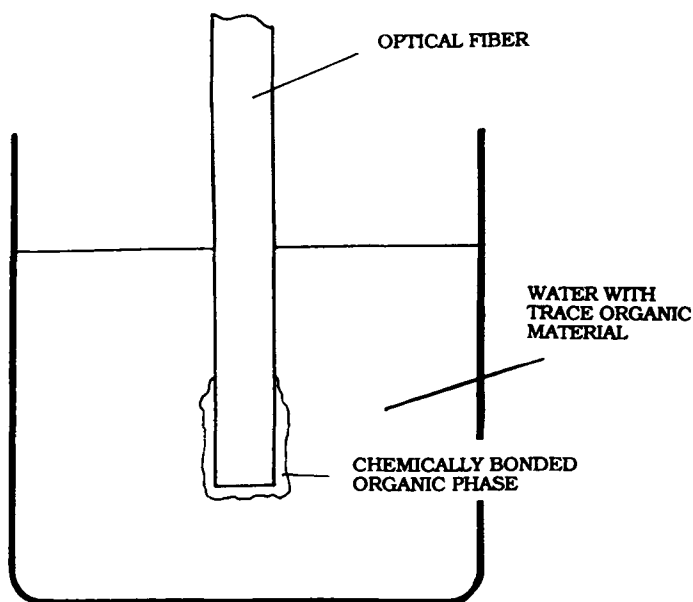


Figure 1. Solid phase microextraction method based on chemically modified fused silica fibers.

addition of the desorption module.^{5,6} These inconveniences are eliminated in the solid phase microextraction (SPME) technique based on chemically modified fused silica fibers.^{7,8} These fibers are widely used in optical communication and often referred to as optical fibers. Their diameters vary between 0.05 to 1 mm.

Chemical modification of these fibers is achieved by the preparation of the surface involving etching procedures followed by chemical attachment of various moieties. The stationary phases bonded to the surface of silica are similar to those used in fused silica GC columns or HPLC columns.

The SPME process consists of a few simple steps. The fiber, with immobilized organic film, is inserted into the water matrix sample (Figure 1). The organic components are extracted from water into the nonpolar phase. The whole microextractor, located on the tip of the fiber, is then inserted directly into the conventional gas chromatographic injection port such as "split-splitless" or "on column" type. The organic analytes are thermally desorbed and analyzed.

The fused silica fiber is contained inside a Hamilton 7000 series syringe during these operations (Figure 2). The syringe facilitates convenient operation of the SPME device and protects the fiber from damage during the introduction into the injector of a gas chromatograph and storage. The metal plunger wire assembly, which is originally supplied with the syringe, is removed and replaced with a fused silica optical fiber. Prior to placing the fiber inside the plunger, a drop of epoxy is placed on the end of the fiber and allowed to harden. This holds the fiber in position in the syringe. The length of the fiber is determined experimentally and depends on the injector of the gas chromatograph.

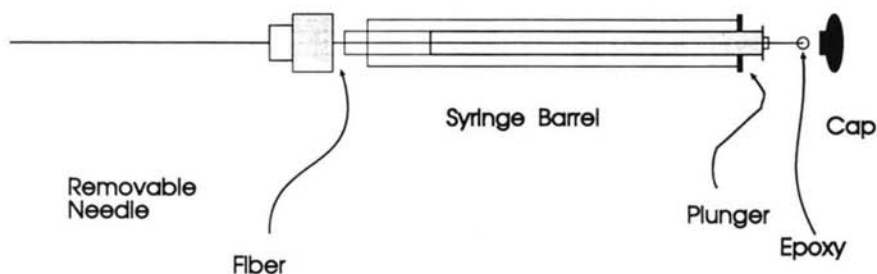


Figure 2. Construction of solid phase microextraction (SPME) device.

In addition to the improved convenience of the sample transfer into the chromatographic instrument, SPME method differs significantly in the extraction part of the process compared to the cartridge method. The extraction procedure does not require prior sampling of aqueous material since *in vivo* or *in vitro* sampling can be conveniently performed. The microextractor can be directly inserted into the fluid stream. The simple geometry of the fiber eliminates plugging caused by particulate matter present in real samples. Also, due to the small size of the fiber, not all of the organic compounds are extracted, but rather the equilibrium described by the partition coefficient between water and organic stationary phase for a given analyte is established. Therefore the SPME method can be made selective by appropriate choice of specifically designed organic phase. The partitioning between the aqueous phase and the organic coating can be described through the distribution constant, K :

$$K = \frac{C_s}{C_{aq}} \quad (1)$$

where C_s is the concentration in the stationary phase and C_{aq} is the concentration in the water. The partition ratio, k' , is therefore:

$$k' = \frac{C_s V_s}{C_{aq} V_{aq}} = \frac{n_s}{n_{aq}} = K \frac{V_s}{V_{aq}} \quad (2)$$

where n_s and n_{aq} are the number of moles in the stationary and aqueous phases, respectively, and V_s and V_{aq} are the volumes of the respective phases. Rearranging Equation 2 yields:

$$n_s = K \frac{V_s n_{aq}}{V_{aq}} \quad (3)$$

substituting $C_{aq} V_{aq}$ for n_{aq} results in:

$$n_s = K V_s C_{aq} = A C_{aq} \quad (4)$$

where $A = K V_s$.

A linear relationship between concentration of analytes in aqueous samples and detector response is expected based upon the relationship in Equation 4. The slope of the linearity curve can be used to determine the partition coefficient for a given analyte if the volume of the stationary phase is known. Furthermore, the sensitivity of the fiber can be adjusted by changing the volume (thickness or area) of the stationary phase.

The linear dynamic range of the method typically extends several orders of magnitude for coatings similar to chromatographic stationary phase materials.⁷ The limit of quantization depends on the partition coefficient and the thickness of the coating and can be as low as few ppt, which was obtained for chlorinated solvents.⁸ In this case the amount of the solvents extracted by a thick polyimide coating from a water sample is about 30 pg per component at a 1- $\mu\text{g/L}$ concentration. This amount ensures not only electron capture detection (ECD), but will allow mass spectrometric identification and quantization.

The dynamics of the extraction process is illustrated on Figure 3, which shows an example of a typical relationship between the amount of analyte adsorbed onto the microextractor (peak area) versus the extraction time, which corresponds to the exposure time of the fiber to the water matrix sample. Initially, the amount of analyte adsorbed by the stationary phase increases with the increase in extraction time. This trend is continued until the point of saturation is achieved, which causes the relationship to level off. This situation indicates the state of equilibrium between the concentration of the analyte in the stationary phase and in the water matrix sample and defines optimum extraction time. According to Figure 3, optimum

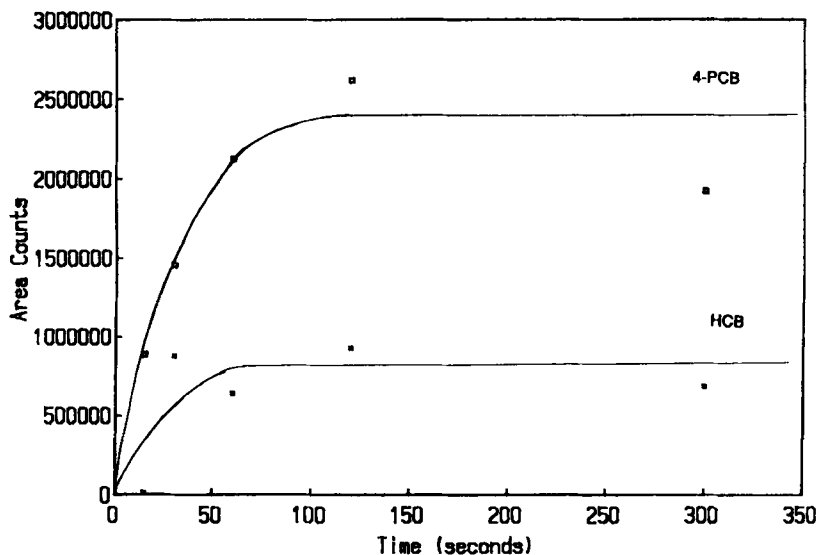


Figure 3. Peak area versus extraction time for hexachlorobenzene and tetrachlorobiphenyl. (From Arthur, C. and J. Pawliszyn. *Anal. Chem.* 62:2148 [1990]. With permission.)

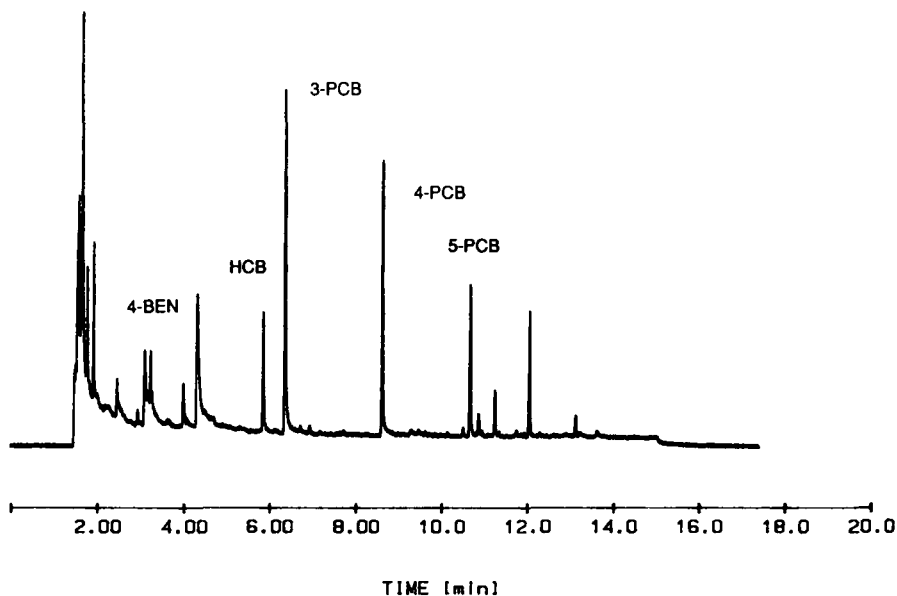


Figure 4. Analysis of chlorinated benzenes and polychlorinated biphenyls with SPME device. (From Arthur, C. and J. Pawliszyn. *Anal. Chem.* 62:248 [1990]. With permission.)

extraction time for uncoated fiber (about 0.1- μm film of silica gel) and polychlorinated biphenyls (PCBs) as analytes is about 1 min.

Figure 4 illustrates the chromatogram corresponding to a PCB mixture in water extracted and analyzed by the SPME method. Peak tailing is larger for the more volatile compounds than the heavier, later eluting components. This is an artifact of thermal focusing that occurs when the analytes are volatilized at 300°C and transferred to a 150°C oven.¹² The heavier compounds benefit from thermal focusing, but the oven is at too high a temperature to allow focusing of the more volatile compounds. The tailing can be alleviated by using cryogenically cooled oven to improve focusing.

An uncoated fiber can also be used to adsorb benzene, toluene, ethyl benzene, and xylenes (BTEX) from aqueous solutions. For this separation (Figure 5) a flame ionization detector (FID) was used, illustrating that a sufficient quantity was adsorbed for FID detection. This expands the general applicability of the fiber as FID detectors are somewhat easier to operate and maintain than ECD detectors. The extraction efficiency in this case is sufficiently high to significantly deplete analyte after 2 to 3 injections if a small volume of aqueous material (1 to 2 mL) is sampled. A larger sample volume (100 mL) is thus recommended if multiple injections are necessary.

Moderate levels of organic interferences and variation in ionic strength of aqueous solution do not significantly change the extraction equilibria.⁸ However, large amounts of organic solvent could be added intentionally to introduce partitioning selectivity, as is commonly done in liquid chromatography.

The fiber method has great potential for the analysis of highly sorptive compounds that can be difficult to sample without loss of analyte. Losses to storage bottles and transfer lines could potentially be eliminated by sampling in situ and analyzing the fiber in the field using portable GC instrumentation.

Possible applications of this technique include sampling of both surface and ground water samples, either in situ or in the laboratory. It could potentially be used in on-line process applications or clinical analysis. Both of these applications benefit from the simplified sample preparation. The coating can be designed for either a broad scan of the organic contaminants (nonselective fiber coating) or selective sampling. This method, when combined with laser desorption, could reduce the sample extraction and analysis to a fraction of a minute.⁹ Curie point heating and microwave desorption¹⁰ are alternative desorption methods. The fiber also shows promise as a method of studying the adsorption properties of polymers and for obtaining information about partitioning in liquid chromatographic systems.

Figure 6 illustrates the advantages of the SPME method compared to solvent procedure. Chromatograms from Figure 6a corresponds to optical fiber technique using C-18 coating and Figure 6b to liquid-liquid extraction with chloroform. In

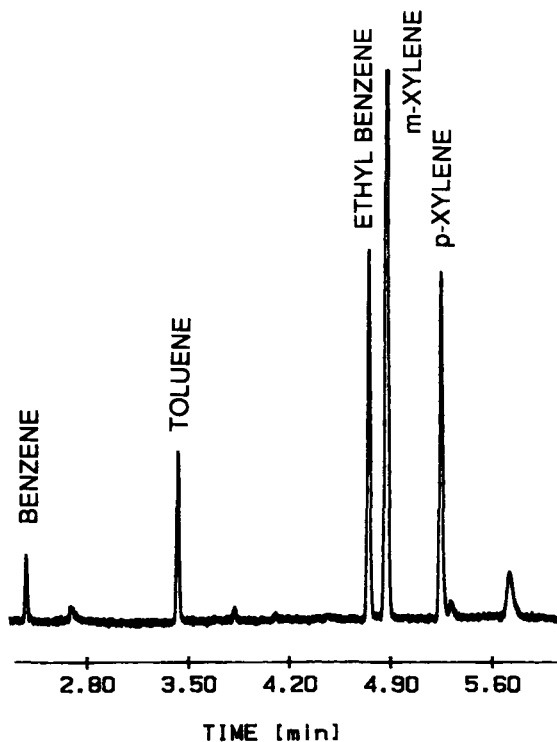


Figure 5. Separation of benzene, toluene, ethylbenzene, and xylenes after desorption from fused silica fiber.

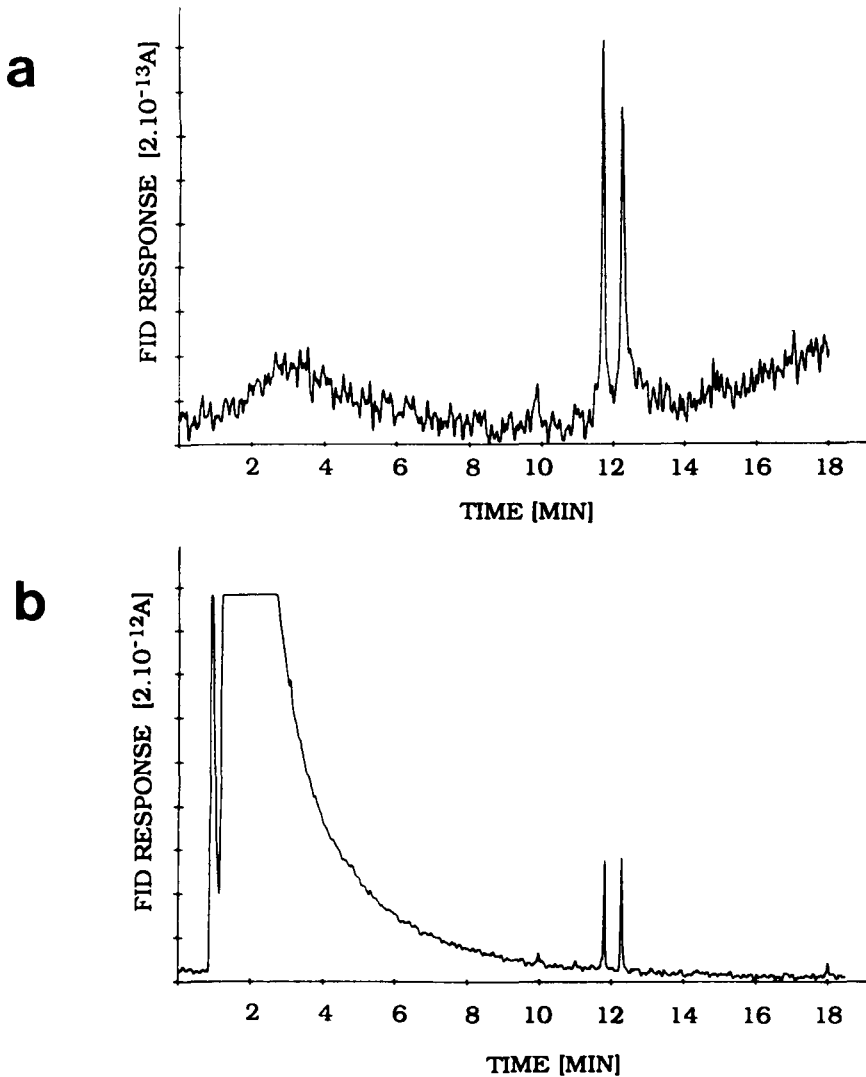


Figure 6. A comparison between the chromatograms corresponding to fused silica fiber method (a) and solvent extraction (b) of a sewage treatment plant water sample. (From Belardi, R. and J. Pawliszyn. *Water Poll. Res. J. Canada* 24:179 [1989]. With permission.)

both cases the same effluent from a sewage treatment plant was analyzed under the same chromatographic conditions. Results are similar, however the total extraction time was about an hour for solvent method and 2 min for the fused silica fiber technique. The SPME device facilitates easy sampling in the field. In addition, when organic solvents are used in the preparation step, the corresponding large peak, together with possible impurities, can mask volatile analytes (Figure 6b).

SUPERCRITICAL FLUID EXTRACTION OF ENVIRONMENTAL SAMPLES

Supercritical fluid extraction processes are well accepted by chemical engineers.¹¹⁻¹⁷ This method exploits the properties of the gas at temperatures and pressures near the critical point (Figure 7). It combines both distillation and extraction in a single process since both vapor pressure and phase separation are involved. The major features of supercritical extraction include low toxicity of the supercritical carbon dioxide and its low cost and high chemical inertia; low temperature extractions of nonvolatile compounds; selectivity of the process through density programming (by varying the fluid pressure); rapid extractions because of low viscosity of fluids, high diffusivities, and perfect wettability compared to liquids; easy separation of the solute from the mixture by lowering the pressure; and low energy consumption due to low temperatures of adsorption and desorption compared to a high thermal energy requirement for distillation. In the food industry, the nontoxic properties of supercritical carbon dioxide and low extraction temperatures have been recognized. Several interesting applications have been proposed, including the extraction of caffeine from coffee and the extraction of hops, spices, and tobacco.¹⁸ The speed and low energy cost of supercritical fluid extraction have allowed many important industrial applications such as coal extraction,¹⁹ regeneration of activated carbon beds used in wastewater treatment,²⁰ and even desalination

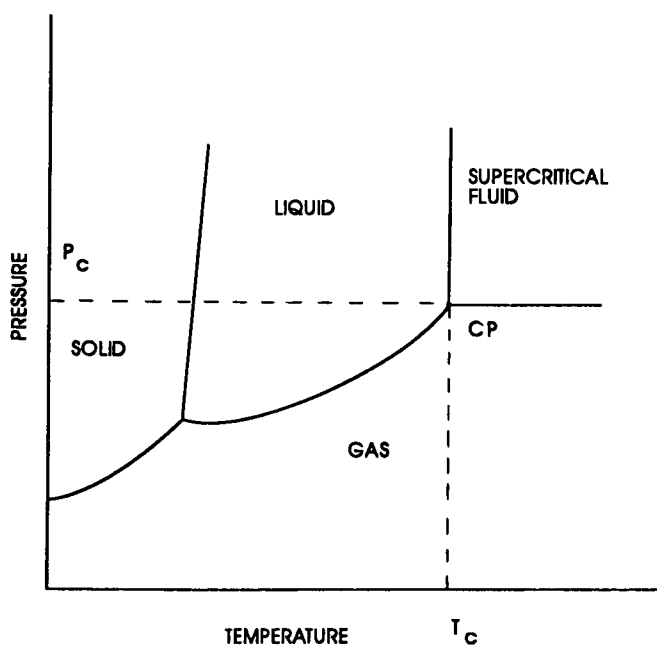


Figure 7. Supercritical fluid region.

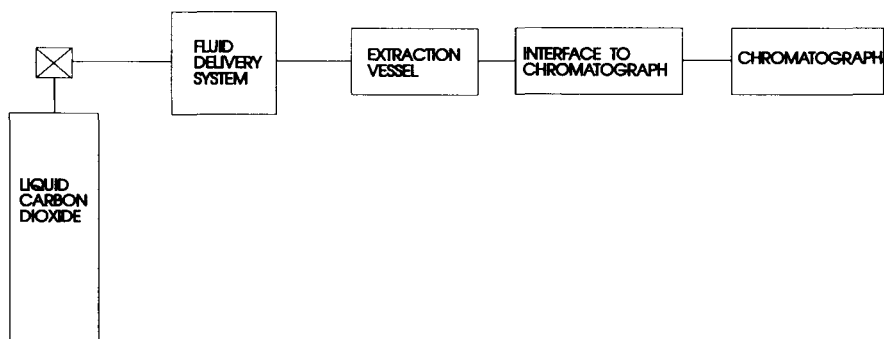


Figure 8. Instrumentation for analytical scale supercritical fluid extraction.

of seawater.²¹ The direct extraction of organic components from water solutions has also been accomplished.^{22,23} Supercritical fluid extraction is currently under intensive investigation with an increasing number of new practical applications. For example, it was recently discovered that even high molecular weight polar molecules such as proteins and peptides can be dissolved in the fluids by using reverse micelles and microemulsions produced by addition of surfactant.^{24,25}

The interesting properties of supercritical fluids can also improve analytical scale extraction. A lot of research involving analytical application of this method has been reported since 1986 and has been summarized in recent review papers.^{27,28,29} SFE is slowly being recognized to be the preferred alternative to commonly used Soxhlet extractions in many analytical applications involving environmental materials. This method facilitates very rapid and efficient separation of organic contaminants from the matrix. Current instrumentation for supercritical fluid extractions consists of a source of high pressure fluid, extraction vessel, restrictor, and interface to the chromatograph (Figure 8). All components are connected in series. Syringe or dual piston pumps are used to supply fluid to the extraction vessel. They are very expensive devices and their price determines the overall cost of the supercritical fluid extraction.²⁹ They operate using a moving piston equipped with a polymeric seal, and therefore they are sometimes unreliable for the delivery of fluids whose critical temperatures are below (Xe) or slightly above (CO₂, N₂O) room temperature. The main reason for this is that the supercritical fluid has a much lower viscosity than normal liquid and therefore the pump is prone to leaks past the piston seals. In order to prevent these problems, cooling the pump heads is necessary.^{30,31} In addition the moving seal deteriorates much faster when used with supercritical fluids because of the pressure deep cycles produced during operation and charging of the device. To limit these problems and lower the cost of the instrumentation, a thermal expansion pump has been proposed. This fluid delivery system is based on the heating of a high pressure vessel filled with the liquid gas.^{32,33} This pump can be designed to be a small size, without using polymeric seals, and can be operated by a car battery, which allows field application.

The extraction vessel can be a specially designed high pressure container,³⁴ but for extracting organics from solid matrices, a standard housing for an HPLC pre-column or commercially available finger-tight unit is the least expensive and most effective solution. The solid sample is simply packed in place of the column packing and the whole assembly is fitted into the supercritical fluid line.³⁵ The fluid flow is forced around the particles of the sample matrix, similarly as in chromatographic-packed columns, and therefore facilitates efficient removal of the extracted material, which is then transported outside the vessel. A restrictor is used to provide a pressure drop between the extraction vessel and the interface to the chromatographic instrument which is close to 1 atm (Figure 8). This restrictor usually consists of a piece of small in diameter fused silica tubing. The diameter of the tubing is between 10 to 40 μm and determines the flow of the extraction fluid through the system. For example, a 20- μm restrictor provides the flow of expanded gas of about 150 mL/min, while a 30- μm restrictor, 300 mL/min.³⁶ This corresponds to about three orders of magnitude smaller volumetric flow rates of the compressed fluid in the extractor. The main purpose of the fluid flow is to transfer the extracted material from the extraction vessel for collection at the interface to the chromatograph. The higher the flow, the more efficient transport. However, increased flow can cause loss of analytes during collection because of volatilization. It also requires use of high volume pumps and large amounts of the fluid which adds to the cost and inconvenience of the method. Therefore it is important to optimize the flow rates, especially for frequently used applications. For example, in the case when desorption rates of analytes are kinetically limited, it is more optimum to operate extraction at close to static conditions.³⁷

The components of the gas mixture coming out of the restrictor can be conveniently collected for further chromatographic analysis. However, it should be remembered that the organic components are likely to form an aerosol and escape to the atmosphere. In order to prevent this loss, the collection of the extract should be done by trapping it in an organic solvent. It is also possible to perform direct deposition of the analytes on the front of the capillary column by using a cool on-column injector. The instrumental arrangement is shown in Figure 9. The fused silica restrictor is inserted directly into the front of the capillary column.^{34,39} The organic components of the extract mixture are adsorbed at the front of the column placed in the cooled "on-column" injector. Rapid vaporization of the deposited material together with the cryo oven can be used to sharpen the injection band. Temperature-programmed gas chromatographic analysis then follows, facilitating high resolution analysis. The on-line approach allows ultratrace analysis since all deposited material is introduced onto the column. The main difficulty in practically implementing the direct deposition method is the large amount of gas which flows in the system. The majority of the gas is vented through the metal sheath inserted in the septum, but a significant portion of it flows through the column. This introduces additional strain on the detector.

Extraction of the environmental samples often results in a very complex organic mixture produced which require use of sequential chromatographic clean-up tech-

SCF Delivery system

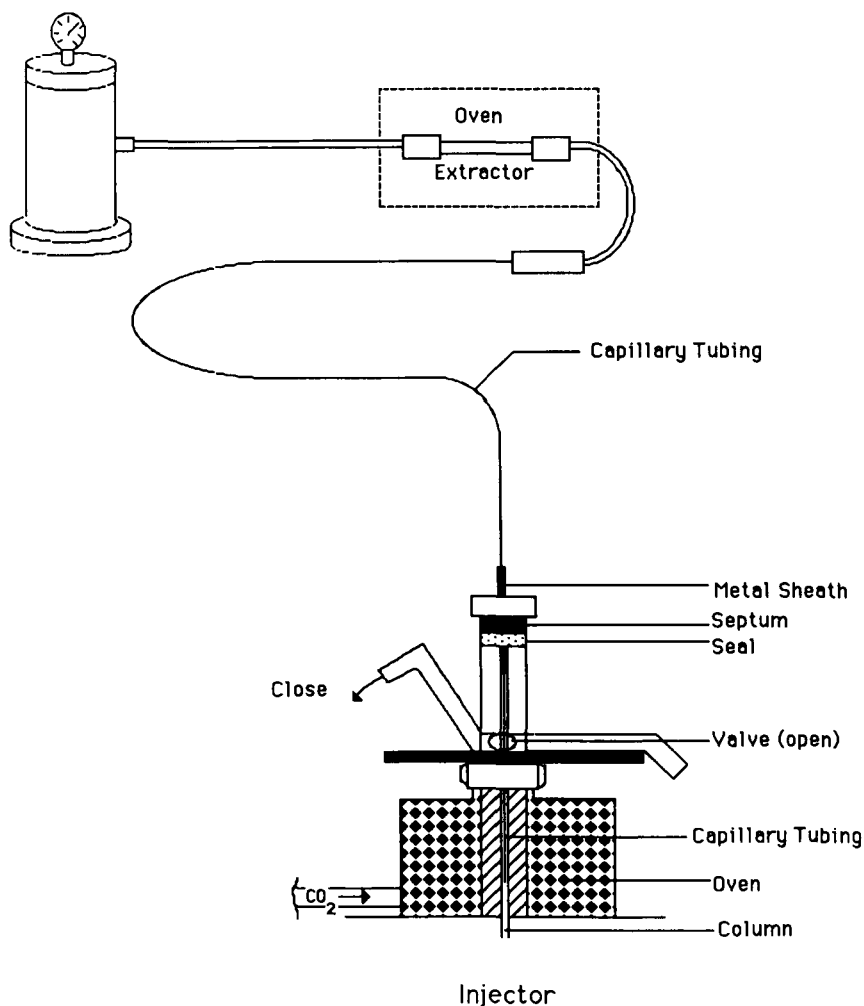


Figure 9. On-line SFE-GC system. (From Alexandrou, N. and J. Pawliszyn. *Water Poll. Res. J. Canada* 24:207 [1989]. With permission.)

niques before the capillary GC analysis. Supercritical fluid extractions hold the promise of eliminating this step since some degree of extraction selectivity can be obtained by varying its density and composition of the fluid.

The most popular gases which exist as supercritical fluids at conditions close to ambient temperature and pressure are shown in Table 1. Solubility properties of the compressed gases can be approximated by the solubility parameters:⁴⁰

$$S = 1.25 P_c^{1/2} \left[\frac{P^G}{\rho^L} \right] \quad (5)$$

where P_c is critical pressure in atmospheres, ρ^G is reduced density of supercritical fluid used in extraction, and ρ^L is the reduced density of the fluid in its liquid state. The factor $P_c^{1/2}$ corresponds to "chemical effect," which relates to the molecular structure, and ρ^G/ρ^L to the "state effect," which depends on the pressure in the system. The simple diagram comparing this solubility of various compressed gases between themselves and the normal liquids is shown in Figure 10. This diagram suggests that highly compressed CO_2 ($\rho^L = \rho^G$) has a solubility parameter of about 10.6, which is close to that of pyridine. Supercritical carbon dioxide is the most popular fluid due to its low toxicity and cost. Not all substances, however, are very soluble in this relatively nonpolar solvent. The addition of a more polar or high affinity solvent can significantly change the extraction properties of the fluid. This approach is widely applied in liquid chromatographic separations,^{41,42} where the elution properties of the mobile phase are modified by changing its composition. Similarly, in supercritical fluid extraction, this principle of modifying properties of the fluid has been used. For example, the addition of the methanol to the supercritical mixture significantly improves the recovery rates of polycyclic aromatic hydrocarbons. This method has been used to first remove low molecular weight, nonpolar compounds and then to remove more polar polycyclic hydrocarbons with additions of methanol.³⁵ The critical temperatures of fluid are significantly increased when adding modifier.⁴³ Therefore, the extraction must proceed at higher temperatures to ensure supercritical fluid conditions.

Initially, analytical researchers used directly fundamental concepts developed by chemical engineers, which are based on analyte solubilities in supercritical fluids,²¹⁻²⁶ to explain their results and optimize SFE conditions. However, in many instances significant discrepancies between experimental results and theory have been observed. The main reason for the disagreement is the difference in concentration levels of the compound of interest in the matrix. In engineering applications, the objective is to remove a product, which is present in the raw material at levels often exceeding 1%. In this situation the effect of the matrix present in the extraction vessel is limited. Engineers are not concerned with trace amounts of product which remains adsorbed onto the matrix. Under such conditions the solubilities of the compound of interest in the fluid determine the efficiency of the overall extraction. Also, the extraction mixtures are simple with the main component being a product.

Table 1. Properties of Some Gases Suitable for Supercritical Fluid Extraction

Compound	bp(°C) at 1 atm ^a	T _c (°C)	P _c (atm)	ρ_c (g·cm ⁻³)
Carbon dioxide	-78.5	31.3	72.9	0.448
Ammonia	-33.4	132.3	111.3	0.24
n-Propane	-44.5	96.8	42.0	0.220
Chlorotrifluoromethane	-81.4	28.8	39.0	0.58
Nitrous oxide	-89	36.5	71.4	0.457
Xenon	-107.1	16.6	58.0	1.105

^a 1 atm = 1.01 × 10⁵ pascal.

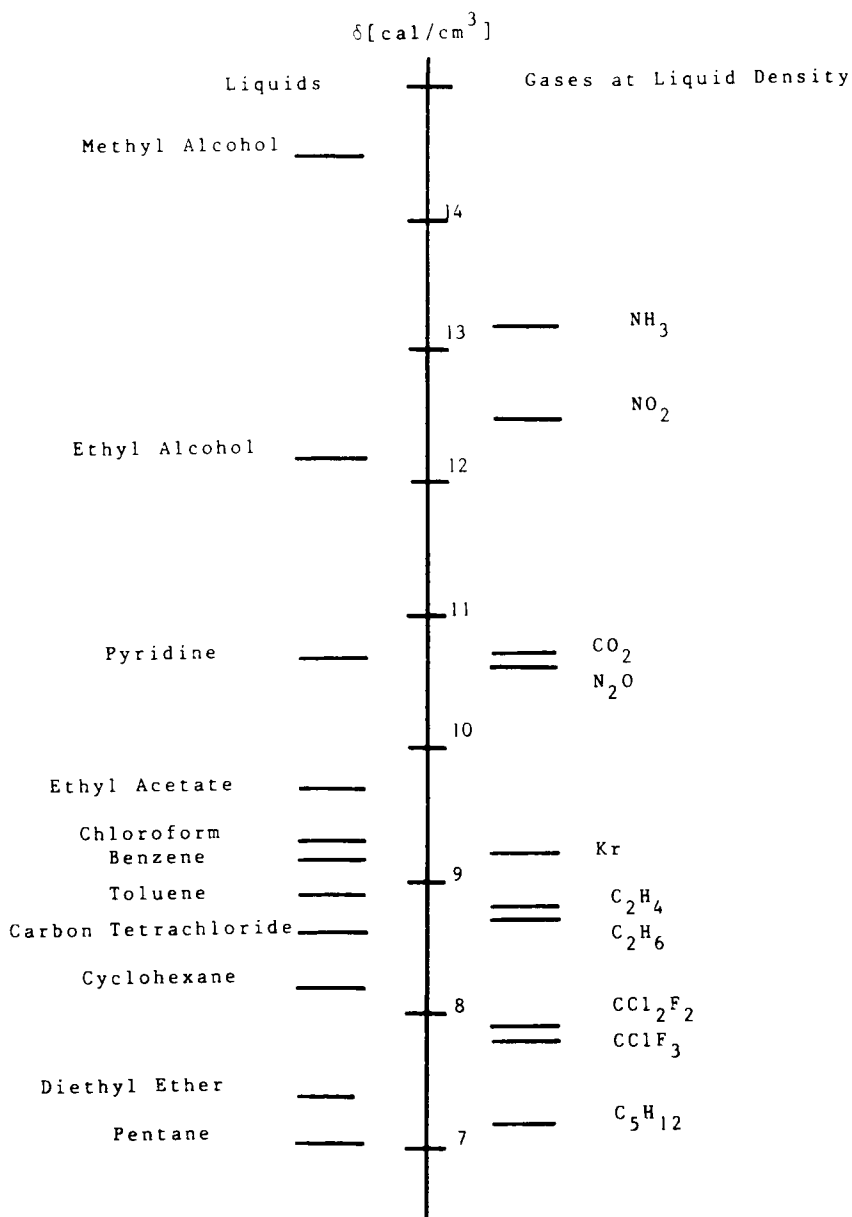


Figure 10. Solubility parameter for most important supercritical fluids and normal liquids. (Adapted from Giddings, J., M. Myers, L. McLaren, and R. Keller. *Science* 162:67 [1968]. With permission.)

Therefore, engineers were able to develop sophisticated fractionating techniques for their processes, which are based upon solubility diagrams of solids in pure fluids (such as the cross-over region method).⁴⁴ On the other hand, the analytical chemist's objective is to remove quantitatively traces of target organic contaminants adsorbed onto the matrix, which limits applicability of engineering approaches for analytical uses. First, it is very difficult to saturate the fluid with the target components since they are present often in ppt levels in the matrix. Second, the concentration level of interferences can vary significantly from sample to sample and the absolute level is, in most cases, much higher compared to the target compound. This will lead to unpredictable solubility properties of the fluid mixture since the impurities will act as modifiers. In addition, for trace levels of analytes, the effects associated with the presence of the matrix in the extraction vessel, known to us from chromatographic experience, are becoming important. For example, partitioning of analytes between the porous surface of the matrix and the fluid and chemisorption of analytes on the active sites is expected to occur in this case. Therefore dynamics of the mass transport from the surface of the matrix to the bulk of the fluid will limit the extraction rates considering high flow rates of the fluid in the extractor. This transport process consists of three distinct steps: desorption of analytes from the matrix surface, solvation of the material in the fluid, and diffusion of it to the bulk of the solvent.³⁷ To properly optimize analytical SFE, it is necessary to define which of these steps determine the overall extraction time. Clear evidence of these effects is frequently observed. For example, during research directed towards development of rapid SFE procedures to quantitatively remove native polychlorinated dibenzo-p-dioxins and polychlorinated dibenzofurans from flyash samples, it was discovered that these compounds are strongly bound to the matrix; they are most likely chemisorbed onto the original active sites where they were formed.^{37,45} The large energy barrier associated with dissociation of the analyte-matrix complex prohibits removal of contaminants (Figure 11). This is in contrast to the case when analytes are physically adsorbed onto the matrix when the equilibrium defined by the corresponding partition coefficient is reached rapidly, limited only by the diffusion. To facilitate extraction of chemisorbed organic contaminants, it is necessary to destroy the matrix by acid etching.³⁷ In addition, it was found that replacing CO₂ with more polar N₂O also results in quantitative removal. The dramatic difference between SFE efficiencies obtained for CO₂ and N₂O, structurally similar molecules, is somewhat unexpected particularly since their solubility parameters are similar (Figure 10). The initial results related to the removal of the native dioxins and furans from flyash using this approach indicate that the fluid molecules of nitrous oxide are involved in a specific interaction with the matrix which lowers the activation barrier for desorption of chemisorbed molecules and therefore facilitates rapid extraction.³⁷ By recognizing this fact, it is possible to improve performance of the extraction method. For example, the difference in extraction efficiencies between CO₂ and N₂O can be used effectively to clean up complex organic mixtures which are present in the flyash. Weakly adsorbed interferences can be removed first with CO₂, followed by extraction of compounds of interest with N₂O.³⁷

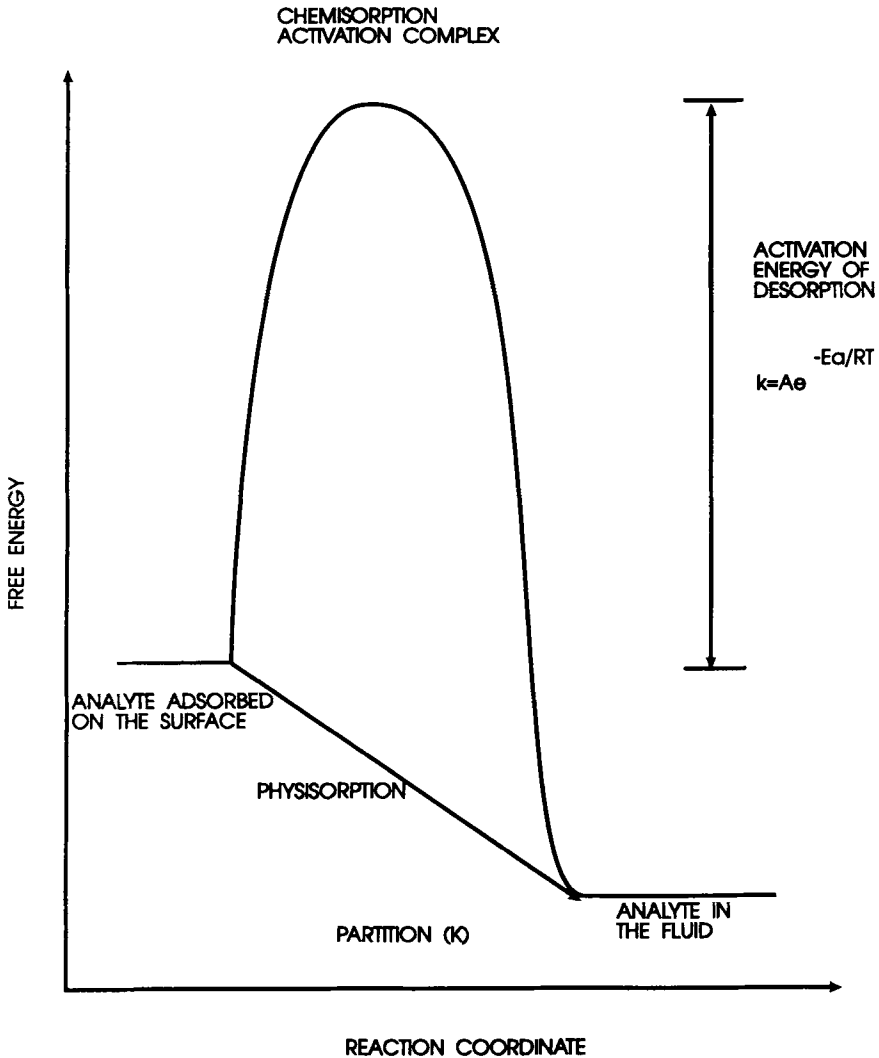


Figure 11. Free energy versus reaction coordinate indicating the difference in energy requirement for desorption of chemisorbed and physisorbed species.

This example indicates that partial fractionation of organic contaminants can be achieved by optimizing supercritical fluid extraction directly from the matrix. However, in the majority of important complex environmental samples such as soil, pulp, or fish tissue, this simple procedure is not expected to be satisfactory due to poor selectivity of the matrix and large number of interferences. Therefore additional clean-up procedures need to be used before GC/MS analysis. At present time this is accomplished most effectively with column chromatography or solid phase ex-

traction methods which use organic solvents. These solvents can be replaced by supercritical fluids. The principle of such a separation scheme is based on varying the partitioning of organic components between the stationary phase and the mobile fluid in such a way that the interferences are eluted first, followed by removal of target compounds. This process can be obtained by applying sorbents specific to the components of interests and/or using selective fluid mixtures (modifiers, different fluids) and/or varying the extraction pressures.⁴⁶

In most cases the process of removing trace organic components from solid matrices using the dynamic method and the system outlined in Figure 8 is expected to occur far from the partition equilibrium. The continuous, usually high flow of fluid through the extraction vessel leaches the organic components from the sample matrix to the collection volume. In the cases where the overall dynamics of the process is determined by the transport of analytes through the porous matrix, the extraction rates can be enhanced by using ultrasonic waves which produce convection of the fluid in micropores and therefore increase this transport. For example, the use of sonic waves enhances extraction efficiency of caffeine from coffee beans.⁴⁷ However, it should be remembered that supercritical fluids are naturally characterized by large convection currents.⁴³

To this point we have discussed the removal of organic components from solid matrices. Aqueous samples can be extracted as well using supercritical gases. However, the rate limited step in this process is the diffusion of analytes in the aqueous phase, similarly to the liquid-liquid extraction. The presence of water traces in the extract mixture might cause a problem in subsequent chromatographic analysis. The extraction vessel design for the extraction of liquids is very complex compared to the simple column type used for solid matrices. In addition, in trace analysis the concentration of organic components in the aqueous samples is very low, which requires a large volume extraction vessel to accommodate enough aqueous sample for satisfactory analysis.

The whole process can be significantly simplified if an indirect approach rather than a direct one is taken. In the first step, the organic components present in the water matrix are adsorbed on a sorbent such as XAD resin, Tenax GC, or solid phase extraction material. After drying the sorbent, the supercritical fluid extraction of the organics follows. Figure 12 shows an example of the system which was used to extract chlorinated organics from the aqueous matrix.^{33,39} Initially, the water sample is pushed through the cartridge using pressure produced by dry nitrogen supplied from a pressure cylinder. The extracted water is drained into a waste bottle. After the water sample is exhausted, dry nitrogen is purged through the extraction vessel which removes moisture. This process can be performed at elevated temperatures to shorten drying time. The higher the temperature, the faster the drying process; however, an increase in the loss of volatiles might occur. The same temperature can be used in the next step involving supercritical fluid extraction of the solid sorbent. Transition from adsorption to the extraction process is achieved by changing the position of the valves fitted into the system (Figure 12a). The source of carbon dioxide is connected directly to the extraction vessel and the extraction

flows to the restrictor which determines the magnitude of the flow. In practice, the switching is achieved with the help of a single electronically activated 10-port valve as indicated in Figure 12b. The timing of the whole process can be controlled with the help of a microprocessor. Good recoveries of the nonvolatile pollutants from water were obtained using this simple and easy to automate method.^{33,39} The isolation process described dries the sorbent at elevated temperatures. A similar objective can be achieved by using a vacuum,⁵ but this approach requires additional expensive and cumbersome instrumentation.

A similar approach, as illustrated in Figure 12, can be used in determining the total amount of organic components in aqueous suspension. The tightly packed sorbent can be used as a filter. The organics from water are absorbed on the sorbent, while the particulate matter is trapped in the bulk of the packing. Therefore, after

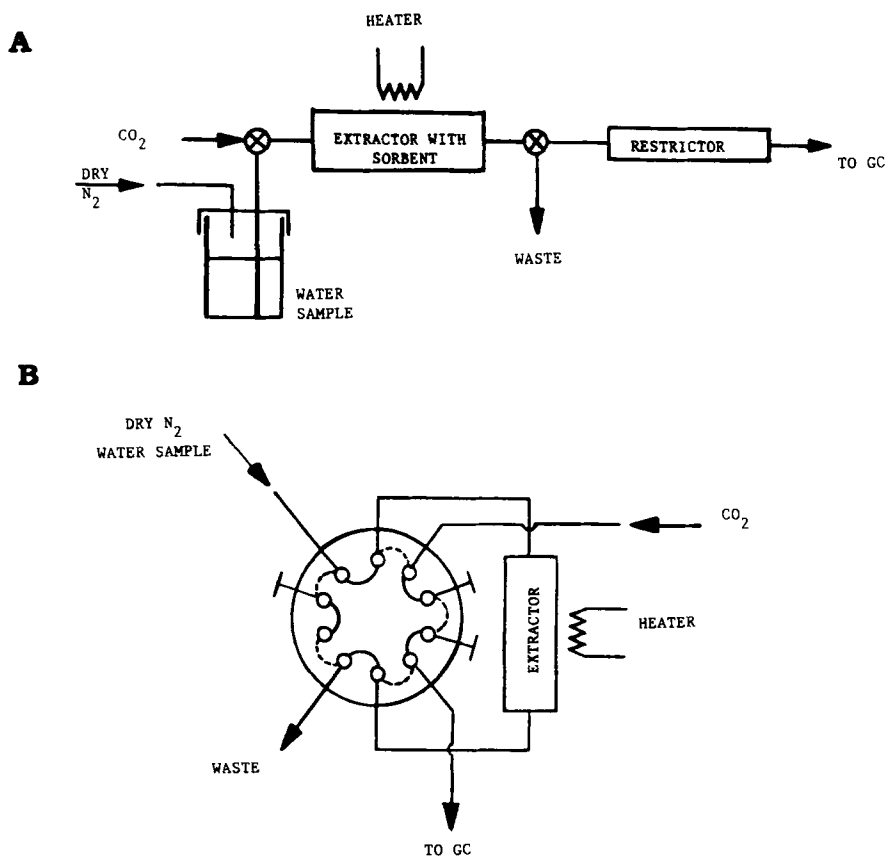


Figure 12. Schematics of system for indirect supercritical fluid extraction of organics present in aqueous matrix samples. (A) Principle of the method; (B) control of the process with a single 10-port valve. (From Giddings, J., M. Myers, L. McLaren, and R. Keller. *Science* 162:67 [1968]. With permission.)

extraction, the total amount of organic material present in the suspension can be analyzed. If, on the other hand, separate values for water phase and solid suspended material is required, the sample should be first centrifuged to separate the aqueous and solid phases before appropriate extraction procedures.

GAS EXTRACTION OF VOLATILE ORGANICS FROM AQUEOUS SAMPLES WITH HOLLOW FIBER MEMBRANES

Polymeric membranes are currently used for many diverse applications, such as microporous filtration, ultrafiltration, reverse osmosis, dialysis, electro dialysis, and gas separation.⁴⁸ These membranes are supplied in many different forms and shapes. They can separate molecules based on size, shape, or solubility characteristics. The most useful geometry for analytical applications is a hollow fiber. In such a system the aqueous sample containing the volatile species is passed through the inside of the hollow fiber. Analytes diffuse through the inner solution to the membrane wall, diffuse across the fiber's walls, and are absorbed at the fiber's outside wall, and finally they are removed by gas stripping.

Hollow fiber membranes provide a much larger surface area per volume over a wider variety of flows than both the static headspace and purge and trap methods, which are often used as sample preparation steps prior to GC analysis. This results in a much faster mass transfer of analytes from aqueous phase to gas and therefore more rapid determinations. The large surface area-to-volume ratio remains undisturbed even at high or low fluid flows. Gas flow can be increased without changing the liquid flow and vice versa.

A variety of volatile species have been successfully removed from water in industrial processes by using hollow fiber membranes. Separation of chlorinated solvents from water have been accomplished with this method.⁴⁹ To this date only a small number of analytical investigations involving this approach for volatile organic determinations have been conducted. Hollow fiber membranes have been used successfully as a mass spectrometer interface.⁵⁰⁻⁵⁵ It was also used as a preparation method for gas chromatographic analysis.^{56,57} To date only two types of hollow fiber membranes have been explored in analytical applications: a microporous hollow fiber membrane and a nonporous silicone rubber membrane. An analytical scale extraction module requires only a single hollow fiber to warrant low level determinations. These units can be made very inexpensively using a Teflon[®] or a glass tube (Figure 13). The ends are sealed with epoxy and one end is attached to a pump. Water containing the volatile components is pumped through the fiber. Gas enters the teflon tube via fused silica tubing and flows around the fiber countercurrent to the water flow. The volatile components diffuse across the membrane and into the gas stream which flows into 0°C hexane for the off-line method or directly into a cryogenically cooled GC injector for the on-line method (Figure 14). As a precautionary measure a Nafion dryer is placed between the module and the GC. The dryer is selectively permeable to water and will remove any water vapor before the gas enters the GC. This will prevent water condensation in the injector and damage to the capillary column. Water may be present in the

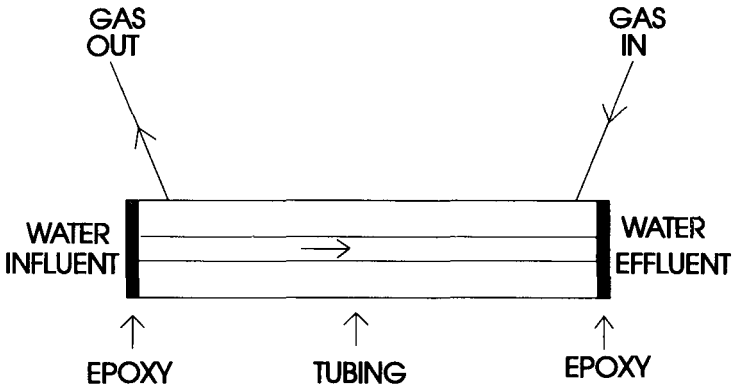


Figure 13. Analytical-scale hollow fiber membrane (HFM) module.

gas initially, particularly when the ambient air is used as the stripping gas (in field applications) or when seepage through the membrane occurs.

To ensure that the results obtained in this method are quantitative, it is necessary to completely remove all target analytes from the aqueous samples. In this case the results will not be affected by changes of the extraction parameters, such as temperature variations. Changes in these factors are very difficult to compensate by

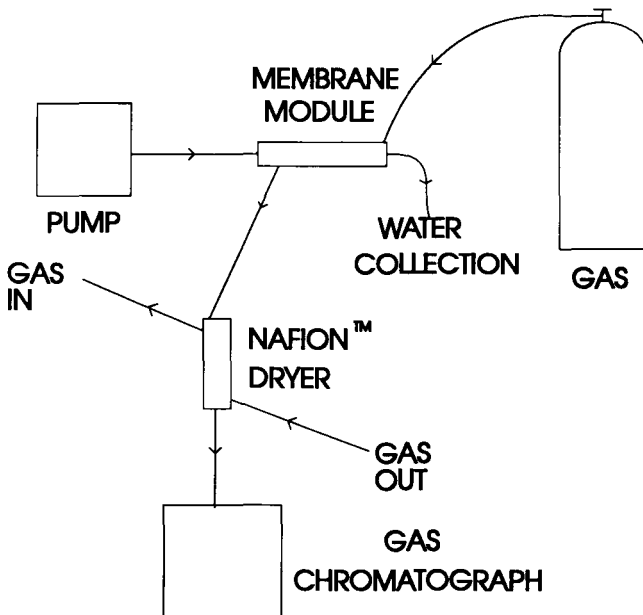


Figure 14. On-line HFM-GC system.

using internal standards. To achieve quantitative extraction, careful optimization of experimental conditions is required. Here, the example of such a process is performed for microporous polypropylene hollow fibers. These membranes are available in different dimensions. The wall thickness is approximately 30 μm and pore size varies from $0.05 \times 0.15 \mu\text{m}$ to $0.065 \times 0.19 \mu\text{m}$. These pores can cover 30 to 40% of the surface area. These pores do not get wet when the membrane is exposed to water due to the hydrophobic character of the polymer. Several inner diameters of fibers are available ranging from 100 to 400 μm . The transfer of volatile compounds from water to gas occurs through direct contact of the two phases. Figure 15 illustrates the interface between the air-filled membrane pores and the liquid-filled fiber lumen.

Mass transport across the membrane is driven by the concentration difference across the interface. When equilibrium is reached, the concentration in the gas phase C_g , can be related to the concentration in the aqueous phase, C_a , by Henry's law constant, H :

$$H = \frac{C_g}{C_a} \quad (6)$$

Hence, the rate of transport is directly related to the volatility and hydrophobicity of the compound.

Three separate resistances to overall mass transfer across the membrane are involved: (1) diffusion from the liquid-filled fiber lumen across the liquid film layer to the membrane surface, (2) diffusion through the gas-filled membrane pores, and (3) diffusion through the air film layer to the outside of the membrane. This is represented by:

$$\frac{1}{K_L} = \frac{1}{k_l} + \frac{1}{k_m H} + \frac{1}{k_g H} \quad (7)$$

where K_L is the overall mass transfer coefficient, k_l is the liquid phase mass transfer coefficient, k_m is the membrane mass transfer coefficient, and k_g is the gas phase mass transfer coefficient. This equation may be used to calculate the overall mass transfer coefficient.

The behavior of the system can be predicted from the equation describing the ratio of influent concentration to effluent concentration for a single pass through the fiber.⁴⁹

$$\frac{C_1}{C_2} = \frac{\exp [(K_L a L / v) (1 - R)] - R}{1 - R} \quad (8)$$

In this equation, C_1 is the influent concentration, C_2 is the effluent concentration, a is the ratio of surface area to volume of the liquid phase which is equal to $4/d$ where d is the inner diameter of the fiber, L is the active length of the fiber, v is

the linear flow rate, and $R = Q_w/Q_g H$ where Q_w is the volumetric water flow rate and Q_g is the volumetric gas flow rate. This equation neglects parabolic flow profile, which is expected at typical analytical conditions, but provides a good qualitative understanding which parameters should be varied to improve the performance of the system. Increasing the length of the fiber and decreasing its diameter or the linear velocity of the aqueous sample in the lumen will improve the removal efficiency.

The analytical data obtained for extraction of chlorinated solvents and illustrated on Figure 16 support these conclusions.⁵⁷ The smaller diameter of the fiber and slower flow rate, the better extraction efficiencies. The removal of solvents is quantitative when 100- μm fiber and 30 mm/sec linear flow rate is used. The detection limit of the method is in low parts per trillion level, in direct on-column system showed on Figure 14, since all extracted and trapped material is analyzed.

CONCLUSIONS

Continuous development of new materials and technology such as fused silica optical fibers, hollow fiber membranes, or high pressure components, applications of which have been discussed in this chapter creates an opportunity to devise new and better analytical procedures. The methods described are capable to vastly reduce use of toxic organic solvents in the analytical laboratory. These procedures are more efficient, faster, and less costly when compared to the orthodox solvent extraction techniques. They are also more suitable for automation and for field operation.

ACKNOWLEDGMENTS

Robert Belardi and Catherine Arthur have performed most of the experimental work related to the solid phase microextraction; Nick Alexandrou and Michael Lawrence have investigated applications of supercritical fluid extraction; and Katie Pratt has been involved in hollow fiber research.

This work was supported in part by the Natural Sciences and Engineering Research Council of Canada (NSERC), Imperial Oil of Canada, Varian Canada, and Ontario Ministry of Environment.

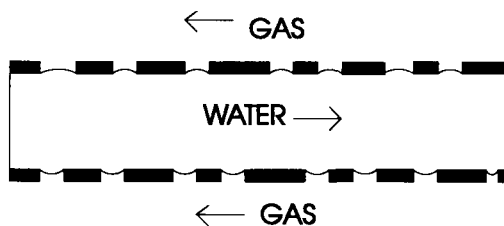


Figure 15. Porous hollow fiber membrane.

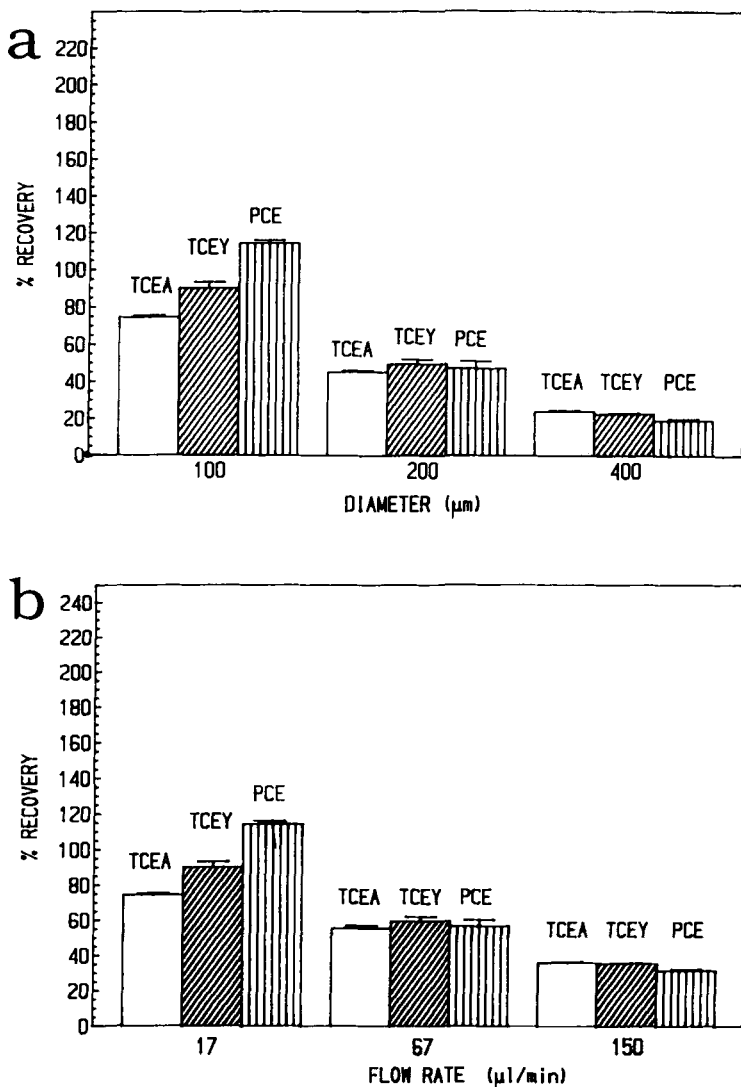


Figure 16. Analytical data obtained for gas extraction of chlorinated solvents from water.

REFERENCES

1. Rushway, R. *J. Chromatogr.* 211:135 (1981).
2. Junk, G., and J. Richard. *Anal. Chem.* 60:451 (1988).
3. Hoke, S., E. Brueggemann, L. Baxter, and T. Trybus. *J. Chromatogr.* 357:429 (1986).
4. Green, D., and D. LePape. *Anal. Chem.* 59:669 (1987).

5. Pankow, J., M. Ligocki, M. Rosen, L. Isabelle, and K. Hart. *Anal. Chem.* 60:40 (1988).
6. Pankow, J., and L. Isabelle. *J. Chromatogr.* 237:25 (1982).
7. Belardi, R., and J. Pawliszyn. *Water Poll. Res. J. Canada* 24:179 (1989).
8. Arthur, C., and J. Pawliszyn. *Anal. Chem.* 62:2148 (1990).
9. Pawliszyn, J., and S. Liu. *Anal. Chem.* 59:1475 (1987).
10. Neu, H., W. Merz, and H. Panzel. *HRC&CC* 7:382 (1982).
11. "Extraction with Supercritical Gases," *Angew Chem. Int. Ed. Engl.* 17:701 (1978).
12. Williams, D. *Chem. Eng. Sci.* 36:1769 (1981).
13. Paulaitis, M. et al. *Rev. Chem. Eng.* 1:179 (1982).
14. McHugh, M., and V. Krukonis. *Supercritical Fluid Extraction*, (Stoneham, MA: Butterworth Publishers, 1986).
15. Squires, T., and M. Paulaitis, Eds. "Supercritical Fluids," ACS Symposium Series, #329 (1987).
16. B. Charpentier and M. Sevenants, Eds. "Supercritical Fluid Extraction and Chromatography," ACS Symposium Series, #366 (1988).
17. K. Johnson and J. Penninger, Eds. "Supercritical Science and Technology," ACS Symposium Series, #406 (1989).
18. Zosel, K. U.S. Patent 3,806,619 (1974).
19. Coenan, H. et al. U.S. Patent 4,485,003 (1984).
20. Modell, M. U.S. Patent 4,061,566 (1977).
21. Texaco Inc. U.S. Patent 3,318,805 (1982).
22. De Fillippi, R., and J. Vivian. U.S. Patent 4,349,415 (1982).
23. Shimshick, E. U.S. Patent 4,250,331 (1981).
24. Lembert, R., R. Fuller, and K. Johnson. *J. Phys. Chem.* 94:6021 (1990).
25. Smith, R., J. Fulton, J. Blitz, and J. Tingey. *J. Phys. Chem.* 94:781 (1990).
26. Berkman, E., and R. Smith. *J. Phys. Chem.* 94:345 (1990).
27. Hawthorne, S. *Anal. Chem.* 62:633a (1990).
28. Vannoort, R., J. Chervet, H. Lingerman, G. DeJong, and U. Brinkman. *J. Chromatogr.* 505:45 (1990).
29. Lopez-Avila, V., N. Dodohiwala, and W. Beckert. *J. Chromatogr. Sci.* 28:468 (1990).
30. Greibrokk, T. et al. *J. Chromatogr.* 371:145 (1986).
31. Greibrokk, T. et al. *Anal. Chem.* 56:2681 (1984).
32. Pawliszyn, J. *HRC* 13:199 (1990).
33. Lawrence, M., M. Colquhoun, and J. Pawliszyn. "Indirect Supercritical Fluid Extraction of Polychlorinated Dibenzo-p-Dioxins in Rainwater," in Proceedings of the 1990 International Symposium on Measurements of Toxic and Related Pollutants; U.S. EPA Report Number EPA/600/9-90/026, Raleigh, NC (1990), p. 123.
34. Wright, B., C. Wright, R. Gale, and R. Smith. *Anal. Chem.* 59:38 (1987).
35. Hawthorne, S., and D. Miller. *J. Chromatogr. Sci.* 24:258 (1986).
36. Hawthorne, S., and D. Miller. *J. Chromatogr.* 403:77 (1987).
37. Alexandrou, N., and J. Pawliszyn. *Anal. Chem.* 61:2770 (1989).
38. Wright, B., S. Frye, D. McMinn, and R. Smith. *Anal. Chem.* 59:640 (1987).
39. Alexandrou, N., and J. Pawliszyn. *Water Poll. Res. Canada* 24:207 (1989).
40. Giddings, J., M. Myers, L. McLaren, and R. Keller. *Science* 162:67 (1968).
41. Snyder, L., and J. Kirkland. *An Introduction to Modern Liquid Chromatography*, 2nd ed. (New York: John Wiley & Sons, Inc., 1979).
42. Glajch, J., and J. Kirkland. *J. Anal. Chem.* 55:319A (1983).

43. Gulari, E. et al. "Supercritical Fluids," T. Squires, and M. Paulaitis, Eds., ACS Symposium Series #329 (1987).
44. Chimowitz, E., and K. Pennisi. *AIChE J.* 32:1665 (1986).
45. Alexandrou, N., M. Lawrence, and J. Pawliszyn. "Supercritical Fluid Extraction of Fly Ash Samples for Rapid Determination of Polychlorinated Dibenzo-p-Dioxins and Dibenzofurans," in Proceedings of the 1990 International Symposium on Measurements of Toxic and Related Pollutants; U.S. EPA Report Number EPA/600/9-90/026, Raleigh, NC (1990), p. 123.
46. King, J. J. *Chromatogr. Sci.* 27:355 (1989); Alexandrou, N., M. Lawrence, and J. Pawliszyn. "Clean-Up of Complex Organic Mixtures using Sorbents and Supercritical Fluids," 1991 International Symposium on Supercritical Fluid Chromatography, Park City, UT, January 1991.
47. Wright, B. et al. "Supercritical Fluid Extraction and Chromatography," B. Charpentier and M. Sevenants, Eds. ACS Symposium Series #366, (1988), p. 44.
48. Warren, D. *Anal. Chem.* 56:1529A (1984).
49. Semmens, M., R. Qin, and A. Zander. *AWWA J.* 81:162 (1989).
50. Savickas, P., M. LaPack, and J. Tou. *Anal. Chem.* 61:2332 (1989).
51. Kallos, G., and N. Mahle. *Anal. Chem.* 55:813 (1983).
52. Bier, M., and R. Cooks. *Anal. Chem.* 59:597 (1987).
53. Jones, P., and S. Yang. *Anal. Chem.* 47:1000 (1975).
54. Westover, L., J. Tou, and J. Mark. *Anal. Chem.* 46:568 (1974).
55. Brodbelt, J., R. Cooks, J. Tou, G. Kallos, and M. Dryzga. *Anal. Chem.* 59:454 (1987).
56. Stetter, J., and Z. Cao. *Anal. Chem.* 62:182 (1990).
57. Pawliszyn, J., and K. Pratt. "Rapid Isolation of Volatile Organics from Water Samples with Gas Elimination Device Constructed from Microporous Hollow-Fibres," Paper #1009, 1990 Pittsburgh Conference, New York, March 1990.



Taylor & Francis

Taylor & Francis Group

<http://taylorandfrancis.com>

CHAPTER 14

Model Studies on the Solid Supported Isolation, Derivatization, and Purification of Chlorophenols and Chlorophenoxy Acetic Acid Herbicides

Jack M. Rosenfeld and Y. Moharir

INTRODUCTION

Solid supported processes are a standard approach to simplifying sample preparation for determination of organic contaminants in the environment and are now almost a standard feature of many such analytical procedures. All aspects of sample preparation have been performed on solid supports. Columns of reverse phase supports have been used for primary isolation of organics from water.¹ Separation of analytes from interferences has carried out on normal phase supports such as silica gel.^{2,3} In addition to these chromatographic techniques, solid supported reactions were used effectively in the determination of stable compounds such as dioxins or polychlorinated biphenyls. After primary isolation, the labile components of the isolates were destroyed by solid supported oxidation reagents. In this technique oxidizing agents, such as concentrated sulfuric acid or potassium perman-

ganate, are deposited onto the surface of silica gel.⁴ When an isolate is passed over, such solid supported reagent compounds that are susceptible to oxidation are destroyed, whereas the more stable analytes are recovered.

In addition to the simplifying manual techniques, solid supported processes have also been preferred in automated systems for sample preparation. For example, one of the first automated sample preparation techniques was based on the isolation of organics from plasma via adsorption on XAD-2 a styrene-divinyl-benzene cross-linked copolymeric macroreticular resin.⁵ Use of in-line and off-line solid supported reactions in automated and semiautomated determination of drugs by high pressure liquid chromatography has been described and reviewed.^{6,7}

We reported preparation of electrophoric derivatives for gas chromatography by solid supported reactions. Carboxylic acids and phenols were derivatized directly from aqueous phase⁸⁻¹⁰ or with prior adsorption¹¹⁻¹³ using XAD-2 as the solid support. The lipophilicity of the analyte was one determinant of the reaction rate. More lipophilic compounds which were readily adsorbed from water reacted faster than more hydrophilic species. The treatment of the resin during preparation with either hydrochloric acid or ethylene diamine tetraacetic acid also had a major effect on reaction yield. Both of these treatments remove metals adsorbed on the surface of the resin,⁹ and when the amount of metals on the resin surface is reduced, the reaction yield is also reduced. From these two sets of data, it was argued that the resin functioned both as an adsorbent and the adsorbed metals as catalysts.⁹

Previous work focused on sample preparation from biological material but appeared to have application to the determination of chlorophenoxy acetic acid herbicides and their phenolic breakdown products from drinking water. Derivatization is an important step in sample preparation of aqueous samples for determination of these analytes. The principal reactions reported to date for purposes of gas chromatographic determination of parent herbicides and corresponding phenols are pentafluorobenzoylation as well as silylation with cyano-containing reagents.^{14,15} Derivatization with pentafluorobenzyl bromide (PFBBBr), however, is currently used in a standard EPA procedure, but the process is complex and involves use of toxic catalysts.¹⁴

To circumvent some of these problems and to provide a basis for automating sample preparation, pentafluorobenzoylation of these analytes directly from water using XAD-2 supported reactions was investigated. In conjunction with the simultaneous isolation/derivatization procedure, we also developed a procedure for in-line chromatographic separation of derivatized analytes from each other and from interferences.

EXPERIMENTAL

Apparatus

The pentafluorobenzyl (PFB) derivatives of pure analytes were determined on a Hewlett-Packard (H-P) 5790 GC equipped with a pulse linearized ECD and a J & W fused capillary column DB-1, 30 M × 0.321 mm with film thickness 0.25

μm . The output of the detector was monitored on a H-P 3390A recording integrator. Hydrogen was used as a carrier gas with linear velocity of 62 cm/sec at 180°C and 10% methane in argon was used as a makeup gas at a flow rate 15 mL/min.

Reagents

Pentafluorobenzyl bromide was purchased from Caledon Laboratories, Georgetown, Ontario. The macroreticular resin, XAD-2, a cross-linked copolymer of styrene/divinylbenzene was obtained from BDH Laboratories, Toronto, Ontario, and was cleaned and stored as previously described.^{2,3} Florisil and basic alumina were purchased from Supelco (Canada) Oakville Ont. Disposable 1-mL Supelclean columns used for packing the Florisil and basic Alumina semipreparative column and a vacuum module were also purchased from Supelco (Canada) Oakville Ont. Solvents were purchased from the usual commercial suppliers, such as Fisher, BDH, and Aldrich Canada. Pure analytes were obtained from the EPA Repository.

All glassware was silylated by standard procedures. Glassware and plasticware were washed with methylene dichloride, methanol, acetonitrile, and dried prior to use.

Preparation of Pentafluorobenzyl Derivatives

The PFB derivatives of pure analytes were prepared by stirring the organic acid in acetone with PFBBBr and K_2CO_3 at ambient temperature for 18 hr. Reaction work-up consisted of evaporating the acetone, extracting the residue with CH_2Cl_2 and finally washing the organic phase with distilled water. The PFB esters were purified by thin-layer chromatography.

Derivatization and Isolation

Three hundred milligrams of XAD-2 were added to a 16 \times 100 mm screw cap vial and wetted with 300 μL of acetonitrile. Four milliliters 0.1 *M* of phosphate buffer at pH 7.4 were added to these vials. For the initial studies all four model compounds were added at a concentration of 1.25 $\mu\text{g}/\text{mL}$. For studies on the chromatographic separation, the investigation was carried out on solutions of buffer containing 5 ng/mL of each of the following: 2,4-dichlorophenol (2,4-DiClPh), 2,4,5 trichlorophenol (2,4,5-TriClPh), and 2,4-dichlorophenoxy acetic acid (2,4-DiClPAA).

The reaction was initiated by adding 150 μL of a solution of PFBBBr in hexane (1/9 v/v), and the reaction mixture was shaken for 2 hr in a water bath at 40°C. After this time the resin was isolated by filtration in a 5-mL Supelclean cartridge and washed with distilled water and the water removed by suction. For the studies of the reaction characteristics, the analytes were eluted directly from the resin with hexane, followed by CH_2Cl_2 , and then 10% EtOH/Et₂O (v/v).

For experiments on chromatographic separation, a different procedure was used. After removal of bulk water by filtration, 100 μL of acidified 2,2-dimethoxypropane

was added as a water scavenger and allowed to remain in contact with the resin for 15 min. Excess scavenging reagent and products of hydrolysis (acetone and methanol) were removed with a gentle stream of nitrogen at room temperature. The cartridge was then inserted linked in series to a 1-mL cartridge containing Florisil and a 1-mL cartridge containing basic alumina. Derivatized phenols were eluted from the XAD-2-Florisil-alumina link with 30 mL (three column volumes) hexane/toluene (95/5 v/v). The Florisil and Alumina columns were split. In one experiment the PFB ester of 2,4-DiCIPAA was eluted with 30 mL 25% and 30 mL 50% CH_2Cl_2 in hexane. In a second experiment the Florisil column was linked to a silica gel column and the link was washed with 30 mL 25% and 30 mL 50% CH_2Cl_2 in hexane; analyte eluted in the latter eluant.

Gas Chromatography

Samples were analyzed by gas chromatography with electron capture using the column described earlier and the following temperature conditions: 170 to 215°C at 4°C/min; 215 to 300°C at 20°C with a 2-min hold at 300°C.

Calculation of Yield

Reaction yield was calculated based on recovery of radiolabel when the reaction was carried out with C^{14} 2,4-DiCIPAA. The PFB ester, but not parent 2,4-DiCIPAA eluted from the chromatographic systems described earlier, accordingly recovered radiolabel represented reaction yield for carboxylic acids.

RESULTS AND DISCUSSION

Definition of the Problem

Development of analytical techniques for determination of herbicides and related compounds requires that several distinct problems be addressed. First, the herbicides are carboxylic acids, but the degradation products are phenols and both functionalities must be derivatized. In principle, under alkaline conditions, the weak acid (phenol) and strong (carboxylic) acid would be ionized and would react. Second, numerous interferences are found in surface water, drinking water, and on laboratory glassware. The most common are mammalian fatty acids which are derivatized to electrophoric derivatives¹⁶ and material found in plastic-ware such as phthalates that is endogenously electrophoric.¹⁷

Simultaneous Adsorption/Derivatization

The derivatization of chlorophenoxy acetic acids and corresponding phenols was investigated as an approach to development of a simultaneous determination of all pertinent analytes. Model compounds studied were 2,4-DiCIPh, 2,4,5-TriCIPh, and 2,4-DiCIPAA. Derivatization of organic acids in heterogeneous aqueous/organic systems requires that the pH is sufficient to ionize the acid; and at alkaline pH,

Table 1. Derivatives Recovered from Different Reaction and Chromatographic Conditions

Analytes	Aqueous Phase		Normal Phase Used for Chromatography	
	0.1 N NaOH	0.1 M Phosphate Buffer pH 7.4	Florisil	Alumina
		No product		
Phenols ^a	PFB-ether	No product	PFB-ether	PFB-ether
2,4-DiCIPh	PFB-ether	PFB-ether	PFB-ether	PFB-ether
2,4,5-TriCIPh	PFB-ether	PFB-ether	PFB-ether	PFB-ether
Acids ^b	PFB-ester	PFB-ester	PFB-ester	PFB-ester
2,4-DiCIPAA	No product	PFB-ester	PFB-ester	No product

^a e.g., Cannabinoids;^{11,13} indoleamines.⁸

^b Straight saturated and unsaturated carboxylic acids with 9 to 24 carbon atoms;^{9,10} carboxylic acid metabolites of cannabinoids.¹³

both the chlorophenols and 2,4-DiCIPAA should be expected to react. In our hands, however, the PFB ester of 2,4-DiCIPAA was not recovered at alkaline conditions. As expected, however, the PFB ethers of 2,4-DiCIPh, 2,4,5-TriCIPh and penta-chlorophenol were formed and isolated (Table 1).

The reason for this is not clear. It may be that the parent 2,4-DiCIPAA or the PFB ester is unstable to alkaline conditions. This possibility was suggested by the fact that the PFB ester of 2,4-DiCIPAA could not be recovered from chromatography on basic alumina, but was recovered from Florisil. This was the only PFB derivative that could not be successfully chromatographed on the alkaline normal phase. The requirement of simultaneous adsorption and derivatization of parent herbicide and the phenolic breakdown products was not met under the usual conditions that would be expected for derivatization of carboxylic acids and phenols.

Unlike all other phenols studied to date,^{8,11,13} however, it was possible to effect simultaneous adsorption/derivatization of the chlorophenols with PFBBr on XAD-2 at pH 7.4. This reflects the lower pKa of the halogenated compounds. Since carboxylic acids readily react at this pH, both parent herbicide and the degradation product could be isolated as the PFB esters under the identical reaction conditions.

Derivatization of analytes, while necessary, was insufficient for developing methods of high sensitivity. The matrix of lipophilic compounds that can interfere, even when limited to ordinary laboratory reagents and water, is quite complex. Separation of derivatized analyte from interferences was essential particularly if natural waters (e.g., well water) are to be analyzed.

Chromatographic Separation

A primary requirement of any separation technique is effective transfer of analyte to the chromatographic phase. In the case of solid supported reaction, such transfer involved two steps: elution from the resin in high yield and transfer to the normal phase without undue spreading of the derivative over the length of the column, thus reducing the effectiveness of the chromatographic procedure. This combination of requirements dictated the elution from the resin in the most lipophilic solvent possible and this required development of effective drying conditions.

After derivatization the reaction products remain adsorbed on a surface that is coated with water. The coating of water inhibits contact of eluant with the resin surface, thus making the elution inefficient. As a result, 50 to 70% of derivatized analyte is eluted in hexane while the remainder requires elution with increasingly more polar solvents, which also dissolves some of the water retained on the surface (Table 2). If the latter group of solvents were used to elute from the resin onto normal phase, there would be no effective separation of derivatized analyte from interferences because such solvents are very powerful eluants.

The first step of the separation problem was thus drying of the resin; a standard requirement following adsorption of analyte from water using a reverse phase column composed of alkylsilica or XAD-2. This is usually performed by heating in conjunction with exposure to a stream of nitrogen or by exposing the solid support to a vacuum and preferably with a flow of nitrogen. Such a procedure, however, cannot be used when determining the low molecular weight, and hence volatile, analytes under investigation. Accordingly, a water scavenger, acidified 2,2-dimethoxypropane (which reacts with water to form acetone and methanol) was added to the resin. After treatment of resin with this reagent the residual 2,2-dimethoxypropane, methanol, and acetone could be evaporated with a slow flow of nitrogen, at room temperature and at atmospheric pressure. When the resin was dried in this manner, all the analytes eluted from the resin in hexane without interference from residual water, drying agent, or reaction products. This hexane eluate was then directly transferred to a column of Florisil and all reaction products (PFB derivatives of analytes and interferences) eluted from the resin were found to be retained on this normal phase. Two successive washes with 5 mL of hexane did not remove the derivatives from the Florisil.

Florisil alone, however, was not effective at separating the PFB derivatives of the phenolic analytes from the interferences since both these products eluted with 5% Toluene in hexane (Figure 1A). As a result a linked system consisting of an XAD-2-Florisil-basic alumina was investigated. This linked system allowed isolation of PFB ethers in a cleaner isolate (Figure 1B) with the alumina retaining some of the interfering compounds.

A difficulty was encountered with PFB ester of 2,4-DiCIPAA which could not be recovered from this basic alumina (Table 1). The unexpected behavior for this PFB derivative necessitated further development of the linked system. In the first modification, the alumina column was removed after elution of the PFB-ethers of

Table 2. Elution of PFB Derivatives from XAD-2 Without Using a Drying Procedure

Analyte	Percent of Total Recovered PFB Derivative in Solvents Used to Wash XAD-2		
	Hexane	CH ₂ Cl ₂	10% EtOH/Et ₂ O
2,4-DiCIPh	60	15	25
2,4,5-TriCIPh	60	30	10
2,4-DiCIPAA	50	25	24

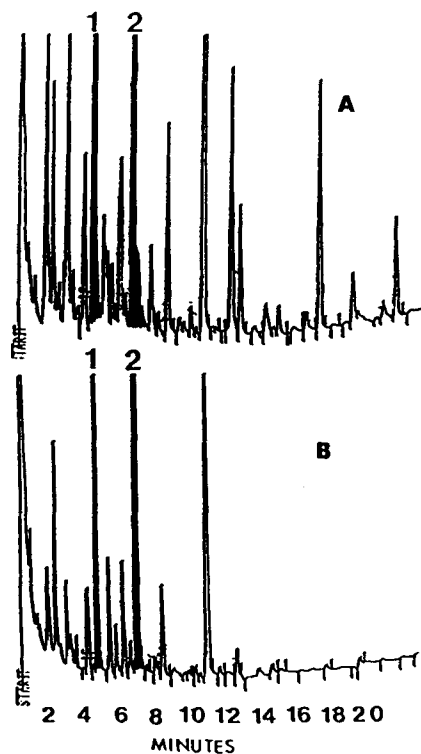


Figure 1. GC/ECD traces of the chlorinated phenol fraction from: (A) the XAD-2 reactor bed-Florisisil link and (B) XAD-2 reactor bed-Florisisil-basic alumina link. Peaks corresponding to PFB ethers of 2,4-dichlorophenol (1) and 2,4,5-trichlorophenol (2) are darkened.

the chlorophenols and the PFB ester of 2,4-DiCIPAA was then eluted from the Florisisil with 25% CH_2Cl_2 in hexane, which produced only a partial recovery (40 to 60%), and 50% CH_2Cl_2 in hexane, which eluted an additional 30 to 40% of the product. There was little separation of analyte from interferences (Figure 2). As expected, the major interferences could be attributed to PFB esters of the mammalian fatty acids — dodecanoic acid, tetradecanoic acid, hexadecanoic (palmitic), acid octadecanoic (stearic) acid, and unsaturated octadecanoic (linoleic and linolenic) acids. Separation of analyte from interferences was not improved by elution with different solvent systems.

The PFB ester of 2,4-DiCIPAA, however, could be considerably purified by linking the Florisisil column to a silica gel column. In this case, the analyte was eluted from the XAD-2-Florisisil-silica gel link. A substantial proportion of the interferences were eluted with 25% CH_2Cl_2 in hexane (Figure 3A), and the PFB ester of 2,4-DiCIPAA was eluted with 50% CH_2Cl_2 in hexane (Figure 3B) from this linked system.

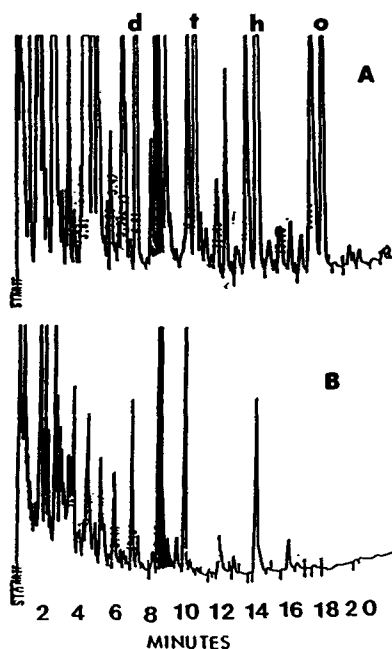


Figure 2. GC/ECD traces of eluates from the XAD-2 reactor bed-Florisil link: (A) 25% CH_2Cl_2 /hexane and (B) 50% CH_2Cl_2 /hexane. Peak corresponding to PFB ester of 2,4-dichlorophenoxy acetic acid is darkened. PFB esters of: d = dodecanoic acid, t = tetradecanoic acid, h = hexadecanoic (palmitic) acid, and o = octadecanoic (stearic) acid.

The schematic diagram for the separation of the PFB ethers of the chlorophenols and the PFB ester of 2,4-DiCIPAA from each other and from the interferences is shown in Figure 4.

Despite the extensive chromatography, the yield of PFB ester of 2,4-DiCIPAA is 66 ± 5 ($n = 6$) for the entire process. In ten experiments spread over several weeks, the phenolic analytes could be reproducibly recovered in the 5% toluene in hexane eluants from the Florisil/alumina-linked columns and after splitting the link, and acidic fractions were recovered in the 50% CH_2Cl_2 in hexane eluant from the XAD-2-Florisil-silica gel link.

FUTURE DIRECTIONS

This work has shown that it is possible to use solid supports for simultaneous isolation and derivatization of organic acids from water. Use of solid supports simplifies sample preparation because the isolation/reaction requires only agitation and work-up involves isolation of the reactor bed filtration and elution. By eluting onto a chromatographic support, the recovery of the derivatives from the reactor bed can be combined with chromatographic separation. Use of water-compatible solid supports, chemical drying, and in-line chromatographic purification are steps that are rugged and can readily be combined into automated techniques.

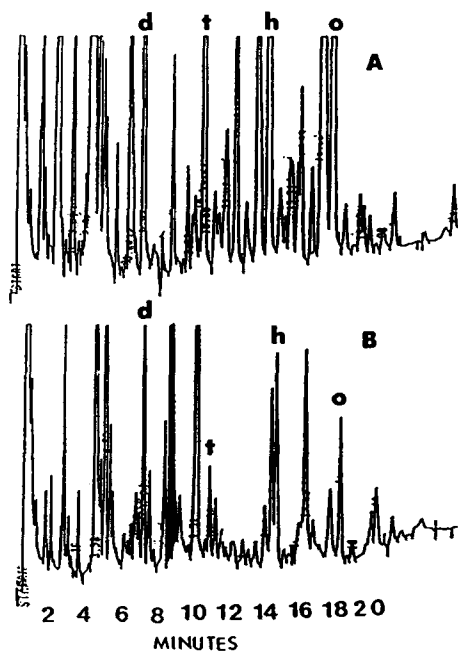


Figure 3. GC/ECD traces of eluates from the XAD-2 reactor bed-Florisol-silica gel link: (A) fatty acid fraction and (B) chlorophenoxyacetic acid fraction. Peak corresponding to PFB ester of 2,4-dichlorophenoxy acetic acid is darkened. PFB esters of: d = dodecanoic acid, t = tetradecanoic acid, h = hexadecanoic (palmitic) acid, and o = octadecanoic (stearic) acid.

Future investigations will focus on methods to increase the reaction rate and to improve separations. Recent developments that could prove important in these studies are the commercial availability of XAD-16 which, like XAD-2, is a polyaromatic, but with a specific surface area that is 2.5 times larger. This would increase the binding of analyte to the surface and would therefore be expected to increase the reaction rate. Separations of the derivatized analytes from interferences may be greatly enhanced by the highly efficient Empore disks. These disks are also designed to reduce the amount of solvent required to elute the derivatized analytes and this is expected to increase speed of analysis and reduce costs.

One of the difficulties with applying the technique to the analysis of environmental samples is the slow reaction rate of the polar analytes.^{9,12,13} The current lack of understanding of the reaction mechanism requires that optimization of yield and rate be carried out empirically; however, this approach has limitations. A delineation of the reaction mechanism would be useful in this regard. Another problem is the organic acids that can be present in the environment. These will derivatize in conjunction with the phenoxyacid herbicides as well as the chlorophenols. A possible approach to this problem was described using the fatty acids that are present on laboratory glassware, but the concentration in the environment can be expected to be considerably higher. Analysis of such samples may require more power separation techniques such as supercritical fluid extraction or chromatography.

5. St. Onge, L. M., E. Dolar, M.-A. Anglim, and C. J. Least. "Improved Determination of Phenobarbital, Primidone, and Phenytoin by Use of a Preparative Instrument for Extraction, Followed by Gas Chromatography," *Clin. Chem.* 25(8):1373—1376 (1979).
6. Xie, K.H., S. Colgan, and I. S. Krull. "Solid Phase Reactions and Derivatization in HPLC," *J. Liq. Chromatogr.* 6(s-2):125—151 (1983).
7. Colgan, S., I. S. Krull. "Derivatization of Ethylene Bromide with Silica-Supported Silver Picrate for Improved High-Performance Liquid Chromatographic Detection," *Anal. Chem.* 58:2366—2372 (1986).
8. Rosenfeld, J. M., G. M. Brown, C. H. Walker, and C. H. Sprung. "Use of Impregnated Reagents in the Pentafluorobenzoylation of Indoleamine Metabolites," *J. Chromatogr.* 325:309—313 (1985).
9. Rosenfeld, J. M., M. Mureika-Russell, and S. Yeroushalmi. "Solid Supported Reagents for the Simultaneous Extraction and Derivatization of Carboxylic Acids from Aqueous Matrix," *J. Chromatogr.* 358:137—146 (1986).
10. Rosenfeld, J. M., M. C. Orvidas, and O. Hammerburg. "Simplified Methods for the Preparation of Microbial Fatty Acids for Analysis by Gas Chromatography with Electron Capture Detection," *J. Chromatogr.* 378:9—17 (1986).
11. Rosenfeld, J. M., R. McLeod, and R. L. Foltz. "Solid Supported Reactions in the Determination of Cannabinoids," *Anal. Chem.* 58:716—721 (1986).
12. Rosenfeld, J. M., M. Love, and M. Mureika-Russell. "Solid Supported Sample Preparation Method for Prostaglandins: Integration of Procedures for Isolation and Derivatization for Gas Chromatographic Determination." *J. Chromatogr.* 489:263—272 (1989).
13. Rosenfeld, J. M., Y. Moharir, and S. D. Sandler. "Selective Sample Preparation for the Determination of 11-Nor-9-Carboxy-delta-9-Tetrahydrocannabinol from Human Urine by Gas Chromatography with Electron Capture Detection," *Anal. Chem.* 61:925—928 (1989).
14. Federal Register Part VIII. Environmental Protection Agency 58 (1984).
15. Bertrand, M. J., A. W. Ahmed, B. Sarrasin, and V. N. Mallet. "Gas Chromatographic and Mass Spectrometric Determination of Chlorophenoxy Acids and Related Herbicides as Their (Cyanoethyl)dimethylsilyl Derivatives," *Anal. Chem.* 59:1302—1306 (1987).
16. Greving, J. A., J. H. G. Jonkman, De Zeeuw. "Determination of Carboxylic Acids in the Picomole Range After Derivatization with Pentafluorobenzyl Bromide and Electron Capture Gas Chromatography," *J. Chromatogr.* 148:389—395 (1978).
17. Junk, G. A., M. A. Avery, and J. J. Richard. "Interferences in Solid Phase Extraction Cartridges Using C-18 Bonded Porous Silica Cartridges," *Anal. Chem.* 60:1347—1350 (1988).



Taylor & Francis

Taylor & Francis Group

<http://taylorandfrancis.com>

CHAPTER 15

A Surface Acoustic Wave Piezoelectric Crystal Aerosol Mass Microbalance*

W. D. Bowers and R. L. Chuan

The feasibility of applying surface acoustic wave (SAW) piezoelectric crystal technology to the measurement of subnanogram levels of particles and parts-per-million levels of sulfur dioxide has been demonstrated. Improvements necessary for implementing the development of a practical instrument for the real-time measurement of very low aerosol mass and ambient gases have been identified. Mass sensitivity comparisons of a 158-MHz SAW piezoelectric microbalance and a conventional 10-MHz quartz crystal microbalance (QCM) showed that the SAW crystal was 266 times more sensitive. This is in good agreement with the theoretical value of 250. Frequency stability of a single SAW resonator was six parts in 10^8 over 1 min.

Response to temperature change is found to be very linear over the range +30 to -30°C . Response to pressure change is found to exhibit an aging effect whereby

* Reprinted by permission of the American Institute of Physics. The majority of this chapter first appeared in *Rev. Sci. Instrum.*, 60, 1297, 1989.

after one complete cycle of pressure variation from 1 atm to 70 mmHg and back to 1 atm, the SAW response to pressure change decreases by an order of magnitude. A strong response to 15 ppm SO₂ has been demonstrated on a chemically coated SAW crystal. With improvements, SO₂ measurements at the parts-per-billion level should be achievable.

INTRODUCTION

In situ measurement and collection of aerosol particles in the upper atmosphere have been conducted by NASA teams on a continuing basis since 1979, as a part of a broader research program in the climatic effects of stratospheric aerosols and gases. During the ensuing years the general characteristics of these aerosols have been established. They appear to be delineated into three groups by size and composition, with the two upper-size groups being made up predominantly of volcanic eruption materials, and the third, a small particle group yet unidentified as to origin. There is no clear evidence that any of the three groups is anthropogenic in origin. As we look into the future course of this type of research, two areas need to be addressed. One is the question of the conversion of sulfur dioxide gas to sulfuric acid or sulfates, and the other question is the identification and origin of the very fine particles which are generally carbon rich. A principal instrument for the characterization of stratospheric aerosol particles has been the QCM cascade impactor which collects and weighs particles in up to 10 size bands.¹⁻³ The development of the QCM instrument, to a significant extent supported by NASA,^{4,5} has resulted in its use in diverse research areas in numerous laboratories in the United States and Western Europe.

It now appears that for the pursuit of the two problems cited here the capability of the QCM-type instrument should be improved in two areas: higher sensitivity, in order to measure the mass of the very small particles, and the ability to measure certain gases (particularly SO₂) concurrently with measurement of sulfates in order to address the question of gas-to-particle conversion. This improvement is possible through the adaptation of a new type of piezoelectric crystal device, commonly referred to as the SAW device, which potentially can be three orders of magnitude more sensitive than the conventional bulk piezoelectric device as used in the QCM instrument.

The application of the SAW device in mass-measuring instruments has been principally in the area of chemical sensing, in which a reactive coating applied to the surface of a SAW device responds specifically to a given gas through a mass change which, in turn, results in a frequency change.^{6,7} There has been increased research activity in the last several years in the analytical chemistry community based on the SAW technology.⁸⁻¹¹ We report here our initial work in demonstrating the feasibility of using a SAW crystal to detect aerosols,¹⁶ followed by a brief discussion of our most recent work describing the next generation of particulate mass sensing instrument based on a new 200 MHz SAW resonator which has a lower limit-of-detection of 3×10^{-12} g.

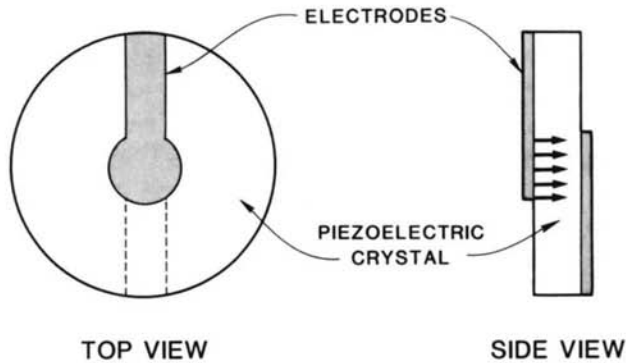


Figure 1. 10-MHz piezoelectric crystal excitation is across the bulk crystal.

PRINCIPLE OF OPERATION

In the piezoelectric crystal used as the sensing element in the QCM instrument, the electric-field-excited mechanical oscillation takes place within the bulk of the crystal, since the driving electrodes are placed across the crystal, as depicted in Figure 1. The electric field is applied across the crystal disc. Depending on the orientation of the crystal axes with respect to the electric field vector, different modes of vibration can be excited. The shear mode excited in the so-called AT-cut crystal is particularly sensitive to the thickness (or mass) of the crystal and is the one used for mass sensing. The sensitivity of the crystal is proportional to the square of its frequency in the fundamental mode, f_0 :

$$\Delta f = \alpha f_0^2 \Delta m/A \quad (1)$$

where α is a constant, $\Delta m/A$ is the change in mass per unit area on the crystal which produces a frequency change Δf . For a 10-MHz AT-cut crystal, the sensitivity reduces to about 10^9 Hz/g. This is about the practical limit for a piezoelectric crystal operating in bulk vibration. To increase the fundamental frequency (and thereby the sensitivity) would mean reducing the thickness of the crystal. A 10-MHz crystal has a thickness of about 0.015 cm; any thinner crystal would be much too fragile to be of any practical value.

There is, however, a different mode of excitation of a piezoelectric crystal that produces a much higher frequency (for the same thickness or more) and this is the Rayleigh mode surface acoustic wave. In this mode of operation the electrodes are placed on the same side of the crystal, Figure 2, so that the electric field, instead of being directed normal to the surface, is parallel to and penetrates only a shallow depth into the crystal, Figure 2. This mechanism has been described in detail by Wohljen.^{6,7}

When two sets of interdigital electrodes are placed over a crystal at a distance L apart, a standing wave is set up if $L = N\lambda$, where N is an integer and λ is the

wavelength of the surface acoustic wave. The frequency f is equal to v/λ , where v is the surface acoustic wave phase velocity. The wavelength is dependent on the spacing, s , between the interdigital electrodes, being twice the spacing. The surface velocity for quartz is about 3000 m/sec. Thus, if electrodes can be spaced a distance 15 μm apart, $f = v/2s = 10^8 = 100$ MHz. SAW crystals operating greater than 200 MHz have been fabricated and used for gas vapor detection.¹² Compared to the 10-MHz AT-cut bulk piezoelectric crystal in use now, the sensitivity can be increased by up to three orders of magnitude. The thickness of this type of crystal is about 1 mm, which makes it quite robust, in fact, much more so than the 10-MHz AT-cut crystals used in the QCM.

With photolithographic techniques it is fairly easy to produce closely spaced electrodes. Furthermore, by depositing two sets of electrodes on the same crystal blank, it is possible to use one set for sensing and the other set for temperature and pressure compensation, such as depicted in Figure 3, and produce a beat frequency, as is done now in the QCM with two separate crystals. There should be no problem with depositing aerosol particles on the surface (either adhesive coated or not) as has been done with the current QCM instrument to make particle mass measurements.

EXPERIMENTAL

The SAW device used in these investigations was purchased from Microsensor Systems, Inc. (Fairfax, VA). The unit consists of the dual RF drive electronics, model RFM-158A, dual RF buffer amplifier/power supply/coating fixture, model

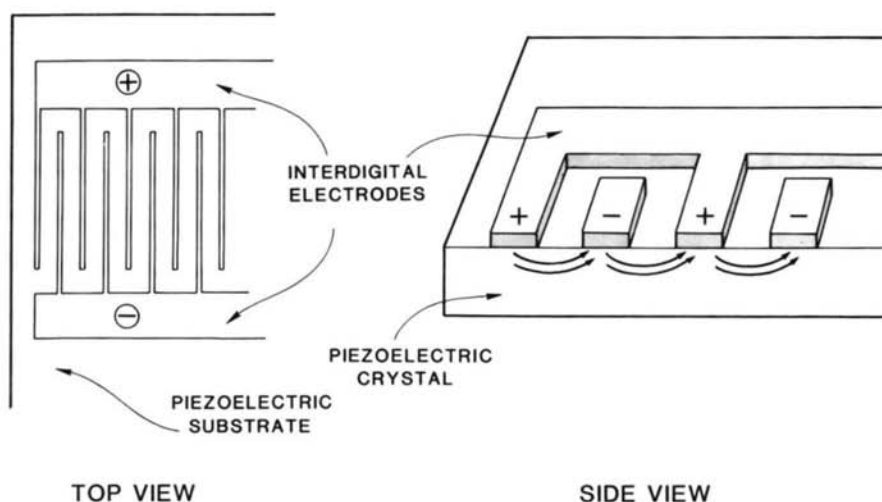


Figure 2. SAW piezoelectric crystal excitation is parallel to the surface of the crystal. (a) Close-up view of interdigital electrodes on surface of crystal; (b) cut-away side view illustrating RF excitation is along the upper most surface layer of the piezoelectric crystal.

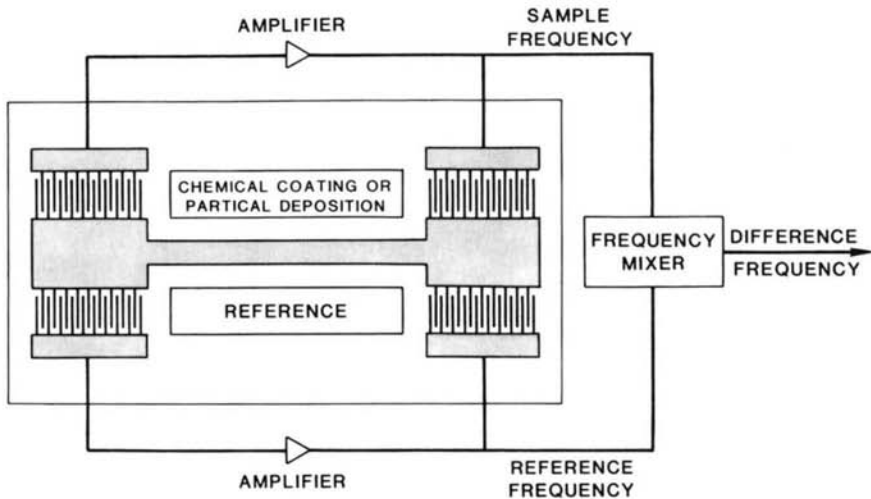


Figure 3. The signal from the particle deposition side and/or coated delay line is mixed with the signal from the reference and the difference frequency monitored.

SPM-158, and dual 158-MHz SAW sensor, model SD-158A. The 158-MHz SAW sensor is comprised of two independent SAW oscillators fabricated on a single piece of quartz and mounted on a TO-8 type header which fits into a 12-pin socket on the RF drive electronics board. The signals generated by the two individual SAW delay lines are mixed electronically to produce a frequency that is the difference between the two delay lines. This frequency is then processed into a TTL-compatible signal and displayed on a conventional frequency counter, Phillips PM 6674/02.

The mass sensitivity comparison was made between the SAW crystal and a conventional 10-MHz QCM instrument in a side-by-side comparison. For the SAW device, aerosol particles were deposited onto the center portion of the region between the two sets of interdigital electrodes (Figure 3). A standard-stage 8 nozzle, designed for a flow rate of 2 L/min, was used to deposit the particulates. This is the same nozzle normally found in the QCM and used for NASA Langley aerosol research. The aerosol mass concentration is measured with a standard laboratory type California Measurements PC-3 10-stage QCM with only the stage 8 nozzle in place. The air sample is delivered to the two systems by a single pump to assure identical air samples in both devices.

Chemically coated SAW crystals and 10-MHz QCM crystals were challenged with SO_2 vapor and their responses compared. A 15-ppm SO_2 test vapor was generated using a permeation tube (VICI Metronics) at room temperature. The air carrier gas was dehumidified using Drierite followed by a particulate filter before use. In the "bypass" position, the dry and particulate-free airstream flows over the permeation tube, into a four-way valve, and out to a charcoal filter. A second dry and particulate-free airstream is drawn through the remaining side of the four-way

valve, through the QCM or over the SAW crystal depending on which crystal was being challenged and into another charcoal filter. When the valve is switched to the "challenge" position, the SO₂ airstream is diverted to the coated sensor, absorbed by the coating, resulting in a frequency shift, and detected. After 15 to 30 sec, the valve is returned to the bypass position and clean air flushes the coated crystal.

RESULTS AND DISCUSSION

We define the sensitivity of the piezoelectric device as $\sigma = -\Delta f/\Delta m$, where Δf is the frequency change due to an addition of Δm in mass. The limit of detection (LOD) is $L = (3/\sigma)\delta f$, which is the least count in mass increment for a least count of frequency, δf . Since the sensitivity is proportional to the square of the frequency, Equation 1, and if $f_s =$ SAW frequency and $f_b =$ bulk crystal frequency, then $\sigma_s/\sigma_b = (f_s/f_b)^2$ and $L_s/L_b = (\delta f_s/\sigma_s)(\sigma_b/\delta f_b)$. Substitution and rearrangement gives $L_s/L_b = (f_b/f_s)^2 (\delta f_s/\delta f_b) = (f_b/f_s)(\delta f_s/f_b)(f_b/\delta f_b)$. The quantity $\delta f/f$ is the stability of the piezoelectric device. For the QCM, at $f_o = 10^7$ Hz, the stability is about one part in 10^7 over a 10-min period, which implies a detection limit of 3×10^{-9} g (for $\sigma_b \approx 10^9$ Hz/g). For the 158-MHz SAW device, its sensitivity would be $(f_s/f_b)^2 = (15.8)^2 = 250$ times greater than the QCM. In order to lower the detection limit by two orders of magnitude, 3×10^{-11} g, it would require, using the relationship described here, a SAW frequency stability of 1.5 parts in 10^8 . When two SAW crystals are used in dual-difference mode, the stability of the beat-frequency would be two parts in 10^8 .

The SAW crystals were used as received and aged for several days at room temperature before use as recommended by Microsensor, Inc. Once aged, the difference frequency of the two delay lines was monitored to determine the frequency stability of the sensor. The stability of the SAW device was found to be one part in 10^7 over a several second period which is acceptable for the detection of gaseous vapors. However, the measurement of particulates typically requires several minutes to collect sufficient sample and it was found that the stability was eight parts in 10^5 over 5 min. The individual SAW delay lines were then monitored and the same instability was observed. Under these conditions the SAW only possesses a LOD 2.5 times lower than the QCM.

It was discovered during the initial stages of the SAW mass calibration that the frequency fluctuations decreased drastically when one of the SAW delay lines stopped oscillating due to a mass overload. This behavior was investigated further and it was found that a frequency stability of six parts in 10^8 over a 1-min period was obtained when one of the delay lines was overloaded with a thick grease.

Since a stable oscillation could be obtained with a single delay line, the two delay lines must be interacting resulting in the instability. Outside evaluation of the 158-MHz delay line confirmed that there was cross-talk between the two delay lines and this was the main cause of the frequency instability.¹⁵ All experiments described here were performed using a single delay line and monitoring the fundamental frequency and recording the frequency every second.

Temperature and Pressure Effects

Since the SAW microbalance must operate in a variety of environments, the 158-MHz SAW crystal was evaluated over wide ranges of temperature and pressure to investigate its stability and performance. First, the stability of the SAW device was examined as a jet of air impinged upon it. Just as in the case of the QCM 10-MHz bulk crystal, the impingement of an air jet results in a finite but small and unchanging shift in the frequency. Whereas in the QCM this flow-induced frequency shift, in the case of stage 8 size band, is about 15 Hz, for the SAW crystal the change is about 100 Hz. In either case this has no effect on the measurement of mass deposition.

The effect of pressure was investigated by placing the entire SAW test fixture into a pressure chamber and the pressure varied from 760 to 70 mm Hg. The results of two pressure cycles are shown in Figure 4. Since there were temperature variations due to pump-down and repressurization, the end points have been corrected for frequency shift due to temperature change. There appears to be an aging effect in which the effect of pressure on the frequency diminishes as time goes on. Since this is the frequency of a single SAW resonator, and not the difference of beat

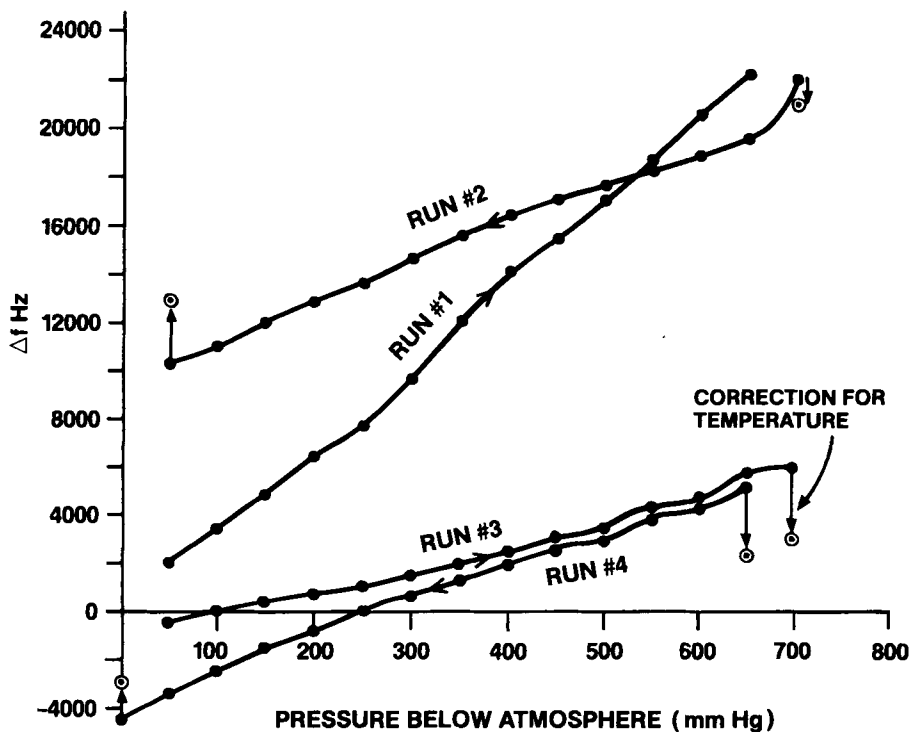


Figure 4. Response of 158-MHz SAW delay line with pressure.

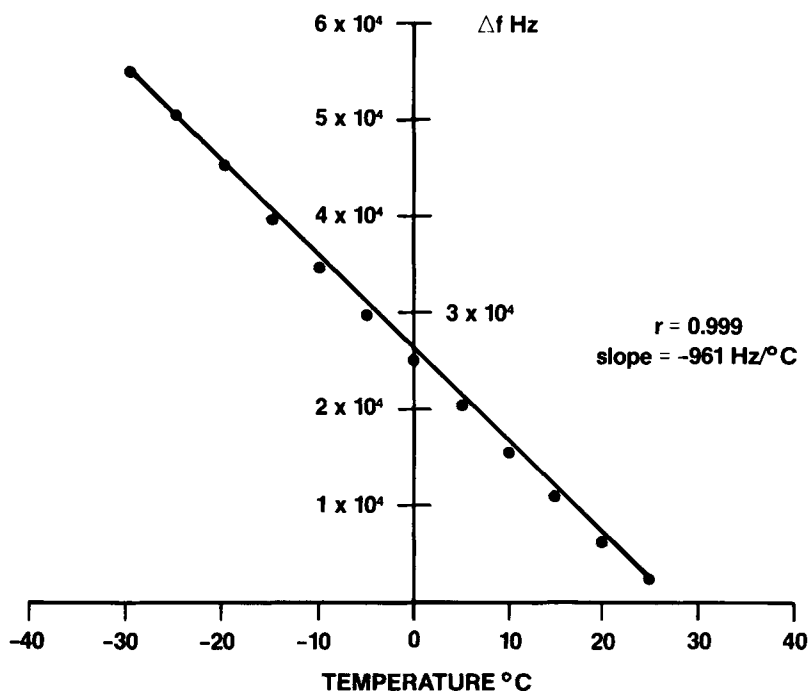


Figure 5. Response of 158-MHz SAW delay line with temperature.

frequency, the latter probably will exhibit even less pressure dependence as observed with the 10-MHz bulk crystal. In any event it appears from the data that once the instrument is at altitude for a few minutes, the pressure dependence of frequency should be negligible over the typical deviation from level flight of a few millibars. The aged slope in the data seems to be about 5 Hz/mmHg, which would be well within the overall noise band of any device.

The stability and performance characteristics of the SAW sensor were investigated from +30 to -30°C temperature range. A thermocouple was mounted on the aluminum bracket near the SAW crystal, and the entire SAW instrument placed in a large zip-lock plastic bag. The bag was loosely sealed around the AC power cable, signal out cables, thermocouple lead, and Tygon tube which supplied 500 mL/min dry purge air. The dry air purge was used to keep water vapor from freezing on the SAW device. This assembly was placed in a styrofoam chest containing dry ice, and the temperature and frequency readings were recorded. The response of a single SAW delay line versus temperature is shown in Figure 5.

The response is quite linear with a correlation coefficient of 0.999 at the 1% level and a slope of $-961 \text{ Hz}/^{\circ}\text{C}$ which corresponds to a 0.001% frequency variation for each degree Celsius. The linear response over this temperature range indicates that a second SAW delay line made on the same substrate and used as a reference would reduce the variation with temperature, as observed with the 10-MHz bulk crystal, and would be somewhat less than $100 \text{ Hz}/^{\circ}\text{C}$.

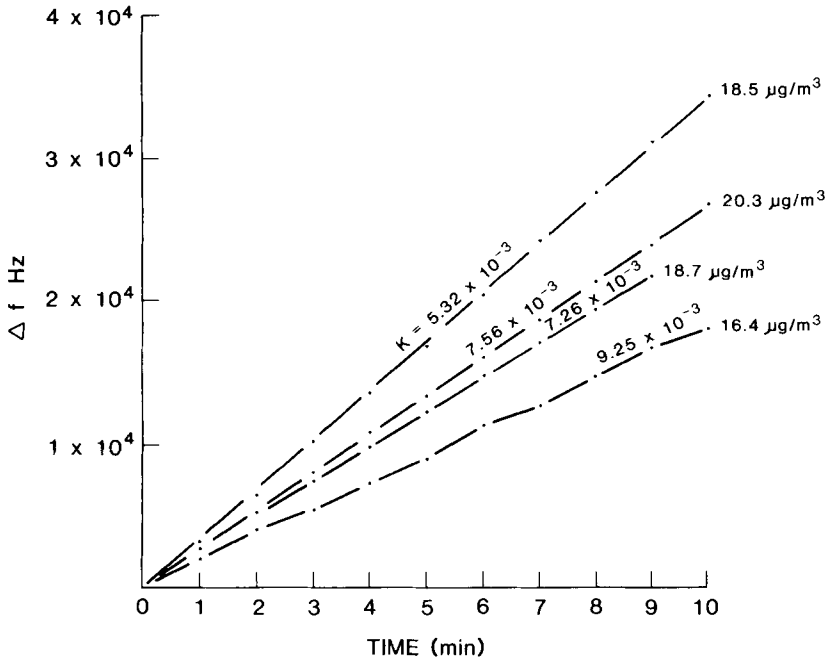


Figure 6. Aerosol mass accumulation on single 158-MHz SAW delay line.

Mass Sensitivity of SAW Crystal

As stated in Equation 1, the sensitivity of a piezoelectric device takes the form:

$$\Delta f = \alpha f_o^2 \Delta m / A \tag{1}$$

where α is a constant and A is the area over which mass is deposited. From this it is seen that the sensitivity is proportional to the square of the nominal frequency. Because the 10-MHz QCM is a well-established device with a history of calibration supporting its operation, it was used as a reference to calibrate the 158-MHz SAW device. As an aerosol mass measuring system the QCM operates with the relationship:

$$C = k \Delta f / \Delta t \tag{2}$$

where C is the aerosol mass concentration in $\mu\text{g}/\text{m}^3$; k the sensitivity coefficient which includes the factors α , f_o^2 , and A in the basic sensitivity equation plus the sampling flow rate; and $\Delta f / \Delta t$ is the frequency change rate in hertz per minute.

The results of four calibration runs are shown in Figure 6 in terms of frequency change with time at a constant aerosol concentration as measured with the PC-3 QCM. The sensitivity coefficient, k , for each run is shown and there are significant

variations in the value of k through these four runs. There are several possible explanations, some based on our experience with the conventional 10-MHz crystal. The most important is probably the location of the aerosol deposition on the SAW crystal. Between runs 1 and 2 the impaction nozzle was removed to allow the removal of the SAW crystal for cleaning. The sensing region between two sets of interdigital electrodes is about 0.22 mm, while the deposition spot measures about 1.20 mm. (The stage 8 impaction jet has a diameter of 0.8 mm, and the deposition spot is typically about 1.5 times the jet diameter.)

The changes in k from run 2 through 4 may be due to saturation effects, the nonlinear response of the crystal from overloading. This aspect of the behavior of the SAW crystal has not been specifically investigated, but is being addressed in our continuing studies of the device as an aerosol instrument.

The relative sensitivity of the SAW crystal over that of the bulk crystal can be derived from the k value. For the stage 8 setup, as was used in the calibration experiment:

$$C = k_Q (\Delta f/\Delta t)_Q \quad (3)$$

where $k_Q = 0.33$ if it is a bulk crystal. For the SAW setup:

$$C = 1/\beta k_s (\Delta f/\Delta t)_s \quad (4)$$

where $\beta = 0.233$ represents the ratio of the SAW sensing area to the impaction spot size. Using average values from run 1:

$$k_s = (18.5 \times 0.233)/3472 = 0.00124$$

$$k_s/k_Q = 0.00124/0.33 = 0.00376$$

Since k is inversely proportional to the crystal response sensitivity, αf_o^2 ,

$$(\alpha f_o^2)_s / (\alpha f_o^2)_Q = 1/0.00376 = 266$$

The theoretical sensitivity ratio is the ratio of the square of the nominal frequencies:

$$(158/10)^2 = 250$$

This difference of about 6% is considered acceptable, in view of the overall accuracies involved in the calibration scheme.

If we consider a sampling interval of 10 min, with a frequency/noise level of 10 Hz over that period, then a signal-to-noise ratio of 3 would lead to a frequency shift rate of 30 Hz/10 min and the corresponding aerosol concentration would be $C = 0.00124 \times 3 = 0.0037 \mu\text{g}/\text{m}^3$. For particles of 0.3- μm diameter and density of 1.6 g/cm^3 , this would be equivalent to a number density, N , of 0.16 cm^{-3} . If the frequency instability, especially that of the beat frequency, can be improved to

2 Hz, the minimum concentration that can be measured would be $C = 0.00074 \mu\text{g}/\text{m}^3$ and $N = 0.033 \text{ cm}^{-3}$.

Detection of Sulfur Dioxide

Preliminary investigations were conducted on the detection of SO_2 vapor at the low parts-per-million concentration level with the SAW sensor. Initially, work was carried out with a conventional bulk crystal operating at 10 MHz in order to compare the response characteristics between the two sensors.

10-MHz Bulk Crystal

Triethanolamine (TEA) was used as the liquid phase to coat the surface of the bulk piezoelectric crystal and the SAW device for the detection of SO_2 .¹³⁻¹⁴ The major interference in the detection of SO_2 with triethanolamine is water vapor. Therefore, all water vapor was removed from the airstream using Drierite. A small drop of 5% (w/w) TEA and methanol was placed on the crystal and the solvent allowed to evaporate. The TEA left on the surface of the crystal is smeared over the crystal surface with a Q-tip to provide an even coating over the crystal's active sensing area. The crystal is replaced in its housing and the QCM reassembled. The mass of TEA deposited is determined by the resulting frequency shift. Several coating thicknesses were investigated and their response to 15 ppm SO_2 vapor recorded.

The SO_2 vapor diffuses into the TEA coating on the crystal, increasing the mass load and the resulting frequency change detected. A rapid and reversible response is necessary if one wants to make several real-time measurements in a short time period. A 5 to 6 μg of coating of TEA gave a rapid linear response to SO_2 , with a frequency shift of 250 Hz. After 3 sec, nonlinearity began as the coating became saturated. When the SO_2 vapor was removed from the airstream, it took up to 5 min before baseline was achieved. This was with a 10- to 15-sec exposure to SO_2 .

Thinner coats, 0.8 and 0.9 μg , gave lower frequency shifts, 60 Hz, but achieved baseline in 1 to 2 min. The linear range of the thinner coatings were noticeably less than the thicker layers and seemed to be more susceptible to degradation by water vapor.

SAW Device

The 5% TEA solution was too concentrated to be used with the SAW device because a small aliquot severely overloaded the crystal and damped the oscillation. A 0.2% (v/v) TEA solution in methanol was prepared and used to coat the SAW crystal. The configuration of the SAW sensor made it difficult to coat only one of the delay lines due to their close proximity. Because we were only using one of the delay lines, the coating procedure was easier to perform. The SAW crystal was dipped into the TEA solution so that only one delay line was covered with the solution; it was then removed from the TEA solution and set aside to dry.

The thickness of an organic layer on a SAW device can be approximated⁷ by the following equation:

$$\Delta f = (k_1 + k_2)f_o^2hp \quad (5)$$

where k_1 and k_2 are -9.33×10^{-8} and $-4.16 \times 10^{-8} \text{ m}^2 \text{ sec/kg}$, respectively; f_o is the fundamental frequency, h is the thickness in meters, ρ is the density of the applied layer in kg/m^3 , and Δf is the frequency shift in hertz from the applied layer. Using a 15,454-Hz TEA coating shift and a density of 10^3 kg/m^3 , the thickness of the layer h was calculated to be 500 \AA , which is within the operating range of the SAW device.

The sensor was then challenged with SO_2 vapor in the same manner as the QCM crystal. A linear response was observed for the first several seconds of the exposure upon which saturation occurred, Figure 7. This figure shows the frequency shift of three separate runs with a 15 ppm SO_2 vapor challenge. The response characteristics are quite similar to the bulk 10-MHz crystal, but the baseline recovery was much faster with the SAW device than with the bulk crystal. It took 10 to 20 sec to recover from the SO_2 challenge, and the SAW device seemed to have a higher stability than did the bulk crystal. To determine the response reproducibility, two runs were conducted in which the sensor was challenged with SO_2 nine times and the frequency shift recorded each second for 10 sec. The two runs were taken

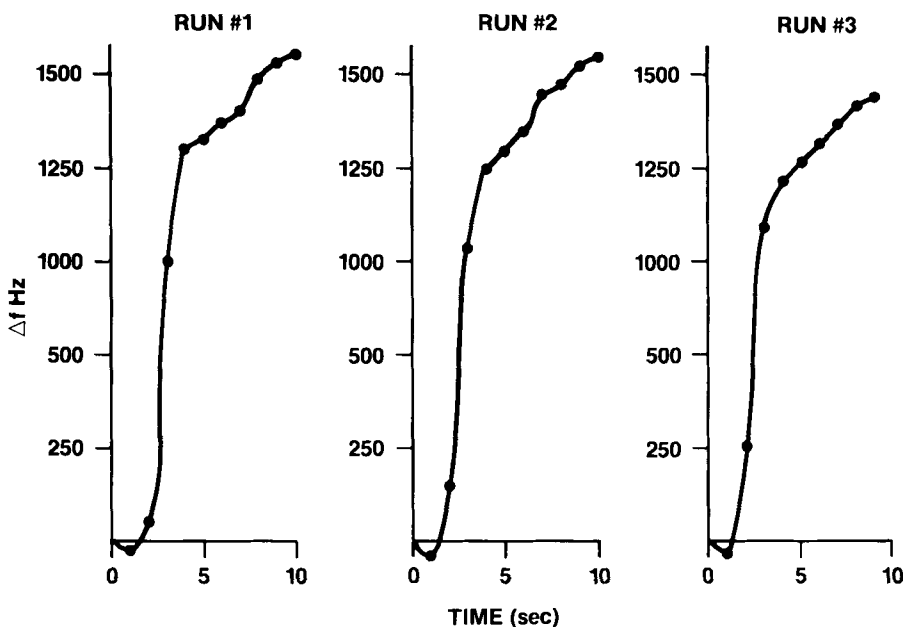


Figure 7. Response of triethanolamine-coated 158-MHz delay line challenged with 15 ppm SO_2 .

several hours apart. The average frequency shifts from the first set of nine challenges were -1315 Hz, -1362 Hz, and -1473 Hz taken at 4, 5, and 6 sec, respectively. The deviation from this average was 11% for all three integration periods. The second run showed similar results with -910 Hz, -1029 Hz, and -1136 Hz at 4, 5, and 6 sec. The deviation from the average was 10% over the nine challenges. The lower response in the second run was probably due to water vapor absorption, which deactivated some of the surface of the coating.

RECENT WORK

Surface acoustic wave (SAW) piezoelectric sensors typically used by researchers in analytical applications are based on SAW delay lines whose operation was described above. Since the time this chapter was prepared we have continued our investigations and have developed a new type of SAW microbalance based on a 200 MHz SAW resonator instead of a conventional delay line.¹⁶

The 200 MHz SAW resonator is similar in construction as the delay line with interdigital electrodes deposited onto the surface of an ST quartz substrate, but contains additional passive elements deposited on its surface. The SAW resonator consists of two transducer electrode arrays that convert the electrical energy into mechanical energy and a set of reflector arrays on each end of the crystal. Unlike the delay line, the resonator's frequency of oscillation is determined by the configuration of the reflector arrays. The mechanical energy traveling along the surface of the crystal is reflected back towards the transducer setting up a standing wave trapping the acoustic energy within the crystal by the constructive interference of the reflected waves. The resonator is therefore a high Q device since the energy is not lost on the ends of the crystal.

The 200 MHz SAW crystal package consists of two individual ST-cut quartz 200 MHz SAW resonator crystals (reference and sensing) mounted on a gold plated six pin base that plugs directly into a circuit board, 6 cm o.d., that contains the power conditioning components, SAW oscillator circuits and signal conditioning electronics. The problem of cross-talk encountered with the 158 MHz delay lines was eliminated by using two individual SAW resonators. Excellent temperature compensation was maintained by mounting the two SAW crystals on a single gold plated package which acts as a thermal base.

The limit-of-detection is a function of both the mass sensitivity of the crystal, which is determined by the operating frequency, and the background noise of the system. The inherent noise of an instrument is typically one of the major parameters in determining the lower limit-of-detection as it directly relates to the signal-to-noise ratio. This was the major limitation of the 158 MHz SAW delay line. Depending on the application, microgravimetric measurements can be made over a period as short as several seconds or up to several hours. The frequency stability of the 200 MHz SAW system and a 10 MHz bulk crystal were measured under identical conditions and compared. The stability of the 200 MHz saw resonator, $\delta f/f$, was better than 5×10^{-9} which is an order of magnitude better than the 10 MHz bulk crystal, 1×10^{-7} . On an absolute basis, the noise of the 200 MHz

SAW resonator is on the same order as the bulk crystal, better than ± 1 Hz. This is also a tremendous improvement over the stability of the 158 MHz SAW delay line (see Results and Discussion above).

A dramatic improvement in the lower limit-of-detection using SAW devices is realized due to high mass sensitivity of the 200 MHz SAW resonator (a result of the operating frequency) coupled with its high frequency stability. The lower limit-of-detection of the 200 MHz SAW resonator was measured to be 3×10^{-12} g which is 1000 times lower than the 10 MHz bulk crystal.

ACKNOWLEDGMENTS

This work was supported by NASA SBIR contracts NAS1-18412, and NAS1-18653.

REFERENCES

1. Chuan, R. L. *J. Aerosol Sci.* 1:111—114 (1969).
2. Chuan, R. L. *Fine Particles*, B. Y. H. Liu, Ed. (New York: Academic Press, 1976), pp. 763—775.
3. Chuan, R. L., D. C. Woods, and M. P. McCormic. *Science* 211:830—832 (1981).
4. NASA Spin Off 82, 96—97.
5. NASA Tech Brief, Vol. 7 (1983).
6. Wohltjen, H., and R. Dessey. *Anal. Chem.* 51:1458—1464 (1979).
7. Wohltjen, H. *Sensors Actuators*. 5:307—325 (1984).
8. Wohltjen, H., and R. Dessey. *Anal. Chem.* 51:1465—1470 (1979).
9. Wohltjen, H., and R. Dessey. *Anal. Chem.* 51:1470—1475 (1979).
10. Nieuwenhuizen, M. S., A. J. Nederlof, and A. W. Barendsz. *Anal. Chem.* 60:230—235 (1988).
11. Nieuwenhuizen, M. S., and A. J. Nederlof. *Anal. Chem.* 60:236—249 (1988).
12. Wohltjen, H., A. W. Snow, W. R. Barger, and D. S. Ballantine. *IEEE Trans. Ultrasonics Ferro Elect. Freq. Control* 34:172—178 (1987).
13. Karmarker, F. H., and G. G. Guilbault. *Anal. Chim. Acta.* 71:419—424 (1974).
14. Cooke, S., T. S. West, and P. Watts. *Anal. Proc.* 17:2—5 (1980).
15. Nova Systems P.O. Box 355, Villa Park, IL, report to Fentometrics, July, 1987.
16. Bowers, W. D. and R. L. Chuan, *Rev. Sci. Instrum.*, 60, 1297, 1989.
17. Bowers, W. D., R. L. Chuan, and T. M. Duong, *Rev. Sci. Instrum.*, 63, 1624, 1991.

LIST OF AUTHORS

L. R. Alexander, Toxicology Branch, Centers for Disease Control,
Atlanta, Georgia 30333

S. S. Berman, Institute for Environmental Chemistry, National Research Council
of Canada, Montreal Road, Ottawa, CANADA KIA 0R9

D. A. Blyth, Geo Centers, Inc., Ft. Washington, Maryland, 20744

W. D. Bowers, Femtometrics, 1001 West Seventeenth Street, Suite R,
Costa Mesa, California 92627

R. L. Chuan, Femtometrics, 1001 West Seventeenth Street, Suite R,
Costa Mesa, California, 92627

R. L. Eatherton, Department of Chemistry, Washington State University,
Pullman, Washington 99164-4630

G. A. Eiceman, Department of Chemistry, New Mexico State University,
Las Cruces, New Mexico 88003-0001

L. E. Elias, Applied Aerodynamics Laboratory, Institute for Aerospace
Research, National Research Council, Ottawa, Ontario, CANADA K1A 0R6

Donald F. Gurka, Methods Research Branch, U. S. Environmental Protection
Agency, 944 East Harmon, Las Vegas, Nevada 89109

H. Hatano, International Institute of Technological Analysis, Health Research
Foundation, Institut Pasteur de Kyoto 5F, Kyoto 606, JAPAN

N. C. Herud, Institute of Clinical Biochemistry, Rikshospitalet, 0027,
Oslo 1, NORWAY

H. H. Hill, Jr., Department of Chemistry, Washington State University,
Pullman, Washington 99164-4630

S. G. Isaacs, Toxicology Branch, Centers for Disease Control,
Atlanta, Georgia 30333

E. Jellum, Institute of Clinical Biochemistry, Rikshospitalet, 0027,
Oslo 1, NORWAY

F. W. Karasek, Department of Chemistry, University of Waterloo,
Waterloo, Ontario, CANADA N2L 3G1

S. H. Kim, EIWA U.S.A., P.M. Box 777, 1419 York Road,
Lutherville, Maryland 21093-6014

Benjamin P.-Y. Lau, Food Research Division, Health and Welfare Canada,
Tunney's Pasture, Ottawa, CANADA K1A 0L2

A. H. Lawrence, Applied Aerodynamics Laboratory, Institute for Aerospace
Research, National Research Council, Ottawa, Ontario, CANADA K1A 0R6

J. C. Marr, Fenwick Laboratories, Ltd., 5595 Fenwick Street, Halifax,
Nova Scotia, CANADA B3H 4M2

J. W. McLaren, Institute for Environmental Chemistry, National Research
Council of Canada, Montreal Road, Ottawa, CANADA K1A 0R9

D. G. McMinn, Department of Chemistry, Gonzaga University, Spokane,
Washington 99258

Y. Moharir, Department of Pathology, McMaster University, 1200 Main Street
West, Hamilton, Ontario, CANADA L8N 3Z5

M. A. Morrissey, Department of Chemistry, Washington State University,
Pullman, Washington 99164-4630

L. L. Needham, Toxicology Branch, Centers for Disease Control,
Atlanta, Georgia 30333

A. Ngo, SCIEEX, 55 Glen Cameron Road #202, Thornhill, Ontario,
CANADA L3T 1P2

T. Ohkawa, Department of Chemistry, Faculty of Science, Kyoto University,
Kyoto 606, JAPAN

D. G. Patterson, Jr., Toxicology Branch, National Center for Environmental
Health and Injury Control, Centers for Disease Control,
Atlanta, Georgia 30333

Janusz Pawliszyn, Department of Chemistry and Waterloo Centre for
Groundwater Research, University of Waterloo,
Waterloo, Ontario, CANADA N2L 3G1

M. A. Quilliam, National Research Council of Canada, 1411 Oxford Street,
Halifax, Nova Scotia, CANADA B3H 3Z1

S. Rokushika, Department of Chemistry, Faculty of Science, Kyoto University,
Kyoto 606, JAPAN

J. M. Rosenfeld, Department of Pathology, McMaster University, 1200 Main Street West, Hamilton, Ontario, CANADA L8N 3Z5

John J. Ryan, Food Research Division, Health and Welfare Canada, Tunney's Pasture, Ottawa, CANADA K1A 0L2

R. St. Louis, Department of Chemistry, Washington State University, Pullman, Washington 99164-4630

C. B. Shumate, Department of Chemistry, Washington State University, Pullman, Washington 99164-4630

B. I. Shushan, SCIEEX, 55 Glen Cameron Road #202, Thornhill, Ontario, CANADA L3T 1P2

W. F. Siems, Department of Chemistry, Washington State University, Pullman, Washington 99164-4630

K. W. M. Siu, Institute for Environmental Chemistry, National Research Council of Canada, Montreal Road, Ottawa, CANADA K1A 0R9

A. P. Snyder, U.S. Army Chemical Research, Development and Engineering Center, Aberdeen Proving Ground, Maryland 21010

Glenn E. Spangler, Environmental Technologies Group, Inc., 1400 Taylor Avenue, Baltimore, Maryland 21204

B. A. Thomson, SCIEEX, 55 Glen Cameron Road #202, Thornhill, Ontario, CANADA L3T 1P2

A. K. Thorsrud, Institute of Clinical Biochemistry, Rikshospitalet, 0027, Oslo 1, NORWAY

H. Y. Tong, Ciba-Geigy Corp., Additives Division, Building LNS-2, 444 Saw Mill River Road, Ardsley, New York 10502

W. E. Turner, Toxicology Branch, Centers for Disease Control, Atlanta, Georgia 30333

J. Visentini, Department of Chemistry, University of Montreal, Montreal, Quebec, CANADA L8N 3Z5

Dorcas Weber, Food Research Division, Health and Welfare Canada, Tunney's Pasture, Ottawa, CANADA K1A 0L2



Taylor & Francis

Taylor & Francis Group

<http://taylorandfrancis.com>

INDEX

- acetaldehyde, marijuana vapor content 66
- acetic acid, ion mobility spectrum 35, 37, 38
- acetone reactant ions 66, 88—96
 - t-caryophyllene sensitivity 88—90, 95—96, 98, 99
 - marijuana detection applications 106—108
 - proton affinity 103
 - temperature effects 98—99
 - Δ_9 -tetrahydrocannabinol sensitivity 90, 98, 107—108
- adenocarcinoma, pancreatic 143
- Agent Orange 136, 140—143, 148, 149
- airborne organic vapors, ion mobility spectrometry 13—25
 - field studies 16—17, 21—23
 - instrumentation 15
 - ion mobility profiles 16—21
 - laboratory studies 16, 17—21
 - procedures 16—17
 - proton/electron affinities 14
 - wind direction effects 16—17
- alkylamines, ion mobility spectrum 43
- ammonia, solubility parameters 265
- ammonium ion, proton affinity 103
- ammonium reactant ions, 87—88
 - cannabidiol sensitivity 93
 - cannabinoid sensitivity 103—106
 - cannabinol sensitivity 93
 - t-caryophyllene sensitivity 87, 89, 96, 99
 - generation of 104—106
 - ionization sequence 103—104
 - marijuana detection applications 106—109
 - proton transfer reactions 103—105
 - temperature effects 96, 98—99
 - Δ_9 -tetrahydrocannabinol sensitivity 87, 91—93
- aniline, ion mobility spectrum 43—46
- anthracene, ion mobility spectrum 34
- 9,10-anthraquinone, mass spectrum 229
- antimony, as flyash water leachate 180, 191
- aqueous samples
 - hollow fiber membrane extraction 271—275
 - supercritical fluid extraction 269—271
- Aroclor 54—56
- aromatic amines, ion mobility spectrum 43—46
- aromatic hydrocarbons, ion mobility spectrum 27—34
- arsenic
 - chemical speciation 198—201, 203—204
 - as flyash water leachate 180, 191
 - marine specimen content 198—201, 203—204
- arsenobetaine 199—200, 203—204
- arsenocholine 199—200, 203—204
- atmospheric pressure ionization 14, 209—217
 - heated nebulizer 210—212, 213—216
 - ion spray 210, 211, 212—216
- 1,2-benzanthrene, ion mobility spectrum 33, 34
- benzene
 - chlorinated 258, 259
 - ion mobility spectrum 33, 34
 - proton affinity 103
- benzene-water partitioning 179—180, 183, 186
- benzodiazepines, skin-surface sampling 5
- 3,4-benzpyrene, ion mobility spectrum 34
- Biller-Biemann enhancement routine 232
- bomb detection 4—5
- bromazepam, ion mobility spectrum 10

- butyric acid, ion mobility spectrum 34, 35, 38
- cadmium, as flyash water leachate 180, 190, 191
- caffeine, supercritical fluid extraction 261
- cannabichrome, nonvolatility 66
- cannabidiol
 - ammonium reactant ion sensitivity 93
 - hydronium reactant ion sensitivity 82—83
 - ion mobility spectrum 82, 83, 85, 86, 93
 - nonvolatility 66
 - proton transfer reaction 102
- cannabinoids
 - ammonium reactant ion sensitivity 103—106
 - ion mobility spectrum 79, 81—83
 - pyrolyzation 67—68
- cannabinol
 - ammonium reactant ion sensitivity 93
 - hydronium reactant ion sensitivity 82—83
 - ion mobility spectrum 82, 83, 85, 86, 93
 - nonvolatility 66
 - proton transfer reaction 102—103
- Cannabis sativa* 66
- capillary gas chromatography 221
- capillary zone electrophoresis 210
- caproic acid, ion mobility spectrum 35, 37, 38
- caprylic acid, ion mobility spectrum 35, 37, 38
- carbon, plasma elemental intensity chromatogram 250
- carbon dioxide, solubility parameters 265, 266, 267
- carbon tetrachloride, solubility parameters 266
- caryophyllene, marijuana vapor content
 - detection 106, 108
 - ion mobility spectrum 79, 81, 106, 108
 - mass spectrum 106, 108
 - proton transfer reaction 101—102
- β -caryophyllene, marijuana vapor content, 66, 110
- t-caryophyllene, marijuana vapor content
 - acetone reactant ion sensitivity 88—90, 95—96, 98, 99
 - ammonium reactant ion sensitivity 87, 89, 96, 99
 - hydronium reactant ion sensitivity 74, 79, 80, 96, 99
 - ion mobility spectrum 74, 79, 80, 87, 88—90, 95—96
 - mass spectrum 80, 87, 89, 95, 90, 97
 - proton transfer reaction 101
 - temperature effects 96, 99
- caryophyllene oxide, proton transfer reaction 101—102
- chemistry, instrumental analytical 1
- chloracne 145
- chlorinated solvents, hollow fiber membrane extraction 271, 274, 275
- chlorine, plasma elemental intensity chromatogram 250
- chloroform, solubility parameters 266
- chlorophenols
 - chromatographic separation 283—286, 287—288
 - derivatization 282—284
- chlorophenoxy acetic acid
 - chromatographic separation 283—288
 - derivatization 282—284
- 4-chlorophenyl phenyl ether, 244
- chlorotrifluoromethane, solubility parameters, 265
- chromatography, *see* specific types of chromatography
- chrysene, ion mobility spectrum 34
- coal, supercritical fluid extraction 261
- cocaine, skin-surface sampling 5
- coffee, decaffeination 261—262
- collidine, ion mobility spectrum 37—39, 44
- corona-spray 60—64
- cresol, ion mobility spectrum 36, 37
- cumene, ion mobility spectrum 34
- cyclohexane, solubility parameters 266
- decaffeination 261—262
- derivatization 280—284
- detector
 - diode array 222
 - electron capture 14
 - high detection selectivity 221
 - multichannel 222

- dexamethasone, atmospheric pressure ionization 214—216
- diazepam, ion mobility spectrum 10
- dibenzofurans, *see also* polychlorinated dibenzofurans
 dimethyl 231, 232, 234
 ethyl 231, 232, 234
- dibenzothiophene, isomers 231, 233
- 2,4-dichlorophenol, derivatization 281—283
- 2,4-dichlorophenoxy acetic acid 55—57
 chromatographic isolation 284—286, 288
 derivatization 281—283
 supercritical fluid chromatography 55—57
- Diehls-Alder reaction 101
- diethyl ether, solubility parameters 266
- digital signal processing 9
- dimethylarsenic acid 200—201
- 2,3-dimethylnaphthalene, ion mobility spectrum 34
- dimethylsulfoxide, ion mobility spectrometry 13
 field studies 21, 23
 instrumentation 15
 laboratory studies 17—18
- d-dimonene, marijuana vapor content 74, 77, 78
- diode array detector 222
- diphenyl, ion mobility spectrum 34
- dipropylenglycolmonomethylether, ion mobility spectrometry 13
 field studies 17, 24
 instrumentation 15
 laboratory studies 17—18
- doxepin, overdose 5—6
- drugs, skin-surface sampling 5—6
- dynamite, detection 4—5
- electron capture detector 14
- electrospray 195, 196, 203—205, 210
- ethanol, marijuana vapor content 66
- ethylacetate, marijuana vapor content 66
- ethyl acetate, solubility parameters 266
- ethyl alcohol, solubility parameters 266
- ethylene benzene
 ion mobility spectrum 34
 solid phase microextraction 258, 259
- ethylene glycol dinitrate 4
- β -farnescene, marijuana vapor content 66
- fatty acids, ion mobility spectrum 32, 34—35
- fibroblast, water leachate toxicity test 185—186, 189—191
- flame ionization detection 222, 258
- fluoranthene, ion mobility spectrum 34
- flyash, as water leachate 179—194
 benzene-water partitioning 179—180, 183, 186
 composition 180—181
 dioxin content 184—185, 187—188
 gas chromatography 183, 187
 gas chromatography-mass spectrometry 183—184, 187—188
 inductively-coupled plasma analysis 180, 185
 inorganic compound content 185—186
 organic compound content 186, 189, 190
 supercritical fluid extraction 267
 two-dimensional gel electrophoresis 185—186
- forensic chemistry 5—6
- Fourier transform infrared hyphenated techniques 241—250
 commercially available 249
 computer software 247—248
 future developments 249—250
 gas chromatography-mass spectrometry 241—244, 247
 gas chromatography-matrix isolation, 244—247
 gas chromatography-supercritical fluid 245, 248
 lightpipe technique 243, 244, 247
 plasma elemental analysis 249, 250
- gas chromatography
 flame ionization detection 222
 ion mobility spectrometry 49—55
 supercritical fluid 245, 246
 two-dimensional 224
 water leachate analysis 183, 187
- gas chromatography-mass spectrometry
 Fourier transform infrared 241—244, 247
 involatile compound analysis 221—222
 parallel column 224—237
 automated comparisons 232—237

- chromatogram comparisons
 - 230—232
- methyl silicone phase 228
- peak detection algorithm, 232—233
- phenyl-methyl silicone phase
 - 228—229, 233—237
- retention indices 233—236
- stationary phase 228
- total ion chromatogram 228—230, 232
- as third-column chromatography, 226
- volatile organic compound analysis
 - 241—242
- water leachate analysis 183—184, 187—188
- gas extraction, with hollow fiber membranes 271—275
- gasoline, nonselective positive-ion chromatogram 52—54
- gel electrophoresis, two-dimensional 185—186
- graphite furnace atomic absorption spectrometry 197
- guanosine, atmospheric pressure ionization 213—214, 215, 216
- heated nebulizer 210—212, 213—216
- helium plasma elemental analysis 249, 250
- 1,2,3,4,7,8-heptachlorodibenzo-p-dioxin, as flyash water leachate 181, 184, 187, 188
- herbicides
 - chromatographic separation 283—286, 287—288
 - derivatization 282—284
- hexachlorodibenzo-p-dioxin
 - as flyash water leachate 181, 184, 187, 188
 - mass spectrometry 164, 165, 171, 173, 176
- hexachlorofuran, mass spectrometry 164, 165, 171, 173, 176
- hexachlorophene, 145
- high performance liquid chromatography fluorescence detector 221
 - with UV adsorption detection 222
- high performance liquid chromatography-electrospray mass spectrometry 180, 185, 195, 196, 203—205
- high performance liquid chromatography-mass spectrometry
 - incompatibility 195—196
 - interfacing techniques 195
 - involatile compound analysis 221—222
- high performance liquid chromatography-mass spectrometry-inductively-coupled plasma 196
 - arsenic speciation, 198—201
 - limitations, 197—198
 - marine sample analysis, 198—203
 - sample introduction, 197
 - tin speciation, 201—203
- high resolution mass spectrometry, of polychlorinated dibenzo-p-dioxins/dibenzofurans 119—154
 - calibration curves 128, 129
 - experimental methodology 121—139
 - fasting vs. nonfasting samples 126
 - interference peaks 165, 171
 - internal standard recovery 134—136
 - in vivo/in vitro studies 124—125
 - isotope ratios 128, 132—133
 - limit of detection 160, 161
 - limit of quantification 138
 - mass chromatograms 168—170
 - method performance 138—139
 - method validation studies 122—126
 - occupational exposure study 147—148
 - quality assurance 126—139
 - quality control 126—128
 - sample cleaning 121—122
 - sample preparation 156
 - Seveso, Italy study 143—145
 - signal-to-noise ratio 134, 137
 - standard solutions 157
 - study sample size 134
 - Vietnam veteran study 126, 140—143, 149
- hollow fiber membrane extraction 271—275
- hops, supercritical fluid extraction 261
- hydrocarbons
 - aromatic 27—34
 - as flyash water leachate, 181
 - polycyclic aromatic 181, 189, 224, 265
- hydrogen, plasma elemental intensity chromatogram 250
- hydronium reactant ions, 74—86
 - cannabidiol sensitivity 82—83

- cannabinol sensitivity 82—83
- generation of 104
- t-caryophyllene sensitivity 74, 79, 80, 96, 99
- marijuana detection applications 106—107, 109
- temperature effects 96, 98—99
- Δ_9 -tetrahydrocannabinol sensitivity 82—86
- hyphenated techniques 241, *see also*
 - Fourier transform infrared
 - hyphenated techniques
- indole acetic acid, Fourier transform infrared spectrum 248
- inductively coupled plasma 180, 185, 195, 196, 203—205
- β -iodonaphthalene, ion mobility spectrum 34
- ion mobility mass spectrometry 1—11
 - airborne organic vapor monitoring 13—25
 - field studies 16—17, 21—23
 - instrumentation 15
 - ion intensity profiles 17—21
 - laboratory studies 16, 17—21
 - mobility spectra 17
 - procedures 16—17
 - proton/electron affinities 14, 21, 23
 - wind direction effects 16—17
 - of aromatic amines 43—46
 - of aromatic hydrocarbons 27—34
 - corona-spray 60—64
 - definition 28
 - of fatty acids 32, 34—35
 - field-use chemical sensors 8
 - forensic applications 5—6
 - as gas chromatographic detector 49—55
 - of heterocyclic nitrogen compounds 34, 41—43
 - instrument parameters 4
 - as liquid chromatographic detector 59—64
 - marijuana headspace vapor analysis 65—117
 - acetone reactant ions 69, 88—96, 111
 - ammonium reactant ions 69, 87—88, 110—111
 - cannabinoids 102—106, 110
 - caryophyllene 79, 81, 101—102, 106, 108, 110
 - hydronium reactant ions 74—86, 110
 - ion-molecule reactions 68—69
 - lesser volatile fraction 66
 - marijuana detection applications 66, 106—110
 - membrane inlet 74
 - monoterpenes 74, 77, 78, 99—101
 - nonvolatile fraction 66
 - permeation tube 73
 - smoking apparatus 74, 75
 - temperature studies 96—99
 - vapor pressure 67
 - volatile fraction 66
 - medical applications 5—6
 - of nitrogen-containing compounds 27—29, 34—43
 - of phenolic compounds 29—33, 36, 38
 - plant materials characterization with 6—8
 - proton transfer reaction 68—69, 99—106
 - of pyridine 34, 37—41
 - sample processing time 2
 - spectra resolution enhancement 9—10
 - spectrometer 2, 3
 - of sulfur-containing compounds 27, 45—48
 - as supercritical fluid chromatographic detector 55—59
 - ion spray 210—216
 - isobutylaldehyde, marijuana vapor content 66
 - ketones, polycyclic aromatic 224
 - lead, as flyash water leachate 180, 181, 190, 191
 - lightpipe technique 243, 244, 247
 - d-limonene, marijuana vapor content 66, 99—101
 - lipoproteins, polychlorinated compound association 123—124
 - liquid chromatography-mass spectrometry
 - atmospheric pressure ionization 209—217
 - heated nebulizer 210—216

- ion spray inlet 210—216
- mass spectra 213—214
- sensitivity 215—216
- low resolution mass spectrometry 160, 161, 168—169
 - adduct ion formation 173
 - applications 163
 - interference peaks 163, 165, 171
 - mass chromatogram 168—170
 - reagent blank response 163
 - sample preparation 156
- lutidine, ion mobility spectrum 37—39
- marijuana headspace vapor analysis 65—117
 - acetone reactant ions 69, 88—96, 111
 - ammonium reactant ions 69, 87—88, 110—111
 - cannabinoids 102—106, 110
 - caryophyllene 79, 81, 101—102, 106, 108, 110
 - hydronium reactant ions 68—69, 74—86, 110
 - ion-molecule reactions 68—69
 - lesser volatile fraction 66
 - marijuana detection applications 66, 106—110
 - with mass spectrometry 70—112
 - membrane inlet 74
 - monoterpenes 74, 77, 78, 99—101
 - nonvolatile fraction 66
 - permeation tube 73
 - smoking apparatus 74, 75
 - temperature studies 96—99
 - vapor pressures 67
 - volatile fraction 66
- marine sediment
 - parallel column gas chromatography 227—237
 - polycyclic aromatic compounds 222, 223, 238
- mass spectrometer 221, 222
 - atmospheric pressure ionization 14
 - time-of-flight 2
- mass spectrometry-mass spectrometry, see also ion mobility mass spectrometry; low resolution mass spectrometry; high resolution mass spectrometry
 - applications 163
 - hybrid instrument 158—159, 164—169, 171
 - interference peaks 171
 - operating conditions 158—159
 - reagent blank response 163, 164
 - triple quadrupole system
 - adduct ion formation 171, 173, 174
 - applications 163
 - isotope ratio 164
 - limit of detection 160, 162—163
 - mass chromatogram 168—170
 - operating conditions 159—160
 - retention time span 163—171
 - sample preparation 156
 - standard solutions 157—158
- matrix isolation 244—247
- mercury, as flyash water leachate 181
- methanol, marijuana vapor content 66
- methionine, atmospheric pressure ionization 213—216
- methyl alcohol, solubility parameters 266
- methylarsonic acid 198—200
- methyl esters 56, 59, 60
- 2-methylnaphthalene, nonselective positive-ion chromatogram 53—54
- methylsalicylate vapors, ion mobility spectrometry 13
 - field studies 16—17, 22
 - instrumentation 15
 - laboratory studies, 17—18
- Missouri, dioxin exposure study 145—149
- monobutyltin 202
- monoterpenes, marijuana vapor content 106
 - ion mobility spectrum 74, 77
 - mass spectrum 74, 78
 - proton transfer reaction 99—101
- multidimensional techniques 222, 224
- musk ambrette, ion mobility spectrum 49—50
- β -myrcene, marijuana vapor content 66
 - ion mobility spectrum 74, 77, 78
 - proton transfer reaction 99—101
- naphthalene
 - ion mobility spectrum 33, 34
 - nonselective positive-ion chromatogram 53—54

- nebulizer, heated 210—212, 213—216
- nickel carbonyl, airborne detection 14
- nitrogen compounds
 heterocyclic, ion mobility spectrum 34, 41—43
 ion mobility spectrum 27—29, 34, 41—43
- N-nitrosodimethylamine, Fourier transform infrared spectra 244
- nitrous oxide, solubility parameters 265
- ocimene, marijuana vapor content 66
- octachlorodibenzo-p-dioxin
 as flyash water leachate 181, 184, 187, 188
 mass spectrometry
 hybrid methods 166
 limit of detection 156
 low resolution 160, 161
 sample preparation 156
 triple quadrupole 159—160
- organometallic speciation 195—208
- orthogonal chromatography 222, 224
- overdose, skin-surface sampling 5—6
- paraben 60, 63—64
- particle beam 195
- PCB, *see* polychlorinated biphenyls
- PCDD, *see* polychlorinated dibenzo-p-dioxins
- PCDF, *see* polychlorinated dibenzofurans
- pentacene, ion mobility spectrum 34
- pentachlorodibenzofurans, mass spectrometry 163, 165, 170, 171, 174—176
- pentachlorophenol, wood chip content 7, 9
- pentafluorobenzoylation 280—284
- pentane, solubility parameters 266
- peppermint oil 54
- peptides
 liquid chromatography-mass spectrometry 210
 supercritical fluid extraction 262
- perylene, ion mobility spectrum 34
- β -phellandrene, marijuana vapor content 66
- phenanthracene
 Fourier transform infrared spectrum 244
 ion mobility spectrum 34
- phenanthro(4,5-bcd)thiophene, mass spectrum 229
- phenol
 chlorinated, trace by-products 120
 ion mobility spectrum 36, 37
- phenolic compounds, ion mobility spectrum 29—33, 36, 38
- photoionization 14
- phthalates
 Fourier transform infrared spectrum 244
 as flyash water leachate 181
- picoline, ion mobility spectrum 37—40
- α -pinene, marijuana vapor content 66
 ion mobility spectrum, 74, 77, 78
 proton transfer reaction 99—101
- piperidine, ion mobility spectrum 41—43
- plasma chromatography, *see* ion mobility mass spectrometry
- plasma elemental analysis 249, 250
- polychlorinated aromatic compounds,
 parallel column gas chromatography 226—237
- polychlorinated biphenyls, parallel column gas chromatography 224, 226
- polychlorinated dibenzo-p-dioxins
 adipose tissue content 120
 as flyash water leachates 179—181, 184—185, 187—190
 recovery study 184—185
- high resolution mass spectrometry 119—154
 calibration curves 128, 129
 chromatographic isomer specificity 130, 134
 experimental methodology 121—139
 fasting vs. nonfasting samples 126
 interference peaks 165, 171
 internal standard recovery 134—136
 in vivo/in vitro studies 124—125
 isotope ratios 128, 132—133
 mass chromatograms 168—170
 method performance 138—139
 method validation studies 122—126
 Missouri study 145—147
 occupational exposure 147—148
 quality assurance 126—138
 quality control 126—128

- sample cleaning 121—122
- sample preparation 156
- Seveso, Italy study 143—145
- signal-to-noise ratio 134, 137
- standard solutions 157
- study sample size 134
- Vietnam veteran study 126, 140—143, 149
- low resolution mass spectrometry 155
 - adduct ion formation 173
 - interference peaks 163, 165, 171
 - limit of detection 160, 161
 - mass chromatograms 168—170
 - reagent blank response 163
 - sample preparation 156
- mass spectrometry-mass spectrometry, 155—177
 - hybrid system 166, 167
 - mass chromatograms, 168—170
 - operating conditions, 158—159
 - pseudo-dioxin formation 173
 - reagent blank response 163, 164
 - retention time span 163—171
 - sample preparation 156
 - standard solutions 157—158
- production 120
- supercritical fluid extraction 267
- toxicity 189—190
- triple quadrupole mass spectrometry-mass spectrometry 155—156
 - adduct ion formation 171, 173, 174, 176
 - limit of detection 160, 162—163
 - mass chromatograms 168—170
 - operating conditions 159—160
 - retention time span 163—171
 - sample preparation 156
 - standard solutions 157—158
- polychlorinated dibenzofurans
 - adipose tissue content 120
 - as flyash water leachates 179—180, 181, 187—190
- high resolution mass spectrometry 119—154
 - calibration curves 128, 129
 - experimental methodology 121—139
 - fasting vs. nonfasting samples 126
 - internal standard recovery 134—136
 - in vivo/in vitro studies 124—125
 - isotope ratios 128, 132—133
 - method performance 138—139
 - method validation studies 122—126
 - quality assurance 128—139
 - quality control 126—128
 - sample cleanup 121—122
 - signal-to-noise ratio 134, 137
 - study sample size 134
- mass spectrometry-mass spectrometry 155—177
 - adduct ion formation 173—174
 - detection limits 160—163
 - hybrid system 166
 - sample cleanup 177
 - sample preparation 156
 - standard solutions 157—158
 - triple quadrupole system 159—160, 162
 - toxicity 189—190
- polychlorinated organic compounds, as flyash water leachate 181
- polycyclic aromatic compounds 189
 - airborne particulate samples 224
 - carcinogenicity 220
 - as flyash water leachate 181
- gas chromatography-mass spectrometry 222
 - marine sediment content 222, 223, 238
 - nitrated, 224
 - structure 219, 220
 - supercritical fluid extraction 265
- polymeric membrane extraction 271—275
- polynuclear aromatics, Fourier transform infrared detection 242
- polynucleotides, liquid chromatography-mass spectrometry 210
- n-propane, solubility parameters 265
- proteins, supercritical fluid extraction 262
- proton transfer reaction 68—69
 - cannabinoids 102—106
 - caryophyllene 101—102
 - monoterpenes 99—101
- pyrene, ion mobility spectrum 34
- pyridine
 - ion mobility spectrum 34, 37—41
 - solubility parameters 266
- quinones, polycyclic aromatic 224
- reserpine, atmospheric pressure ionization 214, 215, 216

- serum, polychlorinated dibenzo-p-dioxin/
dibenzofuran content analysis,
120—150
 - experimental methodology 121—139
 - occupational exposure studies
147—148
 - quality assurance 126—139
 - Seveso, Italy study 143—145
 - Vietnam veteran study 126,
140—143, 149
- sesquiterpenes, marijuana vapor content
66, 102, 110
- Seveso, Italy, dioxin exposure study
143—145
- sewage treatment plant effluent, solid
phase microextraction 259—260
- skin-surface sampling, of drugs 5—6
- solid phase microextraction, with fused
silica fibers 254—260
 - applications 259
 - electron capture detection 257
 - with flame ionization detection 258
 - limit of quantization 257
 - partition coefficient 256, 257
 - peak tailing 258
 - sample transfer 256
 - selectivity 256, 258
 - solvent extraction vs. 259—260
- solid supported processes 279—289
 - chromatographic isolation 284—286,
288
 - derivatization 280—284
- solvent-free extraction 253—277
 - gas extraction 271—275
 - sample transfer 256
 - supercritical fluid extraction 261—271
 - analyte deposition 263
 - applications 261—262
 - aqueous samples 269—271
 - extraction time 265, 267
 - gas solubility parameters 264—267
 - instrumentation 262—263
 - matrix 265, 267—271
 - operation principles 261
 - restrictor 263
 - Soxhlet extraction vs. 262
 - viscosity 262
- steroids, liquid chromatography-mass
spectrometry 210, 213
- sulfur-containing compounds, ion
mobility spectrum 27, 45—48
- sulfur dioxide, surface acoustic wave
piezoelectric microbalance
detection 292, 295—296,
301—303
- supercritical fluid extraction 261—271
 - analyte deposition 263
 - applications 261—262
 - aqueous samples 269—271
 - extraction time 265, 267
 - Fourier transform infrared 245, 248
 - gas solubility parameters 264—267
 - instrumentation 262—263
 - ion mobility spectrometry and 55—59
 - matrix 265, 267—271
 - operation principles 261
 - restrictor 263
 - Soxhlet extraction versus 262
 - viscosity 262
- surface acoustic wave piezoelectric
crystal aerosol mass microbalance
291—304
 - frequency stability 291, 296, 299—301
 - limit of detection 296, 303—304
 - mass sensitivity 299—301
 - piezoelectric crystal excitation
293—294
 - pressure change response 291—292,
297—298
 - principle of operation 293—294
 - quartz crystal microbalance comparison
291—294, 296—297, 299
 - Rayleigh mode surface acoustic wave
293, 294
 - resonator 303—304
 - temperature change response 291, 298
 - triethanolamine liquid phase 301—302
- terpenes 102
- terphenyl, ion mobility spectrum 34
- tetrabutylammonium chloride,
atmospheric pressure ionization
214, 215, 216
- 2,3,7,8-tetrachlorobibenzo-p-dioxin
as Agent Orange contaminant 136,
140—143, 148, 149
- as flyash water leachate 181, 184
- Fourier transform infrared spectrum
244, 246
- half-life 143, 145
- high resolution mass spectrometry
120—150, 168—169

- in vivo/in vitro studies 123—124
- limit of detection 138
- limit of quantification 138
- method performance 138—139
- method validation studies 122—124
- quality assurance 128—133, 137—139
- signal-to-noise ratio 137
- standard isotope ratio chart 132, 133
- low resolution mass spectrometry 160, 161, 168—169
- mass spectrometry-mass spectrometry hybrid methods, 158—159, 164, 165, 168—169, 171
- interference peaks, 171
- limit of detection, 156
- low resolution, 160, 161, 168—169
- sample preparation, 156
- standard solutions, 157
- triple quadrupole, 159—160, 168—169
- minimum detection limits, 156
- occupational exposure, 147—148
- Seveso, Italy exposure study, 143—145
- toxicity, 119
- Δ_9 -tetrahydrocannabinol, marijuana vapor content
 - acetone reactant ion sensitivity 90, 98, 107—108
 - ammonium reactant ion sensitivity 87, 91—93, 98, 108, 110—111
 - detection applications, 107—108, 110—111
 - hydronium reactant ion sensitivity 82—86, 98, 108, 110—111
 - ion mobility spectrum 82—87, 91, 93
 - mass mobility spectrum 92
 - proton transfer reaction 102
- thermospray 195, 210
- tin, chemical speciation 201—203, 205, 206
- tobacco, supercritical fluid extraction 261
- toluene
 - ion mobility spectrum 33, 34
 - proton affinity 103
 - solubility parameters 266
- tributyltin 201—202
- 2,4,5-trichlorophenol 120, 145, 146
 - chromatographic isolation 288
 - derivatization 281—238
- tricyclic antidepressants, skin-surface sampling 5—6
- triethanolamine 301—302
- triethylphosphate, ion mobility spectrum 17—21
- 1,2,3-trimethylbenzene, proton affinity 103
- triphenylamine, ion mobility spectrum 44, 45
- Triton-X 100 62
- two-dimensional gas chromatography 224
- two-dimensional gel electrophoresis 185—186
- ultraviolet adsorption detection 222
- urban dust sample, parallel column gas chromatography 227, 234
- valeric acid, ion mobility spectrum 35, 37
- vapor plumes, ion mobility spectrometry 13—25
 - field studies 16—17, 21—23
 - instrumentation 15
 - ion intensity profiles 17—21
 - laboratory studies 16—21
 - mobility spectra 17
 - procedures 16—17
 - proton/electron affinities 14, 21, 23
 - wind direction effects 16—17
- Vietnam veterans, Agent Orange exposure 136, 140—143, 148, 149
- water leachates, 179—194
 - benzene-water partitioning 179—180, 183, 186
 - dioxin recovery study 184—185, 187—188
 - gas chromatography 183, 187
 - gas chromatography/mass spectrometry 183—184, 187—188
 - inductively coupled plasma analysis 180, 185
 - inorganic compound analysis 185—186
 - organic compound analysis 186, 189, 190
 - two-dimensional gel electrophoresis 185—186

wood, ion mobility spectra 6—9

XAD-2 adsorption/derivatization 280,
281—288

XAD-16 287

xenon, solubility parameters 265

xylene

ion mobility spectrum 34

solid phase microextraction 258, 259

xylenol, ion mobility spectrum 36, 37

zinc, as flyash water leachate 181